more fun than anything

Thesis by

Daniel Charles Harris

In Partial Fulfillment of the Requirements

for the Degree of

Doctor of Philosophy

California Institute of Technology

Pasadena, California

1973

(Submitted 6 March 1973)

There is no way this thesis would be finished at this time without the enormous assistance of my Famous Wife who actually performed many of the experiments during a period in which I was incapacitated. Had I been incapacitated longer, this could have been a damned good thesis.

Acknowledgements

All the members of the Gray Group provided me with aid and comfort on many occasions. Therefore I do not take sole responsibility for the shortcomings of this thesis. Dave Ottesen provided extensive help with normal coordinate analysis. George Rossman was of assistance in nearly every phase of the experimental work. Charlie Cowman, Jack Thibeault and Ron Ziolo collaborated in the study of cyclopropenium salts. Charlie Cowman was especially helpful in the interpretation of electronic spectra. Harry Gray could often be collared into useful discussions. I was chagrined when Harry replaced me as Director of Cyclopropenium Research and named my wife to that post.

This research was supported by the National Science Foundation. I was personally supported for three years by a National Science Foundation Fellowship until it went out of the fellowship business in 1971. I am indebted to Richard Nixon for that. I am also indebted to Mr. Nixon for continuing the war in Asia during my entire stay in graduate school and thereby making life that much more exciting at home and lethal abroad.

Caltech has been far more than generous in its support of my part-time and full-time teaching. I am especially indebted to Harry Gray and George Hammond for directing some of my efforts into undergraduate teaching. Mike Bertolucci provided intimate collaboration in this endeavor. Never to be underestimated are the Trolls of Chem 2 who, for three years, provided the most rewarding teaching experience a person could ask for.

Abstract

An exhaustive study of piddling cyclopropenium salts is described. This includes synthesis, characterization and the study of ligand

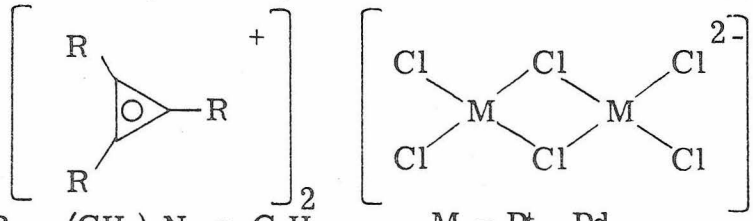

R = $(CH_3)_2N$, n-C_3H_7 M = Pt, Pd

substitution reactions of the $M_2Cl_6^{2-}$ anions. The electronic absorption spectra and vibrational spectra are interpreted. A normal coordinate analysis of the $M_2Cl_6^{2-}$ anions is reported. Startling counterion effects in ligand substitution reactions in CH_2Cl_2 solvent were observed.

The transformation M-M → M-H-M$^+$, in which a metal-metal bond is protonated by strong acid, has been studied in several organometallic systems. Electronic spectra are tentatively interpreted in terms of three-center two-electron M-H-M bonding. The stretching vibrations associated with a W-H-W bridge are assigned. Infrared spectra indicate the presence of isomeric protonated species for several iron compounds. Base strength determination indicates that the replacement of Fe by Ru or replacement of CO by $P(OCH_3)_3$ both increase the basicity of $[(\pi\text{-}C_5H_5)Fe(CO)_2]_2$ by at least 2-3 orders of magnitude.

Ancillary chapters deal with the present state of π-cyclopropenium chemistry, predictions about the infrared spectra of π-cyclopropenium complexes and an original technique for graphical display of the concentrations of the various species present during an acid-base titration in acetic acid. A brief description of my advanced placement freshman chemistry course is included.

TABLE OF CONTENTS

Chapter One. The One That Got Away 1
- Introduction 1
- Properties of Cyclopropenium Salts 1
- Synthesis of π-Cyclopropenium Complexes 10
- References 19

Chapter Two. Great Expectations 23
- References 35

Chapter Three. Synthesis and Properties of $M_2Cl_6^{2-}$ Salts 37
- Introduction 37
- Experimental 39
- Results and Discussion 42
- References 82

Chapter Four. The Infrared Spectrum of the $M_2Cl_6^{2-}$ Anion (M= Pt, Pd) 87
- Introduction 87
- Experimental 89
- Results and Discussion 90
  - Assignment of the Spectra 90
  - Force Constants 98
  - Discussion 101
- Appendix 105
- References 112

Chapter Five. The Reactivity of the $M_2Cl_6^{2-}$ Anion 116
- Cation Exchange 116
- Reaction With Chloride 125
- Reaction With Cyclooctene 140
- Reaction With Acetonitrile 156
- Miscellaneous Reactions 173
- Experimental 179

References 186

Chapter Six. The Protonated Metal-Metal Bond 191
History 191
The Case for Levenson 193
The Silent Majority 198
Electronic Spectra of the Protonated Metal-Metal Bond 206
Vibrational Spectra 228
NMR Studies 276
Potentiometric Base Strength Determination in Acetic Acid 293
A Brief Excursion 295
Experimental 299
References 326

Chapter Seven. Graphical Display of Pernicious Acid-Base Equilibria in Acetic Acid 339
References 368

Chapter Eight. The Philosophy of Chem 2 369

List of Tables

Chapter One

I. Cyclopropenium Salts 2
II. Infrared Spectra 4
III. Force Constants of Aromatic Species 5
IV. Susceptibility of Cyclopropenium Cations to Hydrolysis 7
V. Reduction Potentials 8
VI. Distances (Å) in Some Nickel Complexes of Carbocyclic Rings 12
VII. Electronic Spectra of (L)Ni(1,7-$B_9H_9CHPCH_3$)) Complexes 14

Chapter Two

I. Metal-Olefin Stretching Frequencies 24
II. Selected Vibrational Frequencies of Cyclopentadienyl Complexes 25
III. Skeletal Vibration of Dibenzene-Metal Complexes 27
IV. IR Active Metal-Ring Vibrations 28
V. Vibrations of Coordinated Olefins 30
VI. IR Active Modes of Free Ligands 31
VII. Selected Ligand Vibrations of π-C_6H_6 and π-C_7H_7 Complexes 32

Chapter Three

I. Analytical Data 44
II. Conductivity Measurements 45
III. NMR Measurements 46
IV. Infrared Spectra of $[(n\text{-}C_3H_7)_3C_3]$ Salts in KBr Pellets from 4000-300 cm^{-1} 47
V. Infrared Spectra of $\{[(CH_3)N]_3C_3\}$ Salts in KBr Pellets from 4000-300 cm^{-1} 48
VI. UV-VIS Spectral Data 56
VII. Transitions of $Pt_2Cl_6^{2-}$ 70
VIII. Assignments of Solution Spectra 77
IX. Interatomic Distances (Å) and Angles (Deg) 79
X. Least-Squares Planes in $\{[CH_3)_2N]_3\}_2\{Pt_2Cl_6\}$ 81

Chapter Four

I. FIR Spectra of the Compounds Studied in This Work 93

II. Normal Modes of Vibration of $M_2Y_2X_4$ in D_{2h} Symmetry 94

III. Assignment of the IR-Active Fundamentals of the $M_2Cl_6^{2-}$ Anion 95

IV. Comparison of FIR Spectra 102

Chapter Five

I. Titration of $(N)_2(M_2Cl_6)$ with $(N)(BF_4)$ in CH_2Cl_2 119

II. Titration of $(P)_2(M_2Cl_6)$ with $(N)(BF_4)$ in CH_2Cl_2 122

III. Titration of $(N)_2(M_2Cl_6)$ with $(n\text{-}C_4H_9)_4NCl$ in CH_2Cl_2 130

IV. NMR Measurements 133

V. IR Spectra (360-300 cm^{-1}) 136

VI. Titration of $(N)_2(Pd_2Cl_6)$ with Cyclooctene in CH_2Cl_2 142

VII. Titration of $(N)_2(Pd_2Cl_6)$ with Cyclooctene in CH_2Cl_2 144

VIII. Titration of $(P)_2(Pd_2Cl_6)$ with Cyclooctene in CH_2Cl_2 147

IX. Titration of $(P)_2(Pd_2Cl_6)$ with Cyclooctene in CH_2Cl_2 150

X. Summary of π-Olefin Spectra 154

XI. NMR Spectra of $(CH_3CN)PtCl_3^-$ Salts 161

XII. Infrared and Raman Spectra of $(CH_3CN)PtCl_3^-$ Salts 163

XIII. Electronic Spectra of $(CH_3CN)MCl_3^-$ Salts in CH_3CN 172

Chapter Six

I. Electronic Spectral Data for the Neutral Decacarbonyls with Band Assignments 195

II. Some Selected Eigenvalues of $Mn_2(CO)_{10}$ 198

III. $M_2Cl_9^{3-}$ Structural Data 199

IV. Transition Assignments (kK) of Reflectance Spectra 200

V. Reflectance Spectra of $Cs_3Mo_2Cl_9$ and $K_3W_2Cl_9$ 201

VI. $M_2(RCO_2)_2L_2$ Complexes 204

VII. Electronic Spectra of Group VI Compounds 214

VIII. Electronic Spectra of Group VIII Compounds 223

IX. Vibrations of the M-H-M Unit 229

X. Infrared Spectra 239

XI. Infrared Spectra 240

XII. Infrared Spectra 241
XIII. Raman Spectra 243
XIV. Expected Carbonyl Stretching Modes 248
XV. Assignments of Carbonyl Stretching Modes 249
XVI. Infrared Spectra 256
XVII. Infrared Spectra 264
XVIII. Fe_2P Infrared Spectra 265
XIX. Fe_2PH^+ Infrared Spectra 271
XX. Infrared Spectra 275
XXI. NMR Data 280
XXII. Titration of $[CpFe(CO)_2]_2$ with H_2SO_4 in CH_3CO_2H Followed by NMR 288
XXIII. Base Strength in Acetic Acid Solution 296
XXIV. Base Strength Determination in Acetic Acid Solution 314
XXV. Infrared Spectra 325

List of Spectra

Infrared Spectra

$[P][BF_4]$	49, 91
$[P]_2[Pt_2Cl_6]$	49, 91, 92, 138
$[P]_2[Pd_2Cl_6]$	49, 91, 92
$[N][BF_4]$	50, 51, 91, 92
$[N]_2[Pt_2Cl_6]$	50, 52, 91, 92, 138
$[N]_2[Pd_2Cl_6]$	50, 53, 91, 92
$[(C_6H_5)_4As]_2(Pd_2Cl_6)$	91, 92
$[(C_6H_5)_4As]_2(Pt_2Cl_6)$	91, 92
$[(C_6H_5)_4As][Cl]$	91, 92
$[N]_2[PtCl_4]$	137
$(n\text{-}C_4H_9)_4NCl$	138
$[P][(CH_3CN)PtCl_3]$	162
$[N][(CH_3CN)PtCl_3]$	167
$[N][(C_5H_5N)PtCl_3]$	176
$[Et_4N][HCr_2(CO)_{10}]$	230
$[Et_4N]_2[W_2(CO)_{10}]$	231, 232
$[Et_4N][HW_2(CO)_{10}]$	233, 234, 245
$[Et_4N][DW_2(CO)_{10}]$	235, 236
$[Et_4N][MnCr(CO)_{10}]$	237
$[(C_6H_5)_3P]_2Mn_2(CO)_8$	238
<u>cis</u>-$[CpFe(CO)_2]_2$	252, 253
<u>trans</u>-$[CpFe(CO)_2]_2$	254, 255, 308
$[(Cp)Fe(CO)_2]_2H^+PF_6^-$	258
$[(Cp)Fe(CO)_2]_2$	258, 260
$Cp(CO)Fe\text{-}\mu\text{-}(CO)_2\text{-}FeCp[P(OCH_3)_3]$	261, 262, 263, 308
$Cp(CO)_2Fe\text{-}H\text{-}Fe(CO)(Cp)[P(OCH_3)_3]^+[(C_6H_5)_4B]^-$	268, 270, 308
$Cp(CO)_2Fe\text{-}H\text{-}Fe(CO)(Cp)[P(OCH_3)_3]^+[PF_6]^-$	270
$[CpRu(CO)_2]_2$	273, 274, 277, 278
$\{[CpRu(CO)_2]_2H\}\{B\phi_4\}$	277, 278
$(C_5H_5)_2Ru$	306
$[Et_4N]Br$	321
$NaB(C_6H_5)_4$	322

$(C_6H_5)_3P$ 323

Ultraviolet-Visible Spectra

$[N]_2[Pt_2Cl_6]$ 57,58,67,69
$[P]_2[Pt_2Cl_6]$ 59,60,67,170
$[N]_2[Pd_2Cl_6]$ 61,62,63,171
$[P]_2[Pd_2Cl_6]$ 64,65,66
$[(n\text{-}C_4H_9)_4N]_2[PtCl_4]$ 67
$[N]_2[PtCl_4]$ 174
K_2PtCl_4 72
$Pt_2Cl_6^{2-}$ 74
$[Et_4N]_2[Pt_2Br_6]$ 76
$[P][(CH_3CN)PtCl_3]$ 170
$[P][(CH_3CN)PdCl_3]$ 171
$[N][(C_5H_5N)PtCl_3]$ 177
(allyl alcohol)$PtCl_3^-$ 178
$Mn_2(CO)_{10}$ 194
$Re_2(CO)_{10}$ 194
K_3MoCl_6 201
$Cs_3Mo_2Cl_9$ 201
$K_3W_2Cl_9$ 201
$[(n\text{-}C_4H_9)_4N]_2[Re_2Cl_8]$ 205
$[Et_4N]_2[W_2(CO)_{10}]$ 208
$[Et_4N][HW_2(CO)_{10}]$ 209,210
$[Et_4N][HCr_2(CO)_{10}]$ 211
$W(CO)_6$ 212
$[CpFe(CO)_2]_2$ 217,218,219
$[CpFe(CO)_2]_2H^+$ 218,219
$\{Cp(CO)_2Fe\text{-}H\text{-}Fe(CO)Cp[P(OCH_3)_3]\}\{B(C_6H_5)_4\}$ 220
$Cp(CO)Fe\text{-}\mu\text{-}(CO)_2\text{-}Fe[P(OCH_3)_3]Cp$ 220
$(Cp)_2Ru$ 221
$[CpRu(CO)_2]_2$ 221,222
$\{[CpRu(CO)_2]H^+\}\{HSO_4\}$ 222
$Fe(CO)_5$ 318
$Fe_2(CO)_9$ 318
$[Et_4N][HFe(CO)_4]$ 320

$[Et_4N]_2[Fe_2(CO)_8]$ 320

NMR Spectra

$[P][(CH_3CN)PtCl_3]$ 157
$[N][(CH_3CN)PtCl_3]$ 158
$[CpFe(CO)_2]_2$ 279, 287, 291
$(Cp)(CO)_2Fe\text{-}H\text{-}Fe(CO)[P(OCH_3)_3](Cp)^+$ 282
$(Cp)(CO)Fe\text{-}\mu\text{-}(CO)_2\text{-}Fe[P(OCH_3)_3](Cp)$ 282, 283, 292
$[Et_4N][DW_2(CO)_{10}]$ 294
$HCo[\phi P(OC_2H_5)_2]_4$ 297
$H_2Co[\phi P(OC_2H_5)_2]_4^+$ 298

Raman Spectra

$[P][(CH_3CN)PtCl_3]$ 159
$[N][(CH_3CN)PtCl_3]$ 165
$[N]_2[Pd_2Cl_6]$ 166
$[N][(C_5H_5N)PtCl_3]$ 176
$Mn_2(CO)_8(P\phi_3)_2$ 242
$[Et_4N][MnCr(CO)_{10}]$ 242
$[Et_4N]_2[W_2(CO)_{10}]$ 242
$[Et_4N][DW_2(CO)_{10}]$ 242
$[Et_4N][HW_2(CO)_{10}]$ 242

Chapter One

The One That Got Away

Introduction

Welcome to my thesis. If you read beyond this point, you do so at your own risk. The original goal of this research was to prepare and characterize π-cyclopropenium complexes of transition metals. It is fair to say that this work was a total failure. In this chapter we summarize for posterity other people's syntheses and characterizations of a variety of cyclopropenium salts and π-cyclopropenium complexes.

Properties of Cyclopropenium Salts

An assortment of cyclopropenium salts has been reported since Breslow first prepared the triphenylcyclopropenium cation in 1957.[1] The parent unsubstituted $C_3H_3^{\oplus}$ cation was reported simultaneously by Breslow[2] and Farnum[3] in 1967. It was that report which spurred this research. At least three reviews of cyclopropene chemistry (and cyclopropenium salts) have appeared.[4] Table I lists all of the cyclopropenium cations that have been synthesized of which we are aware.

Three X-ray studies of such salts establish the geometry of cyclopropenium cations. The structure of $[(C_6H_5)_3C_3][ClO_4]$ (Figure 1) shows that the three phenyl rings form a propeller-like structure with twisting angles of 7.6°, 12.1°, and 21.2°. The average C-C

Table I

Cycloprcpenium Salts

Cation	Reference	Cation	Reference	Cation	Reference
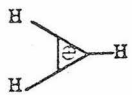	2,3	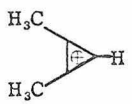 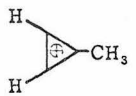	3,9	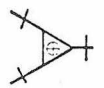 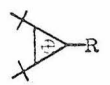	14
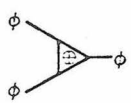 (ϕ = phenyl)	1	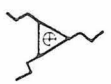 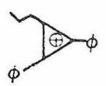	10	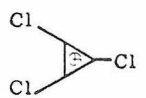 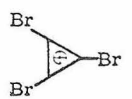	15
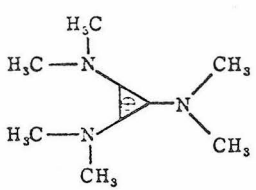	5	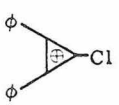 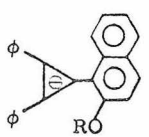	11	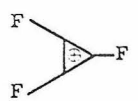	16
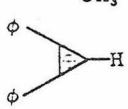	6	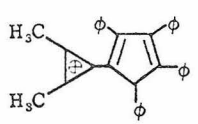	12	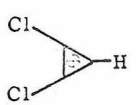 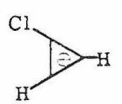	17
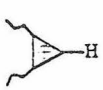	6,7	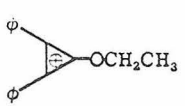	13	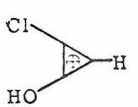 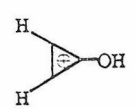	17
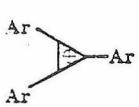 (Ar = several aryl groups)	8			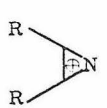	18

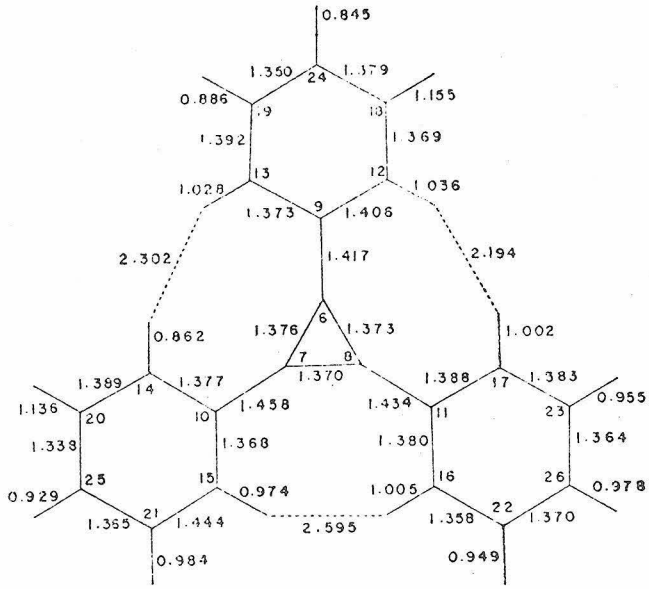

The Structure of the $\phi_3C_3^+$ Cation in $\phi_3C_3{}^+ClO_4{}^-$. From Reference 19. (With Permission)

Figure 1

bond length in the cyclopropenium ring is 1.373Å.[19] The dimethylamine groups of $\{[(CH_3)_2N]_3C_3\}\{ClO_4\}$ are also twisted out of plane of the cyclopropenium ring by 9.9°, 20.8°, and 20.8°, albeit they do not form a propeller-like structure.[20] (Figure 2)

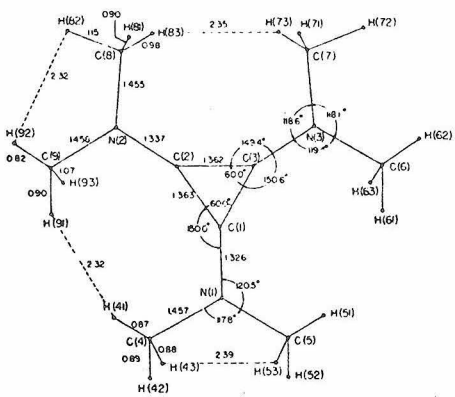

The Structure of the $[(CH_3)_2N]_3C_3^+$ Cation in $[(CH_3)_2N]_3C_3{}^+ClO_4{}^-$. From Reference 20. (With Permission)

Figure 2

The C-C bond lengths have an average value of 1.363Å and the C-N bond lengths are close to those of double bonds, with a value of 1.333Å. In our lab, Jack Thibeault and Ron Ziolo have determined the structure of this same cation in the salt $\{[(CH_3)_2N]_3C_3\}_2\{Pt_2Cl_6\}$.[21] The two crystallographically independent cyclopropenium cations exhibit an average C-N distance of 1.316Å. The C-C bond lengths are somewhat curious as each ring is isosceles with two sides averaging 1.386Å and the third side significantly shorter at 1.344Å. One of these cations is shown in Figure 21, Chapter Three.

The infrared spectrum of the parent $C_3H_3^+$ cation is only expected to have four active fundamentals. These are given in Table II along with the values observed for $C_3D_3^+$.[2b] The only band

Table II[2b]

Infrared Spectra

Vibration	$C_3H_3^+$	$C_3D_3^+$
C-X stretch	3105	2327
C-C stretch	1276	1239
C-X in-plane bending	908	665
C-X out-of-plane bending	736	542

common to substituted cations is the e′ ring breathing mode (C-C stretch) commonly found near 1380-1420 cm^{-1} in alkyl and aryl substituted cations.[4c] In $C_3Cl_3^+$ and $C_3Br_3^+$, this mode occurs at 1312 and 1276 cm^{-1}, respectively.[15] A normal coordinate analysis of these two cations shows significantly high C-C force constants. (Table III)

Table III[15]

Force Constants of Aromatic Species

Species	k_{cc}	k_{cx}
C_6H_6	5.59	4.76
	5.15	4.79
$C_5H_5^-$	5.39	4.79
C_6Cl_6	4.81	2.30
$C_3Cl_3^+$	6.32	2.99
$C_3Br_3^+$	6.46	2.2

Ultraviolet spectra are generally uninformative as the cyclopropenium $\pi \rightarrow \pi^*$ transition in the simple alkyl substituted cations occurs in the vacuum UV.[2b] The lowest energy spin allowed transition of $[(CH_3)_2N]_3C_3^+$ is seen near 43,000 cm^{-1}.[5]

The chemical shift of a proton bound directly to a cyclopropenium ring is ~11 ppm downfield of TMS.[2,3,6a,17,22] Of more interest is the coupling constant, $^1J_{^{13}C-^1H}$, found in $C_3H_3^+$.[2,23] The value of 262-265 Hz indicates 53% s character for the C-H bond.[2b] ^{13}C spectra are also informative. Olah and Mateescu[24] interpret the

^{13}C chemical shift change from +17.8 ppm in $C_3H_3^{\oplus}$ to +38.8 ppm (from CS_2) in $(C_6H_5)_3C_3^{\oplus}$ in terms of charge delocalization onto the phenyl rings. Ray, Colter, and Kurland[25] interpret their own ^{13}C NMR study as indicating insignificant charge delocalization into the phenyl rings. As usual, calculations support both conflicting interpretations, subject to the phase of the moon and the color of the theoretician's socks.[26] A NQR study of $C_3Cl_3^{\oplus}$ was taken to indicate 16% double bond character for each C-Cl bond and considerable sharing of charge by Cl.[27]

Substituted cyclopropenium cations can be remarkably stable, as indicated by values of pK_{R^+} (Table IV) and reduction potentials (Table V). Among the compounds in Table IV, the tripropylcyclopropenium cation is the most resistant to reaction with water. Our own qualitative experience with the tris(dimethylamino)cyclopropenium cation shows it to be exceedingly stable also. Breslow[2b] has used both pK_{R^+} and mass spectroscopic appearance potentials[29] to estimate that the unsubstituted cyclopropenium cation is ca. 19 kcal/mole more stable than the allyl cation in the gas phase and in solution.

$\Delta G = -0.80$ eV

$\Delta G = -0.84$ eV

Table IV[4b, 2b]

Susceptibility of Cyclopropenium Cations to Hydrolysis

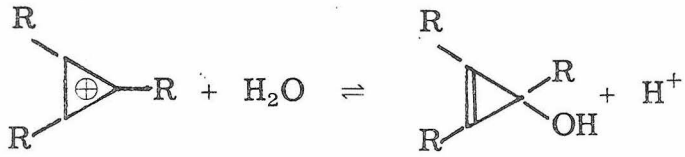

$$K_{R^+} = \frac{[C_3R_3OH][H^{\oplus}]}{[C_3R_3^{\oplus}]}$$

Cyclopropenium Ion	pK_{R^+}	Solvent
dipropyl	2.68	50% acetonitrile
tripropyl	7.2	50% acetonitrile
diphenyl	-0.67	23% ethanol
	0.32	water
propyldiphenyl	3.80	23% ethanol
triphenyl	3.1	50% acetonitrile
	2.80	23% ethanol
	3.18	water
diphenyl (p-anisyl)	4.00	23% ethanol
phenylbis (p-anisyl)	5.16	50% acetonitrile
	5.22	23% ethanol
tris(p-anisyl)	6.50	50% acetonitrile
	6.42	23% ethanol
unsubstituted	-7.4	95% ethanol

Table V[28]

Reduction Potentials

Cyclopropenium Ion	Reduction Potential
triphenyl	-1.13 eV
diphenyl (p-arisyl)	-1.24 eV
tris (p-anisyl)	-1.49 eV

The substituents on a cyclopropenium ring determine with which anions the ring will react. Whereas, for example, the triphenylcyclopropenium cation exists with a chloride anion, cyclopropenium itself does not.[2b, 4b]

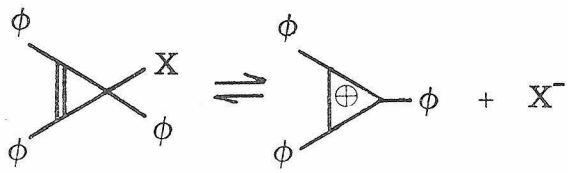

ionic: X = picrate, bromide, chloride, tetrafluoroborate, perchlorate

covalent: X = hydrogen, methoxide, cyanide

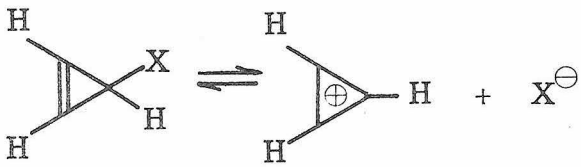

ionic: X = tetrafluoroborate, hexachloroantimonate

covalent: X = chloride, ethoxide

The chlorine atom of 3-chlorocyclopropene is, however, quite mobile. Although it is stationary on the NMR time scale in neat 3-chlorocyclopropene and in CCl_4 at ambient temperature, it migrates rapidly in SO_2 at -40° and in acetonitrile, benzene, and dioxane at ambient temperature. Whereas the highly substituted cyclopropenes form

salts by hydride abstraction by triphenylmethyl cation, neither 1-methylcyclopropene[30] nor cyclopropene[29,31] itself react with this cation.

The aromaticity of the cyclopropenium cation may be contrasted to the "antiaromaticity" of the anion.[32] Breslow has estimated the pK_a of 1,2,3-triphenylcyclopropene to be 51.[33] The vinylic protons of cyclopropene have been found to be more acidic than the methylene protons.[34] The hypothetical anion is

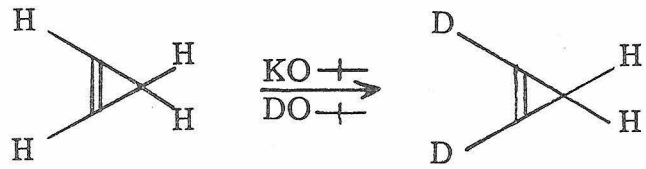

predicted to have a localized electron pair and a barrier to inversion of 52 kcal/mole.[35]

Finally, we include some random observations. The triphenylcyclopropenium cation was observed to dimerize upon irradiation for four hours in 10% H_2SO_4.[36] Cyclopropenium cations behave as

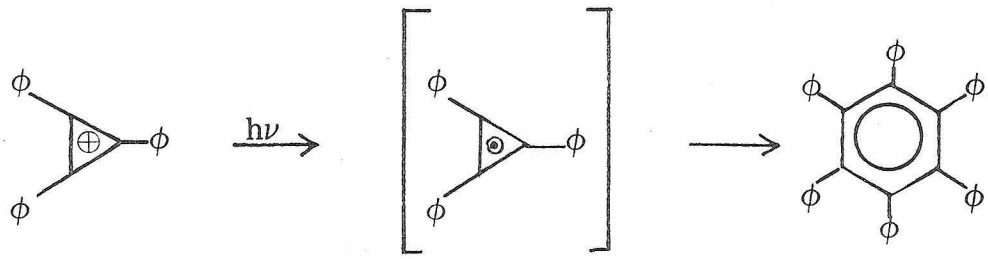

electrophiles and will alkylate aromatic systems in Friedel-Crafts reactions.[4b, 8c]

Synthesis of π-Cyclopropenium Complexes

The first successful preparation of a π-cyclopropenium complex was reported by Gowling and Kettle in 1964.[37] They prepared complexes formulated as Ia and Ib based on elemental analyses and vibrational spectra. In view of the recent work of Olander and Brown[42] (vide infra), it may be better to formulate I as a monomer. Ib exhibited a single sharp CO band at 2039 cm^{-1}.

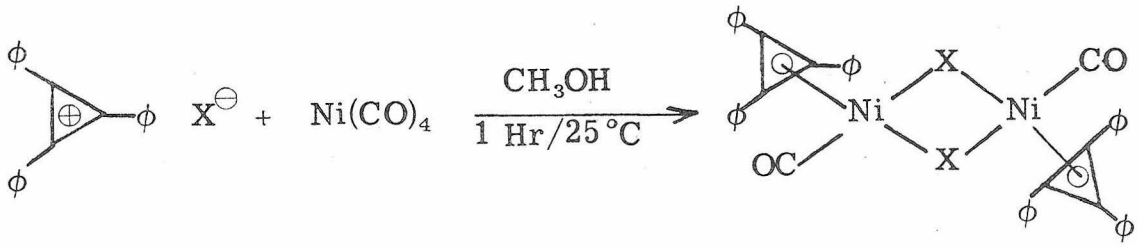

Ia. X = Cl

b. X = Br

This is also in better accord with a monomer than a dimer. Sparingly soluble in tetrahydrofuran and methanol, solutions of these compounds are instantly attacked by air. The solids are more air stable but decomposed in vacuo at 120 °C without subliming.

The data of Gowling and Kettle were very meager but an X-ray study[38] of a derivative of Ia confirmed that a π-complex was indeed

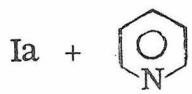

$$\text{Ia} + \text{N} \rightarrow (\pi\text{-}\phi_3C_3)NiCl(C_5H_5N)_2 \cdot (C_5H_5N)$$

II

formed. Treatment of Ia with pyridine afforded the complex II whose structure is given in Figure 3. The ligands form a distorted tetrahedron about nickel, with the same nickel-ring

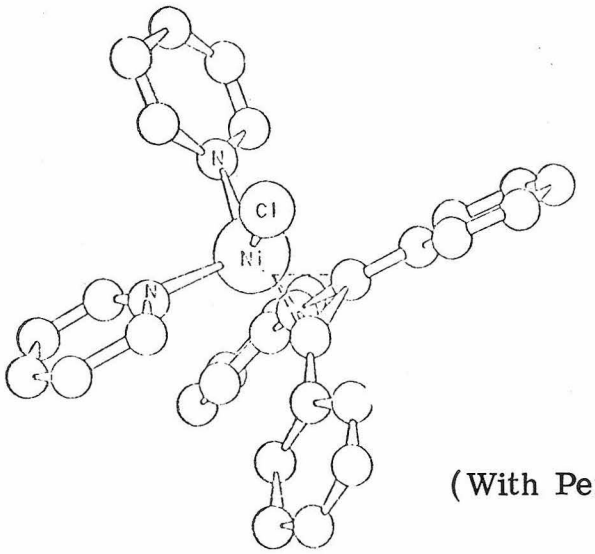

Ni-C = 1.896(9) Å
1.948(9)
1.977(9)
Ni-N = 2.043(8)
2.019(7)
Ni-Cl = 2.322(3)

(With Permission)

The Structure of Complex II. From Reference 38b.
Figure 3

distance found in other π-complexes. The Ni-C distances, therefore, must increase with increasing ring size. The ring C-C distance is 1.422(8)Å compared to 1.373(5)Å in the uncomplexed cation.[19] The phenyl rings are bent back from the plane of the C_3 ring. The effective radius of Ni in this complex is 1.33Å, significantly larger than the ionic radius of Ni(II) and in support of the formulation of this complex as a Ni(O) species. Indeed, no d-d transitions are observed in the UV-VIS spectrum. The first observed transition at 29,000 cm^{-1}

Table VI [39b]

DISTANCES (Å) IN SOME NICKEL COMPLEXES OF CARBOCYCLIC RINGS

Complex	No. of carbon atoms in ring	Ni–C-(ring), Å	Range, Å	Ni–ring, Å
$(\pi\text{-}C_3(C_6H_5)_3)NiCl(py)_2$	3	1.941 (5)	1.896–1.968	1.759
$(\pi\text{-}C_3(C_6H_5)_3)Ni(\pi\text{-}C_5H_5)$	3	1.961 (4)	1.953–1.968	1.779
$[(\pi\text{-}C_4(CH_3)_4)NiCl_2]_2$	4	2.022 (6)	1.997–2.047	1.749
$[(\pi\text{-}C_5H_5)Ni(P(C_6H_5)_2)]_2$	5	2.10 (1)	2.06–2.14	1.74
$(\pi\text{-}C_5H_5)Ni(\pi\text{-}C_3(CH_3)_3)$	5	2.100 (6)	2.060–2.137	1.726
$(\pi\text{-}C_5H_5)NiNO$	5	2.107 (1)		1.72
$(\pi\text{-}C_5H_5)Ni(P(C_6H_5)_3)CF_3$	5	2.11 (1)	2.06–2.16	1.76
$(\pi\text{-}C_5H_5)_2Ni_2C_2(C_6H_5)_2$	5	2.11 (1)	2.05–2.16	1.74
$(\pi\text{-}C_5H_5)NiC_4(CH_3)_4C_5H_5$	5	2.132 (8)	2.098–2.168	1.764
$(\pi\text{-}C_5H_5)NiC_5H_5C_2(COOCH_3)_2$	5	2.130 (6)	2.096–2.148	1.75
$(\pi\text{-}C_5H_5)Ni(P(C_6H_5)_3)C_6H_5$	5	2.139 (4)	2.087–2.195	1.776
$(\pi\text{-}C_5H_5)Ni(P(C_6H_5)_3)C_6F_5$	5	2.141 (8)	2.107–2.184	1.769
$(\pi\text{-}C_5H_5)_2Ni_2(CO)_2$	5	2.15	2.13–2.17	1.78
$(\pi\text{-}C_5H_5)Ni$	5	2.196 (4)		1.83

(ϵ = 2300) is assigned as a charge transfer d-π^* transition. The UV spectrum of the triphenylcyclopropenium group is essentially unchanged in going from the free cation to the π-complex.

Treatment of II with C_5H_5Tl in benzene at room temperature affords the mixed sandwich complex $(\pi\text{-}\phi_3C_3)Ni(\pi\text{-}C_5H_5)$ (III).[39] The structure is shown in Figure 4. The phenyl rings of this air stable compound are bent away from the Ni atom and twisted in a propeller-like fashion.

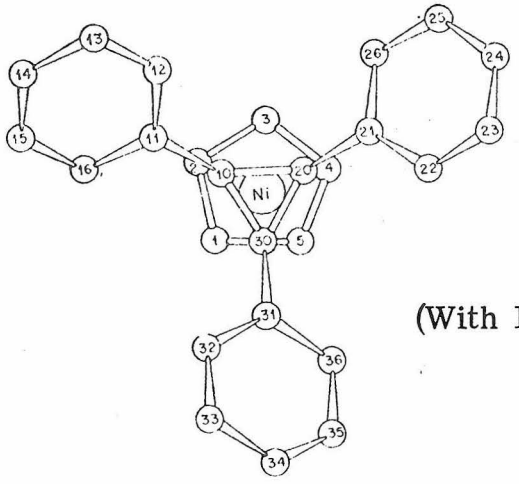

(With Permission)

The Structure of Complex III.
From Reference 39b.

Figure 4

Another mixed sandwich complex in which the cyclopentadienyl ligand is replaced by a 1,7-phosphacarbollyl ligand was reported by Welcker and Todd.[40] The structure this complex is believed to have is shown in Figure 5. The IR spectrum is reported but no bands were

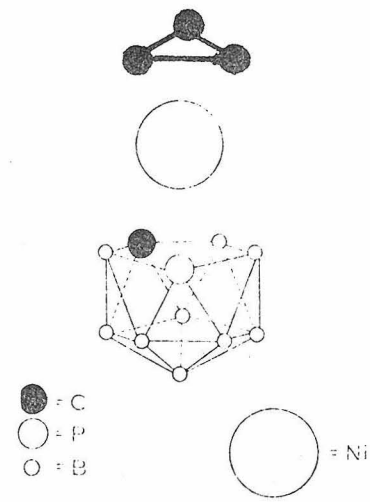

The Proposed Structure of the Skeleton of the 1,7-Phosphacarbollyl Complex Prepared By Welcker and Todd. (Reference 40)
Figure 5

observed between 1445-1080 cm^{-1}. We suspect that this spectrum was just too weak as the cyclopropenium ring breathing mode, if nothing else, ought to occur in this region. The electronic spectra of several complexes were reported, but not interpreted. These are listed in Table VII. Given that the d $\rightarrow \pi^*$ (Ni $\rightarrow \phi_3C_3$) transition of II is assigned at 29,000 cm^{-1} (ϵ = 2300) (~ 355 nm),[38] it is difficult to interpret the spectra in Table VII. To make matters worse, we cannot find any report of the spectrum of the 1,7-phosphacarbollyl group. The lowest energy band is the only one which appears to be

Table VII[40]

Electronic Spectra of (L) Ni(1,7-$B_9H_9CHPCH_3$) Complexes

L	Absorptions (λ(nm)(ϵ))
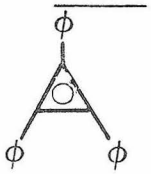	260 (29,600), 300 (27,300), 350 (1100), 420 (490)
	275 (14,000), 313 (4370), 360 (930), 480 (138)
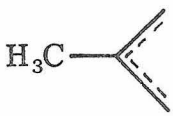	271 (13,800), 308 (5030), 360 (1010), 470 (147)
NO	285 (11,400) 425 (499)

sensitive to the group L. It is reasonable that a M → L(π^*) transition for the allyl complex should be at lower energy than the same transition for a ϕ_3C_3 complex. Simple Hückel theory places the $C_3H_3^{\oplus}$ π^* level 3β above the occupied π level. For the allyl cation, the non-bonding (unoccupied) π level is just $\sqrt{2}\ \beta$ above the occupied level. The interaction of the phenyl groups with the cyclopropenium ring may destroy this argument. The intensity of the L dependent transition seems too low for a charge transfer transition. We see no obvious interpretation of these spectra.

Two π-cyclopropenium complexes of Mo were reported by Hayter.[41] Virtually no data besides the synthetic procedure were given. The synthetic route is given below.

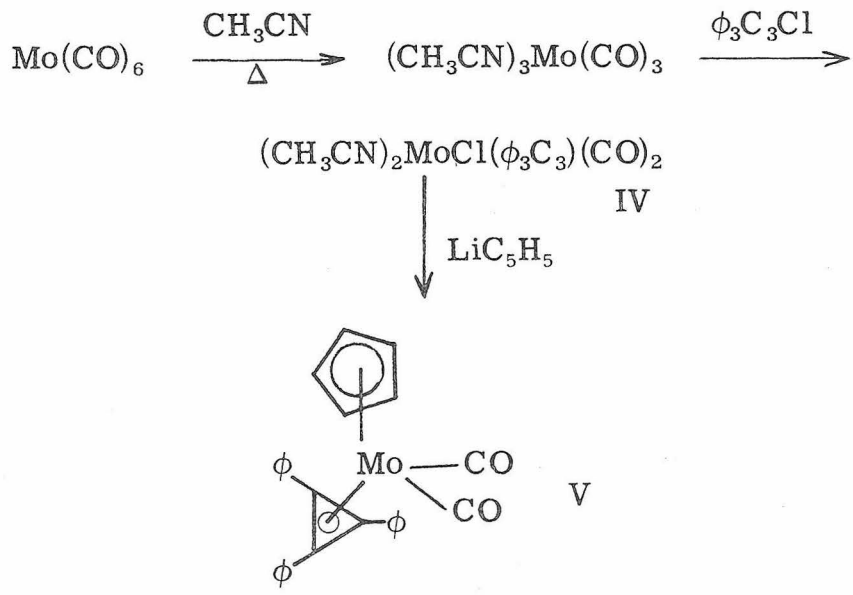

The most noteworthy recent development in π-cyclopropenium chemistry came when Olander and Brown[42] reported several complexes of cyclopropenium groups other than the triphenylcyclopropenium group. By the same route used to prepare I, VI and VII were synthesized. Treatment of VI with NaC_5H_5 gave VIII.

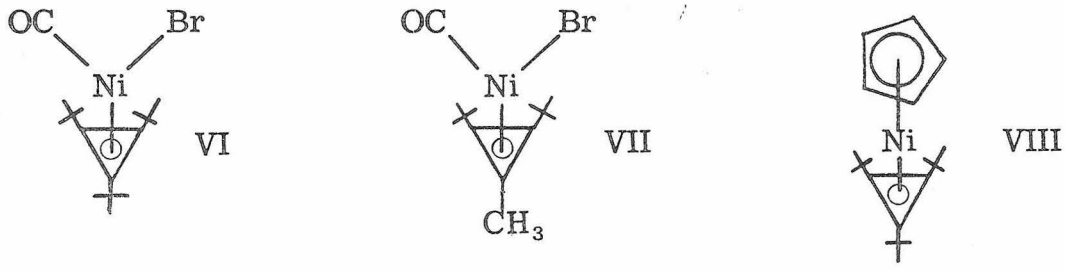

VI takes on CO as follows:

$$\text{VI} + \text{CO} \rightleftharpoons [(t\text{-}C_4H_9)_3C_3]Ni(CO)_2Br$$

$$[(t\text{-}C_4H_9)_3C_3]Ni(CO)_2Br + 2CO \rightleftharpoons Ni(CO)_4 + [(t\text{-}C_4H_9)_3C_3][Br]$$

VI also reacts with $[\phi_3C_3][BF_4]$ to give I as a precipitate.

$$[(t\text{-}C_4H_9)_3C_3]Ni(CO)Br + \phi_3C_3^{\oplus} \xrightarrow{CH_3OH} (\phi_3C_3)Ni(CO)Br\downarrow + (t\text{-}C_4H_9)_3C_3^{\oplus}$$

This last result does not allow us to assess the relative affinity of $\phi_3C_3^{\oplus}$ and $(t\text{-}C_4H_9)_3C_3^{\oplus}$ for nickel because of the production of a precipitate. Nonetheless, it seems reasonable to presume that the tri-t-butyl cation (like tripropyl) is more stable than the triphenylcyclopropenium cation. It is also reasonable to suppose that equilibrium will favor complexation of the less stable cation. If this is the case, reaction of $C_3H_3^{\oplus}$ salts with soluble $(t\text{-}C_4H_9)_3C_3^{\oplus}$ complexes seems like a reasonable way to try to synthesize π-C_3H_3 complexes. Olander and Brown also report that reaction of $[t\text{-}C_4H_9)_3C_3][BF_4]$ with $NaMn(CO)_5$ produces the salt $[(t\text{-}C_4H_9)_3C_3][Mn(CO)_5]$. Not only is this reasonable, but it is unreasonable to expect the complex $[\pi\text{-}(t\text{-}C_4H_9)_3C_3]Mn(CO)_5$ to form as this has two too many valence electrons.

Moiseev <u>et al.</u>[43] report the preparation of IX by bubbling ethylene through a solution of $PdCl_2$ and $\phi_3C_3^{\oplus}Cl^{\ominus}$. The <u>only</u> datum they

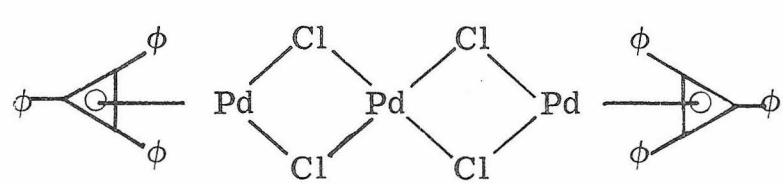

IX

report is elemental analysis so this product must be regarded with some skepticism in view of the work reported in Chapter Three of this thesis.

A handful of unsuccessful attempts to prepare π-cyclopropenium complexes have been reported. Tuggle and Weaver[44] observed the formation of the "iridicycle," X, when trans-$IrCl(CO)[P(CH_3)_3]_2$ was treated with $\phi_3C_3^{\oplus}BF_4^{\ominus}$ in methanol. The structure was determined by X-ray crystallography. Coffey[45] treated

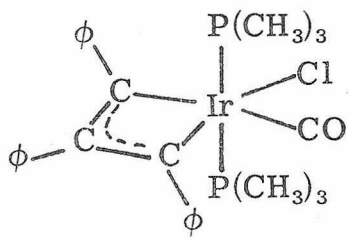

X

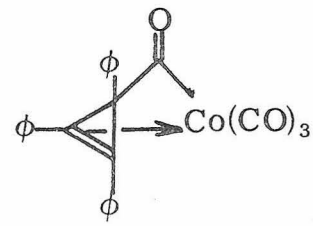

XI

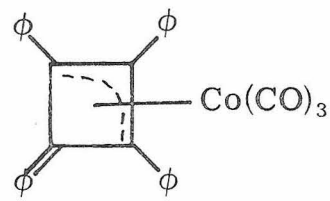

XII

$Co(CO)_4^-$ with $\phi_3C_3^{\oplus}BF_4^{\ominus}$ and observed the formation of a compound formulated as either XI or XII. King and Efraty[46] examined the same reaction using $(CH_3)_3C_3^{\oplus}BF_4^{\ominus}$ and suggest that the data are in better accord with the structure XII. Chatt and Guy[47] observed the formation of $\phi_3C_3^{\oplus}$ salts when reactions were attempted with several platinum compounds.

It was hoped that the present research would produce π-cyclopropenium complexes suitable for studying the metal-cyclopropenium bonding. In particular, several IR vibrations of both the cyclopropenium group itself and of the metal-cyclopropenium linkage would provide a good deal of information on the nature of this bond. (See Chapter Two.) The NMR spectrum of a π-C_3H_3 complex might provide information on charge distribution, hybridization, and dynamic processes such as substitution. Electronic spectra of complexes with less than ten d electrons and relatively simple ligands might shed light on the ligand field strength of a π-cyclopropenium ligand. In suitable complexes, the spectroscopic, structural, and kinetic trans effects of a cyclopropenium ligand could be determined. The total success of our efforts is summarized between the two arrows in the diagram below.

→ ←

References

1. R. Breslow, J. Amer. Chem. Soc., 79, 5318 (1957);
R. Breslow and C. Yuan, Ibid., 80, 5991 (1958).

2. a) R. Breslow, J. T. Groves, and G. Ryan, Ibid., 89, 5048 (1967);
b) R. Breslow and J. T. Groves, Ibid., 92, 984 (1970).

3. D. G. Farnum, G. Mehta, and R. G. Silberman, Ibid., 89, 5048 (1967).

4. a) A. W. Krebs, Angew. Chem. Intnl. Ed. Engl., 4, 10 (1965);
b) I. A. D'yakanov and R. R. Kostikov, Usp. Khim., 36, 1305 (1967); Russ. Chem. Rev., 36, 557 (1967);
c) G. L. Closs, Adv. Alicyclic. Chem., 1, 53 (1966).

5. Z. Yoshida and Y. Tawara, J. Amer. Chem. Soc., 93, 2573 (1971).

6. a) D. G. Farnum and M. Burr, Ibid., 82, 2651 (1960);
b) R. Breslow, J. Lockhart, and H. W. Chang, Ibid., 83, 2375 (1961).

7. R. Breslow and H. Höver, Ibid., 82, 2644 (1960).

8. a) R. Breslow and H. W. Chang, Ibid., 83, 2367 (1961);
b) W. Broser and M. Brockt, Tet. Lett., 5331 (1968);
c) R. West, D. C. Zecher, and W. Goyert, J. Amer. Chem. Soc., 92, 149 (1970).

9. H. Prinzbach, D. Seip, and U. Fischer, Angew. Chem., 77, 258 (1965).

10. R. Breslow, H. Höver, and H. W. Chang, J. Amer. Chem. Soc., 84, 3168 (1962).

11. B. Foehlisch and P. Buergle, Ann. Chem., 701, 67 (1967).

12. H. Prinzbach and U. Fischer, Angew. Chem. Intnl. Ed. Engl., 5, 602 (1966).

13. B. Foehlisch and P. Buergle, Tet. Lett., 2661 (1965).

14. J. Ciabattoni and E. C. Nathan, III, J. Amer. Chem. Soc., 90, 4495 (1968); Ibid., 91, 4766 (1969).

15. R. West, A. Sadô, and S. W. Tobey, Ibid., 88, 2488 (1966).

16. P. B. Sargeant and C. G. Krespan, Ibid., 91, 415 (1969).

17. R. Breslow, G. Ryan, and J. T. Groves, Ibid., 92, 988 (1970).

18. J. Ciabattoni and M. Cabell, Jr., Ibid., 93, 1482 (1971).

19. M. Sundaralingam and L. H. Jensen, Ibid., 88, 198 (1966).

20. A. T. Ku and M. Sundaralingam, Ibid., 94, 1688 (1972).

21. J. Thibeault, Ph.D. Thesis, California Institute of Technology, 1972.

22. D. G. Farnum and C. F. Wilcox, J. Amer. Chem. Soc., 89, 5379 (1967).

23. G. A. Olah, J. M. Bollinger and A. M. White, Ibid., 91, 3667 (1969).

24. G. A. Olah and G. D. Mateescu, Ibid., 92, 1430 (1970).

25. G. J. Ray, A. K. Colter, and R. J. Kurland, Chem. Phys. Lett., 2, 324 (1968).

26. a) R. Basu and S. K. Bose, Theor. Chim. Acta., 4, 94 (1966).
    b) R. Hoffman, R. Bissell and D. G. Farnum, J. Phys. Chem., 73, 1789 (1969).

27. E. A. C. Lucken and C. Mazeline, J. Chem. Soc. A, 153 (1968).

28. R. Breslow, Chem. Brit., 4, 100 (1968).

29. K. B. Wiberg, W. J. Bartley, and F. P. Lossing, J. Amer. Chem. Soc., 84, 3980 (1962).

30. F. Fisher and D. E. Applequist, J. Org. Chem., 30, 2089 (1965).

31. For the synthesis of cyclopropene and deuterated cyclopropenes, see

a) G. L. Closs and K. D. Krantz, J. Org. Chem., 31, 638 (1966);

b) P. B. Shevlin and A. P. Wolf , J. Amer. Chem. Soc., 92, 406 (1970);

c) References cited in R. Srinivasan, Ibid., 91, 6250 (1969).

32. R. Breslow, J. Brown, and J. J. Gajewski, Ibid., 89, 4383 (1967).

33. R. Breslow and K. Balasubramanian, Ibid., 91, 5182 (1969).

34. E. A. Dorko and R. W. Mitchell, Tet. Lett., 341 (1968).

35. D. T. Clark, Chem. Comm. 637 (1969).

36. a) E. E. van Tamelen, R. H. Greeley and H. Schumacher, J. Amer. Chem. Soc., 93, 6151 (1971).

b) E. E. van Tamelen, T. M. Cole, R. Greeley and H. Schumacher, Ibid., 90, 1372 (1968).

37. E. W. Gowling and S. F. A. Kettle, Inorg. Chem., 3, 604 (1964).

38. a) R. M. Tuggle and D. L. Weaver, Ibid., 10, 2599 (1971);

b) D. L. Weaver and R. M. Tuggle, J. Amer. Chem. Soc., 91, 6506 (1969).

39. a) M. D. Rausch, R. M. Tuggle, and D. L. Weaver, Ibid., 92, 4981 (1970);

b) R. M. Tuggle and D. L. Weaver, Inorg. Chem., 10, 1504 (1971).

40. P. S. Welcker and L. J. Todd, Ibid., 9, 286 (1970).

41. R. G. Hayter, J. Organomet. Chem., 13, P1 (1968).

42. W. K. Olander and T. L. Brown, J. Amer. Chem. Soc., 94, 2139 (1972).

43. I. I. Moiseev, M. N. Vargaftik, and Ya. K. Syrkin, Izvest. Akad. Nauk., SSSR, Ser. Khim., 775 (1964); Bul. Acad. Sci., USSR, Chem. Div., 728 (1964).

44. R. M. Tuggle and D. L. Weaver, Inorg. Chem., 11, 2237 (1972); J. Amer. Chem. Soc., 92, 5523 (1970).

45. C. E. Coffey, Ibid., 84, 118 (1962).

46. R. B. King and A. Efraty, J. Organomet. Chem., 24, 241 (1970).

47. J. Chatt and R. Guy, Chem. Ind., 212 (1963).

Chapter Two

Great Expectations

During the long search for a π-cyclopropenium complex, a small amount of coherent thinking about the vibrational spectra of such complexes was undertaken. This chapter deals with the expected features of the spectrum of a π-cyclopropenium complex and what can be learned from such a spectrum. What can we hope to learn from such spectra? Three things come to mind:

a) The strength of the metal-cyclopropenium bond.

b) The effect of coordination on bonding within the ring.

c) The effect of coordination of cyclopropenium on the bonding to other ligands in the complex.

We will review background material on each of these topics before looking at our great expectations.

Allow me to consider the cyclopropenium cation ($C_3H_3^+$) as the second member of the family of C_nH_n ring compounds. For this purpose we will consider the first member of the series to be ethylene. Data on metal-ligand stretching frequencies (where the ligand is the C_nH_n cyclic polyene) are relatively scarce. The metal-ethylene stretch occurs around 400 cm^{-1}. In Zeise's salt, $[K][(C_2H_4)PtCl_3] \cdot H_2O$, $\nu_{Pt-C_2H_4}$ is a strong band at 407 cm^{-1}.[1] Table I lists several Pt-olefin and Pd-olefin stretching frequencies (ν_{M-L}).

Table I[2]

Metal-Olefin Stretching Frequencies

Compound	ν_{M-L} (cm^{-1})		ν_{ML}
$[K][Pt(C_2H_4)Cl_3] \cdot H_2O$	407	trans-$Pt(C_2H_4)(NH_3)Cl_2$	383
$[K][Pt(C_2D_4)Cl_3] \cdot H_2O$	387	trans-$Pt(C_2H_4)(NH_3)Br_2$	383
$[K][Pt(C_2H_4)Br_3] \cdot H_2O$	395	$[Pt(C_2H_4)Cl_2]_2$	408
$[K][Pt(C_3H_6)Cl_3]$	393	$[Pt(C_2D_4)Cl_2]_2$	392
$[K][Pt(trans\text{-}C_4H_8)Cl_3]$	405	$[Pd(C_2H_4)Cl_2]_2$	427

No IR data on ν_{ML} of cyclopropenium complexes have appeared. An assignment has been made of the spectrum of the cyclobutadiene complex $[(CH_3)_4C_4]NiCl_2$.[3] ν_{ML} is assigned as a medium intensity band at 416 cm^{-1}. In addition, there is an IR active metal-ring deformation mode for the C_nH_n rings. This mode, which is observed at 467 cm^{-1} in this Ni complex, is drawn below.

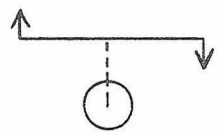

ring tilting mode (δ_t)

A wealth of cyclopentadienyl complexes has been studied. The IR-active metal-ring stretching modes and ring tilting modes are given in Table II. Other modes listed in Table II will be discussed later. The symbols used in this Table and in this discussion are as follows:

Table II

Selected Vibrational Frequencies of Cyclopentadienyl Complexes

Compound	ν_{ML}	δ_t	ν_{CC}	π_{CH}
Cp_2Zn	345	(613)	1410	760
$CpZnC_2H_5$	?	607	1414	747
$CpCdC_2H_5$	n. m.	n. m.	1405	763
Cp_3Ti	413	609	1443	746
	372	570		716
Cp_2TiCl_2	415	595	1441	823
$CpTiCl_3$	414	486	1435	797
Cp_2ZrCl_2	n. m.	n. m.	1441	810
$CpZrCl_3$	n. m.	n. m.	1441	832
Cp_2HfCl_2	330	?	1445	816
Cp_2V	379	422	1425	774
Cp_2VCl	354	416	1426	810
$CpVCl_3$	320	375	1423	826
$CpVC_7H_7$	432	?	1421	803
Cp_3Nb	n. m.	n. m.	1433	749
Cp_4Nb	(359)	(459)	1433	747
Cp_3TaH_3	n. m.	n. m.	1425	825
				795
Cp_2Cr	408	429	1404	766
Cp_2Cr^+	381	479	1421	?
$(CpCrO)_4$	365	(365)	1433	795
$CpCrC_6H_6$	450	(450)	1410	765
Cp_2MoH_2	330	414	1408	763
Cp_2WH_2	312	398	1410	775
$CpMnC_6H_6$	483	535	1409	762
$(Cp_2Tc)_2$	n. m.	n. m.	1410	775
Cp_2ReH	351	412	1408	795
Cp_2Fe	478	490	1408	814
Cp_2Fe^+	423	510	1412	817
Cp_2Ru	379	446	1410	821
Cp_2Os	353	428	1400	823
Cp_2Co	355	464	1412	778
Cp_2Co^+	461	500	1414	820
$CpCoC_6H_6^+$	434	477	1419	---
Cp_2Rh	n. m.	n. m.	1410	847
$CpRhC_6H_6^+$	n. m.	n. m.	1419	759
$CpRhC_5H_6$	n. m.	n. m.	1409	764
Cp_2Ir^+	n. m.	n. m.	1409	818
$CpIrC_5H_6$	n. m.	n. m.	1404	769
Cp_2Ni	355	?	1421	772
$CpNiC_3H_5$	406	451	1404	783
$CpPdC_3H_5$	376	582	1400	741
Cp_2TiCl	350		1445	798
Cp_2TiBH_4	345		1440	800
Cp_2TiI_2	n. m.		1439	819
Cp_2TiBr_2	417		1441	822
Cp_2TiF_2	416		1443	823
$Cp_2Ti(SCN)_2$	410		1439	831
Cp_2VCl_2	n. m.		1433	824

Compound	ν_{ML}	ν_{CC}	π_{CH}
$Cp_2Ti(CO)_2$	458	1423	794
$CpV(CO)_4$	353	1427	?
$[CpV(CO)_3]Cs_2$	n. m.	1427	778
$CH_3COC_5H_4V(CO)_4$	374	1427	?
$[CpCr(CO)_3]_2$	371	1425	840
$CpCr(CO)_3H$	n. m.	1425	759
$CpCr(CO)_3D$	n. m.	1423	706
$CpCr(CO)_3CH_3$	n. m.	1429	846
$[CpCr(CO)_3]Na$	n. m.	1425	696
$[CpCr(CO)_4]BF_4$	431	1433	820
$[CpMo(CO)_3]_2$	330	1439	749
$CpMo(CO)_3H$	n. m.	1418	812
$CpMo(CO)_3D$	n. m.	1416	814
$CpMo(CO)_3Cl$	n. m.	1429	822
$[CpMo(CO)_4]PF_6$	n. m.	1427	?
$[CpW(CO)_3]_2$	347	1418	831
$CpW(CO)_3H$	347	1422	826
$CpW(CO)_3D$	n. m.	1418	826
$CpW(CO)_3CH_3$	352	1421	833
$[CpW(CO)_4]PF_6$	n. m.	1425	?
$CpW(CO)_3Cl$	352	1428	833
$CpW(CO)_3Br$	351	1425	833
$CpW(CO)_3I$	348	1420	?
$CpMn(CO)_3$	370	1425	835
$CpTc(CO)_3$	437	1418	817
$CpRe(CO)_3$	347	1418	824
$[CpFe(CO)_2]_2$	384	1416	813
$[CpRu(CO)_2]_2$	358	1409	813
$[CpOs(CO)_2]_2$	316	1407	820
$CpCo(CO)_2$	378	1401	756
$CpRh(CO)_2$	329	1403	792
$CpIr(CO)_2$	n. m.	1401	812
$[CpNiCO]_2$	(417)	1409	774
$Cp_3Ni_3(CO)_2$	365	1416	794
$[CpPtCO]_2$	469	1395	786
$CpPt(CO)I$	n. m.	1447	798
		1383	

n. m. = not measured

ν	- stretching	ρ_w	- wagging
δ	- deformation	ρ_r	- rocking
δ_t	- ring tilting	ρ_t	- twisting
π	- out-of-plane bending	s	- symmetric
d	- degenerate	as	- asymmetric

The cyclopentadienyl ligand is abbreviated "Cp". For compounds containing two π-cyclopentadienyl ligands, only the asymmetric stretching mode is seen in the IR spectrum. The metal-ligand modes for ferrocene-like compounds are reproduced from reference 4 below. The range of ν_{M-L} for these compounds is 312 cm^{-1} (Cp_2WH_2) to 478 cm^{-1} (Cp_2Fe).

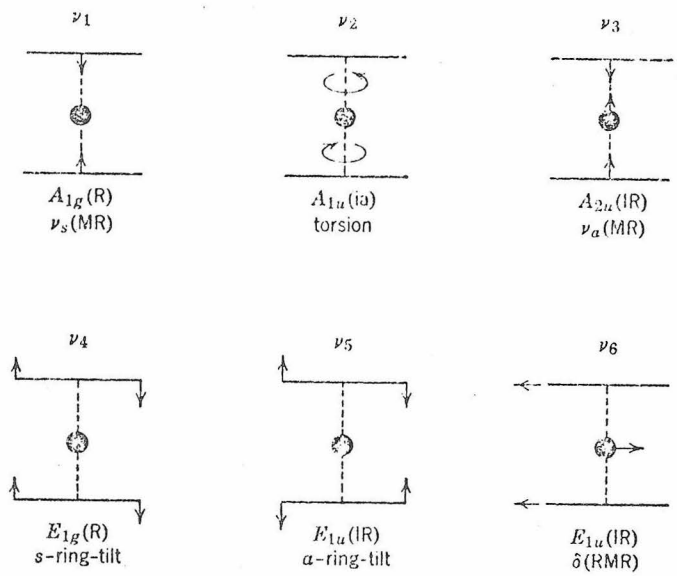

Skeletal vibrations of dicyclopentadienyl metal complexes (D_{5d} symmetry).

Metal-ring vibrations for π-benzene complexes are given in Table III. The values of ν_{M-L} range from 306-459 cm^{-1}. Fritz[3] does not report any ν_{ML} frequencies for π-C_7H_7 or π-C_8H_8 complexes.

Table III[3]

SKELETAL VIBRATIONS OF DIBENZENE-METAL COMPLEXES

Type of vibration	Symm. stretch	Torsion	Asymm. stretch	Symm. ring tilt	Asymm. ring tilt	Ring–M–ring deformation
$(C_6H_6)_2Cr$	270	(305)	459	332	490	(140)
$[(C_6H_6)_2Cr]I$	279	(303)	415	333	466	(144)
$(C_6D_6)_2Cr$	—	—	423	—	479	—
$(C_6H_6)_2Mo$	—	—	362	—	424	—
$[(C_6H_6)_2Mo]I$	—	—	333	—	410	—
$(C_6H_6)_2W$	—	—	331	—	386	—
$[(C_6H_6)_2W]I$	—	—	306	—	378	—
$(C_6H_6)_2V$	—	—	424	—	470	—
$[(C_6H_6)_2Tc]PF_6$	—	—	358	—	431	—
$[(C_6H_6)_2Re]PF_6$	—	—	336	—	396	—

Values in parentheses are determined from combination bands.

Some data are available from recent literature. Although no one has tackled the π-tropylium case, Fritz and Kreiter[5] report low frequency bands for $(\pi\text{-}C_7H_7)V(CO)_3$ at 448 s, 490 s, 526 s, 549 w, and 539 s. (Here s = strong and w = weak). It is not possible to assign these since possible modes in this region include ν_{M-L}, δ_t, δ_{M-C-O}, and ν_{M-C}. Beall and Houk[6] report IR data down to 400 cm^{-1} for eight compounds of the type $(\pi\text{-}C_7H_7)Mo(CO)$-(P)(I) where P is a phosphite or phosphine. Again it is impossible to make a definite assignment. The δ_{M-C-O} frequency could conceivably come where the δ_t mode occurs and all three stretching frequencies (ν_{M-L}, ν_{M-C}, ν_{M-P}) are expected in the 400 cm^{-1} region. The $\pi\text{-}C_8H_8$ case is not much better. Karraker, et al.[7]

have examined the spectra of $U(C_8H_8)_2$ and $Np(C_8H_8)_2$ in the KBr region. Strong bands at 460 cm^{-1} in the Raman spectra of both compounds are conceivably ν_s(M-L). No other bands below 630 cm^{-1} are observed, so this assignment must be very tentative as δ_t and ring deformation modes can occur in this region.

Table IV summarizes these metal-ligand vibrations. As no cyclopropenium data are available, we substitute data for the π-allyl complex $[(\pi\text{-}C_3H_5)PdCl]_2$[8] in its place. The metal-ring stretching force constants for cyclopentadienyl and benzene complexes

Table IV

IR Active Metal-Ring Vibrations

Ring	$\nu_{ML}(cm^{-1})$	$\delta_t(cm^{-1})$	Reference
C_2H_4	383-427	--	2
C_3H_5	401	--	8
$(CH_3)_4C_4$	416	467	3
C_5H_5	312-478	365-613	3
C_6H_6	306-459	386-490	3
C_7H_7	--	--	-
C_8H_8	460 ?(Raman)	--	7

are in the range 1.5-3.9 mdyne/Å.[3] Fritz[3] has pointed out that the reason the metal-ring stretching absorptions are strong in the IR is that the bonds are probably quite polar.

Bonding within the cyclic ligand should be affected by coordination to a metal and this change ought to be reflected by the vibrational spectrum. In olefin complexes, the Chatt-Duncanson-Guy Central Dogma of Metal π-Complexes[9] (sigma donation, pi back bonding) predicts that the C=C bond should be weakened upon coordination. This is reflected by a decrease in $\nu_{C=C}$. The C=C stretch in ethylene occurs at 1623 cm^{-1}. In Zeise's salt this is reduced to 1526 cm^{-1}.[1] (This frequency for Zeise's salt contains both $\nu_{C=C}$ and δ_{CH}, but the magnitude of the change from free to coordinated olefin is similar in cases where coupling to the δ_{CH} mode does not occur.) We also expect C–H wagging (ρ_w) to increase in energy as observed in cyclic C_nH_n complexes (<u>vide infra</u>). This out-of-plane motion is illustrated below. Its frequency should increase

wagging motions of free ethylene

ρ_w (C-H) ν_7 (b_{1u})

ρ_w (C-H) ν_8 (b_{2g})

because of steric interference while wagging toward the transition metal. The manifestation of this in the IR spectra is that the combination band, $\nu_7 + \nu_8$, increases in frequency. In free ethylene, $\nu_7 + \nu_8$ is observed at 1889 cm^{-1} ($\nu_7 = 943$, $\nu_8 = 949$). In Zeise's salt $\nu_7 + \nu_8 = 2048$ cm^{-1} ($\nu_7 = 1023$, $\nu_8 = 1023$).[1] Similar data for other olefin complexes are given in Table V.

Table V

Vibrations of Coordinated Olefins

	$\nu_{C=C}$ (cm^{-1})	$\nu_{C=C}$ (free olefin) (cm^{-1})	Δ^b (cm^{-1})	$\delta_{CH}{}^c$ (cm^{-1}) (combination band)	$\delta_{CH}{}^c$ (cm^{-1}) (free olefin)	Reference
$PtCl_3[(C_3H_5)NH_3]$ [a]	1504	1650	146	2060	1885	10
$PtCl_3[(C_3H_5)_2NH_2]$	1500	1650	150	2070	1935	10
$PtCl_3[(C_3H_5)NH_2(C_2H_5)]$	1503	--	--	2058	--	10
$PtCl_3[(C_3H_5)NH_2(n\text{-}C_8H_{17})]$	1500	--	--	1990	--	10
$PtCl_3[(C_3H_5)NH(C_2H_5)_2]$	1495	--	--	2011	--	10
$PtCl_3[(C_3H_5)_2NH(C_2H_5)]$	1506	1649	143	2065	1955	10
$PtCl_3[(C_3H_5)N(C_2H_5)_3]$	1495	--	--	1990	--	10
$[K][PtCl_3(C_2H_4)] \cdot H_2O$	1526	1623	97	2048	1889	1
$[K][PtCl_3(C_2H_4)] \cdot H_2O$	1428	1515	87	1629	1497	1
$[K][PtBr_3(C_2H_4)]$	1511	1623	112	--	--	2
$[K][PtCl_3(C_3H_6)]$	1505	1649	144	--	--	2
$[K][PtCl_3(trans\text{-}C_4H_8)]$	1522	1681	159	--	--	2
$[K][PtCl_3(cis\text{-}C_4H_8)]$	1505	1672	167	--	--	2
$trans[Pt(C_2H_4)(NH_3)Cl_2]$	1521	1623	102	--	--	2
$trans[Pt(C_2H_4)(NH_3)Br_2]$	1517	1623	106	--	--	2
$[Pt(C_2H_4)Cl_2]_2$	1516	1623	107	--	--	2
$[Pt(C_3H_5)NH(n\text{-}C_8H_{17})]Cl_2]_2$	1513	--	--	2000	--	10
$[Pd(C_2H_4)Cl_2]_2$	1527	1623	96	--	--	2
$Ni(CH_2{=}CHCN)_2$	1446	--	--	--	--	11
$Rh(C_2H_4)_2(C_5H_5)$	1490	1623	133	--	--	12
$Fe(C_2H_4)(CO)_2(C_5H_5)^{\oplus}$	1527	1623	96	--	--	13

[a] C_3H_5 = allyl.

[b] $\nu_{C=C}$(free) - $\nu_{C=C}$(coordinated).

[c] $(\nu_7 + \nu_8)$ in C_2H_4.

Bonding within cyclic C_nH_n ligands is affected just as it is in ethylene. We expect $\nu_{C=C}$ (typically a degenerate ring breathing mode) to decrease from the free ligand value and π_{CH} to increase. (Fritz[3] refers to these modes as ω_{CC} and γ_{CH}, respectively.) These modes are drawn below for C_3H_3 and C_5H_5 rings. Interestingly, the free ligands of D_{nh} symmetry each exhibit just four IR-active modes. (Table VI).

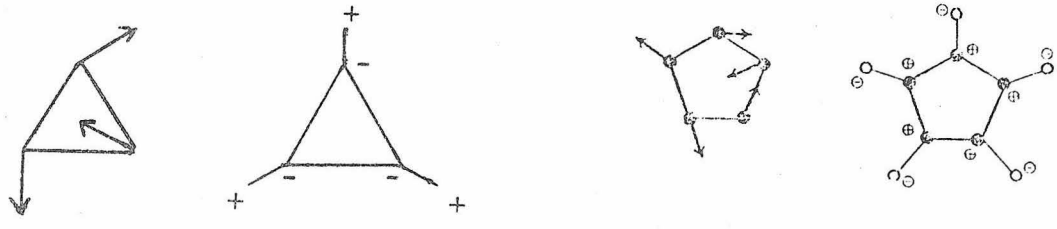

ν_d(CC) π(CH) ν_d(CC) π(CH)

Table VI

IR Active Modes of Free Ligands

	$C_3H_5SbCl_6$[14]	C_5H_5K[3]	C_6H_6[3]	C_7H_7Br[3]	$C_8H_8K_2$[3]
ν_d(CH)	3105	3021	3064	3020	2994
ν_d(CC)	1276	1442	1482	1477	1431
δ_d(CH)	908	1008	1037	992	880
π (CH)	736	701	673	633	684

The only datum available for a cyclobutadiene complex is $\nu_{C=C}$ = 1531 s in $(CH_3)_4C_4NiCl_2$ [3]. ν_{CC} and π_{CH} frequencies for cyclopentadienyl complexes are given in Table II and those of C_6H_6 and C_7H_7 complexes are given in Table VII. The ν_{CC} and π_{CH} modes

referred to in these tables are the same ones given in Table VI. It

Table VII[3]

Selected Ligand Vibrations of π-C_6H_6 and π-C_7H_7 Complexes

	ν_{CC}	π_{CH}		ν_{CC}	π_{CH}
$(C_6H_6)_2Cr$	1426	794	$C_6H_6Cr(CO)_3$	1445	784
$[(C_6H_6)_2Cr]^+$	1430	795	$C_6D_6Cr(CO)_3$	1292	702
$(C_6D_6)_2Cr$	1271	735	$C_6H_6Mo(CO)_3$	1439	763
$(C_6H_6)_2Mo$	1425	773	$C_6D_6Mo(CO)_3$	1285	696
$(C_6H_6)_2W$	1412	798	$C_6H_6W(CO)_3$	1433	776
$(C_6H_6)_2V$, cubic	1416	739	$[C_6H_6Mn(CO)_3]ClO_4$	1453	—
$(C_6H_6)_2V$, monoclinic	1415	742		1433	
$[(C_6H_6)_2Tc]^+$	1443	—	$[(C_6H_6)_2Co_3(CO)_2]^+$	1445	793
$[(C_6H_6)_2Re]^+$	1437	—			776
$CpCrC_6H_6$	1410	779	$[C_7H_7PtBr_2]_2$	1473	744
$CpMnC_6H_6$	1427	808	$[C_7H_7Cr(CO)_2]BF_4$	1450	816
$[CpCoC_6H_6]PF_6$	1449	—	$[C_7H_7Mo(CO)_2]BF_4$	1440	807
$[CpRhC_6H_6]PF_6$, or BF_4^-			$C_7H_7VC_5H_5$	(1421)	784
salt	1449	795	$C_7H_7V(CO)_3$	1431	785

is necessary to specify this because more modes become IR active in the reduced symmetry of the complex. Data for C_8H_8 complexes[7] indicate π_{CH} is nearly unchanged from the free ligand value. ν_{CC} modes are observed at 1470 cm^{-1} in $U(C_8H_8)_2$ and $Np(C_8H_8)_2$. Tables II and VII show substantial decrease in the energy of ν_{CC} modes of C_5H_5, C_6H_6, and C_7H_7 complexes, albeit these shifts are not as great as those of olefin complexes.

The simplest information one could hope to obtain about the effect of a ligand on bonding to other ligands in a complex would be contained in an infrared trans effect. For example, the ν_{PtH} frequency of the compounds trans-$PtHX(PEt_3)_2$ correlates with the trans effect

of the ligand X.[15] As X becomes a stronger trans ligand, ν_{PtH} decreases. A similar effect was observed on ν_{PtCl} in compounds of the type trans-$PtClR(PMe_2\phi)_2$.[16] For square planar compounds of the type $LMCl_3$, we can hope to correlate the ν (M-Cl_{trans}) frequency with the trans effect of the ligand L. In Zeise's salt the force constant for the Pt-Cl bond trans to the ethylene is slightly weaker than the cis Pt-Cl force constants.[1] Presumably the ν(Pt-Cl_{trans}) frequency will decrease as the trans

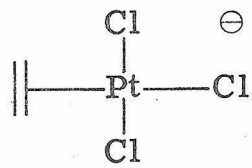

$K(Pt\text{-}Cl_{cis}) = 1.82$ mdynes/Å

$K(Pt\text{-}Cl_{trans}) = 1.78$ mdynes/Å

	C_2H_4	C_2D_4
ν_s(Pt-Cl)	331	329
ν_{as}(Pt-Cl)	339	339
ν(Pt-Cl_{trans})	310	305

effect of L increases. In compounds of the type trans-$PtCl_2L_2$, the ν_{as}(Pt-Cl) frequency is remarkably independent of L, indicating a small cis effect.[17] In cis-$PtCl_2L_2$ compounds, the ν_{PtCl} frequencies are very dependent upon L.[17] Some data are available to show that the trans effect also manifests itself in bridged binuclear complexes. The $\nu_{M\text{-}Cl}$ force constant for bridge bonds decreases when Cl is replaced by ethylene in the terminal position.[2,18]

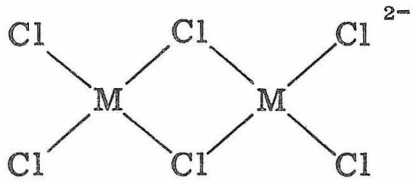

	M = Pt	M = Pd
$K(M\text{-}Cl_{terminal})$	2.02(mdyne/Å)	1.59
$K(M\text{-}Cl_{bridge})$	1.42	1.36
$K_{bridge}/K_{terminal}$	0.70	0.86

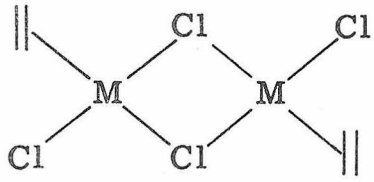

$K(M\text{-}Cl_{terminal})$	2.17	1.71
$K(M\text{-}Cl_{bridge})$	0.69	0.65
$K_{bridge}/K_{terminal}$	0.32	0.38

Great expectations! For a π-C_3H_3 complex we expect ν_d(CC) to decrease ~ 50 cm^{-1} to ~ 1230 cm^{-1}. We expect π_{CH} to increase by 50-100 cm^{-1} to 790-840 cm^{-1}. ν_{ML} should occur near 400 cm^{-1} and δ_t ought to be in the region 400-600 cm^{-1}. We anxiously await the synthesis of a π-C_3H_3 complex. The only data on any π-cyclopropenium complexes are a drop of ν_d(CC) from 1425-1400 cm^{-1} in $(C_6H_5)_3C_3^+$ to either 1370 or 1350 cm^{-1} in $\{[\pi\text{-}C_3(C_6H_5)_3]NiCl(C_5H_5N)_2\} \cdot C_5H_5N$.[19]

References

1. M. J. Grogan and K. Nakamoto, J. Amer. Chem. Soc., 88, 5454 (1966).
2. M. J. Grogan and K. Nakamoto, Ibid., 90, 918 (1968).
3. H. P. Fritz, Adv. Organomet. Chem., 1, 239 (1964).
4. K. Nakamoto, "Infrared Spectra of Inorganic and Coordination Compounds," Wiley-Interscience, New York, 1970 ed.
5. H. P. Fritz and C. G. Kreiter, Chem. Ber., 97, 1398 (1964).
6. T. W. Beall and L. W. Houk, Inorg. Chem., 11, 915 (1972).
7. D. G. Karraker, J. A. Stone, E. R. Jones, Jr., and N. Edelstein, J. Amer. Chem. Soc., 92, 4841 (1970).
8. H. P. Fritz, Chem. Ber., 94, 1217 (1961).
9. J. Chatt, L. A. Duncanson, and R. G. Guy, Nature, 184, 526(1959).
10. R. G. Denning and L. M. Venanzi, J. Chem. Soc., 3241 (1963).
11. H. P. Fritz and G. N. Schrauzer, Chem. Ber., 94, 650 (1961).
12. R. B. King, Inorg. Chem., 2, 528 (1963).
13. E. O. Fischer and K. Fichtel, Chem. Ber., 95, 2063 (1962).
14. R. Breslow and J. T. Groves, J. Amer. Chem. Soc., 92, 984 (1970).
15. J. Chatt, L. A. Duncanson, and B. L. Shaw, Chem. Ind. (London), 859 (1958).
16. M. R. Collier, C. Eaborn, B. Jovanović, M. F. Lappert, L. Manojlović-Muir, K. W. Muir, and M. M. Truelock, Chem. Comm., 613 (1972).

17. D. M. Adams, "Metal-Ligand and Related Vibrations," St. Martin's Press, New York, 1968, pages 74-75.

18. D. M. Adams, P. J. Chandler, R. G. Churchill, J. Chem. Soc. A, 1272 (1967).

19. R. M. Tuggle, Ph.D. Thesis, Carnegie-Mellon University, 1971. We thank Dr. D. L. Weaver for this information.

Chapter Three

Synthesis and Properties of $M_2Cl_6^{2-}$ Salts

Introduction

While attempting to prepare neutral π-cyclopropenium complexes[1] (I) by the same route used to synthesize Zeise's salt (II) (equations 1 and 2), we isolated instead cyclopropenium salts (III) of the bridged, square planar, binuclear anions $Pt_2Cl_6^{2-}$ and $Pd_2Cl_6^{2-}$ (equation 3).

$$C_2H_4 + K_2PtCl_4 \xrightarrow[H_2O]{} [K^+][(C_2H_4)PtCl_3^-] \cdot H_2O + KCl \qquad (1)$$

(II)

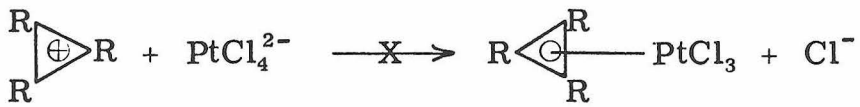

(2)

IV a. $R = (CH_3)_2N-$ I

b. $R = n-C_3H_7-$

$$2\,R_3C_3^+ + 2\,MCl_4^{2-} \xrightarrow[H_2O]{} [R_3C_3^+]_2[M_2Cl_6^{2-}] + 2\,Cl^- \qquad (3)$$

III a. $M = Pt$ $R = (CH_3)_2N-$

b. $M = Pt$ $R = n-C_3H_7-$

c. $M = Pd$ $R = (CH_3)_2N-$

d. $M = Pd$ $R = n-C_3H_7-$

Salts of $Pd_2X_6^{2-}$ (X = Cl, Br) were apparently synthesized as early as 1916[2] but the dimeric nature of these anions was not appreciated until the crystal structure of $[(C_2H_5)_4N]_2[Pt_2Br_6]$ was

determined in 1958.[3,4] The preparation of several quaternary ammonium and arsonium $M_2X_6^{2-}$ salts has been reported.[3,5] A study of the far IR spectra of these anionic species was reported by Adams, Chandler, and Churchill[5] and single crystal polarized optical spectra of the bromides and iodides were reported by Day, Smith, and Williams.[6] In this chapter, we report the synthesis and characterization of IIIa-d. Other members of the Gray research group have determined the crystal and molecular structure of IIIa and studied its single crystal polarized optical spectrum.[7] The results of these other studies are summarized at the end of this section and this writer's interpretation of the polarized spectrum is discussed.

Experimental

General. Analyses were performed by Galbraith Laboratires, Inc., Knoxville, Tennessee. All analytical samples were crystallized three times. Nuclear magnetic resonance spectra were recorded on a Varian A-60A spectrometer and IR spectra were recorded using KBr pellets and a Perkin-Elmer 225 grating infrared spectrometer. Conductivity measurements were made with a Radiometer type CDM2e conductivity meter and a cell with cell constant = 0.57 cm. Melting points were determined using unsealed capillary tubes. UV-VIS measurements were made on a Cary Model 17 spectrophotometer.

Tripropylcyclopropenium Tetrafluoroborate $[(n-C_3H_7)_3C_3][BF_4]$. This was prepared by the method that Breslow, Höver, and Chang[8] used to prepare the corresponding perchlorate. Triphenylmethyl tetrafluoroborate was substituted for triphenylmethyl perchlorate and all other conditions were identical. The crude product, which precipitated from diethyl ether, was obtained in 60% yield and crystallized from ethyl acetate-diethyl ether.

Tris(dimethylamino) cyclopropenium Tetrafluoroborate $\{[(CH_3)_2N]_3C_3\}\{BF_4\}$. This was prepared using the procedure described by Yoshida and Tawara[9] for the preparation of the perchlorate. To a solution of 6.0 ml (10 g, 0.071 mol) C_3Cl_4 in 100 ml CH_2Cl_2 cooled to 0° was added dropwise with stirring ca. 40 ml (0.6 mole) dimethylamine. As the very vigorous initial reaction

subsided, the remaining dimethylamine was added as rapidly as possible. The flask was then tightly stoppered with a ground glass stopper and stirred three hours at 0° and 15 hours at room temperature. The yellow solution with suspended white solid was then refluxed five hours. The mixture was cooled to 0°, shaken well with 200 ml 50% aqueous HBF_4, separated, dried over $MgSO_4$, and concentrated to dryness on a rotary evaporator. The waxy pink residue was crystallized from 22 ml $CHCl_3$ to give 5.1 g (35%) white product after drying. No attempt was made to maximize this yield. Analysis for C and H shows less C than expected. The IR spectrum shows very strong H_2O absorption even after drying the sample three days at 5 μ pressure. The NMR spectrum shows no $CHCl_3$ of crystallization present. We conclude that this material contains ca. 3.5% H_2O by weight. This corresponds to $\{[(CH_3)_2N]_3C_3\}\{BF_4\}\cdot\frac{1}{2}H_2O$.

$[Cy]_2[Pt_2Cl_6]$ (Cy = $[(CH_3)_2N]_3C_3$ or $(n\text{-}C_3H_7)_3C_3$). These were prepared in identical ways so only one preparation will be described. 0.40 g (0.97 mmole) K_2PtCl_4 and 0.25 g (0.99 mmole) $[(n\text{-}C_3H_7)_3C_3][BF_4]$ were dissolved in 8 ml deoxygenated H_2O under N_2. (N_2 atmospheres were used routinely but they are probably not necessary.) The red solution deposited an orange-pink precipitate during 2.2 hours of stirring at 60°C. (Prolonged reaction times did not increase the yield and did cause decomposition of the product.) The solution was filtered in the atmosphere and the product was washed with H_2O. The yield of crude product ranged from 55-78%.

For Cy = $(n-C_3H_7)_3C_3$, the product is crystallized from acetone, in which it is very soluble, to give long pink needles. It is also very soluble in CH_2Cl_2, moderately soluble in CH_3OH and EPA (5:5:2 (vol/vol/vol) ether: isopentane:ethanol) and insoluble in cyclohexane. For Cy = $[(CH_3)_2N]_3C_3$, the product is crystallized from acetone, in which it is somewhat soluble, or CH_2Cl_2-acetone, in which it is more soluble. The product crystallizes as pink to brick red needles or prisms. The pink and red crystals, which often crystallized simultaneously, had identical IR and UV-VIS spectra in KBr pellets. Both compounds and their solutions are air stable, though they undergo solvolysis overnight in acetone at room temperature. (The solutions change from pink or red to yellow.)

<u>$[Cy]_2[Pd_2Cl_6]$(Cy = $(n-C_3H_7)_3C_3$ or $[(CH_3)_2N]_3C_3$).</u> Both compounds were prepared in identical manner without the exclusion of air. 0.45 g (1.7 mmoles) $\{[(CH_3)_2N]_3C_3\}\{BF_4\} \cdot \frac{1}{2}H_2O$ in 10 ml H_2O was added to a solution of 0.50 g (1.7 mmoles) Na_2PdCl_4 in 10 ml H_2O with vigorous magnetic stirring. After five minutes the orange-pink precipitate was filtered, washed with H_2O, and crystallized from CH_2Cl_2-acetone to give orange-red prisms. The compound for which Cy = $(n-C_3H_7)_3C_3$ is crystallized from acetone to give long thin orange-pink needles. Yields ranged from 50-70%. Solubility properties and air stability are similar to the Pt analogs.

Results and Discussion

The cyclopropenium cations IVa[9] and IVb[8] were prepared by literature methods and isolated as the tetrafluoroborate salts. We used BF_4^- wherever possible as a substitute for ClO_4^-, which was used previously,[8,9] to minimize the danger of working with these compounds. The $M_2Cl_6^{2-}$ salts IIIa-d precipitated from aqueous solutions of the cyclopropenium tetrafluoroborates and MCl_4^{2-} (M = Pd, Pt). Previous work[10,11] has established that the monomers and dimers exist in equilibrium in solution so the role of the cation is merely to precipitate the dimer. It is noteworthy, however, that Harris, Livingstone, and Stephenson[3] failed to isolate any salts of $Pt_2Cl_6^{2-}$ even though they isolated salts of the other five anions for which (M = Pt, Pd), (X = Cl, Br, I). The precipitation of $Pt_2Cl_6^{2-}$ or $PtCl_4^{2-}$ from solution is apparently very sensitive to the counterion. Using methyltriphenylarsonium chloride and excess Cl^- (as 2 M HCl), $PtCl_4^{2-}$ is precipitated.[3] Tetrabutylammonium chloride has also been used to prepare salts of $PtCl_4^{2-}$.[12] Pearson and Muir[13] used $[(C_6H_5)_4As]_2[PtCl_4]$ to prepare other compounds but did not state the source of their starting material. On the other hand, Adams, Chandler, and Churchill[5] prepared $[(C_6H_5)_4As]_2[Pt_2Cl_6]$ by merely mixing tetraphenylarsonium chloride and K_2PtCl_4 in H_2O at room temperature (RT). They obtained an immediate precipitate of dimeric product. Our preparation of the $Pt_2Cl_6^{2-}$ salts IIIa and IIIb required heating for two hours to precipitate the products. We do not

understand the apparent kinetic differences between our preparations and that of the tetraphenylarsonium salt.[5] All $Pd_2Cl_6^{2-}$ salts precipitated immediately upon mixing the reactants.

Analytical data for these compounds are shown in Table I. Conductivity measurements (Table II) are consistent with the formulation of these salts as 2:1 electrolytes in acetone and CH_2Cl_2 solution. PMR spectra (Table III) show just three equivalent substituent groups for each cyclopropenium cation. This remains true for the Pt compounds down to -62°. Also, no ^{195}Pt-^{1}H coupling is observed. These data are all consistent with the formulation of IIIa-d as salts.[14] On the other hand, the chemical shifts of the cations in IIIa-d are consistently downfield of those of the BF_4^- salts in acetone and CH_2Cl_2. This indicates some degree of ion pairing in these solvents. In agreement with this, we have observed marked cation dependence of the reactivity of these salts in CH_2Cl_2 solution. In DMSO, the chemical shift of IIIa is the same as the tetrafluoroborate so the ion pairing is probably destroyed in this solvent. DMSO may also solvolyze the anions (vide infra).

The IR spectra recorded in Tables IV and V and Figures 1-5 also support the assignment of these compounds as ionic in the solid state. In particular, all bands in the spectra of IIIa-d above 350 cm^{-1} are due to the cations.[15] The spectra of both the BF_4^- and $M_2Cl_6^{2-}$ salts are very similar so the cyclopropenium groups are not significantly affected by the $M_2Cl_6^{2-}$ anions. The cyclopropenium band which is expected to be most affected by π-coordination to a transition

Table I. Analytical Data

Compound	Color	Melting Point	Analyses							
			C		H		Metal		Cl	
			Found	Calc.	Found	Calc.	Found	Calc.	Found	Calc.
$[(n\text{-}C_3H_7)_3C_3][BF_4]$	white	148°	57.27	(57.17)	8.55	(8.40)	--	--	--	--
$\{[(CH_3)_2N]_3C_3\}\{BF_4\} \cdot \frac{1}{2}H_2O$	white	116-120°	40.88	(40.94)	7.09	(7.25)	--	--	--	--
$[(n\text{-}C_3H_7)_3C_3]_2[Pt_2Cl_6]$	pink	149-150 dec (?)	30.75	(30.88)	4.64	(4.54)	41.59	(41.80)	22.79	(22.79)
$\{[(CH_3)_2N]_3C_3\}_2\{Pt_2Cl_6\}$	red	ca. 190° dec	23.07	(23.01)	3.87	(3.86)	41.70	(41.53)	22.65	(22.64)
$[(n\text{-}C_3H_7)_3C_3]_2[Pd_2Cl_6]$	orange-pink	105-106°	38.10	(38.12)	5.82	(5.60)	27.39	(28.14)	27.86	(28.13)
$\{[(CH_3)_2N]_3C_3\}_2\{Pd_2Cl_6\}$	orange-red	ca. 232° dec	27.96	(28.37)	4.47	(4.76)	27.94	(27.93)	28.30	(27.91)

Table II. Conductivity Measurements

Compound	Molecular Weight	Concentration (M)	Solvent	Conductivity ($cm^2\ ohm^{-1}\ mole^{-1}$)
$[(n-C_4H_9)_4N][I]$	369.4	1.07×10^{-3}	acetone	150
		1.17×10^{-3}	CH_2Cl_2	21
$[(n-C_4H_9)_4N]_2[PtCl_4]$[a]	821.8	5.03×10^{-4}	acetone	110
		5.55×10^{-4}	CH_2Cl_2	16
$[(n-C_3H_7)_3C_3]_2[Pt_2Cl_6]$	933.5	2.84×10^{-4}	acetone	120
		2.47×10^{-4}	CH_2Cl_2	8.2
$\{[(CH_3)_2N]_3C_3\}_2\{Pt_2Cl_6\}$	939.4	4.56×10^{-4}	acetone	130
		4.04×10^{-4}	CH_2Cl_2	14
$[(n-C_3H_7)_3C_3]_2[Pd_2Cl_6]$	756.1	1.19×10^{-3}	acetone	110
		1.19×10^{-4}	acetone	190
		1.34×10^{-3}	CH_2Cl_2	4.2
		1.34×10^{-4}	CH_2Cl_2	11
		6.40×10^{-4}	CH_3OH	160
		2.56×10^{-5}	CH_3OH	280
$\{[(CH_3)_2N]_3C_3\}_2\{Pd_2Cl_6\}$	762.0	5.35×10^{-4}	acetone	140
		5.15×10^{-4}	CH_2Cl_2	24

[a] Ref. 12.

Table III. NMR Measurements

Compound	Solvent	Chemical Shift (ppm downfield of internal TMS)		
		α-CH_2	β-CH_2	CH_3
$[(n-C_3H_7)_3C_3][BF_4]$[a]	$(CD_3)_2CO$	3.32	b	1.08
	CH_2Cl_2	3.15	1.92	1.08
	CH_3CN	3.16	1.90	1.06
	$CHCl_3$	3.16	1.92	1.07
$[(n-C_3H_7)_3C_3]_2[Pt_2Cl_6]$[a,d]	$(CD_3)_2CO$	3.67	2.18	1.16
	CH_2Cl_2	3.67	2.15	1.16
$[(n-C_3H_7)_3C_3]_2[Pd_2Cl_6]$[a]	$(CH_3)_2CO$	3.65	b	1.17
	CH_2Cl_2	3.58	2.15	1.19
$\{[(CH_3)_2N]_3C_3\}\{BF_4\}$[c]	$(CD_3)_2CO$			3.20
	CH_2Cl_2			3.14
	$(CD_3)_2SO$[e]			3.07
	$CHCl_3$[f]			ca. 3.1
$\{[(CH_3)_2N]_3C_3\}_2\{Pt_2Cl_6\}$[c,d]	CH_2Cl_2			3.39
	$(CD_3)_2SO$			3.07
$\{[(CH_3)_2N]_3C_3\}_2\{Pd_2Cl_6\}$[c]	CH_2Cl_2			3.41

a) All $[(n-C_3H_7)_3C_3]$ salts showed a triplet-sextet-triplet pattern for the α-CH_2, β-CH_2 and CH_3 peaks, respectively. All coupling constants are ca. 7.5 Hz.

b) Under solvent peak.

c) All $\{[(CH_3)_2N]_3C_3\}$ salts show a single CH_3 absorption.

d) Examination of the NMR spectrum at 31°, 13°, - 36°, and -62° showed no changes except for decrease of the signal due to sample crystallization.

e) $J_{^{13}C \leftrightarrow H} = 139$ Hz.

f) All samples in this table gave sharp absorption signals except this solution. For this solvent, $\omega_{1/2} \approx 65$ Hz. This is not due to impure compound since the same material in other solvents gave sharp signals.

Table IV. Infrared Spectra of $[(n-C_3H_7)_3C_3]$ Salts in KBr Pellets from 4000 - 300 cm^{-1} [a]

$[(n-C_3H_7)_3C_3][BF_4]$	$[(n-C_3H_7)_3C_3]_2[Pt_2Cl_6]$	$[(n-C_3H_7)_3C_3]_2[Pd_2Cl_6]$
~3430 m, br (H_2O)		
	2970 sh, s	
2970 s	2965 s	2965 s
2940 s	2935 s	2935 s
2880 s	2875 s	2875 s
	2310 w	
2080 w, br	1700 w	
1624 w, br (H_2O)	1625 w	
		1463 s
1457 s	1462 s, br[b]	1453 s
		1445 sh, s
1395 sh, w		
1385 m	1381 s	1382 s
		1357 sh, w
1320 sh, w		1316 w
1305 w[c]		
	1300 w	1300 w
1299 w[c]		
1150 - 1000 s, br[c]		
	1269 m	1270 m
	1246 m	1247 m
	1106 m	1106 m
	1075 w	1074 w
		1039 w
916 w	920 w	919 w
	904 w	905 w
	798 w, br	
771 w[c]		
750 sh, w		
731		
	714 m	714 m
	620 vw	643 w
533 m[c]		
522 m[c]		
467 w		
	345 s	350 s
	311 s	341 s

a) s = strong, m = medium, w = weak, sh = shoulder, br = broad. All spectra were run at ambient temperatures.

b) 1459 s, 1453 sh, s, 1446 s in a weaker sample.

c) These bands are due to BF_4^-. See K. O. Christe and W. Sawodny, Inorg. Chem. 8, 212 (1969).

Table V.. Infrared Spectra of $[((CH_3)_2N)_3C_3]$ Salts in KBr pellets from 4000-300 cm^{-1} [a]

$\{[(CH_3)_2N]_3C_3\}\{BF_4\}$		$\{[(CH_3)_2N]_3C_3\}_2\{Pt_2Cl_6\}$		$\{[(CH_3)_2N]_3C_3\}_2\{Pd_2Cl_6\}$	
300° K	80° K[c]	300° K	80° K[c]	300°K	80° K[c]
~3350-3350 s, br	~3550-3250 s, br	~3550-3350 w, br	~3400 w, br	~3550-3350 w, br	~3410 w, br
3540 m	3530 w				
3470 s	3450 m				
3405 m	3383 m				
3320 w	3227 w				
	3212 w				
	2981 w	3000 w	2993 w	3000 w	2998 w
2960 sh, m	2954 m	2950 sh, m	2954 m	2950 sh, m	2950 w
2930 m	2920 w	2930 m	2915 w	2920 m	2910 w
	2904 w				
2895 m	2889 w	2890 m	2889 m	2880 m	2890 w
2850 w	2839 w	2845 w	2839 w	2840 w	2840 w
2800 w	2790 w	2795 w	2789 w	2790 w	
2415 w	2355 w, br		2352 m	2310 w	
	2330 w, br		2330 m		
2160 w		2155 w		2155 w	
2110 w	2127 w				
2050 w	2065 w				
1820 w		1812 w		1810 w	
1774 w		1767 w		1766 w	
1645 sh, w	1625 sh, w	1637 sh, w	1637 w	1635 w	1640 sh, w
1612 w	1609 w				
	1580 sh, m	1583 sh, m	1586 w	1583 sh, m	1585 sh, m
1562 s, br	1560 s	1560 s, br	1562 s, br	1555 s, br	1565 s, br
	1547 s				
	1472 w				
1460 w	1458 m		1458 w		1456 sh, w
	1454 m	1442 w	1447 m	1437 w	1444 w
	1435 w				
1424 m	1420 m				
	1416 m		1411 m	1415 sh, m	1417 sh, w
1410 s	1405 s	1405 s	1404 s	1402 s	1404 s
		1400 sh, s	1395 m	1398 s	1399 s
1307 w[b]	1306 w[b]				
1301 w					
1296 w[b]					
1223 m	1225 m	1219 m	1222 m	1217 m	1220 m
1150-1010 s, br[b]	1150-1010 s, br[b]				
			1143 sh, m		1144 sh, m
1127 m	1126 w	1133 w	1134 m	1130 w	1133 m
1087 m	1084 m				
	1052 w	1052 w	1059 m	1050 w	1054 w
			1051 m		
1038 m	1037 m	1029 m	1034 m		1033 m
			1026 m	1026 m	
	987 w		988 w		
	792 w		820-775 w, br		
788 m	789 w	781 m	786 m	783 w	784 w
774 sh, w[b]					
	612 w		667 m		
	571 m				
565 w	567 m				
558 w		550 w	550 w		
534 w[b]	533 w[b]				
523 w[b]	521 w[b]				
480 w	489 m				
460 w	465 w				
				454 w	440 w, br
		339 m		345 m	
		314 m		335 s	
310 w, br					
				303 w	

a) Abbreviations are the same used in Table IV

b) These bands are due to BF_4^-.

c) 80° K spectra were only recorded down to 400 cm^{-1}.

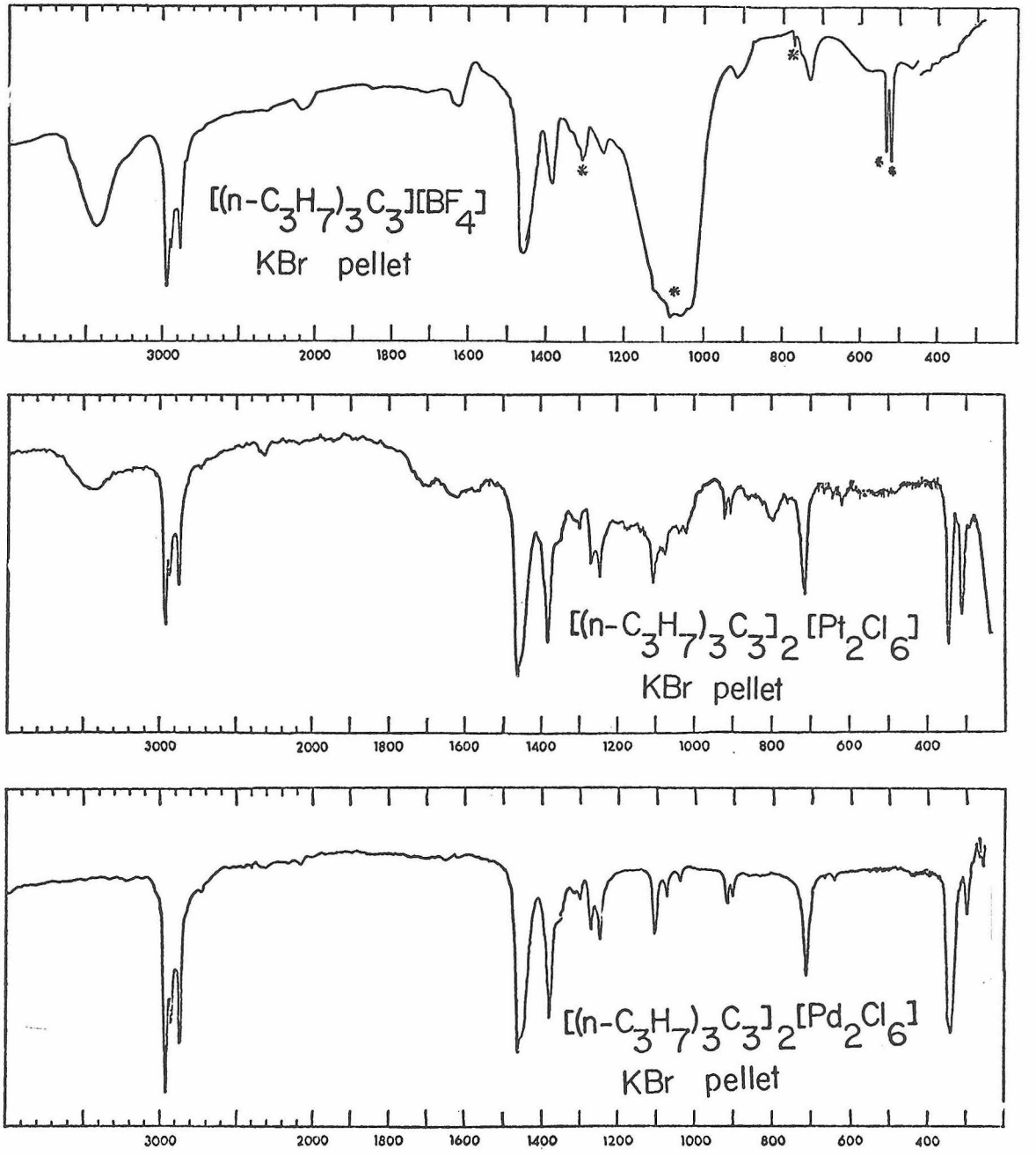
[(n-C3H7)3C3][BF4]
KBr pellet
3000
2000
1800
1600
1400
1200
1000
800
600
400
[(n-C3H7)3C3]2[Pt2Cl6]
KBr pellet
3000
2000
1800
1600
1400
1200
1000
800
600
400
[(n-C3H7)3C3]2[Pd2Cl6]
KBr pellet
3000
2000
1800
1600
1400
1200
1000
800
600
400

Figure 1

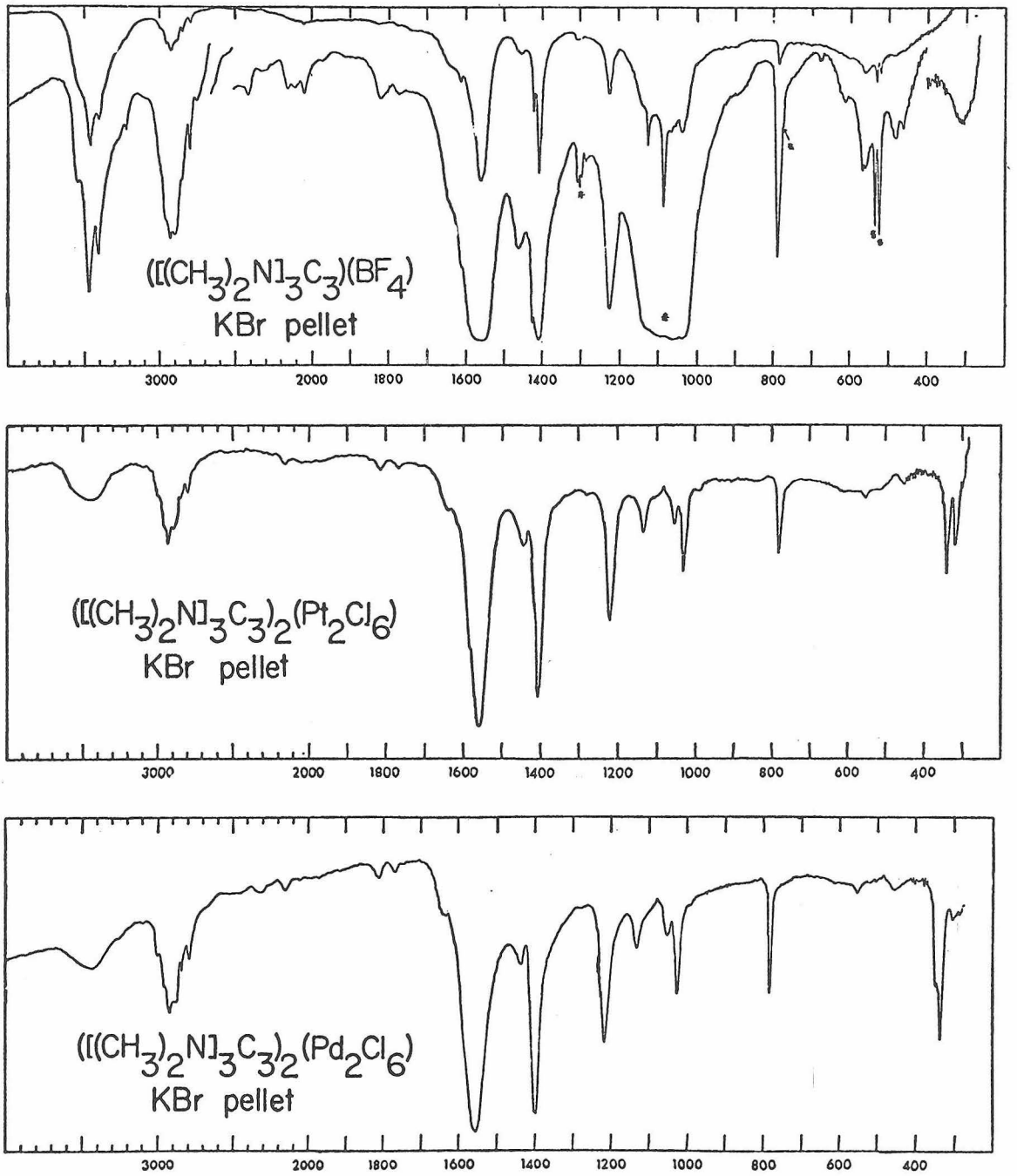
([(CH3)2N]3C3)(BF4)
KBr pellet
3000
2000
1800
1600
1400
1200
1000
800
600
400
([(CH3)2N]3C3)2(Pt2Cl6)
KBr pellet
3000
2000
1800
1600
1400
1200
1000
800
600
400
([(CH3)2N]3C3)2(Pd2Cl6)
KBr pellet
3000
2000
1800
1600
1400
1200
1000
800
600
400

Figure 2

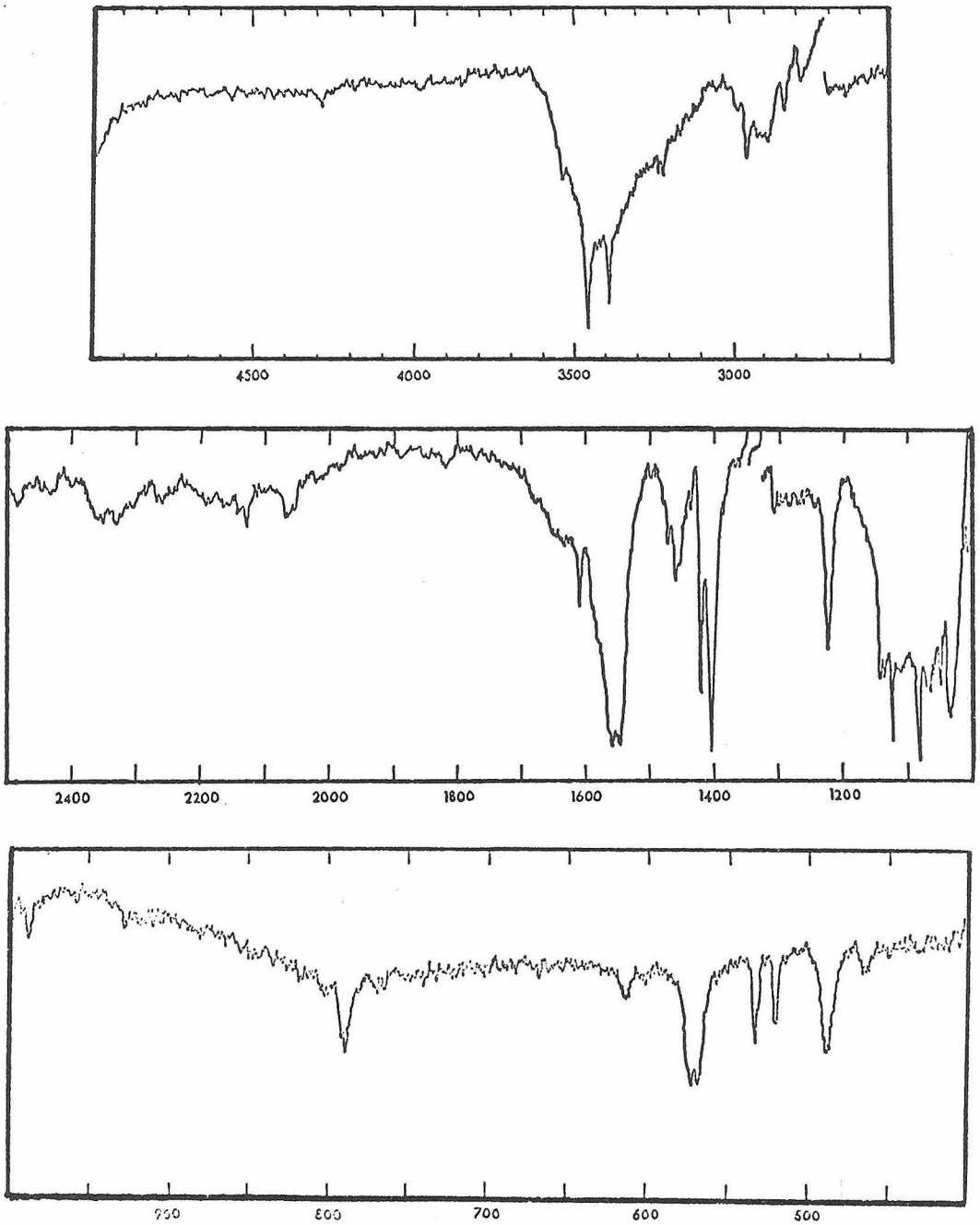

$([(CH_3)_2N]_3C_3)(BF_4)$

KBr pellet – 80°K

Figure 3

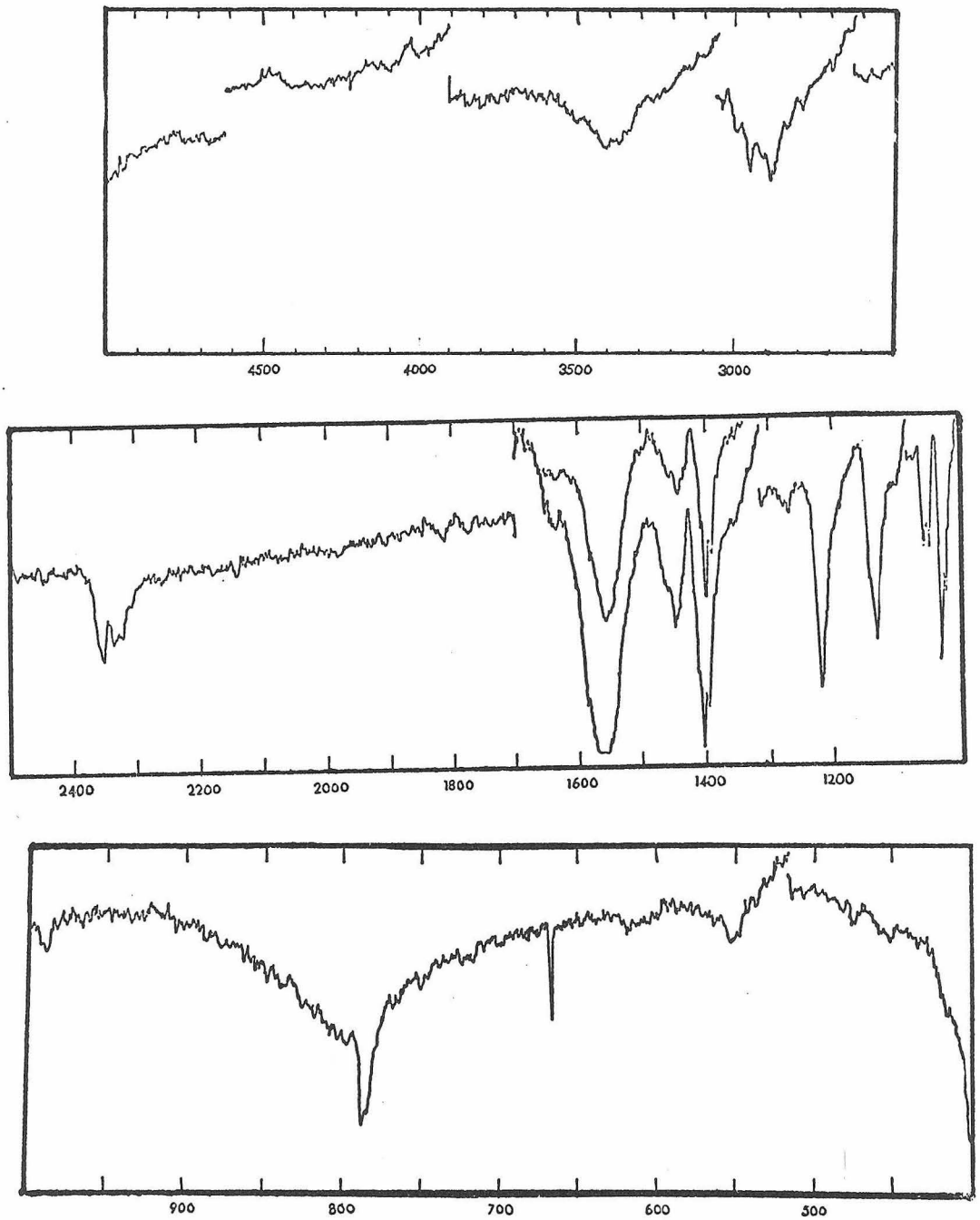

$([(CH_3)_2N]_3C_3)_2(Pt_2Cl_6)$

KBr pellet – 80°K

Figure 4

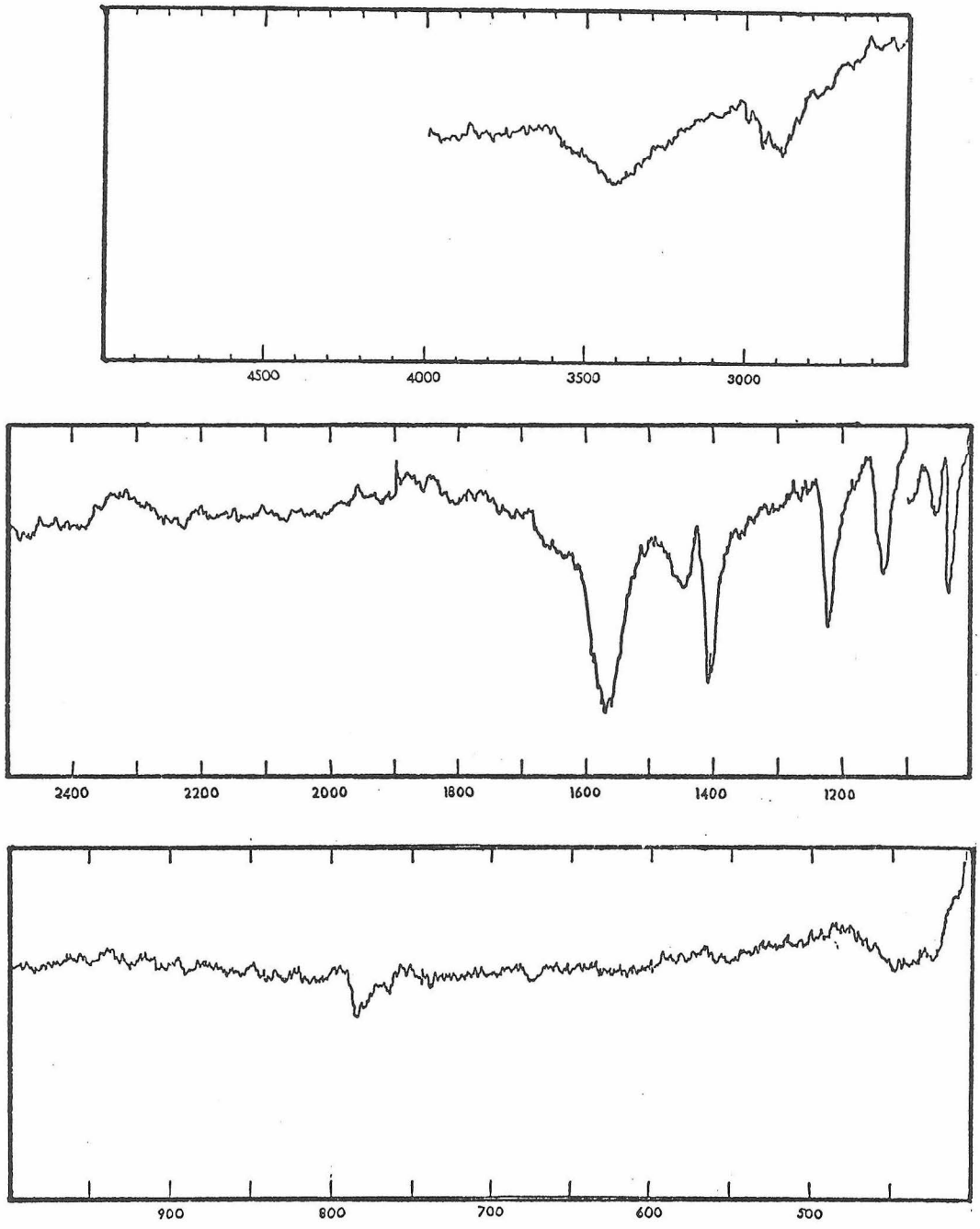

$([(CH_3)_2N]_3C_3)_2(Pd_2Cl_6)$

KBr pellet – 80°K

Figure 5

metal would be the degenerate C=C ring breathing mode, ν_{CC}. Fritz[16] has shown that the ν_{CC} modes of the π-cyclopentadienyl rings in $(\pi-C_5H_5)Pd(\pi-C_3H_5)$ and $[(\pi-C_5H_5)Pt(CO)]_2$ drop more than 40 cm^{-1} from the value found in C_5H_5K. Even larger changes in ν_{CC} are observed in $(\pi-C_6H_6)$[16] and $(\pi-C_2H_4)$[17-22] complexes.[23] The ν_{CC} ring breathing mode in alkyl substituted cyclopropenium cations occurs in the range 1380-1430 cm^{-1}.[24] We observe strong bands at 1381 and 1382 cm^{-1} in IIIb and IIId, respectively. These are hardly shifted from the value of 1385 cm^{-1} found in $[(n-C_3H_7)_3C_3][BF_4]$. The assignment of this band as ν_{CC} is complicated by the fact that the symmetric C-H bending mode of the methyl groups is also expected in this position. Nonetheless, we do not observe any other strong or medium intensity bands in this region of the spectrum, so it appears that no shifting of ν_{CC} is occurring.[25] We have not assigned ν_{CC} in the $[(CH_3)_2N]_3C_3^+$ cation, but, once again, the spectra of IIIa and IIIc are nearly identical to that of the tetrafluoroborate salt. The strongest band in the spectra of the $[(CH_3)_2N]_3C_3^+$ salts is a broad feature near 1560 cm^{-1}. We assign this as the asymmetric C=N stretch.[26] The high frequency of this stretch attests to the importance of the resonance structure Vb.[27]

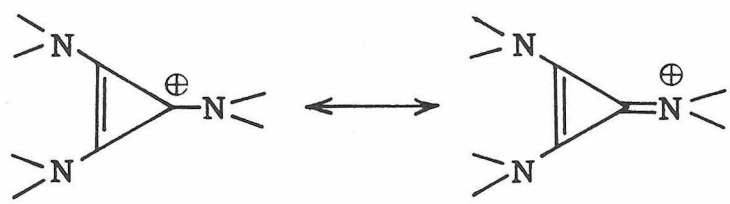

Va Vb

If the cyclopropenium groups interacted strongly with the metals in IIIa-d to form π-complexes, one would expect a new metal-ligand stretching band, ν_{ML}, and a ligand ring-tilting band, δ_t, to appear in the region 300-600 cm^{-1}.[28] No bands which cannot be assigned to the $M_2Cl_6^{2-}$ skeleton are observed in this region.

The UV-VIS spectra reported in Table VI and Figures 6-16 are remarkably similar to the spectra of monomeric MCl_4^{2-} compounds[12, 29] in band positions (see Figure 16). (In Figures 6-16 we abbreviate the cations as follows: N = $\{[(CH_3)_2N]_3C_3^+\}$; P = $[(n\text{-}C_3H_7)_3C_3^+]$.) The solid state (KBr pellet) spectra were generally exceedingly poor, consisting of a series of ill-defined, broad shoulders rising to higher energy. The solution spectra were always obtained with freshly prepared solutions. We found that acetone solutions of IIIa turned from pink to yellow when left overnight at RT. Zeise's Pd dimer, $(C_2H_4)_2Pd_2Cl_4$, has been observed to solvolyze in many mild oxygen-containing solvents (including acetone) but not in dichloroethane.[30] (equation 4)

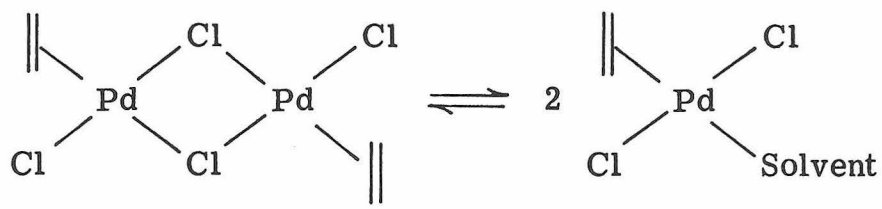

(4)

To see if this was occurring with our compounds, we ran the spectra of both in the solid state and in several solvents. We consider CH_2Cl_2 to be the mildest of our solvents and the peak positions in CH_2Cl_2

Table VI. UV-VIS Spectral Data[a]

Compound	Medium	Spectrum: $\tilde{\nu}_{max}$(kK) (ϵ) ($M^{-1}cm^{-1}$)							
$\{[(CH_3)_2N]_3C_3\}\{BF_4\}$[b]	CH_3OH	43.5 (19,800)							
$[(n\text{-}C_3H_7)_3C_3][ClO_4]$[c]	--	end absorption only							
$\{[(CH_3)_2N]_3C_3\}_2\{Pt_2Cl_6\}$	CH_2Cl_2	~14.5 sh (2)	19.6 (60)	25.1 (161)	31.8 (658)	~38.0 sh (16,000)	43.1 (33,600)		
	$(CH_3)_2CO$	~14.5 sh (2)	19.6 (61)	24.9 (160)					
	CH_3OH	-- --	--	-- --	32.5 --	~39.0 sh (18,000)	43.4 (20,300)		
	KBr pellet 300° K	~32.0 sh	~37.0 sh	~43.0 sh	46.5				
	KBr pellet 80° K	~26.0 sh	~32.0 sh	~37.0 sh	~40.0 sh	~44.8 sh	46.5		
$[(n\text{-}C_3H_7)_3C_3]_2[Pt_2Cl_6]$	CH_3OH	~15.3 sh (4)	20.2 (64)	~25.5 sh (220)	~32.7 (900)	38.6 (3040)	d		
	KBr pellet 300° K	~25.0 sh	~31.0 sh	~37.7 sh	~43.0 sh				
	KBr pellet 80° K	~25.0 sh	~31.0 sh	~38.0 sh	~43.0 sh				
$\{[(CH_3)_2N]_3C_3\}_2\{Pd_2Cl_6\}$	CH_2Cl_2	~16.6 sh (23)	~20.4 sh (376)	22.6 (508)	~29.9 sh (1800)		43.5 (79,100)		
	CH_3OH	~17.6 sh (64)	~20.8 sh (320)	23.1 (544)	30.8 (1690)	~38.0 sh (14,700)	43.3 (57,200)		
	KBr pellet 300° K	~19.2 sh	23.5	~29.4 sh	35.0	42.7			
	KBr pellet 80° K	~19.6 sh	23.8	~30.8 sh	35.0	~40.0 sh	44.6		
$[(n\text{-}C_3H_7)_3C_3]_2[Pd_2Cl_6]$	CH_2Cl_2	~16.1 sh (24)	~20.4 sh (390)	22.8 (512)	~29.4 sh (2200)	~37.7 sh (9500)	43.5 (47,100)		
	$(CH_3)_2CO$	~16.1 sh (25)	~20.0 sh (360)	22.8 (544)	28.7 (3600)				
	CH_3OH	~16.6 sh (21)	~20.4 sh (222)	23.0 (448)	30.7 (1920)	~41.7 sh (15,700)	46,100 (28,400)		
	KBr pellet 300° K	~16.4 sh	~19.5 sh	23.0	~28.6 sh	35.2	~39.1 sh	41.7	
	KBr pellet 80° K	~16.5 sh	~20.0 sh	23.0	~27.8 sh	31.2	35.6	39.2	42.9

a) sh = shoulder

b) Z. Yoshida and Y. Tawara (Ref. 9) report λ_{max} = 233 nm, log ϵ = 4.22 for the perchlorate salt.

c) Ref. 8.

d) No maximum is observed as far as 48,800 cm^{-1} at which point ϵ = 57,800.

correspond fairly well to those of the solids. The CH_2Cl_2 spectra are of much higher quality than the solid state spectra and are probably the most reliable for assigning band energies. As Table VI shows, fresh solutions in acetone and methanol apparently contain intact $M_2Cl_6^{2-}$ anions, albeit the methanol solutions were usually yellower than the pink acetone and CH_2Cl_2 solutions. The much

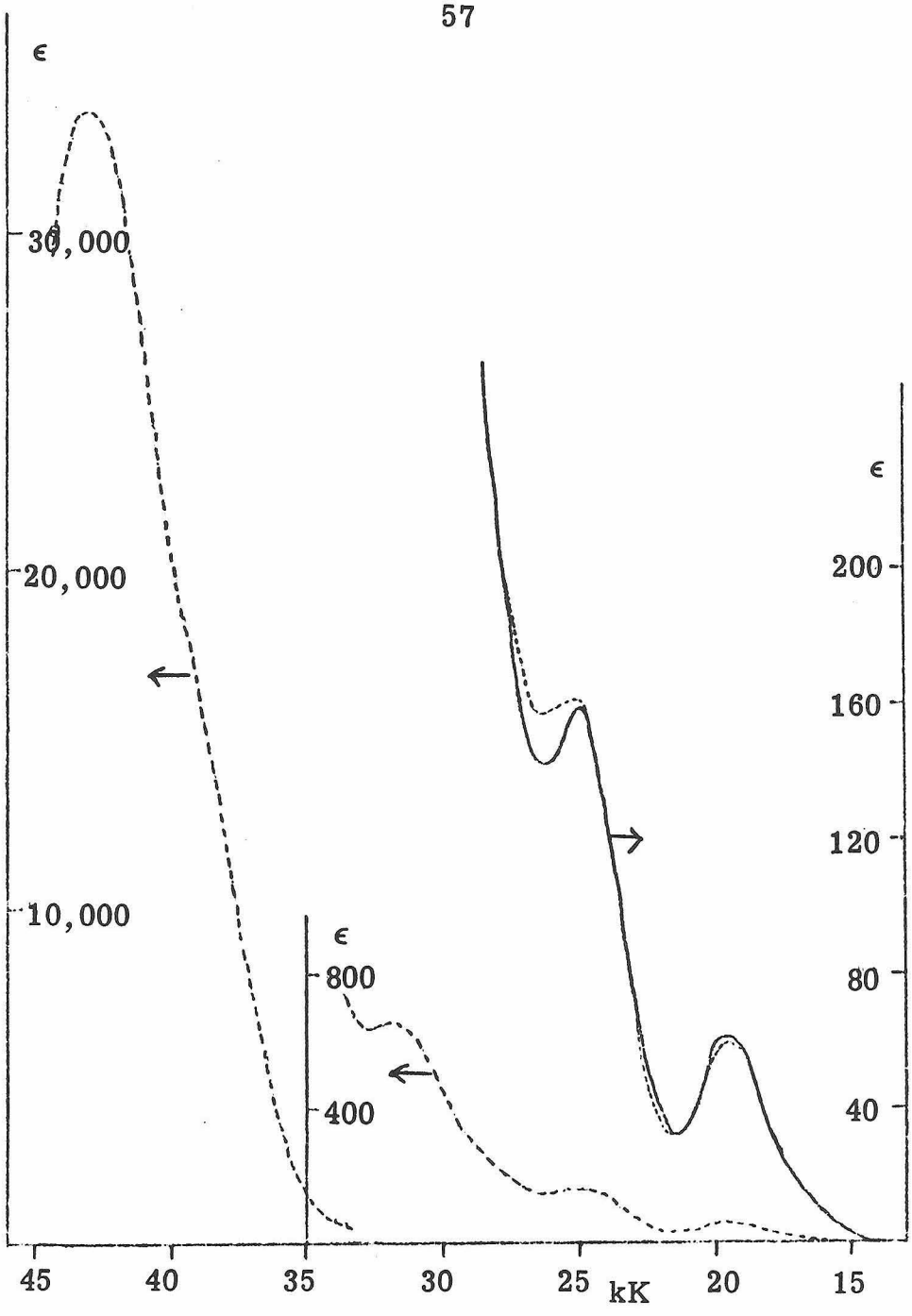

Dotted line: $[N]_2[Pt_2Cl_6]$ in CH_2Cl_2
Solid line: $[N]_2[Pt_2Cl_6]$ in acetone

Figure 6

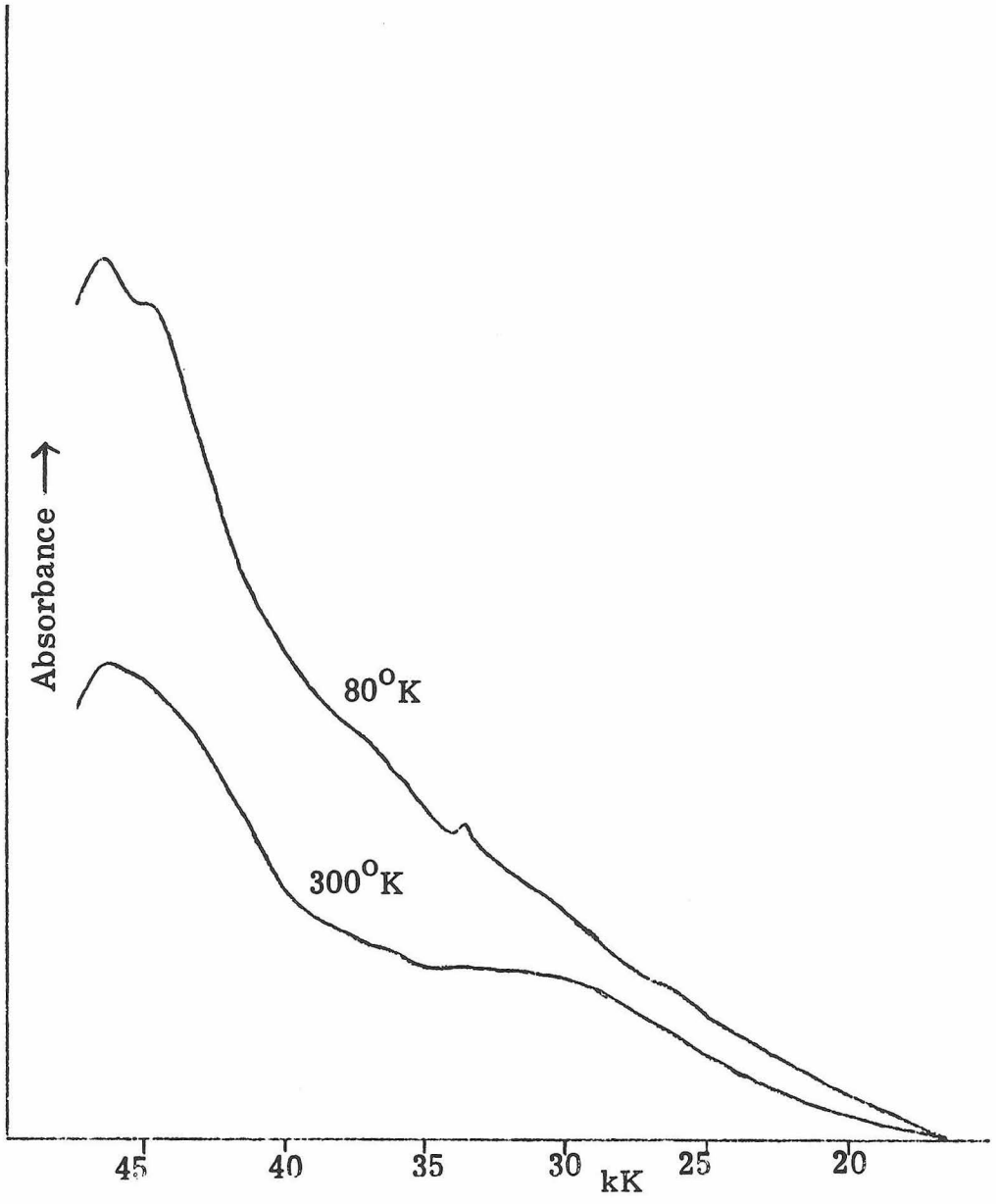

$[N]_2[Pt_2Cl_6]$ in KBr pellet

Figure 7

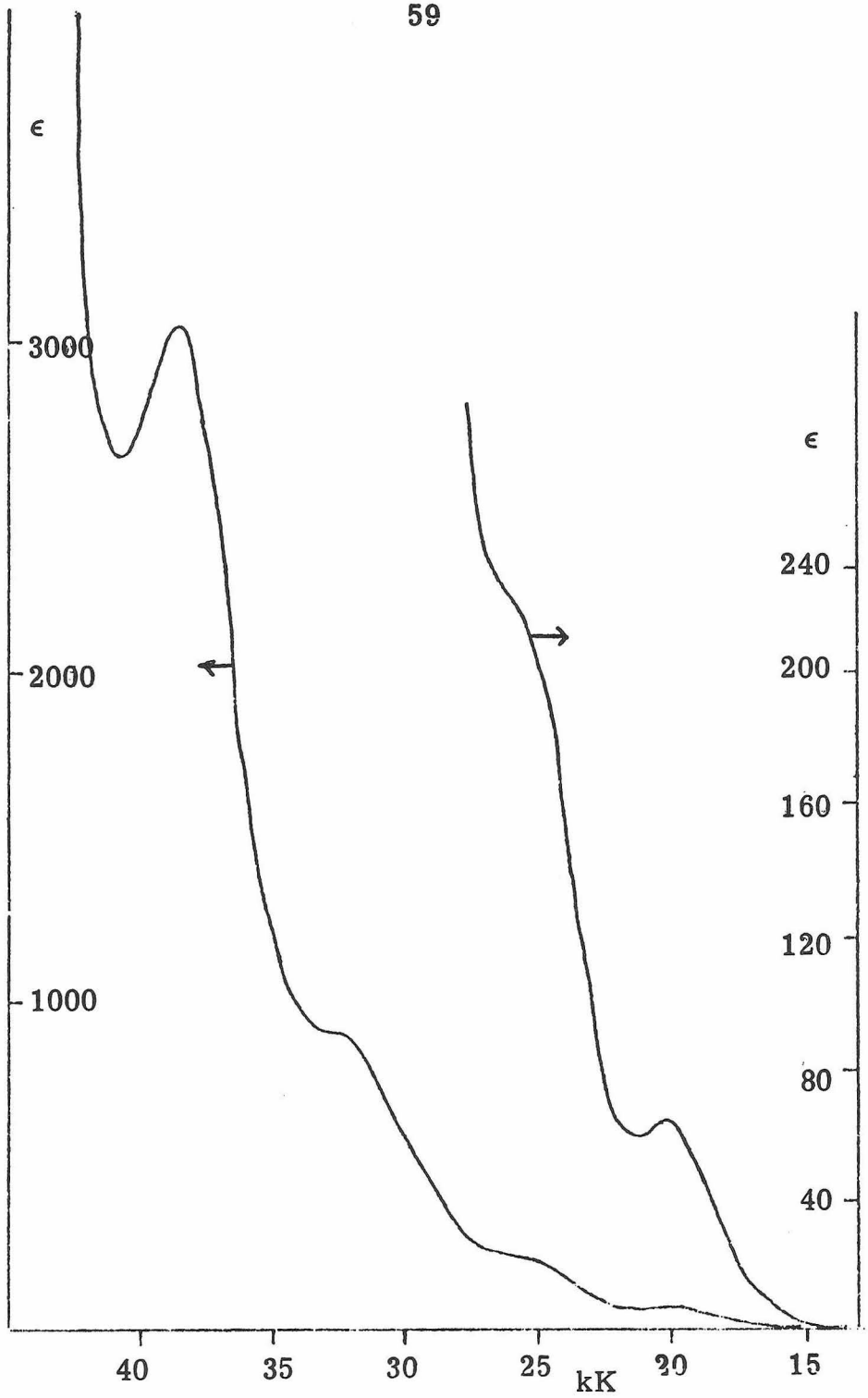

$[P]_2[Pt_2Cl_6]$ in CH_3OH
Figure 8

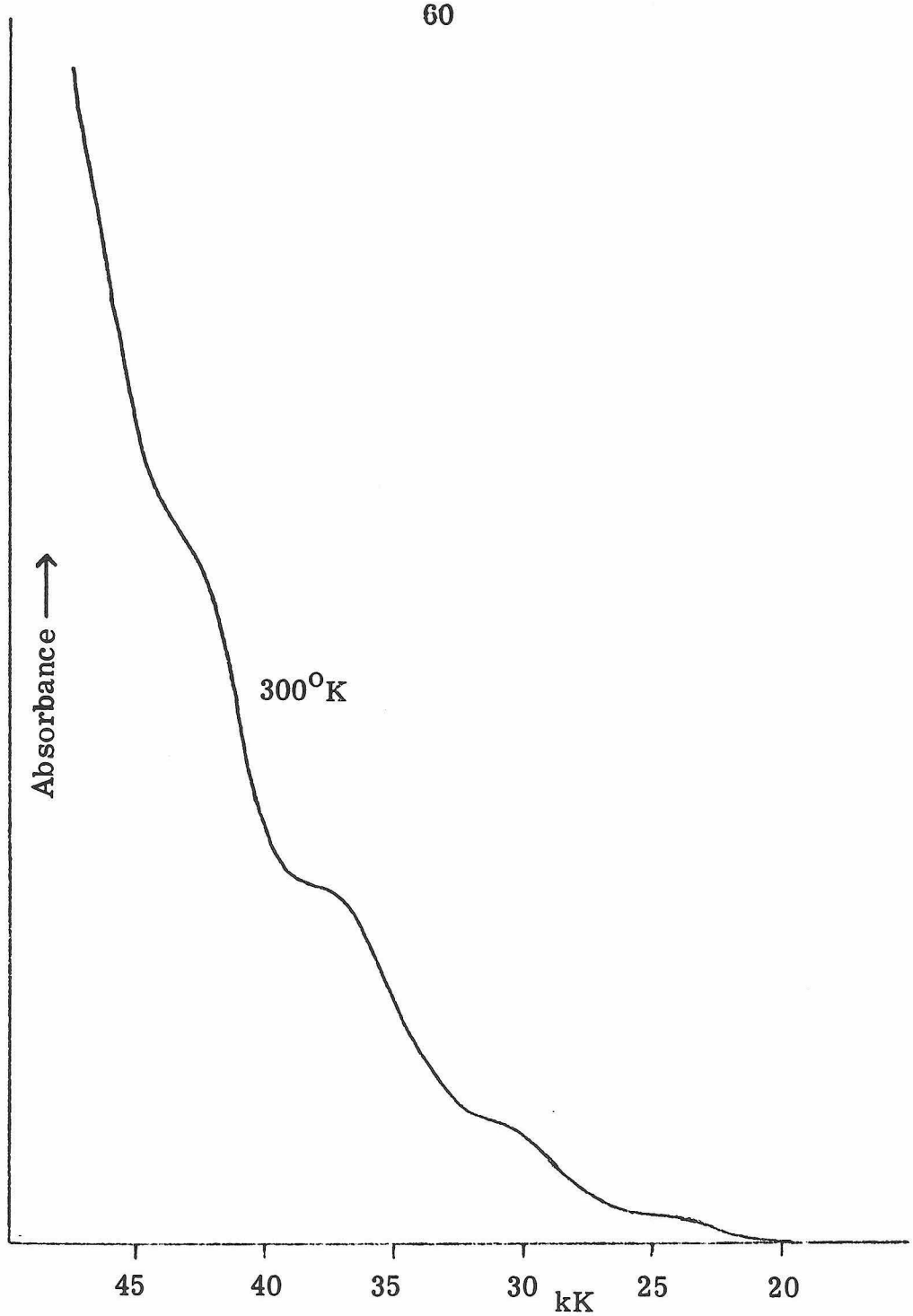

$[P]_2[Pt_2Cl_6]$ in KBr pellet

Figure 9

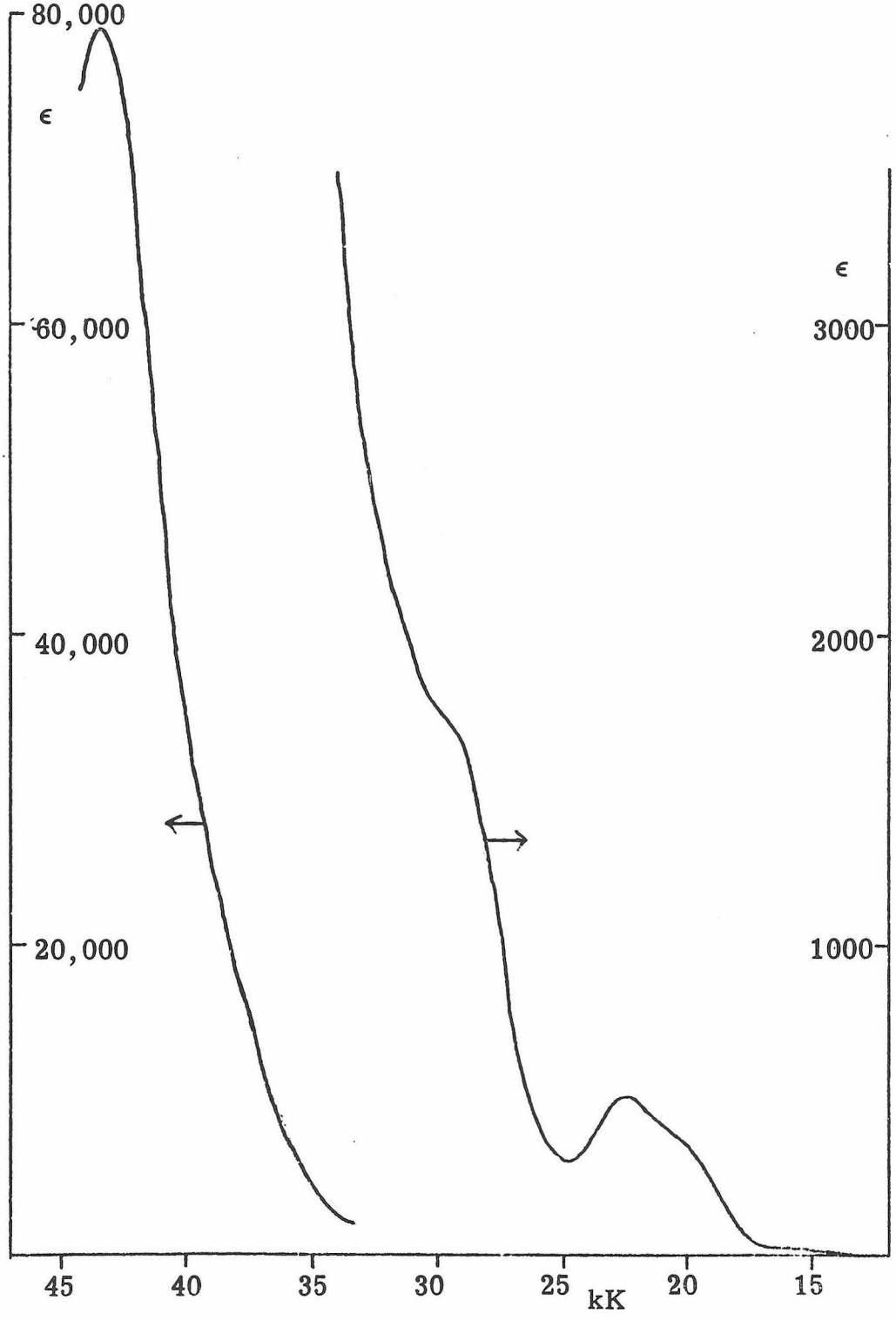

$[N]_2[Pd_2Cl_6]$ in CH_2Cl_2

Figure 10

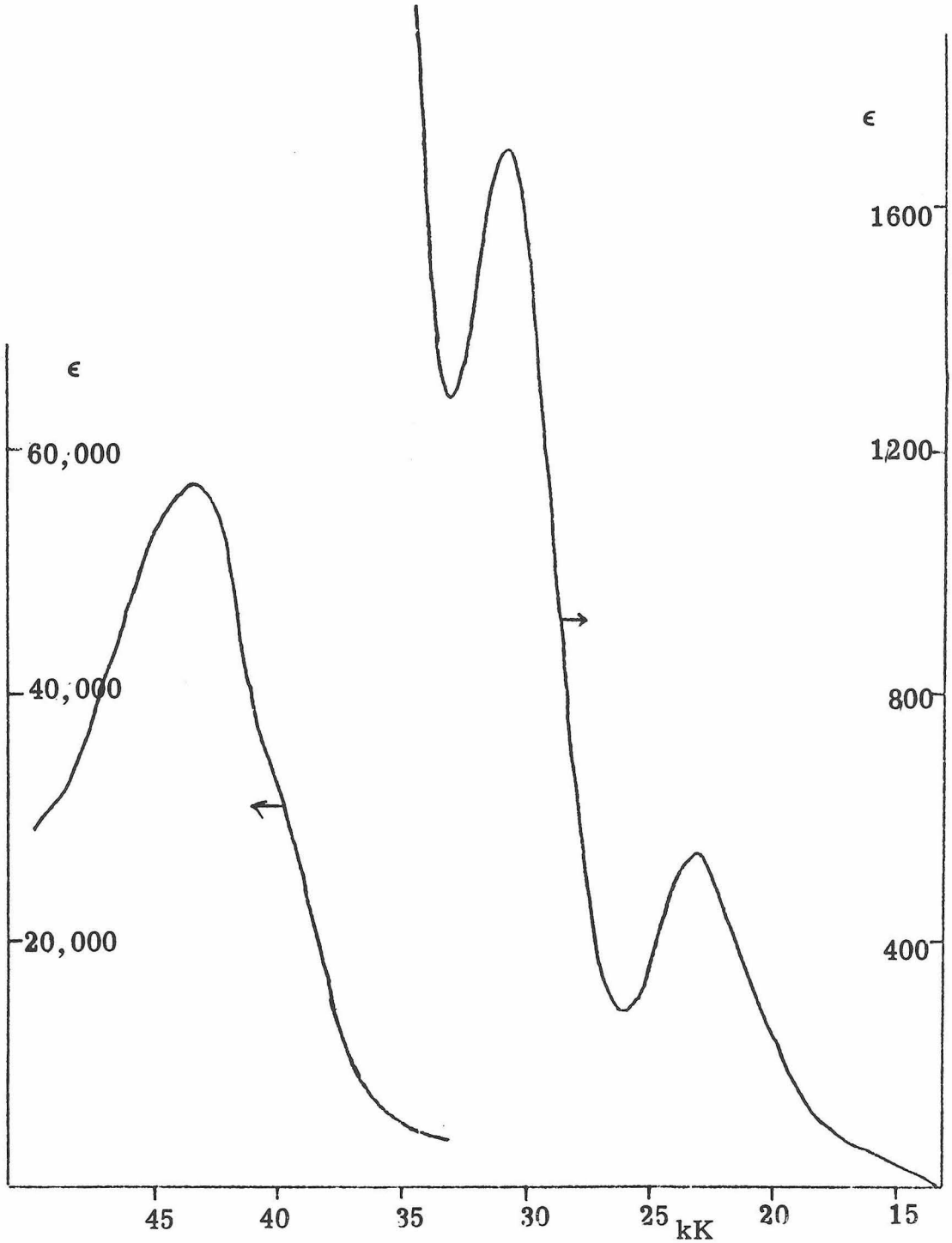

$[N]_2[Pd_2Cl_6]$ in CH_3OH
Figure 11

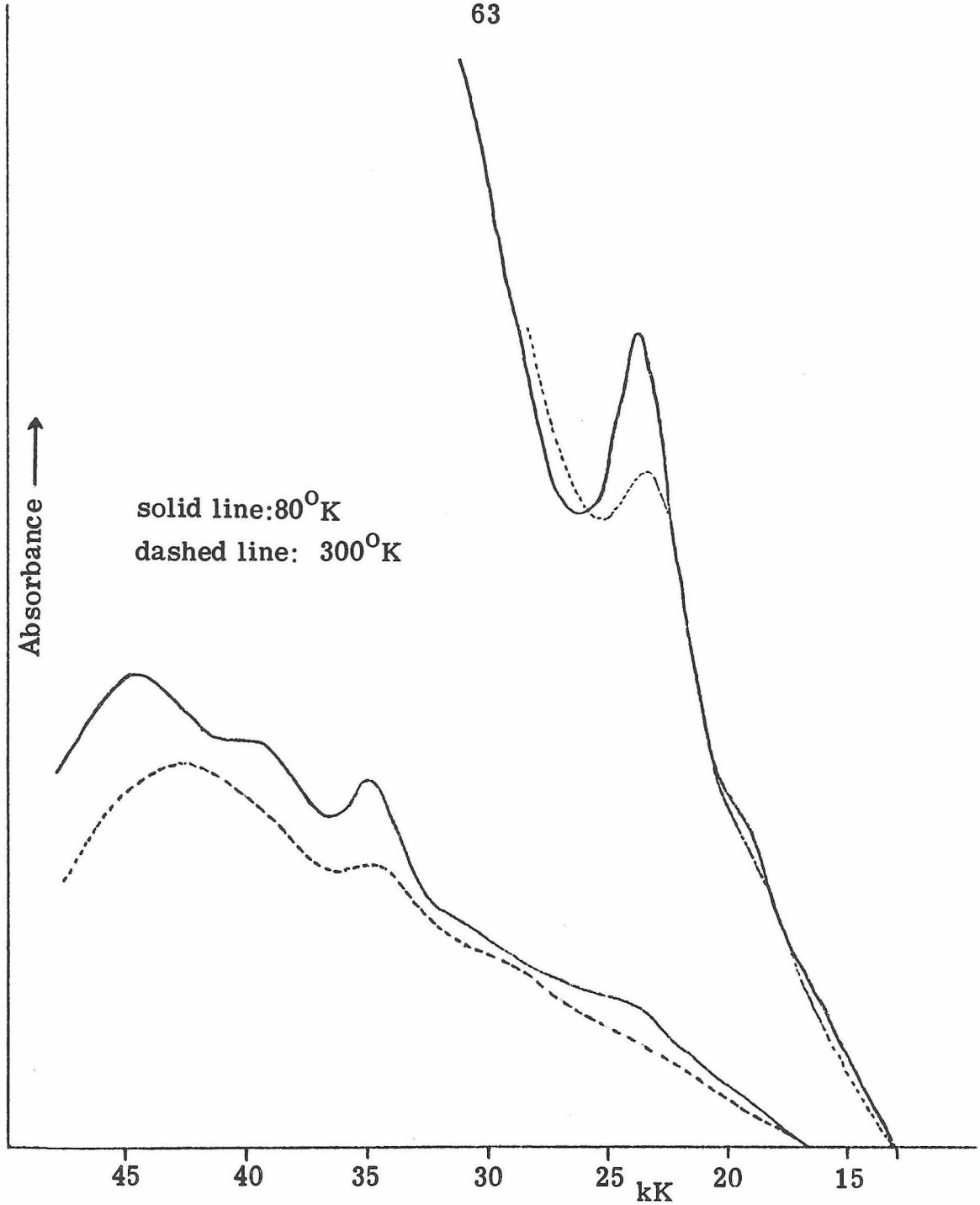

$[N]_2[Pd_2Cl_6]$ in KBr Pellet

Figure 12

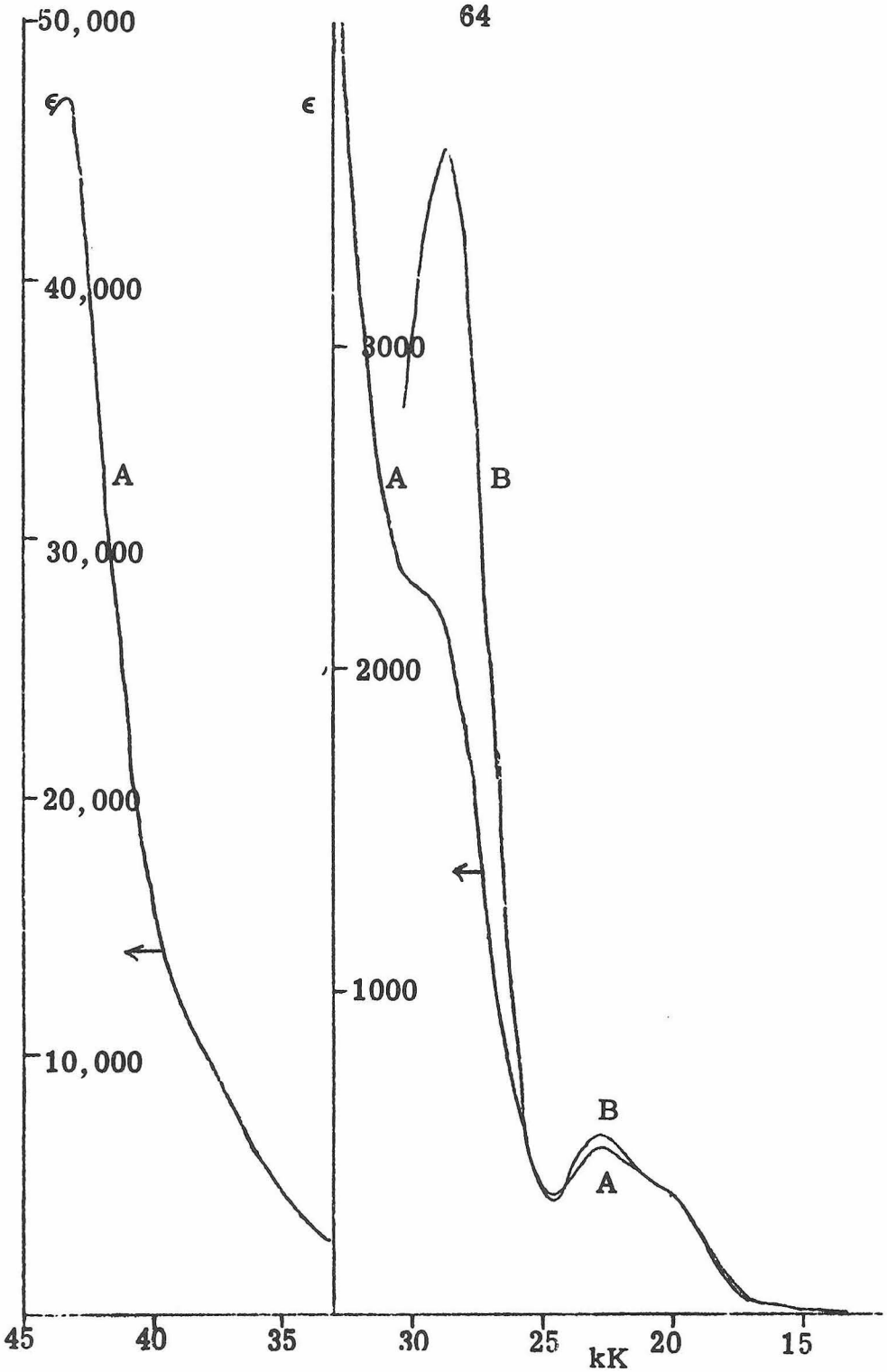

A. $[P]_2[Pd_2Cl_6]$ in CH_2Cl_2

B. $[P]_2[Pd_2Cl_6]$ in acetone

Figure 13

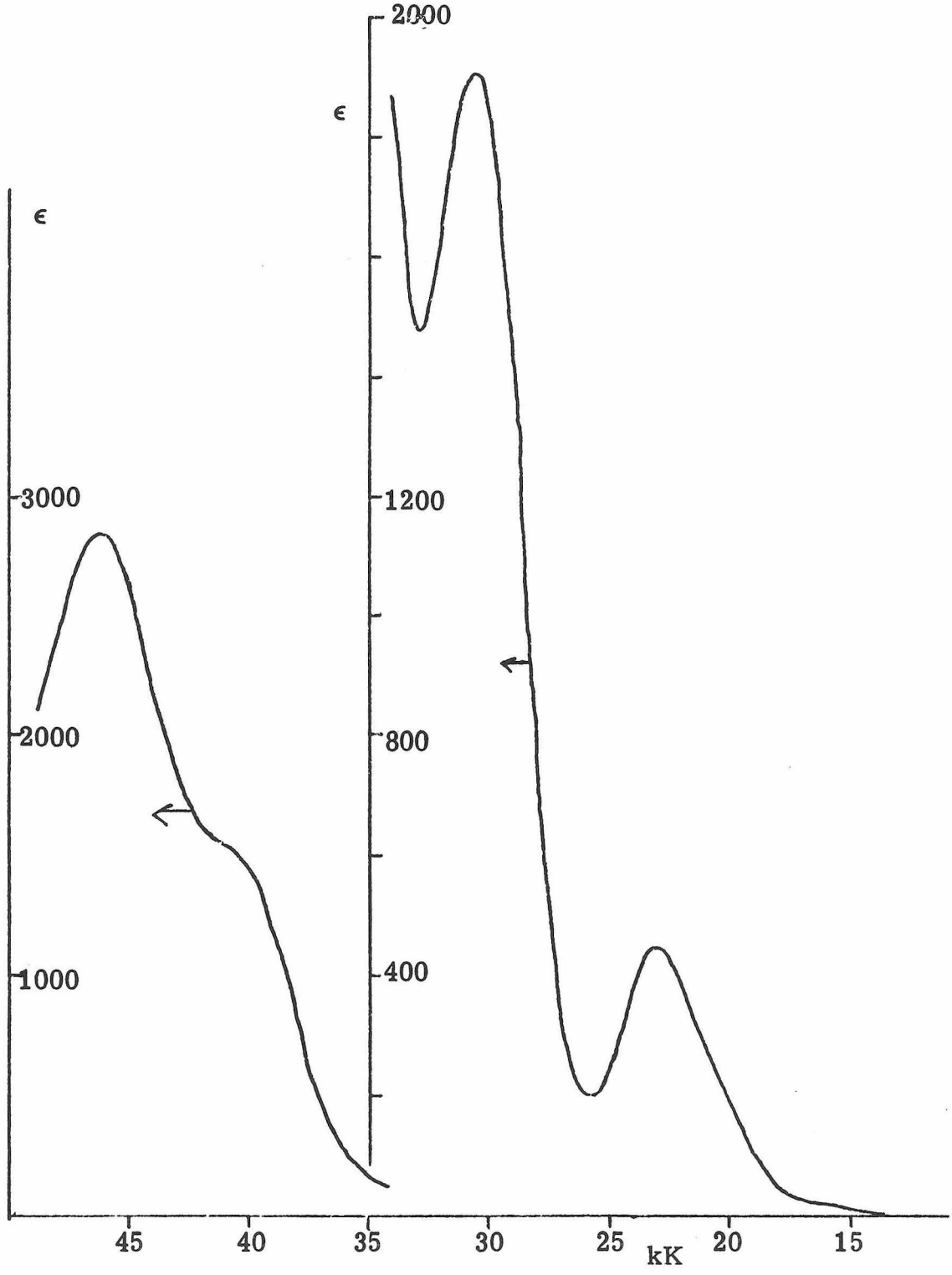

$[P]_2[Pd_2Cl_6]$ in CH_3OH

Figure 14

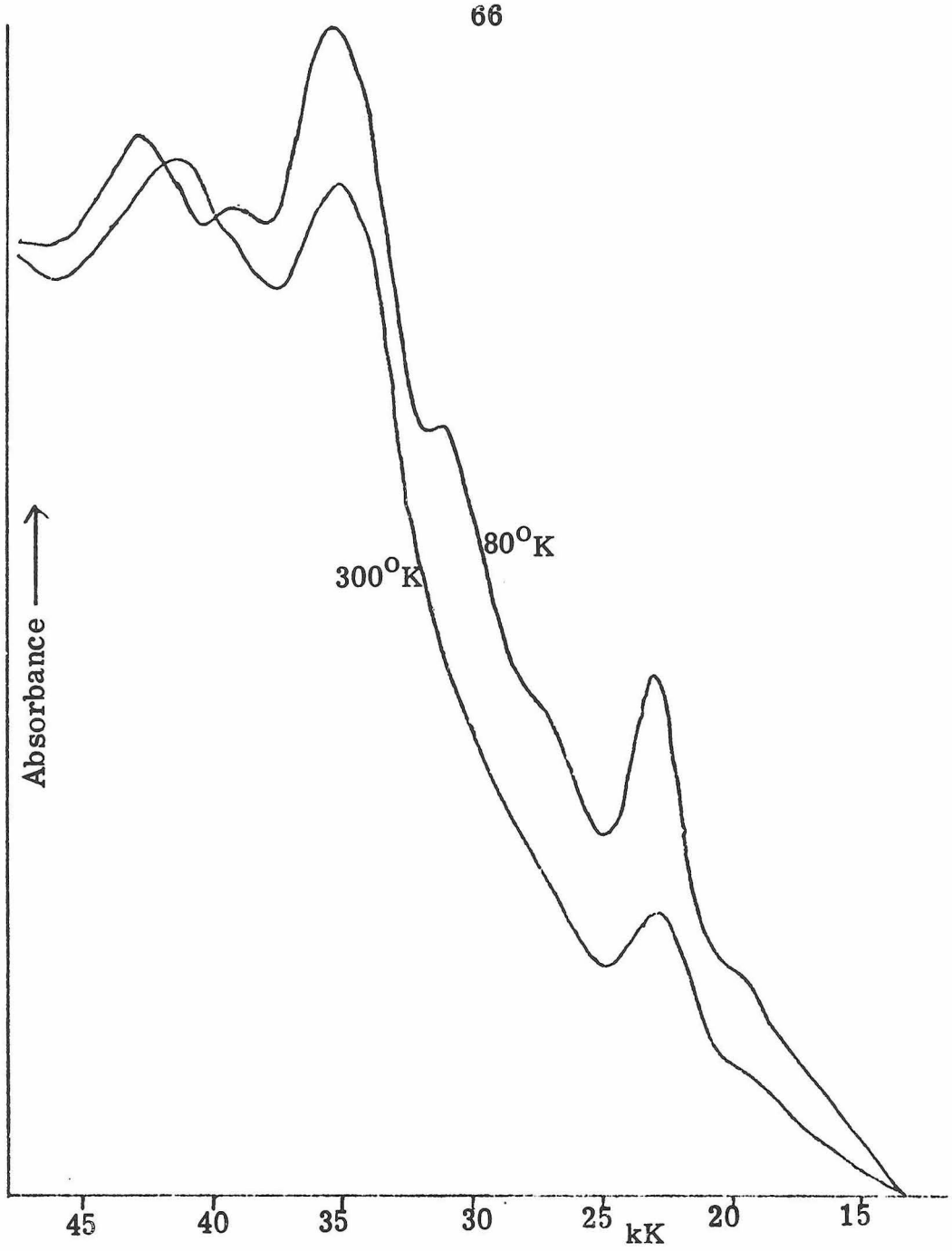

$[P]_2[Pd_2Cl_6]$ in KBr Pellet

Figure 15

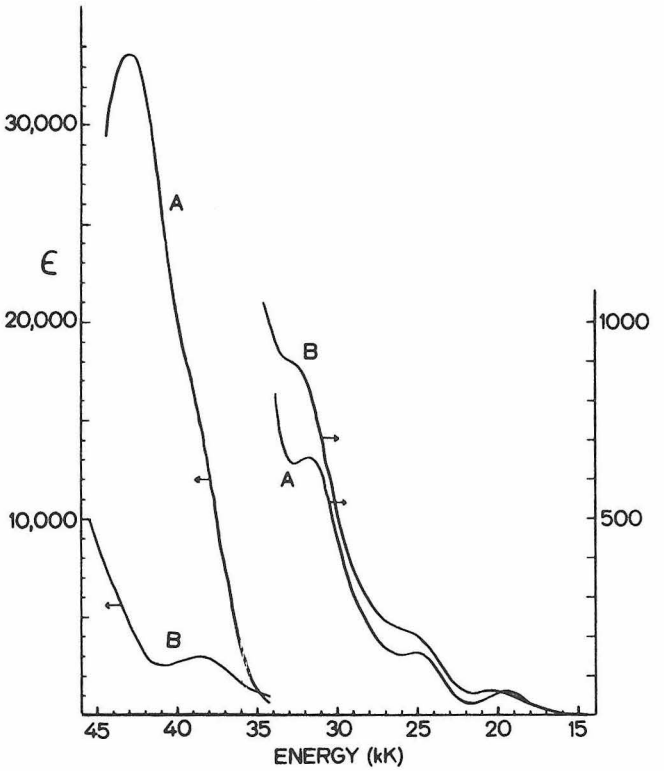

A. $[N]_2[Pt_2Cl_6]$ in CH_2Cl_2
B. $[P]_2[Pt_2Cl_6]$ in CH_3OH

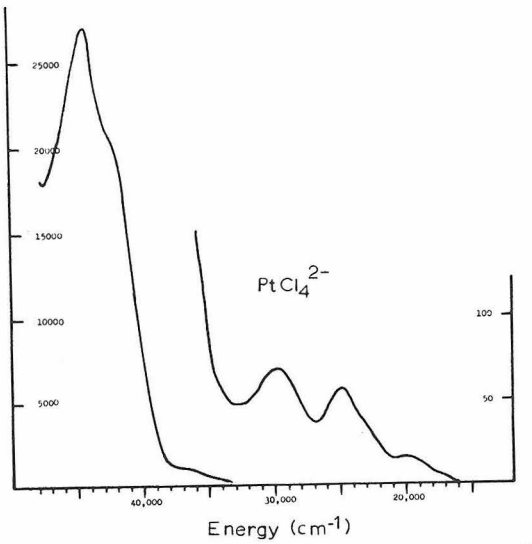

$[(n\text{-}C_4H_9)_4N]_2[PtCl_4]$ in CH_3CN[12]

Figure 16

slower rate of solvolysis of $Pd_2Cl_6^{2-}$ than $(C_2H_4)_2Pd_2Cl_4$ in acetone and methanol is probably due to the greater <u>trans</u> labilizing effect of ethylene in the latter. Attempting to obtain spectra in CH_3CN, we observed slow solvolysis of the $Pt_2Cl_6^{2-}$ anions ($t_{\frac{1}{2}} \approx 20$ min) and "instantaneous" solvolysis of the $Pd_2Cl_6^{2-}$ anions. These solutions were shown to contain monomeric $(CH_3CN)MCl_3^-$ anions.[31]

The single crystal 4°K polarized optical spectrum of $(N)_2(Pt_2Cl_6)$ was heisted from Charlie Cowman and is exhibited in Figure 17. In assigning this spectrum, we chose to ignore previous biases concerning $PtCl_4^{2-}$, especially those of the disreputable Gray <u>et al.</u>[12] Using the coordinate system in Figure 17, the qualitative d-orbital splitting pattern for the dimer in D_{2h} symmetry is as follows:

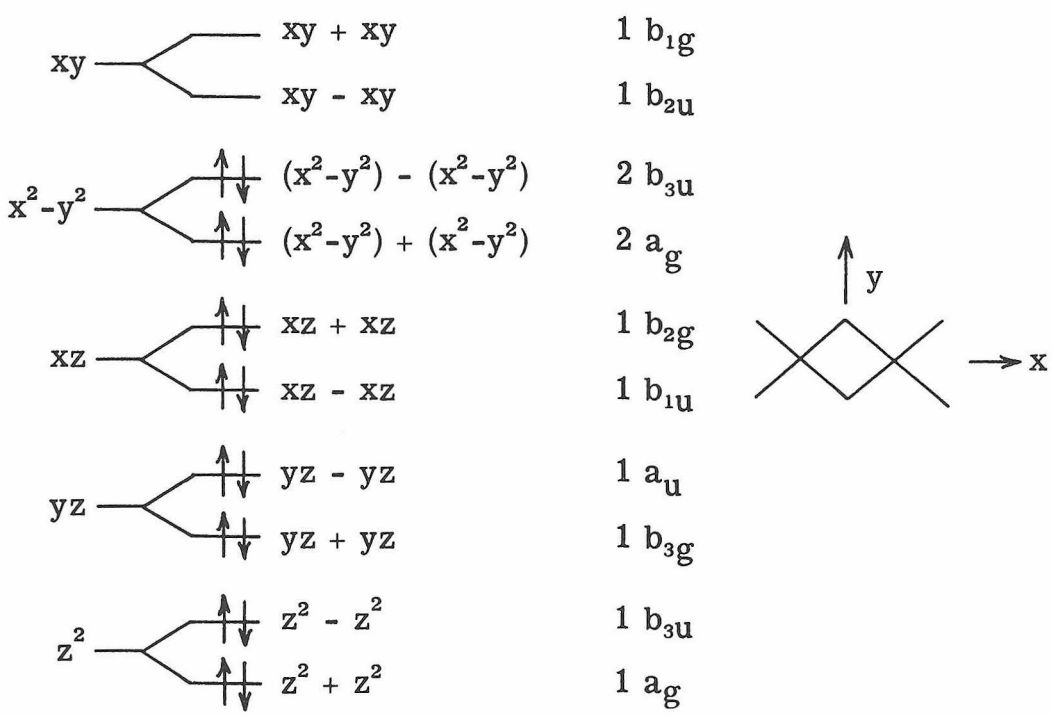

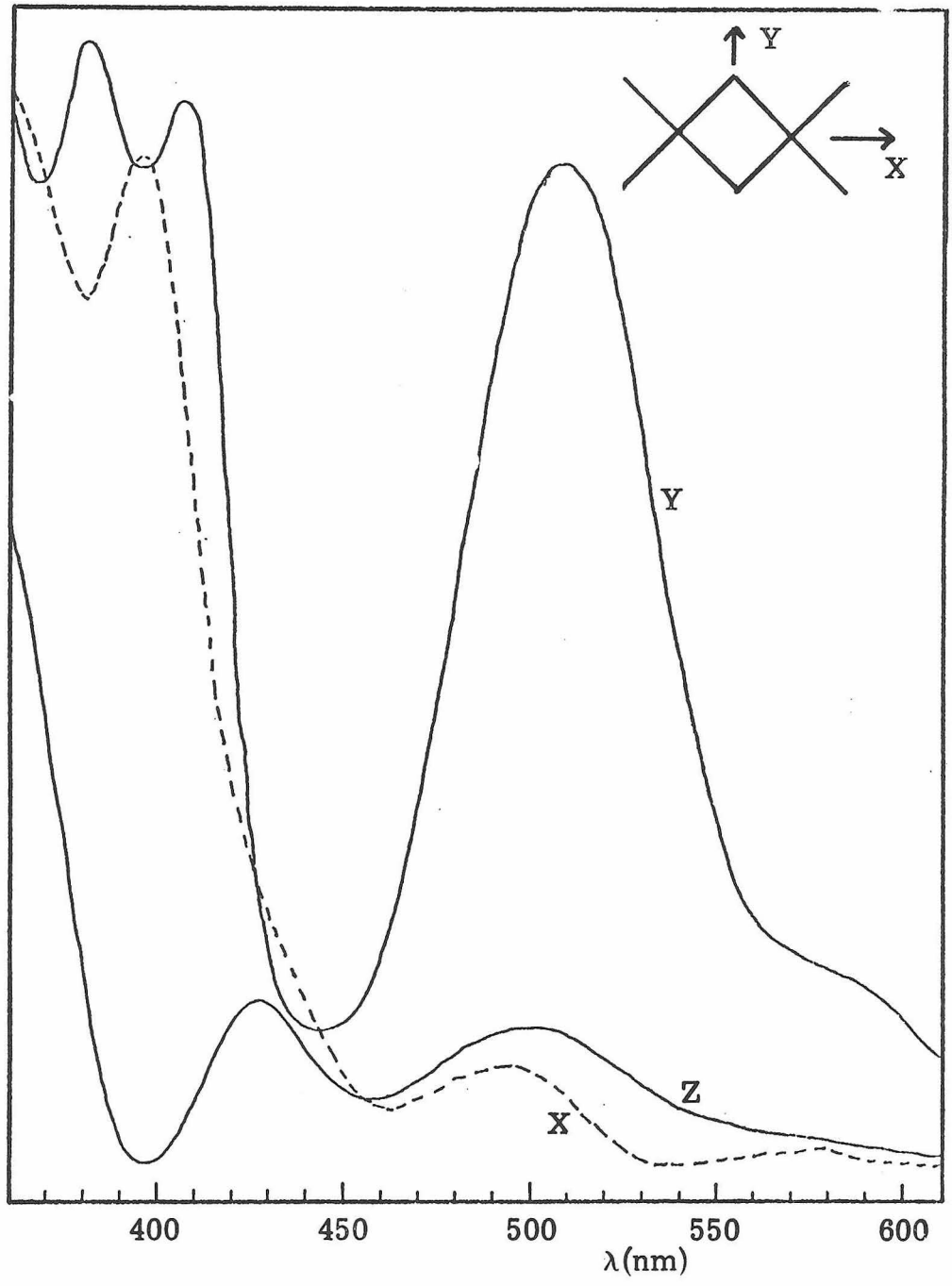

Polarized single crystal optical spectrum of $[N]_2[Pt_2Cl_6]$ resolved into absorption along the three axes defined in the figure above. Courtesy the sweat of C. Cowman.

Figure 17

In using this scheme, we recognize that since the monomer and dimer spectra are so similar in appearance, the splitting between, say, (xz + xz) and (xz - xz) is quite small and all xz and yz levels are nearly degenerate. The various possible transitions are shown in Table VII.

Table VII. Transitions of $Pt_2Cl_6^{2-}$

Designation	Transition	Orbital symmetry of excited state	$^1A_g \rightarrow {}^3X$ polarization	$^1A_g - {}^1X_n$ polarization
α	$2b_{3u} \rightarrow 1b_{1g}$	B_{2u}	–	y
	$2b_{3u} \rightarrow 1b_{2u}$	B_{1g}	x, y	–
	$2a_g \rightarrow 1b_{1g}$	B_{1g}	x, y	–
	$2a_g \rightarrow 1b_{2u}$	B_{2u}	–	y
β	$1b_{2g} \rightarrow 1b_{1g}$	B_{3g}	y, z	–
	$1b_{2g} \rightarrow 1b_{2u}$	A_u	–	–
	$1b_{1u} \rightarrow 1b_{1g}$	A_u	–	–
	$1b_{1u} \rightarrow 1b_{2u}$	B_{3g}	y, z	–
γ	$1a_u \rightarrow 1b_{1g}$	B_{1u}	–	z
	$1a_u \rightarrow 1b_{2u}$	B_{2g}	x, z	–
	$1b_{3g} \rightarrow 1b_{1g}$	B_{2g}	x, z	–
	$1b_{3g} \rightarrow 1b_{2u}$	B_{1u}	–	z
δ	$1b_{3u} \rightarrow 1b_{1g}$	B_{2u}	–	y
	$1b_{3u} \rightarrow 1b_{2u}$	B_{1g}	x, y	–
	$1a_g \rightarrow 1b_{1g}$	B_{1g}	x, y	–
	$1a_g \rightarrow 1b_{2u}$	B_{2u}	–	y

The α transitions are nearly degenerate, as are each set β, γ, and δ. Further, the β and γ transitions are nearly degenerate.

To evaluate singlet-triplet polarizations, we need both spin and orbital symmetries. The transition moment is given by

$$\text{transition moment} \propto \langle \psi_{gs}\, \phi_{gs} | \hat{\mu} | \psi_{es}\, \phi_{es} \rangle$$

where

ψ_{gs} = ground state orbital wavefunction

ϕ_{gs} = ground state spin wavefunction

$\hat{\mu}$ = dipole moment operator

ψ_{es} = excited state orbital wavefunction

ϕ_{es} = excited state spin wavefunction

All $\psi_{gs} = A_g$. All $\phi_{gs} = a_g$. $\hat{\mu} = \begin{pmatrix} b_{1u} - z \\ b_{2u} - y \\ b_{3u} - x \end{pmatrix}$. ψ_{es} is given in Table VII. ϕ_{es}, the triplet spin function, transforms as (b_{1u}, b_{2u}, b_{3u}) in D_{2h} symmetry. For singlet-singlet transitions, $\phi_{es} = a_g$. Evaluating the transition moment integrals, we obtain the results in Table VII.

The spectrum of $PtCl_4^{2-}$ is reproduced from reference 32 in Figure 18. A similar spectrum can be found in reference 33. The energy level scheme and transitions in D_{4h} symmetry will be as follows:

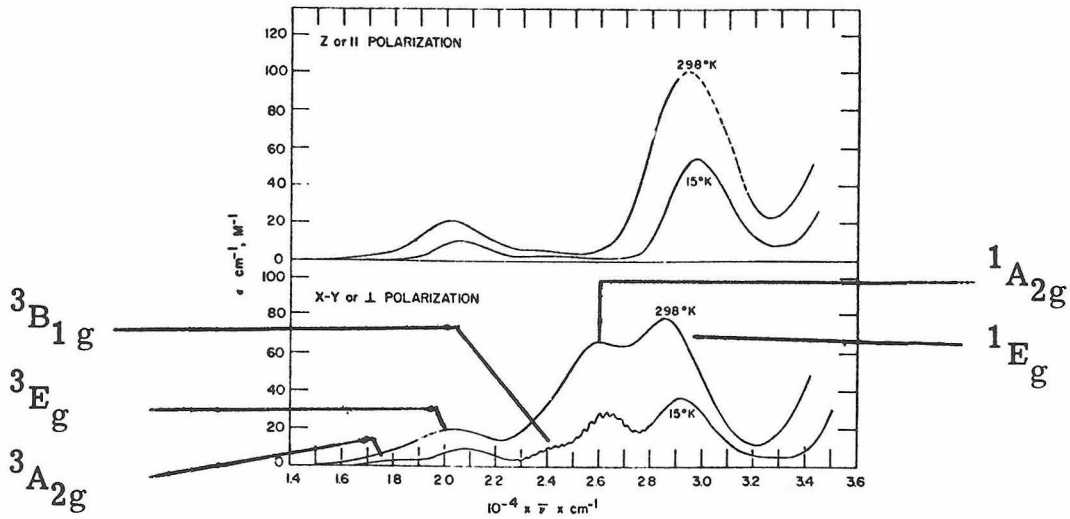

Absorption spectra of a K_2PtCl_4 crystal with polarized light; crystal thickness 46.5 μ.

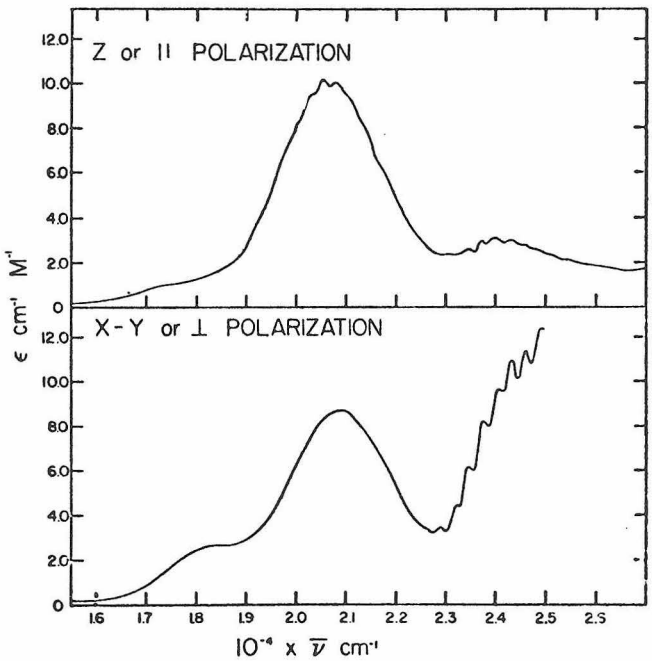

Absorption spectra of a K_2PtCl_4 crystal with polarized light at 15°K.; crystal thickness 113 μ.

Figure 18. (From Reference 32.)

(With Permission)

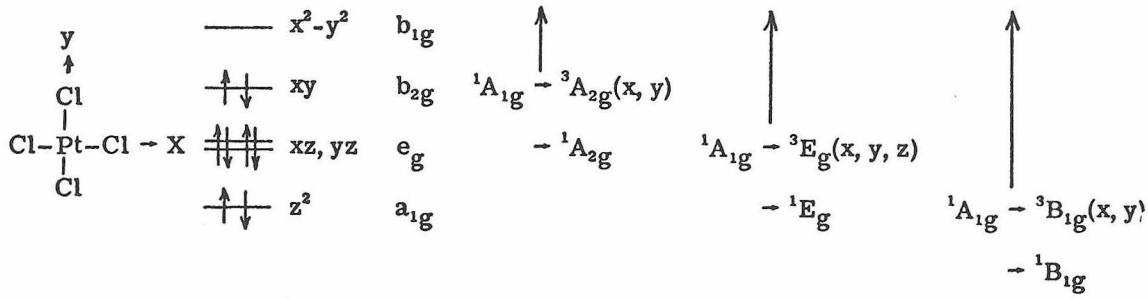

In this diagram, polarizations of the singlet-triplet transitions are shown in parentheses after each transition. Polarization of the singlet-singlet transitions can only come from a vibronic analysis. The polarizations of the three singlet-triplet transitions make the assignment of the first three bands trivial. Our assignments are given in Figure 18. The singlet-singlet assignments are generally agreed upon. The ^3E_g and $^3A_{2g}$ assignments are reversed from that of Gray et al.,[12] but rightfully so.[6, 33]

The dimer spectrum is so similar to the monomer spectrum, both in the solid state and in solution, that assignments should conform very closely to monomer assignments. Our interpretation is given in Figure 19. The lowest energy transition is y polarized, in reasonable agreement with the x, y polarization expected for $^1A_g \rightarrow {}^3B_{1g}$. The next band is the superposition of all the triplet β and γ transitions defined above. This corresponds to the $^1A_g \rightarrow {}^3B_{2g}$ and $^1A_g \rightarrow {}^3B_{3g}$ transitions. In the monomer, this is $^1A_{1g} \rightarrow {}^3E_g$ and Figure 18 clearly shows the expected x, y, z polarization .

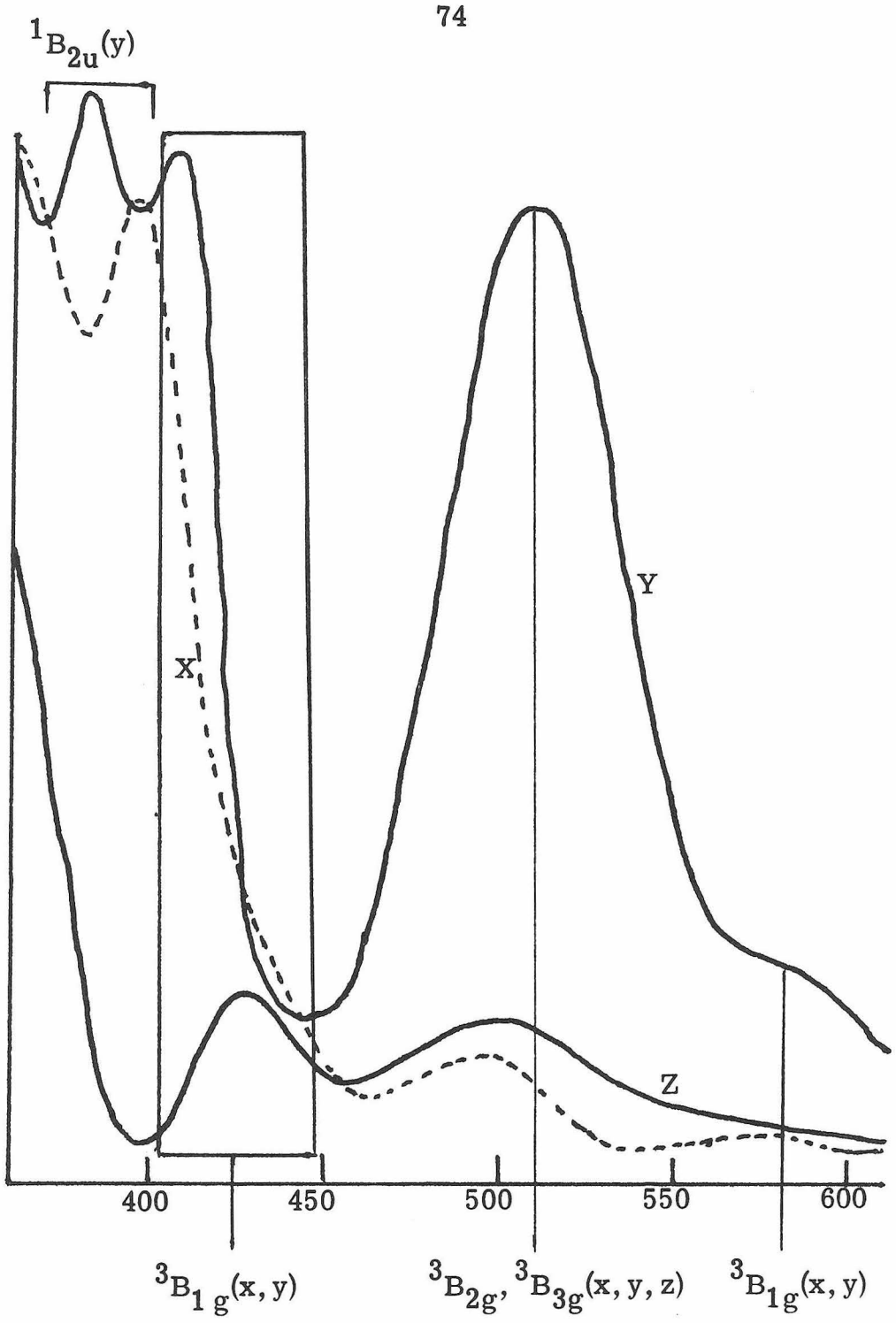

$Pt_2Cl_6^{2-}$ Assignments

Figure 19

The overwhelming y polarization in the dimer spectrum cannot be explained without invoking vibronic interactions, the workings of Zeus or other obfuscations. Common sense says this has to be the same kind of transition seen in the monomer. We assign the set of peaks enclosed in the box in Figure 19 to the $^1A_g \rightarrow {}^3B_{1g}$ transition. This is x, y polarized. We see a strong y band and a shoulder on the x curve at about 430 nm. Both are more intense than the z transition at about 425 nm. The first allowed singlet, $^1A_g \rightarrow {}^1B_{2u}$, is y polarized. The band in the x spectrum at slightly lower energy is either the forbidden x component of this transition or else may be the x component of the $^1A_g \rightarrow {}^3B_{1g}$ transition. In the second case, the 430 nm shoulder would not be real. We feel that this assignment is plausible and almost reasonable. In view of the number of assignments we rejected before adopting this one, it is even more reasonable.

For comparison, the single crystal spectrum of $Pt_2Br_6^{2-}$ is shown in Figure 20.[6] Our assignment is shown in the figure. We feel that this spectrum, albeit poorly resolved, is in excellent qualitative agreement with our spectrum of $Pt_2Cl_6^{2-}$ with respect to relative band positions and intensities. Since this $Pt_2Br_6^{2-}$ spectrum is only resolved into || and ⊥ polarizations, it is possible (likely, we feel) that the second singlet-triplet transition at ~18,000 cm^{-1} is strongly y polarized, as in our spectrum.

Based on this analysis, our assignment of the $M_2Cl_6^{2-}$ solution spectra are given in Table VIII.

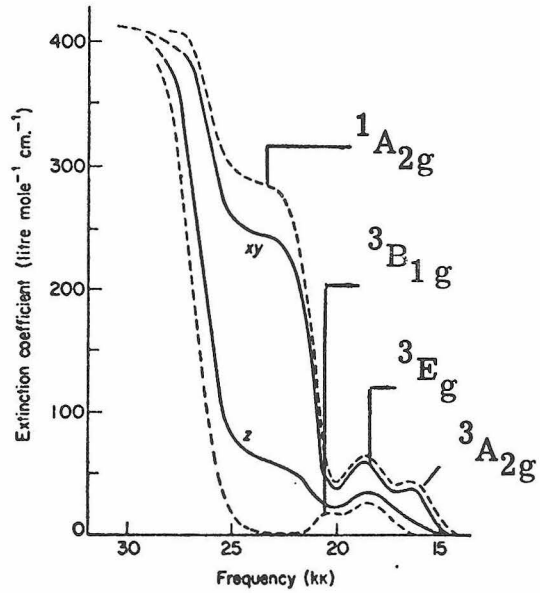

The polarised crystal spectrum of $[N(C_2H_5)_4]_2Pt_2Br_6$. The *xy*-spectrum is measured with the electric vector of the incident light along the crystal extinction direction which lies close to the molecular plane, the *z*-spectrum along the other extinction direction. The dotted lines represent absorption spectra calculated for the electric vector incident parallel and perpendicular to the crystallographic mean-square planes of the molecules

Figure 20. (From Reference 6.)

(With Permission)

Table VIII. Assignments of Solution Spectra

Compound	Solvent	Transitions $^1A_g \rightarrow$ $^3B_{1g}$	$^3B_{2g}$, $^3B_{3g}$	$^1B_{2u}$	$^1B_{1u}$	$^1B_{2u}$ (or charge transfer)	Cation $\pi \rightarrow \pi^*$
$\{[(CH_3)_2N]_3C_3\}_2\{Pt_2Cl_6\}$	CH_2Cl_2	~14.5 sh (2)	19.6 (60)	25.1 (161)	31.8 (658)	~38.0 sh (16,000)	43.1 (33,600)
$[(n-C_3H_7)_3C_3]_2[Pt_2Cl_6]$	CH_3OH	~15.3 sh (4)	20.2 (64)	~25.5 sh (220)	~32.7 (900)	38.6 (3,040)	–
$\{[(CH_3)_2N]_3C_3\}_2\{Pd_2Cl_6\}$	CH_2Cl_2	–	~16.6 sh (23)	~20.4 sh (376)	22.6 (508)	~29.9 sh (1,800)	43.5 (79,100)
$[(n-C_3H_7)_3C_3]_2[Pd_2Cl_6]$	CH_2Cl_2	–	~16.1 sh (24)	~20.4 sh (390)	22.8 (512)	~29.4 sh (2,200)	–

The crystal and molecular structure of IIIa was determined by Jack Thibeault and Ron Ziolo. For completeness, we summarize their findings here. The crystal contains one $Pt_2Cl_6^{2-}$ anion and two crystallographically independent $[(CH_3)_2N]_3C_3^+$ cations. The anion structure is shown in Chapter Four, Figure 1. One cation is shown in Figure 21 of this chapter. In Figure 22 we display a stereo view of the unit cell. Interatomic distances and angles are given in Table IX. Numbering of the atoms is given in Figure 21 and Chapter Four, Figure 1. Deviations of the anion from its least-squares plane are given in Table X. Full details can be found in the thesis of Jack Thibeault.

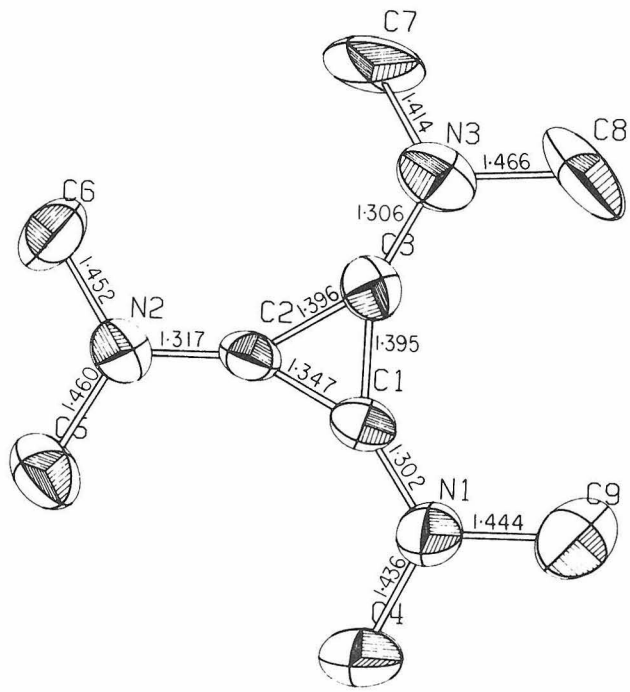

The Structure of Cation I.
Figure 21

Table IX.

Interatomic Distances (Å) and Angles (Deg) [a]

Atoms	Angles	Atoms	Angles
Anion			
Pt1-Cℓ1-Pt2	94.4 (1)	N1-C1-C2	152.4 (12)
Pt1-Cℓ2-Pt2	94.5 (1)	C1-C2-N2	150.9 (10)
Cℓ1-Pt2-Cℓ2	85.2 (1)	N2-C2-C3	148.0 (8)
Cℓ1-Pt1-Cℓ2	84.9 (1)	C2-C3-N3	149.5 (8)
Cℓ5-Pt2-Cℓ6	92.2 (1)	N3-C3-C1	152.6 (11)
Cℓ5-Pt2-Cℓ1	91.1 (1)	C3-C1-N1	146.4 (12)
Cℓ6-Pt2-Cℓ1	91.4 (1)	C1-N1-C9	122.1 (10)
Cℓ1-Pt1-Cℓ3	91.0 (1)	C9-N1-C4	116.6 (8)
Cℓ2-Pt1-Cℓ4	91.4 (1)	C1-N1-C4	120.0 (10)
Cℓ3-Pt1-Cℓ4	92.6 (1)	C2-N2-C5	119.2 (8)
		C5-N2-C6	117.2 (10)
		C2-N2-C6	123.3 (10)
Cation I			
C3-C1-C2	61.1 (7)	C3-N3-C7	121.3 (11)
C1-C2-C3	61.1 (8)	C7-N3-C8	115.4 (11)
C2-C3-C1	57.7 (7)	C3-N3-C8	121.2 (8)

Cation II [b]

Atoms 1-2-3	Angles	Atoms	Distances
C12-C10-C11	58.3 (8)	1-2	1.376 (17)
C10-C11-C12	60.8 (8)	1-2	1.378 (18)
C11-C12-C10	60.9 (8)	1-2	1.343 (15)
N5-C10-C11	150.4 (18)	1-2	1.327 (15)
C10-C11-N5	149.0 (14)		
N5-C11-C12	150.1 (17)	1-2	1.317 (18)
C11-C12-N6	151.3 (19)		
N6-C12-C10	147.8 (8)	1-2	1.324 (16)

Table IX (Continued)

Atoms 1-2-3	Angles	Atoms	Distances
C12-C10-N4	150.8 (9)		
C10-N4-C13	119.3 (12)	2-3	1.446 (14)
C13-N4-C14	118.1 (10)	2-3	1.436 (20)
C10-N4-C14	120.2 (8)		
C11-N5-C15	121.7 (11)	2-3	1.478 (19)
C15-N5-C16	116.8 (9)	2-3	1.465 (17)
C11-N5-C16	119.3 (11)		
C12-N6-C17	119.3 (8)	2-3	1.463 (17)
C17-N6-C18	116.7 (11)	2-3	1.442 (12)
C12-N6-C18	121.2 (10)		

b) Anion and Cation I distances are given in the Figures.

b) The atom numbering scheme for cation II, in the fragment C_{ring}-N(CH_3, CH_3), is 10-4(13, 14), 11-5(15, 16) and 12-6(17, 18).

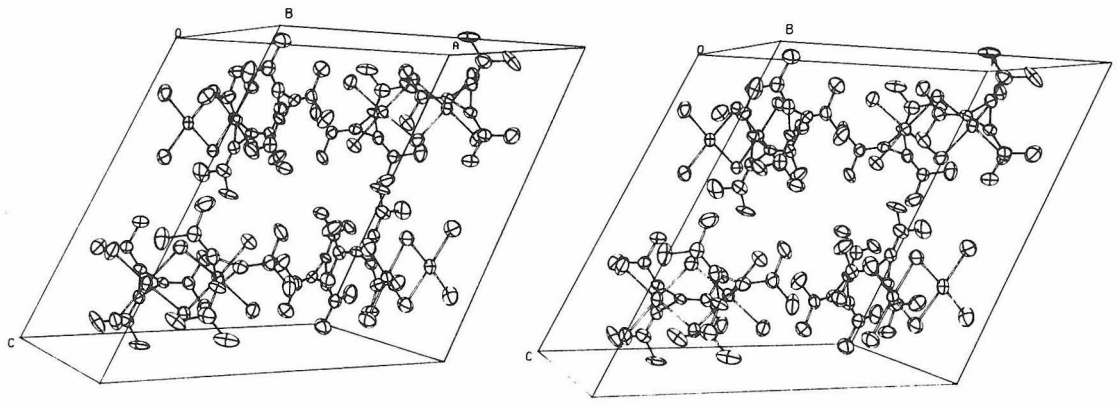

Stereo View of the Unit Cell of $(N)_2(Pt_2Cl_6)$.
Figure 22.

Table X. Least-Squares Planes in $\{[(CH_3)_2N]_3C_3\}_2\{Pt_2Cl_6\}$[a]

Anion		Cation I		Cation II	
Atom	Dev, Å	Atom	Dev, Å	Atom	Dev, Å
Pt1	+0.041	C1	-0.015	C10	+0.030
Pt2	+0.022	C2	+0.000	C11	-0.005
Cℓ1	+0.179	C3	-0.020	C12	+0.016
Cℓ2	+0.182	N1	+0.013	N4	-0.020
Cℓ3	-0.127	N2	+0.007	N5	-0.007
Cℓ4	-0.090	N3	+0.015	N6	-0.015
Cℓ5	-0.123				
Cℓ6	-0.084				

Planes

Anion: $0.339\hat{X} + 0.940\hat{Y} + 0.047\hat{Z} - 0.883 = 0$

Cation I: $0.312\hat{X} + 0.948\hat{Y} + 0.003\hat{Z} - 4.558 = 0$

Cation II: $-0.367\hat{X} + 0.927\hat{Y} - 0.079\hat{Z} + 2.754 = 0$

a) Planes are defined in the real monoclinic coordinates $\hat{X}$, $\hat{Y}$, $\hat{Z}$.

References

1. Relatively few π-cyclopropenium complexes have been reported. For a complete list of such complexes reported as of this writing, see:

   a) E. W. Gowling and S. F. A. Kettle, Inorg. Chem., 3, 604 (1964);

   b) R. M. Tuggle and D. L. Weaver, Ibid., 10, 1504 (1971);

   c) Ibid., 10, 2599 (1971);

   d) D. L. Weaver and R. M. Tuggle, J. Amer. Chem. Soc., 91, 6506 (1969);

   e) R. M. Rausch, R. M. Tuggle, and D. L. Weaver, Ibid., 92, 4981 (1970);

   f) W. K. Olander and T. L. Brown, Ibid., 94, 2139 (1972);

   g) R. G. Hayter, J. Organometal. Chem., 13, P1 (1968);

   h) P. S. Welcker and L. J. Todd, Inorg. Chem., 9, 286 (1970);

   i) I. I. Moiseev, M. N. Vargaftik, and Y. A. Syrkin, Izv. Akad. Nauk SSSR, Ser. Khim., 775 (1964).

2. A. Gutbier and C. Fellner, Z. Anorg. Chem., 95, 169 (1916).

3. C. M. Harris, S. E. Livingstone, and N. C. Stephenson, J. Chem. Soc., 3697 (1958).

4. N. C. Stephenson, Acta Cryst., 17, 587 (1964).

5. D. M. Adams, P. J. Chandler, and R. G. Churchill, J. Chem. Soc. A, 1272 (1967).

6. P. Day, M. J. Smith, and R. J. P. Williams, Ibid., 668 (1968).

7. The crystal structure was studied by J. Thibeault and R. Ziolo. Single-crystal optical spectra were obtained by C. Cowman. Both of these studies consumed enormous energy and required fierce devotion. Thanks, guys.

8. R. Breslow, H. Höver, and H. W. Chang, J. Amer. Chem. Soc., 84, 3168 (1962).

9. Z. Yoshida and Y. Tawara, Ibid., 93, 2573 (1971).

10. J. E. Teggins, D. R. Gano, M. A. Tucker, and D. S. Martin, Jr., Inorg. Chem., 6, 69 (1967).

11. P. M. Henry and O. W. Marks, Ibid., 10, 373 (1971).

12. W. R. Mason III and H. B. Gray, J. Amer. Chem. Soc., 90, 5721 (1968).

13. R. G. Pearson and M. M. Muir, Ibid., 88, 2163 (1966).

14. If a π-cyclopropenyl complex were formed, we expect to observe $^{195}Pt-^{1}H$ coupling to the α-CH_2 protons of IIIb. The Pt would be coupled to the H through one pi bond and two sigma bonds. This is the same case found in the propene complex i and the acetylene complex ii for which $^{3}J_{^{195}Pt-C-C-^{1}H}$ = 40.5 Hz and 29.0 Hz, respectively. (P. D. Kaplan and M. Orchin, Inorg. Chem., 6, 1096 (1967).)

J = 40.5 Hz

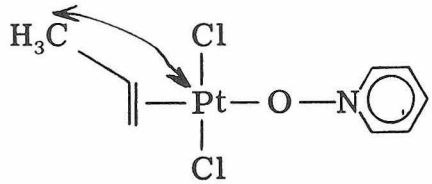

i

J = 29.0 Hz

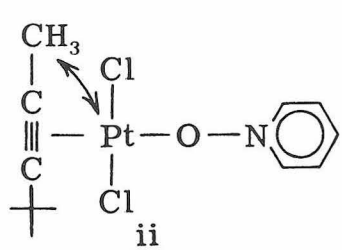

ii

15. Broad bands centered around 3400 cm^{-1} and weaker bands around 1630 cm^{-1} in the spectra of IIIa-d and $[(n-C_3H_7)_3C_3][BF_4]$ are assigned to H_2O present in the KBr pellet. Only in the salt $\{[(CH_3)_2N]_3C_3\}\{BF_4\}$ is this water considered to be part of the crystal. In this case the H_2O bands are much more intense. The bands below 350 cm^{-1} in IIIa-d are skeletal modes of the $M_2Cl_6^{2-}$ anions[5] and will be treated in another paper.

16. H. P. Fritz, Adv. Organometal. Chem., 1, 239 (1964).

17. R. G. Denning and L. M. Venanzi, J. Chem. Soc., 3241 (1963).

18. M. J. Grogan and K. Nakamoto, J. Amer. Chem. Soc., 90, 918 (1968).

19. M. J. Grogan and K. Nakamoto, Ibid., 88, 5454 (1966).

20. H. P. Fritz and G. N. Schrauzer, Chem. Ber., 95, 260 (1962).

21. R. B. King, Inorg. Chem., 2, 528 (1963).

22. E. O. Fischer and K. Fichtel, Chem. Ber., 95, 2063 (1962).

23. In $(\pi-C_8H_8)_2$ complexes, this trend is reversed. In $U(C_8H_8)_2$ and $Np(C_8H_8)_2$, ν_{CC} is observed at 1470 cm^{-1}. (D. G. Karraker, J. A. Stone, E. R. Jones, Jr., and N. Edelstein, J. Amer. Chem. Soc., 92, 4841 (1970).)

24. G. L. Closs, Adv. Alicyclic Chem., 1, 53 (1966).

25. In the Ph. D. Thesis of R. M. Tuggle (Carnegie-Mellon University, 1971), ν_{CC} of the π-cyclopropenyl ligand in $[\pi-C_3(C_6H_5)_3]$-$NiCl(C_5H_5N)_2 \cdot (C_5H_5N)$[1c, d] is tentatively assigned at either 1370 or 1350 cm^{-1}. This is shifted ~50 cm^{-1} from the value of 1425-1400 cm^{-1} found in the free ligand. We thank Dr. D. L. Weaver

for this information.

26. The three C–N stretching vectors transform as a_1' and e' in the idealized molecular point group D_{3h}. Only the e' vibration is allowed. Crystal site symmetry will remove the degeneracy of this vibration and broaden the band.

27. The high frequency of this vibration is not uncommon. Guanidinium salts exhibit ν_{CN} near 1670 cm^{-1}. (P. L. Pickard and G. W. Polly, J. Amer. Chem. Soc., 76, 5169 (1954).) The cation iii exhibits a band at 1610 cm^{-1} due to the NCO^+ linkage. (A. I. Meyers and N. Nazarenko, J. Amer. Chem. Soc., 94, 3243 (1972).)

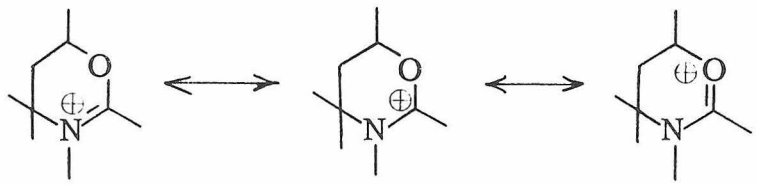

iii

28. Fritz[16] reports ν_{ML} for a cyclobutadiene complex at 416 cm^{-1}, for cyclopentadienyl complexes in the range 312-478 cm^{-1} and for benzene complexes in the range 306-459 cm^{-1}. δ_t bands for these same ligands are reported at 467 cm^{-1}, 365-613 cm^{-1} and 386-490 cm^{-1}, respectively. In (π-C_2H_4) complexes, ν_{ML} is observed in the range 383-427 cm^{-1}[18] and in a π-allyl complex ν_{ML} occurs at 401 cm^{-1}. (H. P. Fritz, Chem. Ber., 94, 1217 (1961).)

29. C. M. Harris, S. E. Livingstone, and I. H. Reece, J. Chem. Soc., 1505 (1959).

30. U. Belluco, M. Nicolini, D. S. Martin, Jr., and D. G. McMane, Inorg. Chem., 8, 2809 (1969).

31. This was shown by IR, polarized solution Raman spectra and NMR. Because of this solvolysis, the acetonitrile spectra reported earlier[29] are not those of the intended anions.

32. D. S. Martin, Jr., M. A. Tucker, and A. J. Kassman, Inorg. Chem., 4, 1682 (1965).

33. O. S. Mortensen, Acta Chem. Scan., 19, 1500 (1965).

Chapter Four

The Infrared Spectrum of the $M_2Cl_6^{2-}$ Anion (M = Pt, Pd)

Introduction

In 1967, Adams, Chandler, and Churchill[1] reported and assigned the far infrared (FIR) spectra (400-60 cm^{-1}) of the ions $M_2X_6^{2-}$ (M = Pt, Pd; X = Cl, Br, I). We recently prepared the compound Ia and determined its structure by X-ray crystallography.[2] The $Pt_2Cl_6^{2-}$ skeleton is symmetrical and nearly planar. The anion

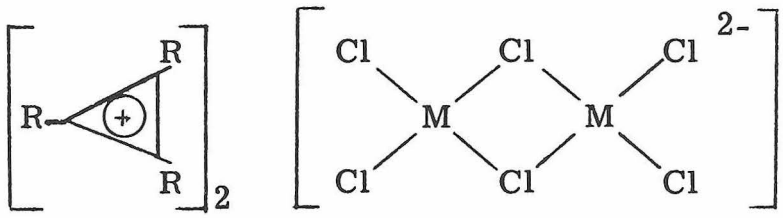

I a M = Pt R = $(CH_3)_2N$-

b M = Pt R = n-C_3H_7-

II a M = Pd R = $(CH_3)_2N$-

b M = Pd R = n-C_3H_7-

$[(C_6H_5)_4As]_2[M_2Cl_6]$

III a M = Pt

b M = Pd

IV = $\{[(CH_3)_2N]_3C_3\}\{BF_4\} \cdot \frac{1}{2}H_2O$

V = $[(n\text{-}C_3H_7)_3C_3][BF_4]$

VI = $[(C_6H_5)_4As][Cl]$

is folded such that the bridging Cl atoms are 0.3Å above the plane of the four terminal Cl atoms (Figure 1). The FIR spectrum of Ia was not in agreement with that reported by Adams, et al.[1] for III a. In view of this, we recorded the FIR spectra (400-33 cm^{-1}) of the compounds

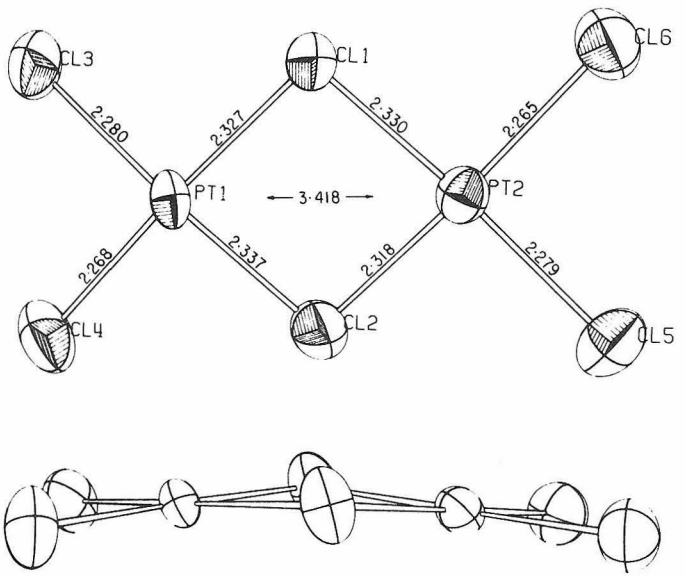

Figure 1. Two views of the $Pt_2Cl_6^{2-}$ anion in $\{[(CH_3)_2N]_3C_3\}_2\{Pt_2Cl_6\}$. Notice the slight fold in the center of the anion such that the two bridging chlorine atoms are 0.3 Å above the plane of the four terminal atoms

I, II, III, IV, V and VI. In this chapter, we present an assignment of the bands we observe for the $M_2Cl_6^{2-}$ skeleton. Our findings differ considerably from the previous assignment.[1]

Experimental

Compounds IIIa and IIIb were prepared by literature procedures.[1] Tetraphenylarsonium chloride hydrate ("$(C_6H_5)_4AsCl \cdot xH_2O$") was obtained from Aldrich Chemical Co. The FIR spectrum of this material and of a sample crystallized from ethanol-ether (M. P. = 259.5 - 261) were identical. KBr pellet spectra (400-220 cm^{-1}) were recorded on a Perkin-Elmer 225 spectrometer. Paraffin pellet spectra (400-33 cm^{-1}) were recorded on a Perkin-Elmer 180 spectrometer. Paraffin pellets were prepared from ~20 mg sample and 0.3 g paraffin. After ~30 min. of thorough grinding in a mortar, the mixture was pressed into a 10 × 21 × 2 mm hole in steel pellet holder on top of a piece of Al foil. The pellet holder and foil were gently heated on a hot plate to barely fuse the pellet. This procedure reduces light scattering by the pellet considerably. After cooling, the foil was removed, excess paraffin was scraped off the holder, and the sample was ready for use. The drawings in Figure 1 were done by ORTEP[3] using the data of our X-ray study.

Results and Discussion

Assignment of the Spectra. – The FIR spectra of three salts of $Pt_2Cl_6^{2-}$ and $Pd_2Cl_6^{2-}$ are shown in Figures 2 and 3 and listed in Table I. The spectra of simple salts of the associated cations are also shown. The spectrum of V in Figure 2 was obtained with a smaller sample than was generally used for the other spectra in Figure 2. Weak bands may be present which are not seen in our spectrum. The KBr pellet spectra are of much higher quality than the paraffin pellet spectra above 250 cm^{-1} so band assignments for modes above 250 cm^{-1} are based on the KBr pellet spectra and assignments below 250 cm^{-1} are based on the paraffin pellet spectra.

We find that the spectrum of $M_2Cl_6^{2-}$ can be analyzed in terms of D_{2h} symmetry despite its small deviation from planarity. The eighteen normal modes of vibration of the $M_2Y_2X_4$ skeleton include eight IR active modes. In conformity with the numbering scheme adopted previously,[1] these modes are described in Table II. Among the IR active modes, ν_{12} will probably occur below 100 cm^{-1} where we did not attempt to assign any bands. We therefore expect seven bands in the IR spectrum above $\sim$100 cm^{-1}.

We will assign the platinum spectra first. The four stretching modes, ν_{13}, ν_{14}, ν_{16} and ν_{17}, should be of highest energy, with terminal stretching somewhat higher than bridge stretching.[1,4] These assignments are given in Table III. In this table we do not distinguish the two MX or MY stretching frequencies by their symmetries. Our force constant calculations could be made to fit any combination of assignments with small variation of the force constants. In some

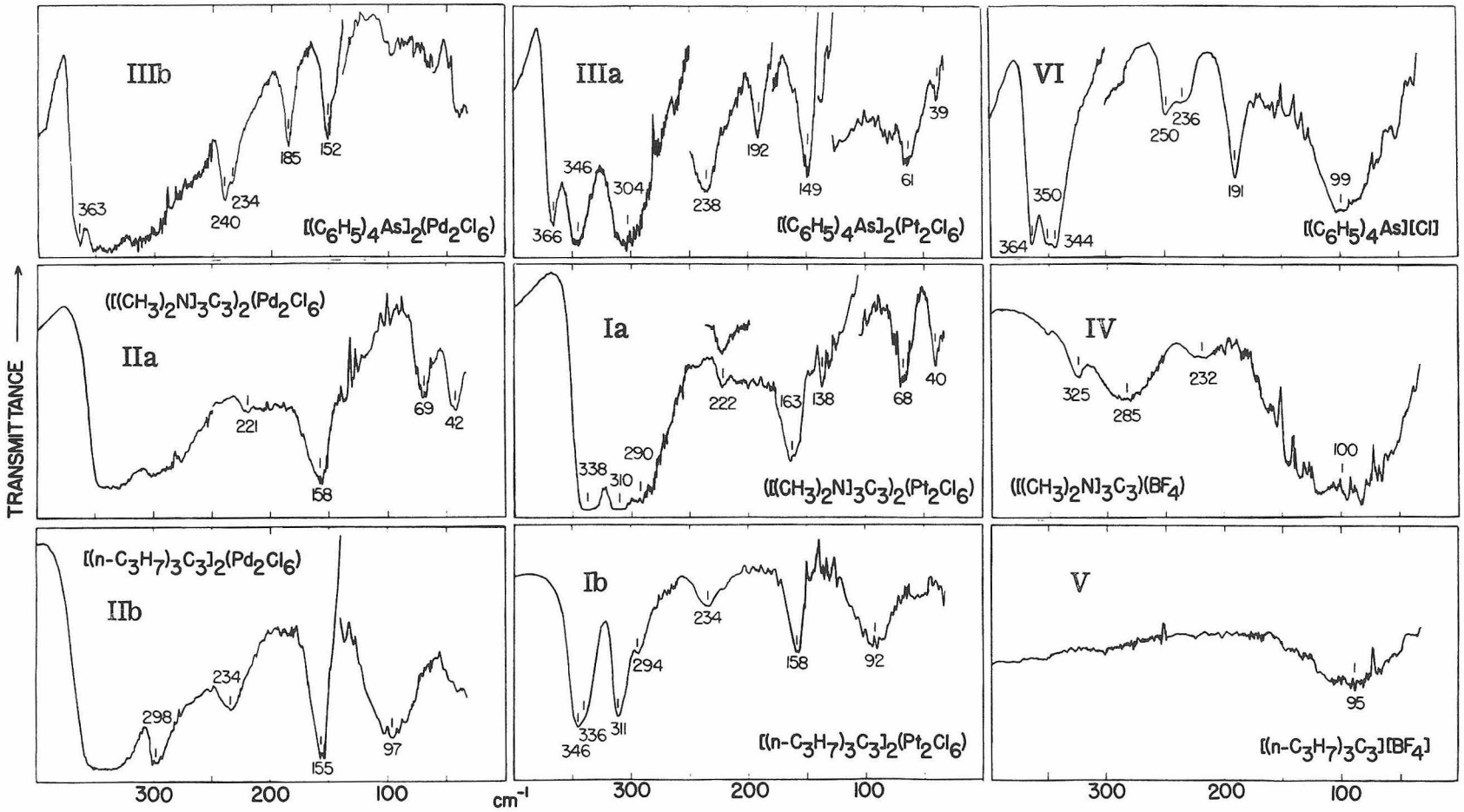

Figure 2. Paraffin pellet FIR spectra (400-33 cm^{-1}) of a series of $M_2Cl_6^{2-}$ salts. (M = Pt, Pd). Cation spectra are given on the right for comparison.

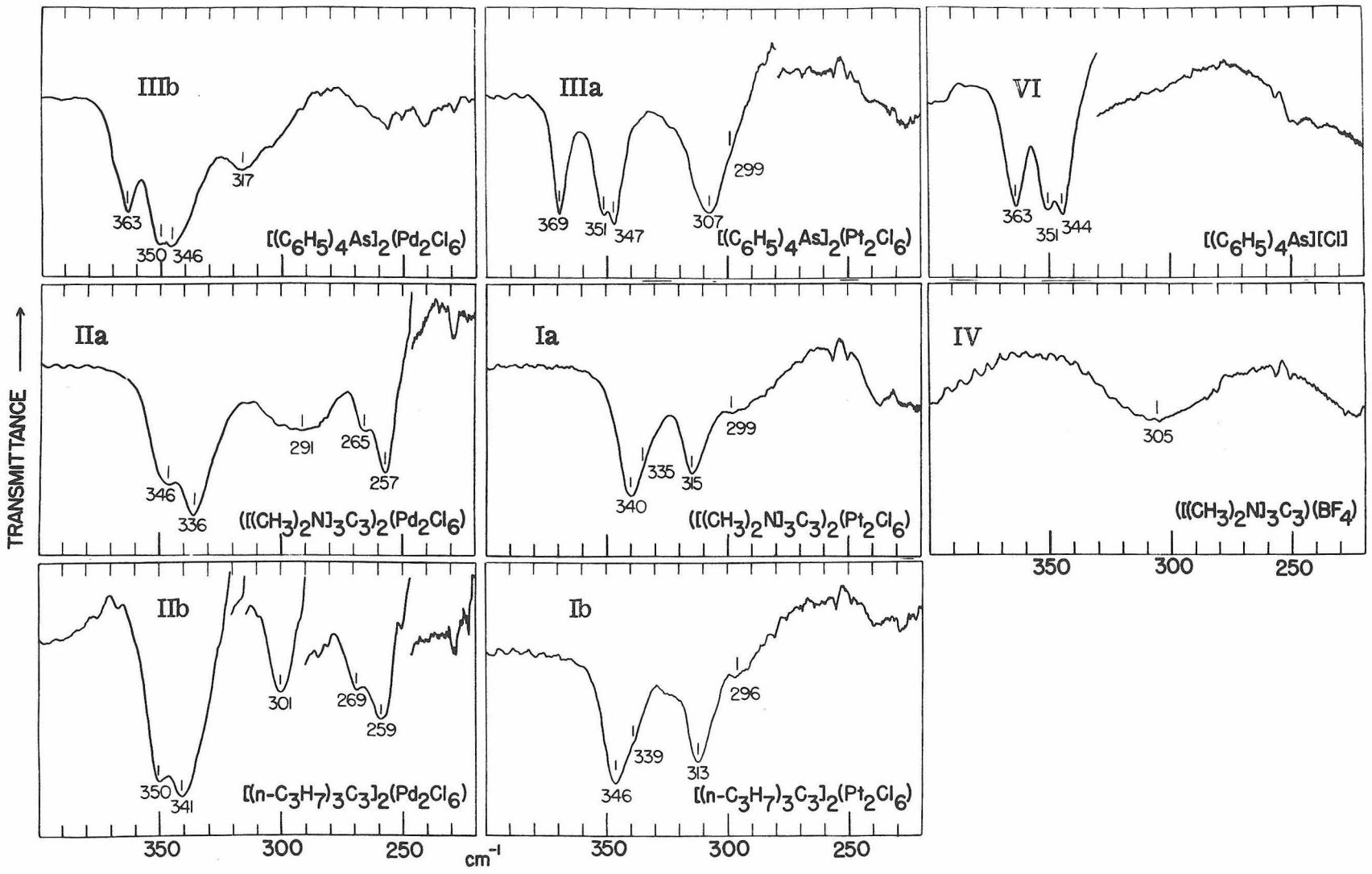

Figure 3. KBr pellet FIR spectra (400-220 cm^{-1}) of the series of compounds shown in Figure 2. No $[(n\text{-}C_3H_7)_3C_3][BF_4]$ was available for these spectra.

Table I

FIR Spectra of the Compounds Studied in this Work[a]

VI		IV		V	IIIa		Ia		Ib		IIIb		IIa		IIb	
363	364				369	366					363	363				
351	350				351						350					
344	344				347	346	340	338	346	346	346		346		350	
							335 sh		339 sh	336 sh			336		341	
			325													
					307	304	315	310	313	311	317				301	298
		305	285		299 sh		299	290	296	294			291			
													265		269	
													257		259	
	250											240				
	236		232			238		222		234		234		221		234
	191					192						185				
						149		163		158		152		158		155
								138								
	99		100	95						92						97
						61		68						69		
						39		40						42		

[a] For each salt, the number on the left is from the KBr pellet spectrum and the number on the right is from the paraffin pellet spectrum.

Table II

Normal Modes of Vibration of $M_2Y_2X_4$ in D_{2h} Symmetry

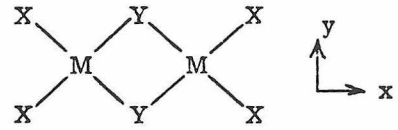

Symmetry	Frequency Number	Approximate Description	Symbol	Activity[a]	Symmetry	Frequency Number	Approximate Description	Symbol	Activity
a_g	ν_1	MX stretch	ν_{MX}	R	a_u	ν_{10}	MX_2 twisting	ρ_t	I
	ν_2	MY stretch	ν_{MY}	R					
	ν_3	MX_2 bend	δ	R	b_{1u}	ν_{11}	MX_2 wagging	ρ_w	IR
	ν_4	M-M stretch (skeletal deformation)	ν_{MM}	R		ν_{12}	out-of-plane deformation		IR
b_{1g}	ν_5	MX stretch	ν_{MX}	R	b_{2u}	ν_{13}	MX stretch	ν_{MX}	IR
	ν_6	MY stretch	ν_{MY}	R		ν_{14}	MY stretch	ν_{MY}	IR
	ν_7	MX_2 rocking	ρ_r	R		ν_{15}	MX_2 rocking	ρ_r	IR
b_{2g}	ν_8	MX_2 wagging	ρ_w	R	b_{3u}	ν_{16}	MX stretch	ν_{MX}	IR
						ν_{17}	MY stretch	ν_{MY}	IR
b_{3g}	ν_9	MX_2 twisting	ρ_t	R		ν_{18}	MX_2 bend	δ	IR

[a] R = Raman, IR = infrared, I = inactive.

Table III

Assignment of the IR-Active Fundamentals of the $M_2Cl_6^{2-}$ Anion

Vibration	Frequency Number	Symmetry	IIIa	Ia	Ib	IIIb	IIa	IIb
ν_{MX}	ν_{13} [a]	b_{2u} [a]	b	340	346	b	346	350
ν_{MX}	ν_{16}	b_{3u}	b	335 sh	339 sh	b	336	341
ν_{MY}	ν_{17} [a]	b_{3u} [a]	307	315	313	317	b	301
ν_{MY}	ν_{14}	b_{2u}	290 sh	299	296	c	265	269
δ	ν_{18}	b_{3u}	238	222	234	c	257	259
ρ_r	ν_{15}	b_{2u}	c	c	c	c	221	234
ρ_w	ν_{11}	b_{1u}	149	163	158	152	158	155

[a] Assignment uncertain.

[b] Interference from cation bands.

[c] Not observed.

cases we were forced to assign very poorly resolved shoulders as fundamentals. Though band broadening due to the presence of many isotopically different species is expected, we require four fundamentals in the Pt-Cl stretching region (~275-350 cm^{-1} [5]) and it is not unreasonable that both ν_{MX} and both ν_{MY} vibrations should be of similar energy.

There remain three vibrations to assign: δ, ρ_r and ρ_w. Only one more band definitely belonging to $Pt_2Cl_6^{2-}$ is seen in the region 100-275 cm^{-1}. This is a medium intensity band near 155 cm^{-1}. All three Pt salts also show a weak but distinct band near 230 cm^{-1}. The spectra of IV and VI also show absorption near 230 cm^{-1}. Further, we cannot rule out the presence of a weak band in this region for V. Because all three Pt salts show bands of similar appearance in this region, we tentatively assign the band near 230 cm^{-1} as a fundamental. This gives us three modes of vibration and two observed bands. Of the three normal modes, δ is expected to occur at highest frequency.[1,4] We assign the band near 230 cm^{-1} to this vibration. We have some basis tochoosebetween ρ_r and ρ_w for the band near 155 cm^{-1}. In Figure 4 we compare vibrations of $Pt_2Cl_6^{2-}$ to those of $PtCl_4^{2-}$.[6,7] The similarity of the π ($PtCl_4^{2-}$) frequency at 168 cm^{-1} to our band at 155 cm^{-1} suggests that we assign $\rho_w \approx 155$ cm^{-1}. Our force constant calculations (<u>vide infra</u>) suggest that ρ_r is at higher energy than ρ_w but we do not observe this band. All of our assignments are given in Table III.

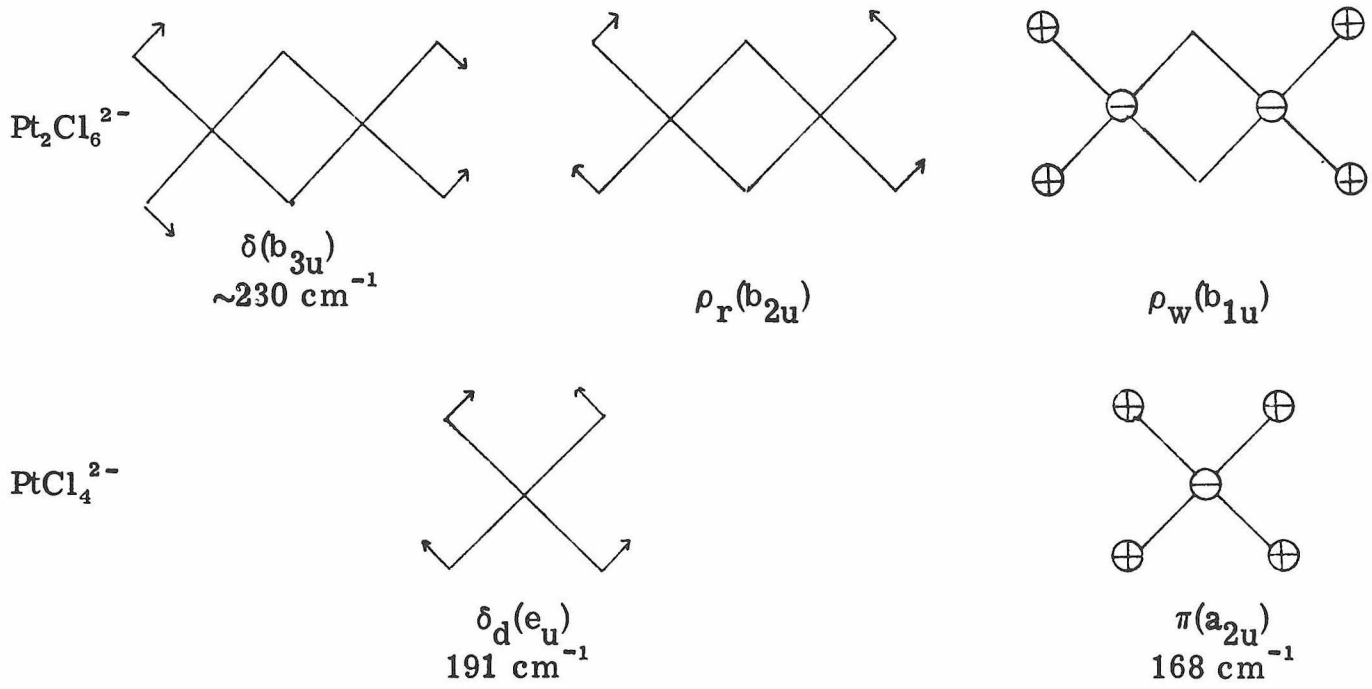

Figure 4. Analogous vibrations (idealized) of $Pt_2Cl_6^{2-}$ and $PtCl_4^{2-}$.

Assignment of the spectra of the $Pd_2Cl_6^{2-}$ salts is facilitated by the appearance of seven absorption bands above 100 cm^{-1}. The spectrum of IIb is the clearest and will be used as an illustration. The four highest energy absorptions are observed at 350, 341, 301, and 269 cm^{-1}. As these are all in the Pd-Cl stretching region, we assign them to ν_{MX} and ν_{MY}. Once again, we are not certain which frequency is associated with which symmetry. The seemingly large splitting of the two ν_{MY} frequencies is not unusual.[8-12] The only surprise in the spectrum is the appearance of the next highest band at 259 cm^{-1}. This is rather high for a bending frequency but since we see the predicted number of bands above 100 cm^{-1} we assign this as the δ fundamental. Since this δ mode at 259 cm^{-1} has b_{3u} symmetry, we tentatively assign the 269 cm^{-1} stretching mode as ν_{14} (b_{2u}). We would not expect two modes of the same symmetry to occur so close together.[13] This would lead to assigning the 301 cm^{-1} band as ν_{17} (b_{3u}). We used these assignments when fitting force constants but emphasize that they are by no means certain. Bands at 234 and 155 cm^{-1} remain to be assigned. The 155 cm^{-1} band is assigned to ρ_w by analogy to $Pt_2Cl_6^{2-}$, leaving ρ_r = 234 cm^{-1}.

<u>Force Constants.</u> Internal coordinates used to calculate all in-plane infrared active frequencies are four terminal M-X stretches (r_i), four bridging M-Y stretches (s_i), and four X-M-Y bends (β_i). The b_{2u} and b_{3u} G matrix blocks are those reported by Adams, <u>et al.</u>[1] with the correct values of the elements P and R reported in the

Appendix. An idealized D_{2h} geometry was used in both cases. The $Pt_2Cl_6^{2-}$ geometry is that observed for Ia.[3] The Pd geometry is based on the structure of Zeise's Pd dimer, $[(C_2H_4)_2PdCl_2]_2$.[14] These geometric parameters are given below.

$Pt_2Cl_6^{2-}$:	$r = 2.273$Å	$\alpha = 92.44°$	$Pd_2Cl_6^{2-}$:	$r = 2.25$Å	$\alpha = 92°$
	$s = 2.328$Å	$\beta = 91.23°$		$s = 2.33$Å	$\beta = 91°$
		$\gamma = 85.07°$			$\gamma = 86°$
		$\delta = 94.46°$			$\delta = 94°$

The angles are defined in the Appendix. Each set of b_{2u} and b_{3u} frequencies is determined from the equation $|G'F' - E\lambda| = 0$, where G' and F' are the symmetrized G and F matrices.[15] This means that the b_{2u} and b_{3u} frequencies are each determined by a 3×3 matrix of force constants. Each matrix is symmetric about the diagonal and hence contains six different force constants. We were able to fit the three observed frequencies of each symmetry with two sets of five force constants. (The value of one of the off-diagonal force constants was taken as zero). Since each F' matrix contained five different elements, ten parameters are the minimum necessary to describe this system.[16] The force field ultimately adopted was

$$
\begin{aligned}
2V = {} & \sum_1^4 F_r(\Delta r_i)^2 + \sum_1^4 F_s(\Delta s_i)^2 + \sum_1^4 F_\beta(\Delta\beta_i)^2 + 2F_{rr}[(\Delta r_1)(\Delta r_2) \\
& + (\Delta r_3)(\Delta r_4)] + 2F_{ss}[(\Delta s_1)(\Delta s_3) + (\Delta s_2)(\Delta s_4)] \\
& + 2F_{\beta\beta}[(\Delta\beta_1)(\Delta\beta_3) + (\Delta\beta_2)(\Delta\beta_4)] \\
& + 2\sum_1^4 F_{rs}(\Delta r_i)(\Delta s_i) + 2\sum_1^4 F_{s\beta}(\Delta s_i)(\Delta\beta_i) + 2F_{rs'}[(\Delta r_1)(\Delta s_2) \\
& + (\Delta r_2)(\Delta s_1) + (\Delta r_3)(\Delta s_4) + (\Delta r_4)(\Delta s_3)] + 2F_{s\beta'}[(\Delta s_1)(\Delta\beta_3) \\
& + (\Delta s_2)(\Delta\beta_4) + (\Delta s_3)(\Delta\beta_1) + (\Delta s_4)(\Delta\beta_2)]
\end{aligned}
$$

Our force constants were chosen to fit the following frequencies within $\pm$ 0.4 cm^{-1}.[27]

	ν_{13}	ν_{16}	ν_{14}	ν_{17}	ν_{18}	ν_{15}
$Pd_2Cl_6^{2-}$ (IIb)	350	341	269	301	259	234
$Pt_2Cl_6^{2-}$ (Ia)	335	340	299	315	222	--

Since we are lacking ν_{15} for $Pt_2Cl_6^{2-}$, it is only possible to determine all ten force constants for $Pd_2Cl_6^{2-}$. These were found by trial and error to be:

F_r = 1.67 mdyne/Å

F_s = 1.24 mdyne/Å

F_β = 4.05 mdyne-Å/rad^2 ⇒ 0.776 mdyne/Å

F_{rr} = 0.09 mdyne/Å

F_{ss} = 0.05 mdyne/Å

$F_{\beta\beta}$ = -0.85 mdyne-Å/rad^2 ⇒ -0.016 mdyne/Å

F_{rs} = -0.04 mdyne/Å

$F_{rs'}$ = 0.16 mdyne/Å

$F_{s\beta}$ = 0.19 mdyne/rad ⇒ 0.082 mdyne/Å

$F_{s\beta'}$ = 0.36 mdyne/rad ⇒ 0.15 mdyne/Å

Units of mdyne/Å are obtained for F_β, $F_{\beta\beta}$, $F_{s\beta}$ and $F_{s\beta'}$ by dividing the first force constant given by rs, rs, s and s, respectively. We attach little significance to the interaction force constants as a considerable variation of several such force constants simultaneously would still allow an excellent fit of the observed frequencies. Calculations for $Pt_2Cl_6^{2-}$, using 163 cm^{-1} as a lower limit for the value of ρ_r, produce the following principal force constants:

$F_r \approx 2.0$ mdyne/Å

$F_s \approx 1.7$ mdyne/Å

$F_\beta \approx 2.3$ mdyne-Å/rad^2 $\Rightarrow$ 0.47 mdyne/Å

It is stated above that our calculations suggest that $\rho_r > \rho_w$. The reason we say this is that the larger the spread of δ and ρ_r, the larger the magnitude of $F_{\beta\beta}$. $|F_{\beta\beta}|$ seems very large already and reversing the assignment of ρ_r and ρ_w would make it even larger.

The internal coordinate β is a poor one for studying bending as considerable stretching of the M-Y bonds occurs along with change of the XMY angles. The potential energy distributions reflected this as all three modes in each symmetry block were mixed extensively with our final choice of Pd force constants. In the case of $Pt_2Cl_6^{2-}$, M-X and M-Y stretching were mixed extensively but bending was fairly well separated.

Discussion. In Table IV we compare our findings for III and VI to those of Adams et al.[1] The first, striking point is that the sharp, medium intensity band near 190 cm^{-1}, which is definitely a $(C_6H_5)_4As^+$ band, is assigned as an $M_2Cl_6^{2-}$ fundamental by Adams, et al. because they do not observe this band in the spectrum of VI. We observe this band in the spectrum of VI as a hydrate obtained commercially and as a crystalline material crystallized from ethanol-ether. We also observe this band in the spectra of III but not in the spectra of I and II. There is no doubt that this is not an $M_2Cl_6^{2-}$ fundamental. Instead, we assign the band near 230 cm^{-1} as a fundamental based on its appearance in Ib and IIb and its absence in V. This is our least certain assignment.

Table IV

Comparison of FIR Spectra[a]

VI			IIIa			IIIb		
This Work		Ref. 1	This Work		Ref. 1	This Work		Ref. 1
363[b]	364[c]	370[d]	369[b]	366[c]		363[b]	363[c]	
351	350	353	351		350 vs[d]	350		353 vs[d]
344	344	349	347	346	346 vs	346		
			307	304	315 m-s	317		305 m
			299 sh		302 m			
								264 w-m
	250	240					240	
	236	234		238			234	
	191			192	186 m-s		185	186 m-s
				149	159 m-s		152	156 s
		139						
	99				98 w-m			97 w
				61				
				39				

[a] Bands for III from Ref. 1 include only those assigned as fundamentals. Complete spectra were not reported. Abbreviations are s = strong, m = medium, w = weak, v = very.

[b] The data of this column come from KBr pellet spectra.

[c] The data of this column come from paraffin pellet spectra.

[d] The data of this column come from Nujol mulls on polyethylene plates.

Another sharp distinction between our work and previous work is the appearance of a pair of bands near 260 cm^{-1} in the KBr pellet spectra of II. We do not see these bands in our paraffin pellet spectra and Adams[1] reports only one band in this region. In our KBr pellet spectrum of IIIb we see almost nothing in this region so these bands are apparently quite sensitive to the cation and to the sampling technique.

The assignment of $\rho_r > \rho_w$ deserves some comment. There has been little consistency in assigning these fundamentals in the past. Adams, et al.[1] assigned $\delta > \rho_w > \rho_r$ for $Pt_2Cl_6^{2-}$ and $Pd_2Cl_6^{2-}$. Adams and Churchill[4] assign $\delta = 144$ cm^{-1}, $\rho_w = 137$ cm^{-1} and ρ_r = (not observed)(148 cm^{-1} calc.) for Au_2Cl_6. Similarly, they assign $\delta > \rho_w$ for Al_2X_6 (X = Cl, Br, I) with ρ_r not observed. In the case of B_2H_6,[17] the assignment of the IR active modes is $\delta = 1177$, $\rho_w = 973$, ρ_r = (not observed)(950 cm^{-1} calc.). On the other hand, for B_2D_6[17a,b,18] the assignment is $\delta = 876$, $\rho_r = 730$, $\rho_w = 720$ cm^{-1}. Where observed, ρ_r and ρ_w are very close. We submit that in the B_2H_6 structure, the ratio ρ_w/ρ_r will be greater than in the planar $Pd_2Cl_6^{2-}$ structure. This is because in the B_2H_6 wag, motion of the terminal atoms takes them toward bridging atoms. In the $Pd_2Cl_6^{2-}$ wag, motion of the terminal atoms does not take them toward bridging atoms. This is exactly reversed in the rocking motion.[19] We illustrate these modes in Figure 5. Given that ρ_r and ρ_w are of very similar energy in B_2H_6 and B_2D_6, it is not unreasonable to assign $\rho_r > \rho_w$ in $Pd_2Cl_6^{2-}$. As discussed above, our force constants support this assignment.

Our $Pd_2Cl_6^{2-}$ stretching force constants, F_r and F_s, are in

reasonable agreement with those of Adams[1] and the ratio F_s/F_r is 0.74. This supports Adams' generalization[4] concerning the difference between structures of the $Pd_2Cl_6^{2-}$ type ($F_s/F_r \approx 0.75$) and the Al_2Cl_6 type ($F_s/F_r \approx 0.5$). Our $Pt_2Cl_6^{2-}$ stretching force constants are also roughly in this range, but we feel they are very imprecise because of the missing fundamental frequency. The value of F_β is large in both cases because bridge bond stretching is also involved in motions of the β coordinates. We expect the true bending force constants, F_α, to be smaller, as in $PtCl_4^{2-}$.[22]

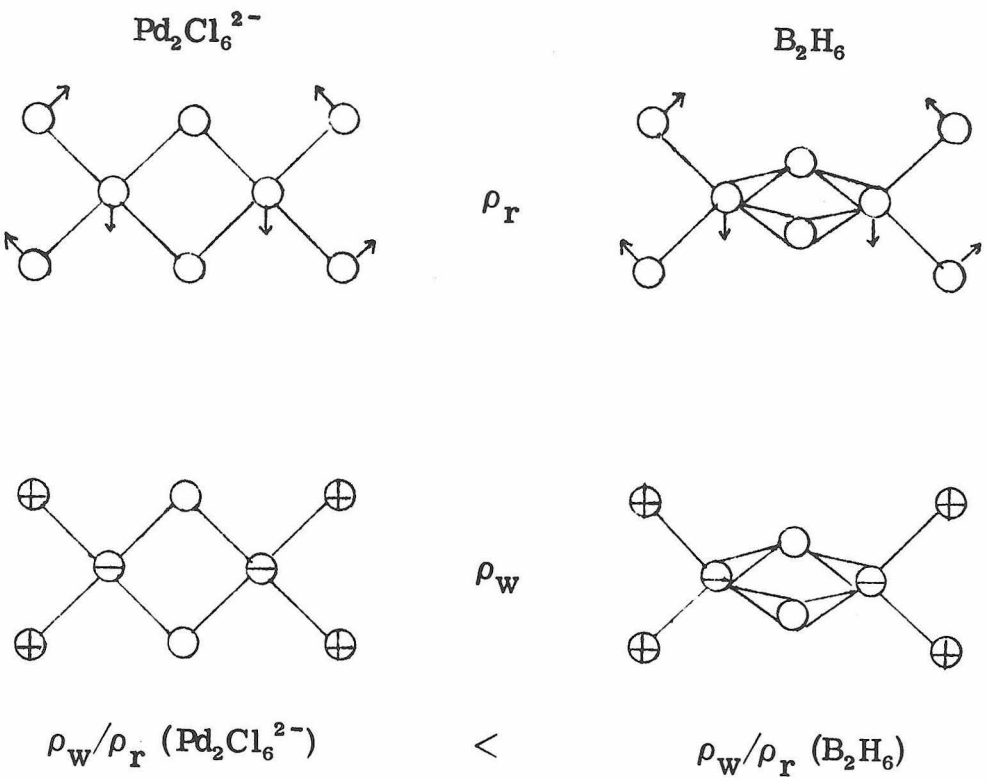

Figure 5. Comparison of the idealized rocking and wagging modes of $Pd_2Cl_6^{2-}$ and B_2H_6.

Appendix

The complete G matrix for $M_2Y_2X_4$ with D_{2h} symmetry has not been given before. Adams, et al.[1] report the in-plane G matrix; but we found a mistake in their element R and the element P was omitted. We now report the complete G matrix, including both in-plane and out-of-plane vibrations. Where possible, we conform to the nomenclature of Adams.[1]

Fourteen internal coordinates for the thirteen in-plane vibrations are defined below, where r and s are stretching motions and α and β are bending motions. Using these internal coordinates,

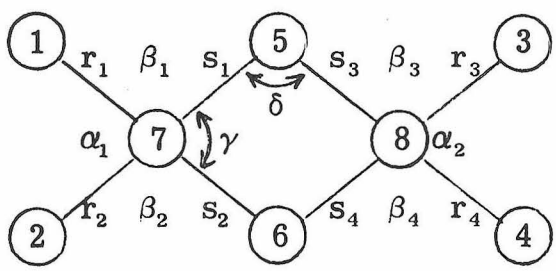

one redundancy appears in the b_{3u} block of the G′ matrix.[15] We have eliminated the redundant row and column of the b_{3u} block given below.

Internal coordinates for the five out-of-plane vibrations could consist of the eight ω and τ coordinates defined below:

ω_1 - motion of atom 1 out of the plane of atoms 7, 5, 6

ω_2 - motion of atom 2 out of the plane of atoms 7, 5, 6

ω_3 - motion of atom 3 out of the plane of atoms 8, 5, 6

ω_4 - motion of atom 4 out of the plane of atoms 8, 5, 6

τ_1 - torsion of atoms 6 and 8 about the 5-7 bond

τ_2 - torsion of atoms 7 and 6 about the 5-8 bond

τ_3 - torsion of atoms 5 and 7 about the 8-6 bond

τ_4 - torsion of atoms 8 and 5 about the 6-7 bond

However, this would introduce three redundancies. Instead, we replace the four τ coordinates by a single θ coordinate defined as follows:

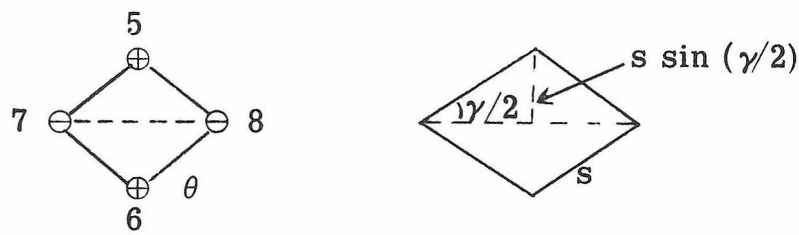

θ is a book-like folding of atoms 5 and 6 out of the plane of the page perpendicular to the 7-8 axis. Atoms 7 and 8 move down enough to compensate for the upward motion of atoms 5 and 6. With the geometry shown above, Wilson's $\vec{s}_{\theta i}$ vectors [23] become

$$|\vec{s}_{\theta 5}| = [s \sin(\gamma/2)]^{-1} \quad \text{out of page}$$

$$|\vec{s}_{\theta 6}| = [s \sin(\gamma/2)]^{-1} \quad \text{out of page}$$

$$|\vec{s}_{\theta 7}| = [s \sin(\gamma/2)]^{-1} \quad \text{into page}$$

$$|\vec{s}_{\theta 8}| = [s \sin(\gamma/2)]^{-1} \quad \text{into page}$$

The $\vec{s}_{\omega i}$ vectors have already been given [24] and vectors for stretching and bending are readily available. [25] G matrix elements follow from the formula [26]

$$G_{tt'} = \sum_{i=1}^{N} \mu_i \vec{s}_{ti} \cdot \vec{s}_{t'i}$$

where μ_i is the reciprocal of the mass of atom i and the sum extends over all atoms common to the vibrations t and t′.

The symmetry coordinates for $M_2Y_2X_4$ are then given by

$$U = \begin{array}{c}
\begin{array}{ccccccccccccccccccc} r_1 & r_2 & r_3 & r_4 & s_1 & s_2 & s_3 & s_4 & \beta_1 & \beta_2 & \beta_3 & \beta_4 & \alpha_1 & \alpha_2 & \omega_1 & \omega_2 & \omega_3 & \omega_4 & \theta \end{array} \\
\left[\begin{array}{ccccccccccccccccccc}
\frac{1}{2} & \frac{1}{2} & \frac{1}{2} & \frac{1}{2} & & & & & & & & & & & & & & & \\
 & & & & \frac{1}{2} & \frac{1}{2} & \frac{1}{2} & \frac{1}{2} & & & & & & & & & & & \\
 & & & & & & & & \frac{1}{2} & \frac{1}{2} & \frac{1}{2} & \frac{1}{2} & & & & & & & \\
 & & & & & & & & & & & & \frac{1}{\sqrt{2}} & \frac{1}{\sqrt{2}} & & & & & \\
\frac{1}{2} & -\frac{1}{2} & -\frac{1}{2} & \frac{1}{2} & & & & & & & & & & & & & & & \\
 & & & & \frac{1}{2} & -\frac{1}{2} & -\frac{1}{2} & \frac{1}{2} & & & & & & & & & & & \\
 & & & & & & & & \frac{1}{2} & -\frac{1}{2} & -\frac{1}{2} & \frac{1}{2} & & & & & & & \\
\frac{1}{2} & -\frac{1}{2} & \frac{1}{2} & -\frac{1}{2} & & & & & & & & & & & & & & & \\
 & & & & \frac{1}{2} & -\frac{1}{2} & \frac{1}{2} & -\frac{1}{2} & & & & & & & & & & & \\
 & & & & & & & & \frac{1}{2} & -\frac{1}{2} & \frac{1}{2} & -\frac{1}{2} & & & & & & & \\
\frac{1}{2} & \frac{1}{2} & -\frac{1}{2} & -\frac{1}{2} & & & & & & & & & & & & & & & \\
 & & & & \frac{1}{2} & \frac{1}{2} & -\frac{1}{2} & -\frac{1}{2} & & & & & & & & & & & \\
 & & & & & & & & \frac{1}{2} & \frac{1}{2} & -\frac{1}{2} & -\frac{1}{2} & & & & & & & \\
 & & & & & & & & & & & & \frac{1}{\sqrt{2}} & -\frac{1}{\sqrt{2}} & & & & & \\
 & & & & & & & & & & & & & & \frac{1}{2} & \frac{1}{2} & -\frac{1}{2} & -\frac{1}{2} & \\
 & & & & & & & & & & & & & & \frac{1}{2} & -\frac{1}{2} & \frac{1}{2} & -\frac{1}{2} & \\
 & & & & & & & & & & & & & & \frac{1}{2} & -\frac{1}{2} & -\frac{1}{2} & \frac{1}{2} & \\
 & & & & & & & & & & & & & & \frac{1}{2} & \frac{1}{2} & \frac{1}{2} & \frac{1}{2} & \\
 & & & & & & & & & & & & & & & & & & 1
\end{array}\right]
\end{array}
\begin{array}{l}
\left.\begin{array}{c} \\ \\ \\ \\ \end{array}\right\} a_g \\
\left.\begin{array}{c} \\ \\ \\ \end{array}\right\} b_{1g} \\
\left.\begin{array}{c} \\ \\ \\ \end{array}\right\} b_{2u} \\
\left.\begin{array}{c} \\ \\ \\ \\ \end{array}\right\} b_{3u} \\
\left.\begin{array}{c} \\ \end{array}\right\} b_{2g} \\
\left.\begin{array}{c} \\ \end{array}\right\} b_{3g} \\
\left.\begin{array}{c} \\ \end{array}\right\} a_u \\
\left.\begin{array}{c} \\ \\ \end{array}\right\} b_{1u}
\end{array}$$

Using these U and G matrices, the blocks of the G′ matrix[15] become

$$a_g \quad \begin{bmatrix} A+D & E+F & H+I & 2T/\sqrt{2} \\ & B+J+K & M+N+P & 2V/\sqrt{2} \\ & & C+R+S & 2W/\sqrt{2} \\ & & & X \end{bmatrix}$$

$$b_{1g} \quad \begin{bmatrix} A-D & E-F & H-I \\ & B-J-K & M-N-P \\ & & C-R-S \end{bmatrix}$$

$$b_{2g} \quad \begin{bmatrix} AA+BB-CC-DD \end{bmatrix}$$

$$b_{3g} \quad \begin{bmatrix} AA-BB+CC-DD \end{bmatrix}$$

$$a_u \quad \begin{bmatrix} AA-BB-CC+DD \end{bmatrix}$$

$$b_{1u} \quad \begin{bmatrix} AA+BB+CC+DD & 2EE \\ & Z \end{bmatrix}$$

$$b_{2u} \quad \begin{bmatrix} A-D & E-F & H-I \\ & B-J+K & M-N+P \\ & & C-R+S \end{bmatrix}$$

$$b_{3u} \quad \begin{bmatrix} A+D & E+F & H+I \\ & B+J-K & M+N-P \\ & & C+R-S \end{bmatrix}$$

where

$$A = G_{r_1 r_1} = \mu_m + \mu_x$$

$$B = G_{s_1 s_1} = \mu_m + \mu_y$$

$$C = G_{\beta_1 \beta_1} = \sigma_r^2 \mu_x + \sigma_s^2 \mu_y + (\sigma_r^2 + \sigma_s^2 - 2\sigma_r \sigma_s \cos\beta)\mu_m$$

$$D = G_{r_1 r_2} = \mu_m \cos\alpha$$

$$E = G_{r_1 s_1} = \mu_m \cos\beta$$

$$F = G_{r_1 s_2} = \mu_m \cos\epsilon$$

$\epsilon = \alpha + \beta$ or $\beta + \gamma$ (whichever is smaller)

$$H = G_{r_1 \beta_1} = -\sigma_s \mu_m \sin\beta$$

$$I = G_{r_1 \beta_2} = -(\mu_m/\sin\beta)[\sigma_s(\cos\alpha - \cos\beta\cos\epsilon) + \sigma_r(\cos\epsilon - \cos\alpha\cos\beta)]$$

$$J = G_{s_1 s_2} = \mu_m \cos\gamma$$

$$K = G_{s_1 s_3} = \mu_y \cos\delta$$

$$M = G_{s_1 \beta_1} = -\sigma_r \mu_m \sin\beta$$

$$N = G_{s_1 \beta_2} = -\mu_m[(\sigma_s/\sin\beta)(\cos\epsilon - \cos\gamma\cos\beta) + (\sigma_r/\sin\beta)(\cos\gamma - \cos\epsilon\cos\beta)]$$

$$P = G_{s_1 \beta_3} = -\sigma_s \mu_m \sin\delta$$

$$R = G_{\beta_1 \beta_2} = (\mu_m/\sin^2\beta)[(\cos\gamma - 2\cos\epsilon\cos\beta + \cos\alpha\cos^2\beta)\sigma_r^2 + (\cos\epsilon - \cos\gamma\cos\beta - \cos\beta\cos\alpha + \cos\epsilon\cos^2\beta)2\sigma_r\sigma_s + (\cos\alpha - 2\cos\beta\cos\epsilon + \cos\gamma\cos^2\beta)\sigma_s^2]$$

$$S = G_{\beta_1\beta_3} = -\sigma_s^2 \mu_y \cos\delta$$

$$T = G_{r_1\alpha_1} = -\sigma_r \mu_m \sin\alpha$$

$$V = G_{s_1\alpha_1} = I$$

$$W = G_{\beta_1\alpha_1} = \mu_x \sigma_r^2 \cos\psi + [(\sigma_r - \sigma_s \cos\beta - \sigma_r \cos\alpha)\sigma_r \cos\psi + (\sin\beta \sin\alpha \sin^2\psi + \cos\epsilon \cos\psi)\sigma_s \sigma_r]\mu_m$$

$$\cos\psi = (\cos\epsilon - \cos\beta\cos\alpha)/\sin\beta\sin\alpha$$

$$X = G_{\alpha_1\alpha_1} = 2\sigma_r^2[\mu_x + (1-\cos\alpha)\mu_m]$$

$$Z = G_{\theta\theta} = \frac{2\sigma_s^2}{\sin^2(\gamma/2)}(\mu_y + \mu_m)$$

$$AA = G_{\omega_1\omega_1} = \mu_x \sigma_r^2 + \frac{\mu_y \sigma_s^2}{\sin^2\gamma}[\sin^2\beta + \sin^2(\alpha+\beta)] + \mu_m\left[\sigma_r + \frac{\sigma_s}{\sin\gamma}(\sin\beta + \sin(\alpha+\beta))\right]^2$$

$$BB = G_{\omega_1\omega_2} = \frac{2\mu_y \sigma_s^2 \sin\beta \sin(\alpha+\beta)}{\sin^2\gamma} + \mu_m\left[\sigma_r + \frac{\sigma_s}{\sin\gamma}(\sin\beta + \sin(\alpha+\beta))\right]^2$$

$$CC = G_{\omega_1\omega_3} = \frac{\mu_y \sigma_s^2}{\sin^2\gamma}(\sin^2\beta + \sin^2(\alpha+\beta))$$

$$DD = G_{\omega_1\omega_4} = \frac{2\mu_y \sigma_s^2 \sin\beta \sin(\alpha+\beta)}{\sin^2\gamma}$$

$$EE = G_{\omega_1\theta} = \frac{\mu_y \sigma_s^2}{\sin\gamma \sin(\gamma/2)}(\sin(\alpha+\beta) + \sin\beta) + \frac{\mu_m \sigma_s}{\sin(\gamma/2)}\left[\sigma_r + \frac{\sigma_s}{\sin\gamma}(\sin(\alpha+\beta) + \sin\beta)\right]$$

$$\sigma_r = r^{-1} \qquad \sigma_s = s^{-1}$$

The numerical values of these elements, when all distances are expressed in Ångstrom units, are:

$Pd_2Cl_6^{2-}$:

A = 0.037605	F = -0.009386	M = -0.004176
B = 0.037605	H = -0.004033	N = 0.003805
C = 0.014417	I = 0.004386	P = -0.004024
D = -0.000328	J = 0.000656	R = -0.003637
E = -0.000164	K = -0.001968	S = 0.000362

$G'(B_{2u})$:

$$\begin{bmatrix} 0.037933 & 0.009222 & -0.008419 \\ & 0.034982 & -0.012006 \\ & & 0.018416 \end{bmatrix}$$

$G'(B_{3u})$:

$$\begin{bmatrix} 0.037277 & -0.009550 & 0.000353 \\ & 0.040228 & 0.003653 \\ & & 0.010419 \end{bmatrix}$$

$Pt_2Cl_6^{2-}$:

A = 0.033332	F = -0.005115	M = -0.002255
B = 0.033332	H = -0.002201	N = 0.002048
C = 0.012644	I = 0.002394	P = -0.002195
D = -0.000218	J = 0.000441	R = -0.001971
E = -0.000110	K = -0.002194	S = 0.000405

$G'(B_{2u})$:

$$\begin{bmatrix} 0.033550 & 0.005005 & -0.004595 \\ & 0.030698 & -0.006500 \\ & & 0.015020 \end{bmatrix}$$

$G'(B_{3u})$:

$$\begin{bmatrix} 0.033114 & -0.005226 & 0.000193 \\ & 0.035967 & 0.001989 \\ & & 0.010267 \end{bmatrix}$$

References

1. D. M. Adams, P. J. Chandler, and R. G. Churchill, J. Chem. Soc. (A), 1272 (1967).

2. J. Thibeault, Ph.D. Thesis, California Institute of Technology, 1972.

3. C.K. Johnson, "ORTEP, a Fortran Thermal-Ellipsoid Plot Program for Crystal Structure Illustrations," Report ORNL-3794, Revised, Oak Ridge National Laboratory, Oak Ridge, Tenn., 1965.

4. D. M. Adams and R. G. Churchill, J. Chem. Soc. (A), 2141 (1968).

5. D. M. Adams, "Metal Ligand and Related Vibrations," St. Martin's Press, New York, 1968, pages 73-75.

6. The abbreviations used in this drawing are d = degenerate , π = out-of-plane vibration.

7. $PtCl_4^{2-}$ assignments are from:

   a) K. Nakamoto, "Infrared Spectra of Inorganic and Coordination Compounds," Wiley-Interscience, New York, 1970 ed., page 115;

   b) P. J. Hendra, J. Chem. Soc. (A), 1298 (1967);

   c) A. Sabatini, L. Sacconi, and V. Schettino, Inorg. Chem., 3, 1775 (1964);

   d) H. Stammreich and R. Forneris, Spectrochim. Acta, 16, 363 (1970).

8. D. M. Adams and P. J. Chandler, J. Chem. Soc. (A), 588 (1969).

9. M. J. Grogan and K. Nakamoto, J. Amer. Chem. Soc., 90, 918 (1968).

10. D. M. Adams and P. J. Chandler, Chem. Comm., 69 (1966).

11. M. J. Taylor, A. L. Odell and H. A. Raethel, Spectrochim. Acta, 24A, 1855 (1968).

12. D. A. Duddell, R. L. Goggin, R. J. Goodfellow, and M. G. Norton, Chem. Comm., 879 (1968).

13. "Fermi resonance" would probably split these states further apart. See E. B. Wilson, Jr., J. C. Decius, and P. C. Cross, "Molecular Vibrations," McGraw-Hill, New York, 1955, pp 197-198.

14. J. N. Dempsey and N. C. Baenziger, J. Amer. Chem. Soc., 77, 4984 (1955).

15. Ref. 13, Chapters 4-6. $G' = UG\tilde{U}$ where $\tilde{U}$ is the transpose of U and U is given in the Appendix. F′ is obtained similarly.

16. Each F′ matrix is given by

$$F'(b_{2u}) = \begin{bmatrix} F_1(b_{2u}) & F_4(b_{2u}) & F_5(b_{2u}) \\ & F_2(b_{2u}) & F_6(b_{2u}) \\ & & F_3(b_{2u}) \end{bmatrix}$$

$$F'(b_{3u}) = \begin{bmatrix} F_1(b_{3u}) & F_4(b_{3u}) & F_5(b_{3u}) \\ & F_2(b_{3u}) & F_6(b_{3u}) \\ & & F_3(b_{3u}) \end{bmatrix}$$

The force constants are determined from

$$\begin{aligned} F_1(b_{2u}) &= F_r - F_{rr} & F_1(b_{3u}) &= F_r + F_{rr} \\ F_2(b_{2u}) &= F_s + F_{ss} & F_2(b_{3u}) &= F_s - F_{ss} \\ F_3(b_{2u}) &= F_\beta + F_{\beta\beta} & F_3(b_{3u}) &= F_\beta - F_{\beta\beta} \\ F_4(b_{2u}) &= F_{rs} - F_{rs'} & F_4(b_{3u}) &= F_{rs} + F_{rs'} \\ F_5(b_{2u}) &= 0 & F_5(b_{3u}) &= 0 \\ F_6(b_{2u}) &= F_{s\beta} + F_{s\beta'} & F_6(b_{3u}) &= F_{s\beta} - F_{s\beta'} \end{aligned}$$

17. a) Ref. 7a, page 125;

b) W. J. Lehmann, J. F. Ditter and I. Shapiro, J. Chem. Phys., 29, 1248 (1958);

c) W. E. Anderson and E. F. Barker, ibid., 18, 698 (1950).

18. a) R. C. Taylor and A. R. Emery, Spectrochim. Acta, 10, 419 (1958);

b) R. C. Lord and E. Nielsen, J. Chem. Phys., 19, 1 (1951).

19. It may seem that the bridging atoms are too far from the terminal atoms to significantly affect the ratio ρ_w/ρ_r. Yet in π-C_nH_n complexes (n = 5, 6), the out-of-plane C-H bend is at markedly higher frequencies than in the free C_nH_n group.[20] For example, in $(\pi - C_6H_6)Cr(CO)_3$, $\Delta\nu = 121\ cm^{-1}$. The major interference to this motion is the metal atom which might hardly seem big enough to affect the C-H bending of a complexed benzene ring. Such a situation is also observed in π-C_2H_4 complexes.[21] The situation in any of these π-complexes is complicated by the somewhat altered nature of the C-H bond upon coordination.

20. H. P. Fritz, Adv. Organomet. Chem., 1, 239 (1964).

21. a) R. G. Denning and L. M. Venanzi, J. Chem. Soc., 3241 (1963).

b) M. J. Grogan and K. Nakamoto, J. Amer. Chem. Soc., 88, 5454 (1966).

22. L. H. Jones, Coord. Chem. Rev., 1, 351 (1966).

23. Ref. 13, page 55 and E. B. Wilson, Jr., J. Chem. Phys., 9, 76 (1941). $\vec{s}_{\theta 5}$ is chosen such that the direction will produce the largest change in the θ coordinate and the magnitude is $1/r_5$ where $r_5 = s \sin(\gamma/2)$. The other $\vec{s}_{\theta i}$ vectors follow from symmetry and the condition that there be no rotation or translation during the vibration.

24. Ref. 13, page 58.

25. Ref. 13, pages 55-58.

26. Ref. 13, page 61.

27. Calculations were done using a program provided by David K. Ottesen of Caltech and written by R.S. Ottinger, Ph.D. Thesis, Oregon State University, 1966.

Chapter Five

The Reactivity of the $M_2Cl_6^{2-}$ Anion

Cation Exchange

At the time these cyclopropenium salts were thought to be π-cyclopropenium complexes, several titrations suggested themselves as useful experiments. For the ensuing discussion, we will often abbreviate the two cyclopropenium cations as follows:

$$(n\text{-}C_3H_7)_3C_3^+ \equiv P$$

$$[(CH_3)_2N]_3C_3^+ \equiv N$$

If a π-N complex were partially ionized (as conductivity suggested), titration of such a solution with excess $(N)(BF_4)$ would reverse the ionization (1).

$$NMCl_3 \rightleftharpoons N^+ + \text{"}MCl_3^-\text{"} \qquad (1)$$

Here M can be either Pt or Pd. The titration of a P complex with a N salt would allow us to evaluate the relative affinity of N and P for the same metal.

As successive aliquots of a solution of $(N)(BF_4)$ in CH_2Cl_2 are added to a solution of $(N)_2(M_2Cl_6)$ (Figures 1 and 2, Table I), the NMR chemical shift of the methyl peak varies smoothly from the value of the metal salt toward that of the tetrafluoroborate salt. As only one sharp methyl resonance is observed, exchange between ionic environments is rapid on the NMR time scale at 60 MHz and

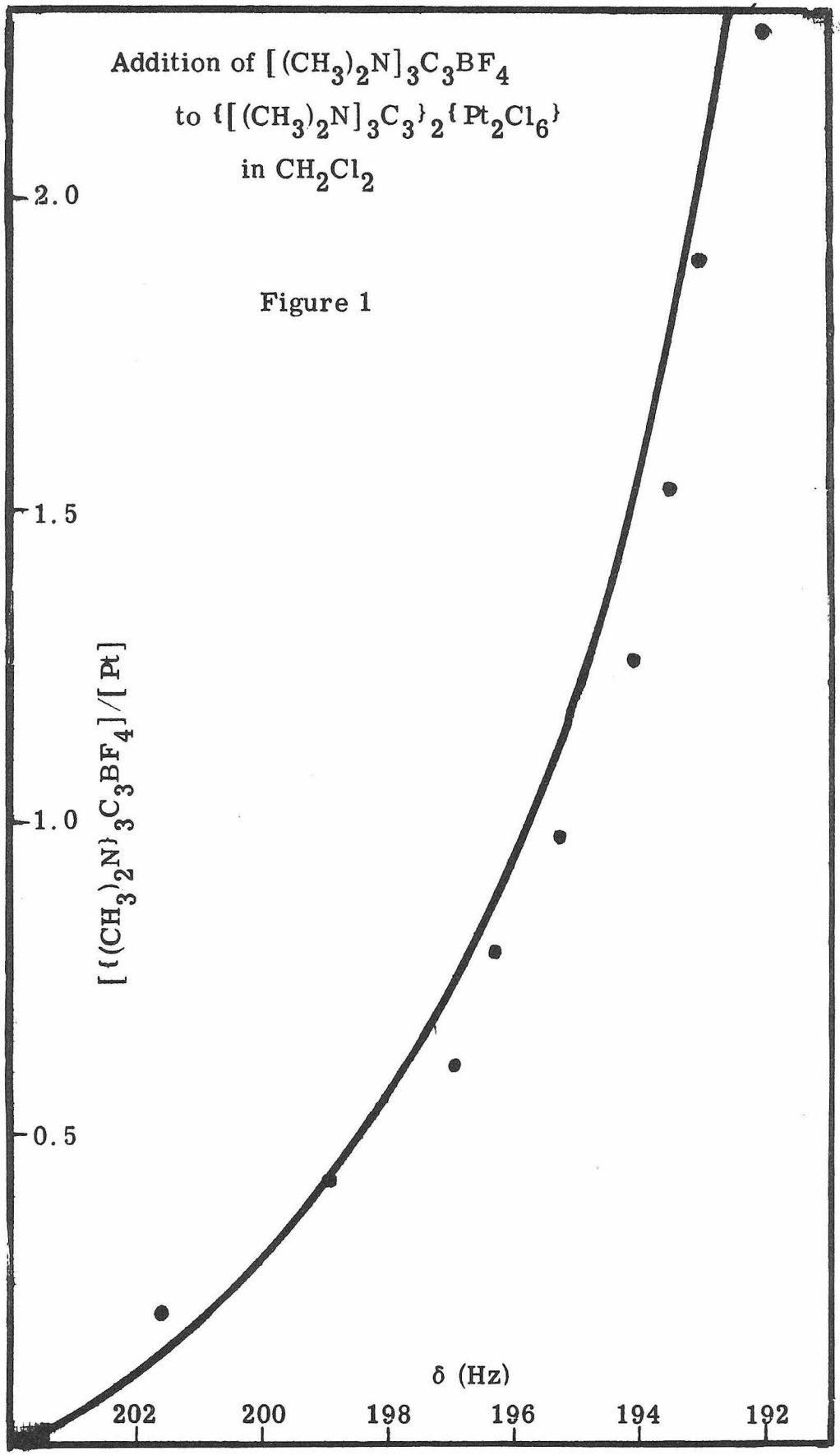
Addition of $[(CH_3)_2N]_3C_3BF_4$
to $\{[(CH_3)_2N]_3C_3\}_2\{Pt_2Cl_6\}$
in CH_2Cl_2
2.0
1.5
1.0
0.5
$[\{(CH_3)_2N\}_3C_3BF_4]/[Pt]$
δ (Hz)
202
200
198
196
194
192

Figure 1

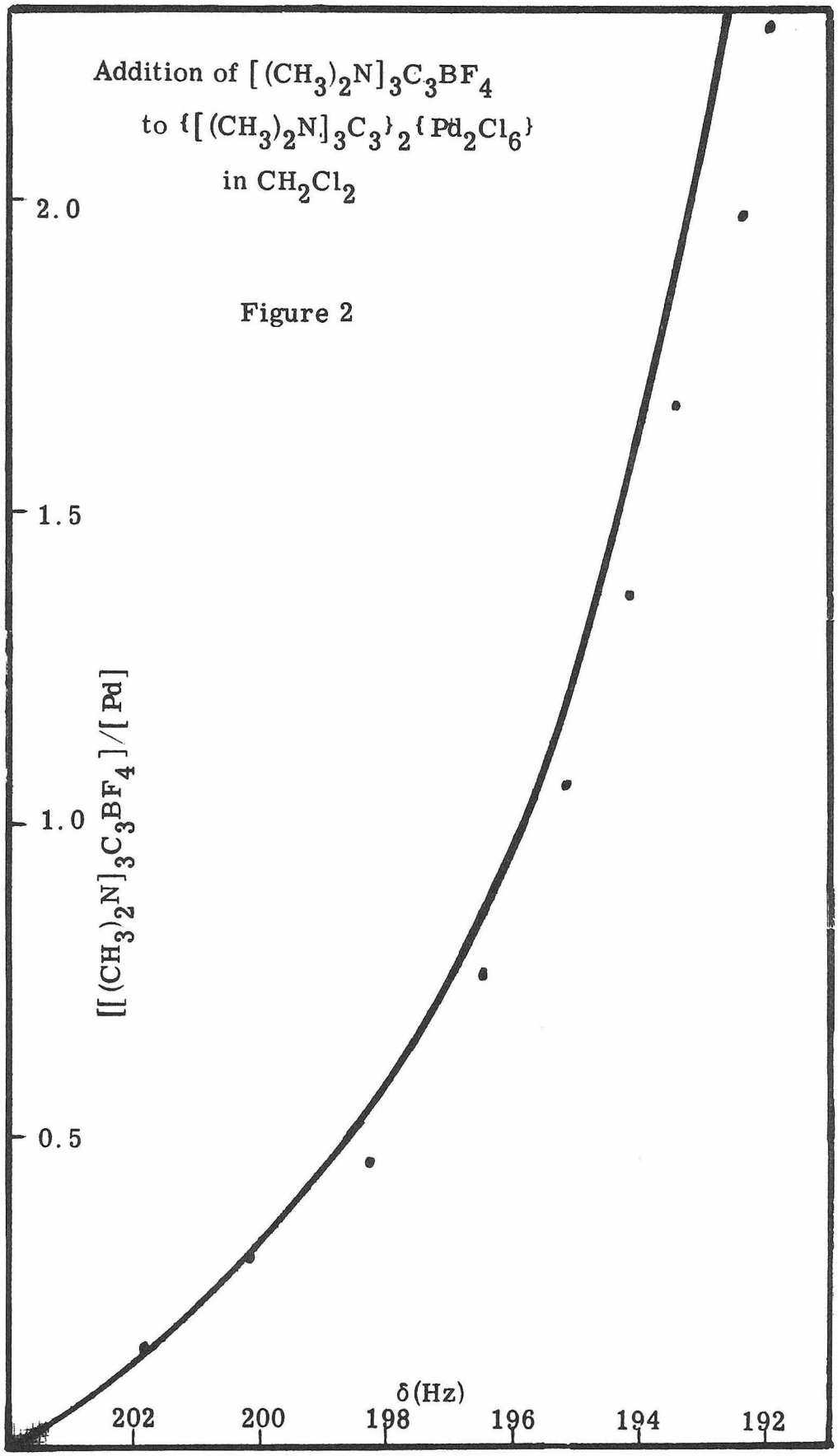
Addition of $[(CH_3)_2N]_3C_3BF_4$
to $\{[(CH_3)_2N]_3C_3\}_2\{Pd_2Cl_6\}$
in CH_2Cl_2
2.0
1.5
1.0
0.5
$[[(CH_3)_2N]_3C_3BF_4]/[Pd]$
δ(Hz)
202
200
198
196
194
192

Figure 2

Table I

Titration of $(N)_2(M_2Cl_6)$ with $(N)(BF_4)$ in CH_2Cl_2[f]

Experiment	μl Titrant Added[b]	Chemical Shift[c]	$[(N)(BF_4)]/[M]$[d]
M = Pt[a]			
A	0	203.82	0
B	23	201.62	0.212
C	23	198.95	0.425
D	20	196.92	0.609
E	20	196.28	0.794
F	20	195.22	0.977
G	30	194.08	1.254
H	30	193.50	1.532
I	40	193.02	1.901
J	40	192.00	2.270
M = Pd[e]			
A	0	204.00	0
B	20	201.80	0.152
C	20	200.12	0.304
D	20	198.20	0.456
E	40	196.48	0.760
F	40	195.10	1.064
G	40	194.12	1.368
H	40	193.40	1.672
I	40	192.35	1.976
J	40	191.96	2.280

[a] 12.10 mg $(N)_2(Pt_2Cl_6)$ in 0.80 ml CH_2Cl_2 + 0.03 ml TMS.

[b] Titrant soln = 60.85 mg $(N)(BF_4) \cdot \frac{1}{2}H_2O$ in 1.00 ml CH_2Cl_2.

[c] Hz downfield of internal TMS

[d] [M] represents the concentration of metal atoms in solution $= 2[M_2Cl_6]$.

[e] 11.92 mg $(N)_2(Pd_2Cl_6)$ in 0.80 ml CH_2Cl_2 + 0.03 μl TMS.

[f] Values in this Table and in Figures 1 and 2 are not corrected for the "true" molecular weight of $(N)(BF_4) \cdot \frac{1}{2}H_2O$ which was not formulated as a hydrate at the time of this experiment. These numbers are based on a molecular weight of 255.1. The correct weight should have been 264.1.

40 °C. The average chemical shift of several samples of the pure tetrafluoroborate was 187.77 (± 0.2) Hz. Using the initial chemical shifts for the metal salts and the anticipated final chemical shift of the tetrafluoroborate, one can calculate the expected chemical shift for any mixture during this titration, if one assumes that the observed chemical shift will be determined by the average of the cyclopropenium cations in the metal and tetrafluoroborate environments.

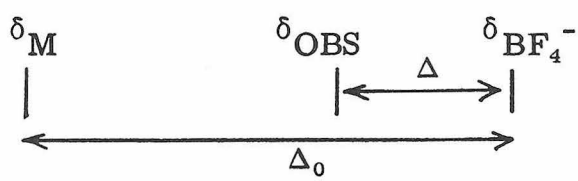

Let δ_M = chemical shift of $[M_2Cl_6^{2-}]$ salt (Hz from TMS)

$\delta_{BF_4^-}$ = chemical shift of $[BF_4^-]$ salt

δ_{OBS} = observed chemical shifts of mixture

Δ_0 = $\delta_M - \delta_{BF_4^-}$

Δ = $\delta_{OBS} - \delta_{BF_4^-}$

Then

$$\alpha \equiv \frac{\Delta}{\Delta_0} = \frac{2[(N)_2(M_2Cl_6)]}{2[(N)_2(M_2Cl_6)] + [(N)(BF_4)]} \qquad (2)$$

The concentration of neutral ion pairs is used in equation (2) (and in all equations below) because free ions will not be important in CH_2Cl_2. The dielectric constant is just too low. Equation (2) allows us to calculate α (and hence δ_{OBS}) and these calculated values are shown by the solid lines in Figures 1 and 2. These calculated values differ by ~0.5 Hz from the observed values in a reasonably

systematic way. This could indicate that the chemical shifts of the two salts are not exactly constant as the solution composition changes and/or that more complex ionic aggregates are formed. Both possibilities are very likely.

The titrations of $(P)_2(M_2Cl_6)$ with $(N)(BF_4)$ in CH_2Cl_2 are described in Table II and a graph for M = Pd is given in Figure 3.

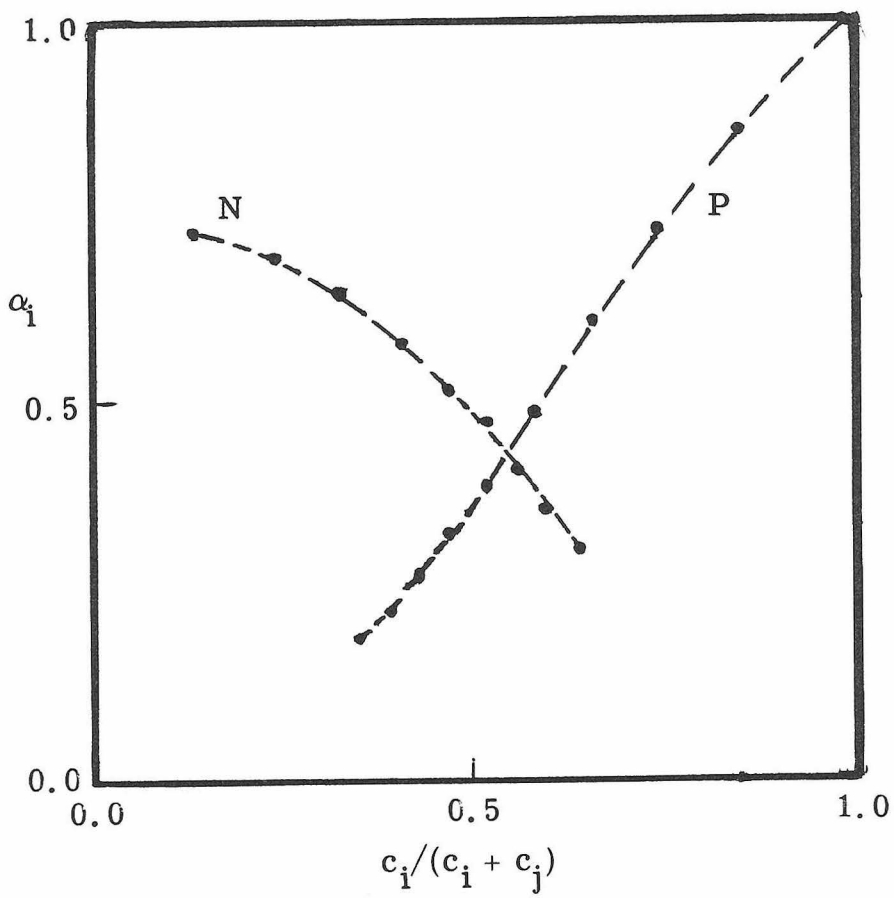

Titration of $[(n\text{-}C_3H_7)_3C_3]_2[Pd_2Cl_6]$ with $\{[(CH_3)_2N]_3C_3\}\{BF_4\}$ in CH_2Cl_2

Figure 3

The lower set of data (M = Pt) in Table II is much less accurate

Table II[a]

Titration of $(P)_2(Pd_2Cl_6)$ with $(N)(BF_4)$ in CH_2Cl_2[b]

Experiment	μℓ(N)(BF₄) added[c]	δ[d] α-CH₂	δ[d] N-CH₃	α[e] α-CH₂	α[e] N-CH₃	M_T[f]	$[(P)_2(M_2Cl_6)]$	$[(P)(BF_4)]$	N_T/M_T	$[(N)_2(M_2Cl_6)]$	$[(N)(BF_4)]$	Total Metal Salt[g]
A	0	16.08	--	1	--	6.45	3.22	0	0	0	0	6.45
B	25	19.42	30.52	0.856	0.722	6.16	2.64	0.82	0.166	0.368	0.28	6.01
C	50	22.45	31.00	0.725	0.692	5.89	2.14	1.62	0.333	0.680	0.60	5.63
D	75	25.15	31.75	0.608	0.645	5.64	1.72	2.21	0.500	0.910	1.00	5.25
E	105	27.98	32.88	0.486	0.577	5.37	1.30	2.77	0.700	1.08	1.59	4.78
F	135	30.20	33.92	0.389	0.514	5.13	1.00	3.13	0.900	1.18	2.25	4.37
G	165	31.70	34.55	0.325	0.476	4.91	0.795	3.31	1.10	1.28	2.83	4.16
H	195	32.95	35.65	0.271	0.409	4.70	0.635	3.43	1.30	1.25	3.61	3.77
I	225	33.98	36.50	0.226	0.357	4.51	0.501	3.49	1.50	1.21	4.35	3.44
J	270	34.83	37.30	0.190	0.308	4.26	0.404	3.45	1.80	1.18	5.31	3.17
					Titration of $(P)_2(Pt_2Cl_6)$ with $(N)(BF_4)$ in CH_2Cl_2[h]							
A	0	11.5	--	1	--	7.24	3.62	0	0	0	0	7.24
B	30	17.5	31.5	0.783	0.661	6.59	2.58	1.43	0.278	0.605	0.620	6.37
C	70	24.5	34	0.531	0.509	5.88	1.56	2.76	0.648	0.970	1.87	5.06
D	100	27.5	35	0.422	0.448	5.44	1.15	3.14	0.926	1.13	2.78	4.56
E	140	30.5	36	0.314	0.388	4.94	0.776	3.39	1.30	1.25	3.92	4.05
F	180	32.5	38	0.242	0.267	4.53	0.548	3.43	1.67	1.01	5.55	3.12
G	220	34	38.5	0.188	0.230	4.18	0.393	3.39	2.04	1.01	6.51	2.81

[a] All concentrations should be multiplied by 10^{-2} to obtain moles/ℓ.

[b] 12.8 mg $(P)_2(Pd_2Cl_6)$ in 0.50 ml CH_2Cl_2 + 0.025 ml TMS.

[c] Titrant solution is 59.6 mg $(N)(BF_4) \cdot \frac{1}{2} H_2O$ in 1.00 ml CH_2Cl_2 in the Pd titration and 53.12 mg in 1.00 ml for the Pt titration.

[d] Hz upfield of high field ^{13}C satellite of CH_2Cl_2.

[e] $\alpha = \Delta/\Delta_o$ (defined in text)

[f] M_T = total concentration of metal atoms = $2[(P)_2(M_2Cl_6)]$ in the initial solutions.

[g] Total Metal Salt = $2\{[(N)_2(M_2Cl_6)] + [(P)_2(M_2Cl_6)]\}$.

[h] 10.14 mg $(P)_2(Pt_2Cl_6)$ in 0.30 ml CH_2Cl_2. δ values in this titration were only determined to ± 0.5 Hz.

than the upper set as the chemical shifts were only measured to the nearest 0.5 Hz. Given that we are dealing with salts, these titrations presumably measure the following equilibrium.

$$(P)_2(M_2Cl_6) + 2(N)(BF_4) \rightleftharpoons (N)_2(M_2Cl_6) + 2(P)(BF_4) \quad (3)$$

$$K = \frac{[(N)_2(M_2Cl_6)][(P)(BF_4)]^2}{[(P)_2(M_2Cl_6)][(N)(BF_4)]^2} \quad (4)$$

The analysis of these data proceeds as follows. Each cation, N and P, has a value of α associated with each point in the titration. Chemical shifts are measured in Hz upfield of the high field ^{13}C CH_2Cl_2 satellite. The values of δ_M and $\delta_{BF_4^-}$ are given below. For the P species, we are measuring the chemical shift of the α-CH_2 protons.

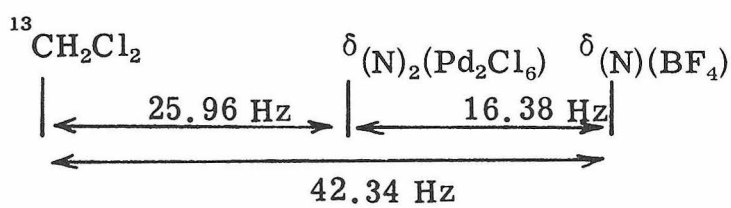

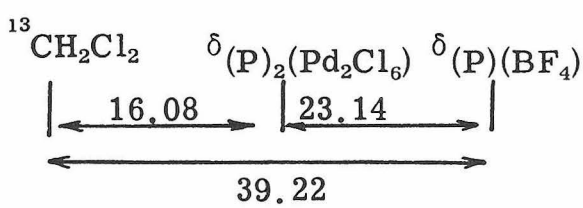

For the Pt titration, $\delta_{(N)_2(Pt_2Cl_6)}$ = 11.5 Hz and $\delta_{(P)_2(Pt_2Cl_6)}$ = 25.85 Hz. We know the total concentration of metal in each solution. We determine α for each cyclopropenium cation ($\alpha = \Delta/\Delta_0$) and various concentrations fall out readily if the chemical shifts depend only on the ratio of the tetrafluoroborate and $M_2Cl_6^{2-}$

associated with each cation.

$$M_T = \text{total concentration of metal atoms} \quad (5)$$

(twice the initial dimer concentration)

$$[(P)_2(M_2Cl_6)] = \tfrac{1}{2}\,\alpha_P M_T \quad (6)$$

$$[(P)(BF_4)] = (1 - \alpha_P)\, M_T \quad (7)$$

$$N_T = \text{total concentration of added N salt} \quad (8)$$

$$[(N)_2(M_2Cl_6)] = \tfrac{1}{2}\,\alpha_N N_T \quad (9)$$

$$[(N)(BF_4)] = (1 - \alpha_N)\, N_T \quad (10)$$

In Figure 3 we plot α_N and α_P vs. the fraction of total cyclopropenium cations in solution represented by N or P. For example, the line labeled N is a plot of α_N vs. $N_T/(N_T + P_T)$ where $P_T(= M_T)$ = total concentration of P. If the equilibrium in equation (3) were unity, we would observe two perpendicular straight lines with slopes of +1 and -1 which cross at the center of the graph. In fact, the two curves are not linear and do not cross at the center of the graph. The equilibrium constant defined by equation (4) is generally near 2 (see Table II). This would indicate that N has a greater affinity for $Pd_2Cl_6^{2-}$ than does P. The $Pt_2Cl_6^{2-}$ titration gives values of K closer to unity. There is a major problem with these calculations, however. The column in Table II labeled "Total Metal Salt" is twice the sum of the calculated values of $[(P)_2(M_2Cl_6)]$ and $[(N)_2(M_2Cl_6)]$. This should equal the known value of M_T in column seven, but it does not. This indicates that the chemical shift behavior is not as simple as I am. For example, species like $(P)(N)(M_2Cl_6)$ will foul this scheme. This experiment was a good idea for a π-complex but a lousy idea for a piddling salt.

In support of the idea that no change in the metal chromophore should occur during these titrations, spectrophotometric examination of these solutions (~ 330-600 nm) shows little or no change in the spectrum as the ratio [N]/[Pd] varies from 1-20 and the ratio [N]/[Pt] varies from 1 to 52.

Reaction with Chloride

Undaunted by these results, we proceed to examine the reaction of $M_2Cl_6^{2-}$ with Cl^-. When a solution of $(N)_2(M_2Cl_6)$ is treated with $(n\text{-}C_4H_9)_4NCl$ in CH_2Cl_2 the chemical shift of the cyclopropenium protons varies smoothly with the amount of added $(n\text{-}C_4H_9)_4NCl$ (Figures 4 and 5). This chemical equilibrium is established rapidly as there is no significant change in the NMR spectrum of a solution in 30 minutes. This is contrary to reactions of the Pt salts with CH_3CN or cyclooctene which are much slower. It seemed reasonable that reaction (11)should be occurring in these solutions.

$$M_2Cl_6^{2-} + 2Cl^- \rightleftharpoons 2MCl_4^{2-} \qquad (11a)$$

$$R + 2C \rightleftharpoons 2P \qquad (11b)$$

$$K_{11} = [P]^2/[R][C]^2 \qquad (11c)$$

Here we have rewritten equation (11a) in the abbreviated form (11b). Subsequent analysis of these titration data did not support reaction (11), so we formulated reaction (12) as another reasonable possibility.

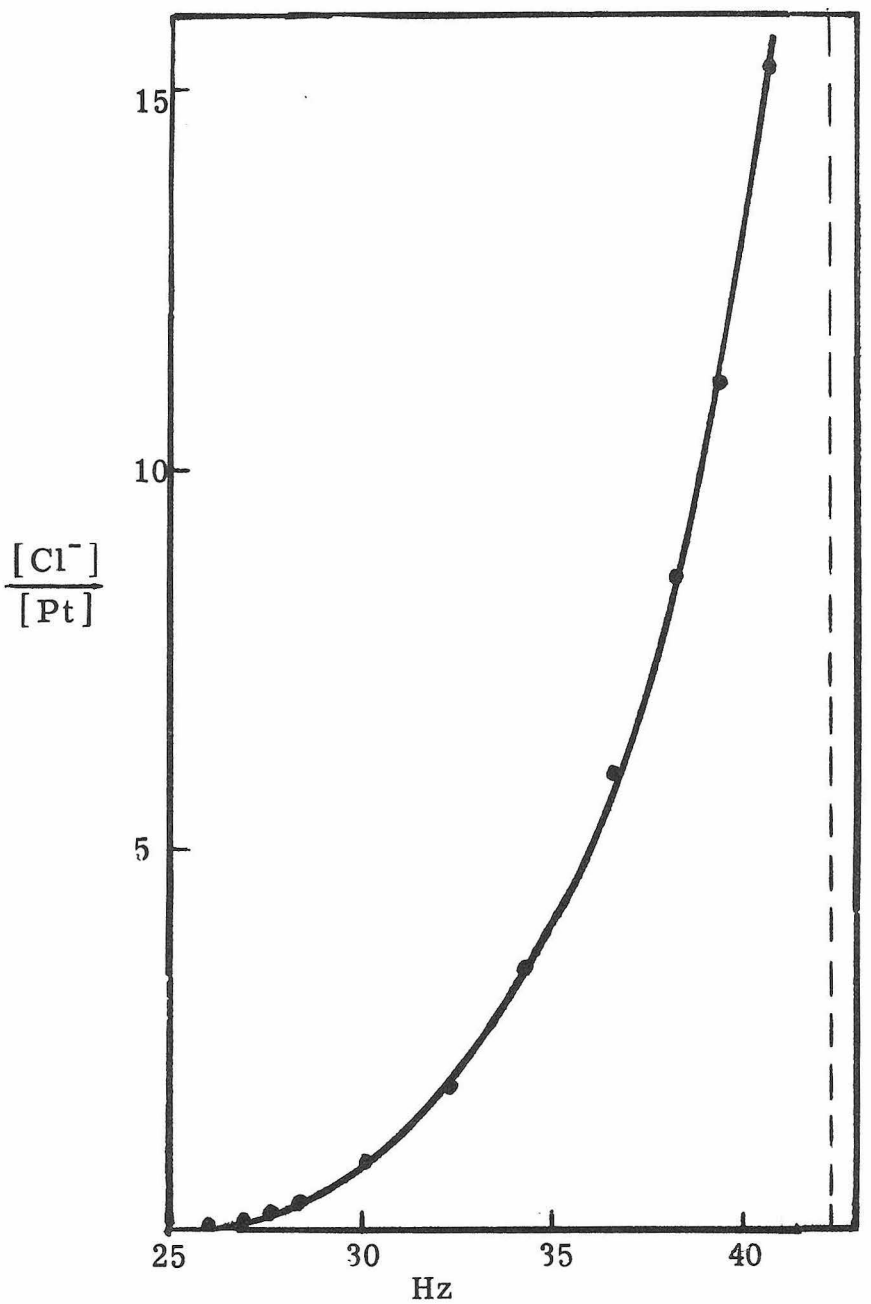

Titration of $\{[(CH_3)_2N]_3C_3\}_2\{Pt_2Cl_6\}$
with $(n\text{-}C_4H_9)_4NCl$ in CH_2Cl_2
Figure 4

$$M_2Cl_6^{2-} + Cl^- \rightleftharpoons \begin{array}{c} Cl \\ | \\ Cl-M-Cl \\ | \\ Cl \end{array} \begin{array}{c} Cl \\ | \\ -M-Cl^{3-} \\ | \\ Cl \end{array} \qquad (12a)$$

$$R + C' \rightleftharpoons P' \qquad (12b)$$

$$K_{12} = [P']/[R][C'] \qquad (12c)$$

In order to extract equilibrium constants from the titration, it is necessary to find the "final" chemical shift value of the cyclopropenium protons when the reaction is complete. Figure 6 shows the variation of the ^1H chemical shift of $(N)(BF_4)$ vs. added $(n\text{-}C_4H_9)_4NCl$ in CH_2Cl_2. We find a variation of about 1 Hz over the first 15 equivalents of added tetrabutylammonium chloride. This gives us an approximate idea of the inherent variation expected for the "final" chemical shift value in our titration. The chemical shift of $(N)(BF_4)$ in CH_2Cl_2 solution is shown with a dotted line in Figures 4 and 5. As this "eyeballs" as a reasonable asymptote of the titration curves, we arbitrarily adopt this as the limiting chemical shift.

The analysis proceeds as follows. For reaction (11),

$$[R] = \tfrac{1}{2}\alpha M_T \qquad (13)$$

$$[P] = (1 - \alpha) M_T \qquad (14)$$

$$[C] = C_T - [P] \qquad (15)$$

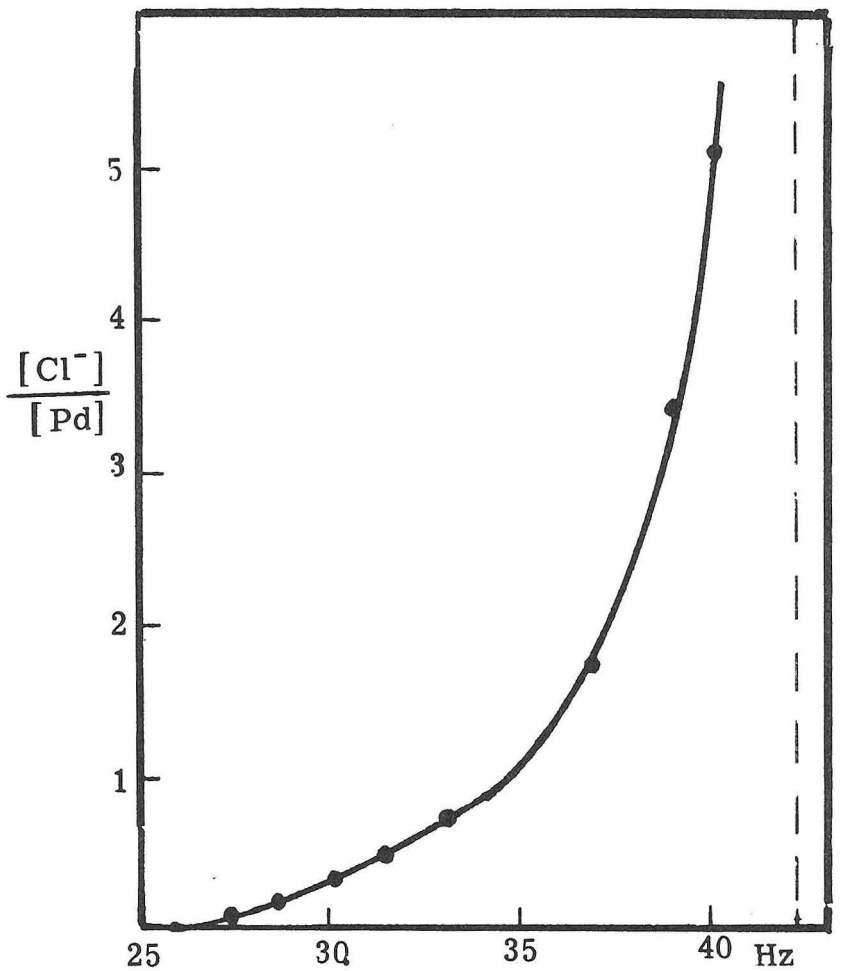

Titration of $\{[(CH_3)_2N]_3C_3\}_2\{Pd_2Cl_6\}$ with $(n\text{-}C_4H_9)_4NCl$ in CH_2Cl_2

Figure 5

Here C_T is the total concentration of added chloride species in solution. For reaction (12),

$$[R] = \tfrac{1}{2}\alpha M_T \tag{16}$$

$$[P'] = \tfrac{1}{2}(1 - \alpha) M_T \tag{17}$$

$$[C'] = C_T - [P'] \tag{18}$$

The analysis of these titrations is given in Table III. Calculations were not made for low values of α because there can be serious errors in α in the region near the poorly defined "final" chemical

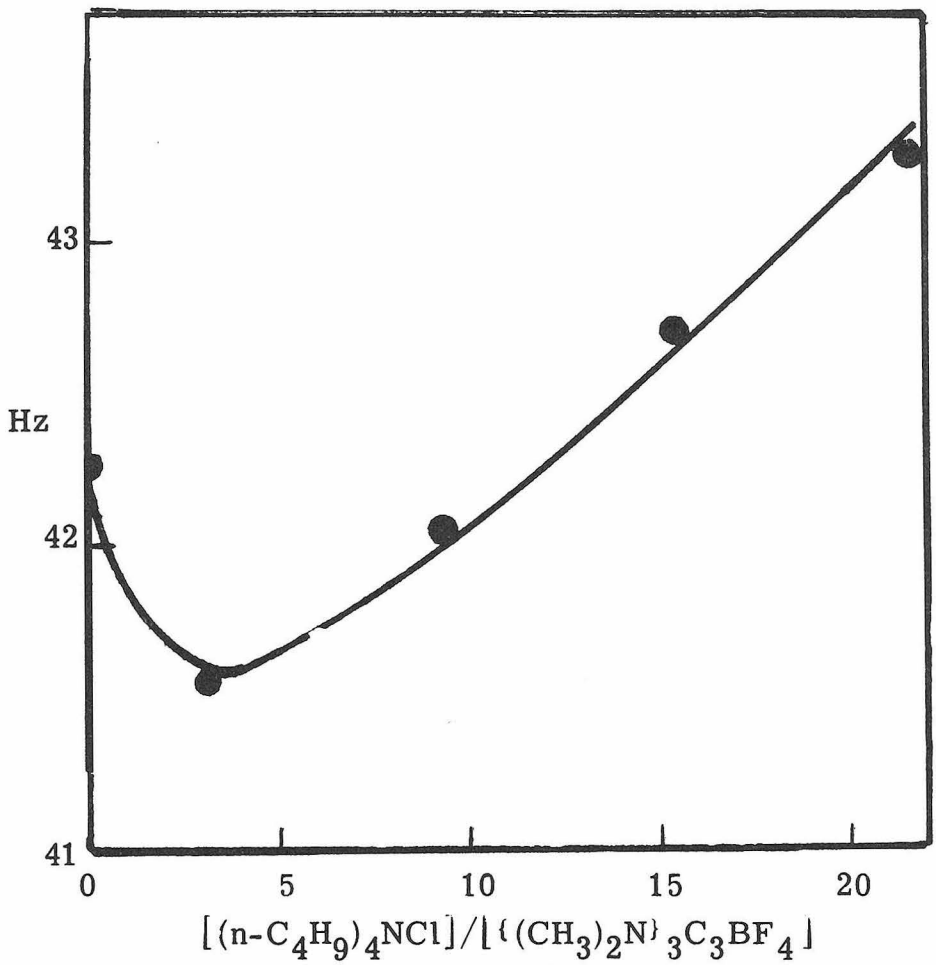

Figure 6

Table III[a]

Titration of $(N)_2(Pt_2Cl_6)$ with $(N\text{-}C_4H_9)_4NCl$ in CH_2Cl_2[c]

Experiment	Total Sample Volume (ml)	$\frac{[Cl]}{M_T}$	δ (Hz)	α	M_T	[R]	[P]	[C]	[P′]	[C′]	K_{11}[b]	K_{12}[b]
A	0.430	0	25.85	1	3.09	-	-	-	-	-	-	-
B	0.445	0.077	26.82	0.917	2.98	-	-	-	-	-	-	-
C	0.470	0.206	27.49	0.901	2.83	1.27	0.281	0.301	0.141	0.441	68.5	25.1
D	0.495	0.334	28.28	0.853	2.68	1.14	0.368	0.530	0.197	0.701	42.1	24.5
E	0.505	0.849	30.08	0.744	2.63	0.978	0.674	1.56	0.338	1.89	19.1	18.2
F	0.525	1.88	32.28	0.610	2.53	0.772	0.987	3.76	0.493	4.26	8.91	15.0
G	0.555	3.42	34.33	0.486	2.40	0.582	1.23	6.96	0.616	7.58	5.37	14.0
H	0.605	5.99	36.62	0.347	2.20	0.381	1.43	11.7	0.717	12.4	3.93	15.1
I	0.655	8.56	38.25	0.248	2.03	-	-	-	-	-	-	-
J	0.705	11.1	39.38	0.179	1.88	-	-	-	-	-	-	-
K	0.805	16.3	40.63	0.104	1.65	-	-	-	-	-	-	-
Titration of $(N)_2(Pd_2Cl_6)$ with $(n\text{-}C_4H_9)_4NCl$ in CH_2Cl_2[d]												
A	0.425	0	25.98	1	4.78	-	-	-	-	-	-	-
B	0.445	0.067	27.44	0.911	4.56	-	-	-	-	-	-	-
C	0.475	0.168	28.69	0.834	4.28	-	-	-	-	-	-	-
D	0.515	0.303	30.15	0.745	3.94	1.47	1.00	0.189	0.503	0.691	1920	49.6
E	0.565	0.471	31.44	0.666	3.59	1.20	1.20	0.493	0.600	1.09	248	45.6
F	0.635	0.707	33.12	0.564	3.20	0.900	1.40	0.865	0.698	1.56	289	49.7
G	0.665	1.72	36.93	0.331	3.05	0.505	2.04	3.20	1.02	4.22	80.7	47.9
H	0.715	3.40	38.97	0.206	2.84	-	-	-	-	-	-	-
I	0.765	5.09	40.08	0.138	2.65	-	-	-	-	-	-	-
Titration of $(P)_2(Pd_2Cl_6)$ with $(n\text{-}C_4H_9)_4NCl$ in CH_2Cl_2[e]												
A	0.425	0	15.70	1	-	-	-	-	-	-	-	-
B	0.445	0.086	15.50	-	-	-	-	-	-	-	-	-
C	0.485	0.259	14.88	-	-	-	-	-	-	-	-	-
D	0.525	1.98	16.88	0.95	3.02	1.4	0.15	5.8	0.076	5.9	0.047	0.89
E	0.575	4.14	~21	0.78	2.75	1.1	0.62	1.1	0.31	11	0.31	2.6

[a] All concentrations should be multiplied by 10^{-2} to obtain units of moles/l. Any quantities depending on $[(n\text{-}C_4H_9)_4NCl]$ are known only to two significant figures though three figures are retained for the sake of calculation.

[b] 1 $mole^{-1}$.

[c] 6.24 mg $(N)_2(Pt_2Cl_6)$ in 0.40 ml CH_2Cl_2 + 0.030 ml TMS.

[d] 7.73 mg $(N)_2(Pd_2Cl_6)$ in 0.40 ml CH_2Cl_2 + 0.025 ml TMS.

[e] 5.99 mg $(P)_2(Pd_2Cl_6)$ in 0.40 ml CH_2Cl_2 + 0.025 ml TMS. This titration is very crude as the α-CH_2 signal of $(n\text{-}C_4H_9)_4NCl$ is very close to the α-CH_2 proton signal of the cyclopropenium cation. By experiment E, these are overlapping.

shift. The data for the two titrations of $(N)_2(M_2Cl_6)$ salts do not support reaction (11) but are in reasonable accord with reaction (12) when the constants K_{11} and K_{12} are calculated. A titration of $(P)_2(Pd_2Cl_6)$ is also shown in Figure 7 and Table III. The

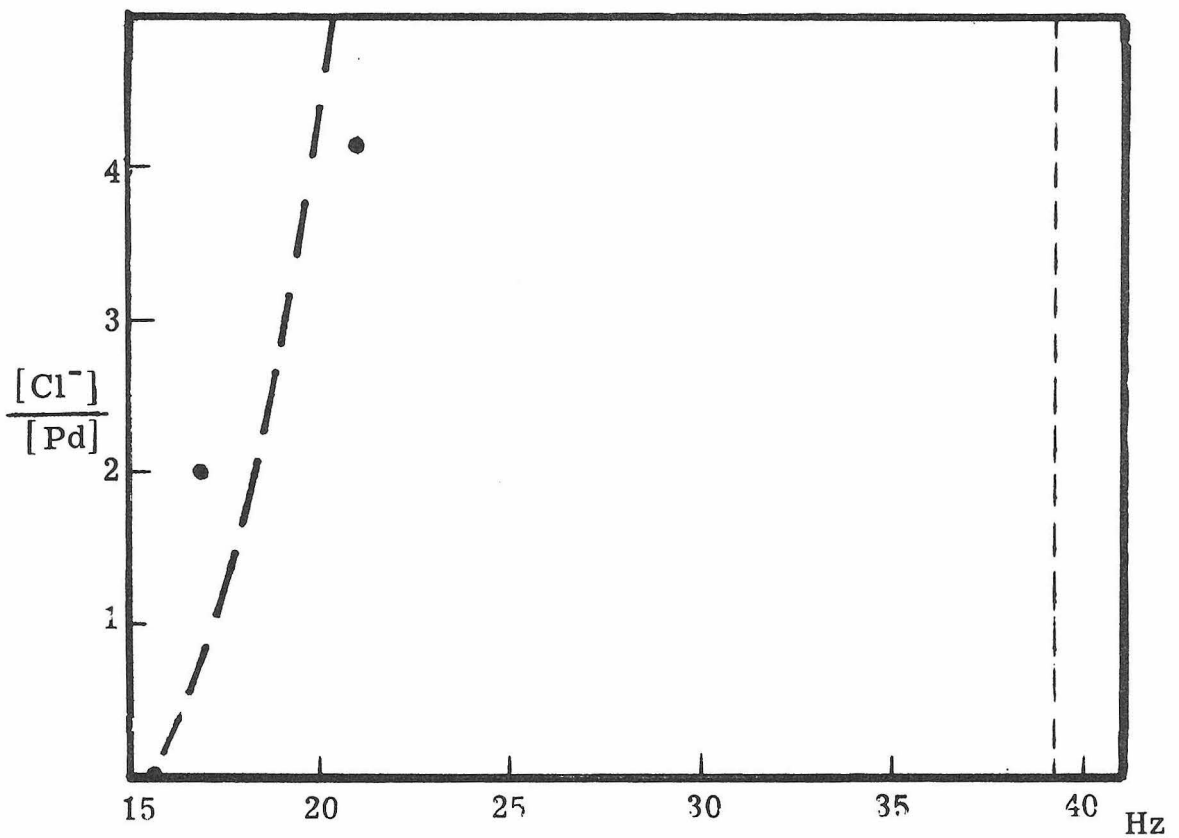

Titration of $[(n\text{-}C_3H_7)_3C_3]_2[Pd_2Cl_6]$
with $(n\text{-}C_4H_9)_4NCl$ in CH_2Cl_2
Figure 7

dotted line in Figure 7 is the chemical shift of $(P)(BF_4)$. This titration is of very poor quality because the α-CH_2 proton signals of P and of $(n\text{-}C_4H_9)_4NCl$ nearly overlap. We make no quantitative statements about this titration but state, rather, that for a given

ratio of added $(n\text{-}C_4H_9)NCl$ to metal, the P reaction proceeds very much less than the N reaction. This cation dependence of the reactivity of these $M_2Cl_6^{2-}$ salts is further illustrated and discussed later in this section.

Before examining other evidence concerning the products in our reactions, we wish to discuss the validity of using the change in chemical shifts to evaluate equilibrium constants. Several other salts of P and N were synthesized during the course of this work and their chemical shifts are given in Table IV. The chemical shift of (N)(Cl) is 3.19 ppm in CH_2Cl_2, close to the value of 3.14 ppm for $(N)(BF_4)$ and well upfield of the 3.39 ppm shift of $(N)_2(Pt_2Cl_6)$ and the 3.41 ppm shift of $(N)_2(Pd_2Cl_6)$. If the exchange (19) were occurring purely statistically, we would expect the observed chemical shift in the $Pt_2Cl_6^{2-}$ titration to move upfield more rapidly than it does.

$$(N)_2(M_2Cl_6) + 2[(n\text{-}C_4H_9)_4N][Cl] \rightleftharpoons [(n\text{-}C_4H_9)_4N]_2[M_2Cl_6] + 2(N)(Cl) \qquad (19)$$

On the other hand, reaction (19) could explain the $(N)_2(Pd_2Cl_6)$ titration reasonably well if no other reaction (such as 12) were even occurring. Chemical shifts, therefore, are a singularly miserable property to use for these titrations. Any discussion of the data in Table III must assume the absence of reactions such as (19) and this is probably not reasonable.

As an interesting tangent to this meandering discussion, if the reaction (19) is not occurring and if reaction (12) is really what is going on, the chemical shift of starting material, $(N)_2(M_2Cl_6)$ is

Table IV

NMR Measurements

Compound	Solvent	Chemical Shift (ppm downfield of internal TMS)		
		α-CH_2	β-CH_2	CH_3
$[(n\text{-}C_3H_7)_3C_3][BF_4]$ [a]	$(CD_3)_2CO$	3.32	b	1.08
	CH_2Cl_2	3.15	1.92	1.08
	CH_3CN	3.16	1.90	1.06
	$CHCl_3$	3.16	1.92	1.07
$[(n\text{-}C_3H_7)_3C_3][Br]$ [a,g]	$CHCl_3$	3.26	1.90	1.03
$[(n\text{-}C_3H_7)_3C_3]_2[Pt_2Cl_6]$ [a,d]	$(CD_3)_2CO$	3.67	2.18	1.16
	CH_2Cl_2	3.67	2.15	1.16
$[(n\text{-}C_3H_7)_3C_3]_2[Pd_2Cl_6]$ [a]	$(CH_3)_2CO$	3.65	b	1.17
	CH_2Cl_2	3.58	2.15	1.19
$\{[(CH_3)_2N]_3C_3\}\{BF_4\}$ [c]	$(CD_3)_2CO$			3.20
	CH_2Cl_2			3.14
	$(CD_3)_2SO$ [e]			3.07
	$CHCl_3$ [f]			ca. 3.1
$\{[(CH_3)_2N]_3C_3\}\{Cl\}$ [c,h]	CH_2Cl_2			3.19
$\{[(CH_3)_2N]_3C_3\}\{B(C_6H_5)_4\}$ [c]	CH_2Cl_2 [i]			2.92
	$(CH_3)_2CO$			3.03
$\{[(CH_3)_2N]_3C_3\}_2\{PtCl_4\}$ [c]	CH_2Cl_2			3.25
$\{[(CH_3)_2N]_3C_3\}_2\{Pt_2Cl_6\}$ [c,d]	CH_2Cl_2			3.39
	$(CD_3)_2SO$			3.07
$\{[(CH_3)_2N]_3C_3\}_2\{Pd_2Cl_6\}$ [c]	CH_2Cl_2			3.41

[a] All $[(n\text{-}C_3H_7)_3C_3]$ salts showed a triplet-sextet-triplet pattern for the α-CH_2, β-CH_2, and CH_3 peaks, respectively. All coupling constants are ca. 7.5 Hz.

[b] Under solvent peak.

[c] All $\{[(CH_3)_2N]_3C_3\}$ salts show a single CH_3 absorption.

[d] Examination of the NMR spectrum at 31°, 13°, -36°, and -62° showed no changes except for decrease of the signal due to sample crystallization.

[e] $J_{^{13}C-^1H}$ = 139 Hz.

[f] All samples in this table gave sharp absorption signals except this solution. For this solvent, $\omega_{1/2} \approx 65$ Hz. This is not due to impure compound since the same material in other solvents gave sharp signals.

[g] Chemical shifts for this salt were based on an assumed value of 7.27 ppm for the shifts of solvent $CHCl_3$.

[h] $J_{^{13}C-^1H}$ = 141 Hz.

[i] Phenyl multiplet occurs at δ 6.9 - 7.5 ppm. Area (CH_3)/Area (C_6H_5) = 1.13 (calculated ratio is 1.11).

that much more interesting. In Table IV we see that the chemical shifts of the tetrafluoroborate, chloride, tetrachloroplatinate, and tetraphenylborate salts of N are all 0.2-0.5 ppm upfield of the $M_2Cl_6^{2-}$ salts. This suggests that there may be some form of "ring current" in the

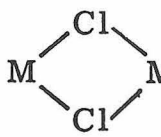

M unit which deshields the N cation. Since the chemical shift of the "$Cl_3M-Cl-M-Cl_3^{3-}$ salt" is near that of the tetrafluoroborate, this "ring current" is not operative in the linearly bridged species. Just an idea I thought I'd throw out.

It was very surprising, to say the least, that these titration data were not in accord with equation (11). Henry and Marks[1] examined the equilibrium between $Li_2Pd_2Cl_6$ and LiCl in acetic acid.[2] Among the models (20), (21), and (22), only (20) is in accord with their spectrophotometric data. K_{20} was found to be 0.1 M^{-1} at 25°.

$$Li_2Pd_2Cl_6 + 2LiCl \overset{K_{20}}{\rightleftharpoons} 2Li_2PdCl_4 \qquad (20)$$

$$LiPdCl_3 + LiCl \overset{K_{21}}{\rightleftharpoons} Li_2PdCl_4 \qquad (21)$$

$$Li_2Pd_2Cl_6 + LiCl \overset{K_{22}}{\rightleftharpoons} Li_2Pd_2Cl_7 \qquad (22)$$

Equation (22) is analogous to equation (12) which seems to describe our systems. Teggins, et al.[3] obtained evidence for the existence of $Pt_2Br_6^{2-}$ in equilibrium with $PtBr_4^{2-}$ in aqueous solution. These authors also postulate the species I to explain some of their observations. One should bear in mind that Br^- is a much better

bridging ligand than Cl^-.

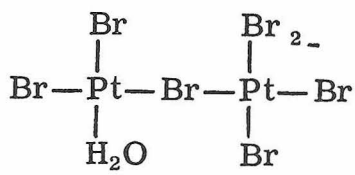

I

Since the chemical shift evidence is poor and ambiguous, at best, we sought qualitative IR evidence concerning the reaction product. These results are given in Table V. The IR spectrum of $(N)_2(Pt_2Cl_6)$ in CH_2Cl_2 in both CsI and AgCl cells[4] shows two bands in the region 360-300 cm^{-1} at 341 and 315 cm^{-1}. In Figure 8 we see that the spectrum of a CH_2Cl_2 solution of $(N)_2(Pt_2Cl_6)$ containing a large excess (approximately saturated) of $(n\text{-}C_4H_9)_4NCl$ shows just one broad band at ~ 322 cm^{-1}. For comparison, a spectrum of authentic $(N)_2(PtCl_4)$ (KBr pellet) shows one fairly sharp band at 315 cm^{-1}. The spectrum of $[(n\text{-}C_4H_9)_4N]_2[PtCl_4]$[6] in $CHCl_3$ solution (Figure 9) shows one sharp band at 316 cm^{-1}. Similarly, the spectrum of $(N)_2(Pd_2Cl_6)$ with a large excess of $(n\text{-}C_4H_9)_4NCl$ shows one broad absorption at 321 cm^{-1} (and a weak, perhaps insignificant band at 300 cm^{-1}). We feel that these data are consistent with the formation of MCl_4^{2-} (reaction (11)) and not with the formation of $Cl_3M\text{-}Cl\text{-}MCl_3^{3-}$. The $M_2Cl_7^{3-}$ species would be expected to show terminal M-Cl stretching at a frequency 10-30 cm^{-1} higher than ~ 320 cm^{-1} as well as a bridging M-Cl-M stretch in or below the region of the spectrum examined. The observation of a single

Table V

IR Spectra (360-300 cm^{-1})

Sample	Solvent	Cell	Absorptions (cm^{-1})
$(N)_2(Pt_2Cl_6)$	CH_2Cl_2	CsI or AgCl	341, 315
$(N)_2(Pt_2Cl_6)$ + excess $(n\text{-}C_4H_9)_4NCl$	CH_2Cl_2	AgCl	~ 322 br
$(N)_2(PtCl_4)$	KBr pellet	--	315
$(N)_2(Pd_2Cl_6)$ + excess $(n\text{-}C_4H_9)_4NCl$	CH_2Cl_2	AgCl	~ 321 br, 300 w
$(P)_2(Pt_2Cl_6)$	$CHCl_3$	polyethylene	344, 313
$(P)_2(Pt_2Cl_6)$ + excess $(n\text{-}C_4H_9)_4NCl$	$CHCl_3$	polyethylene	339, ~ 313 sh
$[(n\text{-}C_4H_9)_4N]_2[PtCl_4]$	$CHCl_3$	polyethylene	316
$[(n\text{-}C_4H_9)_4N]_2[PtCl_4]$ + excess $(n\text{-}C_4H_9)_4NCl$	$CHCl_3$	polyethylene	314

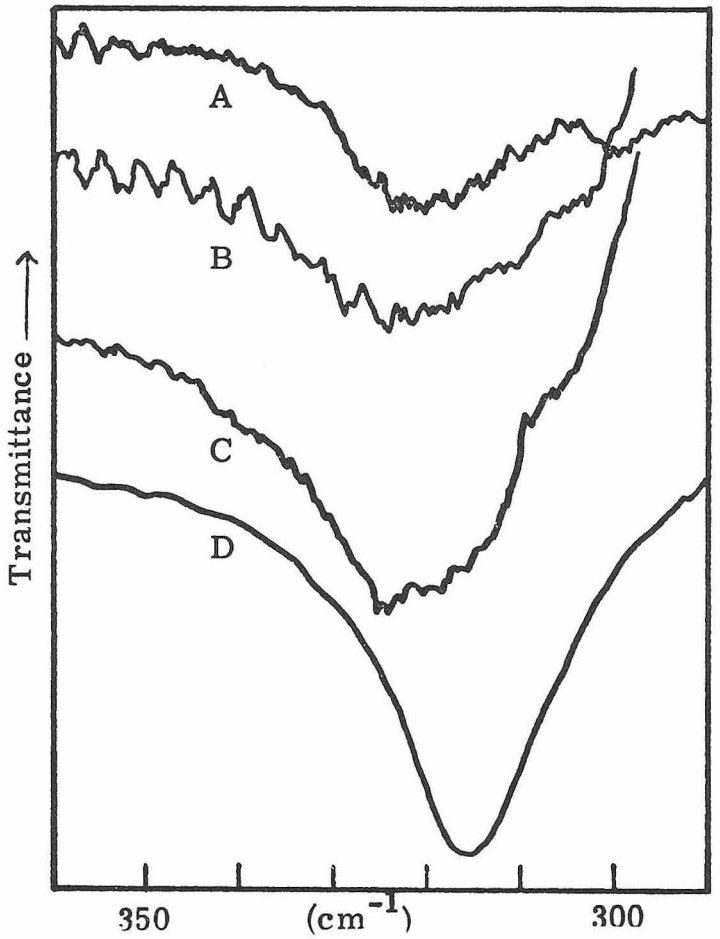

A. $(N)_2(Pd_2Cl_6)$ plus excess $(n\text{-}C_4H_9)_4NCl$ in CH_2Cl_2

B. $(N)_2(Pt_2Cl_6)$ plus excess $(n\text{-}C_4H_9)_4NCl$ in CH_2Cl_2

C. different sample with same components as B

D. solid $(N)_2(PtCl_4)$ in KBr pellet

Figure 8

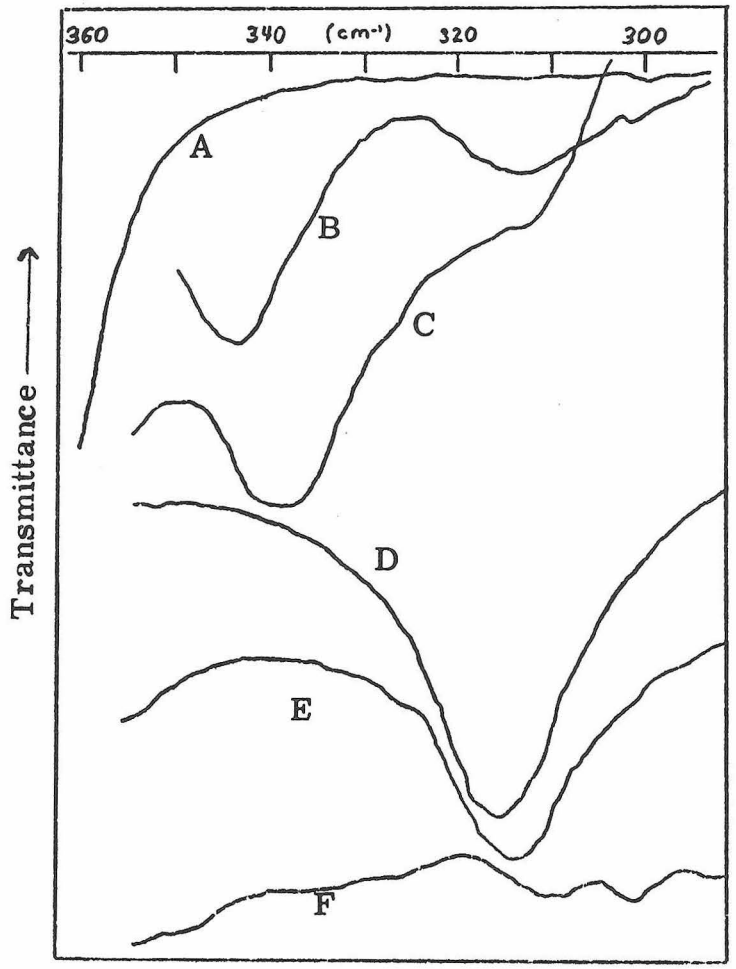

A. Chloroform in polyethylene cell

B. $(P)_2(Pt_2Cl_6)$ in $CHCl_3$

C. $(P)_2(Pt_2Cl_6)$ plus excess $(n\text{-}C_4H_9)_4NCl$ in $CHCl_3$

D. $[(n\text{-}C_4H_9)_4N]_2[PtCl_4]$ in $CHCl_3$

E. $[(n\text{-}C_4H_9)_4N]_2[PtCl_4]$ plus excess $(n\text{-}C_4H_9)_4NCl$ in $CHCl_3$

F. $(n\text{-}C_4H_9)_4NCl$ in $CHCl_3$

Figure 9

band near 320 cm^{-1} in these solutions is consistent with the formation of MCl_4^{2-}.

On the other hand, the spectrum of $(P)_2(Pt_2Cl_6)$ is nearly unchanged by the addition of a large excess of $(n\text{-}C_4H_9)_4NCl$ in $CHCl_3$ solution (Figure 9). This agrees with the NMR titration, Figure 7, which shows little effect of $(n\text{-}C_4H_9)_4NCl$ on $(P)_2(Pd_2Cl_6)$ in CH_2Cl_2 compared to $(N)_2(Pd_2Cl_6)$ (Figure 5). We feel that this is a real, marked cation dependence of these reactions. Whether reaction (11) or (12) is occurring (we favor (11)), <u>the P cation markedly reduces the equilibrium constant</u>.

To make matters worse, we examined the change in the visible spectrum of $(N)_2(Pt_2Cl_6)$ upon addition of $(n\text{-}C_4H_9)_4NCl$ in CH_2Cl_2. The spectrum of pure $(N)_2(PtCl_4)$ in CH_2Cl_2 shows bands at 20,000 (ϵ = 16.9) and 24,770 cm^{-1} (ϵ = 53.2). The spectrum of $(N)_2(Pt_2Cl_6)$ shows bands at 19,600 (ϵ = 28.7 per Pt) and 25,100 (ϵ = 76.6 per Pt). Addition of 1.94 and 4.86 equivalents of $(n\text{-}C_4H_9)_4NCl$ to $(N)_2(Pt_2Cl_6)$ causes a slight ($\lesssim$ 10%) <u>increase</u> in absorption of the two bands. If $PtCl_4^{2-}$ were formed, we would expect a decrease of these bands. The concentrations involved are $M_T = 1.83 \times 10^{-3}M$, $(n\text{-}C_4H_9)_4NCl = 0$, 3.54×10^{-3} and $8.88 \times 10^{-3}M$. Without knowledge of the equilibrium constant we cannot say how great α should be. But the direction of change of the spectrum is <u>not</u> in accord with reaction (11). This experiment deserves a careful repetition if one is to study the equilibrium with chloride.

In summary, NMR chemical shifts are in accord with reaction (12) but are subject to many effects that render their significance questionable. The qualitative change of the IR spectra do not agree with equation (12) and could agree with equation (11). The changes in the visible spectra do not support reaction (11).

Reaction with Cyclooctene

Hardly fazed by these results, we now examine a more interesting reaction of these $M_2Cl_6^{2-}$ salts with the olefin cyclooctene. In two separate experiments, the titration of $(N)_2(Pd_2Cl_6)$ with cyclooctene in CH_2Cl_2 produced a smooth change in the chemical shift of the N protons (Figure 10). The chemical shift asymptotically approaches a value estimated as 35.60 Hz upfield of the high field ^{13}C solvent satellite. Analysis of these data in Table VI gives us an equilibrium constant of 0.7 for reaction (23) at 40 °C.

$$(N)_2(Pd_2Cl_6) + 2C_8H_{14} \overset{K_{23}}{\rightleftharpoons} 2[N][(C_8H_{14})PdCl_3] \qquad (23a)$$

$$R + 2C_8 \rightleftharpoons 2\,P \qquad (23b)$$

$$K_{23} = [P]^2/[R][C_8]^2 \qquad (23c)$$

When this same reaction is carried out spectrophotometrically, we find $K_{23} \approx 3$ at 21 °C. (Table VII and Figure 11.) The agreement between the spectrophotometric titration and the NMR titration shows that chemical shifts can be a reliable function of the extent of reaction if no complications from ion pairing are operating.

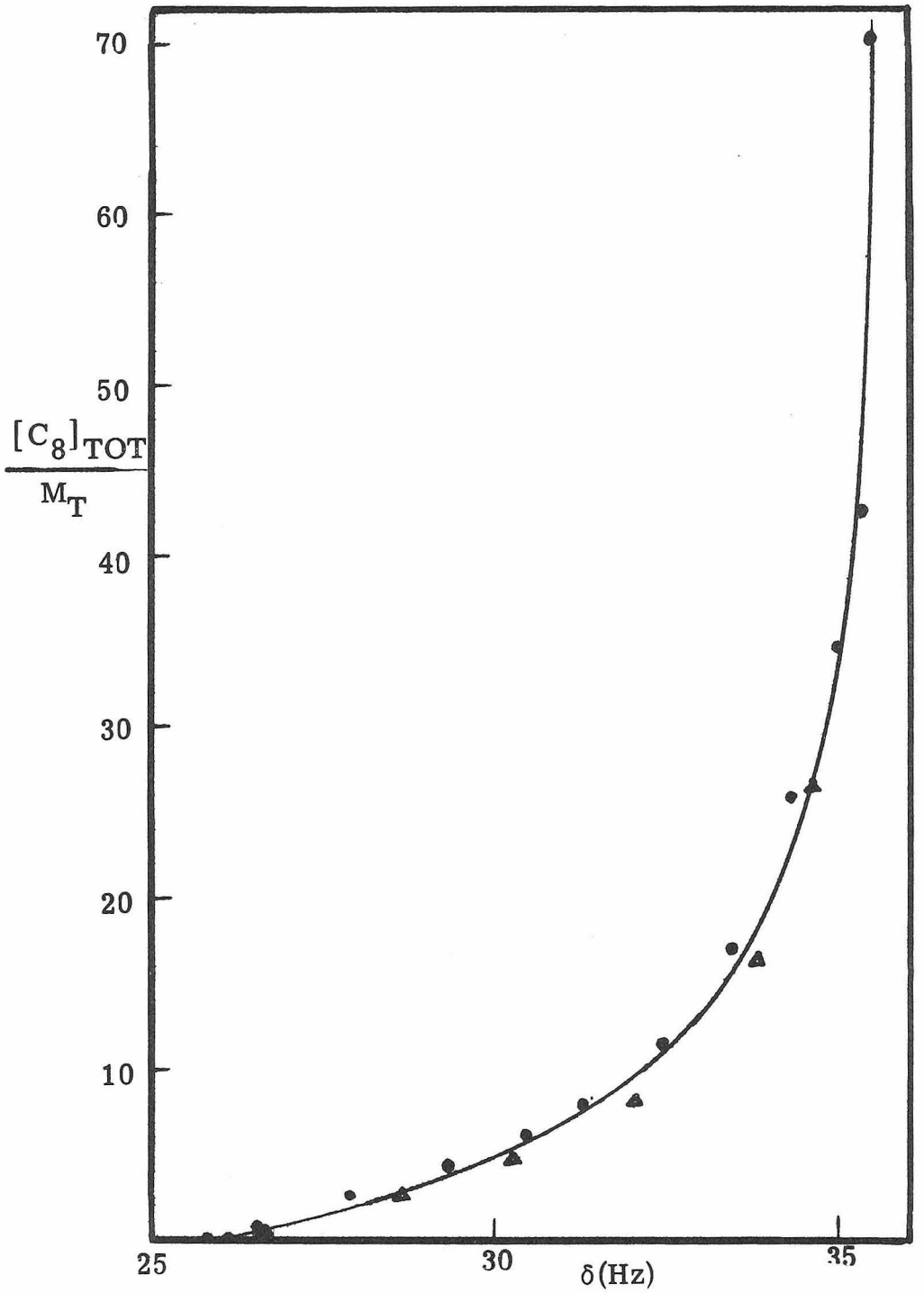

Titration of $(N)_2(Pd_2Cl_6)$
with cyclooctene in CH_2Cl_2

o Experiment I

▲ Experiment II

Figure 10

Table VI[a]

Titration of $(N)_2(Pd_2Cl_6)$ with Cyclooctene in CH_2Cl_2

Followed by NMR at 40°C

Experiment	Total Sample Volume (ml)	$\frac{[C_8]_{TOT}}{M_T}$	δ(Hz)	α[d]	M_T	R	P	$[C_8]_{TOT}$	$[C_8]_{FREE}$	K[e]
Experiment I[b]										
A	0.375	0	25.86	1	5.72	2.86	0	0	0	--
B	0.395	0.714	26.58	0.926	5.43	2.51	0.405	3.88	3.48	0.540
C	0.445	2.50	27.90	0.790	4.82	1.91	1.01	12.0	11.0	0.438
D	0.495	4.29	29.32	0.645	4.33	1.40	1.54	18.6	17.0	0.584
E	0.545	6.07	30.46	0.528	3.94	1.04	1.86	23.9	22.0	0.686
F	0.595	7.86	31.30	0.441	3.61	0.796	2.02	28.3	26.3	0.739
G	0.615	11.4	32.44	0.324	3.49	0.566	2.36	39.9	37.5	0.696
H	0.645	16.8	33.48	0.218	3.33	0.362	2.60	55.9	53.3	0.659
I	0.695	25.7	34.32	0.131	3.09	--	--	79.4	--	
J	0.745	34.6	35.00	0.062	2.88	--	--	99.8	--	
K	0.845	42.5	35.34	0.027	2.54	--	--	108	--	
L	0.945	70.4	35.50	0.010	2.27	--	--	160	--	
Experiment II[c]										
A	0.425	0	26.12	1	6.42	3.21	0	0	0	--
B	0.475	0.421	26.67	0.942	5.74	2.70	0.334	2.42	2.08	0.946
C	0.500	2.53	28.68	0.730	5.46	1.99	1.47	13.8	12.3	0.717
D	0.525	4.63	30.24	0.565	5.20	1.47	2.26	24.1	21.8	0.728
E	0.565	8.00	32.04	0.376	4.83	0.908	3.02	38.6	35.6	0.790
F	0.665	16.4	33.82	0.188	4.10	--	--	--	--	--
G	0.685	26.5	34.60	0.106	3.99	--	--	--	--	--
										0.68 av.

[a] All concentrations should be multiplied by 10^{-2} to obtain units of moles/ℓ.

[b] 8.18 mg $(N)_2(Pd_2Cl_6)$ in 0.35 ml CH_2Cl_2 + 0.025 ml TMS.

[c] 10.40 mg $(N)_2(Pd_2Cl_6)$ in 0.40 ml CH_2Cl_2 + 0.025 ml TMS.

[d] Assuming a limiting chemical shift of 35.60 Hz.

[e] ℓ/mole.

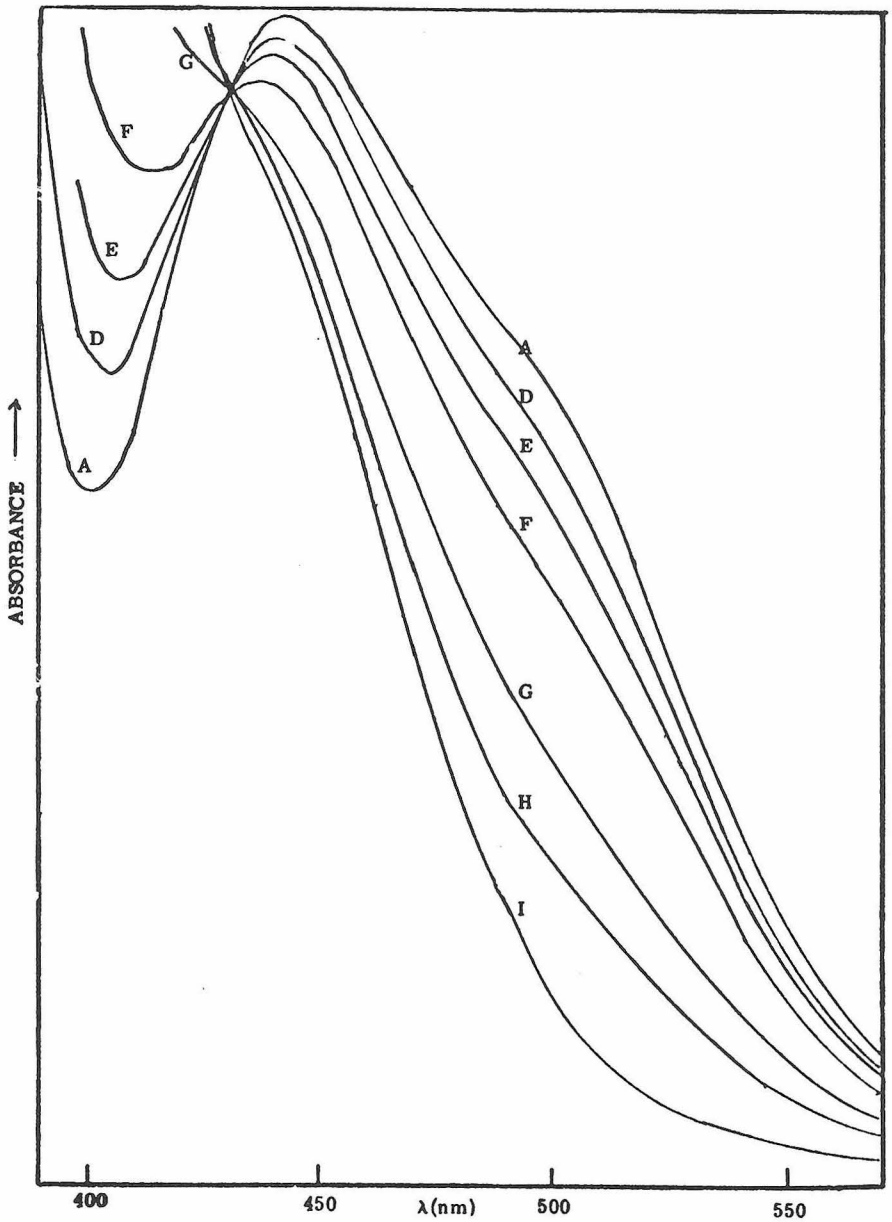

Titration of $(N)_2(Pd_2Cl_6)$
with cyclooctene in CH_2Cl_2
Figure 11

Table VII[a]

Titration of $(N)_2(Pd_2Cl_6)$ with Cyclooctene in CH_2Cl_2

Followed Spectrophotometrically at 21 °C

Experiment	A_{490}	A_{500}	A_{510}	α_{490}	α_{500}	α_{510}	α_{avg}	$\frac{[C_8]_{TOT}}{M_T}$	$[C_8]_{TOT}$	P	R	$[C_8]_{FREE}$	K^b
A	.466	.429	.383	1	1	1	1	0	0	0	0.609	0	--
B	.454	.416	.371	.962	.960	.961	.961	0.899	1.10	0.0472	0.586	1.05	3.47
C	.445	.405	360	.934	.927	.926	.929	1.80	2.19	0.0868	0.566	2.10	3.02
D	.432	.395	.350	.893	.897	.894	.894	2.70	3.29	0.129	0.544	3.16	3.06
E	.403	.364	.322	.801	.808	.803	.804	5.62	6.85	0.238	0.490	6.61	2.65
F	.360	.321	.280	.665	.672	.668	.688	11.2	13.7	0.404	0.407	13.3	2.27
G	.272	.229	.193	.388	.392	.387	.389	29.0	34.2	0.745	0.236	33.5	2.09
H	.209	.176	.144	.190	.231	.229	.216	45.0	54.8	0.955	0.132	53.8	2.39
I	.149	.100	.070	0	0	0	0	687	--	--	--	--	
													2.7 average

[a] All solutions have $M_T = 1.218 \times 10^{-3}$ M. All concentrations should be multiplied by 10^{-3} to obtain units of moles/ℓ.

[b] ℓ/mole.

Titration with a neutral reactant in this case eliminates the problems of new types of ionic association which destroyed the value of the titrations with $(n\text{-}C_4H_9)_4NCl$. Since the equilibrium constant decreases from 21°C to 40°C, the reaction is exothermic. We do not feel that it is justified to assign a value to ΔH based on just two points.

In contrast to the simple behavior of $(N)_2(Pd_2Cl_6)$, titration of $(P)_2(Pd_2Cl_6)$ with cyclooctene produced a curve of chemical shifts that loops back on itself as more olefin is added. (Figure 12, Table VIII). This suggests that at least two reactions occur and that the chemical shift of the first product lies further upfield than that of the second product. In agreement with this, spectrophotometric titration (Figure 13, Table IX) shows an isosbestic point at 462 nm through addition of the first 1.2 equivalents of olefin (curves A-E, Figure 13a). Further olefin addition (curves F-I, Figure 13b) wrecks the isosbestic point and reduces the original absorption maximum at 437 nm to a shoulder in the final spectrum (curve I).

These data are in qualitative accord with Scheme I. In particular, the species II would possess both $[PdCl_4]$ and $[(ol)PdCl_3]$ (ol = olefin) chromophores. The product III would possess only the latter chromophore. The $[(ol)PdCl_3]$ chromophore should exhibit its first d-d transition at higher energy than the $[PdCl_4]$ chromophore.[7] We see in Figure 13a, curve F, that the first reaction product (II) has a maximum near 430 nm. This is consistent with

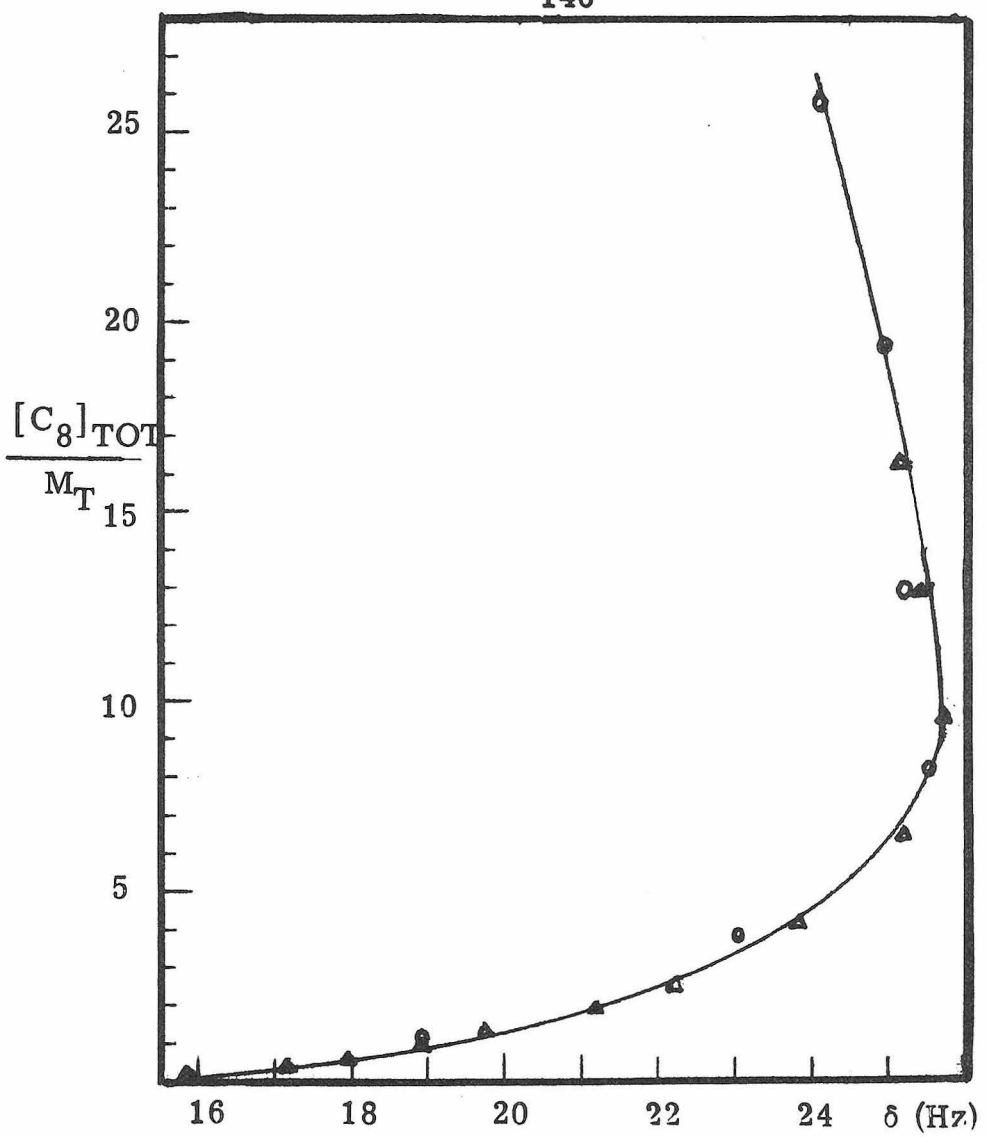

Titration of $(P)_2(Pd_2Cl_6)$
with cyclooctene in CH_2Cl_2

○ Experiment I

△ Experiment II

Figure 12

Table VIII[a]

Titration of $(P)_2(Pd_2Cl_6)$ with Cyclooctene in CH_2Cl_2

Followed by NMR at 40 °C

Experiment	Total Volume (ml)	$[C_8]_{TOT}/M_T$	δ (Hz)	M_T	$[C_8]_{TOT}$
Experiment I[b]					
A	0.375	0	15.84	6.09	0
B	0.395	0.268	17.16	5.78	1.55
C	0.415	0.537	17.94	5.50	2.95
D	0.440	0.872	18.96	5.19	4.52
E	0.465	1.21	19.72	4.91	5.93
F	0.510	1.81	21.22	4.48	8.11
G	0.560	2.48	22.26	4.08	10.1
H	0.585	4.16	23.86	3.90	16.2
I	0.615	6.17	25.28	3.71	22.9
J	0.665	9.53	25.76	3.43	32.7
K	0.715	12.9	25.46	3.19	41.1
L	0.765	16.2	25.18	2.98	48.5
Experiment II[a]					
A	0.430	0	15.86	4.99	0
B	0.530	1.07	18.92	4.05	4.34
C	0.555	3.74	23.05	3.87	14.5
D	0.595	8.02	25.58	3.61	29.0
E	0.640	12.8	25.25	3.36	43.0
F	0.700	19.3	24.94	3.07	59.3
G	0.760	25.7	24.17	2.83	72.8

[a] All concentrations should be multiplied by 10^{-2} to obtain units of moles/ℓ.

[b] 8.63 mg $(P)_2(Pd_2Cl_6)$ in 0.35 ml CH_2Cl_2 + 0.025 ml TMS.

[c] 8.14 mg $(P)_2(Pd_2Cl_6)$ in 0.40 ml CH_2Cl_2 + 0.030 ml TMS.

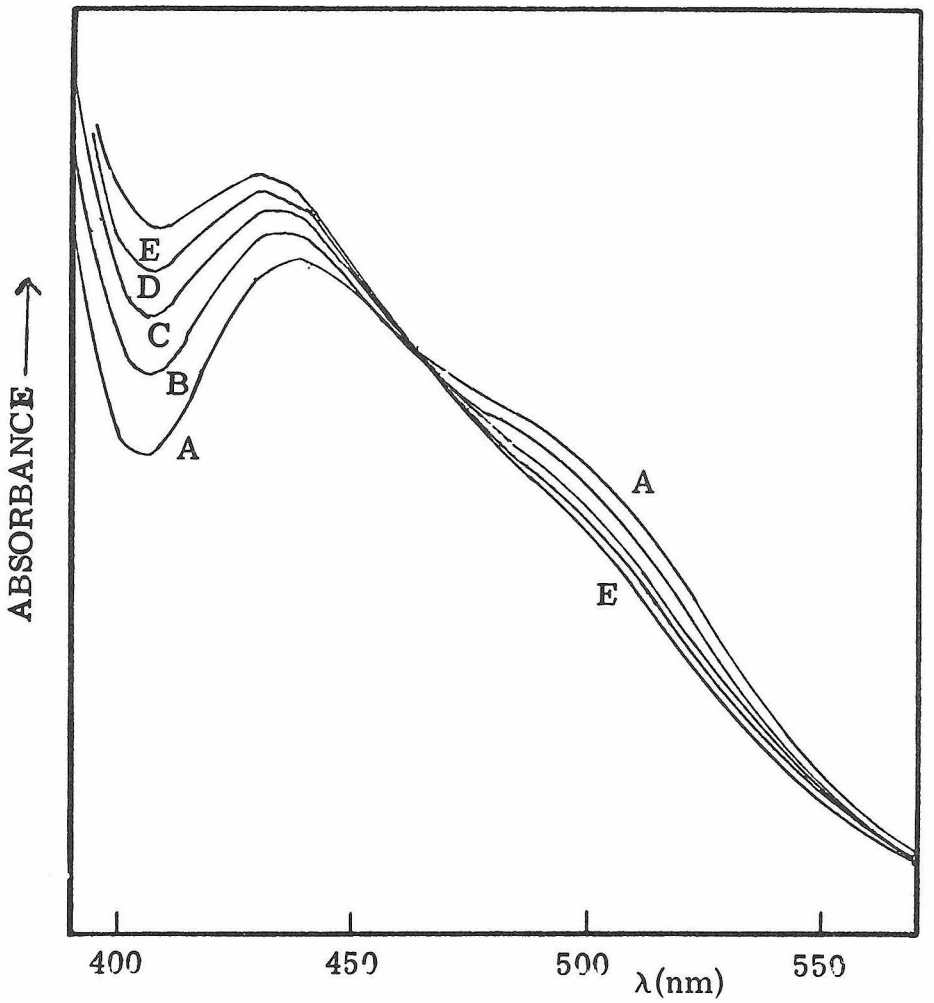

Titration of $(P)_2(Pd_2Cl_6)$
with cyclooctene in CH_2Cl_2
Figure 13a

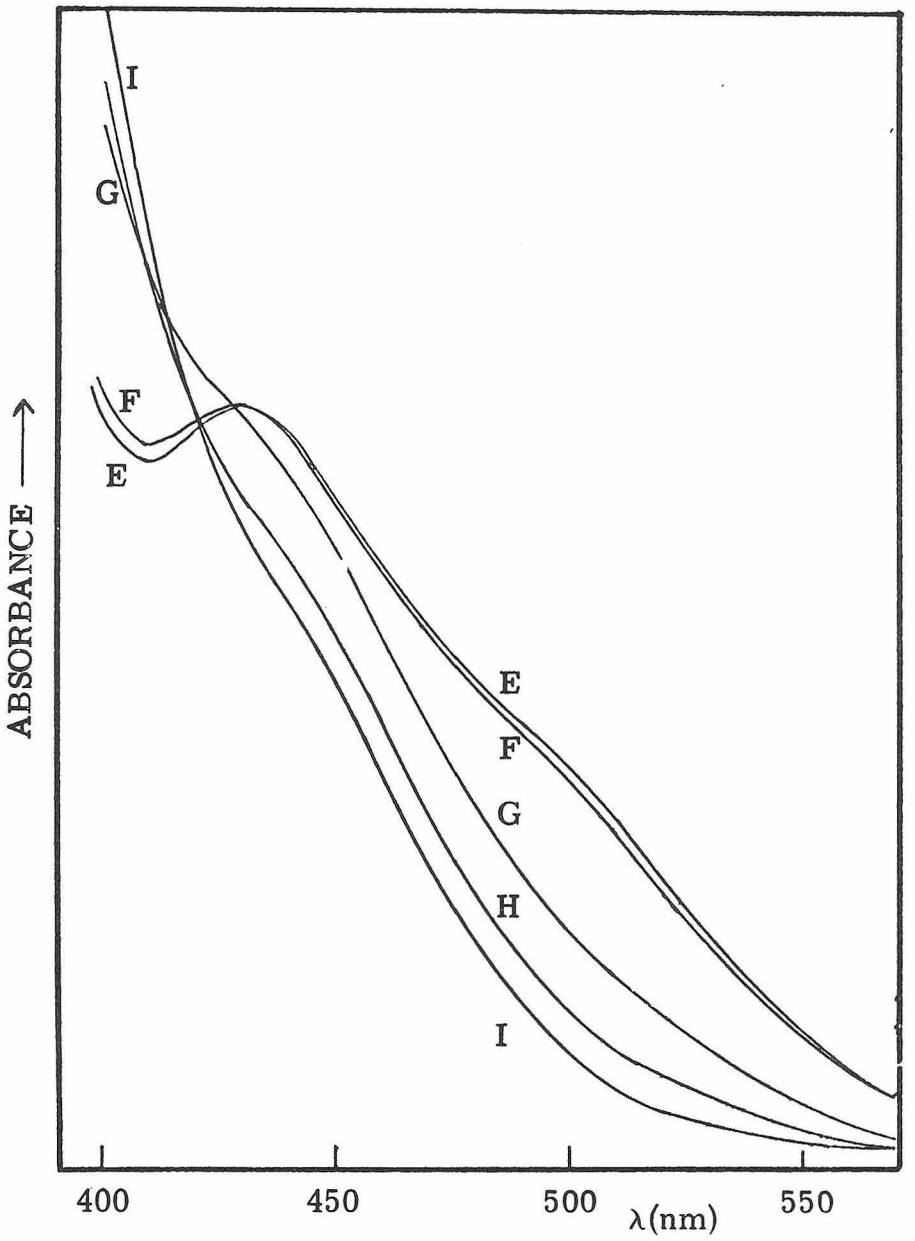

Titration of $(P)_2(Pd_2Cl_6)$
with cyclooctene in CH_2Cl_2

Figure 13b

Table IX

Titration of $(P)_2(Pd_2Cl_6)$ with Cyclooctene in CH_2Cl_2

Followed Spectrophotometrically at 21 °C

Experiment	$[C_8]_{TOT}$ / M_T [a]	Absorbance [c] 570	560	550	540	530	520	510	500	490	480	470	460	450	440	430	420	410	400
A	0	087	122	169	232	306	381	448	504	543	574	604	644	693	725	708	625	531	539
B	0.404	082	115	159	218	287	358	425	478	532	557	596	645	706	752	750	684	612	631
C	0.808	076	108	150	206	270	338	404	458	504	544	592	648	716	769	778	731	672	703
D	1.21	075	104	145	198	250	326	388	444	490	535	589	650	722	780	800	764	718	756
E	1.62	072	100	138	189	248	311	374	427	476	526	583	652	722	792	819	792	761	810
F	2.02	069	095	131	179	237	297	358	413	463	514	574	643	729	788	819	804	778	830
G	10.1	036	049	068	092	132	158	199	248	306	382	470	570	662	745	809	862	950	1130
H	20.2	021	030	049	054	074	098	129	169	223	294	382	477	573	652	720	801	934	1172
I [b]	262	014	018	026	032	046	060	086	118	172	238	328	424	514	600	692	810	996	1270

[a] $M_T = 3.80 \times 10^{-3}$ moles/ℓ.

[b] Solution I contains $M_T = 1.19 \times 10^{-3}$ M. Absorbance values are corrected for concentration so that they are directly comparable to solutions A-H.

[c] Absorbance was measured on a 0-0.5 absorbance unit scale so true absorbances are half the value given in this Table. The numbers 570-390 are wavelengths in nm. The absorbances are expressed without decimal points: 087 = 0.087; 1264 = 1.264.

Scheme I

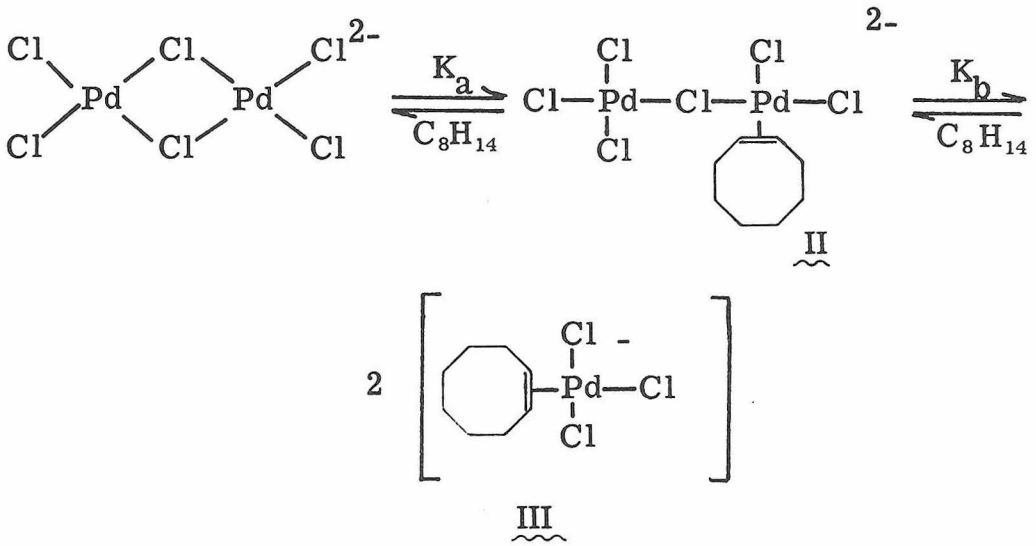

the presence of a $[PdCl_4]$ chromophore in the first product. The final product (Figure 13b, Curve I) exhibits a visible spectrum similar to that of the final product of the titration of $(N)_2(Pd_2Cl_6)$ (Figure 11, Curve I). We have been unable to extract the equilibrium constants K_a and K_b from the spectrophotometric titration. Since these constants are potentially available from these data, values of the absorbance measured in Figure 13 are included in Table IX.

Infrared evidence for this reaction is not very informative. At a ratio $[C_8]_{TOT}/M_T \approx 15$ in CH_2Cl_2 solution (AgCl cell), we see a medium intensity band at 339 cm^{-1} and a weaker band at 306 cm^{-1}. This spectrum is qualitatively correct for the reactant, II or III.

If our interpretation of the $(P)_2(Pd_2Cl_6)$ titration is correct, this is the first time anyone has ever observed a monohalogen-bridged Pd or Pt dimer. Pearson and Muir[14,15] postulated such an intermediate in the reaction of $Pt_2Br_6^{2-}$ with olefins and amines.

Their kinetic data are consistent with Scheme II in which Y is the attacking species and S is solvent.

Scheme II

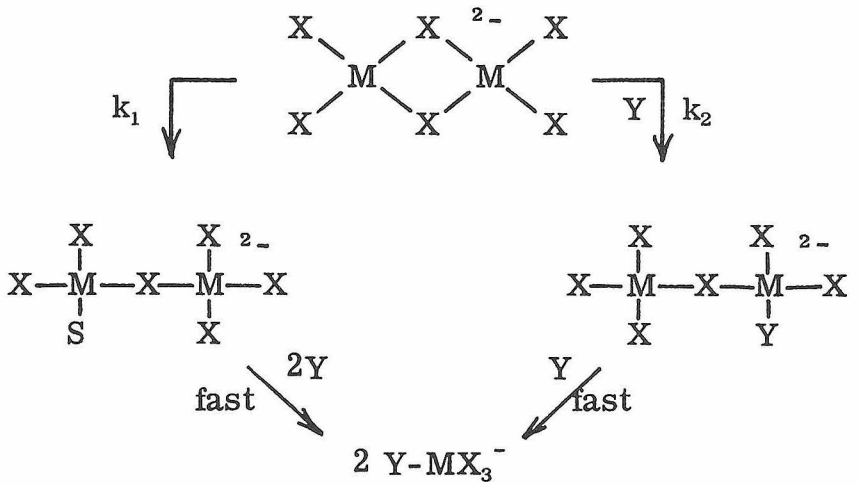

We feel that the monohalogen-bridged intermediate is now a reality and will be more important for Br and I complexes. In our reaction with cyclooctene, the bulk of the tripropylcyclopropenium cation and the fair size of the cyclooctene reagent apparently account for the observation of the monobridged intermediate as a distinct intermediate. In view of this, we expect that this intermediate ought to be more prevalent in the chemistry of bulky reagents.[26]

Reaction of cyclooctene with $(N)_2(Pt_2Cl_6)$ or $(P)_2(Pt_2Cl_6)$ is much slower than reaction with $Pd_2Cl_6^{2-}$. Whereas the Pd solutions equilibrate "instantly", the Pt solutions require several hours to reach equilibrium. This presents problems in measuring the equilibrium constant because solutions of $Pt_2Cl_6^{2-}$ in a solvent as

mild as CH_2Cl_2 are unstable. (With respect to what? Solvolysis by CH_2Cl_2 seems unreasonable. Perhaps there is a slight reaction with water.) A solution of $(P)_2(Pt_2Cl_6)$ in CH_2Cl_2 left overnight exposed to the air shows a 10% decrease in the 500 nm absorption and a 10% increase in the 400 nm band. Solutions of $(P)_2(Pt_2Cl_6)$ and cyclooctene left long enough to reach equilibrium (generally 10-20 hours) showed spectral changes that could not be the result of reaction only with olefin. Hence, the equilibrium could not be measured quantitatively. At any given wavelength, however, one can construct a titration curve such as that in Figure 14. In this plot we see that the absorbance approaches its final value linearly

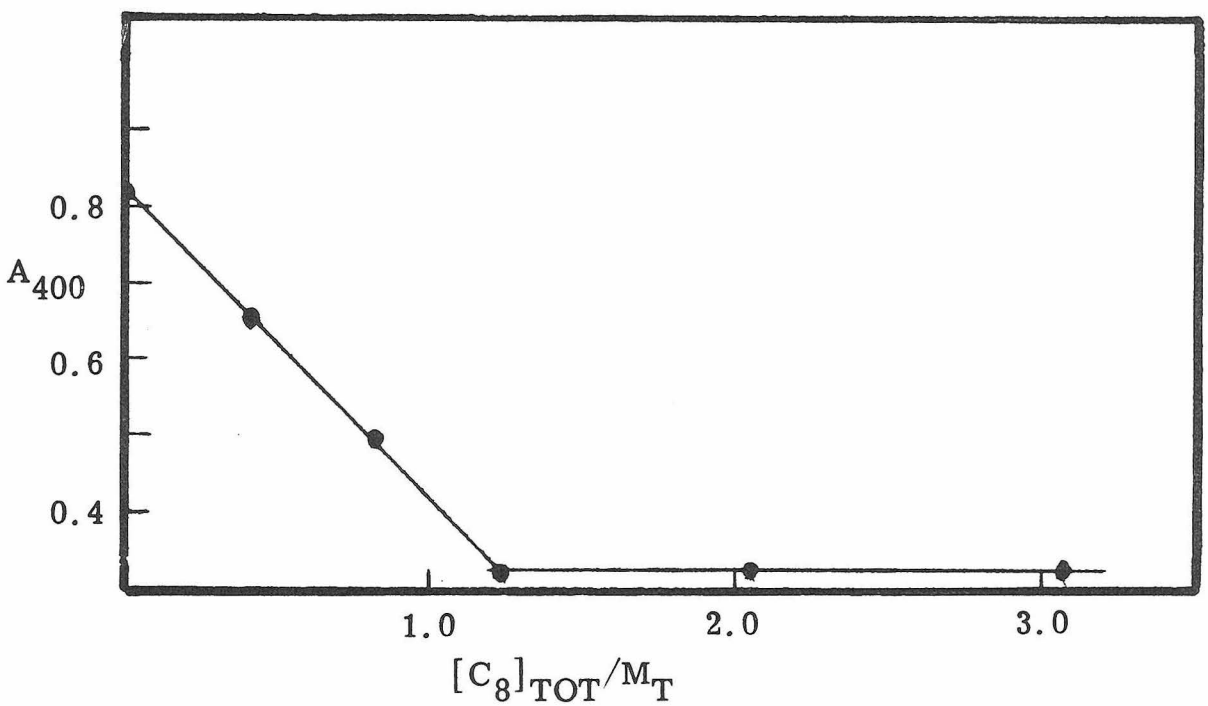

Titration of $(P)_2(Pt_2Cl_6)$
with cyclooctene in CH_2Cl_2
Figure 14

and then levels off immediately. To establish the linearity more accurately, more points were collected in a titration illustrated in Figure 15. Absorbances measured at both 400 and 500 nm fall off linearly, but not with the same slope. The difference in slope is due to whatever reaction causes the change in the $(P)_2(Pt_2Cl_6)$ spectrum in the absence of olefin. Both lines intercept the limiting absorbance value near $[C_8]_{TOT}/M_T = 1.0$. This establishes the stoichiometry and supports reaction (24) as the next reaction.

$$(P)_2(Pt_2Cl_6) + 2C_8H_{14} \overset{K_{24}}{\rightleftharpoons} 2[P][(C_8H_{14})PtCl_3] \qquad (24)$$

The linear nature of the titration curves tells us that K_{24} is very large. Assuming that 5% dissociation of the π-olefin complex at the 50% titration point could go unnoticed (an overestimate), we establish an approximate lower limit on K_{24} of 4×10^5 l/mole.[10] Our visible spectra of Pt and Pd olefin complexes are summarized in Table X.

Table X

Summary of π-Olefin Spectra

Compound	Range (nm)	Spectrum [$\bar{\nu}_{max}$ (ϵ)]
$[P][(C_8H_{14})PdCl_3]$	750-290	31,900 (~4400)
$[N][(C_8H_{14})PdCl_3]$	750-290	~23,000 sh (~300); 31,500 (~4500)
$[P][(C_8H_{14})PtCl_3]$	750-360	~22,000 sh (~20)
$[K][C_2H_4)PtCl_3]$[8]	--	23,900 (40); 30,350 (340); 33,450 (605)...

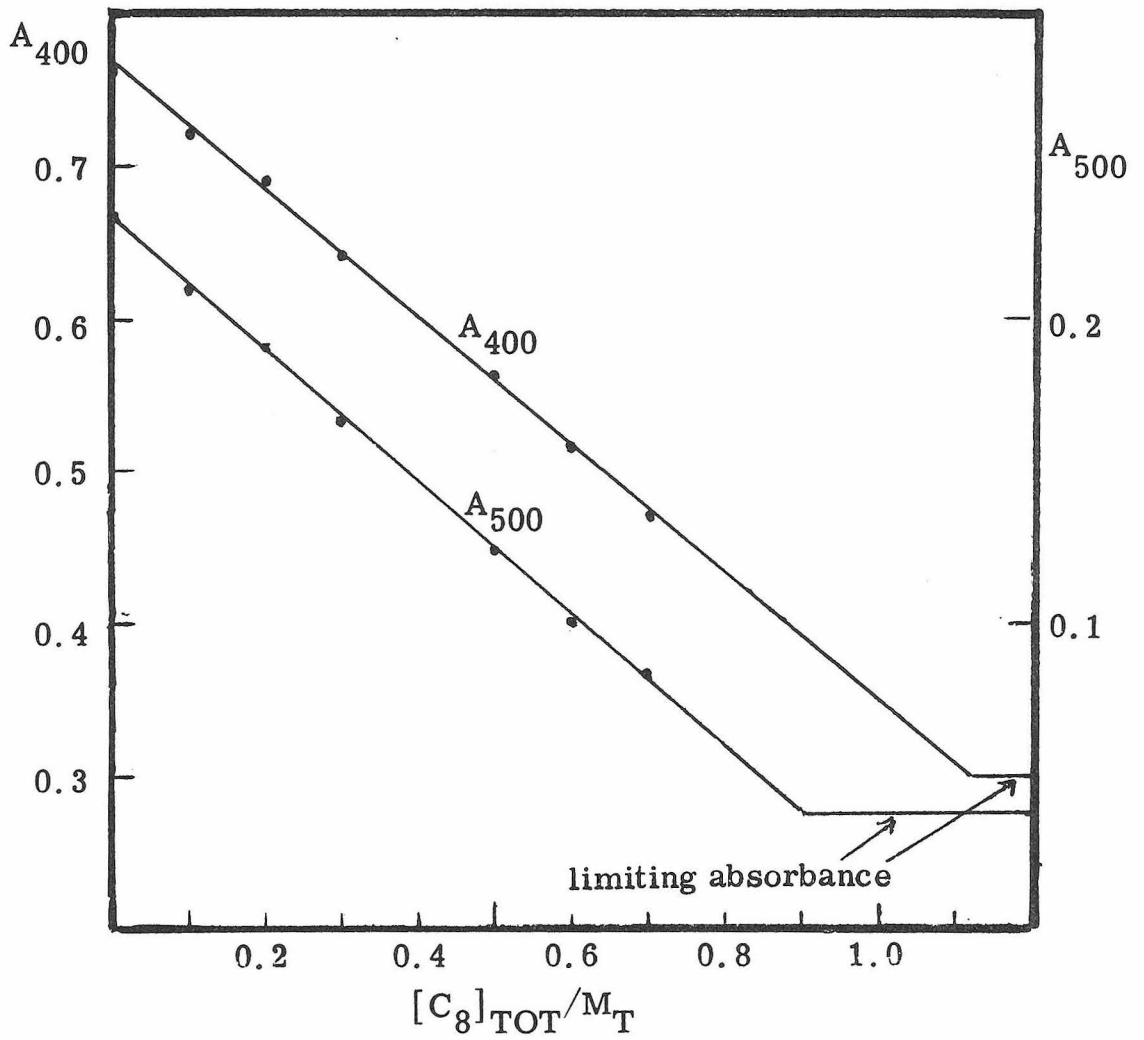

Titration of $(P)_2(Pt_2Cl_6)$
with cyclooctene in CH_2Cl_2
Figure 15

IR evidence concerning the Pt product is poor. A solution containing $[C_8]_{TOT}/M_T = 2$ in CH_2Cl_2 in a AgCl cell showed one broad band at 328 cm^{-1}. The spectrum of Zeise's salt shows two bands at 339 and 310 cm^{-1}.[11] Perhaps these absorptions are closer together and broader in the cyclooctene complex. Attempting to obtain a Raman spectrum of this solution, we instead observed strong emission with a maximum at 15,100 cm^{-1}. This compares to emission from solid Zeise's salt at 14,300 cm^{-1}[12] and emission from K_2PtCl_4 at 12,700 cm^{-1}.[13]

We can compare our equilibrium constants to previous work[8b] on Pt and Pd monomers. This is shown below

$$Pd_2Cl_6^{2-} + 2(C_8H_{14}) \underset{CH_2Cl_2}{\rightleftharpoons} 2[Pd(C_8H_{14})Cl_3^-] \quad K \approx 3 \text{ (l/mole)} \qquad (25)$$

$$Pt_2Cl_6^{2-} + 2(C_8H_{14}) \underset{CH_2Cl_2}{\rightleftharpoons} 2[Pt(C_8H_{14})Cl_3^-] \quad K \gtrsim 10^5 \text{(l/mole)} \qquad (26)$$

$$PdCl_4^{2-} + (ol) \underset{H_2O}{\rightleftharpoons} (ol)PdCl_3^- + Cl^- \quad K \approx 10 \text{ (dimensionless)} \qquad (27)$$

$$PtCl_4 + (ol) \underset{H_2O}{\rightleftharpoons} (ol)PtCl_3^- + Cl^- \quad K \approx 10^3 \text{ (dimensionless)} \qquad (28)$$

The previous work was done with a variety of olefins, not including cyclooctene.

Reaction with Acetonitrile

When we attempted to record the spectra of $M_2Cl_6^{2-}$ salts in acetonitrile, we observed that solutions of the M = Pt salts turned

from pink to yellow in the course of about an hour at room temperature. The studies described in this section establish conclusively that solvolysis occurs according to equation (29)

$$M_2Cl_6^{2-} + 2CH_3CN \overset{K_{29}}{\rightleftharpoons} 2\left[CH_3CN-\underset{\underset{Cl}{|}}{\overset{\overset{Cl}{|}}{M}}-Cl^-\right] \qquad (29)$$

All four cases for which M = Pt, Pd and cation = P, N have been studied in solution. In addition, crystals of $[N][(CH_3CN)PtCl_3]$ have been isolated and studied as a solid.

That one acetonitrile molecule per metal atom becomes coordinated is established for M = Pt by integration of the acetonitrile and cation absorptions in the proton NMR spectra (Figures 16 and 17) and by elemental analysis of crystalline $[N][(CH_3CN)PtCl_3]$

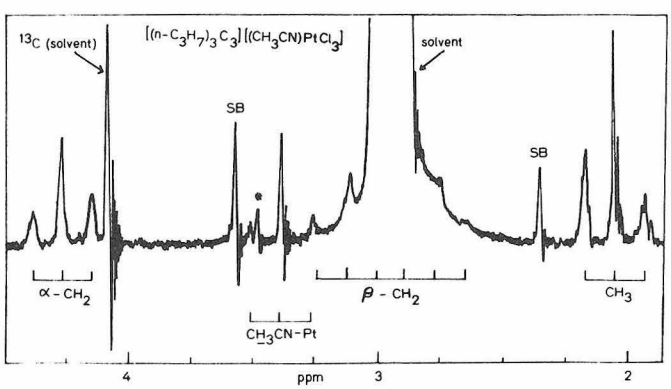

NMR spectrum of $[P][(CH_3CN)PtCl_3]$ in CH_3CN. Peaks labeled SB are spinning side bands. The peak marked with an asterisk is unidentified.

Figure 16

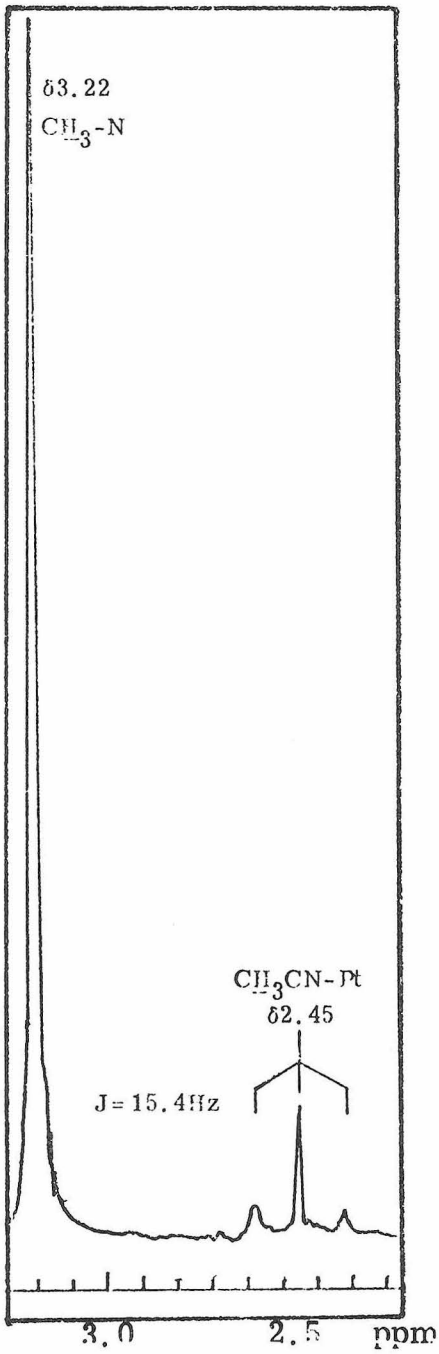

NMR spectrum of
$[N][(CH_3CN)PtCl_3]$ in CH_2Cl_2
Figure 17

(see Experimental Section). For example, in Figure 17, the ratio of the areas of the cation and acetonitrile signals is 5.99:1 (theoretical = 6.00:1). Further, the failure to observe a signal for free CH_3CN in a CH_2Cl_2 solution of $[N][(CH_3CN)PtCl_3]$ establishes that the equilibrium constant, K_{29}, is large for M = Pt.

That the acetonitrile is sigma bonded is supported by the Raman and NMR spectra. ν_{CN} shifts to <u>higher</u> energy than that of free CH_3CN upon sigma coordination.[16,17] We observe a strong Raman band for free CH_3CN at 2253 cm^{-1} and a much weaker combination band at 2294 cm^{-1}. Solutions of $[P][(CH_3CN)PtCl_3]$ also show two weak peaks at 2306 and 2336 cm^{-1} (Figure 18).

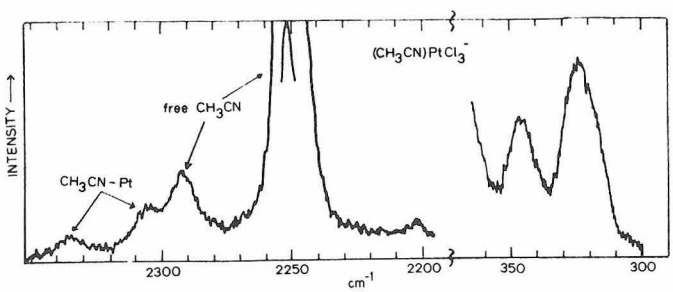

Raman spectrum of $[P][(CH_3CN)PtCl_3]$ in acetonitrile.

Figure 18

Similar infrared spectra have been obtained for $(C_2H_4)PtCl_2(CH_3CN)$.[18] The infrared spectra of solid $[N][(CH_3CN)PtCl_3]$ and of $[P][(CH_3CN)PtCl_3]$ (as an oil obtained by evaporation of a CH_3CN solution) show only exceedingly weak absorption in the 2300 cm^{-1} region. The NMR spectra summarized in Table XI exhibit $J_{^{195}Pt-^1H} \approx 15$ Hz for coordinated CH_3CN. This is similar to the coupling observed in <u>cis</u>- and <u>trans</u>-$(C_2H_4)PtCl_2(CH_3CN)$.[5,18] The chemical shift of coordinated CH_3CN (~ 0.4 ppm downfield of free CH_3CN) is also similar to that observed by other workers.[5,18]

Infrared (Figure 19) and Raman (Figure 18) spectra, summarized in Table XII, are in good agreement with a C_{2v} planar structure. The three M-Cl stretches transform as $2a_1[\nu(M\text{-}Cl_{\underline{trans}})$ and $\nu_s(Cl\text{-}M\text{-}Cl)] + b_1[\nu_{as}(Cl\text{-}M\text{-}Cl)]$.[19] All of these modes are both IR and Raman active. It is commonly found in such systems that ν_{as} is the strongest IR band. For both Pt and Pd compounds, we observe a strong band in the region 328-340 cm^{-1} and one or two weaker bands. Corresponding to these weak IR bands are strong Raman bands. No Raman band appears at the position of ν_{as}. Since a_1 vibrations are usually the strongest in a Raman spectrum, it is eminently reasonable to assign the central band as $\nu_{as}(b_1)$ and the two flanking bands as $\nu_s(a_1)$ and $\nu(M\text{-}Cl_{\underline{trans}})(a_1)$.

A conflict arises in distinguishing the two a_1 bands. We generally expect ν_s to be of lower energy than ν_{as}. This means the low energy Raman band would be ν_s. On the other hand, if

Table XI

NMR Spectra of $(CH_3CN)PtCl_3^-$ Salts

Compound	Solvent	Cation Chemical Shifts[a] α-CH_2	β-CH_2	CH_3	Coordinated CH_3CN Chemical Shift	$J_{^{195}Pt-^1H}$(Hz)
$[P][(CH_3CN)PtCl_3]$[b]	CH_3CN	3.28	1.97	1.07	2.39	15
$[N][(CH_3CN)PtCl_3]$	CH_3CN			3.08	2.38	15
$[N][(CH_3CN)PtCl_3]$[c]	CH_2Cl_2			3.22	2.45	15.4
$[N][(CH_3CN)PdCl_3]$[d]	CH_2Cl_2			--	2.27	--

[a] ppm downfield of internal TMS.

[b] All couplings within propyl groups are ~ 7.5 Hz giving triplets for the α-CH_2 and CH_3 groups. The β-CH_2 sextet is partly obscured by solvent.

[c] The ^{195}Pt satellites have a greater half-width than the central CH_3CN peak. $\omega_{1/2}$ (central peak) = 1.0 Hz. $\omega_{1/2}$ (satellites) = 1.7 Hz. See reference 28.

[d] This spectrum was obtained with ~ 10 mg $[N]_2[Pd_2Cl_6]$ in 250 μl CH_2Cl_2 plus 50 μl CH_3CN. Integration of the single cyclopropenyl methyl peak (at 3.28 ppm) and the coordinated CH_3CN peak shows a ratio of 20:1. This indicates that the reaction is only ~ 1/3 complete under these conditions.

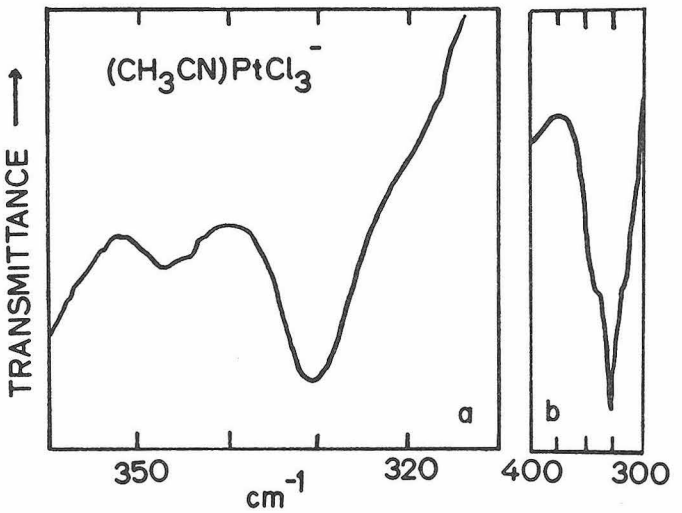

a. Infrared spectrum of $[P][(CH_3CN)PtCl_3]$ in acetonitrile.

b. Infrared spectrum of the oily residue obtained by concentrating the solution to dryness.

The band cut off the left side of the spectrum is δ(CCN) of the solvent.

Figure 19

Table XII

Infrared and Raman Spectra of $(CH_3CN)PtCl_3^-$ Salts[a]

Infrared

	Cell	ν_s(Cl-M-Cl)(a_1)[b]	ν_{as}(Cl-M-Cl)(b_1)	ν(M-Cl_{trans})(a_1)[b]
[P][$(CH_3CN)PtCl_3$]	CsI	347 m	330 s	~ 319 sh, w
[N][$(CH_3CN)PtCl_3$]	CsI	345 m	330 s	~ 317 sh, w
	AgCl	~344 br, w	328 br, m	~ 316 sh, br, w
[P][$(CH_3CN)PdCl_3$]	AgCl	--	340 s	302 vw
[N][$(CH_3CN)PdCl_3$]	AgCl	--	339 s	~ 300 vw

Raman[c]

	ν_s(Cl-M-Cl)(a_1)[b]	ν_{as}(Cl-M-Cl)(b_1)	ν(M-Cl_{trans})(a_1)[b]	CH_3CN 380 cm^{-1} Band Depolarization Ratio[d]	CH_3CN Bands[e]
[P][$(CH_3CN)PtCl_3$]	347 (65%) [0.44]	--	324 (59%) [1.00]	0.93	2306, 2336
[N][$(CH_3CN)PtCl_3$]	346 (90%) [0.28]	--	325 (90%) [1.00]	0.97	2305, 2334
[P][$(CH_3CN)PdCl_3$]	348 (24%) [0.34]	--	302 65%) [1.00]	0.83	f
[N][$(CH_3CN)PdCl_3$]	346 (23%) [0.31]	--	301 (31%) [1.00]	0.89	f

[a] Unless otherwise stated, all spectra were recorded in CH_3CN solution. Pt solutions were aged 5-24 hrs and Pd solutions were aged 0.5-4 hrs. Abbreviations: s = strong; m = medium; w = weak; v = very; sh = shoulder; br = broad.

[b] $\nu_{M-Cl}(a_1)$ modes may be reversed. See the text for a discussion of this assignment.

[c] Raman listings are in the following order: frequency (cm^{-1})
(depolarization ratio as % of CH_3CN 380 cm^{-1} band depolarization)
[relative integrated intensity].

[d] $I_\perp/I_\parallel$ for a solvent band known to be depolarized.

[e] Free CH_3CN exhibits ν_{CN} at 2253 cm^{-1} and a combination band at 2294 cm^{-1}.

[f] Not measured.

acetonitrile exerts a stronger trans effect than Cl, we expect $\nu(M\text{-}Cl_{trans})$ to be of lower energy than either ν_s or ν_{as}.[20] Spaulding, et al.[18,5] observed that in trans-$(C_2H_4)PtCl_2(CH_3CN)$ there is no $^{195}Pt\text{-}^{1}H$ (ethylene) coupling at room temperature but that in the cis isomer the coupling is observed. They interpret this as indicating a greater trans effect for CH_3CN than for Cl.[21] We feel that this is sufficient evidence to assign $\nu_s > \nu_{as} > \nu(M\text{-}Cl_{trans})$.[22]

The Raman spectrum of solid $[N][(CH_3CN)PtCl_3]$ is shown in Figure 20 and the spectra of solid samples of $[N]_2[Pt_3Cl_6]$ and $[N]_2[Pd_2Cl_6]$ are shown in Figure 21. In all cases the metal-halogen stretching absorptions (300-350 cm^{-1}) are disappointingly weak. The IR spectrum of $[N][(CH_3CN)PtCl_3]$ in a KBr pellet is shown in Figure 22. Following the vibrational analysis of Zeise's salt,[11] we expect nine vibrations of the $APtCl_3$ unit (where A is acetonitrile taken as a monatomic ligand). Of these, one will be a Pt-A stretch, three are Pt-Cl stretches, three are in-plane bending and two are out-of-plane bending. All are IR and Raman active. We have already assigned the $\nu_{M\text{-}Cl}$ vibrations. ν_{MA} will probably be higher than ν_{MCl}.[23] In free CH_3CN there is a CCN bend at 380 cm^{-1}. We do not see such a band in the spectrum of solid $[N][(CH_3CN)PtCl_3]$ (Figure 22). We also do not see an obvious candidate for ν_{MA}. Both of these must be very weak and should occur in the same region of the spectrum. The broad band in the IR spectrum at 295 cm^{-1} is a cation absorption. The

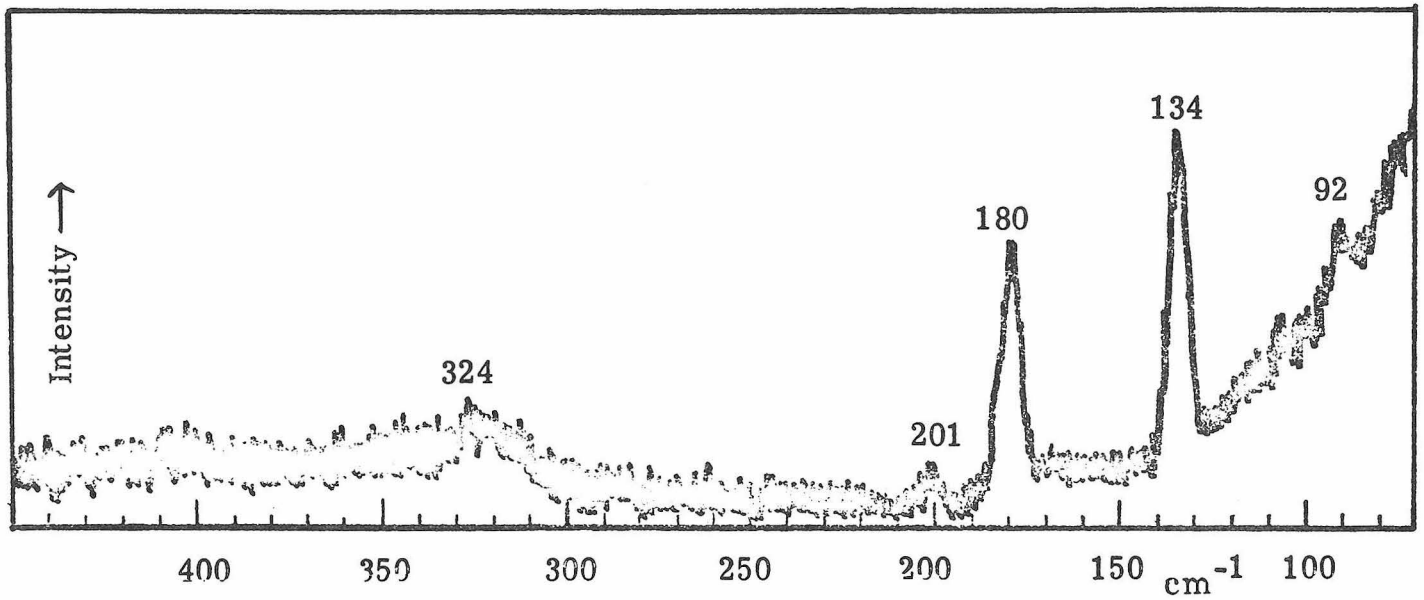

Raman Spectrum of Solid $\{[(CH_3)_2N]_3C_3\}\{(CH_3CN)PtCl_3\}$.
Bands at 180 and 134 cm^{-1} are artifacts of the spectrometer.

Figure 20

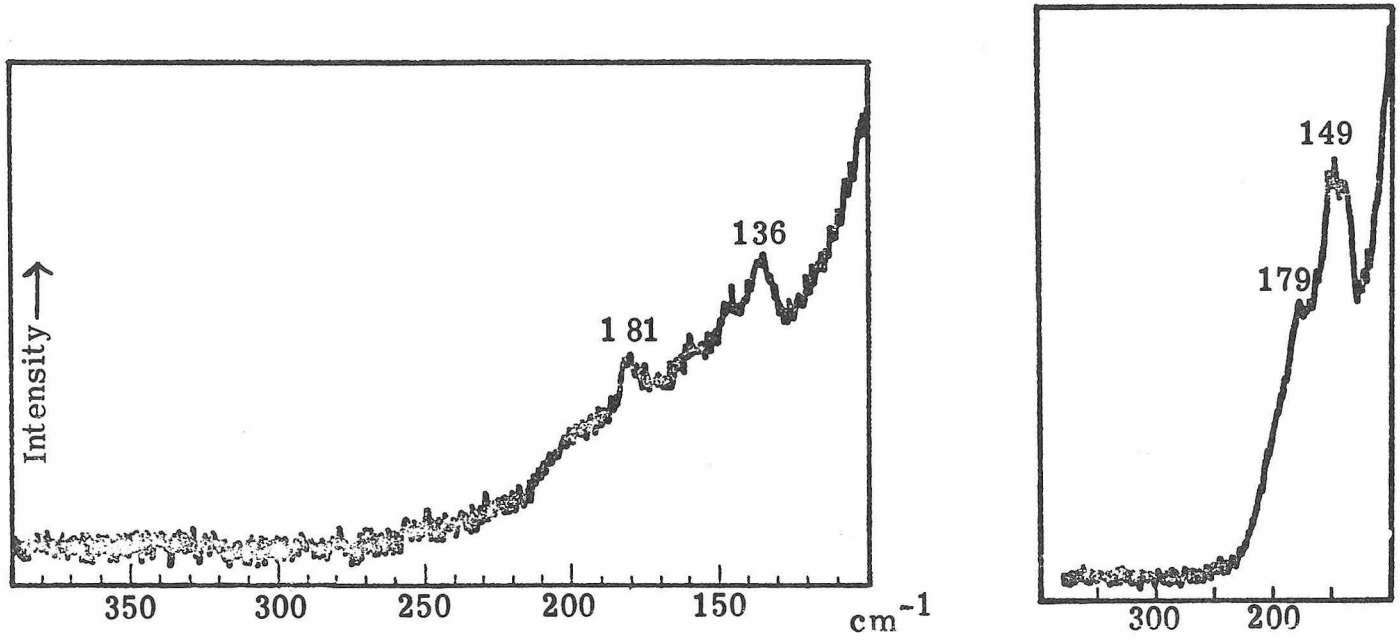

Raman spectra of (left) $[N]_2[Pd_2Cl_6]$ and (right) $[N]_2[Pt_2Cl_6]$ as solid samples. The spectrometer gives bands at ca. 180 and 135 cm^{-1} which are artifacts.

Figure 21

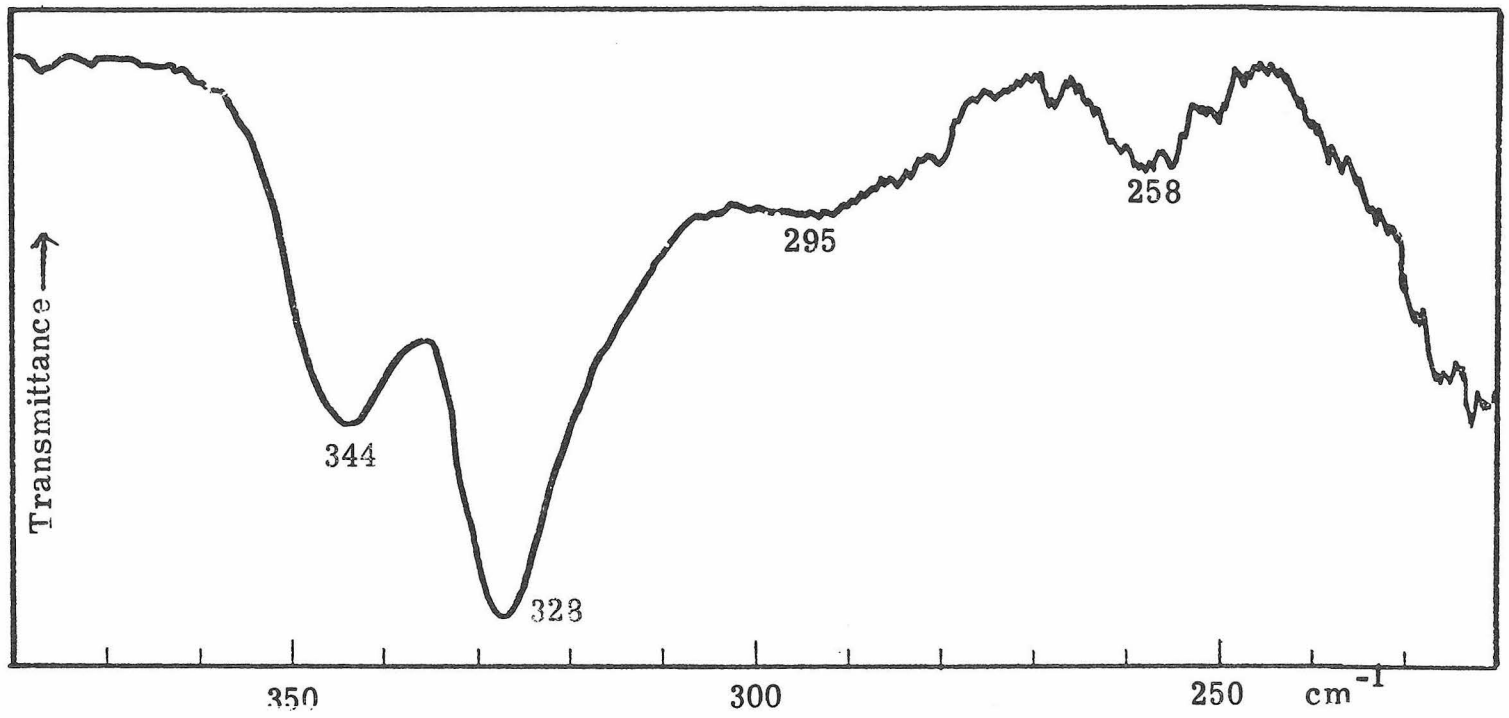

KBr Pellet Infrared Spectrum of [N] [$(CH_3CN)PtCl_3$]

Figure 22

remaining IR and Raman data are insufficient to assign the various bending modes.

To establish that we are observing just one product, a simple spectrophotometric titration of $(P)_2(Pd_2Cl_6)$ with CH_3CN in CH_2Cl_2 was done. In Figure 23 a three point titration is shown. The isosbestic point at 416 nm establishes that no significant intermediate product is present. The equilibrium constant for reaction (29) is 5×10^{-2} l/mole in this case.

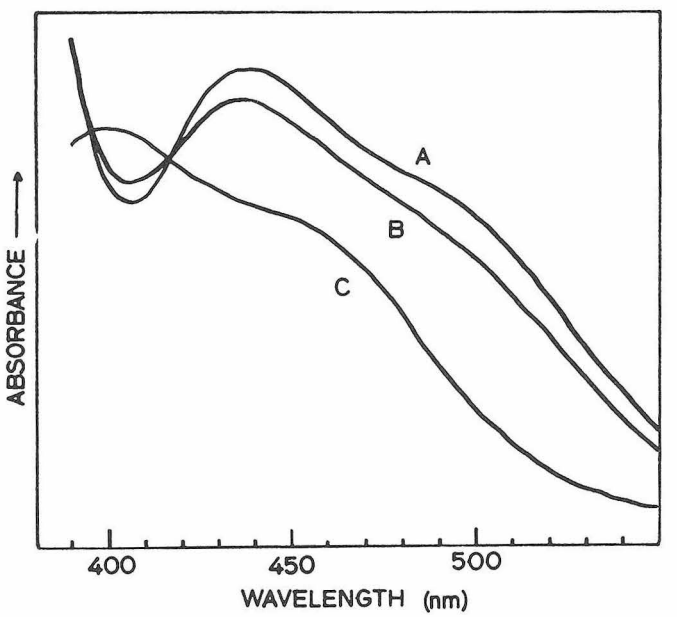

Spectrophotometric Titration of $[P]_2[Pd_2Cl_6]$ with CH_3CN in CH_2Cl_2.

$[CH_3CN]_{TOT}/M_T$ = A. 0
B. 47.6
C. 1 060

Figure 23

The UV-VIS spectra of the acetonitrile complexes are shown in Figures 24-25 and summarized in Table XIII. We interpret the spectrum in C_{2v} symmetry using the coordinate system and character table below.

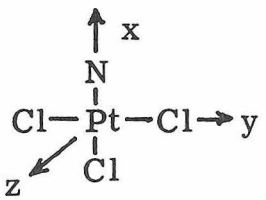

C_{2v}	E	$C_2(x)$	$\sigma(xz)$	$\sigma(yz)$		
A_1	1	1	1	1	x	x^2, y^2, z^2
A_2	1	1	-1	-1		yz
B_1	1	-1	1	-1	z	xz
B_2	1	-1	-1	1	y	xy

The order of the d orbitals is qualitatively estimated to be as follows:

———	$x^2 - y^2$	(a_1)
—↑↓—	xy	(b_2)
—↑↓—	xz	(b_1)
—↑↓—	yz	(a_2)
—↑↓—	z^2	(a_1)

This gives rise to the following transitions in order of increasing energy

$^1A_1 \rightarrow {}^1B_2$ allowed

$^1A_1 \rightarrow {}^1B_1$ allowed

$^1A_1 \rightarrow {}^1A_2$ forbidden

$^1A_1 \rightarrow {}^1A_1$ allowed

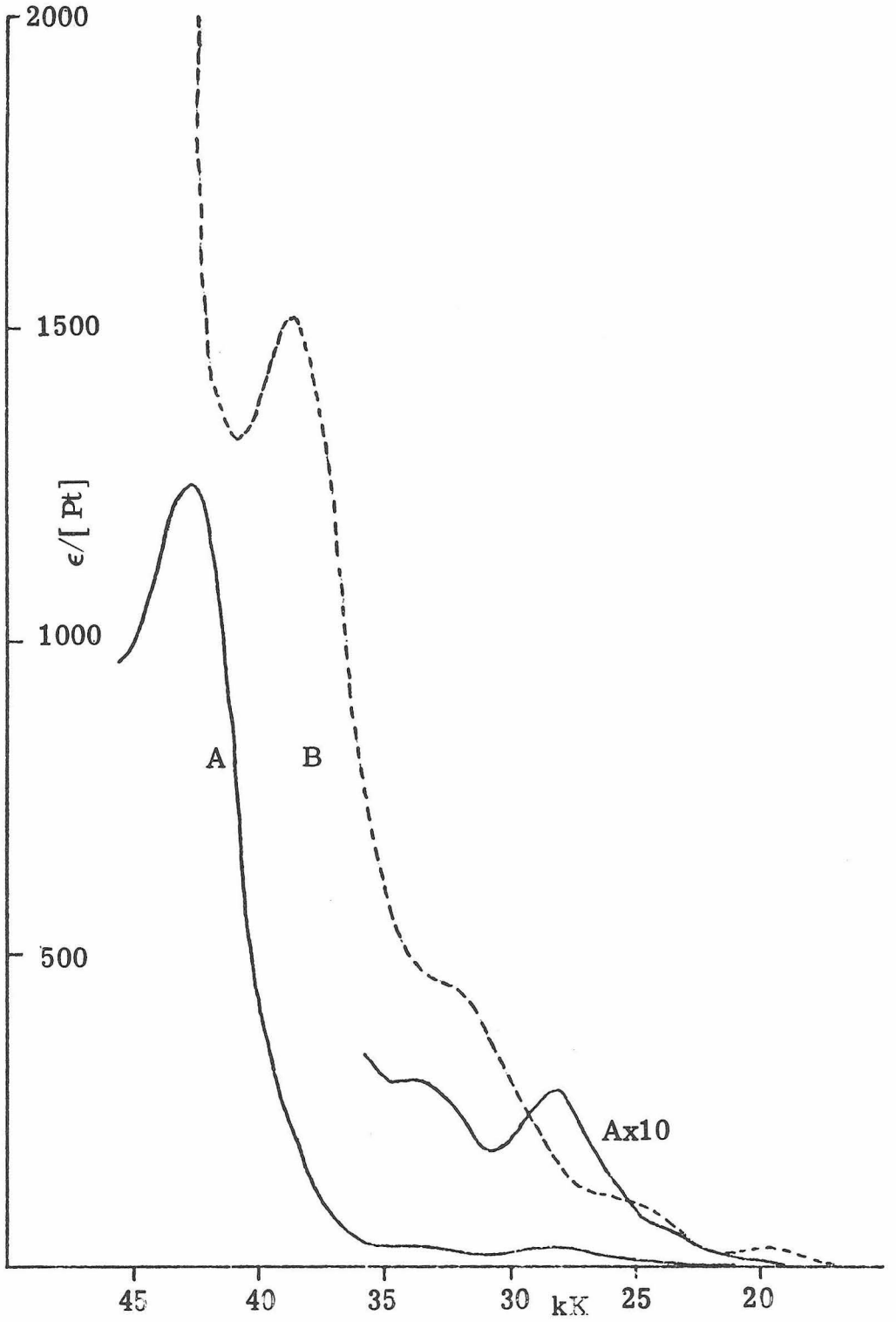

A. $[P][(CH_3CN)PtCl_3]$ in CH_3CN
B. $[P]_2[Pt_2Cl_6]$ in CH_3OH

Figure 24

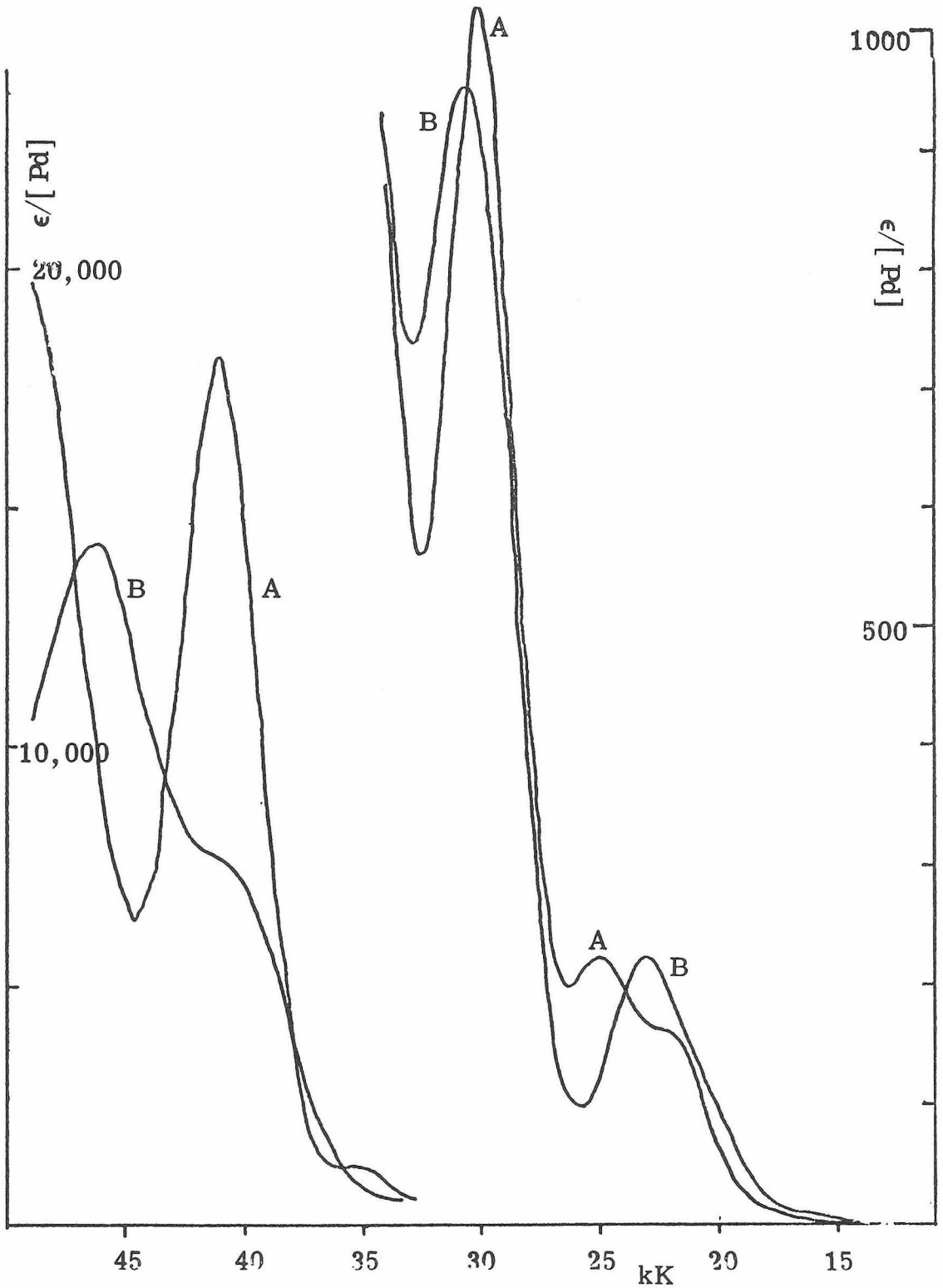

A. $[P][(CH_3CN)PdCl_3]$ in CH_3CN
B. $[P]_2[Pd_2Cl_6]$ in CH_3OH

Figure 25

Table XIII

Electronic Spectra of $(CH_3CN)MCl_3^-$ Salts in CH_3CN[a]

$[P][(CH_3CN)PdCl_3]$	$[P][(CH_3CN)PtCl_3]$	$[N][(CH_3CN)PtCl_3]$	Assignment	Analogous $PtCl_4^{2-}$ Absorption[c]	Analogous $Pd_2Cl_6^{2-}$ Absorption[d]
~17.5 sh[b] (10)	~23.0 sh (4)	~23.3 sh	$^1A_1 \rightarrow {}^3B_2$	20.24 (16.6)	~16.1 sh (24)
~22.2 sh (161)	28.2 (29)	28.3	$^1B_2$	24.75 (59.6)	~20.4 sh (390)
25.0 (222)	33.7 (30)	~33.0 sh	$^1B_1$	29.50 (66.4)	22.8 (512)
30.1 (1020)	~39.0 sh (1250)	~38.5 sh	$^1A_1$	37.03 (404)	~29.4 sh (2200)
~35.7 sh (1230)	42.7	42.9	charge transfer		
41.0 (18,200)			charge transfer		

[a] $\bar{\nu} \times 10^{-3}$ cm^{-1} (ϵ, ℓ mole^{-1} cm^{-1}).

[b] sh = shoulder. ϵ is for $\bar{\nu}$ given.

[c] From CH_3CN solution data from reference 6.

[d] $[P]_2[Pd_2Cl_6]$ in CH_2Cl_2 from this work.

This scheme matches the observed spectrum very nicely and the assignments are given in Table XIII. In this table we also compare these spectra to those of $PtCl_4^{2-}$ and $Pd_2Cl_6^{2-}$. When account is made of the higher ligand field strength of CH_3CN, these spectra correlate nicely. The perturbation from a D_{4h} effective ligand field is apparently not very great in view of the intensities of the transitions of $(CH_3CN)PtCl_3^-$.

Miscellaneous Reactions

Treatment of $(N)_2(Pt_2Cl_6)$ with one equivalent (phosphine/Pt = 1) of $P(OCH_3)_3$ in CH_2Cl_2 results in an equilibrium mixture of $(N)_2(Pt_2Cl_6)$, $(N)_2(PtCl_4)$ and (by difference) $[(CH_3O)_3P]_2PtCl_2$. The first two compounds co-crystallized from solution and could be picked apart by hand. The IR spectrum of $(N)_2(PtCl_4)$ shows just one band at 315 cm^{-1} in the ν_{PtCl} region. The NMR spectrum shows only one sharp absorption for the cation at δ 3.25 ppm. The visible spectrum (Figure 26) is unmistakably that of $PtCl_4^{2-}$. We did not examine the solution to identify $[(CH_3O)_3P]_2PtCl_2$. Presumably the reaction is

$$Pt_2Cl_6^{2-} + 2P(OCH_3)_3 \rightleftharpoons PtCl_4^{2-} + [(CH_3O)_3P]_2PtCl_2 \quad (30)$$

This is the first known case[14,15] of unsymmetrical cleavage of an $M_2X_6^{2-}$ anion.

Reaction of $(N)_2(Pt_2Cl_6)$ with an equivalent of pyridine similarly produces an equilibrium mixture of starting material and product.

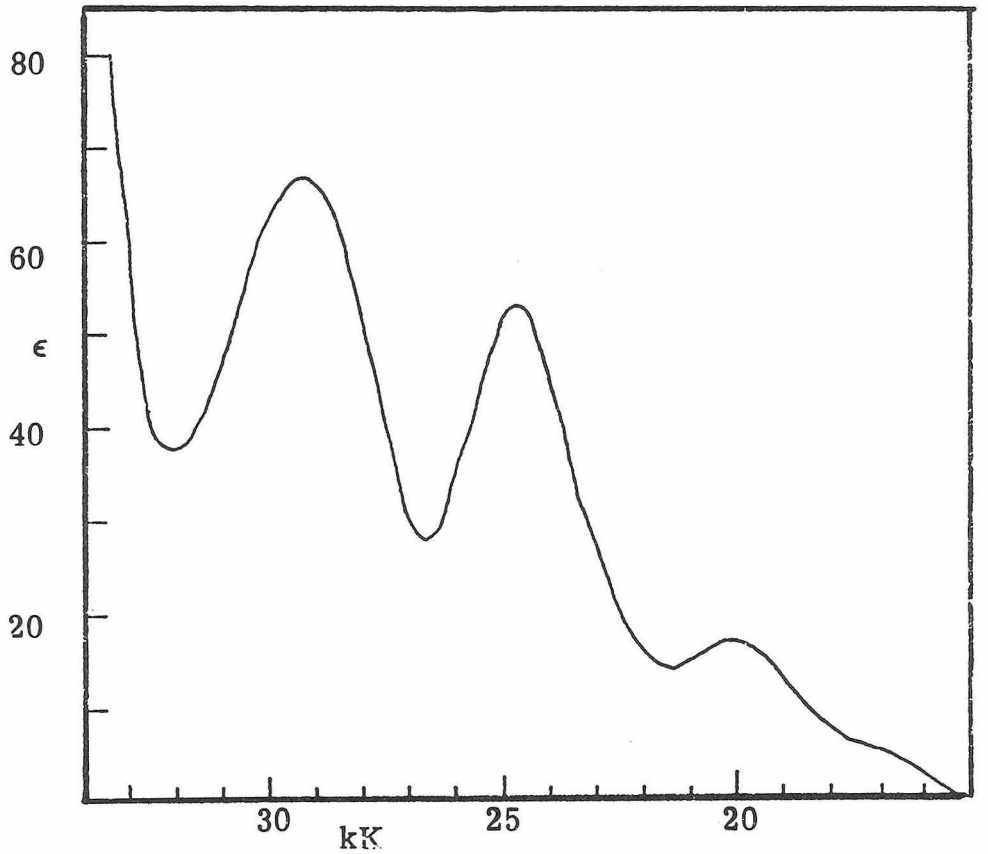

$[N]_2[PtCl_4]$ in CH_2Cl_2

Figure 26

$$Pt_2Cl_6^{2-} + 2C_5H_5N \rightleftharpoons 2(C_5H_5N)PtCl_3^- \qquad (31)$$

The product was isolated as a yellow solid, slightly contaminated by starting material. The IR and Raman spectra (Figure 27) can be rationalized if we assume that ν_s(Cl-Pt-Cl) and ν_{as}(Cl-Pt-Cl) are nearly degenerate. The assignment would be

$$\nu_s(\text{Cl-Pt-Cl}) = 327\ \text{cm}^{-1}$$
$$\nu_{as}(\text{Cl-Pt-Cl}) = 325\ \text{cm}^{-1}$$
$$\nu(\text{Pt-Cl}_{trans}) = 314\ \text{cm}^{-1}$$

The visible spectrum (Figure 28) somewhat resembles that of (olefin)$PtCl_3^-$ complexes (Figure 29), indicating the high ligand field strength of pyridine and possibly even the decent π-acceptor strength of this ligand.

When $(P)_2(Pt_2Cl_6)$ was mixed with an equivalent of NaSCN in acetone, an orange material was formed whose IR spectrum indicates a mixture of N-bonded and S-bonded species.[24] We assign these modes as follows:

	N-bonded	S-bonded
ν(CN)	2110 m	2140 s
ν(CS)	774 m	719 m
δ(SCN)	480 w	429 w

In addition, two broad Pt-Cl stretches are seen at 348 and 323 cm^{-1}. The cyclopropenium α-CH_2 chemical shift is in the range expected for a dimer. We have insufficient evidence to speculate on the structure of the reaction products.[25]

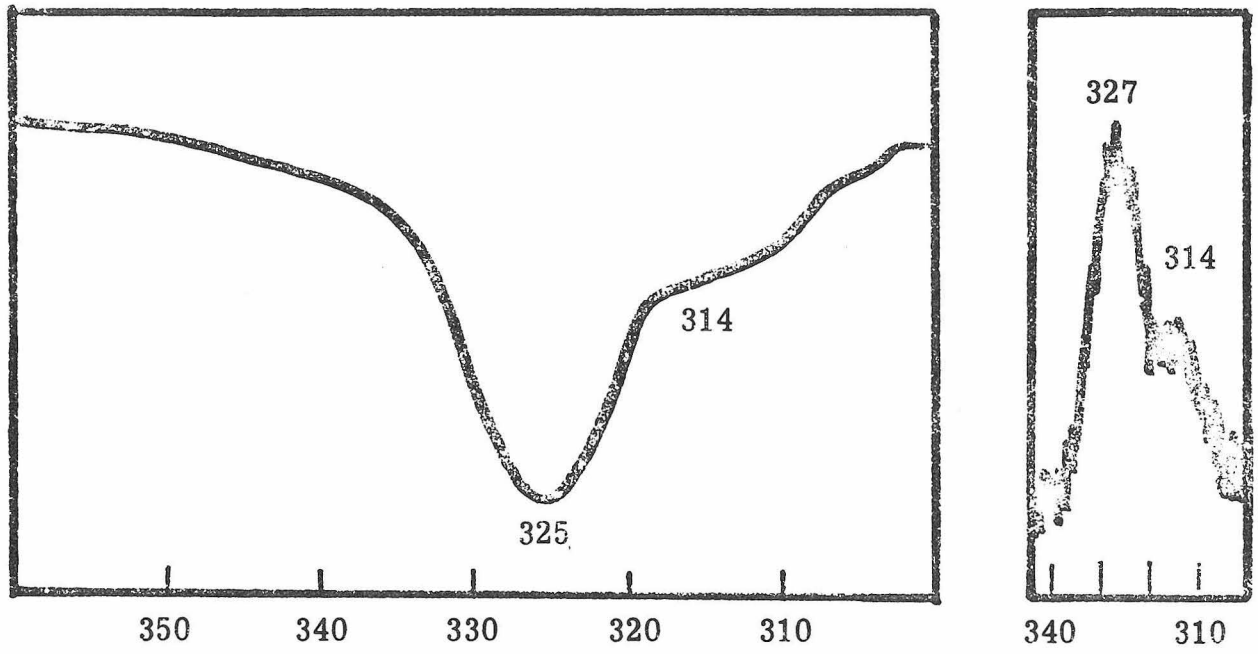

Infrared (left)(KBr pellet) and Raman spectra of solid $[N][(C_5H_5N)PtCl_3]$.

Figure 27

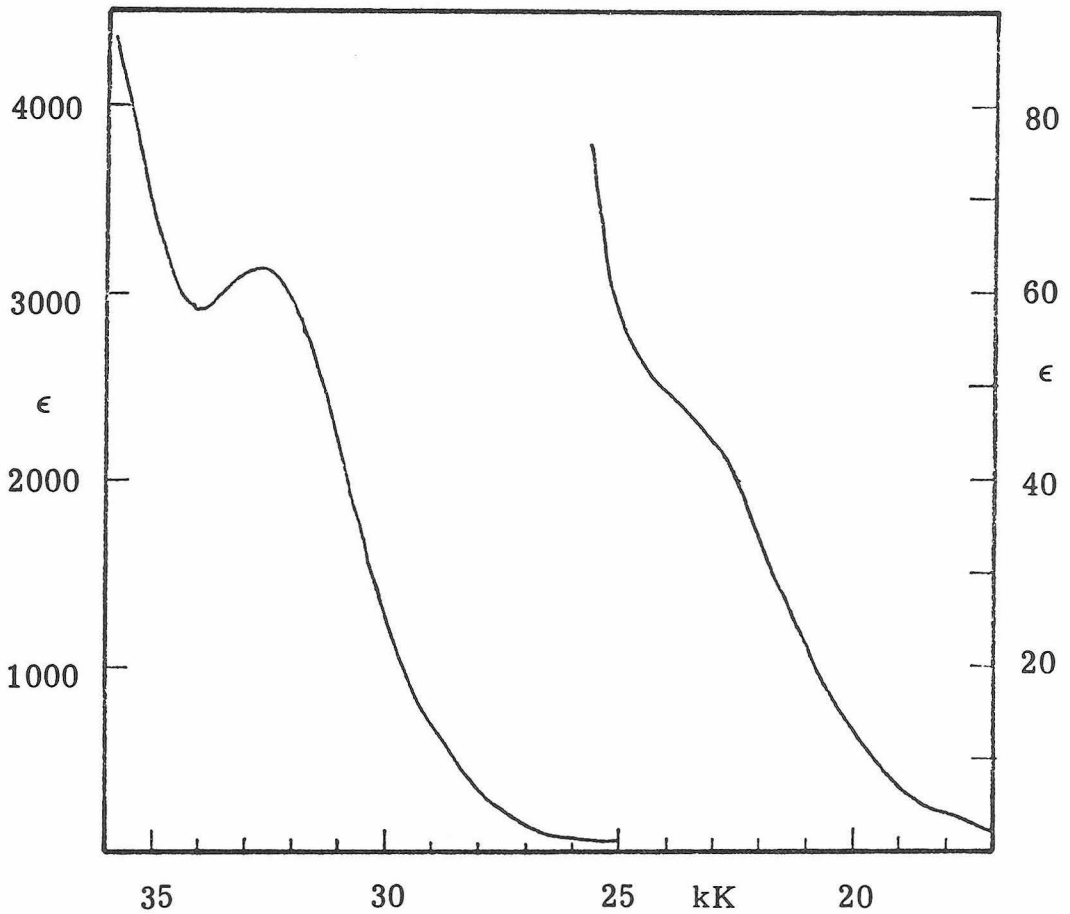

$[N][(C_5H_5N)PtCl_3]$ in CH_2Cl_2
Figure 28

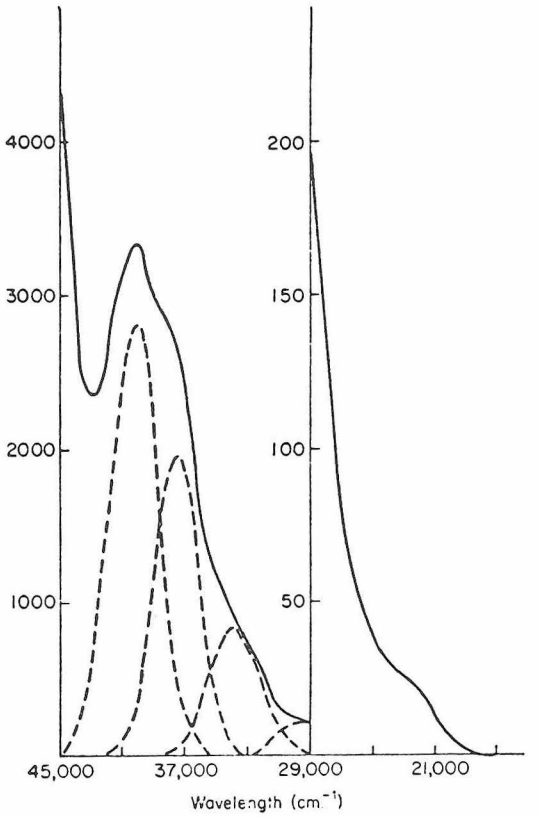

(allyl alcohol) $PtCl_3^-$ (Reference 9)

Figure 29

(With Permission)

In an attempt to examine the reaction with cyanide, we discovered that the cyclopropenium ring is attacked by cyanide. A reaction more complicated than (32) must occur because we observe five peaks in the NMR spectrum of the product of $(N)(BF_4)$ and KCN.

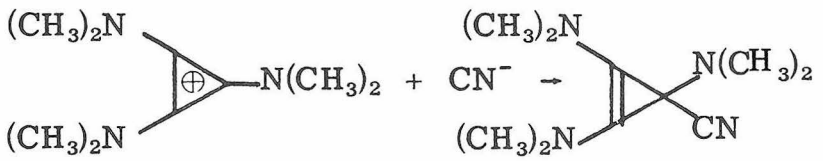

(32)

Experimental

NMR Titrations. Titrations with $(n\text{-}C_4H_9)_4NCl$, cyclooctene, $(N)(BF_4)$ and $(P)(BF_4)$ were performed on a Varian A60-A spectrometer operating at ca. 40 °C. In a typical experiment, ~ 10 mg cyclopropenium salt was weighed into an NMR tube and 0.40 ml spectroquality CH_2Cl_2 and 30 μl TMS was added volumetrically by syringe. The volume of this solution was assumed to be 0.430 ml and additional aliquots of titrant solution were assumed to be additive. No corrections were made for volumes of mixing. After each aliquot of titrant was added from a 250 μl syringe, the spectrum was scanned 2-3 times using a 100 Hz sweep width. Chemical shifts were measured in Hz upfield of the high field $^{13}CH_2Cl_2$ satellite. (In some initial experiments, chemical shifts were measured in Hz downfield of internal TMS using a 250 or 500 Hz sweep width. In titrations of $[(CH_3)_2N]_3C_3^+$ salts, the

methyl chemical shift was used. In titrations of $(n\text{-}C_3H_7)_3C_3^+$ salts, the chemical shift of the α-CH_2 protons was followed. Reproducibility of the chemical shift from one scan to the next was typically better than ± 0.1 Hz. Absolute accuracy is, of course, much less because of the instability of the spectrometer. $(n\text{-}C_4H_9)_4NCl$ is very hygroscopic and its weight was only measured to two places in preparing titrant solutions. The actual amount of $(n\text{-}C_4H_9)_4NCl$ used in any titration could easily be in error by 30%, so exact data from these titrations must not be taken too seriously. Cyclooctene was redistilled (B.P. 38°, aspirator pressure) before use. Final solutions of cyclooctene complexes are all yellow.

Spectrophotometric Titrations. 10-50 mg cyclopropenium salt was dissolved in 25 ml CH_2Cl_2. 2.6 ml aliquots of this stock solution were treated with varying quantities of titrant solution and the final solutions were made up to a constant volume by adding more solvent. Spectra were determined on a Cary 17 at *ca.* 20°.

CH_3CN Solution Studies. Solutions of $(CN_3CN)MCl_3^-$ were prepared by dissolving the appropriate cyclopropenium $M_2Cl_6^{2-}$ salt in spectroquality CH_3CN. Pd solutions remained a constant bronze-yellow color from the moment of mixing. Pt solutions turned from their initial pink color to yellow in less than two hours. Pt solutions used for these studies were aged 5-24 hours and Pd solutions were aged 0.5-4 hours.

Infrared spectra were recorded on a Perkin-Elmer 225 spectrometer. Both CsI and AgCl cells were used as specified in Table XII. In general, Pt salts were not reactive toward CsI, but Pd salts did react with a CsI cell.

Raman spectra were obtained with a Cary 81 laser Raman spectrometer using a He-Ne (6328 Å) laser. Depolarization ratios are expressed as a percent of the depolarization ratio observed for the solvent 380 cm^{-1} band. (The CH_3CN 380 cm^{-1} band is a depolarized degenerate C-C-N bending mode.) Ideally this solvent band should exhibit a depolarization ratio ($I_\perp/I_\parallel$) of 0.75. In fact, we observe values of 0.83-0.97. Both ν_{MCl} bands always exhibited $I_\perp/I_\parallel < (I_\perp/I_\parallel)_{380\ band}$ and are therefore polarized (a_1 symmetry). Band intensities were measured by tracing the peaks on mm ruled graph paper and counting the enclosed squares. Overlapping peaks were resolved by eye prior to this count.

<u>$\{[(CH_3)_2N]_3C_3\}\{(CH_3CN)PtCl_3\}$</u>. $(N)_2(Pt_2Cl_6)$ was dissolved in CH_3CN to produce a nearly saturated solution after an hour of stirring at room temperature. The solution was filtered and allowed to stand 1-3 days with a loose aluminum foil cap until yellow crystals began to form. (Seed crystals may be obtained by precipitating a small quantity of solution with hydrocarbon.) Crystallization was continued for a day at 0° and a day at -20°. The crystals are orange when isolated by filtration and washed with ether. An analytical sample was dried 3 days at 10 μ/25 °C. Anal. Calcd for $C_{11}H_{21}N_4PtCl_3$: C, 25.85; H, 4.14; Pt, 38.17; Cl, 20.81. Found: C, 25.93; H, 3.99; Pt, 39.22; Cl, 20.80. MP 164° dec. IR: (KBr pellet, 2000-300 cm^{-1}) 1810 vw, 1764 vw, 1640 sh, w, 1550 br, vs, 1444 w, 1415 m, 1400 s, 1282 vw, 1221 m, 1132 w, 1052 w, 1026 m, 958 vw, 784 m, 618 vw, 558 vw, 454 vw,

344 m, 328 m, 316 sh, w. NMR data are given in Table XI and Figure 17. A Raman spectrum of this solid is shown in Figure 20.

$\{[(CH_3)_2N]_3C_3\}\{Cl\}$. 0.85 g $(N)(BF_4)$ dissolved in 10 ml H_2O is passed through a column of 4 g Mallinckrodt Amberlite IRA 400 anion exchange resin loaded with KCl. The eluate is concentrated and passed a second time through a fresh anion exchange column to remove all traces of BF_4^- from the IR spectrum of the hygroscopic white solid.

$[(n\text{-}C_3H_7)_3C_3][X]$ (X = Cl, Br). These oils, which could not be crystallized from H_2O, EtOH, CH_2Cl_2 or C_6H_6, are obtained by ion exchange in the same manner as (N)(Cl) above.

$\{[(CH_3)_2N]_3C_3\}\{B(C_6H_5)_4\}$. 0.08 g $(N)(BF_4)$ in 2 ml H_2O was added to a filtered solution of 0.12 g $NaB(C_6H_5)_4$ in 4 ml H_2O with vigorous magnetic stirring. The voluminous white precipitate was filtered, washed with water, and crystallized from acetone-ether. MP 187-188°.

Reactions of $Pt_2Cl_6^{2-}$:

with $P(OCH_3)_3$ - 0.20 mmoles $(N)_2(Pt_2Cl_6)$ in 2 ml CH_2Cl_2 was treated with 0.40 mmoles $P(OCH_3)_3$ in 50 μl CH_2Cl_2. The salt dissolved with a slight release of heat to give a red solution which was left at room temperature 3.5 hrs. No crystals formed after 2 hrs at -20°, so 0.5 ml acetone was added to produce a little precipitate. After another hour at -20°, 2 ml more acetone was added and the solution deposited a pink microcrystalline product laced with large, well formed red needles after standing overnight

at -20°. The red needles were picked out by hand and identified as starting material by their IR spectrum. The pink product was redissolved in CH_2Cl_2/acetone and 50 μl $P(OCH_3)_3$ solution (0.4 mmoles) was added. No product crystallized after 2 days at -20°, so the solution was cooled on dry ice for 6 hours to produce pink microcrystalline product which was washed with ether and dried in vacuo. This product (MP 218 dec) was identified as $(N)_2(PtCl_4)$ from its spectra. NMR (CH_2Cl_2): δ 3.25 ppm (singlet) (No $P(OCH_3)$ is seen. It would occur at δ 3.50 ppm (J = 10.5 Hz).) IR: $[(CH_3)_2N]_3C_3^+$ spectrum plus one peak at 315 cm^{-1} (ν_{PtCl}) in a KBr pellet. UV(CH_2Cl_2): ~17,000 sh (ϵ = 5.5), 20,000 (16.9), 24,770 (53.2), 29,240 (67.0). (Cf.literature[6] spectrum of $[(n\text{-}C_4H_9)_4N]_2[PtCl_4]$ in CH_3CN: ~17,500 sh (ϵ = 6.5), 20,240 (16.6), 24,750 (59.6), 29,500 (66.4).) Raman (solid): 328, 306.

with pyridine - 76 mg (0.081 mmoles) $(N)_2(Pt_2Cl_6)$ was treated with 0.18 mmoles pyridine in 1 ml CH_2Cl_2. The red solution began to deposit some yellow crystals after ~5 min, and the solution turned yellow on standing overnight at RT. Yellow crystals mixed with red crystals of starting material continued to come out for a day at -20°. The product was filtered, redissolved in 3 ml CH_2Cl_2, treated with 1 μl pure pyridine, and the solution was filtered. It was concentrated to ~1.5 ml on a hot plate and 2 ml acetone was added. The yellow solution was left at -20° to crystallize for 3 days. The yellow product is always contaminated by red starting material. A sample of product and starting material

was separated as much as possible by hand. Anal. Calcd for $\{[(CH_3)_2N]_3C_3\}\{(C_5H_5N)PtCl_3\}$, $C_{14}H_{23}N_4PtCl_3$: C, 30.63; H, 4.22; Pt, 35.54; Cl, 19.37. Found: C, 29.51; H, 3.69; Pt, 36.02; Cl, 18.52. MP ~ 160-170 dec. NMR (CH_2Cl_2): δ_{CH_3} = 3.18 ppm. Pyridine - not observed. (This sample was either badly out of tune or contained a paramagnetic impurity. The CH_3 resonance was broadened and the much weaker pyridine signal is lost in the baseline.) IR(KBr pellet, 4000-270 cm^{-1}): 3110 w, 3065 w, 3035 w, 3015 w, 2930 w, 2890 w, 2750 w, 2695 w, 1604 w, 1589 sh, m, 1561 br, s, 1474 w, 1449 m, 1420 m, 1405 s, 1222 m, 1211 m, 1151 w, 1073 w, 1063 w, 1029 w, 820 w, 786 w, 782 m, 700 m, 460 vw, 325 m, 314 sh, w. The Raman spectrum appears in Figure 27. UV(CH_2Cl_2, Figure 28): ~17,500 sh (ϵ = 3), ~23,500 sh (47), 32,600 (3110).

<u>with SCN^-</u> - 4.6 mg (0.056 mmole)NaSCN and 22 mg (0.047 mmole) $(P)_2(Pt_2Cl_6)$ were dissolved in 1.5 ml acetone. The solution was stirred at room temperature for 6 hrs and it turned from pink to orange early in the reaction. A small amount of white precipitate formed after the first few minutes. The orange solution was removed by pipette and concentrated to dryness <u>in vacuo</u> to produce an orange oily residue. NMR (acetone): α-CH_2, 3.60; β - CH_2, 2.27; CH_3, 1.23. IR(KBr pellet, 4000-290): 3440 br, m, 2960 s, 2930 s, 2870 s, 2140 s, 2110 m, 1636 w, 1620 w, 1462 br, s, 1380 s, 1353 vw, 1338 vw, 1311 w, 1247 m, 1220 sh, w, 1103 w, 1072 w, 1040 w, 917 w, 855 w, 774 m, 719 m, 480 w, 429 w, 348 m,

323 m. This oil could not be eluted from an alumina column with acetone and the components were only slightly separated on a silica gel column.

Reaction of $(N)(BF_4)$ and NaCN. 0.08 g $(N)(BF_4)$ and 0.07 g (~ 3 equivalents) KCN were stirred 15 minutes in 2 ml H_2O at 50 °C to form an orange-red oil soluble in CH_2Cl_2. A small amount of crystalline material also formed in the aqueous phase. NMR of the oil in CH_2Cl_2 shows peaks at 191, 189.5, 143. 141.5, and 138 Hz downfield of TMS with relative intensities 45 : 14 : 60 : 14 : 37, respectively. Addition of $(N)(BF_4)$ and H_2O to this solution shows that none of the five peaks can be attributed to these two substances.

References

1. P. M. Henry and O. W. Marks, Inorg. Chem., 10, 373 (1971).

2. In aqueous solution, the $Pd_2Cl_6^{2-}$ dimer is not formed to any appreciable extent and above $[Cl^-] = 0.1$ M, $PdCl_4^{2-}$ is the predominant species. (A. Aguiló, Adv. Organomet. Chem., 5, 327 (1967).

3. J. E. Teggins, D. R. Gano, M. A. Tucker, and D. S. Martin, Jr., Inorg. Chem., 6, 69 (1967).

4. It is unfortunately necessary to specify the type of IR cell and to determine that the cell is inert toward these samples. Several platinum halides have been found to react with halide cells.[5] In our work, $(N)_2(Pd_2Cl_6)$ in CH_2Cl_2 reacted immediately with a CsI cell.

5. L. Spaulding, B. A. Reinhardt, and M. Orchin, Inorg. Chem., 11, 2092 (1972).

6. W. R. Mason, III, and H. B. Gray, J. Amer. Chem. Soc., 90, 5721 (1968). This material was obtained from C. Cowman.

7. We have tried in vain to find reports of the visible spectra of Pd-olefin complexes. We did find that the color of $(C_2H_4)_2Pd_2Cl_4$ is yellow.[2] In the case of Pt, however, $PtCl_4^{2-}$ shows its first few absorptions at 17,500 ($\epsilon = 6.5$), 20,240 (16.6), 24,750 (59.6).[6] Zeise's salt, $[K][(\pi\text{-}C_2H_4)PtCl_3] \cdot H_2O$ shows its first two bands at 23,900 ($\epsilon = 40.1$), 30,350 (340), 33,450 (605).[8] The band at 24,750 in $PtCl_4^{2-}$ is generally considered to be the first d-d spin allowed transition.[6] In

contrast, the band at 23,900 is taken as a spin allowed d-d transition in Zeise's salt.[9] There is a contradiction here because ethylene ought to be higher in the spectrochemical series than Cl.

8. a) J. W. Moore, Acta Chem. Scand., 20, 1154 (1966);
b) F. R. Hartley, Chem. Revs., 799 (1969).

9. R. G. Denning, F. R. Hartley, and L. M. Venanzi, J. Chem. Soc., 1322 (1967).

10. $K_{24} = [P]^2/[R][C_8]^2_{FREE}$. $M_T = 4.09 \times 10^{-3}$ M. $P = (0.95) \cdot (\frac{1}{2} M_T) = 1.95 \times 10^{-3}$ M. $R = \frac{1}{2}(M_T - P) = 1.07 \times 10^{-3}$ M. $[C_8]_{FREE} = (0.05)(C_8)_{TOT} = (0.05)(\frac{1}{2})M_T = 0.10 \times 10^{-3}$ M. $K = (1.95 \times 10^{-3})^2/(1.07 \times 10^{-3})(0.10 \times 10^{-3})^2 \approx 4 \times 10^5$.

11. M. J. Grogan and K. Nakamoto, J. Amer. Chem. Soc., 88, 5454 (1966).

12. Solutions of Zeise's salt in water do not emit appreciable radiation at RT. The solid had to be cooled to observe this emission. P. Natarajan and A. W. Adamson, J. Amer. Chem. Soc., 93, 5599 (1971).

13. P. D. Fleischauer and P. Fleischauer, Chem. Revs., 199 (1970).

14. M. M. Muir and E. M. Cancio, Inorg. Chim. Acta, 4, 565 (1970).

15. R. G. Pearson and M. M. Muir, J. Amer. Chem. Soc., 88, 2163 (1966).

16. R. A. Walton, Quart. Rev., 19, 126 (1965).

17. π-CH_3CN group exhibit $\nu_{CN} \sim 200\ cm^{-1}$ lower than free CH_3CN. (M. Farona and K. Kraus, Inorg. Chem., **9**, 1700 (1970).

18. T. Weil, L. Spaulding, and M. Orchin, J. Coord. Chem., **1**, 25 (1971).

19. ν = stretching, s = symmetric, as = asymmetric.

20. a) D. M. Adams, "Metal-Ligand and Related Vibrations," St. Martin's Press, New York, 1968, p. 73. For other infrared trans effects in square planar Pt complexes see:

    b) M. R. Collier, C. Eaborn B. Jovanović, M. F. Lappert, L. Manojlović-Muir, K. W. Muir, and M. M. Truelock, Chem. Comm., 613 (1972)

    c) J. Chatt, L. A. Duncanson, and B. L. Shaw, Chem. Ind. (London), 859 (1958).

21. Lack of coupling to Pt implies that ethylene is undergoing a rapid dissociation-association. Mere propeller-like rotation of the ethylene (for which the activation energy is very probably lowered by CH_3CN which is a stronger π acceptor than Cl) is not sufficient to eliminate the Pt-C_2H_4 coupling since ^{103}Rh-C_2H_4 coupling is observed to exist in the high temperature limiting spectrum of $CpRh(C_2H_4)_2$. (R. Cramer, J. B. Kline, and J. D. Roberts, J. Amer. Chem. Soc., **91**, 2519 (1969).)

22. In Zeise's salt, three bands are observed at 339, 331, and 310 cm^{-1}.[11] The lowest energy band is assigned as

$\nu(M\text{-}Cl_{trans})$ and the highest energy band is assigned as ν_{as}. This is reasonable in this case because the 339 cm^{-1} band is stronger than the 331 cm^{-1} band.

23. In reference 20a, Chapter 6, we find $\nu_{Pt\text{-}N}$ for various amine complexes to be near 500 cm^{-1}. CH_3CN will be bound more weakly than amines so ν_{PtA} should be lower than 500 cm^{-1}.

24. a) Reference 20a, page 327.

For other recent references on the problem on N-bonded vs. S-bonded thiocyanate, see:

b) C.J. Horn and T. M. Brown, Inorg. Chem., **11**, 1970 (1972);

c) D. F. Gutterman and H. B. Gray, Inorg. Chem., **11**, 1727 (1972);

d) J. L. Lauer, M. E. Peterkin, J. L. Burmeister, K. A. Johnson, and J. C. Lim, Inorg. Chem., **11**, 907 (1972);

e) J. B. Melpolder and J. L. Burmeister, Inorg. Chem., **11**, 911 (1972);

f) M. W. Adlard and G. Socrates, J. Chem. Soc. Dal., 797 (1972).

25. The interesting bridged species **i** and **ii** have been observed and should be considered when speculating on the product of this reaction. For a leading reference, see M. C. Hall, J. A. J. Jarvis, B. T. Kilbourn, and P. G. Owston, J. Chem. Soc. Dal., 1544 (1972).

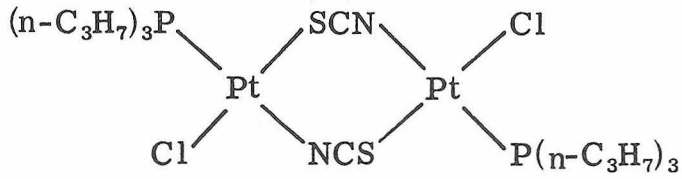

i

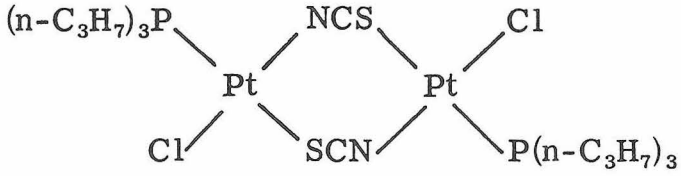

ii

26. For a recent report on a very large kinetic cation dependence, see J. P. Collman, J. N. Cawse, and J. I. Brauman, J. Amer. Chem. Soc., 94, 5905 (1972).

27. Very peculiar differences between a central peak and its ^{195}Pt satellites have been observed. See K. Thomas, J. T. Dumler, B. W. Renoe, C. J. Nyman, and D. M. Roundhill, Inorg. Chem., 11, 1795 (1972).

Chapter Six

The Protonated Metal-Metal Bond

History

Late one night, working in the basement of the now-defunct Gates Laboratory, I had given up research for the day from sheer disgust. The syntheses of π-cyclopropenium complexes had failed in most conceivable ways, taking as its toll one NMR probe, some gas chromatography equipment, and most of my short supply of sanity. I opened up the latest issue of the Journal of the Chemical Society, Section A, and saw that a reasonable piece of work developed from dumping polynuclear carbonyl compounds in 98% H_2SO_4 and watching protons play hopscotch between the metals.[1] I had sitting in my refrigerator a bottle of $[(\pi\text{-}C_5H_5)Fe(CO)_2]_2$ and thought this would be an excellent candidate for such a dump-and-run experiment. The hope was that a proton would find its way between the two iron atoms as follows:

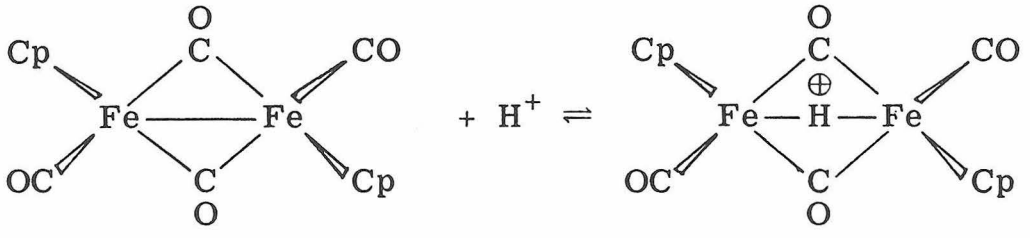

I

In fact, a metal-bound hydrogen signal was observed at τ36 ppm. This chemical shift was near the upper limit of observed proton

shifts at the time of this study,[2] and I was immediately confident that the proton was indeed bound to both metal atoms. The structure of the product was subsequently shown to be II

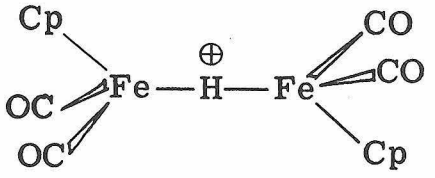

II

which is even more interesting than I as only a proton held the two halves of the cation together. I later found that Davison, et al.[3] had observed this high field NMR signal eight years before I did, and while my own work was in progress, Symon and Waddington[4] reached the same conclusion I did about the structure of II.

From this random start, a sensible project suggested itself. Levenson[5] studied the electronic spectra of a series of compounds with metal-metal bonds and assigned a strikingly intense transition near 30,000 cm^{-1} to the $\sigma \rightarrow \sigma^*$ transition. With a series of compounds available with protonated metal-metal bonds, I thought it would be easy to study the electronic effects of protonation. The simple-minded thought was that a $\sigma \rightarrow \sigma^*$ transition would split into two transitions when the metal-metal bond is protonated (Figure 1). It is therefore reasonable to start with Levenson's case for the $\sigma \rightarrow \sigma^*$ assignment.

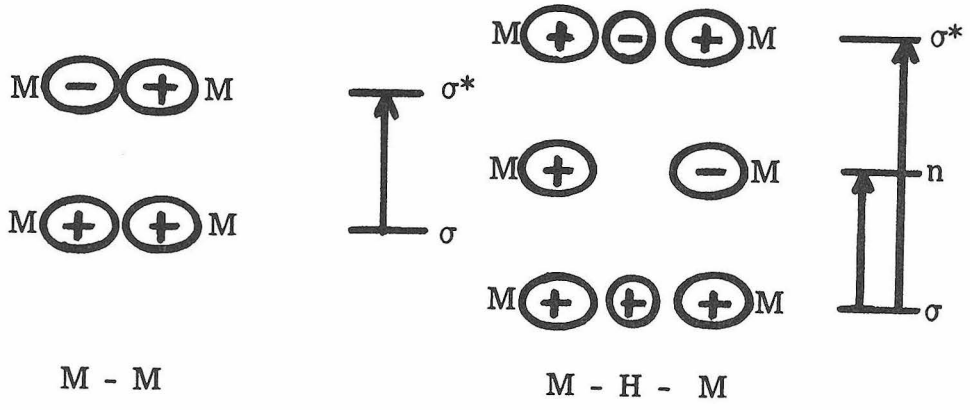

Figure 1.

The Case for Levenson

Two examples of Levenson's spectra and his assignments of four different spectra are given in Figure 2[6] and Table I. The coordinate system is chosen such that the z axis is colinear with the metal-metal bond (Figure 3). The d_{xz}, d_{yz}, and d_{xy} orbitals are referred to collectively as the $d\pi$ orbitals. The various combinations of ligand antibonding orbitals are called the π^* orbitals. My own summary of Levenson's substantial case for the $\sigma \rightarrow \sigma^*$ assignment is now given. The organization and emphasis is mine.

1. $Mn_2(CO)_{10}$ possesses the staggered D_{4d} metal-metal bonded structure in the solid state.[7] (Figure 3) Infrared spectra fully support such a structure in solution.[8,9]

2. The band assigned as the $\sigma \rightarrow \sigma^*$ transition is fully allowed by the selection rules of the molecular point group and has an observed extinction coefficient of $\sim 30,000$ l mole^{-1} cm^{-1}. The band is polarized parallel to the metal-metal axis. Given a $^1A_1$

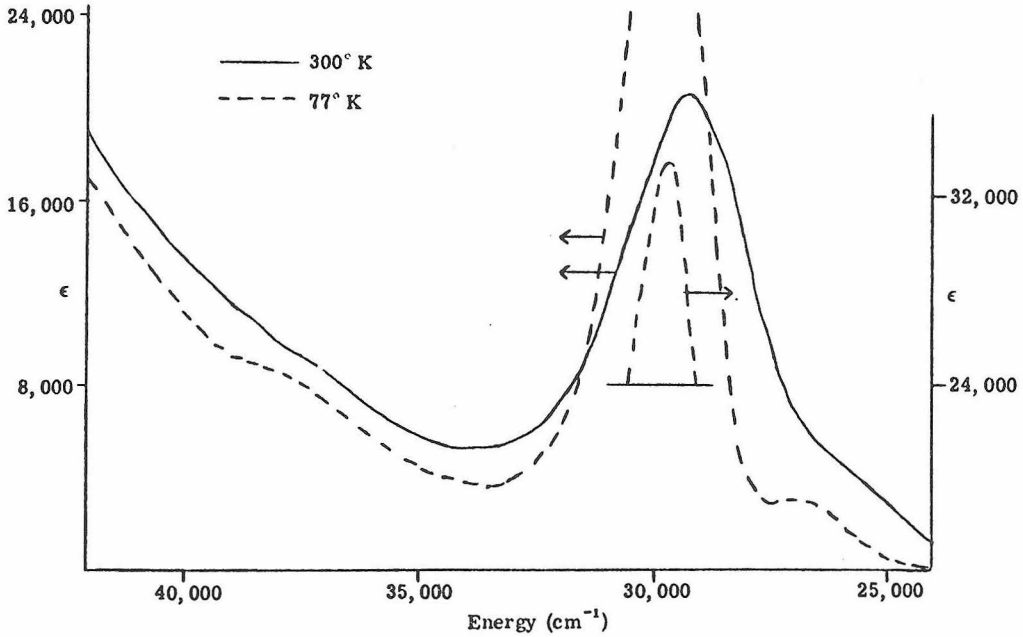

Electronic spectra of $Mn_2(CO)_{10}$ in 3-PIP.

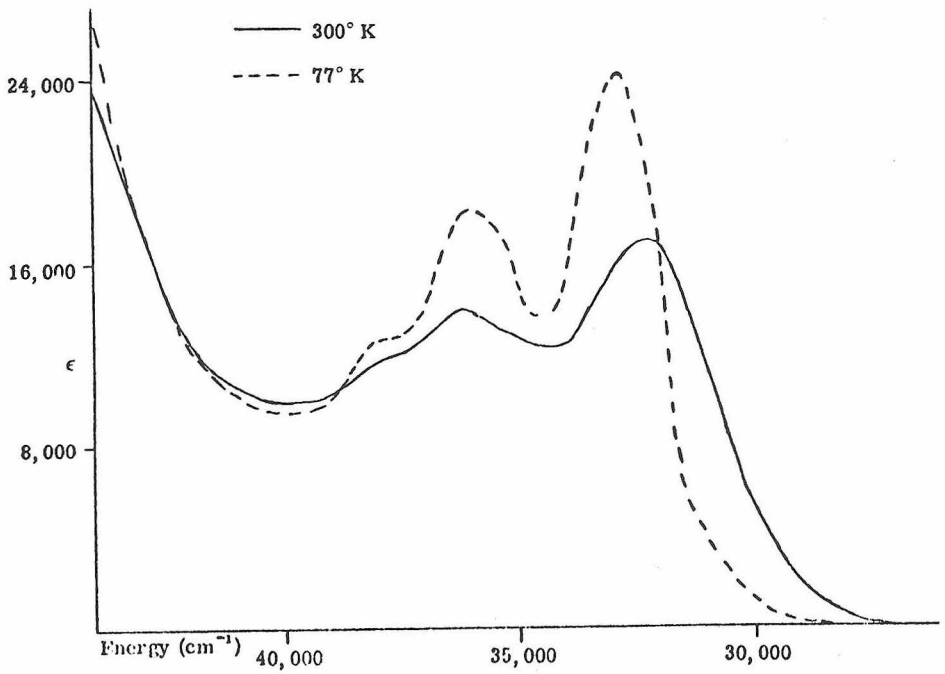

Electronic spectra of $Re_2(CO)_{10}$ in 3-PIP.

Figure 2. (Reference 5)

Table I[5]

Electronic Spectral Data for the Neutral Decacarbonyls with Band Assignments

Complex	Band Energy (cm^{-1})[a]	e	Assignment[c]
$Mn_2(CO)_{10}$	26,700	2,900	$d\pi \rightarrow \sigma^*$
	29,740	33,700	$\sigma \rightarrow \sigma^*$
	37,600	8,200	$d\pi \rightarrow \pi^*$
	49,100[b]	84,400	$M \rightarrow \pi^*$
$Tc_2(CO)_{10}$	32,400	26,600	$\sigma \rightarrow \sigma^*$
	35,500	12,700	$\sigma \rightarrow \pi^*$
	38,200	11,200	$d\pi \rightarrow \pi^*$
	51,500[b]	104,000	$M \rightarrow \pi^*$
$Re_2(CO)_{10}$	32,800	24,000	$\sigma \rightarrow \sigma^*$
	36,000	18,100	$\sigma \rightarrow \pi^*$
	38,100	12,500	$d\pi \rightarrow \pi^*$
	$>$52,500[b]	$>$100,000	$M \rightarrow \pi^*$
$MnRe(CO)_{10}$	31,950	20,100	$\sigma \rightarrow \sigma^*$
	36,000	11,400	$\sigma \rightarrow \pi^*$
	37,700	9,900	$d\pi \rightarrow \pi^*$
	51,700[b]	86,600	$M \rightarrow \pi^*$

[a]At 77° K in 3-PIP.

[b]At 300° K in acetonitrile.

[c]σ^* refers to the antibonding d_{z^2} combination; π^* refers to any of the antibonding ligand orbital combinations.

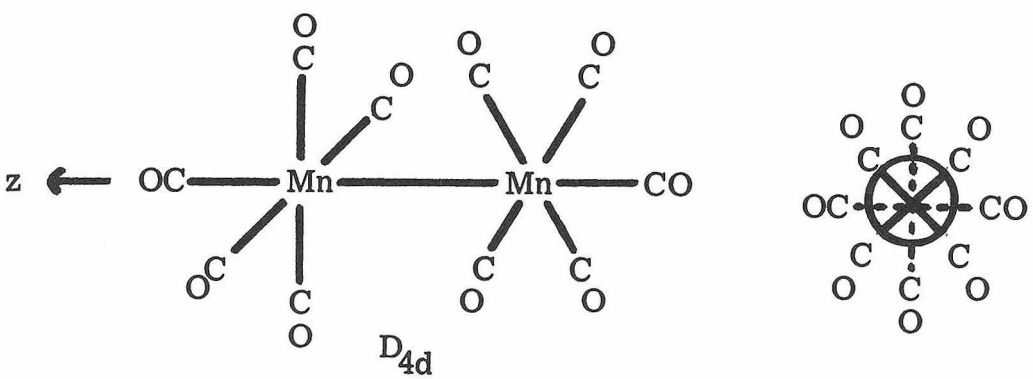

Figure 3. The structure of $Mn_2(CO)_{10}$.

ground state, only a $^1A_1 \rightarrow {}^1B_2$ transition is fully allowed and z polarized. The $\sigma \rightarrow \sigma^*$ transition fulfills these requirements. The band assigned as $\sigma \rightarrow \sigma^*$ in $MnRe(CO)_{10}$ does not split into two components at 80°K as it might if the transition were degenerate in the parent D_{4d} $Mn_2(CO)_{10}$ molecule.

3. For the first row carbonyls, $Cr(CO)_6$, $Fe(CO)_5$, and $Ni(CO)_4$, the energy of the first $M \rightarrow L(\pi^*)$ charge transfer band increases systematically as the ionization energy of the compound increases.[10,11] This presumably reflects a constant π^* energy level and a highest filled d orbital whose energy varies with the metal. Using this correlation one would expect the first $M \rightarrow L(\pi^*)$ band of $Mn_2(CO)_{10}$ to occur at least 10,000 cm^{-1} higher than the 29,200 cm^{-1} position assigned to the $\sigma \rightarrow \sigma^*$ transition. We feel that this is a somewhat vulnerable argument because one is comparing mononuclear and binuclear compounds. It would not be surprising if the correlations obeyed by one family of compounds do not apply directly to the other. However, a 10,000 cm^{-1} deviation is very unlikely.

The energy of the first $M(d\pi) \rightarrow L(\pi^*)$ charge transfer bands of $Cr(CO)_6$, $Mo(CO)_6$, and $W(CO)_6$ varies by only 1100 cm^{-1}, decreasing down the column.[11] The $\sigma \rightarrow \sigma^*$ transition of the $M_2(CO)_{10}$ (M = Mn, Tc, Re) <u>increases</u> in energy going down the column. The ionization energy of the mononuclear compounds[10b] increases slightly going down the column whereas the ionization energy of the binuclear compounds[12] decreases going down the

column. This is taken as evidence that the highest filled orbital in the different classes of compounds is different. In the mononuclear compounds, the highest filled orbital is certainly the $t_{2g}(d\pi)$ orbital. For the binuclear (d^7) compounds the z^2 or $x^2 - y^2$ orbitals must be occupied in some way in the ground state.

The $\sigma \rightarrow \sigma^*$ transition in $MnCr(CO)_{10}^-$ does not show the large drop in energy (relative to the neutral compounds) expected for a $M \rightarrow L(\pi^*)$ transition. All of these data together show that the transition in question does not obey the trends observed for $M \rightarrow L(\pi^*)$ transitions in mononuclear complexes.

4. Semiempirical molecular orbital calculations produce energy levels which place the $\sigma \rightarrow \sigma^*$ transition in the proper range, both absolutely and relative to the other transitions. (Table II) The calculated MO scheme is in good qualitative and semiquantitative agreement with observed photoelectron spectra.[12]

5. If we accept that the transition is not a $M \rightarrow L$ charge transfer band, the only other d-d transition which meets the symmetry requirements given in paragraph 2 is a $d_{xy_{A,B}} \rightarrow d_{x^2 - y^2_{B,A}}$ transition. The notation means that an electron goes from a d_{xy} orbital on one atom to an unoccupied $d_{x^2 - y^2}$ orbital on the other atom. The one-electron orbital energy of this transition is calculated to be $\gtrsim 20,000\ cm^{-1}$ above the energy of the band assigned as $\sigma \rightarrow \sigma^*$. We point out that this is an $e_2 \rightarrow e_2$ transition and <u>the different states produced by the $(e_2)^3(e_2)^1$ configuration could be very different from the one-electron energy levels</u>.

Table II[5]

Some Selected Eigenvalues of $Mn_2(CO)_{10}$

Energy (cm^{-1})		Level	
+ 620		$8b_2$	p
- 5,580		$10e_1$	p
- 18,060		$9e_3$	π^*
- 18,530		$8e_2$	$d_{x^2-y^2}$
- 18,600		$2a_2$	π^*
- 19,730		$8a_1$	π^*
- 20,430		$2b_1$	π^*
- 21,410		$7e_2$	π^*
- 21,960		$9e_1$	π^*
- 22,790		$8e_3$	π^*
- 24,480		$7b_2$	π^*
- 25,120		$8e_1$	π^*
- 27,590		$7e_3$	π^*
- 28,710		$6e_2$	π^*
- 30,300		$7e_1$	p, π^*
- 33,080		$7a_1$	s, p
- 39,420		$6b_2$	σ^* d_{z^2} comb.
- 65,340	highest filled level →	$6a_1$	σ_b d_{z^2} comb.
- 66,620		$5e_2$	d_{xy}
- 67,290		$6e_3$	d_{xz}, d_{yz}
- 69,390		$6e_1$	d_{xz}, d_{yz}
-102,950		$5b_2$	σ^1_{ax}

6. The $\sigma \rightarrow \sigma^*$ energies vary in a very reasonable way with other molecular properties. As the sample temperature is lowered the band shifts to significantly higher energy (500-1000 cm^{-1} greater). This large effect is in accord with the idea that at lower temperature the average M-M distance decreases as the population of the second vibrational state decreases. The $\sigma \rightarrow \sigma^*$ energy also increases as the M-M force constant[13] increases.

The Silent Majority

Though Levenson has presented what we feel are reasonably convincing arguments in favor of the $\sigma \rightarrow \sigma^*$ transition, no other case of metal-metal bonded compounds that we are aware of shows

any similar spectroscopic behavior. One interesting series of compounds is $M_2Cl_9^{3-}$ (M = Cr, Mo, W) whose structure is a face shared bioctahedron (Table III). The metal-metal distance

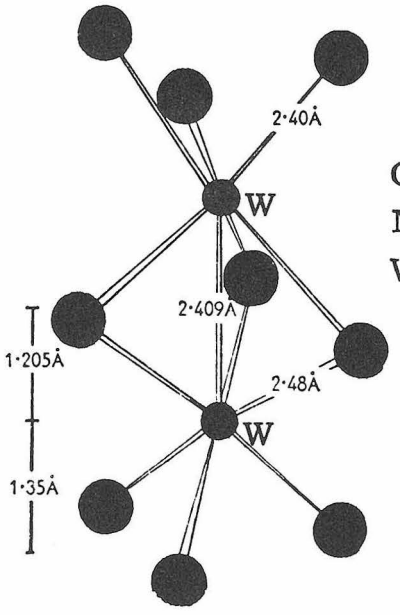

$W_2Cl_9^{3-}$ (Ref. 16)

Table III. $M_2Cl_9^{3-}$ Structural Data.

	M-M (Å)	M-Cl terminal	M-Cl bridging	Reference
Cr	3.12	2.34	2.52	14
Mo	2.66	2.38	2.49	15
W	2.41	2.40	2.48	16

decreases drastically on going from Cr to W. Further, the Cr atoms are displaced from the centers of their Cl_6 octahedra away from the neighboring Cr atom. In $W_2Cl_9^{3-}$ the case is reversed, and the two W atoms are displaced from the centers of their octahedra toward each other.[15] For comparison of intermetallic distances, the Cr-Cr distance in metallic chromium is 2.49 Å and the W-W distance in metallic tungsten is 2.74 Å.[17] These structural data fully support the presence of a W-W bond in $W_2Cl_9^{3-}$ and the absence of a Cr-Cr bond in $Cr_2Cl_9^{3-}$.

As the M(III) ions are formally d^3, magnetic susceptibility data is of interest. $Cr_2Cl_9^{3-}$ shows the expected μ_{eff} 3.76 B.M. (per Cr atom) for a d^3 ion.[18] Further, the susceptibility shows the expected temperature dependence. On the other hand, $W_2Cl_6^{3-}$ has a temperature independent magnetic susceptibility giving μ_{eff} = 0.43 B.M.[18] $Mo_2Cl_9^{3-}$ also exhibits a low magnetic moment of 0.6 B.M.[17] A normal coordinate analysis of $W_2Cl_9^{3-}$ [19] indicates a W-W force constant of 1.15 mdyne/Å, compatible with a single W-W bond.

Electronic spectra support the notion of metal-metal bonds in $Mo_2Cl_9^{3-}$ and $W_2Cl_9^{3-}$ and the absence of a bond in $Cr_2Cl_9^{3-}$. The spectra of $CrCl_6^{3-}$ and $Cr_2Cl_9^{3-}$ are essentially identical and readily interpreted in terms of an octahedral crystal field about Cr(III).[20] A d^3 species is expected to show the low-lying transitions given in Table IV.

Table IV[20]

Transition Assignments (kK) of Reflectance Spectra

	$^4A_{2g}$ →			
Compound	$^4T_{2g}$	$^4T_{1g}$	^2E_g, $^2T_{1g}$	$^2T_{2g}$
Cs_3CrCl_6	13.0	18.3	14.1 sh	--
$Cs_3Cr_2Cl_9$	12.6	18.0	14.1 ? sh	--
K_3MoCl_6	19.2	24.0	9.65	14.8

For comparison, the spectra of K_3MoCl_6, $Cs_3Mo_2Cl_9$, and $K_3W_2Cl_9$ are shown in Figure 4. WCl_6^{3-} has never been

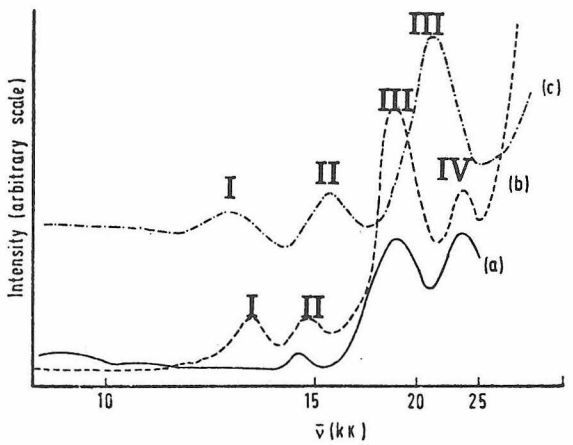

Near-i.r.–visible region reflectance spectra of (a) K_3MoCl_6; (b) $Cs_3Mo_2Cl_9$; and (c) $K_3W_2Cl_9$ (displaced vertically for clarity)

Figure 4. (Reference 20) (With Permission)

prepared. The principal difference in the spectra of $MoCl_6^{3-}$ and $Mo_2Cl_9^{3-}$ is the absence of a band near 10 kK in the latter and the presence of a new band at 13.5 kK. The bands are listed in Table V.

Table V[20]

Reflectance Spectra of $Cs_3Mo_2Cl_9$ and $K_3W_2Cl_9$

Compound	Band I	Band II	Band III	Band IV
$Cs_3Mo_2Cl_9$	11.75, 12.75 sh, 13.5	15.2	19.25	23.75
$K_3W_2Cl_9$	12.9	16.7	22.3	--
$K_3W_2Cl_9$ (in H_2O)[21]	13.2	15.9	21.9	--
	(ϵ = 50)	(ϵ = 160)	(ϵ = 473)	

Bands I and II of $Mo_2Cl_9^{3-}$ boggle any octahedral crystal field interpretation, or so the experts say. The ϵ values[17] indicate that bands I and II are spin forbidden (ϵ = 20 and 30). Crystal field theory cannot reconcile these energies with the $^4A_{2g} \rightarrow {}^2E_g$, $^2T_{1g}$ and $^4A_{2g} \rightarrow {}^2T_{2g}$ transitions. The interpretation of Smith and Wedd[20] goes as follows: The t_{2g} orbitals point between ligands and will overlap t_{2g} orbitals on the neighboring metal atom. The e_g orbitals point at the ligands and are relatively unaffected by a neighboring metal atom. The $^4A_{2g} \rightarrow {}^2X$ transitions are all $(t_{2g})^3 \rightarrow (t_{2g})^3$ transitions whose energies will be influenced by the presence of a neighboring metal atom. The $^4A_{2g} \rightarrow {}^4X$ transitions are all $(t_{2g})^3 \rightarrow (t_{2g})^2(e_g)^1$ transitions which will be less affected (why ?) by the presence of a neighboring metal atom. Bands I and II are the $^4A_{2g} \rightarrow {}^2X$ transitions, with energies changed on going from $MoCl_6^{3-}$ to $Mo_2Cl_9^{3-}$. Bands III and IV are the $^4A_{2g} \rightarrow {}^4X$ transitions with relatively constant energies in monomer and dimer. In support of this, Bands III and IV show nearly a 1000 cm^{-1} red shift in $Cs_3Mo_2Br_9$ while Band I is unshifted and band II is $\sim$500 cm^{-1} red shifted.

If you believe this interpretation, fine. If you don't swallow this interpretation, fine. The indisputable fact is that $W_2Cl_9^{3-}$, which certainly appears to have a metal-metal bond, shows no striking $\sigma \rightarrow \sigma^*$ transition comparable to Levenson's compounds. The presence of a metal-metal bond apparently provides only a small perturbation on the electronic structure of each octahedral metal unit.

(It is not clear to me what the MO scheme for $W_2Cl_9^{3-}$ would look like. Based on d^3 monomeric units, the $\sigma(d_{z^2})$ orbital between the two W atoms is unoccupied in $W_2Cl_9^{3-}$. Presumably the metal-metal bond results from π overlap of the monomer t_{2g} orbitals.)

Another class of compounds for which crystallographic data indicate single or multiple metal-metal bonding is $M_2(RCO_2)_2L_2$ in which L is a monodentate ligand. The structures of several such compounds are given in Table VI. The electronic spectra of the Rh dimer[23] and an isoelectronic Ru dimer[24] have been interpreted in terms of several totally unconvincing schemes involving multiple metal-metal bonding. Though the interpretations are just B.S., the spectra are unequivocally unlike the Levenson spectra. The spectra show two systems of bands near 600 nm and 450 nm. The 600 nm band is sensitive to the nature of L and the 450 nm band is relatively insensitive. The different explanations[23,24] do not agree on whether the σ^* orbital is involved in the transitions or even what the bond order is in these compounds. Neither band in question is very intense and the first transition with $\epsilon > 1000$ in $[Rh(CH_3CO_2)_2(H_2O)]_2$ occurs at ~ 260 nm.

Another series of compounds exemplified by Mo_2Cl_8[25] and $Re_2Cl_8^{2-}$[26] apparently possess quadruple metal-metal bonds based on crystallographic data. (Mo-Mo = 2.138(4)Å, Re-Re = 2.241(7)Å.[27]) The spectrum of $Re_2Cl_8^{2-}$ is shown in Figure 5.[29]

Table VI[22]

$M_2(RCO_2)_2L_2$ Complexes

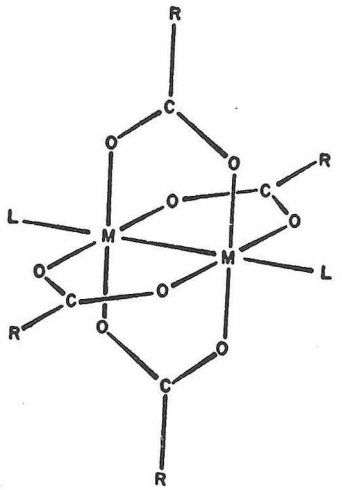

M	R	L	M-M (Å)	$\bar{\nu}_{M-M}$ (Raman)
Cr	CH_3	H_2O	2.362(1)	--
Cu	CH_3	pyridine	2.630(3)	--
Mo	CH_3	--	2.11(1)	406
Mo	CF_3	--	2.090(4)	397
Mo	CF_3	pyridine	2.129(2)	367
Mo	CH_3	pyridine	--	363
Re	C_6H_5	Cl	2.235(2)	--
Ru	C_3H_7	Cl	2.28(4)	--
Rh	CH_3	H_2O	2.386(1)	--

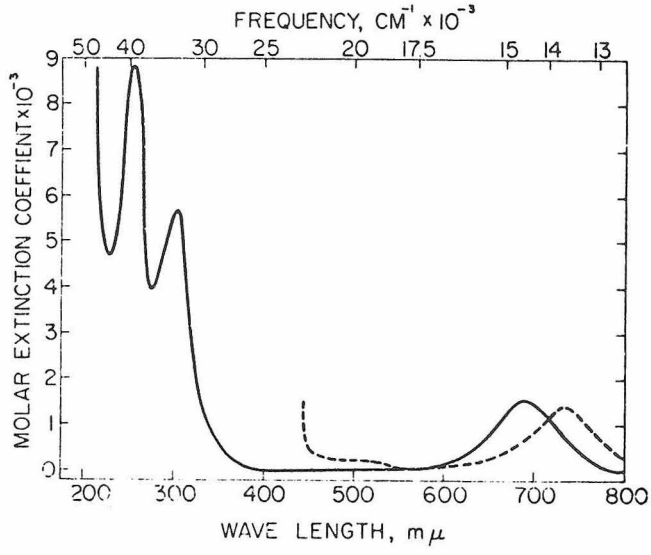

Solid curve: the absorption spectrum of $[(n\text{-}C_4H_9)_4N]_2[Re_2Cl_8]$, 14 mg. per 100 ml. of methanol (containing 1 ml. of concentrated aqueous HCl per 100 ml.). Dashed curve: a portion of the spectrum of $[(n\text{-}C_4H_9)_4N]_2[Re_2Br_8]$ in acetone.

Figure 5[29] (With Permission)

Cotton[26] has interpreted the lowest energy of $Re_2Cl_8^{2-}$ at 14.5 kK as a $\delta[(b_{2g})^2] \rightarrow \sigma_n[(b_{2g})^1(a_{2u})^1]$ transition in which σ is a non-bonding σ orbital. 4°K single crystal polarized optical spectra obtained by Charlie Cowman of this lab show vibronic structure consistent with a $\delta[(b_{2g}^2)] \rightarrow \delta^*[(b_{2g})^1(b_{1u})^1]$ transition.[28] The next highest energy bands are at 32.8 and 39.2 kK with ϵ values of about 6000 and 9000, respectively. Either one could be analogous to Levenson's $\sigma \rightarrow \sigma^*$ transition (in position and intensity) but Cotton[27] assigns these as $\delta \rightarrow \delta^*$ and $\pi \rightarrow \sigma_n$ transitions.

The vast majority of compounds thought to have metal-metal bonds do not walk up to you and say, "Look at my beautiful intense $\sigma \rightarrow \sigma^*$ transition!" In many cases, this could be simply because the σ orbital is not the highest (or nearly highest) occupied

level and the σ^* orbital is not the lowest (or nearly lowest) unoccupied level. What do seem to be associated with metal-metal bonds are new or altered low energy transitions not present in corresponding monomeric compounds. These are of widely variable intensity. We call the class of compounds which does not hit you on the head with an obvious $\sigma \rightarrow \sigma^*$ transition "The Silent Majority."

Electronic Spectra of the Protonated Metal-Metal Bond

Certainly the most sensible experiment to study the effect of protonation of the metal-metal bond would be to protonate the $Mn_2(CO)_{10}$ family of compounds studied by Levenson. Unfortunately our attempts at such protonation using 98% H_2SO_4 in a variety of organic solvents were futile. $Mn_2(CO)_{10}$, $[(C_2H_5)_4N][MnCr(CO)_{10}]$[40] and $Mn_2(CO)_8[P(C_6H_5)_3]_2$[72, 73] could not be protonated under our conditions. Experiments with "super acid" media would be worthwhile. Davison et al.[3] did observe the following change in the spectrum of $Mn_2(CO)_{10}$ when it was dissolved in 98% H_2SO_4:

$Mn_2(CO)_{10}$ in $CHCl_3$: 29.2 kK (ϵ = 22,800)

$Mn_2(CO)_{10}$ in 98% H_2SO_4: 25.7 kK (ϵ = 1140)

These are all the data they report, and we have not examined this compound in neat H_2SO_4. Clearly there is room for experimentation here.

The series of compounds $M_2(CO)_{10}^{2-}$ and $HM_2(CO)_{10}^{-}$ [30-40] (M = Cr, Mo, W) is especially interesting because the dianions are isoelectronic and isostructural[30, 30a] with Levenson's compounds.

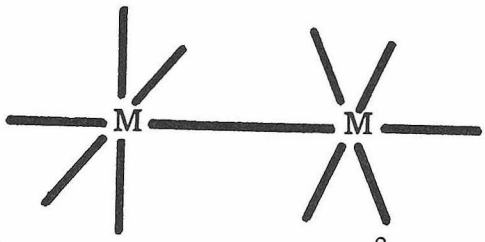

D_{4d}

staggered geometry

$Cr_2(CO)_{10}^{2-}$	Cr-Cr = 2.97(1) Å	Reference 30
$Mo_2(CO)_{10}^{2-}$	Mo-Mo = 3.123(7)	Reference 30
$Mn_2(CO)_{10}$	Mn-Mn = 2.923(3)	Reference 7
$Tc_2(CO)_{10}$	Tc-Tc = 3.036 (6)	Reference 41

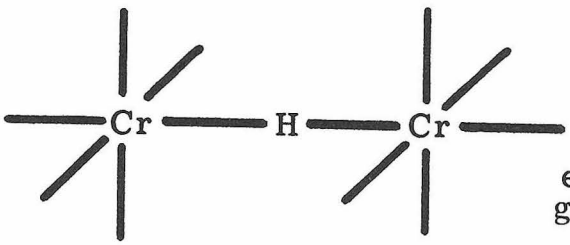

D_{4h}

eclipsed geometry

$HCr_2(CO)_{10}^-$	Cr-Cr = 3.406(9) Å	Reference 30

The electronic spectra of $W_2(CO)_{10}^{2-}$, $HW_2(CO)_{10}^-$, and $HCr_2(CO)_{10}^-$ are given in Figures 6-9. For comparison, the spectrum of $W(CO)_6$ is reproduced from reference 11 in Figure 10. Solubility problems precluded the determination of any ϵ values. The absorption bands for these compounds are listed in Table VII. In several samples we have been able to estimate that the 27 kK band of $W_2(CO)_{10}^=$ and $HW_2(CO)_{10}^-$ and the 23.6 kK band of $HCr(CO)_{10}^-$ have ϵ values on the order of 10^3. The shoulder at ~ 24 kK in the spectrum of $W_2(CO)_{10}^{2-}$ was found to be of variable intensity in spectra of different samples. The solid line in Figure 6 shows the best spectrum we obtained. We believe this

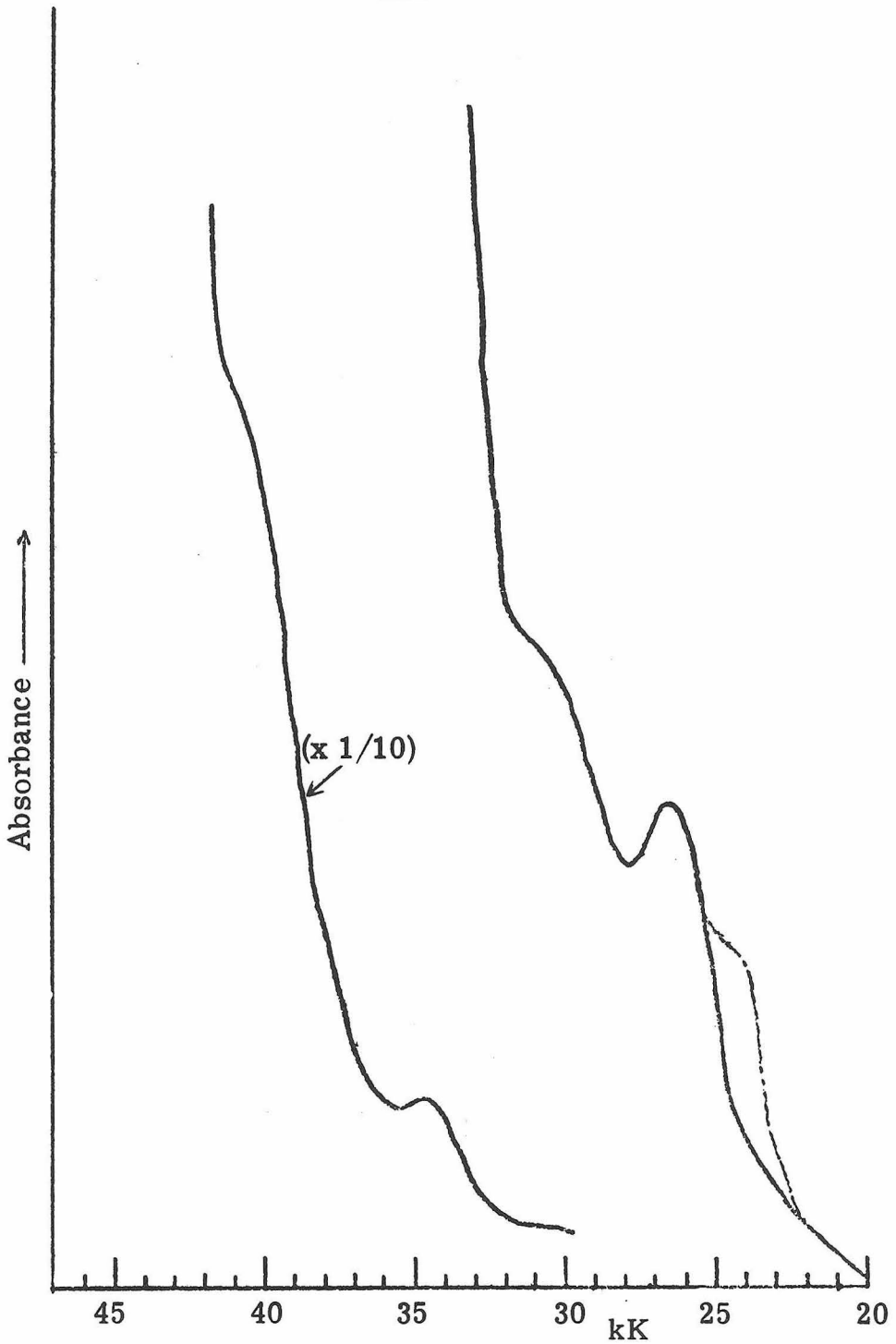

$[(C_2H_5)_4N]_2[W_2(CO)_{10}]$ in Ethanol

Figure 6

(Note for posterity: This spectrum is entirely wrong.)

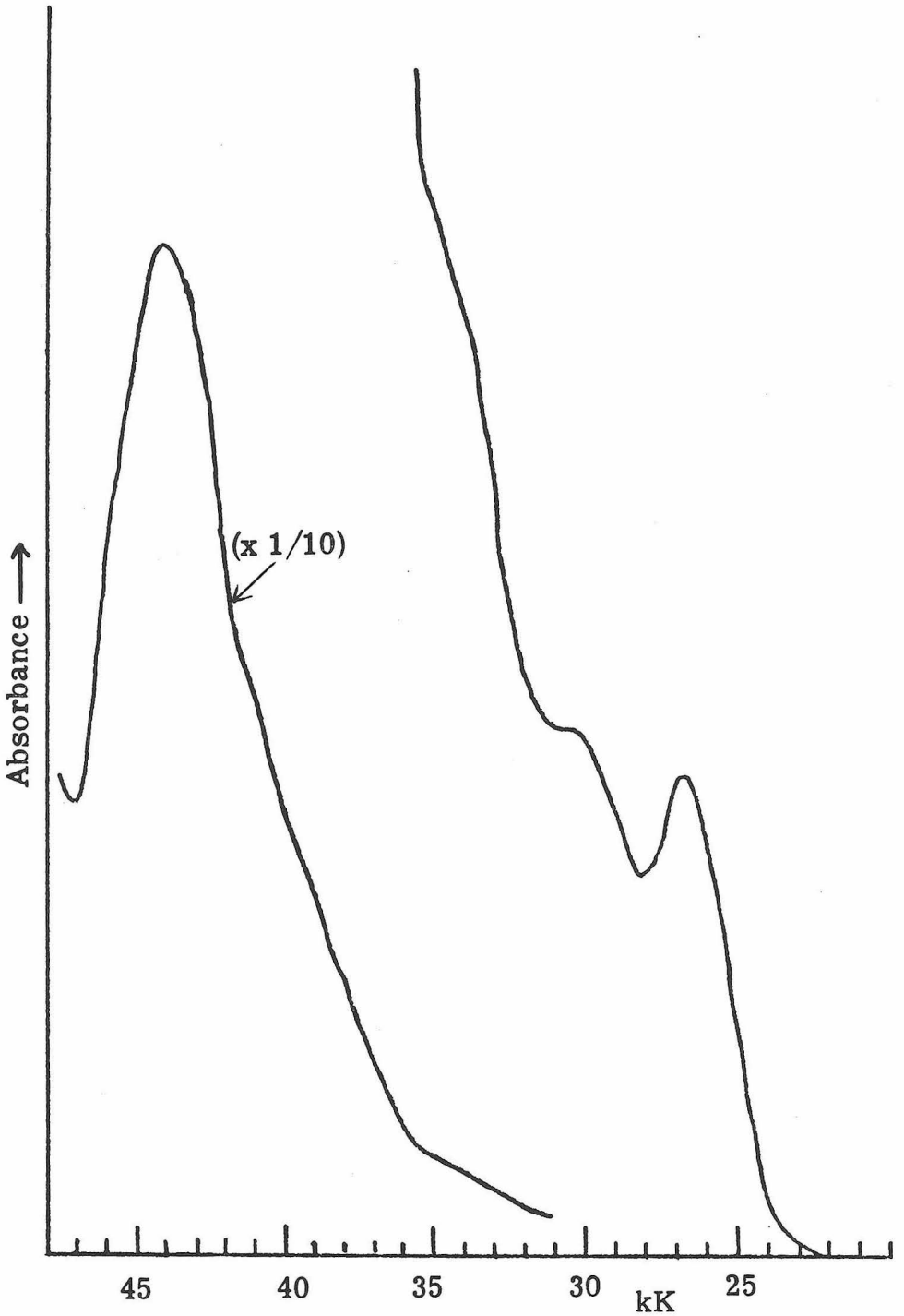

$[(C_2H_5)_4N][HW_2(CO)_{10}]$ in Ethanol

Figure 7

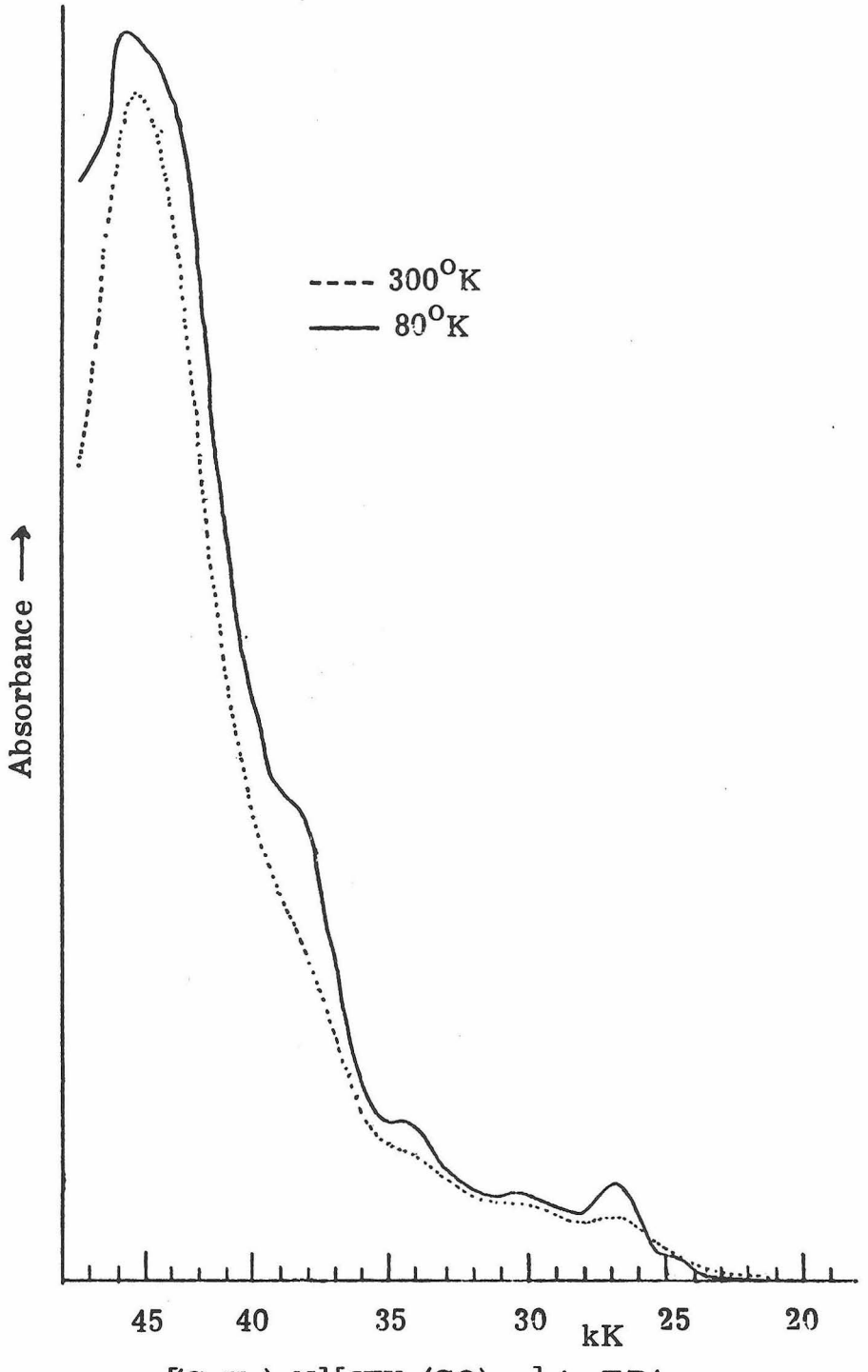

$[(C_2H_5)_4N][HW_2(CO)_{10}]$ in EPA

Figure 8

Absorption Spectrum of $[Et_4N][HCr_2(CO)_{10}]$ in Ethanol or Tetrahydrofuran Solution

Figure 9

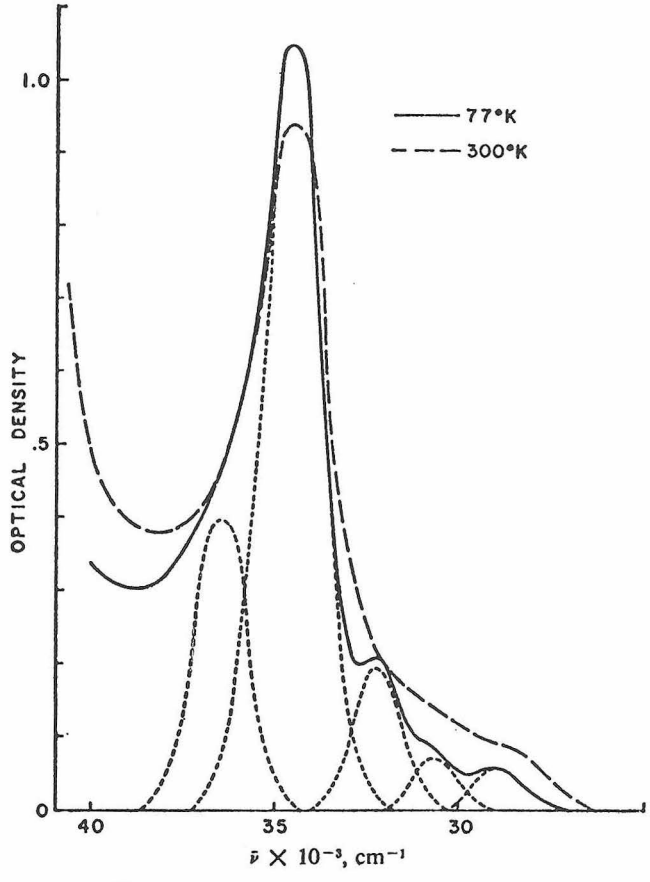

Electronic spectra of $W(CO)_6$ in EPA (0.80×10^{-4} *M* solution) at 300 and 77°K.

Figure 10. (Reference 11)

(With Permission)

24 kK band is due to the green impurity often present in samples of yellow $W_2(CO)_{10}^{=}$.

Table VII is arranged to emphasize the excellent correspondence between the monomer and dimer spectra with the exception of the lowest energy band. (~ 27 kK for W and 23.6 kK for Cr.) Further, $W_2(CO)_{10}^{2-}$ and $HW_2(CO)_{10}^{-}$ have nearly identical spectra! The spectrum of $Cr_2(CO)_{10}^{2-}$ is not listed because we were unable to obtain a pure sample of this compound. However, a roughly equimolar mixture of $Cr_2(CO)_{10}^{2-}$ and $HCr_2(CO)_{10}^{-}$ (based on the IR spectrum) gave a spectrum that was superimposable on the spectrum of pure $HCr_2(CO)_{10}^{-}$. We feel it is safe to say that $Cr_2(CO)_{10}^{2-}$ and $HCr_2(CO)_{10}^{-}$ have essentially identical spectra, as with the W analogs. To summarize these observations, the spectra of $M_2(CO)_{10}^{2-}$ and $HM_2(CO)_{10}^{-}$ are identical and differ from the spectra of $M(CO)_6$ only in the presence of an additional low energy band in the dimers.

We are strongly inclined to assign this low energy transition of $M_2(CO)_{10}^{2-}$ and $HM_2(CO)_{10}^{-}$ to the $\sigma \rightarrow \sigma^*$ and $\sigma \rightarrow n$ transitions, respectively. The other transitions would correspond to monomer transitions. Because this is a dimer, we have twice as many orbitals in our basis set and it is possible to see more transitions than we see in the monomer even though each monomer transition has a corresponding dimer transition. In D_{4h} symmetry the $\sigma \rightarrow n$ transition is allowed but the $\sigma \rightarrow \sigma^*$ transition is forbidden for $HM_2(CO)_{10}^{-}$. The same energy is found for the $M_2(CO)_{10}^{2-}$ $\sigma \rightarrow \sigma^*$

Table VII

Electronic Spectra of Group VI Compounds

$W(CO)_6$[a]	$W_2(CO)_{10}^{=}$[b]	$HW_2(CO)_{10}^{-}$[c]		$Cr(CO)_6$[a]	$HCr(CO)_{10}^{-}$[b]	$M(CO)_6$
		CH_3CH_2OH	EPA-80°K			Assignments[d]
--	[24.4][e]	--	24.7 sh[f]	--	--	--
--	26.7	26.8	26.9	--	23.6	--
28.3(1000)	--	--	--	--	--	$^1A_{1g} - {}^3T_{1g}$
29.95(1680)	~30.8 sh	30.5	30.5	29.5(700)	~28 sh	$^1A_{1g} - {}^1T_{1g}$
31.85(3250)	--	--	~32.3 sh	31.55(2670)	~32 sh	$^1A_{1g} - {}^1T_{1g}$
34.65(17,600)	34.7	~34.5 sh	34.7	35.7(13,100)	--	$^1A_{1g} - {}^1T_{1u}$[h]
37,100(7400)[g]	--	--	--	38.85(3500)	--	$^1A_{1g} - {}^1T_{2g}$
39,550(9600)	~40.8 sh	~39 sh	~38.8 sh	--	--	$^1A_{1g} - {}^1T_{1u}$[h]
43,750(208,000)	--	--	44.7	43.6(85,100)	--	$^1A_{1g} - {}^1T_{1u}$[h]

[a] From reference 11. Acetonitrile solution. ϵ values in parentheses.

[b] Ethanol solution of tetraethylammonium salt.

[c] Tetraethylammonium salt.

[d] Reference 11.

[e] This band is due to an impurity.

[f] This band is weak and only seen at liquid nitrogen temperatures. It may be a spin-forbidden transition.

[g] This band is not seen in the net absorption spectrum. It is obtained from Gaussian analysis.

[h] Charge transfer.

transition and the $HM_2(CO)_{10}^-$ $\sigma \rightarrow n$ transition so the energy level diagram probably looks as follows in which $\Delta_1 = \Delta_2$.

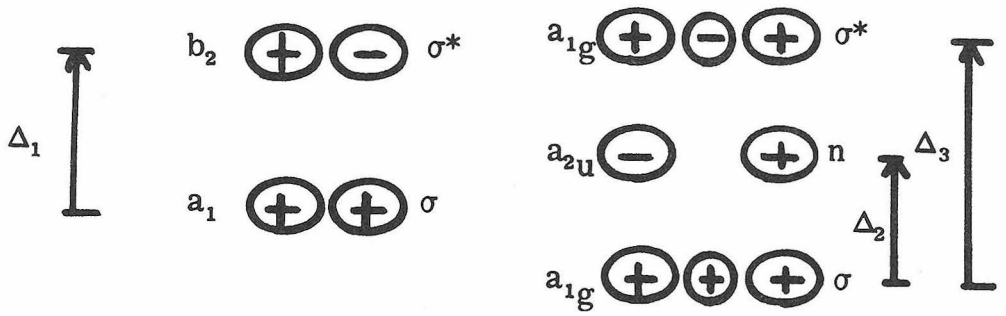

allowed D_{4d} D_{4h} allowed forbidden

It is very interesting and hard to believe that the $\sigma \rightarrow \sigma^*$ and $\sigma \rightarrow n$ transitions have the same energy. I have not really convinced myself of this scheme but if it is true then perhaps the energy factors which determine the internuclear distances in $M_2(CO)_{10}^{2-}$ and $HM_2(CO)_{10}^-$ are such that the minimum energy of the protonated system is reached when the σ orbital is just stabilized relative to the n orbital as much as it would be stabilized compared to the σ^* orbital in $M_2(CO)_{10}^{2-}$. There is a faint trace of plausibility in this notion. Only faint.

We have examined the spectra of compounds containing both protonated and unprotonated Fe-Fe and Ru-Ru bonds. $[CpFe(CO)_2]_2$ is known to exist in both <u>cis</u> and <u>trans</u> forms[42,43] in the solid state and as an equilibrium mixture in solution.[44-56] We will show later in this chapter that protonation leads to a species containing no carbonyl bridges. This conclusion was reached independently by Symon and Waddington.[4] The phosphite

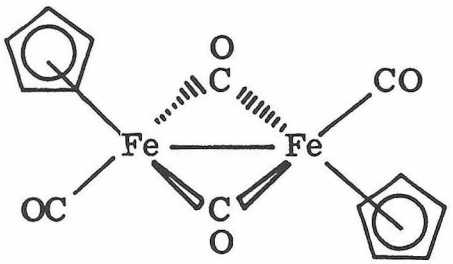

Fe-Fe = 2.534(2)Å

Reference 42

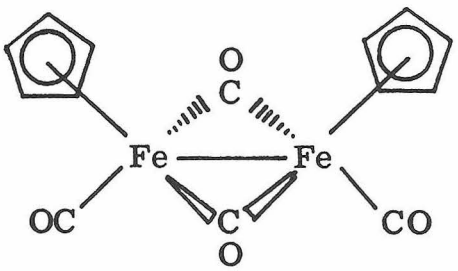

Fe-Fe = 2.531(2)Å

Reference 43

substituted complex III was prepared by the method of Haines and DuPreez.[57-59]

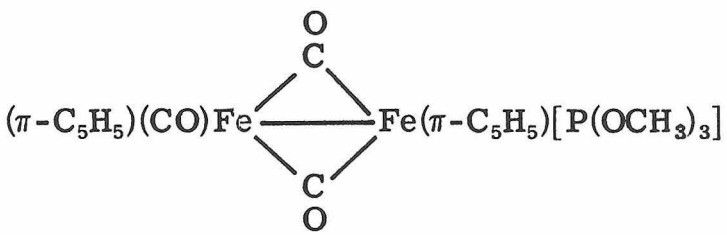

III

We have also studied the analogous Ru dimer, $[CpRu(CO)_2]_2$,[60-62] in both its protonated and unprotonated forms. Non-bridged adducts of these Fe and Ru compounds with Lewis acids other than $H^{\oplus}$ are known.[63-66]

Our electronic spectra are shown in Figures 11-16 and listed in Table VIII. The numbering of bands (Roman numerals) in the iron spectra corresponds to the band numbers in Table VIII. We interpret the iron spectra as follows. The unprotonated compounds all show at least three common absorptions, labeled Bands I-III in Table VIII. Band II of the phosphite substituted dimer is split by 1100 cm^{-1} at 80°K. We believe this is vibrational

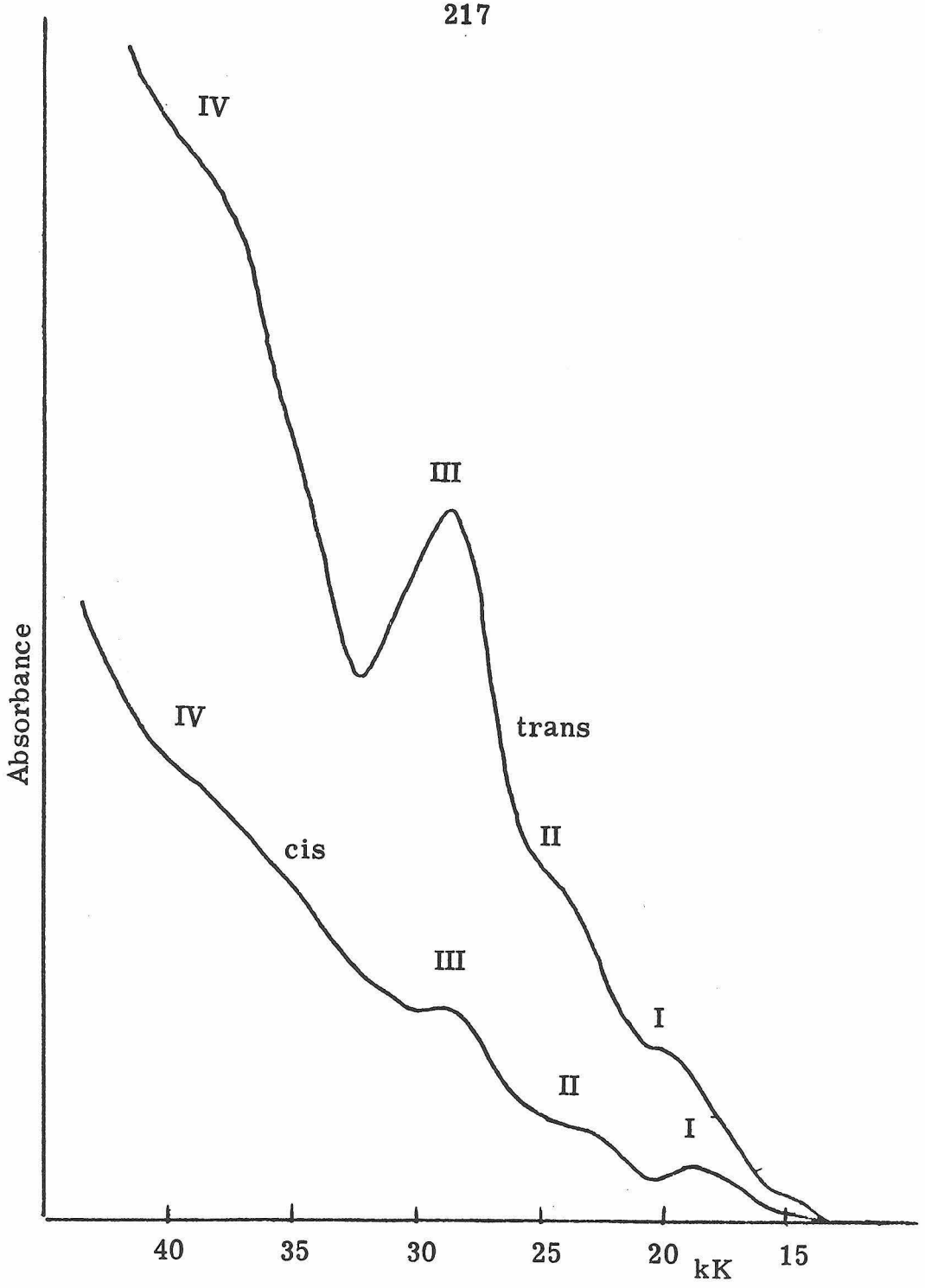

$[CpFe(CO)_2]_2$ KBr Pellet Absorption Spectra at $80^{o}K$

Figure 11

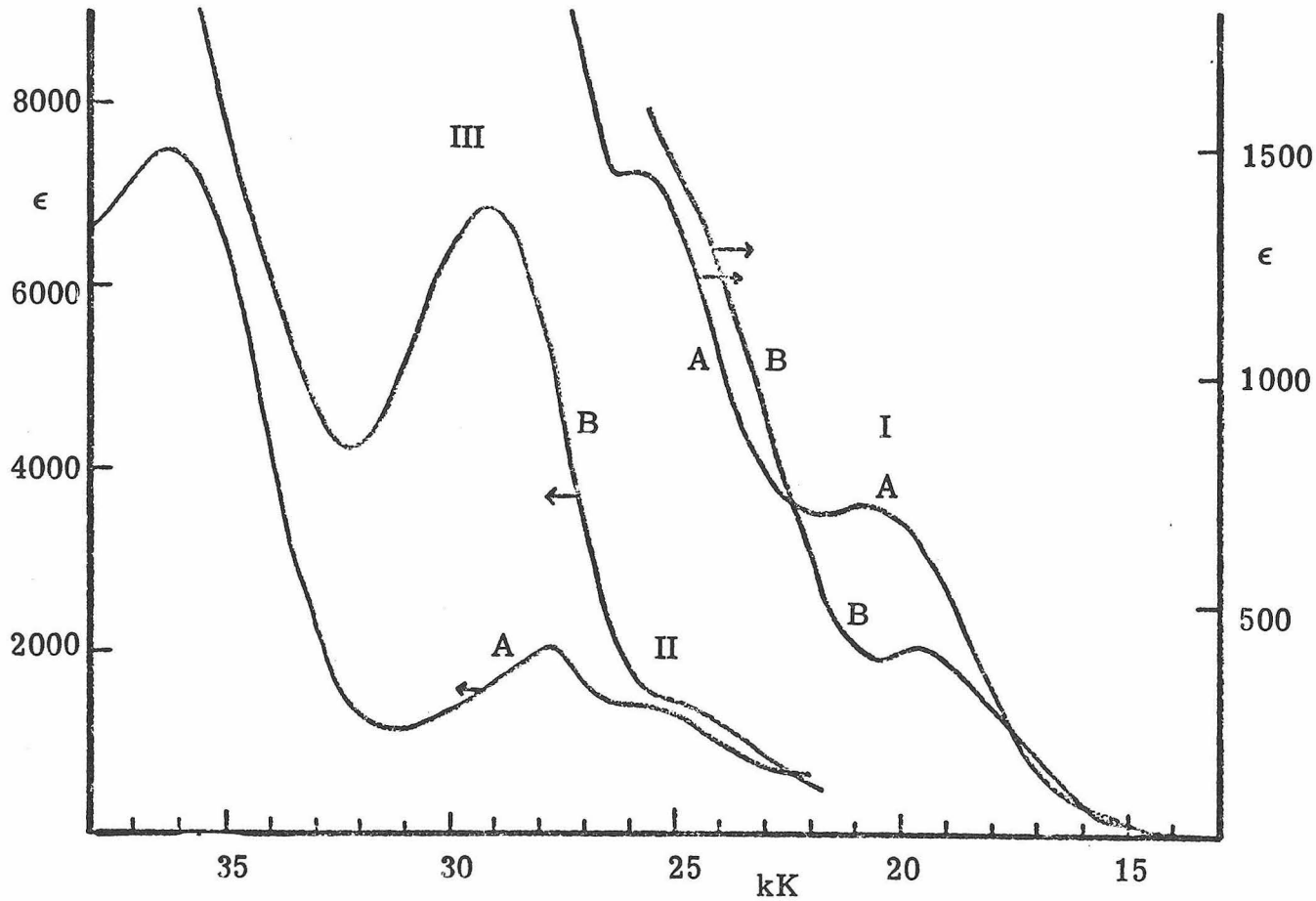

Absorption Spectra in Acetic Acid Solution

A. $[CpFe(CO)_2]_2H^+$

B. $[CpFe(CO)_2]_2$

Figure 12

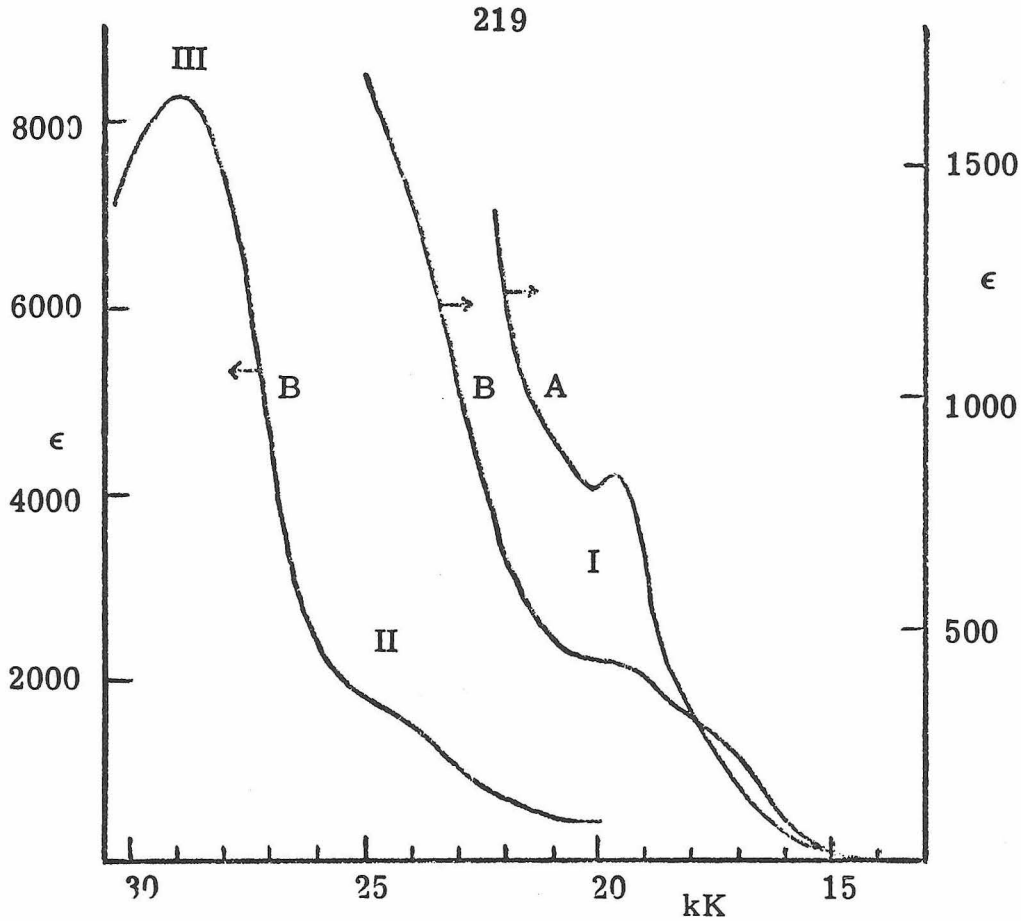

Absorption Spectra in Acetone Solution

A. $[CpFe(CO)_2]_2H^+$

B. $[CpFe(CO)_2]_2$

Figure 13

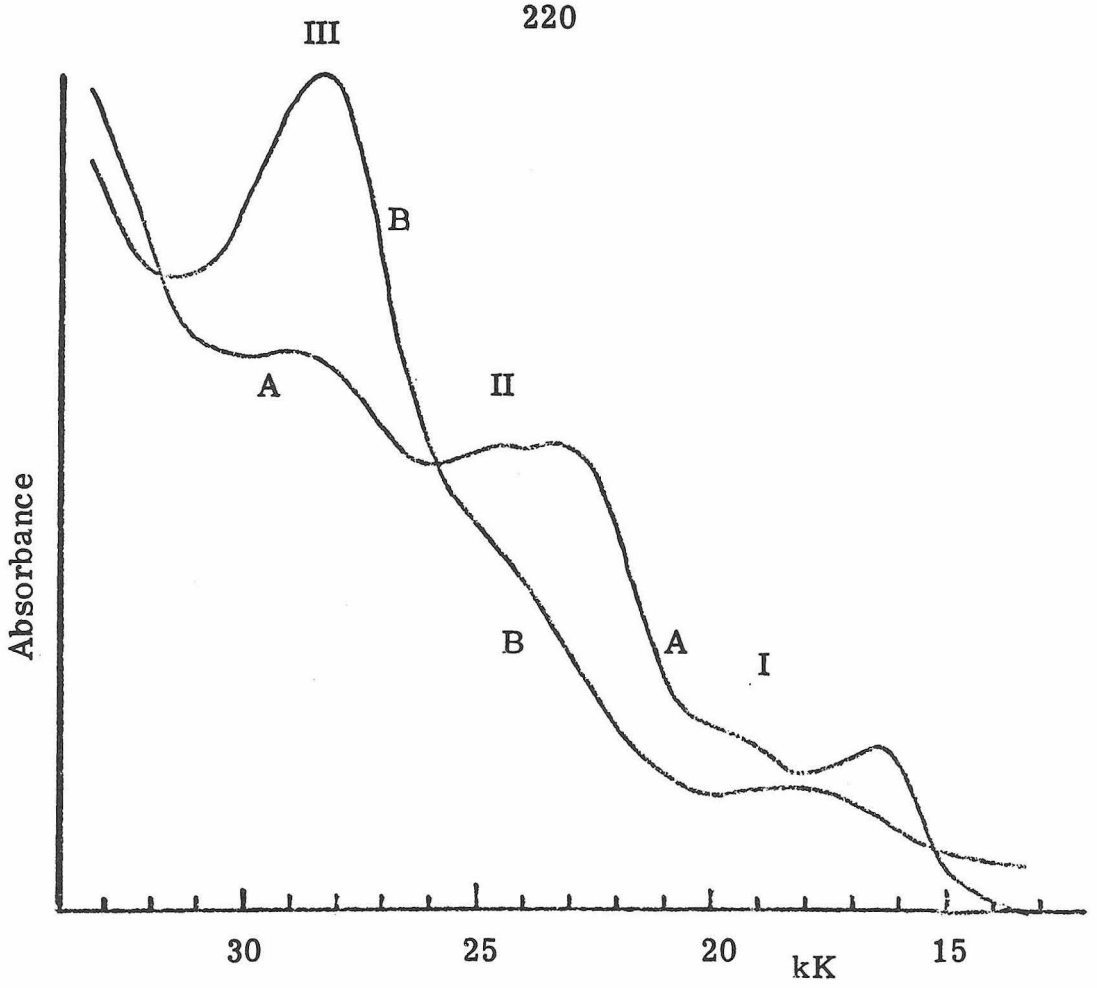

KBr Pellet Absorption Spectra ($80^{o}K$)

A. $\{Cp(CO)_2Fe\text{-}H\text{-}Fe(CO)Cp[P(OCH_3)_3]\}\{B(C_6H_5)_4\}$

B. $Cp(CO)Fe\text{-}\mu\text{-}(CO)_2\text{-}Fe[P(OCH_3)_3]Cp$

Figure 14

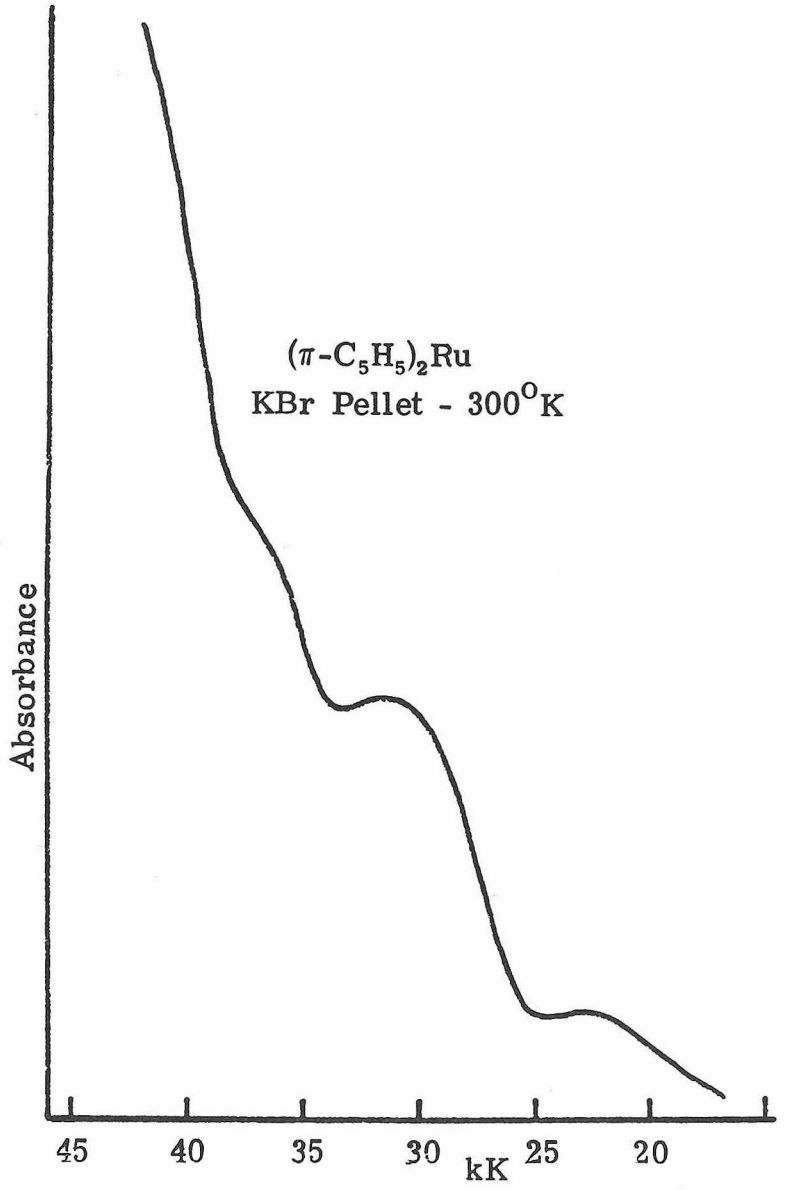
$(\pi\text{-}C_5H_5)_2Ru$
KBr Pellet - 300°K
Absorbance
45
40
35
30
kK
25
20

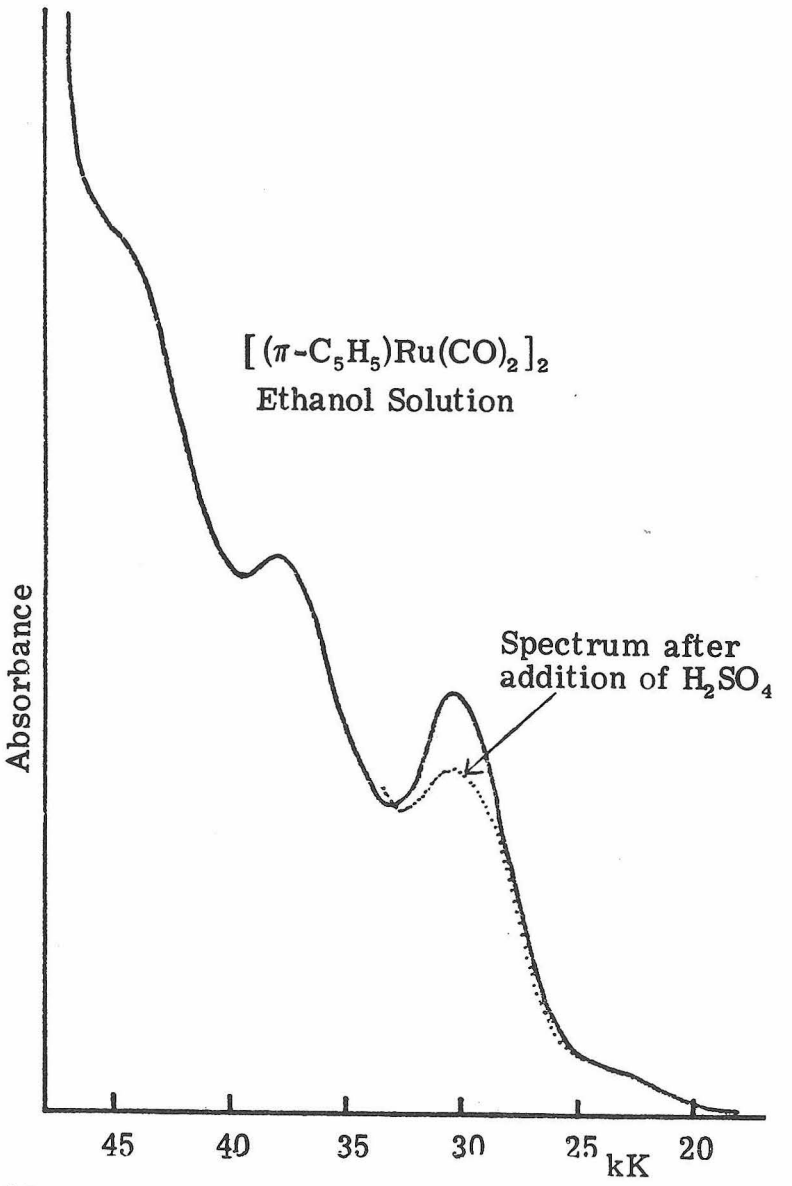
$[(\pi\text{-}C_5H_5)Ru(CO)_2]_2$
Ethanol Solution
Spectrum after addition of H_2SO_4
Absorbance
45
40
35
30
25
kK
20

Figure 15

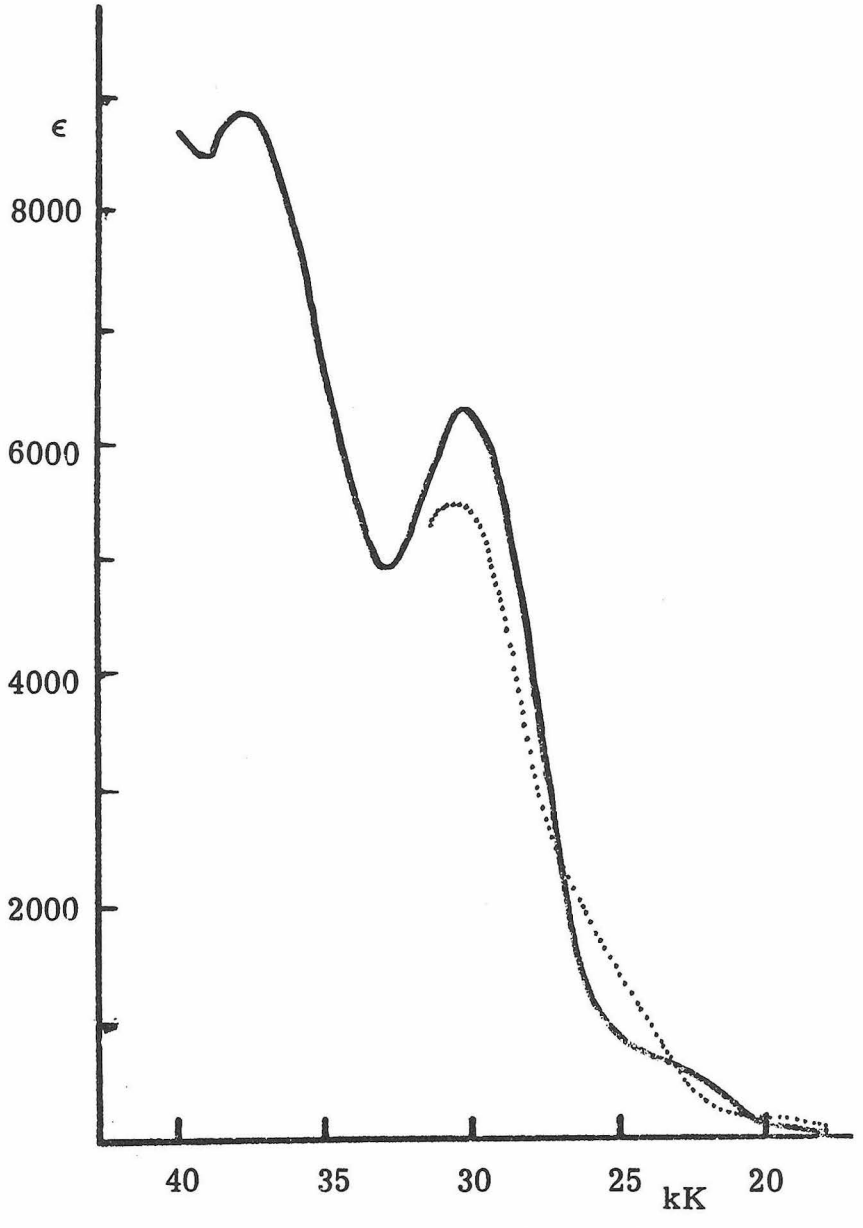

Absorption Spectra in Acetic Acid Solution

—— $[CpRu(CO)_2]_2$

----- $\{[CpRu(CO)_2]H^+\}\{HSO_4^-\}$

Figure 16

Table VIII[a]

Electronic Spectra of Group VIII Compounds

Compound		Band I	Band II	Band III	Band IV
Trans-$[CpFe(CO)_2]_2$(KBr pellet -80°K)	~15 sh	19.0	~24 sh	29.4	~37 sh
Cis-$[CpFe(CO)_2]_2$ (KBr pellet -80°K)		19	~24 sh	28.6	~37 sh
$[CpFe(CO)_2]_2$ (Acetic acid solution)		19.6 (401)	~24.4 sh (1300)	29.3 (2010)	
$[CpFe(CO)_2]_2$ (Acetone solution)	~17.5 sh (270)	~19.8 sh (432)	~24 sh (1400)	29.0 (8240)	
$\{[CpFe(CO)_2]_2H^{\oplus}\}\{HSO_4^{\ominus}\}$ (Acetic acid solution)		20.8 (728)	25.7 (1440)	27.9 (7530)	36.1
$\{[CpFe(CO)_2]_2H^{\oplus}\}\{HSO_4^{\ominus}\}$ (Acetone solution)		19.6, ~21 sh (835) (880)			
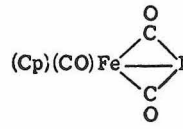 $(Cp)(CO)Fe$—$Fe(Cp)[P(OCH_3)_3]$ (KBr pellet -80°K)		18.2	~24 sh	28.4	
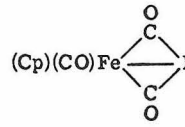 $(Cp)(CO)Fe$—$Fe(Cp)[P(OCH_3)_3]$ (CH_3CN solution)		17.9 (520)		29.2 (4150)	
$\{Cp(CO)_2Fe\text{-}H\text{-}Fe(CO)(Cp)[P(OCH_3)_3]^{\oplus}\}\{HSO_4^{\ominus}\}$ (KBr pellet -80°K)		16.4 ~19.5 sh	23.3, 24.4	29.1	
$[CpRu(CO)_2]_2$ (ethanol solution)		~23 sh	30.3	38.0	~44.5 sh
$[CpRu(CO)_2]_2$ (acetic acid solution)		~23 sh (600)	30.3 (6300)	37.6 (8800)	
$\{[CpRu(CO)_2]_2H^+\}\{HSO_4^-\}$ (acetic acid solution)[b]		~25 sh (1400)	30.5 (5400)		
Cp_2Ru (KBr pellet -300°K)		23.3	31.4	~37 sh	

[a] Energies in kK. ϵ values in parentheses.

[b] This sample may not really be protonated. See the section on infrared spectra for a discussion of this problem.

structure. Lower energy shoulders may be triplet transitions. The protonated species, $[CpFe(CO)_2]_2H^{\oplus}$, shows essentially the same spectrum as $[CpFe(CO)_2]$. In acetone a very poorly resolved shoulder at ~ 21 kK also appears. So far we have the same behavior found in the Cr and W compounds, viz., the spectra of protonated and unprotonated forms are nearly identical. In the phosphite substituted protonated dimer, IV, Band I splits into two absorptions separated by 3000 cm^{-1}. The unsubstituted

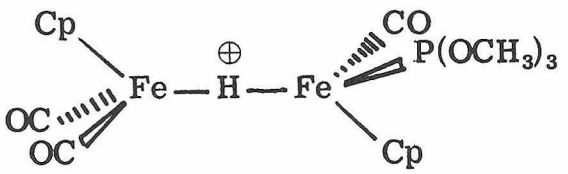

IV

species is believed to exist in the C_{2h} conformation, V, in

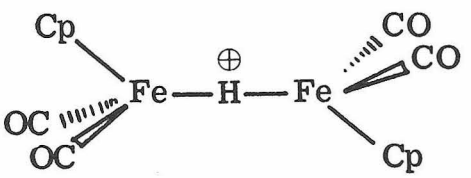

C_{2h}

V

solution.[4,78] In C_{2h} symmetry, the $\sigma \rightarrow n$ transition is allowed but the $\sigma \rightarrow \sigma^*$ transition is not.[105] The phosphite substituent lowers the symmetry to C_1 or, at best, C_s. In either case, both the $\sigma \rightarrow n$ and $\sigma \rightarrow \sigma^*$ transitions are allowed in the reduced symmetry. This is summarized in Figure 17. The two bands of IV at 16.4 and 19.5 kK are therefore assigned as $\sigma \rightarrow n$ and

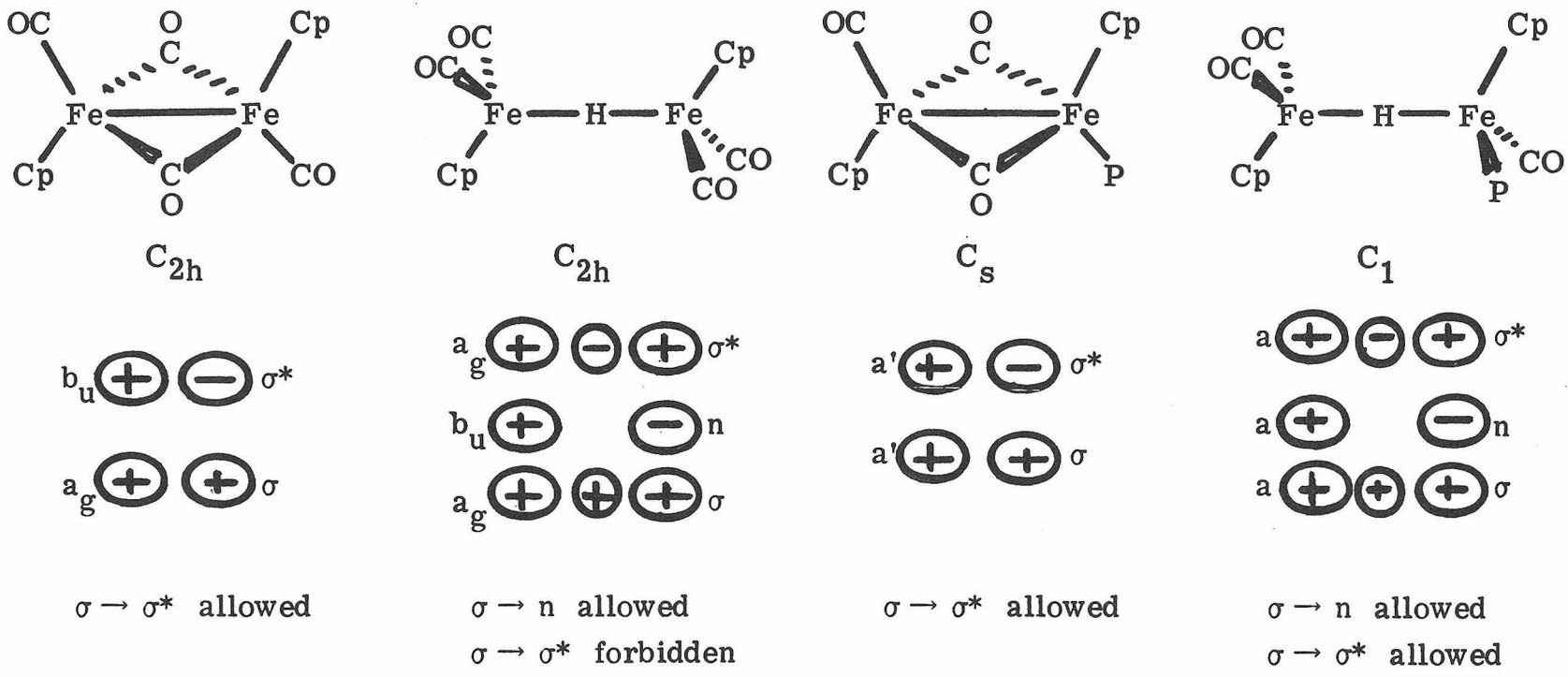

$\sigma \rightarrow \sigma^*$ allowed

$\sigma \rightarrow n$ allowed
$\sigma \rightarrow \sigma^*$ forbidden

$\sigma \rightarrow \sigma^*$ allowed

$\sigma \rightarrow n$ allowed
$\sigma \rightarrow \sigma^*$ allowed

Figure 17. Summary of M-M and M-H-M Transitions.

$\sigma \rightarrow \sigma^*$, respectively. In the unsubstituted compound only the $\sigma \rightarrow n$ transition is seen.[105]

The assignment of Band I in the unprotonated dimers as a $\sigma \rightarrow \sigma^*$ transition is exceedingly tenuous. We do not even begin to propose a molecular orbital scheme to try to show that the σ level is the highest occupied (or nearly highest occupied) level. We do note that $CpFe(CO)_2H$, which can be considered to be a "hydrogen-capped" half of $[CpFe(CO)_2]_2$ is yellow[67] so Band I is certainly associated with the M-M bond, whatever the exact transition happens to be. Further, the Fe-Fe bond in these compounds is universally accepted[43,59a] to be a normal 2-electron bond. Moreover, one-electron oxidation of these iron-dimers[59a,b] is believed to remove one electron from the Fe-Fe bond. This strongly supports the σ level as being the highest occupied level.

An empirical observation, in agreement with Levenson, is that phosphine substitution lowers the energy of the $\sigma \rightarrow \sigma^*$ transition. One phosphine substituent lowers the energy of Band I in our compounds from ~19.5 kK to 18.2 kK. Two phosphine substituents in the compound VI[59a] lower Band I to 15.4 kK. The spectrum reported[59a] for VI (but not interpreted) is 15.4 (ϵ = 497), 27.0 sh (ϵ = 4950). These bands correspond to Bands I and III and Band II is apparently not resolved. The one-electron oxidation product of VI, in which the electron is believed to have

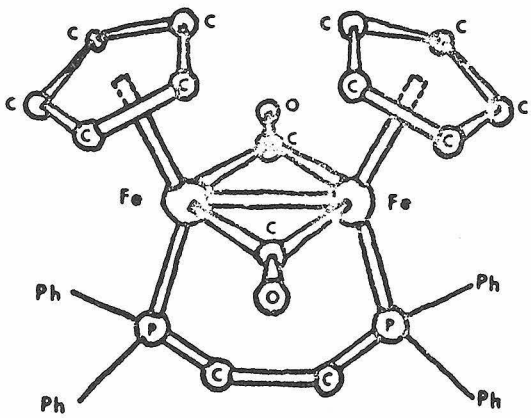

VI
(Reference 59a)

(With Permission)

been removed from the metal-metal σ bond,[59a] has the following spectrum: 15.5 (ϵ = 1680), 19.5 (ϵ = 3250), 22.7 sh (ϵ = 8080), 37.7 (ϵ = 39,600). I suggest that the $\sigma \rightarrow \sigma^*$ transition is the 15.5 kK band, indicating that the $\sigma \rightarrow \sigma^*$ energy separation is less than the separation of the σ level and the next filled level <u>below</u> it. This orbital gives rise to an $X \rightarrow \sigma$ transition at 19.5 kK in the oxidized species.

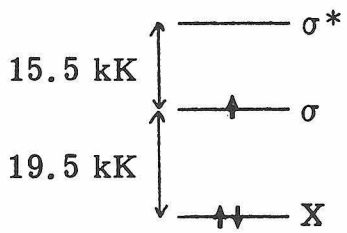

Partial energy level scheme for the oxidized product $VI^{\oplus}$

Now to throw a wrench in the machinery. Figure 15 shows a more than coincidental resemblance between the spectra of ruthenecene (Cp_2Ru) and $[CpRu(CO)_2]_2$. Sohn <u>et al.</u>[68] list the following absorptions for Cp_2Fe and Cp_2Ru (ϵ values are given in parentheses):

	A	B	C	D	E	F
Cp_2Fe	18.9	22.7	30.8	37.7	41.7	50.0
	(7)	(91)	(49)	(1600)	(3500)	(51,000)
Cp_2Ru	26.0	31.0	36.6	42.0	46.1	>51.3
	(5)	(200)	(150)	(2000)	(4200)	(>50,000)
	triplet transition	ligand field d-d transitions		charge transfer		

The reported position of Band A for Cp_2Ru (26.0 kK) does not agree with our spectrum in Figure 15 which shows a broad band at 23.3 kK. The rest of our spectrum agrees with Sohn's. If we believe the data of Sohn (probably an excellent bet), then Bands B, C, and D correspond approximately to our bands II, III, and IV. Band I is much too intense to be a triplet so even though the energy corresponds to Sohn's Band A, we feel that it is reasonable to assign the transition differently. The nagging fact remains, however, that our only spectrum of Cp_2Ru looks just like $[CpRu(CO)_2]_2$. On this note I will terminate this section.

Vibrational Spectra

We have obtained infrared spectra of all of the compounds prepared for the study of the protonated metal-metal bond. Raman spectra of several compounds were also determined. Our main interest is to determine the frequencies of the vibrations associated with the protonated metal-metal bond. In an excellent comprehensive review article, Kaesz and Saillant[69] point out that most

$\nu_{M\text{-}H\text{-}M}$ frequencies that have been observed are in the region $\sim 1100 \pm 300$ cm^{-1}. The highest assigned M-H-M frequency listed in this paper is 1585 cm^{-1} for $H_4Ru_4(CO)_{12}$. However, the list of observed M-H-M frequencies is very small. For many compounds believed to contain a M-H-M linkage, no absorption associated with this unit can be assigned, even when the corresponding M-D-M compound is also examined.[70,71] We will examine the Cr family of compounds first and then treat the iron family.

For a linear M-H-M unit, two stretching vibrations and one bending vibration are expected. These are shown in Table IX.

Table IX

Vibrations of the M-H-M Unit

Description	Designation	Picture	Activity in D_{4h}
asymmetric stretch	ν_{as}		IR
symmetric stretch	ν_s		Raman
bend	δ		IR

When M is a metal, we expect the order $\nu_{as} > \delta > \nu_s$.

The KBr pellet IR spectra of $HCr_2(CO)_{10}^-$, $W_2(CO)_{10}^{2-}$, $HW_2(CO)_{10}^-$, $DW_2(CO)_{10}^-$, $MnCr(CO)_{10}^-$, and $Mn_2(CO)_8(P\phi_3)_2$ are presented in Figures 18-26 and listed in Tables X through XII. Comparison spectra of $(C_2H_5)_4NBr$ and $P\phi_3$ are available in the Experimental section. Raman spectra are shown in Figure 27 and listed in Table XIII. Comparison of the spectra of $W_2(CO)_{10}^{2-}$,

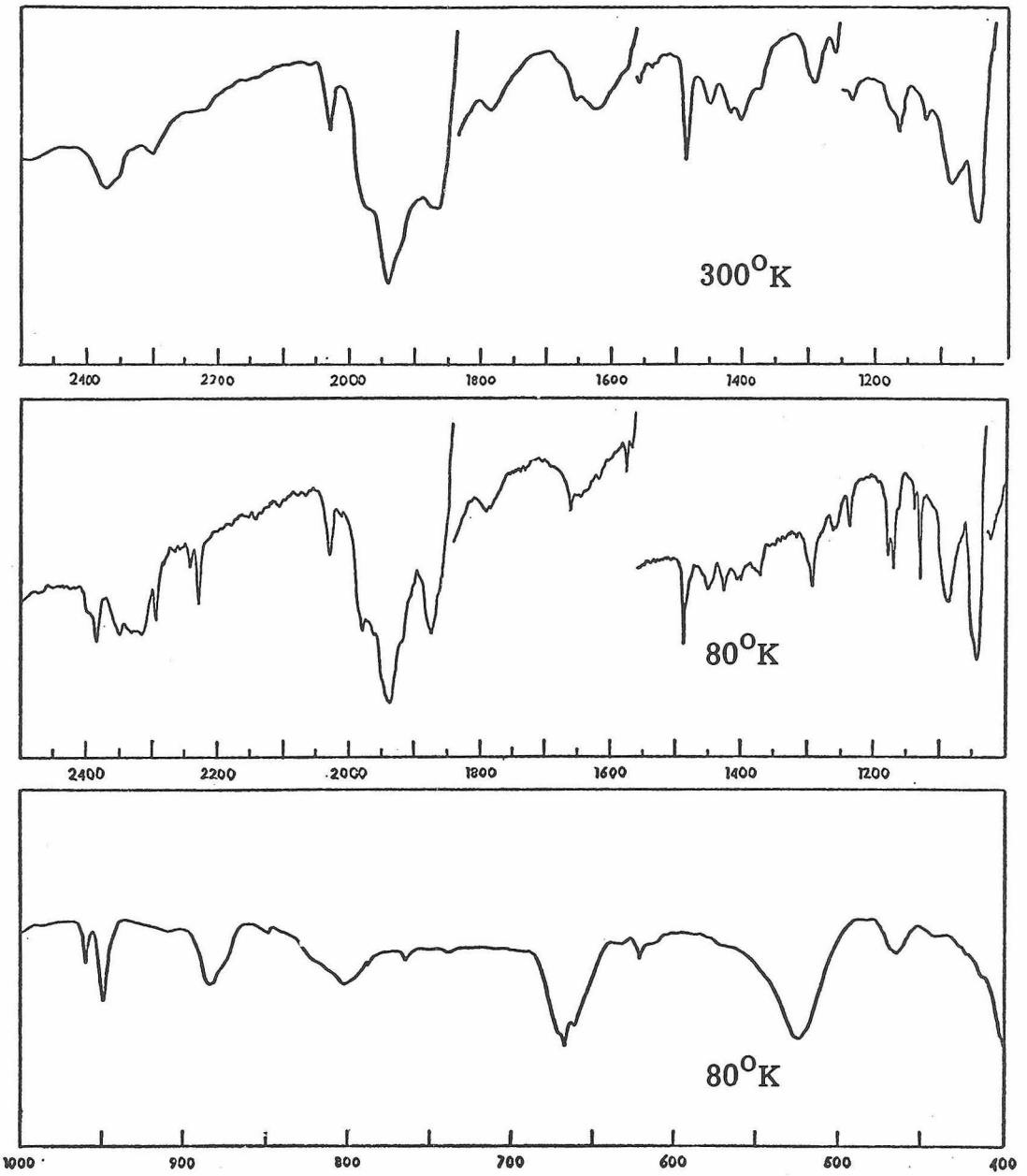

KBr Pellet Spectra of $[(C_2H_5)_4N][HCr_2(CO)_{10}]$

Figure 18

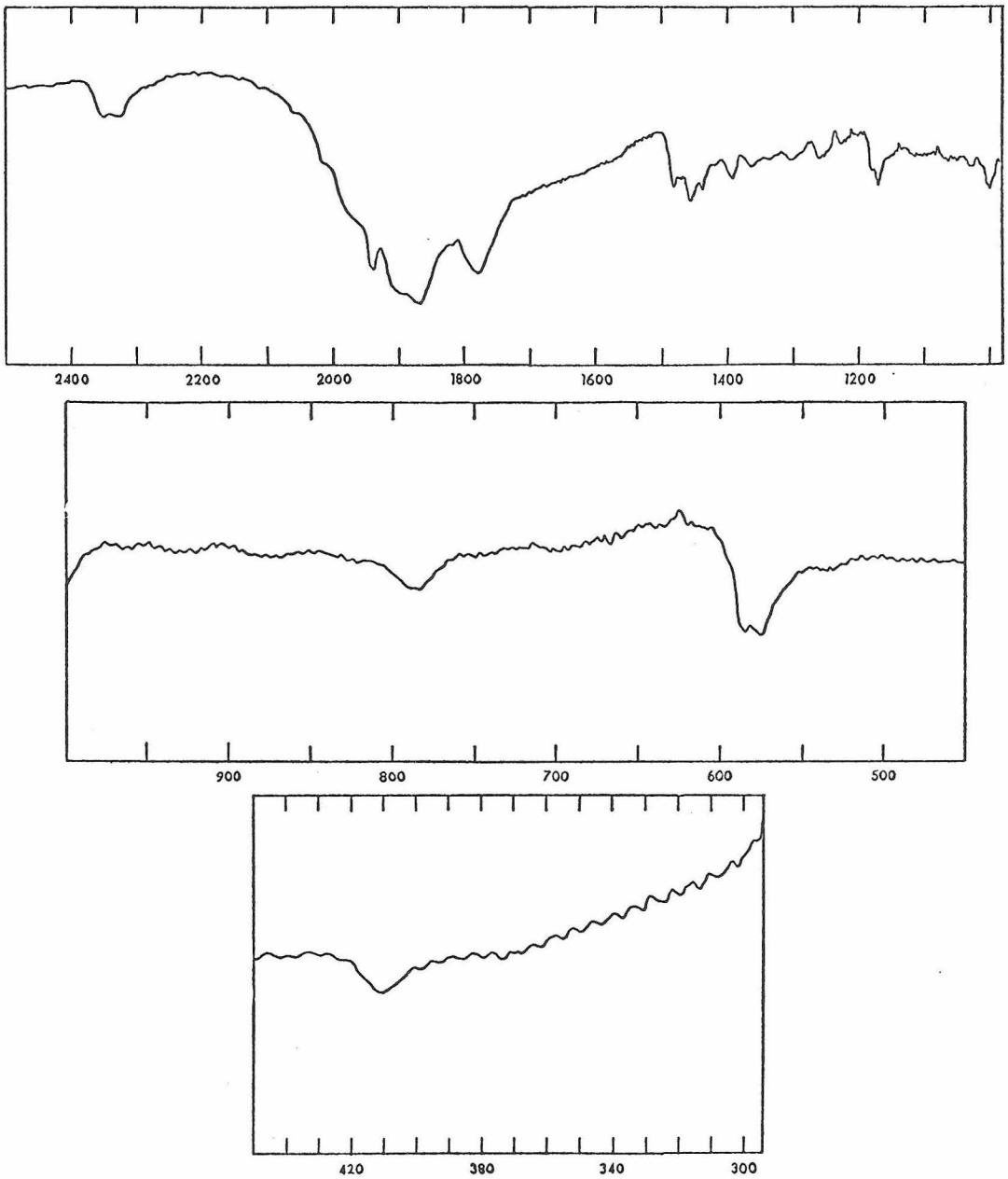

$[(C_2H_5)_4N]_2[W_2(CO)_{10}]$
KBr Pellet - 300°K

Figure 19

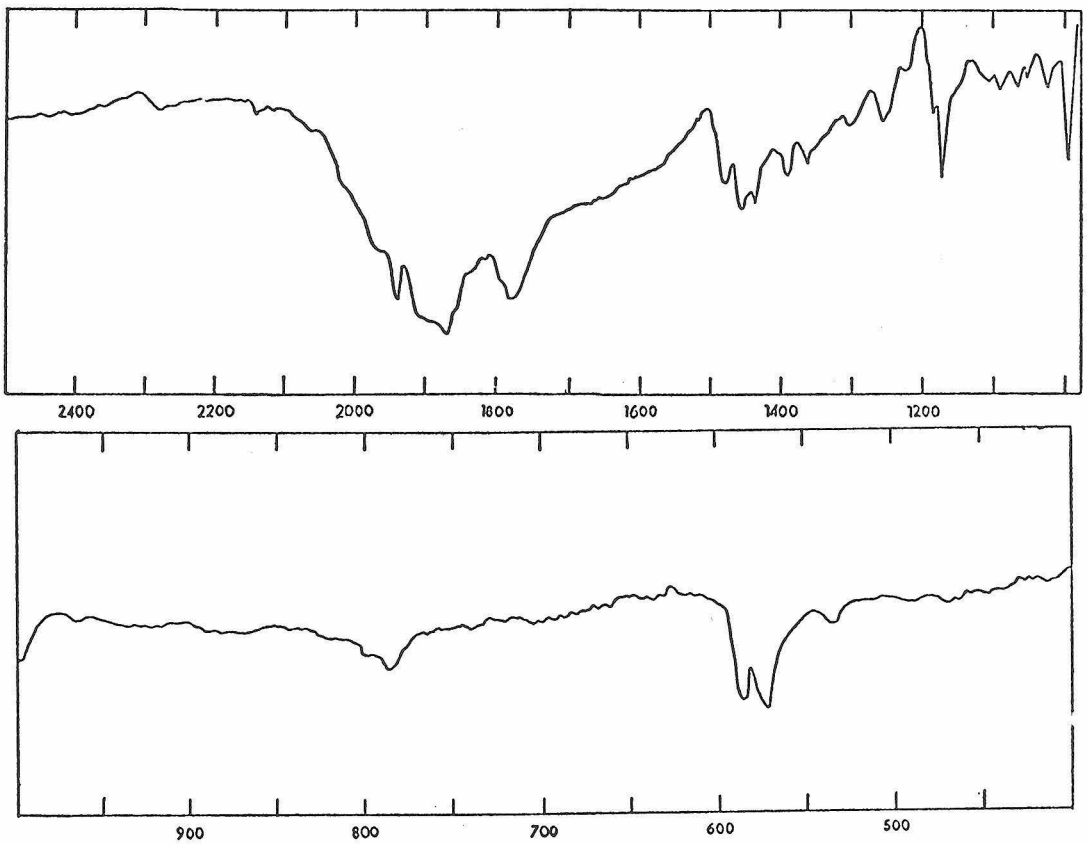

$[(C_2H_5)_4N]_2[\overline{W}_2(CO)_{10}]$
KBr Pellet - $80^{o}K$

Figure 20

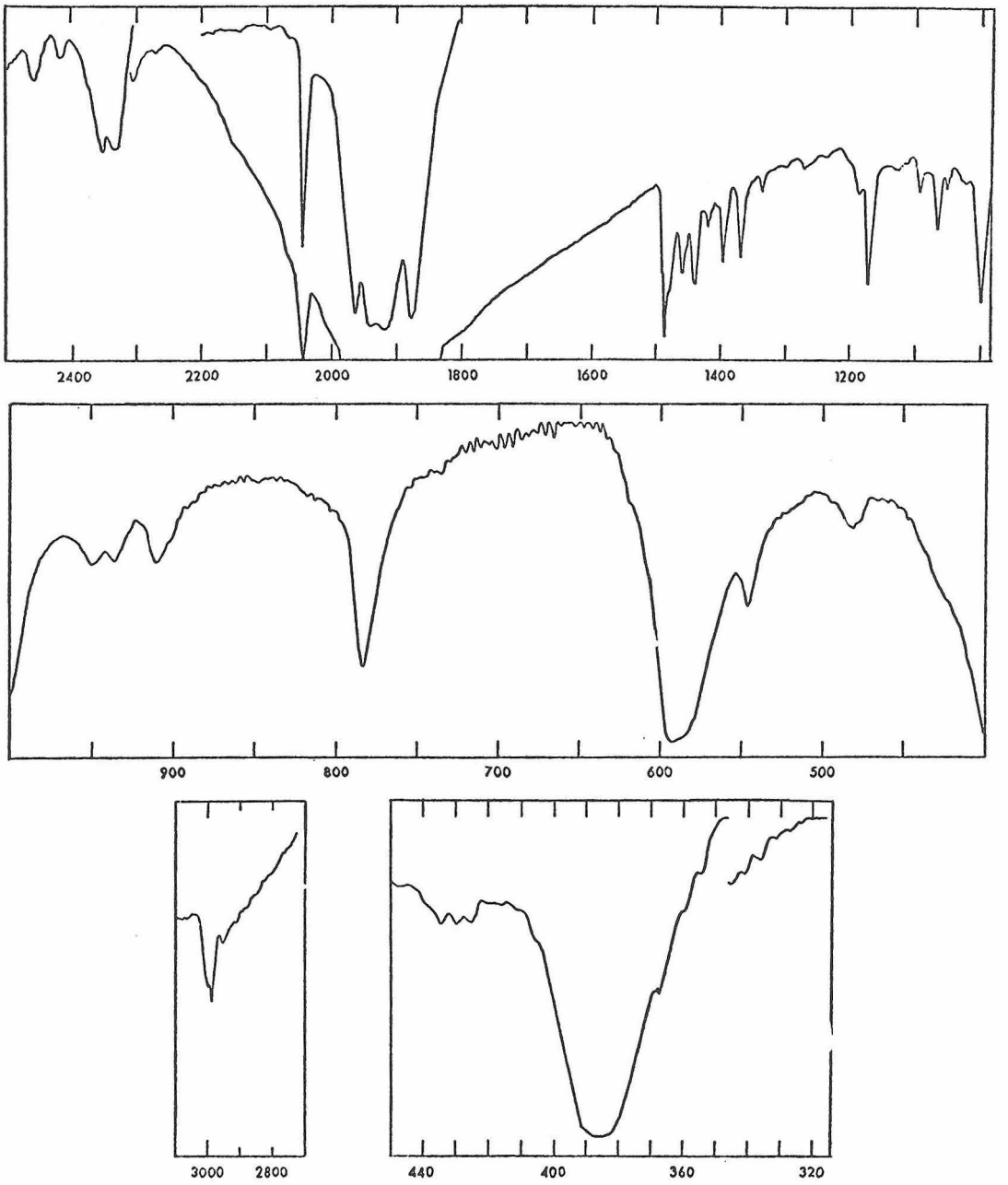

$[(C_2H_5)_4N][HW_2(CO)_{10}]$
KBr Pellet - 300°K

Figure 21

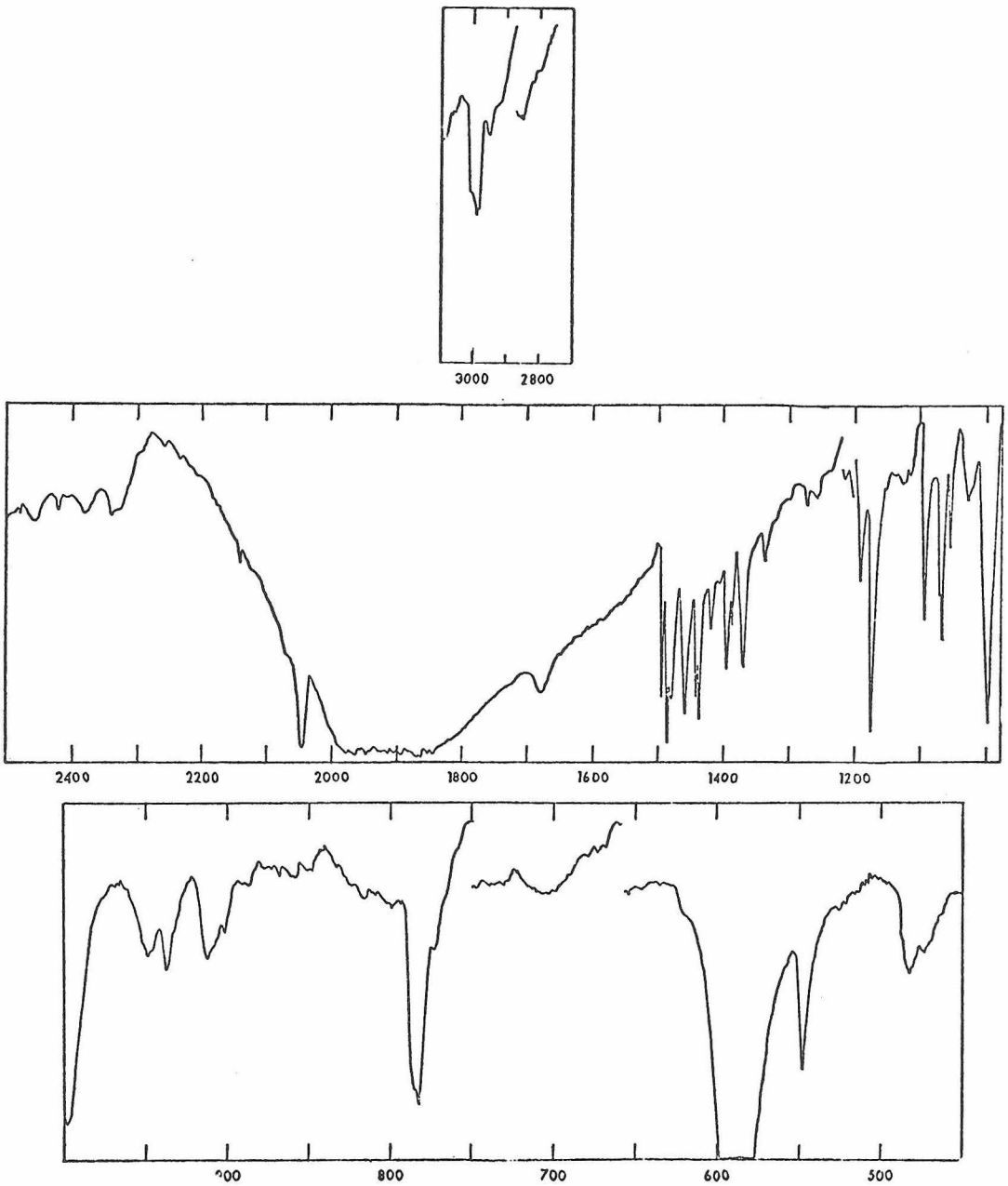

$[(C_2H_5)_4N][HW_2(CO)_{10}]$
KBr Pellet - $80^{o}K$

Figure 22

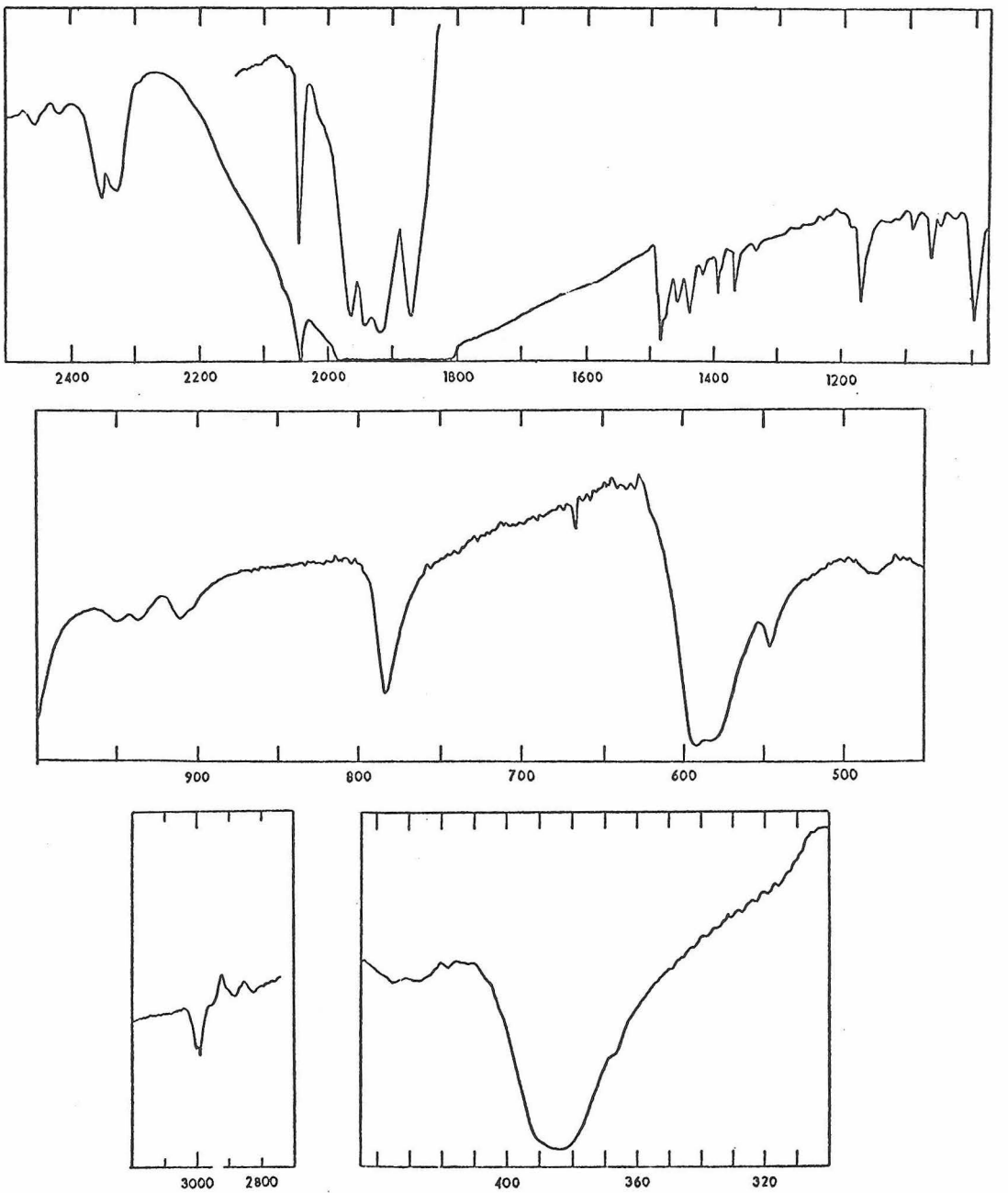

$[(C_2H_5)_4N][DW_2(CO)_{10}]$
KBr Pellet - 300°K

Figure 23

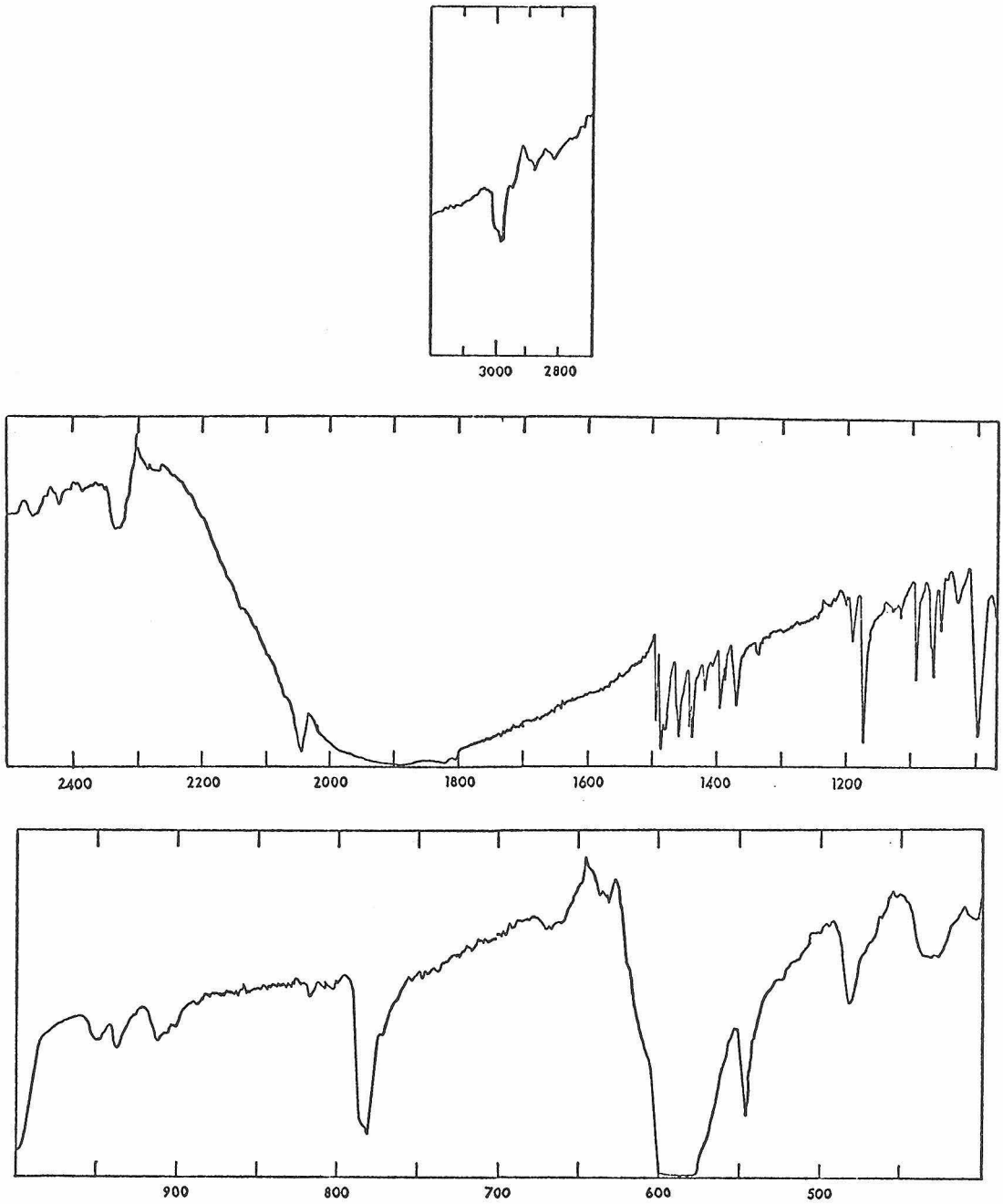

$[(C_2H_5)_4N][DW_2(CO)_{10}]$
KBr Pellet - $80^{o}K$

Figure 24

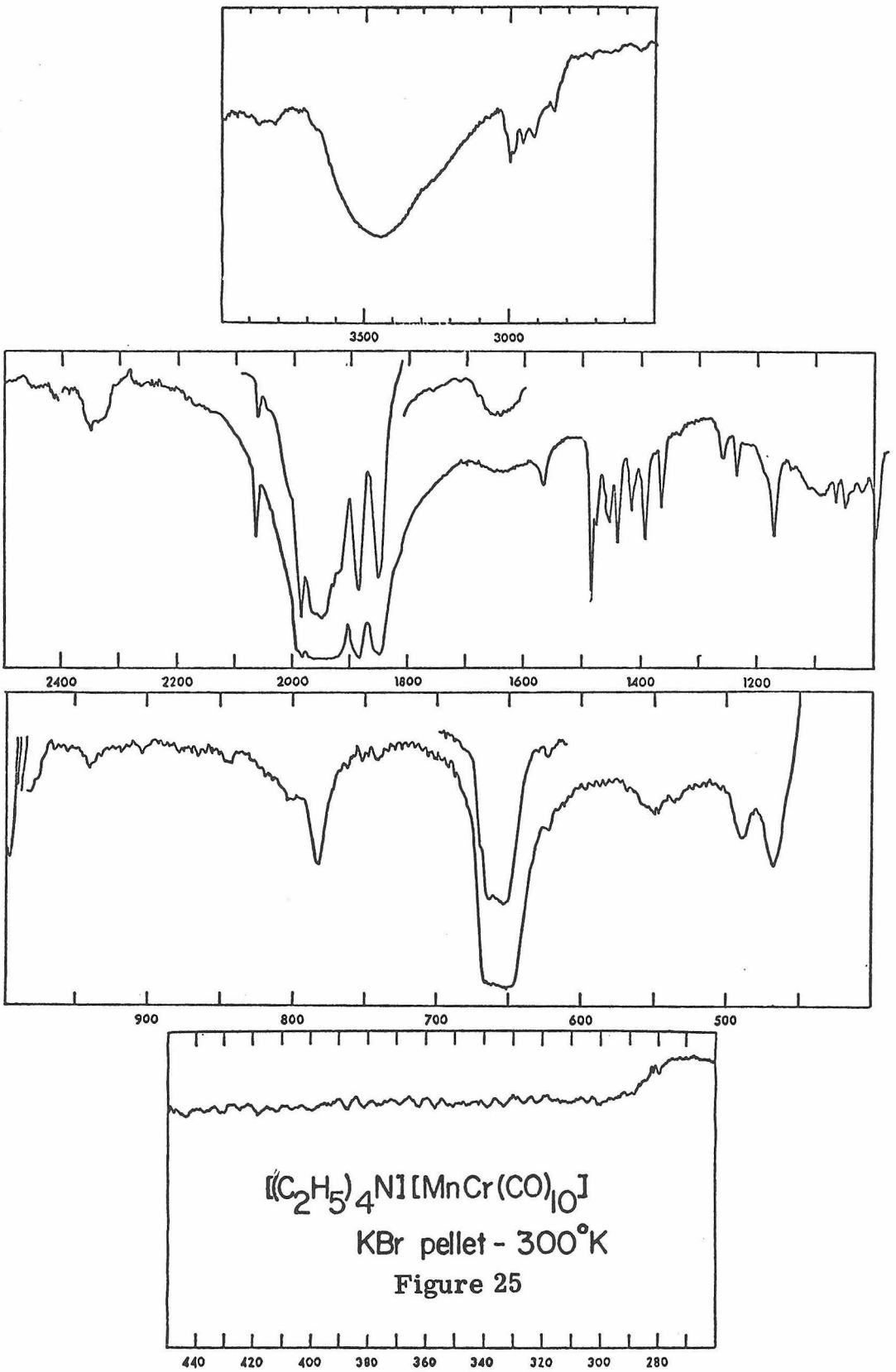

$[(C_2H_5)_4N][MnCr(CO)_{10}]$

KBr pellet - 300°K

Figure 25

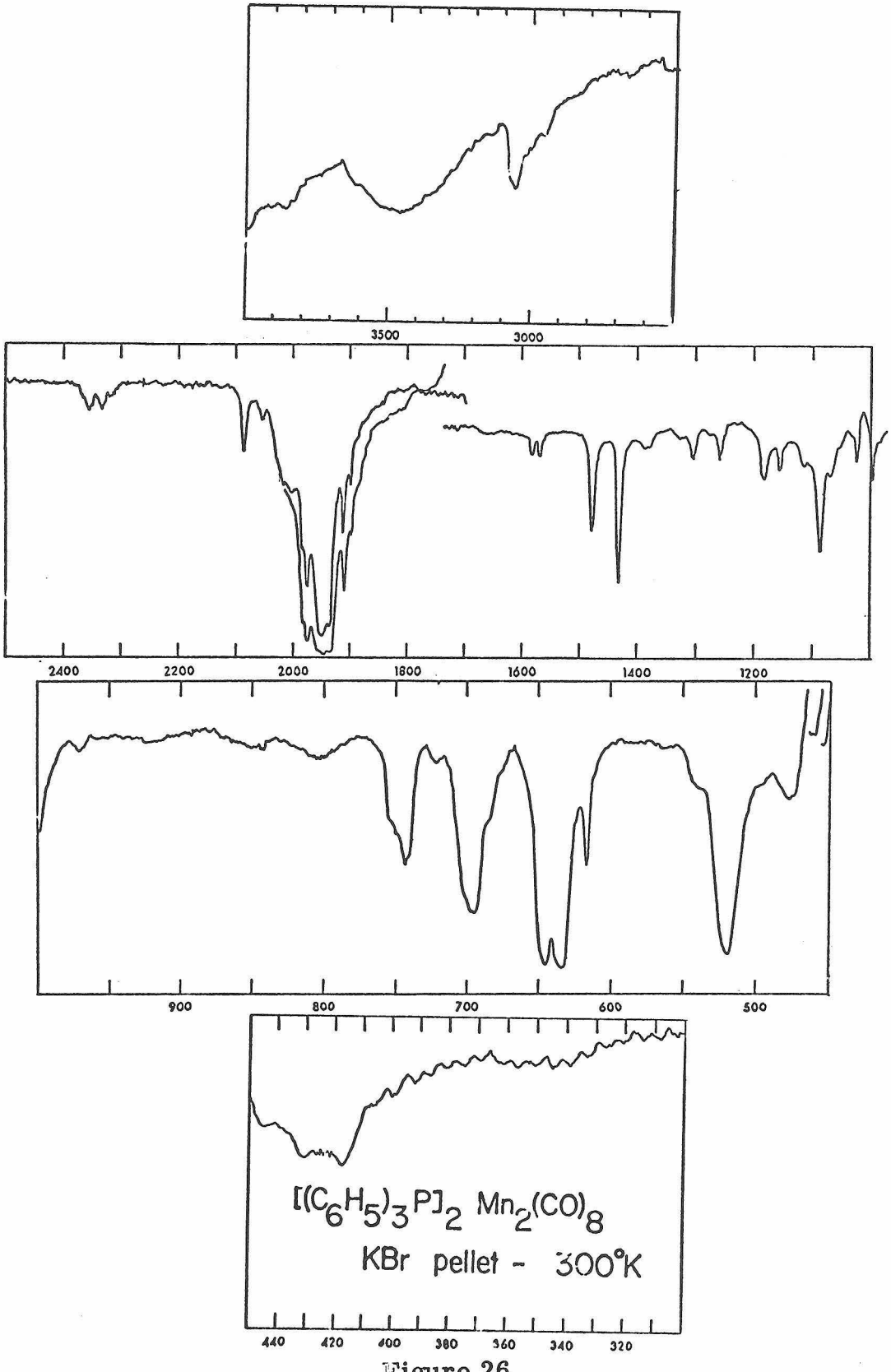
3500
3000
2400
2200
2000
1800
1600
1400
1200
900
800
700
600
500
[(C6H5)3P]2 Mn2(CO)8
KBr pellet - 300°K
440
420
400
380
360
340
320

Figure 26

Table X. Infrared Spectra

$[(C_2H_5)_4N][HCr_2(CO)_{10}]$

300° (2500-1000 cm^{-1})	80° (2500-400 cm^{-1})
2371 br, m	2375 m
2356 sh, w	2350 m
	2325 br, m
2301 w	2294 m
	2242 w
	2229 m
2030 w	2028 m
1970 sh, m	1980 m
	1962 m
1940 s	1937 s
	1920 sh, m
1870 m	1874 m
1785 w	1790 w
1655 w	1660 w
1624 br, m	~1645 br, w
	1574 w
	1566 w
	1488 m
1485 m	1485 w
1450 w	1450 w
1418 w	1426 w
	1406 vw
1401 w	1400 vw
1374 w	1370 w
1291 w	1292 w
1258 w	1260 w
1234 w	1236 w
1175 sh, w	1177 m
	1170 m
1162 w	1162 w
	1137 w
1123 w	1129 m
1084 m	1087 m
1042 m	1043 s
	960 w
	949 m
	873 m
	803 br, m
	764 vw
	667 m
	661 m
	621 w
	524 m
	466 w

Table XI. Infrared Spectra

$[(C_2H_5)_4N]_2[W_2(CO)_{10}]$		$[(C_2H_5)_4N][W_2H(CO)_{10}]$		$[(C_2H_5)_4N][W_2D(CO)_{10}]$	
300°	80°	300°	80°	300°	80°
(2200-300 cm^{-1})	(2200-400 cm^{-1})	(3100-2800 cm^{-1}) (2200-300 cm^{-1})	(3100-2800 cm^{-1}) (1800-450 cm^{-1})	(3100-2800 cm^{-1}) (2200-300 cm^{-1})	(3100-2800 cm^{-1}) (1800-400 cm^{-1})
		2996 m		3000 m	
		2988 m	2990 m	2989 m	2990 m
		2952 w	2950 w		
				2880 vw	2880 w
				2823 vw	2823 vw
2013 sh, w	2015 sh, w	2045 s	2045 s	2045 s	
1975 sh, m	1965 sh, m	1964 vs		1964 vs	
1939 s	1939 s	1939 vs		1940 vs	
1898 sh, s	1898 sh, s	1919 vs		1917 vs	
1870 s	1869 s	1873 vs		1871 vs	
1780 s	1779 s				
		---	1680 m	---	---
		1489 sh, m	1495 m	1489 sh, w	1494 m
1483 w	1480 w	1485 m	1486 m	1484 m	1486 m
		1478 m	1480 m	1477 m	1481 m
			1461 m		
1457 w	1455 w	1458 m	1459 m	1457 w	1458 m
			1455 sh, m		
1438 w	1436 w	1439 m	1442 m	1438 w	1442 m
		1428 m	1438 m		1437 m
			1419 w	1418 w	1418 w
1392 w	1390 w	1394 m	1394 m	1394 w	1394 m
			1387 w	1388 sh, w	1386 w
			1378 sh, m		
1365 vw	1362 w	1367 m	1369 m	1366 w	1369 m
1304 vw	1303 vw	1335 vw	1336 w	1334 vw	1336 w
		1273 vw	1273 vw		
1261 w	1255 w		1259 vw		
	1225 vw		1216 vw		
1190 w	1185 w	1186 w	1192 m		
1171 w	1173 m	1172 m	1174 s		1191 w
			1125 vw	1170 m	1174 s
	1105 vw				1127 vw
	1090 vw	1093 w	1092 m		1116 vw
				1092 w	1093 m
	1066 vw	1066 w	1066 m		1068 m
	1052 vw	1052 vw	1055 m	1065 w	1063 m
1029 vw	1024 vw	1024 vw	1028 w	1050 w	1035 w
1000 w	997 m	1000 m	998 s	1029 vw	1028 w
		950 w	949 m	998 m	998 s
		936 w	937 m	950 w	950 w
		911 w	912 m	936 w	937 w
			902 w	911 w	912 w
786 w	786 w	783 m	782 s		902 w
			773 w	783 m	783 s
			706 br, w		772 sh, w
				667 vw	669 br, w
		592 s			634 w
534 m	586 m	586 sh, s	~588 vs		608 sh, m
575 m	572 m			592 vs	
	534 w	546 w	548 m	584 sh, vs	~587 vs
		482 w	483 m		
			474 m	546 w	548 m
				481 w	482 m
411 w					470 sh, w
		385 s		435 w	432 w
				427 w	
				385 vs	

Table XII. Infrared Spectra

$[(C_6H_5)_3P]_2Mn_2(CO)_8$	$[(C_2H_5)_4N][MnCr(CO)_{10}]$
300°	300°
(4000-300 cm^{-1})	(4000-300 cm^{-1})
3060 w	3450 br, m
2355 vw	3015 sh, w
2333 vw	3000 w
2086 w	2990 w
2055 vw	2956 vw
~ 2010 sh, w	2920 vw
1983 vw	2850 vw
1975 s	2068 vw
1949 vs	~ 2010 sh, m
1935 vs	1988 vs
1912 w	1963 vs
1899 vw	1952 vs
1584 vw	~1925 sh, vs
1569 vw	1888 vs
1480 m	1853 vs
1434 m	1640 br, w
1390 vw	1566 w
1383 vw	1485 s
1325 vw	1477 m
1307 w	1454 m
1260 w	1440 m
1184 w	1417 m
1158 w	1393 m
1116 vw	1365 m
1088 m	1260 w
1072 vw	1236 w
1026 w	1184 sh, w
998 w	1172 m
804 br, vw	1093 br, w
752 sh, m	1065 vw
744 m	1050 vw
722 vw	1022 vw
696 m	998 m
686 sh, m	940 vw
646 s	802 w
632 s	783 m
617 m	663 vs
540 sh, w	654 vs
520 s	550 br, w
477 m	489 m
430 w	468 m
417 w	419 br, w

A. $Mn_2(CO)_8(P\phi_3)_2$
B. $[(C_2H_5)_4N][MnCr(CO)_{10}]$
C. $[(C_2H_5)_4N]_2[W_2(CO)_{10}]$
D. $[(C_2H_5)_4N][DW_2(CO)_{10}]$
E. $[(C_2H_5)_4N][HW_2(CO)_{10}]$

Bands labeled with asterisks are artifacts.

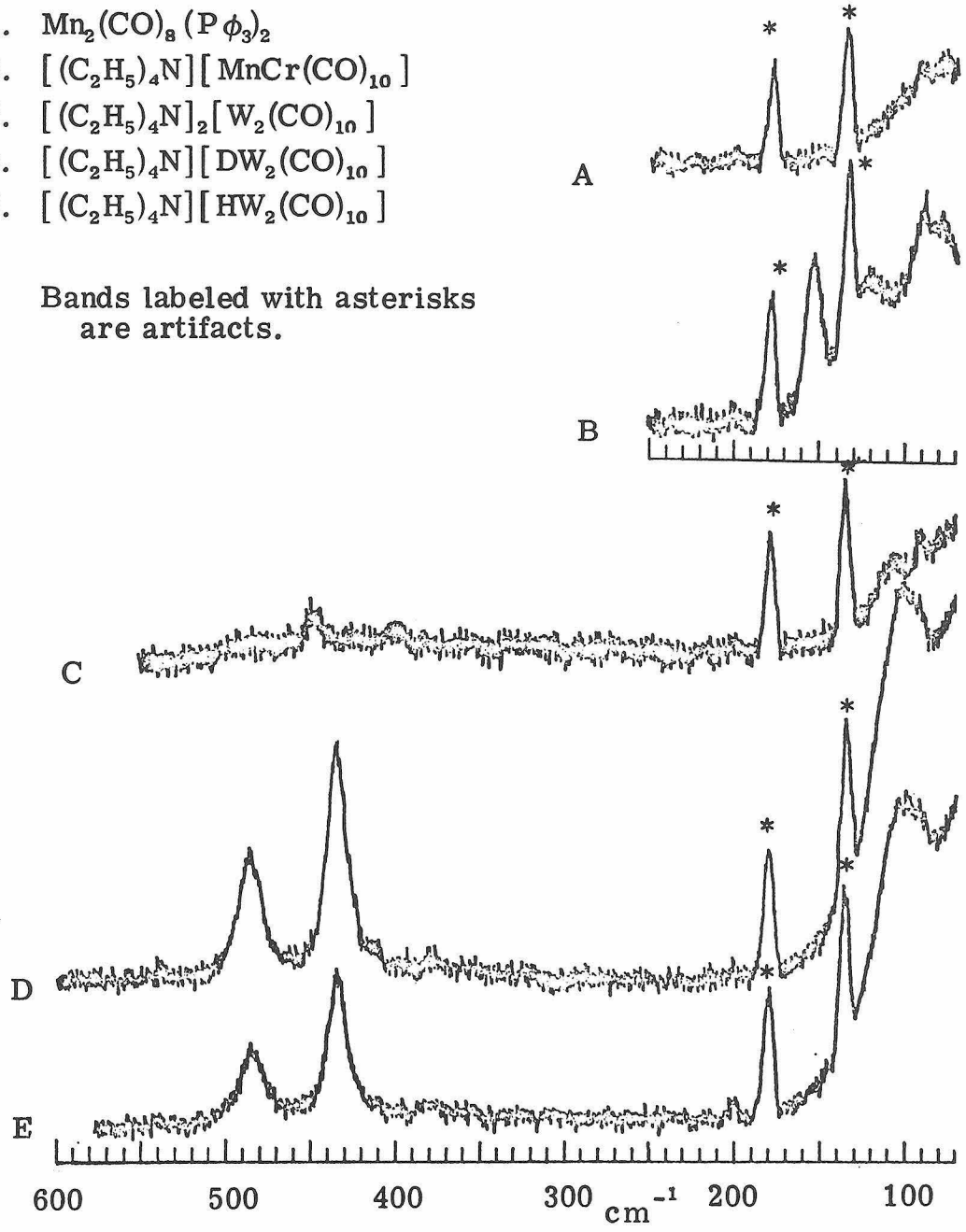

Raman Spectra

Figure 27

Table XIII

Raman Spectra[a]

Compound	Region Covered (cm^{-1})	Spectrum[b]
$[(C_2H_5)_4N][HW_2(CO)_{10}]$	70-2880	101 (48), 136 (59), 181 (46), 380 (6), 415 sh (7), 436 (81), 487 (40), 672 (5), 1115 (4), 1296 (6), 1458 (8), 1851 (19), 1891 (3), 1963 (52), 2069 (18)
$[(C_2H_5)_4N][DW_2(CO)_{10}]$	70-2170	101 (50), 135 (40), 180 (32), 378 (3), 436 (62), 486 (32), 1852 (12), 1963 (32), 2068 (12)
$[(C_2H_5)_4N]_2[W_2(CO)_{10}]$	70-550, 1600-2220	91 (10), 108 (11), 136 (57), 179 (44), 401 (8), 450 (13)
$[(C_2H_5)_4N][MnCr(CO)_{10}]$	70-2240	80 (16), 90 (25), 122 (8), 134 (61), 156 (45), 180 (44), 400 (11), 420 (32)
$Mn_2(CO)_8(P\phi_3)_2$[c]	70-200	91 (7), 135 (47), 179 (35)
KBr[d]	70-260	135 (15), 180 (10)

[a] Solid samples.

[b] Entries are $\bar{\nu}_{max}$ and, in parentheses, relative intensities.

[c] This orange compound slowly burned in the 6328 Å laser. All other samples in this Table are yellow.

[d] This sample shows that bands at 135 and 180 cm^{-1} are an artifact of our Cary 81 Lemon Raman Spectrometer.

$HW_2(CO)_{10}^-$, and $DW_2(CO)_{10}^-$ show only one band which might be attributed to the M-H-M linkage. At room temperature, the spectra of $HW_2(CO)_{10}^-$ and $DW_2(CO)_{10}^-$ are identical. However, at liquid nitrogen temperature a medium intensity band at 1680 cm^{-1} appears in $HW_2(CO)_{10}^-$. This is shown most clearly in Figure 28 which was obtained with a different KBr pellet sample from the one used for Figures 21 and 22. (In all cases where 300°K and 80°K spectra are given, the same sample was used for both spectra.) This 1680 cm^{-1} band is not present in spectra of $W_2(CO)_{10}^{2-}$ and $DW_2(CO)_{10}^-$. We have run enough different samples of these compounds to be absolutely certain that this is not an artifact. George McGovern would be 3000% sure of this result. Since no other fundamental is expected in this region, we assign this band as ν_{as}(M-H-M).

Unfortunately, no corresponding ν_{as}(M-D-M) can be found in the spectrum of $DW_2(CO)_{10}$. Using the procedure outlined in the next paragraph, we anticipate ν_{as}(M-D-M) to be at 1190 cm^{-1}. A medium intensity band due to the tetraethylammonium cation occurs in this region. The next best thing is to look for the other two M-H-M vibrations. To our knowledge, nobody has ever assigned a M-H-M bend.

A study of $HMn(CO)_5$ and $DMn(CO)_5$ led Risen[74] to assign bands at 731 and 612 cm^{-1} as containing substantial H-Mn-C bending motion. Paauwe[70] has speculated that a very questionable band in $HCr(CO)_{10}^-$ at 536 cm^{-1} might be the δ(Cr-H-Cr) vibration.

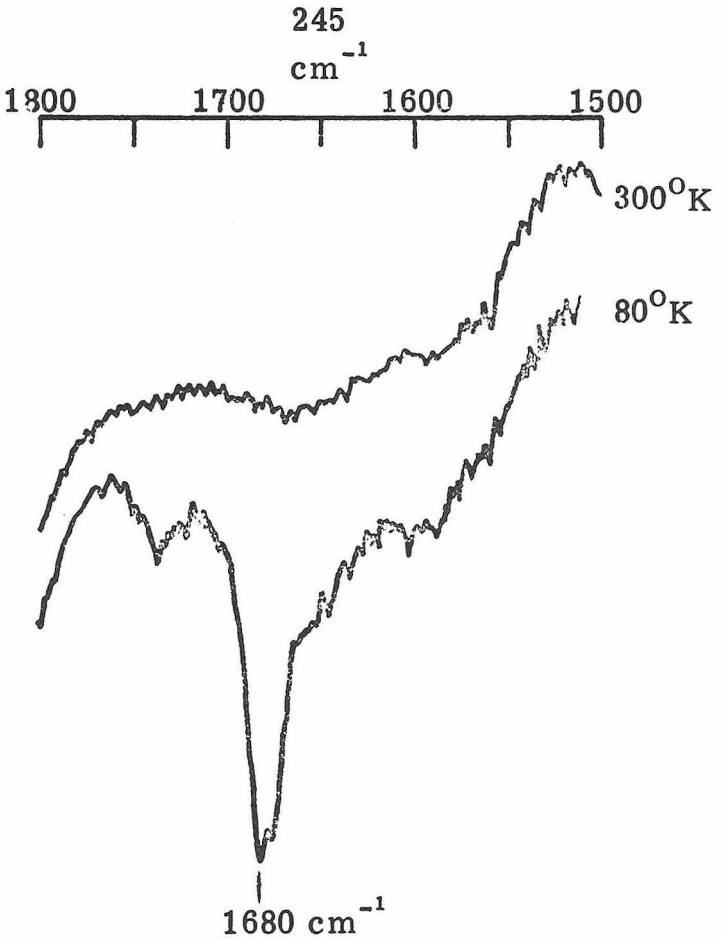

Dramatic Change in the Spectrum of
$[Et_4N][HW_2(CO)_{10}]$ on Cooling

Figure 28

In our spectra of $HW_2(CO)_{10}^-$ and $DW_2(CO)_{10}^-$ we find no bands in this, or any other region, present in one compound and absent in the other.

So we try the last possibility. The Raman active ν_s mode is expected to be a very low frequency vibration because it involves only heavy metal motion and no H motion. To estimate its frequency, we made the following primitive calculation. Assume that we actually have a three particle system in which the end units

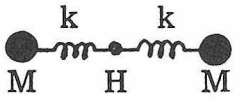

have mass M_M equal to the mass of a $W(CO)_5$ unit. The stretching frequencies of this system are[75]

$$\nu_{as} = \frac{1}{2\pi} \sqrt{k\mu}$$

$$\nu_s = \frac{1}{2\pi} \sqrt{k/M}_M$$

where $$\mu = \frac{2M_M + M_H}{M_M M_H}$$

M_H = mass of hydrogen atom

k = force constant of M-H bond

Putting in a value of 1680 cm^{-1} for ν_{as}, we expect ν_s for <u>both</u> $HW_2(CO)_{10}^-$ and $DW_2(CO)_{10}^-$ to occur at 67 cm^{-1}. This frequency

must be regarded with due recognition of the crude procedure by which it was derived.[76] The Raman spectra (Fig. 27) show a strong band at 101 cm^{-1} present in both $HW_2(CO)_{10}^-$ and $DW_2(CO)_{10}^-$ but absent in the spectrum of $W_2(CO)_{10}^{2-}$. This band is tentatively assigned to ν_s.

The only other task we will attempt with these spectra is the assignment of the ν_{CO} frequencies. The predictions are given in Table XIV and the assignments are given in Table XV. The assignment for $HCr_2(CO)_{10}^-$ was done by Paauwe[70] and our assignment of $HW_2(CO)_{10}^-$ is based on the analogous $HCr_2(CO)_{10}^-$ assignment. The availability of both Raman and IR data makes this assignment very straightforward. The assignment of $MnCr(CO)_{10}^-$ is implicit in the paper by Anders and Graham[40] and is based on the similarity of the spectrum of $MnCr(CO)_{10}^-$ to separate $Mn(CO)_5X$ and $Cr(CO)_5Y$ spectra. Finally, the two strong bands of $Mn_2(CO)_8(P\phi_3)_2$ are taken as the fundamentals. The assignment of the e_1 band is based on the splitting observed in the KBr pellet.

The only additional comment on these spectra is an explanation of the very low ν_{CO} frequencies of $W_2(CO)_{10}^{2-}$. The appearance of bands below 1800 cm^{-1} led the early investigators of these compounds to assume that carbonyl bridges were present. X-ray work on $Cr_2(CO)_{10}^{2-}$ and $Mo_2(CO)_{10}^{2-}$ show that only terminal carbonyls are present. Noting that $(\pi\text{-}C_5H_5)V(CO)_3^{2-}$ and $Fe(CO)_4^{2-}$ exhibit ν_{CO} modes at 1748, 1645, and 1730 cm^{-1}, Kaska[33] explains the $M_2(CO)_{10}^{2-}$ spectra in terms of strong back bonding due to the

Table XIV

Expected Carbonyl Stretching Modes

Structural Formula	Point Group	IR Active Modes	Raman Active Modes
$M_2(CO)_{10}$	D_{4d}	$2b_2 + e_1$	$2a_1 + e_2 + e_3$
$HM_2(CO)_{10}$	D_{4h}	$2a_{2u} + e_u$	$2a_{1g} + b_{1g} + e_g$
$MM'(CO)_{10}$	C_{4v}	$4a_1 + 2e$	$4a_1 + b_1 + b_2 + 2e$
$M_2(CO)_8L_2$[a]	D_{4d}	$b_2 + e_1$	$a_1 + e_2 + e_3$

[a] Axial substitution

Table XV

Assignments of Carbonyl Stretching Frequencies

$HCr_2(CO)_{10}^-$ THF Solution[a] IR	Raman	Assignment[a]	$HCr_2(CO)_{10}^-$ KBr Pellet IR	$HW_2(CO)_{10}^-$ KBr Pellet IR	Solid Raman	Assignment	$Cr_2(CO)_{10}^{2-}$ [b] THF Solution[a] IR	Raman	Assignment[a]
	2064 w	a_{1g}			2069 m	a_{1g}		2010 m	a_1
2029 m		a_{2u}	2030 w	2045 s		a_{2u}	1918 s		b_2
	1963 vs	b_{1g}	1970 sh,m	1964 vs	1963 s	b_{1g}	1895 vs		e_1
1938 vvs		e_u	1940 s	1939 vs }		e_u		1888 vs	e_2
	1904 vw	e_g		1919 vs }			1869 sh		
	1886 s	a_{1g}			1891 w	e_g	1825 m		b_2
1877 vs		a_{2u}	1870 m	1875 vs		a_{2u}		1814 s	a_1
					1851 m	a_{1g}	1805 m	1802 w	
								1768 vw	
							1756 m		

$W_2(CO)_{10}^{2-}$ KBr Pellet IR	Assignment	$MnCr(CO)_{10}^-$ THF Solution[c] IR	Assignment[d]	KBr Pellet IR	$Mn_2(CO)_8(P\phi_3)_2$ $CHCl_3$ Solution[e] IR	KBr Pellet	Assignment
2013 sh,w	a_1	2063 w	a_1 (Mn)	2068 vw		2086 w	
1975 sh,m				2010 sh,m		2055 vw	
1939 s	b_2	1990 s	a_1 (Cr)	1988 vs		2010 sh,w	
1898 sh,s				{ 1963 vs		1983 vw	
1870 s	e_1	1950 vs	e (Mn)	1952 vs			
1780 s	b_2	1925 m	a_1 (Mn)	1925 sh,vs	1980 sh	1975 s	b_2
		1896 s	e (Cr)	1888 vs	1956 vs	1949 vs }	e_1
		1865 m	a_1 (Cr)	1853 vs		1935 vs }	
						1912 w	
						1899 vw	

[a] Reference 70.

[b] See also reference 33 for a discussion of the marked solvent dependence of these spectra.

[c] Reference 40.

[d] These assignments are implicit, but not explicit, in reference 40. The designations (Mn) and (Cr) imply separate vibrations of the $Mn(CO)_5$ or $Cr(CO)_5$ halves of the molecule.

[e] Reference 72.

very low oxidation state of the metal. This is very reasonable.

The infrared spectra of the iron compounds are particularly interesting because previous studies[47,61] have shown that geometric isomerism in these compounds can be elucidated by the study of the infrared spectra. The ν_{CO} region is especially useful for this purpose. Manning[47] studied the spectrum of $[CpFe(CO)_2]_2$ as a function of solvent. He concluded that the <u>cis</u> (VII) and <u>trans</u> (VIII) isomers are in equilibrium and that a non-bridged isomer (IX) is present in negligible amounts.

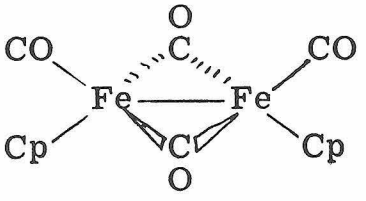

VII

$\rightleftharpoons$

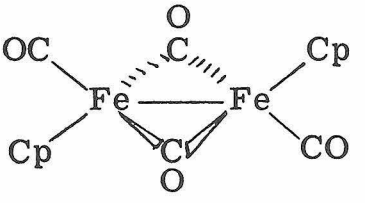

VIII

$\rightleftharpoons$

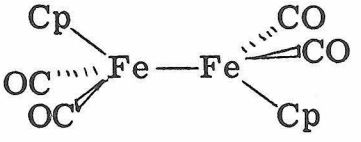

IX

VII		VIII	
ν_{CO}:	~1780	ν_{CO}:	~1780
	~1805		~1960
	~1960		
	~2000		

Solutions containing both cis and trans isomers generally show four ν_{CO} bands owing to the near coincidence of two of the bands of VII with those of VIII. (That more than four bands are really present was confirmed by studying the region of the first overtone of ν_{CO}.) Manning[47] estimates the following cis/trans ratios:

Solvent	Cis (VII)/trans (VIII)
cyclohexane	36 : 64
carbon disulfide	43 : 57
benzene	51 : 49
nitrobenzene	71 : 29
dimethylsulfoxide	86 : 14

The more polar cis isomer predominates in the more polar solvents.

Crystallization of $[CpFe(CO)_2]_2$ from a wide variety of solvents at $\sim 0°$ gives pure trans isomer as black (intense red) plates. At lower temperatures (-78°), pure cis isomer can be isolated, also as black crystals. Crystal structure determination[42,43] has confirmed the nature of VII and VIII. Both have identical Fe-Fe bond lengths (2.53Å), but the cis isomer has a book-like fold about the Fe-Fe axis such that the two Fe_2CO planes have a dihedral angle of 164°. Presumably this bend is away from the side of the molecule with the cyclopentadienyl groups.

Our spectra of the pure cis and trans isomers are given in Figures 29-32 and listed in Table XVI. The ν_{CO} band positions,

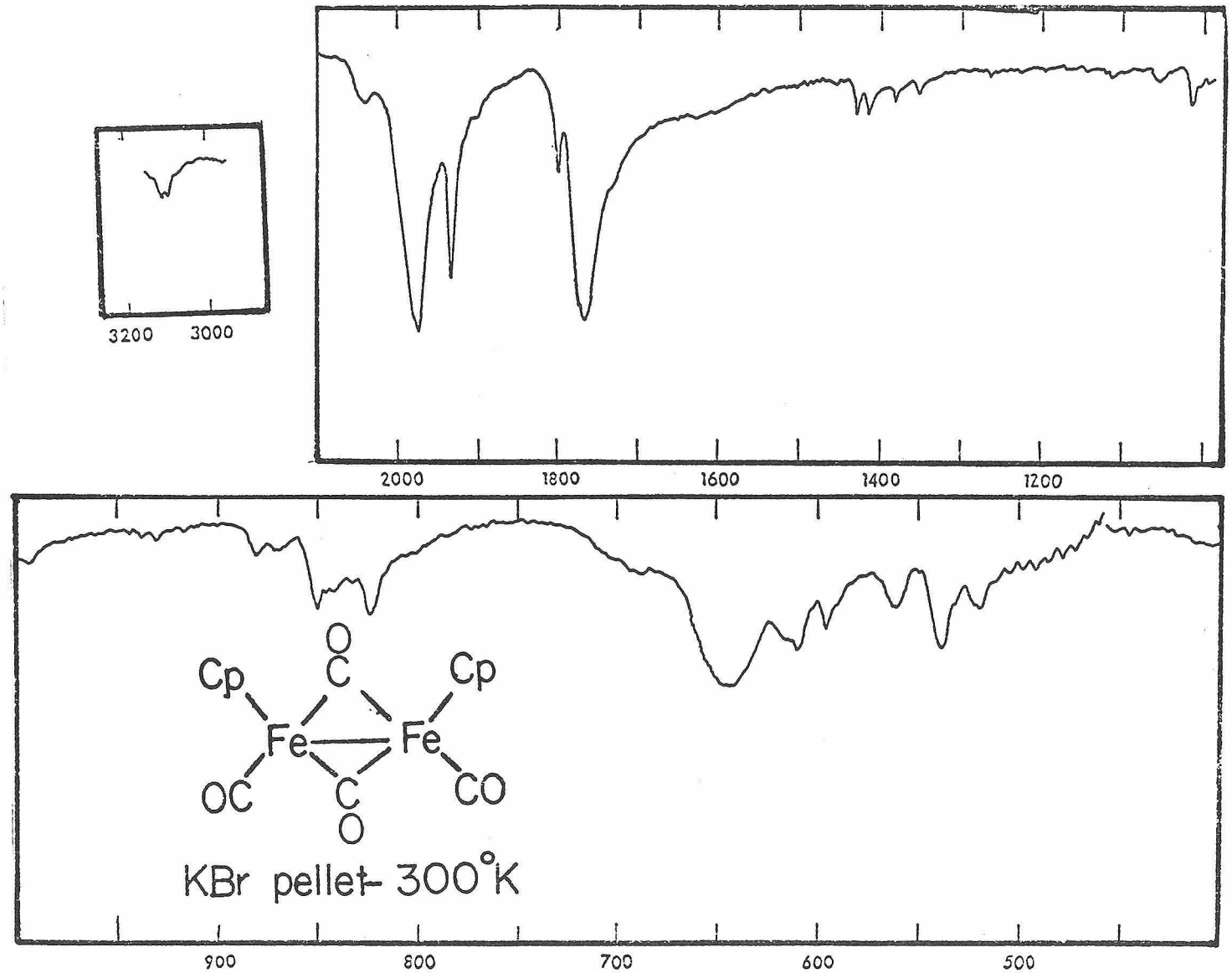
3200
3000
2000
1800
1600
1400
1200
Cp
O
C
Cp
Fe
Fe
OC
C
CO
O
KBr pellet- 300°K
900
800
700
600
500

Figure 29

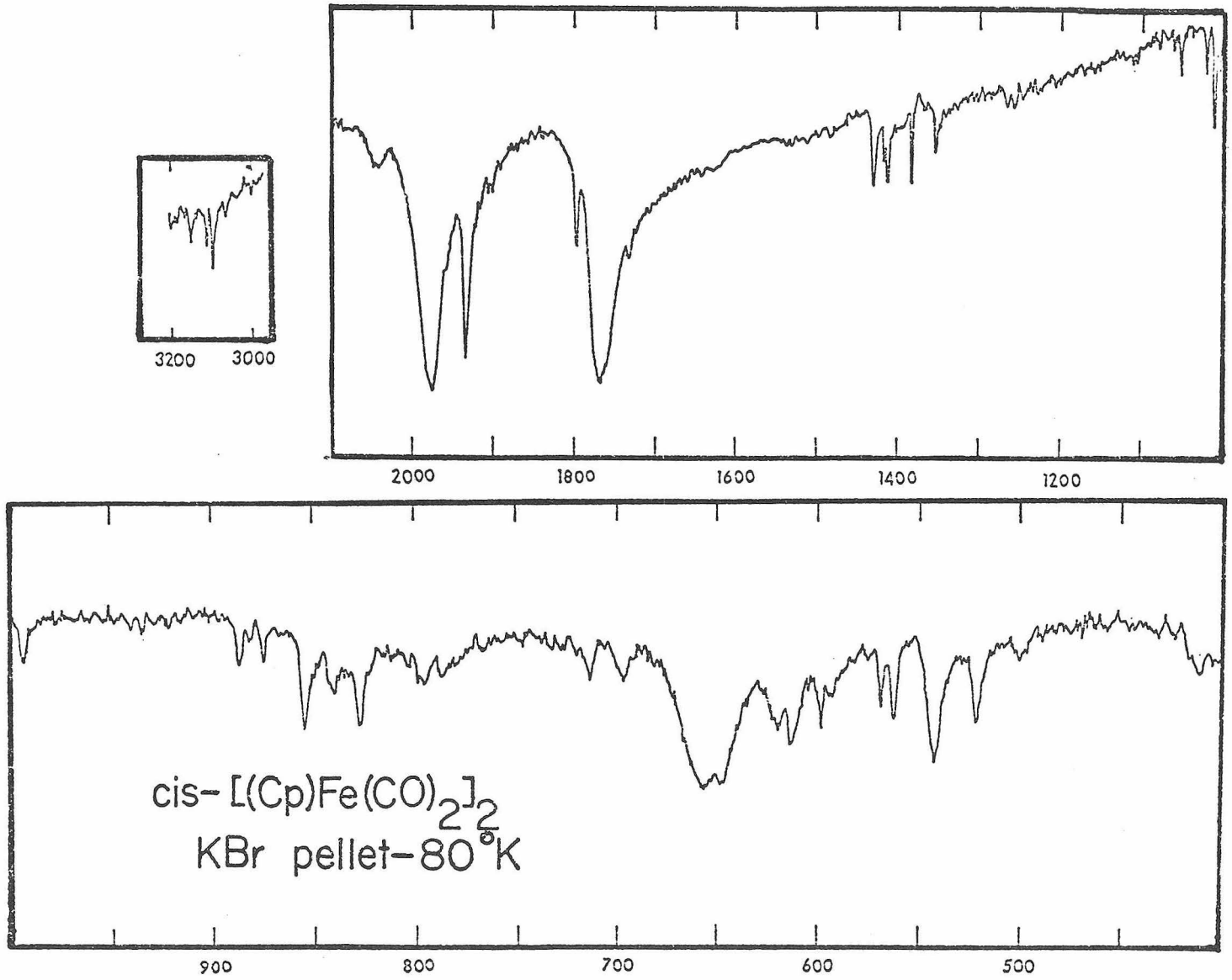
3200
3000
2000
1800
1600
1400
1200
cis-[(Cp)Fe(CO)2]2
KBr pellet-80°K
900
800
700
600
500

Figure 30

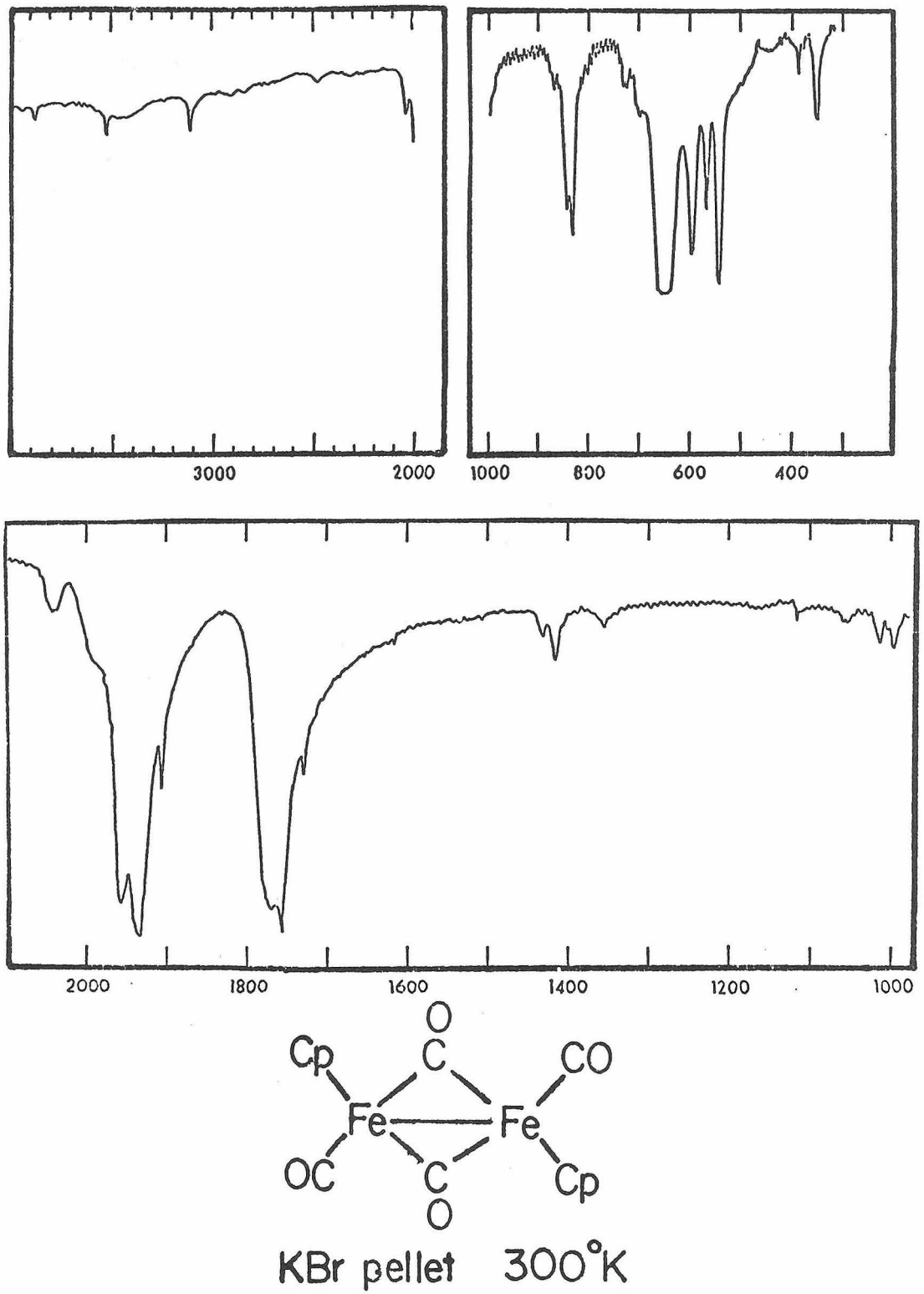
3000
2000
1000
800
600
400
2000
1800
1600
1400
1200
1000
O
Cp
C
CO
Fe
Fe
OC
C
Cp
O
KBr pellet 300°K

Figure 31

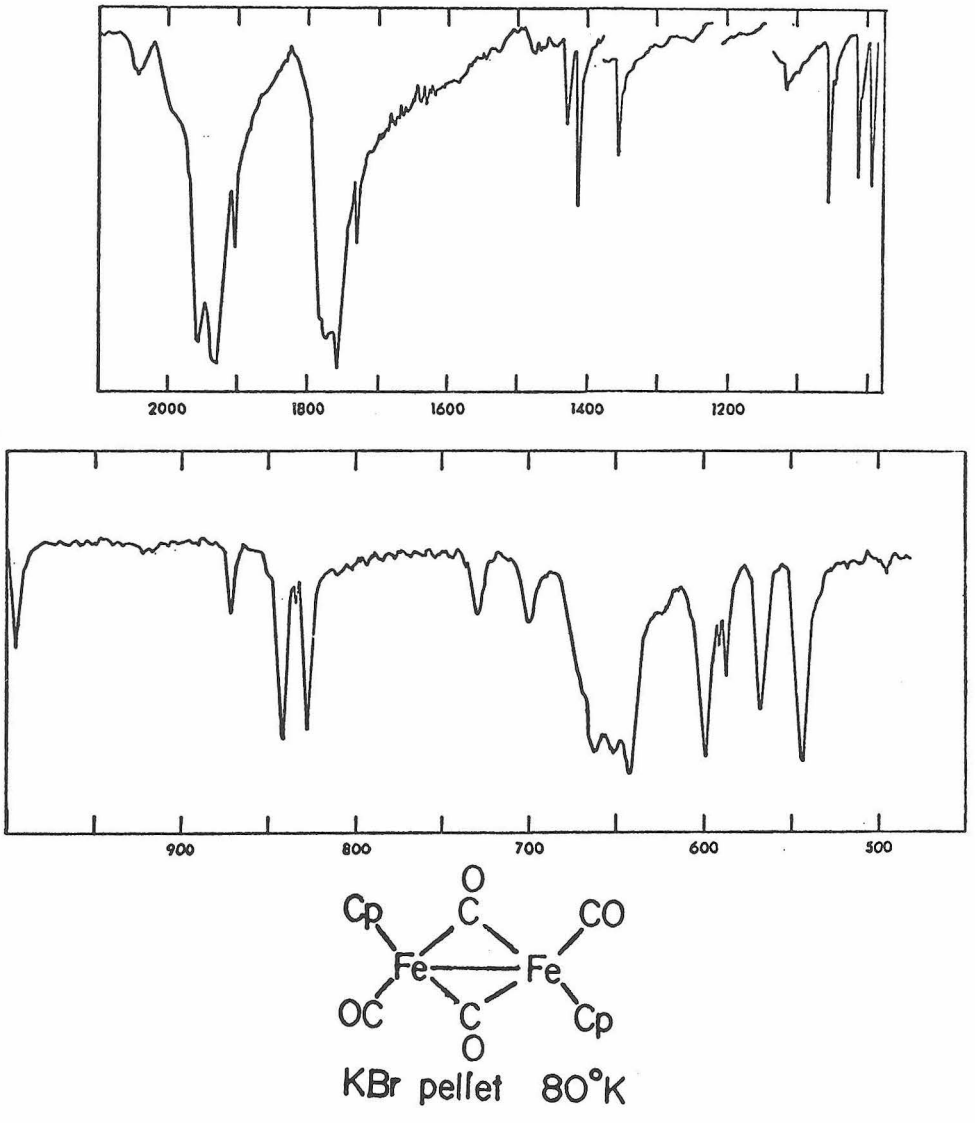
2000
1800
1600
1400
1200
900
800
700
600
500
O
C
Cp
CO
Fe
Fe
OC
C
Cp
O
KBr pellet 80°K

Figure 32

Table XVI. Infrared Spectra

cis-$[(\pi\text{-}C_5H_5)_2Fe(CO)_2]_2$		trans-$[(\pi\text{-}C_5H_5)_2Fe(CO)_2]_2$	
300° (3200-400 cm^{-1})	80° (3200-400 cm^{-1})	300° (4000-320 cm^{-1})	80° (2100-470 cm^{-1})
3111 w	3149 w		
3096 w	3110 w	3880 vw	
	3095 w	3520 w	
2040 w	2044 w	3109 w	
1976 vs	1976 vs	2044 w	2045 w
1933 s	1934 s	1990 sh, w	1990 sh, w
1906 w		1957 vs	1957 vs
1800 m	1798 m	1933 vs	1932 vs
1768 vs	1769 vs	1906 w	1904 w
~1735 sh, m	1733 w	1770 vs	1775 vs
1431 w	1431 m	1756 vs	1759 vs
1417 w	1417 w	1730 w	1732 w
	1413 m	1431 w	1429 w
1383 w	1384 m	1415 w	1414 m
1355 w	1355 w	1355 vw	1357 w
	1267 vw		
	1259 vw	1117 vw	1116 w
1057 w	1054 w	1056 vw	1056 m
	1022 w		1048 vw
1015 w	1014 m	1013 w	1014 m
	1007 w		1010 sh, w
	993 w	997 w	995 m
	887 w		
881 w	881 vw		
871 w	874 w		872 w
850 m	854 m		
844 sh, m	840 w	841 m	842 m
833 sh, m		830 m	834 vw
825 m	828 m		828 m
	797 w	725 w	729 w
	787 w	698 sh, w	700 w
	714 w		663 s
688 sh, w, br	697 w	649 m, br	652 s
	656 m		643 s
644 m, br	649 m		624 sh, vw
616 sh, w	620 w	594 m	599 s
610 m	613 m		592 vw
596 w	598 w		588 w
	569 w	565 m	558 m
561 w	562 w	543 m	543 s
538 m	543 m	386 w	
519 m	522 m	348 w	
	500 w		
	411 w		

in excellent agreement with those reported by Bryan *et al.*,[43] are given below:

	cis-$[CpFe(CO)_2]_2$		*trans*-$[CpFe(CO)_2]_2$
	2040 w		2044 w
ν_s(terminal) →	1976 vs		1990 sh, w
ν_{as}(terminal) →	1933 s	ν_{as}(terminal) → {	1957 vs
	1906 w		1933 vs
ν_s(bridge) →	1800 m		1906 w
ν_{as}(bridge) →	1768 vs	ν_{as}(bridge) → {	1770 vs
	~1735 sh, m		1756 vs
			1730 w

The four fundamentals of the *cis* isomer are shown by arrows and assigned according to Manning.[47] (Manning's assignments are exceedingly tenuous so these shouldn't be taken too seriously.) The splitting of the fundamentals of the *trans* isomer is a solid state effect, not seen in solution.

Symon and Waddington[4] studied the infrared spectrum of the protonated species, $[CpFe(CO)_2]_2H^+$. Their conductimetric titration of $[CpFe(CO)_2]_2$ with BCl_3 in liquid HCl, as well as our own integration of NMR signals, establishes that $[CpFe(CO)_2]_2$ is a *monobasic* species. This fact, and the exceptionally high field of the NMR signal (see NMR section of this chapter) support the idea that the proton is in a bridging position between the two iron atoms. No IR bands associated with the Fe-H-Fe (or Fe-D-Fe) bridge have been observed.[77] Symon and Waddington[4] have

shown that $[CpFe(CO)_2]_2H^+$ has <u>two</u> infrared absorptions in the terminal ν_{CO} region and none in the bridging region. This strongly supports the C_{2h} structure X:

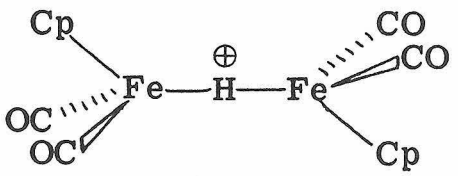

ν_{CO}: ~2040
~2010

X

This species is unstable (we concur) and goes to $CpFe(CO)_3^+$ and $[CpFe(CO)_2]_2$ as the only identifiable products (Figure 33).

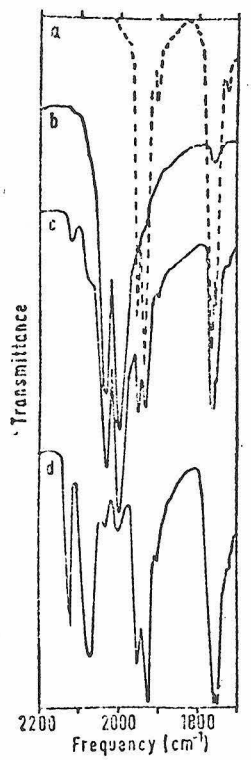

The i.r. spectrum of $[(\pi\text{-}C_5H_5)Fe(CO)_2]_2H^+PF_6^-$ in the carbonyl region as a function of time. a, $[(\pi\text{-}C_5H_5)Fe(CO)_2]_2$, b, $[(\pi\text{-}C_5H_5)Fe(CO)_2]_2H^+PF_6^-$ initially, c, the same after 2 h in the i.r. beam, and d, the same after 18 h in the i.r. beam

Figure 33
(From reference 4)

(With Permission)

When we treated $[CpFe(CO)_2]_2$ with gaseous HBr in $CHCl_3$, we observed <u>three</u> bands in the terminal ν_{CO} region (Figure 34). We observed a very weak band at 2120 cm^{-1}, the position of one of the two bands of $CpFe(CO)_3^+$. This assures us that the intense band at 2052 is <u>not</u> due to $CpFe(CO)_3^+$ since the bands would have to be nearly the same intensity if they were both due to $CpFe(CO)_3^+$. One reasonable explanation of this spectrum is that both <u>trans</u> (X) and <u>gauche</u> (XI) isomers are present in this solution. The two highest frequencies are in reasonable agreement with those found by Symon and Waddington[4]

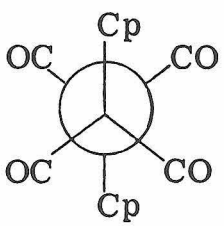

$\nu_{CO} \approx 2052$
2011

<u>trans</u>-X (C_{2h})

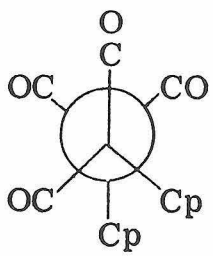

$\nu_{CO} \approx 2052$
2011
2011
1953

<u>gauche</u>-XI (C_2)

for the <u>trans</u> isomer. It is not at all unreasonable to expect the four bands of the <u>gauche</u> isomer to occur in this region also. The 2011 band is broad enough to contain several absorptions. The 2052 band is rather sharp, indicating that the two bands which comprise it are nearly perfectly degenerate or this explanation is wrong.

A very reasonable explanation which invokes no accidental degeneracies is that the three bands are due to the presence of a single rotamer, XII. This rotamer has only <u>three</u>-IR active ν_{CO}

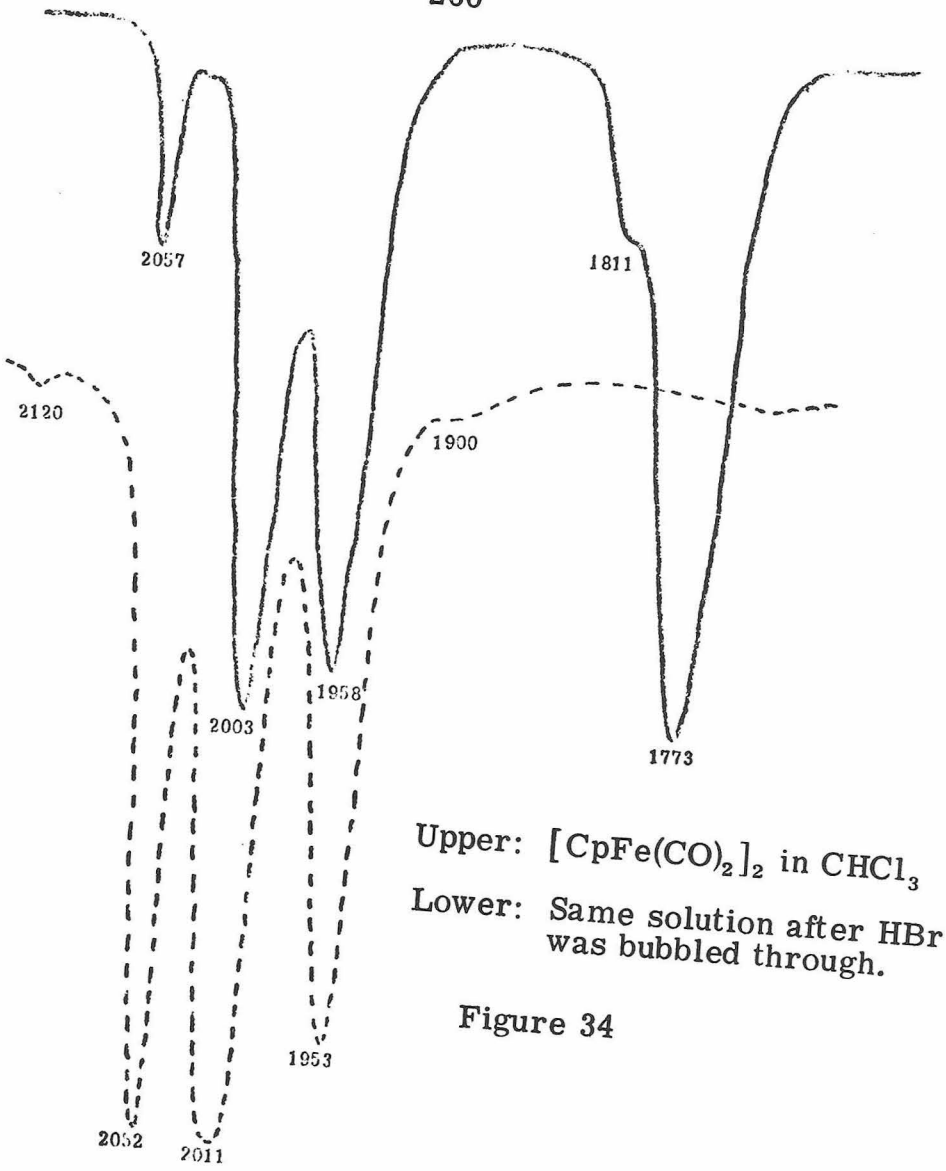

Upper: $[CpFe(CO)_2]_2$ in $CHCl_3$

Lower: Same solution after HBr was bubbled through.

Figure 34

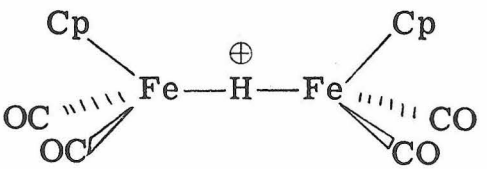

XII (C_{2v})

modes. It has been postulated as a minor (but observable) isomer in solutions of $[CpRu(CO)_2]_2$.[61] A third explanation, which we cannot rule out, is that HBr attacked the iron dimer to do more than just protonate it.

The KBr pellet infrared spectrum of a sample of $Cp(CO)Fe\text{-}\mu\text{-}(CO)_2\text{-}FeCp[P(OCH_3)_3]$ (hereafter "Fe_2P"), crystallized from benzene-petroleum ether at -20 °C, is shown in Figures 35 and 36 and listed in Table XVII. A $CHCl_3$ solution of Fe_2P gives the IR spectrum shown in Figure 37. In Table XVIII

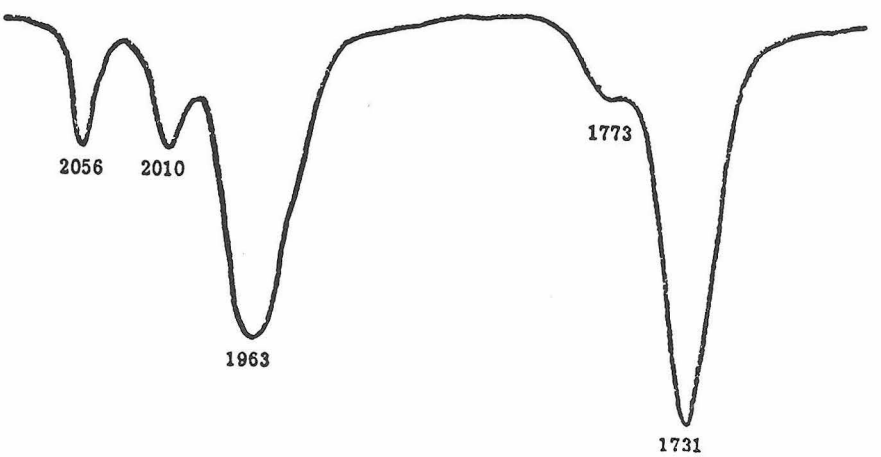

$CHCl_3$ Solution Infrared Spectrum of
$Cp(CO)Fe\text{-}\mu\text{-}(CO)_2\text{-}FeCp[P(OCH_3)_3]$

Figure 37

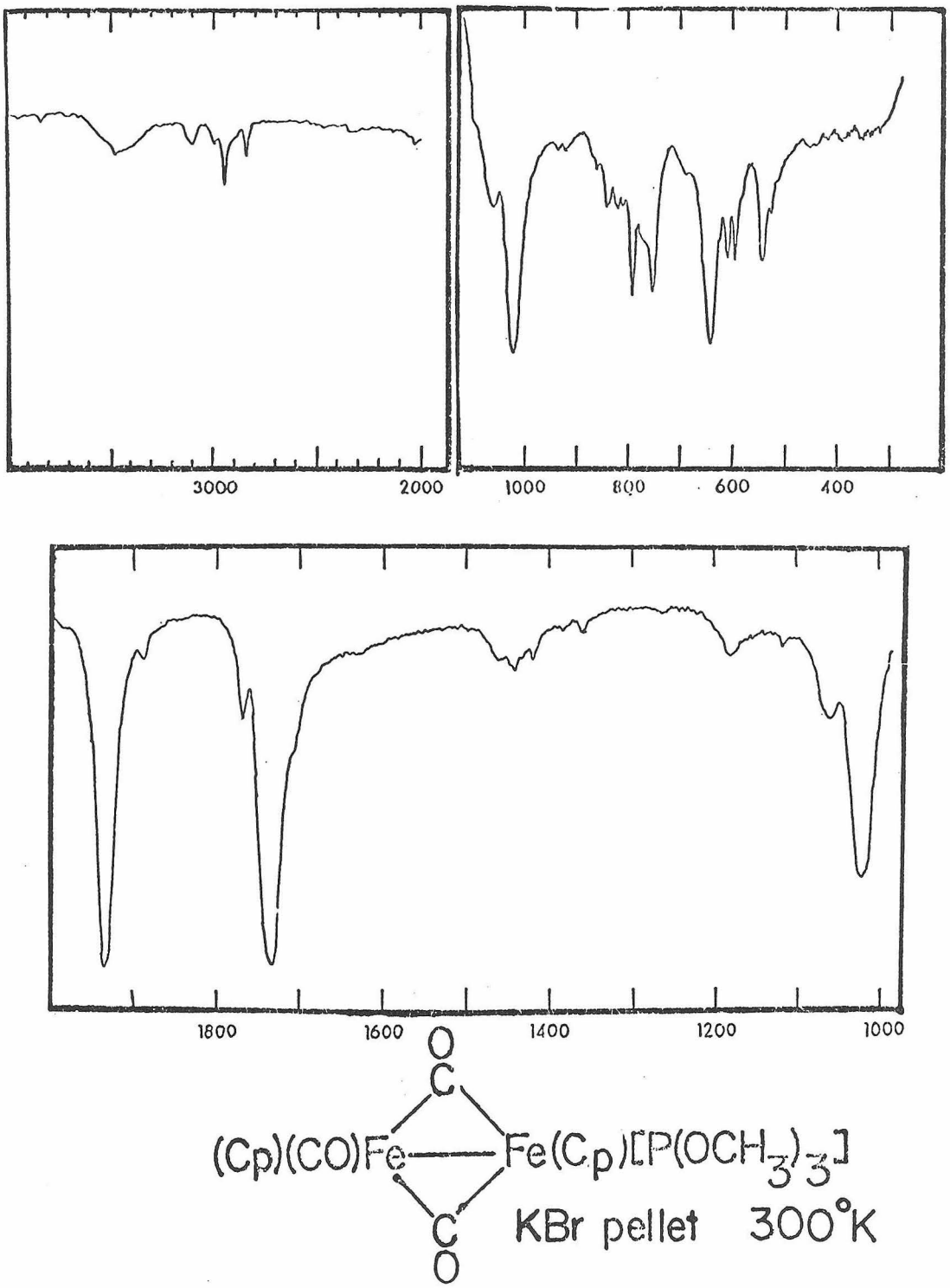
3000
2000
1000
800
600
400
1800
1600
1400
1200
1000
O
C
(Cp)(CO)Fe
Fe(Cp)[P(OCH3)3]
C
O
KBr pellet 300°K

Figure 35

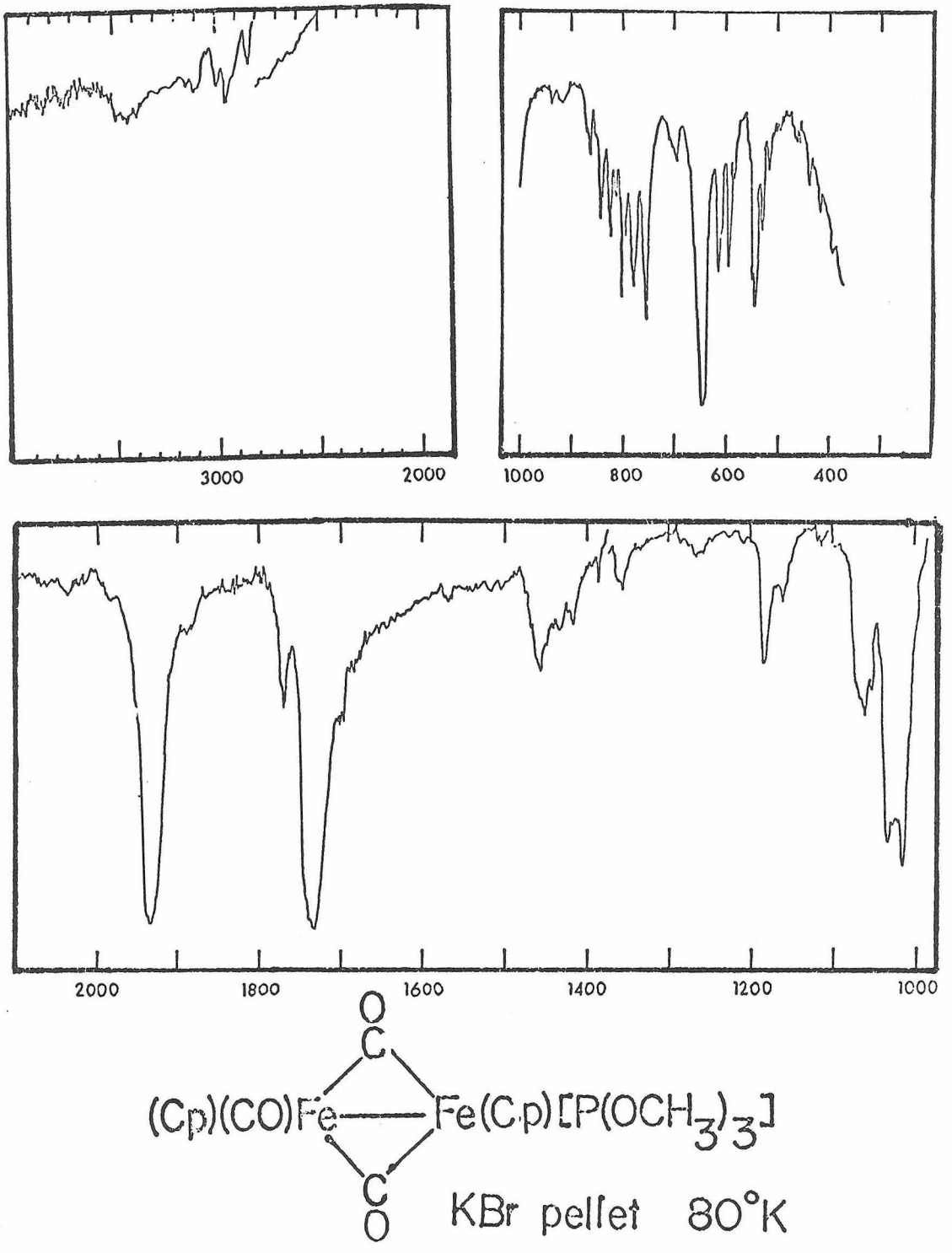
3000
2000
1000
800
600
400
2000
1800
1600
1400
1200
1000
O
C
(Cp)(CO)Fe
Fe(Cp)[P(OCH3)3]
C
O
KBr pellet 80°K

Figure 3

Table XVII. Infrared Spectra

$(Cp)(CO)Fe\text{-}\mu\text{-}(CO)_2\text{-}Fe(Cp)[P(OCH_3)_3]$		$(Cp)(CO)_2Fe\text{-}H\text{-}Fe(CO)(Cp)[P(OCH_3)_3]^+B(C_6H_5)_4^-$	
300° (3200-400 cm^{-1})	80° (3200-400 cm^{-1})	300° (3200-300 cm^{-1})	80° (3200-400 cm^{-1})
3105 w	3100 w	3110 w	3109 w
3000 w	3000 w	3085 w	3080 w
2950 w	2950 w	3050 m	3051 m
2845 w	2840 w	3025 w	3021 w
	2030 w	3000 w	3006 vw
1983 vw	1984 w		2994 w
1933 vs	1932 vs	2980 w	2979 w
1887 w	1888 sh, w	2960 w	2961 w
1770 m	1770 m	2850 vw	2842 w
1733 vs	1733 vs	2060 sh, w	2057 sh, w
1707 sh, m	1700 sh, w	2035 vs	2035 vs
	1684 sh, w	1984 vs	1982 vs
	1569 vw	1955 s	1956 vs
1460 w	1455 m		1909 vw
1441 w			1820 w, br
	1432 w		1776 w, br
1419 w		1579 w	1580 w
	1415 w		1575 w
1383 vw	1385 w	1480 w	1480 m
1359 vw	1358 w	1476 w	1476 m
1180 w	1263 vw		1463 vw
	1183 m		1456 vw
1118 vw	1160 w		1447 w
		1440 vw	1438 w
1059 m	1059 m	1426 m	1426 m
	1050 vw	1421 sh, w	1418 sh, w
1024 s	1032 s		1384 vw
	1014 s	1360 vw	1360 vw
938 vw	937 vw		1302 vw
922 vw	917 vw	1267 vw	1269 w
	870 vw		1260 sh, w
860 vw	862 w	1181 w	1184 m
840 vw	843 m	1174 sh, w	
	839 m		1162 m
820 w	823 m	1150 w	1151 w
810 w	813 w	1063 sh, w	
793 m	800 s	1044 s	1044 s
770 sh, m	779 s	1030 s	1031 s
753 m	753 s		1020 sh, s
690 sh, w	694 w		941 vw
641 s	647 vs		875 vw
610 m	613 s	859 w	860 w
596 m	597 s	850 w	852 w
	582 w	843 w	844 w
544 m	548 s		804 m
	543 s	800 m	800 m
527 w	528 m	757 sh, w	759 w, br
	514 m	743 m	744 m
	462 vw		740 m
	438 vw	734 s	735 m
	417 vw		732 sh, m
	392 vw	708 s	709 m
			706 m
			703 m
			657 w
		640 w	641 w
		627 w	625 w
		615 w	613 w
			610 w
		605 m	603 m
			599 vw
			594 vw
		584 w	587 w
		564 sh, w	570 w
			559 w
			553 m
		545 m	546 m
			539 w
		502 w	502 w
		479 w	481 w
			476 w
		462 w	
			409 w
			400 w

Table XVIII

Fe_2P Infrared Spectra

Physical State	
KBr pellet	1983 vw, 1933 vs, 1887 w, 1770 m, 1733 vs, 1707 sh, m
$CHCl_3$ solution	2056 m, 2010 m, 1963 s, 1773 m, 1731 s
Cyclohexane solution[a]	1964 (7.7), 1944 (2.3), 1750 (10)

[a] Relative intensities in parentheses. From reference 57.

we list the bands in the ν_{CO} region of the solid sample, of the $CHCl_3$ solution, and of a cyclohexane solution reported by Haines and DuPreez.[57] We suggest that cis, trans, and non-bridged isomers are all apparent in these spectra. In the solid sample we believe only one isomer is present with a ν_{CO} (terminal) = 1933 cm^{-1}. In $CHCl_3$ the other bridged isomer is predominant (ν_{CO} = 1963) and a non-bridged isomer (ν_{CO} = 2056, 2010 + one band hidden under 1963 band) is also present. In cyclohexane, both bridged species (ν_{CO} = 1964, ν_{CO} = 1944) are present, but no non-bridged isomer is present. Manning[47] found the ratio of cis/trans isomers of the unsubstituted compound $[CpFe(CO)_2]_2$ to be 36 : 64 in cyclohexane. We estimate from his data that this ratio is approximately 60 : 40 in chloroform. On the assumption

that more cis-Fe_2P will be present in $CHCl_3$ than in cyclohexane, we make the following assignments:

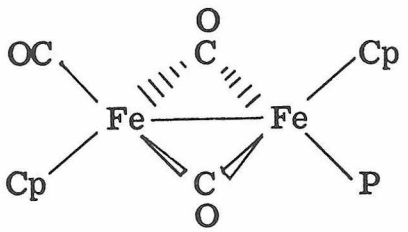

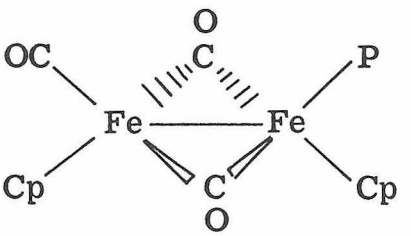

trans	cis
ν_{CO} (terminal) =	ν_{CO} (terminal) =
1933 (in KBr pellet)	1963 (in $CHCl_3$)
1944 (in cyclohexane)	1964 (in cyclohexane)

$(Cp)(CO)_2Fe—Fe(CO)(Cp)(P)$

non-bridged

ν_{CO} (terminal) =

$$\left.\begin{array}{r} 2056 \\ 2010 \\ \sim 1963 \end{array}\right\} \text{(in } CHCl_3\text{)}$$

This assumption implies that the trans isomer is present in solid crystallized from benzene-petroleum ether at -20° and that the cis isomer predominates in solution, even in non-polar solvents. Even if the assignment of cis and trans isomers is reversed, the spectra strongly imply that the predominant form in solution is the opposite isomer of the one isolated as a solid. Variable temperature NMR experiments analogous to those on $[CpFe(CO)_2]_2$[44,45]

would undoubtedly shed light on this equilibrium. If this assignment of a non-bridged species is correct, it suggests that the medium intensity band at 2057 cm^{-1} in the $CHCl_3$ solution of $[CpFe(CO)_2]_2$ (Figure 34) is also due to a non-bridged species.

When an acetic acid solution of Fe_2P is treated with H_2SO_4, the monobasic red dimer picks up a proton to form green Fe_2PH^+. The high field NMR signal again suggests that the hydrogen atom is in a bridging position. Pouring this solution into a solution of $NaB\phi_4$ in H_2O precipitates the crystalline green salt $(Fe_2PH^+)(B\phi_4^-)$ which can be recrystallized from acetone-ether. Extensive efforts by Dick Stanford of this department to find a suitable crystal for an X-ray crystal structure determination failed. All crystals examined were twinned in so subtle a fashion that some twins were apparent only after a diffraction experiment.

The infrared spectrum of $(Fe_2PH^+)(B\phi_4^-)$ in a KBr pellet is shown in Figures 38 and 39 and listed in Table XVII. When we attempted to prepare the PF_6^- salt by an analogous route, we obtained a green precipitate which gave the KBr pellet spectrum shown in Figure 40. All attempts to crystallize this material from acetone-ether failed. We also obtained a green solution of Fe_2PH^+ by bubbling HBr (or DBr) through a solution of Fe_2P in $CHCl_3$. These solutions showed no bands (even when frozen at 80 °K) that could be identified as ν(Fe-H-Fe). These spectra are summarized in Table XIX. It appears that we have a mixture of isomers in the PF_6^- salt, supported in a way by our inability to

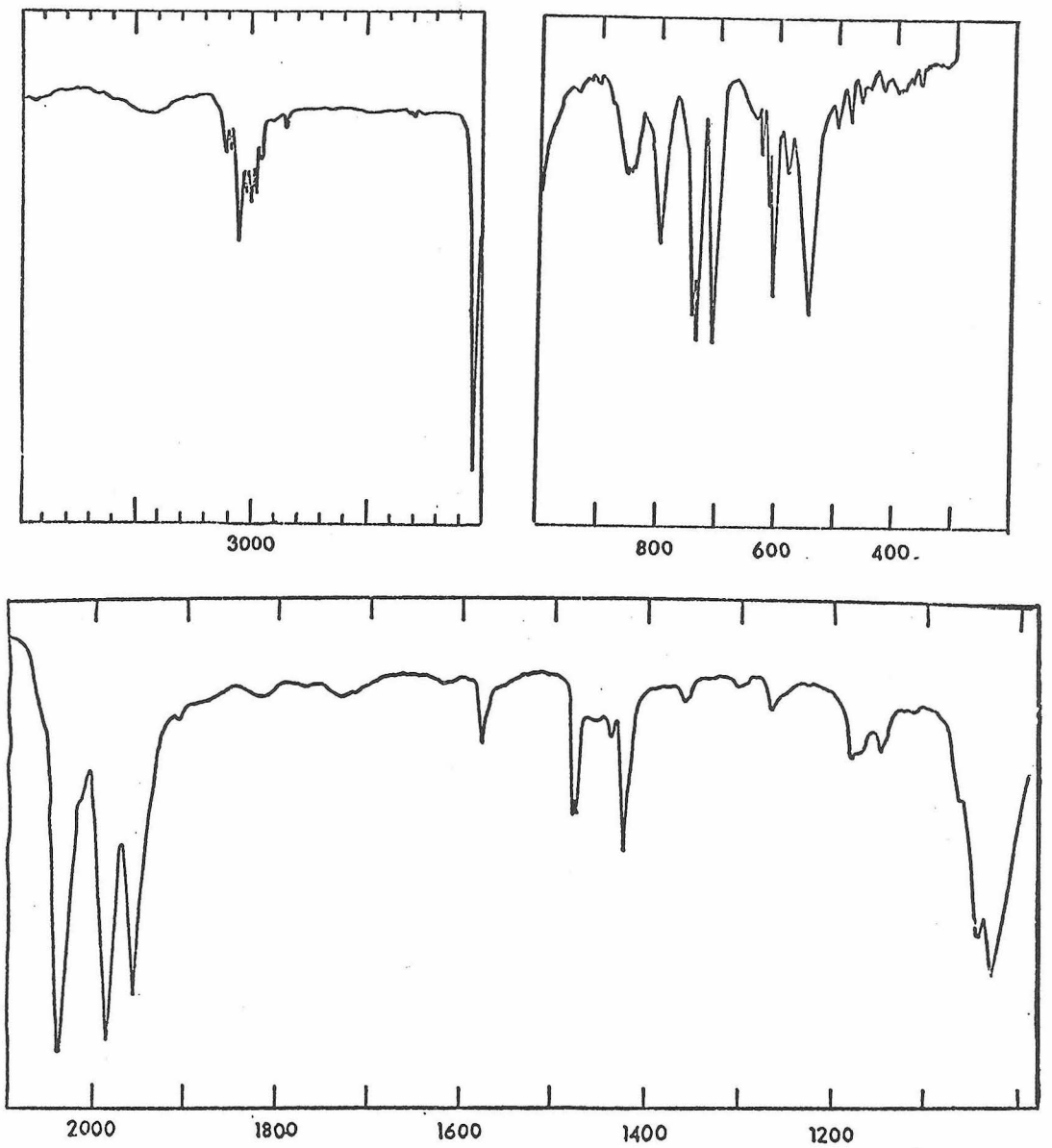

$(Cp(CO)_2Fe\text{-}H\text{-}Fe(CO)(Cp)[P(OCH_3)_3])^+ [(C_6H_5)_4B]^-$

KBr pellet 300°K

Figure 38

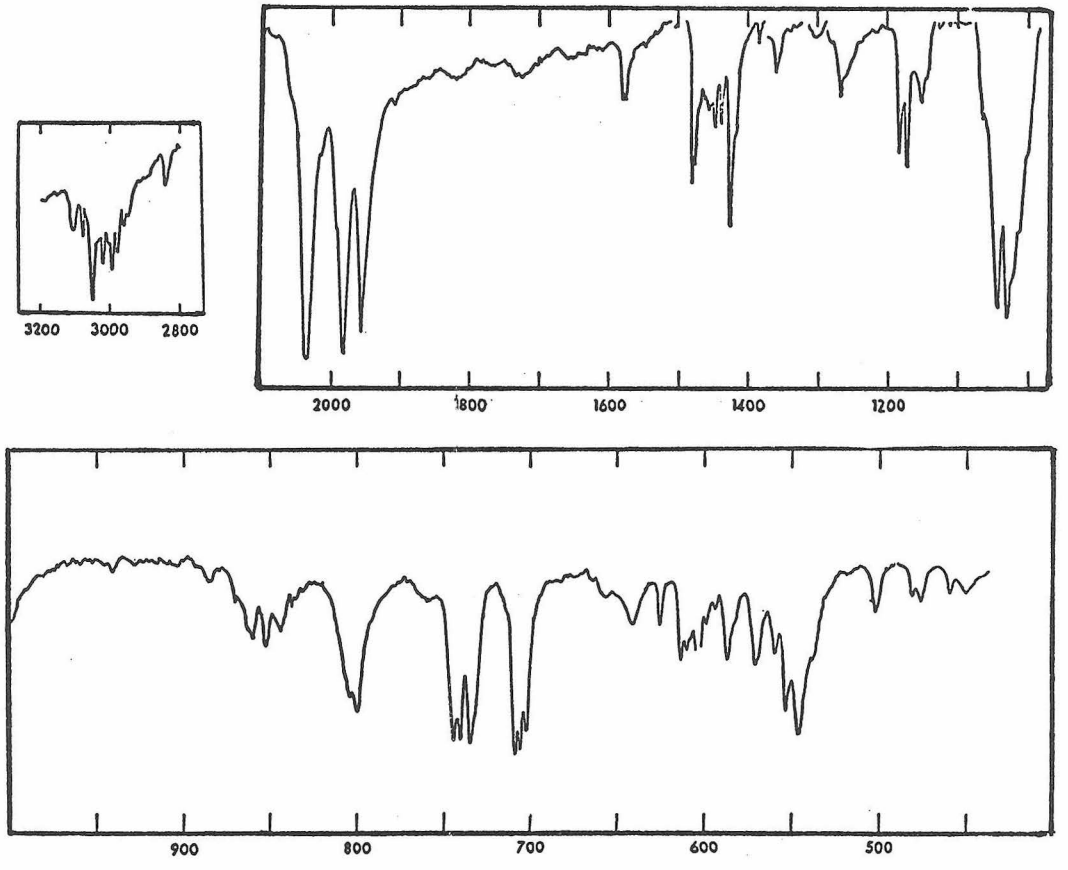

$(Cp(CO)_2Fe\text{-}H\text{-}Fe(CO)(Cp)[P(OCH_3)_3])^+ [(C_6H_5)_4B]^-$

KBr pellet 80°K

Figure 39

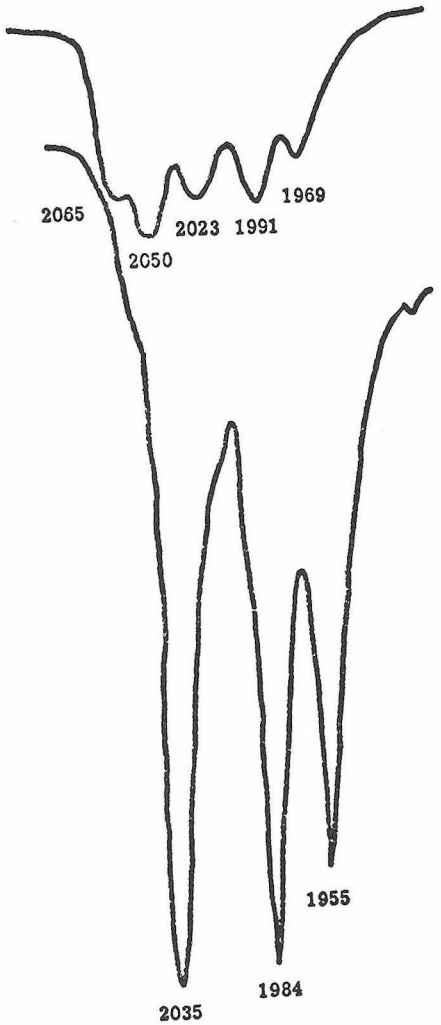

KBr Pellet Infrared Spectra
of Salts of the Cation
$Cp(CO)_2Fe\text{-}H\text{-}Fe(CO)Cp[P(OCH_3)_3]^+$

Upper: PF_6^- salt
Lower: $B(C_6H_5)_4^-$ salt

Figure 40

Table XIX

Fe_2PH^+ Infrared Spectra

Physical State	Spectrum
$(Fe_2PH^+)(B\phi_4^-)$ in KBr pellet	2060 sh, w, 2035 vs, 1984 vs, 1955 s
$(Fe_2PH^+)(PF_6^-)$ in KBr pellet	2065 s, 2050 s, 2023 s, 1991 s, 1969 s
$(Fe_2PH^+)(Br^-)$ in $CHCl_3$ at 80 °K[a]	2068 w, 2037 s, 1994 s, 1974 m

[a] Prepared by bubbling HBr through a solution of Fe_2P at room temperature and then freezing the solution in a AgCl cell.

crystallize this material. The two most obvious isomers are XIII and XIV.[106]

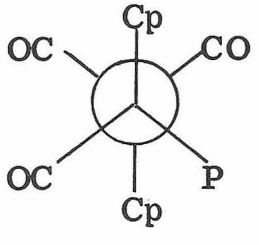

XIII

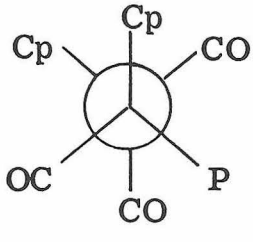

XIV

The most recent investigation of $[CpRu(CO)_2]_2$[61] invoked two (cis and trans) bridged isomers and two non-bridged rotamers to explain the appearance of the ν_{CO} absorptions in various solvents.

An interesting trend, on which there is general agreement, is that non-bridged isomers become more important as we go down the column (Os > Ru > Fe). The iron compound shows only traces of non-bridged isomer in solution and none in the solid. The ruthenium compound shows a significant fraction of non-bridged isomer in solution but, again, only bridged isomer in the solid. The osmium compound is non-bridged, both in solution and in the solid.[52]

Our spectra of solid $[CpRu(CO)_2]_2$ are shown in Figures 41 and 42 and listed in Table XX. Very weak bands due to a hydrocarbon impurity in our sample are present in the 2800-3000 cm^{-1} region. Careful comparison of the spectra of different samples containing variable amounts of this impurity enable us to say with confidence that none of the bands listed for this spectrum are due to the impurity.

Protonation studies of this compound were very vexing. When saturated <u>orange</u> solutions of $[CpRu(CO)_2]_2$ in acetic acid were treated with H_2SO_4, NMR experiments showed a quantitative uptake of H^+ to form <u>green</u> solutions of $[CpRu(CO)_2]_2H^+$. These solutions could be poured into $NaB\phi_4$ in H_2O to give <u>light green</u> precipitate. When we studied the UV-VIS absorption spectra of the more dilute <u>yellow</u> solutions of $[CpRu(CO)_2]_2$ in acetic acid or ethanol, addition of H_2SO_4 (in stoichiometric amounts or in large excess) produced <u>no color change</u>. When we did this experiment with nearly saturated solutions on a preparative scale,

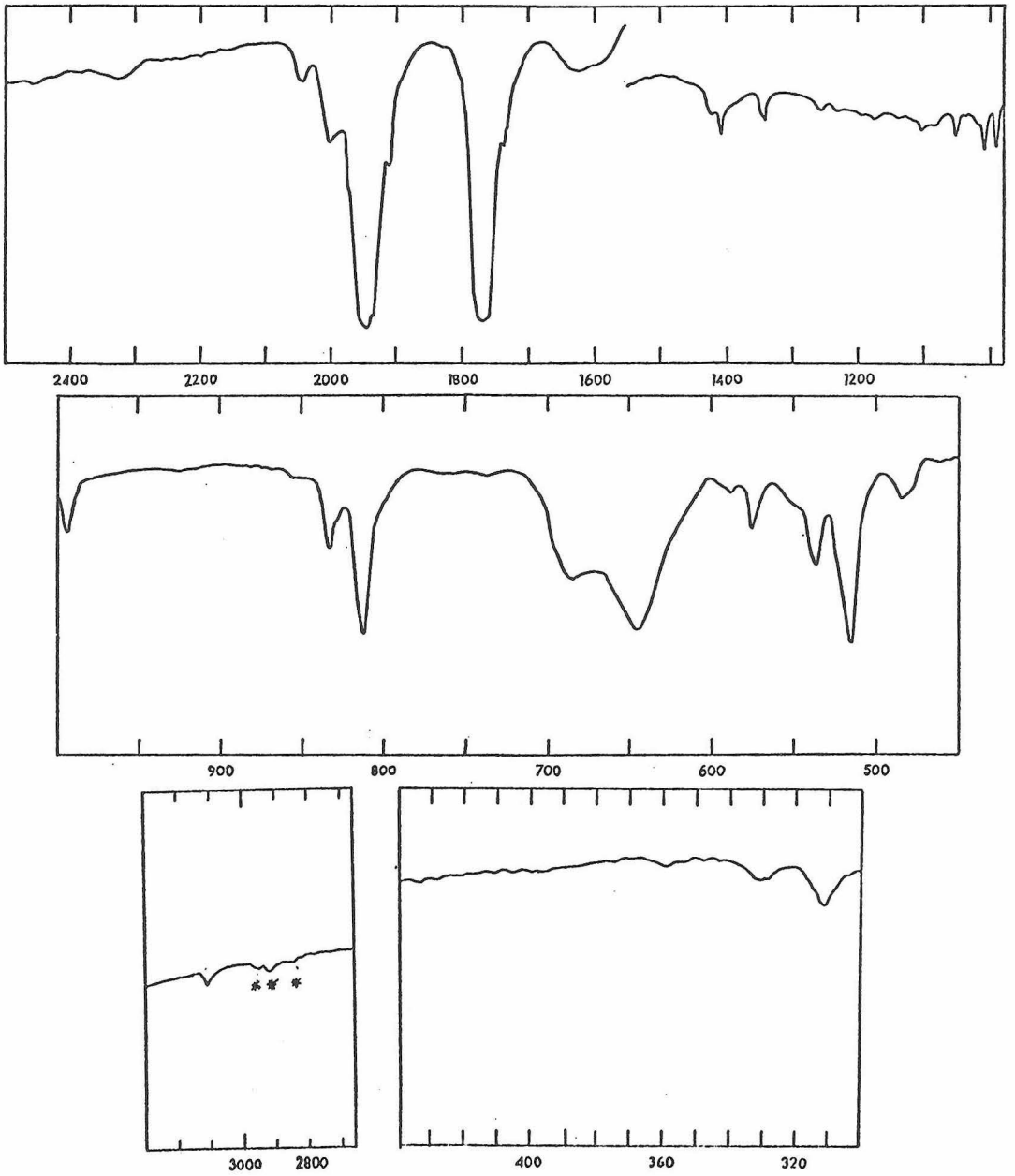

$[(\pi\text{-}C_5H_5)Ru(CO)_2]_2$
KBr Pellet - 300°K

(Asterisks denote hydrocarbon impurity)

Figure 41

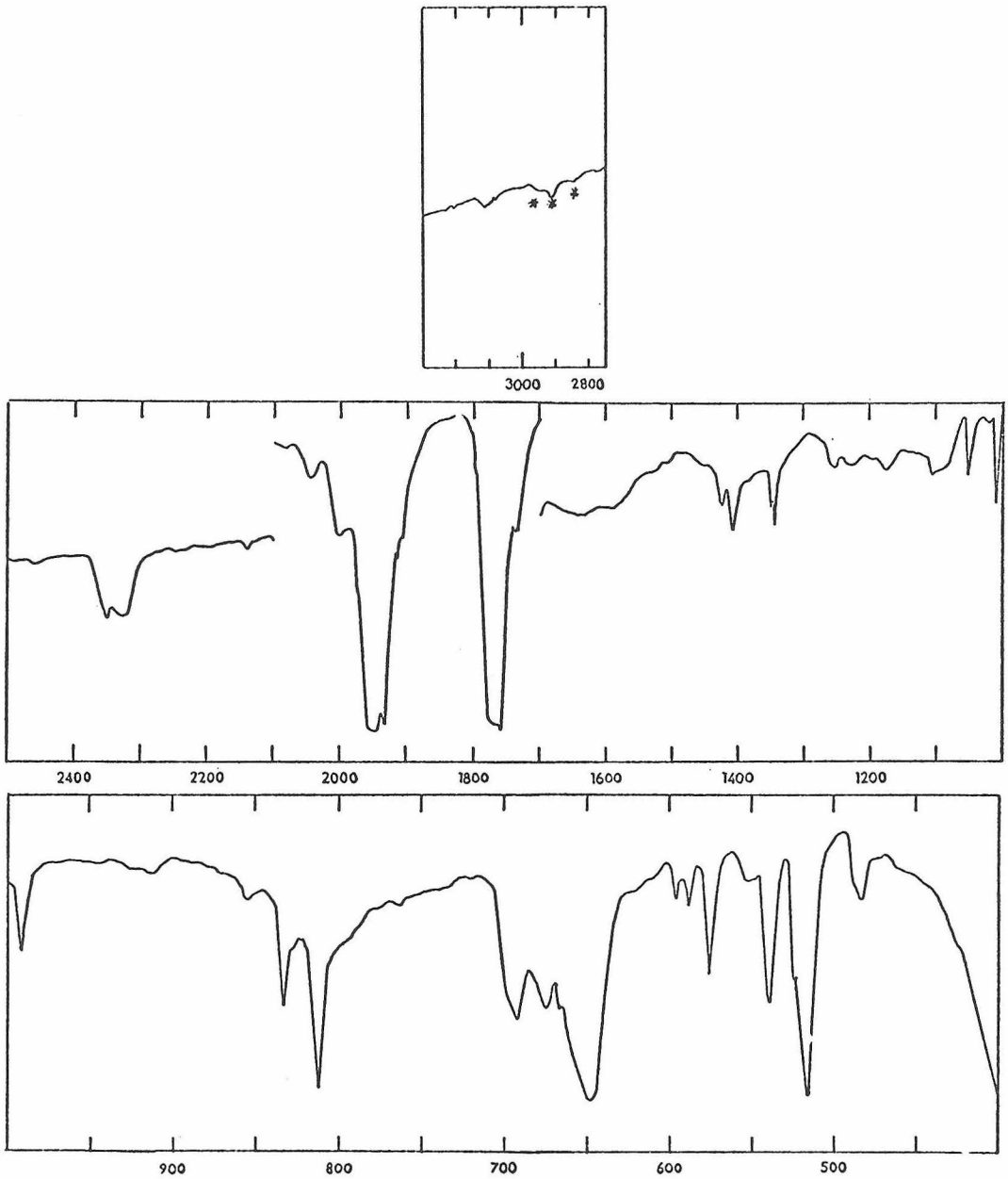

$[(\pi\text{-}C_5H_5)Ru(CO)_2]_2$
KBr Pellet - $80^{o}K$

(Asterisks denote hydrocarbon impurity)

Figure 42

Table XX. Infrared Spectra

$[(\pi\text{-}C_5H_5)Ru(CO)_2]_2$		Fig. 44
300°	80°	300°
(3300-300 cm^{-1})	(3300-400 cm^{-1})	(2500-300 cm^{-1})
3110 vw	3114 vw	
	2352 m	2335 br, w
	2327 m	
		2058 m
2045 w	2045 w	2050 w
		2043 s
		2032 s
2002 m	2003 m	2001 s
		1997 sh, w
1974 sh, m	1975 sh, m	1989 sh, w
1945 vs	1950 vs	1951 br, m
1934 s	1933 s	
1912 vw	1913 vw	
1907 sh, vw	1906 vw	
1798 sh, vw	1797 sh, vw	1808 sh, w
1770 br, vs	1768 vs	1769 m
	1759 vs	
1738 vw	1737 vw	
1732 vw	1732 vw	
1627 br, w	1640 br, w	
		1578 w
		1478 w
1424 w	1424 w	1425 m
1409 w	1407 w	1414 sh, w
1402 sh, w		
1348 sh, w	1349 w	
1343 w	1344 w	
1256 vw	1255 vw	
1233 br, vw	1230 br, vw	
1178 vw	1176 vw	1150 w
1105 vw	1105 vw	
1053 w	1052 w	1059 w
		1029 w
1009 w	1009 w	1008 w
993 w	991 w	999 w
	855 vw	853 w
833 w	833 m	834 w
812 m	813 s	813 w
		745 w
685 sh, m	692 m	735 w
	675 m	715 w
	666 m	708 m
645 m	648 s	650 br, w
	596 w	625 w
587 vw	588 w	613 w
575 w	575 m	605 w
549 sh, w	552 w	600 w
536 w	540 m	537 w
523 sh, w	524 m	522 w
515 m	516 s	518 w
484 w	484 w	499 w
330 br, vw		
311 w		315 w

we again found no color change on addition of H_2SO_4 (stoichiometric or in large excess). Addition of these large scale yellow acidified solutions to $NaB\phi_4$ in H_2O gave a yellow precipitate whose infrared spectrum is shown in Figures 43 and 44 and listed in Table XX. Though these Figures are labeled as a mixture of $[CpRu(CO)_2]_2$ and $[CpRu(CO)_2]_2H^+$, as I look at them now, they may not be. The new peaks near 2050 and 2000 cm^{-1} correspond to weaker peaks in the spectrum of unprotonated $[CpRu(CO)_2]_2$. (See Table XX.) Since no NMR solution (in which we could positively identify a Ru-bound hydrogen) ever remained yellow, I believe that the samples precipitated in these preparative experiments are just a redistribution of the multitudinous isomers of $[CpRu(CO)_2]_2$. Figure 43 is, by the way, the most dramatic example we have ever seen of an infrared spectral change on cooling a sample. The same sample was used for both spectra in this Figure.

NMR Studies

When a solution of $[CpFe(CO)_2]_2$ in acetic acid is treated with a large excess of 98% H_2SO_4 ($H_2SO_4/[CpFe(CO)_2]_2 \gtrsim 100$), a signal appears in the metal hydride region of the ^1H NMR spectrum at τ 36.3 ppm (Figure 45). The unusually large chemical shift suggested immediately that the hydrogen atom is associated with both iron atoms, i.e., it is in a bridging position. Though we reached this correlation of chemical shift with structure (bridging or terminal position) independently, many other workers have now

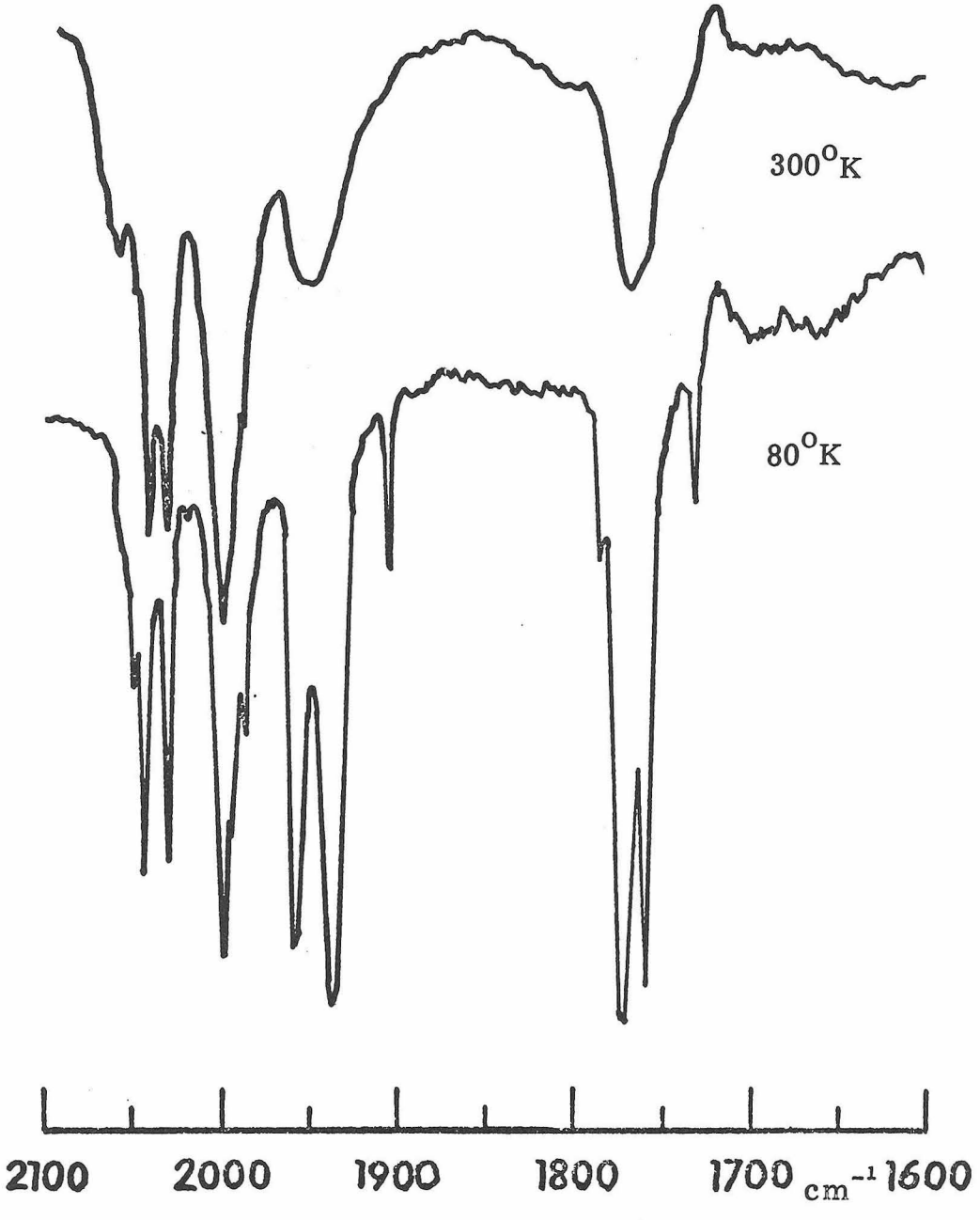

KBr Pellet Spectrum of Mixture of
$[CpRu(CO)_2]_2$ and $\{[CpRu(CO)_2]_2H\}\{B\phi_4\}$

Figure 43

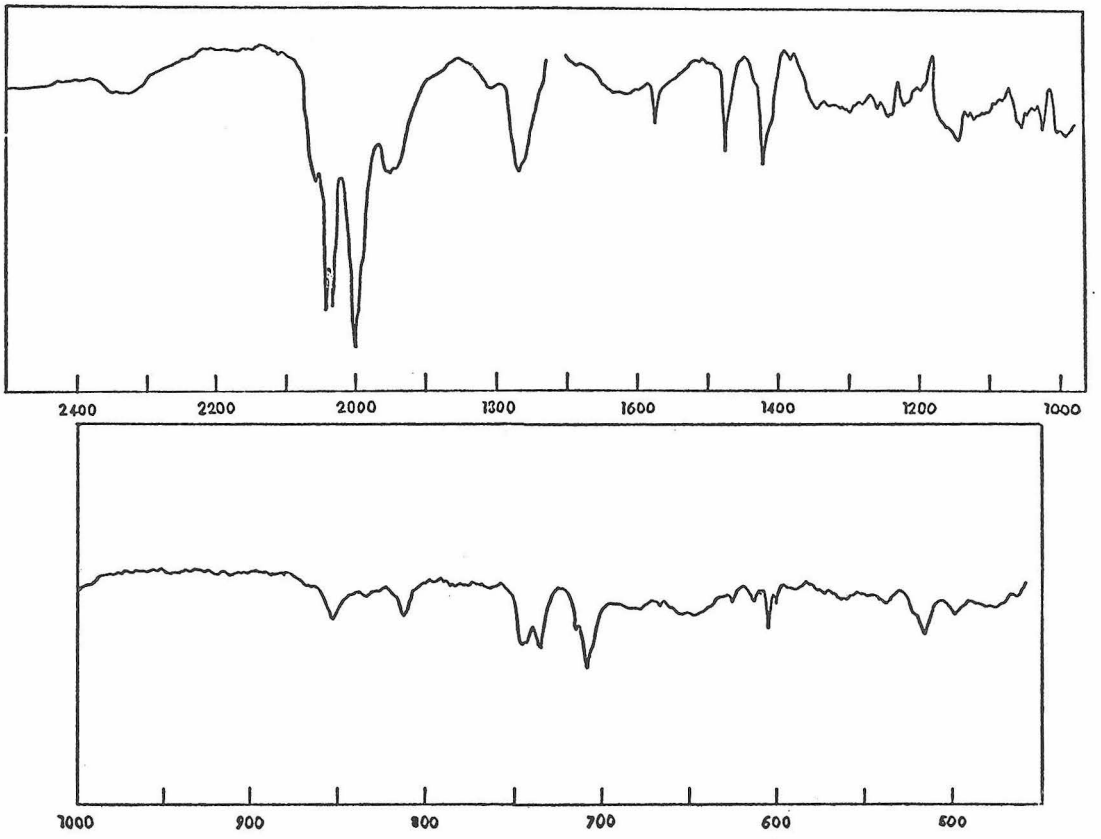

KBr Pellet Spectrum of Mixture of
$[CpRu(CO)_2]_2$ and $\{[CpRu(CO)_2]_2H\}\{B\phi_4\}$

Figure 44

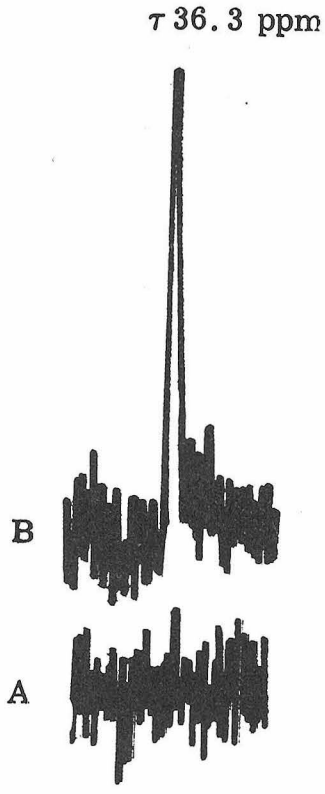

A. 0.07g $[CpFe(CO)_2]_2$ plus 0.5 ml CH_3CO_2H

B. Same solution after addition of 0.15 ml 98% H_2SO_4

Figure 45

made this same correlation. A summary of chemical shifts and a brief discussion of the validity of the correlation can be found in reference 69. In addition to the examples cited in this excellent review article, we have found several other examples which support the correlation.[79-88]

In addition to the appearance of a hydride signal at τ 36.3 ppm, the chemical shift of the cyclopentadienyl groups bound to iron shift from δ 4.89 ppm to 5.34 ppm. This deshielding is consistent with the positive charge introduced upon protonation. Very similar ^1H NMR spectral changes are seen when $[CpRu(CO)_2]_2$ is protonated by 98% H_2SO_4 in CH_3CO_2H. (See Table XXI.) Examination of the spectrum of $[CpFe(CO)_2]_2H^+$ at

Table XXI

NMR Data

Compound	Solvent	τ_H[a]	$\delta(C_5H_5)$	$J_{^{31}P-C_5H_5}$ (Hz)	δ (CH_3)	$J_{^{31}P-CH_3}$ (Hz)
$[(\pi\text{-}C_5H_5)_2Fe(CO)_2]_2$	CH_3CO_2H	--	4.89	--	--	--
	$(CH_3)_2CO$	--	4.98[b]	--	--	--
	CH_3CN	--	4.83	--	--	--
$[(\pi\text{-}C_5H_4CH_3)Fe(CO)_2]_2$	$(CH_3)_2CO$	--	4.86, 4.63[c]	--	--	--
$\{[(\pi\text{-}C_5H_5)_2Fe(CO)_2]_2H^+\}\{HSO_4^-\}$	CH_3CO_2H	36.3	5.34	--	--	--
	$(CH_3)_2CO$[d]	36.5	5.37	--	--	--
	H_2SO_4	35.7[a]	4.2[e]	--	--	--
$\{[(\pi\text{-}C_5H_4CH_3)Fe(CO)_2]_2H^+\}\{HSO_4^-\}$	$(CH_3)_2CO$	38[f]	5.34, 5.19[c]	--	--	--
$(\pi\text{-}C_5H_5)(CO)Fe\text{-}\mu\text{-}(CO)_2\text{-}Fe[P(OCH_3)_3](\pi\text{-}C_5H_5)$	$CDCl_3$	--	4.66, 4.51	0.9	3.53	11
	CH_3CO_2H	--	4.67, 4.53	1.5	3.50	11
	$(CD_3)_2CO$	--	4.67, 4.56	1.0	3.50	11
$\{(\pi\text{-}C_5H_5)(CO)_2Fe\text{-}H\text{-}Fe(CO)(\pi\text{-}C_5H_5)[P(OCH_3)_3]^+\}\{HSO_4^-\}$	CH_3CO_2H	36.3[g]	5.21, 4.95	1.5	3.82	11.5
$[(\pi\text{-}C_5H_5)Ru(CO)_2]_2$	CH_3CO_2H	--	5.33	--	--	--
$\{[(\pi\text{-}C_5H_5)Ru(CO)_2]_2H^+\}\{HSO_4^-\}$	CH_3CO_2H	29.1	5.82	--	--	--

[a] Hydride of protonated species.

[b] Calculated assuming the chemical shift of internal cyclohexane = 1.45 ppm.

[c] Low field peak is ~10% as intense as high field peak.

[d] At -45°C (220 MHz) this sample showed the following changes:

17°C: τ 4.63 ($\omega_{\frac{1}{2}}$ = 1.4 Hz), τ 36.5 ($\omega_{\frac{1}{2}}$ = 2 Hz)

-45°C: τ 4.62 ($\omega_{\frac{1}{2}}$ = 48 Hz), τ 36.4 ($\omega_{\frac{1}{2}}$ = 48 Hz)

The sample is nearly a glass at -45°.

[e] Relative to external TMS.

[f] $\omega_1 \approx$ 20 Hz at ambient temperature (~ 40°C).

[g] $J_{^{31}P-^1H}$ = 44 Hz.

-45 °C shows marked line broadening but no splitting of the C_5H_5 or Fe-H-Fe signals. We attribute the broadening to the greatly increased viscosity of this solution at -45 °. Bullit, et al.[44] observed separate signals for cis and trans isomers of $[CpFe(CO)_2]_2$ at low temperature (-55 °) but we expect that the barrier to rotation about the Fe-H-Fe bond, assuming it is linear, is extremely small.[89]

Protonation of $[\pi\text{-}CH_3C_5H_4)Fe(CO)_2]_2$ in CH_3CO_2H with H_2SO_4 is similar to the protonation of unsubstituted compounds except that two peaks appear in the cyclopentadienyl region of the spectrum in both the protonated and unprotonated material (Table XXI). The low field peak amounts to only ~ 10% of the high field peak and has nearly the same chemical shift as the $[CpFe(CO)_2]_2$ compounds. We believe this is a $[CpFe(CO)_2]_2$ impurity present in the bottle of $[(\pi\text{-}CH_3C_5H_4)Fe(CO)_2]_2$ obtained from Alpha and used without further purification. The hydride signal at $\tau \sim 38$ ppm is ~ 20 Hz wide at ambient temperature. We do not know the cause of this.

The protonation of Fe_2P gives Fe_2PH^+ in which we also believe the proton is bridging the iron atoms (Figure 46). The cyclopentadienyl group of Fe_2P which is bound to iron bound to phosphorus appears as a doublet, $J_{^{31}P-^{1}H} = 1.0$ Hz in $(CD_3)_2CO$ (Figure 47). The other C_5H_5 group is not coupled to ^{31}P. In the protonated form, Fe_2PH^+, both cyclopentadienyl absorptions have

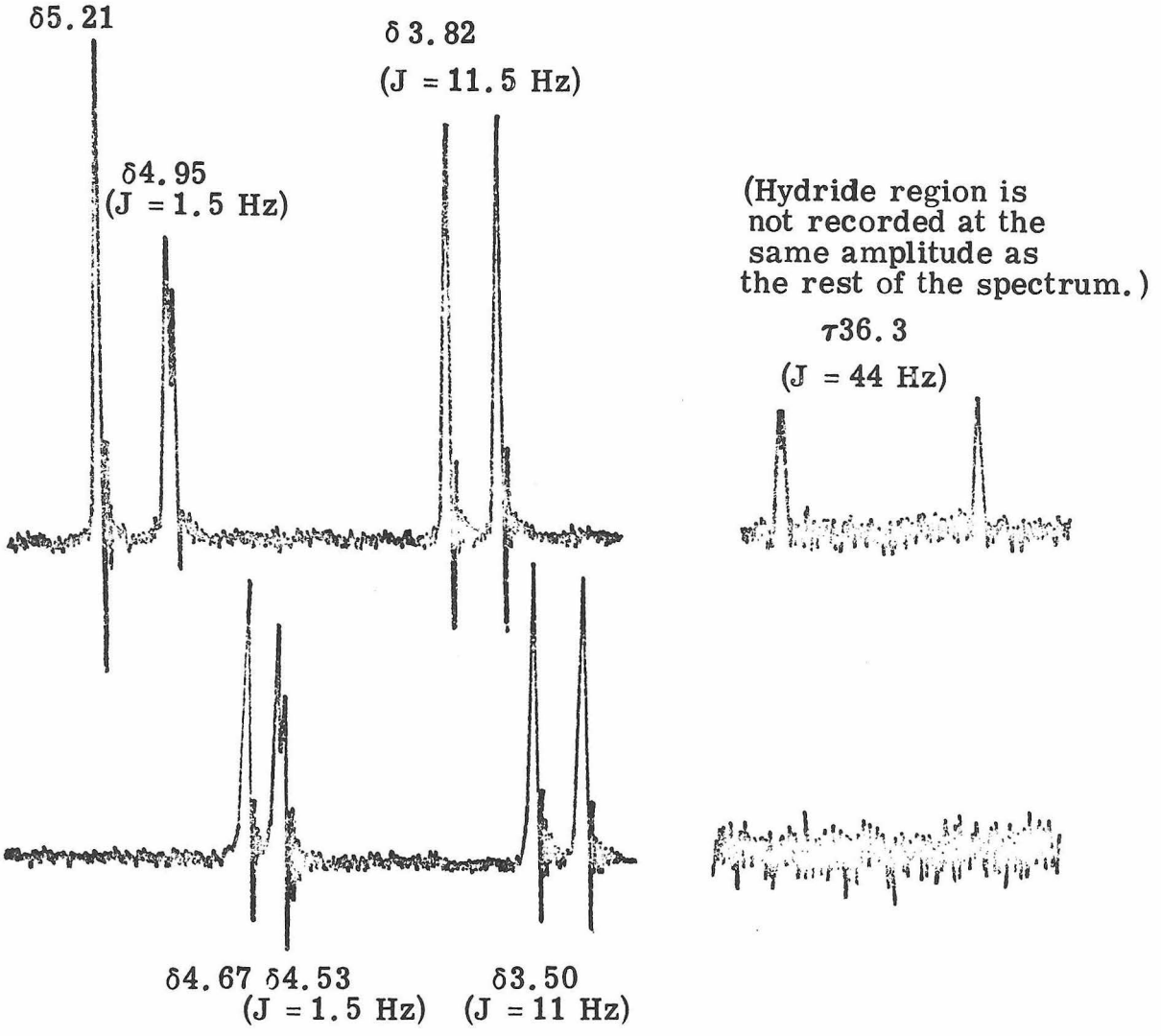

NMR Spectra: Upper - $(\pi\text{-}C_5H_5)(CO)_2Fe\text{-}H\text{-}Fe(CO)[P(OCH_3)_3](\pi\text{-}C_5H_5)^+$
Lower - $(\pi\text{-}C_5H_5)(CO)Fe\text{-}\mu\text{-}(CO)_2\text{-}Fe[P(OCH_3)_3](\pi\text{-}C_5H_5)$

Both Spectra Were Recorded in CH_3CO_2H Solution at 60 MHz

Figure 46

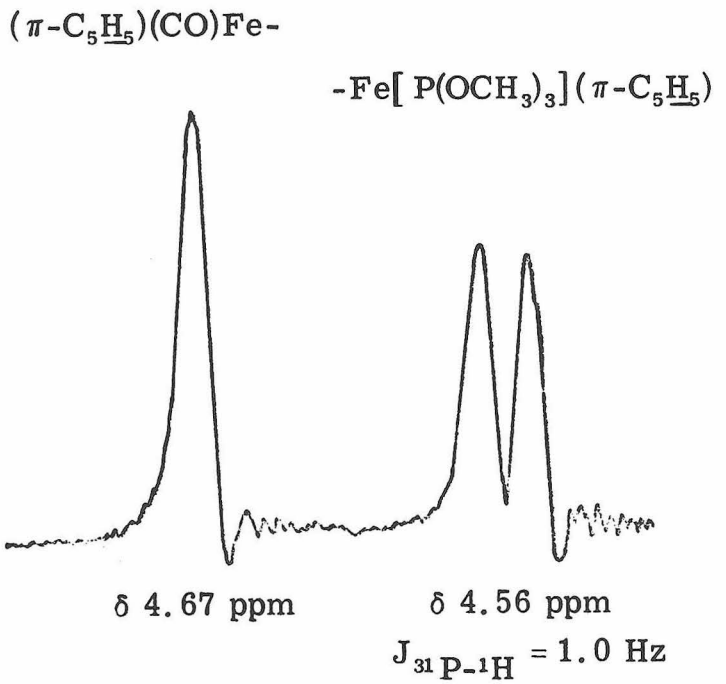

Figure 47. Cyclopentadienyl Region of $(\pi\text{-}C_5H_5)(CO)Fe\text{-}\mu\text{-}(CO)_2\text{-}Fe[P(OCH_3)_3](\pi\text{-}C_5H_5)$ in $(CD_3)_2CO$ Solution

the same appearance as in Fe_2P but they are both shifted downfield about 0.5 ppm. This also supports the notion that the proton is associated with both iron atoms. If only one were protonated, we would expect a big downfield shift for only one of the cyclopentadienyl absorptions. The bridging hydrogen appears as a doublet, $J_{^{31}P-^{1}H} = 44$ Hz. This is the same magnitude as the coupling found in XV and XVI in which ^{1}H is terminal and ^{31}P is bridging.[82,90]

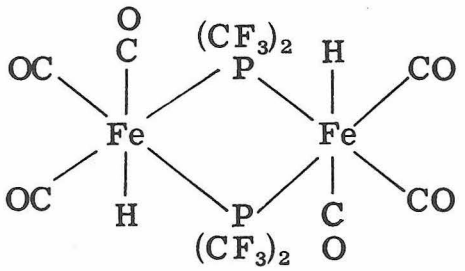

XV τ_H = 15.82 ppm

$J_{^{31}P-^{1}H}$ = 44.7 Hz

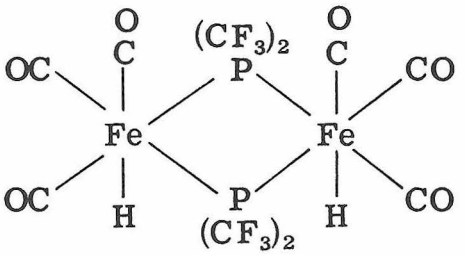

XVI τ_H = 15.60 ppm

$J_{^{31}P-^{1}H}$ = 41.8 Hz

An interesting and structurally useful technique to apply to these compounds would be to obtain spectra under conditions of very high sensitivity such that ^{57}Fe satellites can be observed. To our knowledge, ^{57}Fe-^{1}H coupling has been observed only once, for the compound XVII.[91,92]

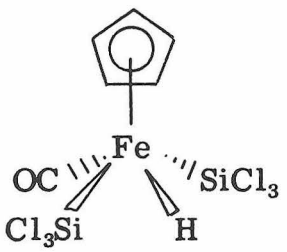

XVII τ_H = 21.64 ppm

$J_{^{57}Fe-^{1}H}$ = 14.5 Hz

$J_{^{29}Si-^{1}H}$ = 20 Hz

Davison, et al.[3] have shown that the appearance of ^{183}W-^{1}H satellites could be used to distinguish structures XVIII, XIX, and XX. Unfortunately, though it is easy to eliminate structure XIX, distinguishing XVIII and XX is only possible if very weak satellites (~ 1%) of the central signal can be detected and integrated

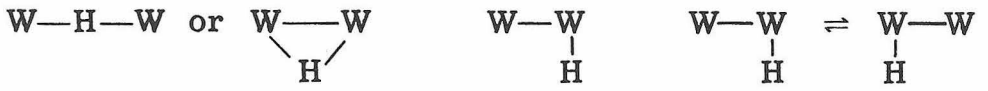

XVIII XIX XX

accurately. Strenuous efforts by Hayter[32] to find these satellites in the spectrum of $HW_2(CO)_{10}^-$ failed. Whitesides and Maglio[93] succeeded in observing these satellites but pointed out further ambiguities in distinguishing XVIII from XX. Using ^{57}Fe satellites will be more difficult by an order of magnitude because of the even lower natural abundance of ^{57}Fe. (^{57}Fe - 2.25% natural abundance, I = 1/2; ^{183}W - 14.28% natural abundance, I = 1/2.)

An attempt to protonate $[CpFe(CO)_2]_2$ in ethanol (0.07 g $[CpFe(CO)_2]_2$, 0.5 ml ethanol, 0.05 ml H_2SO_4) failed to produce any hydride signal as far as τ 43 ppm. Not much iron dimer dissolved in this solvent mixture. Insolubility or, more likely, the competitive basicity of ethanol, produced this negative result. An attempt to do this protonation in CH_3CN was more interesting and enigmatic. The strong C_5H_5 signal moves downfield from δ 4.83 ppm in the neutral compound to 5.44 ppm when acid is added. In addition, a small peak (~ 10% relative area) at 5.21 ppm appears in the spectrum of the acidified solution. No absorption in the hydride region could be found as far as τ 43 ppm. The C_5H_5 peak is strong and sharp in the acidic solution. Our only suggestion is that some sort of exchange process broadens the

hydride signal out of existence. This would be an extension of the behavior observed for $[CpFe(CO)_2]_2$ in CH_3CO_2H (sharp line) and $[(\pi\text{-}CH_3C_5H_4)Fe(CO)_2]_2$ in CH_3CO_2H (broad line, $\omega_{\frac{1}{2}} \approx 20$ Hz at 40 °C). The nature of this exchange process is totally unknown. A useful experiment might be to study the temperature dependence of the spectrum of the CH_3CN solution.

It was possible to make a quantitative estimate of the base strength of $[CpFe(CO)_2]_2$ in CH_3CO_2H solution. Addition of successive aliquots of 4.10 M H_2SO_4 in CH_3CO_2H to a solution of $[CpFe(CO)_2]_2$ caused the $[CpFe(CO)_2]_2$ cyclopentadienyl signal at 4.89 ppm to decrease in intensity as the cyclopentadienyl signal at 5.34 ppm of protonated product grew. This sequence is shown in Figure 48 and detailed in Table XXII. The signals are weaker in the final solution (number 10, Fig. 48) than in the initial solution because the spectrometer was not re-tuned after addition of each aliquot of acid. Relative intensities were determined by several integrations in both directions and only the integration of spectrum number 2 is believed to contain a large error. These data were fitted to the equilibrium below.

$$[CpFe(CO)_2]_2 + H_2SO_4 \rightleftharpoons \{[CpFe(CO)_2]_2H^+\}\{HSO_4^-\}$$

$$K = \frac{[\{[CpFe(CO)_2]_2H^+\}\{HSO_4^-\}]}{\{[CpFe(CO)_2]_2\}\{H_2SO_4\}}$$

The product was taken as an iron pair because of the low dielectric constant of CH_3CO_2H. (See Chapter Seven.) The apparent

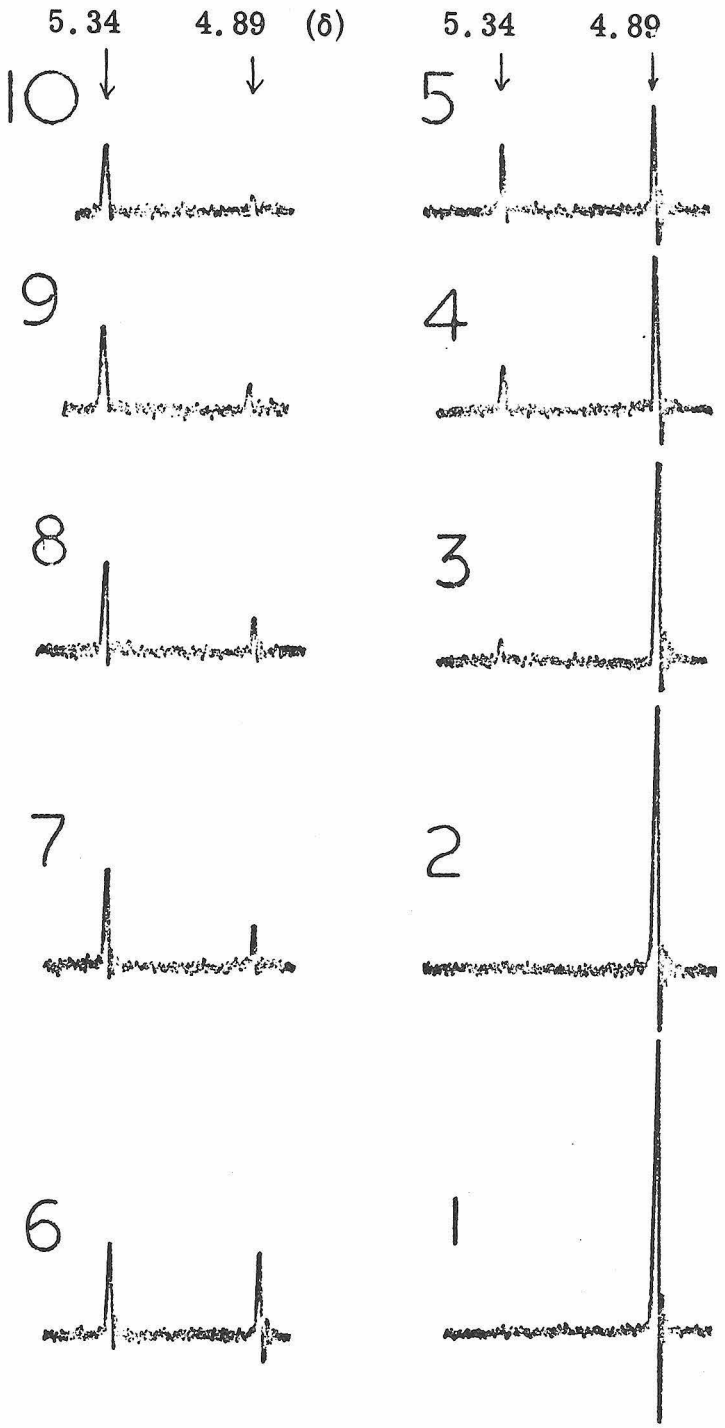

Titration of $[(\pi\text{-}C_5H_5)Fe(CO)_2]_2$ with H_2SO_4 in CH_3CO_2H

Figure 48

Table XXII

Titration of $[CpFe(CO)_2]_2$ with H_2SO_4 in CH_3CO_2H Followed by NMR[a]

Experiment	μl Acid Added[b]	Total Sample Volume[c] (ml)	$[H_2SO_4]_{TOT}$[d]	$[Fe_2]_{TOT}$[e]	$\frac{[HFe_2^+]}{[Fe_2]}$	$[H_2SO_4]_{corrected}$[f]	K[g]
1	0	0.500	--	0.0496	--	--	--
2	15	0.515	0.119	0.0481	0.05	0.117	0.42
3	50	0.565	0.470	0.0439	0.15	0.464	0.32
4	50	0.615	0.766	0.0405	0.44	0.754	0.58
5	50	0.665	1.02	0.0373	0.87	1.00	0.87
6	60	0.725	1.28	0.0342	1.4	1.26	1.1
7	70	0.795	1.52	0.0312	2.5	1.50	1.7
8	60	0.855	1.70	0.0292	3.0	1.68	1.8
9	60	0.915	1.86	0.0272	3.5	1.84	1.9
10	100	1.015	2.08	0.0245	6.1	2.06	3.0

[a] 60 M Hz spectrometer operating at ~40°C. All concentrations are in units of moles/l.

[b] 4.10 M H_2SO_4 in CH_3CO_2H.

[c] Assuming volumes are purely additive, i.e., no ΔV_{mixing}.

[d] Total acid added.

[e] Total base present.

[f] H_2SO_4 concentration corrected for amount that reacted with base.

[g] $K = [[CpFe(CO)_2]_2H^+]/\{[[CpFe(CO)_2]_2]\,[H_2SO_4]_{corrected}\}$. Units are 1 $mole^{-1}$.

equilibrium constant increases with increasing H_2SO_4 concentration, undoubtedly as an effect of the increased activity of H_2SO_4 as the concentration varies from 0.1 M to 2.1 M. In order to extrapolate the values of K to zero acid concentration, we apply Harris' Theorem, viz.,

> Any set of real data which shows a monatomic increase or decrease will approximate a straight line when the logarithm of that data is plotted.

(This theorem is the theoretical foundation for all Arrhenius plots and linear free energy relationships, among other things.) Such a plot is given in Figure 49 and is used to estimate $K = 10^{-0.8}$ l mole^{-1} at infinite dilution. The unfilled circle in this Figure is the point calculated from experiment number 2 which we believe to contain very considerable error.

Similar titrations of $[CpRu(CO)_2]_2$ and Fe_2P (Figures 50 and 51) were performed, but these bases were too strong for this technique. Within experimental error, all of the added H_2SO_4 was consumed by base until one equivalent had been used up. This allows us to establish lower limits on the equilibrium constants of $\sim 10^2$ l mole^{-1} for both $[CpRu(CO)_2]_2$ and Fe_2P. An interesting observation, however, is that mixtures of $[CpRu(CO)_2]$ and $[CpRu(CO)_2]H^+$, like mixtures of $[CpFe(CO)_2]_2$ and $[CpFe(CO_2)_2]_2H^+$, show sharp cyclopentadienyl peaks. In contrast, a mixture of Fe_2P and Fe_2PH^+ (Figure 51, experiments 2 and 3) show broad

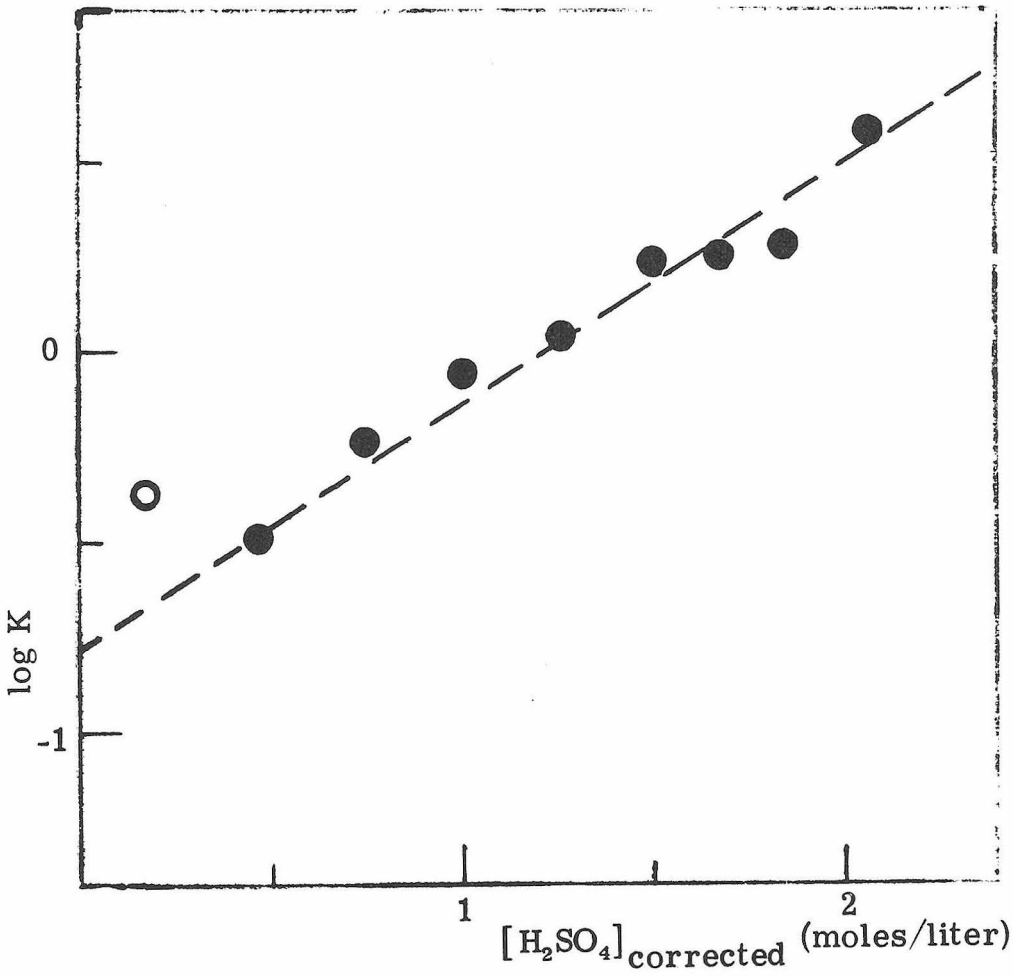

Titration of $[(\pi\text{-}C_5H_5)Fe(CO)_2]_2$ with H_2SO_4 in CH_3CO_2H.
Application of Harris' Theorem.
Figure 49.

lines for both the C_5H_5 and CH_3 protons. An explanation might be that Fe_2P and Fe_2PH^+ exchange the bridging proton between them and the other compounds do not. Again, a study of the temperature dependence of a solution of Fe_2P plus Fe_2PH^+ would be useful.

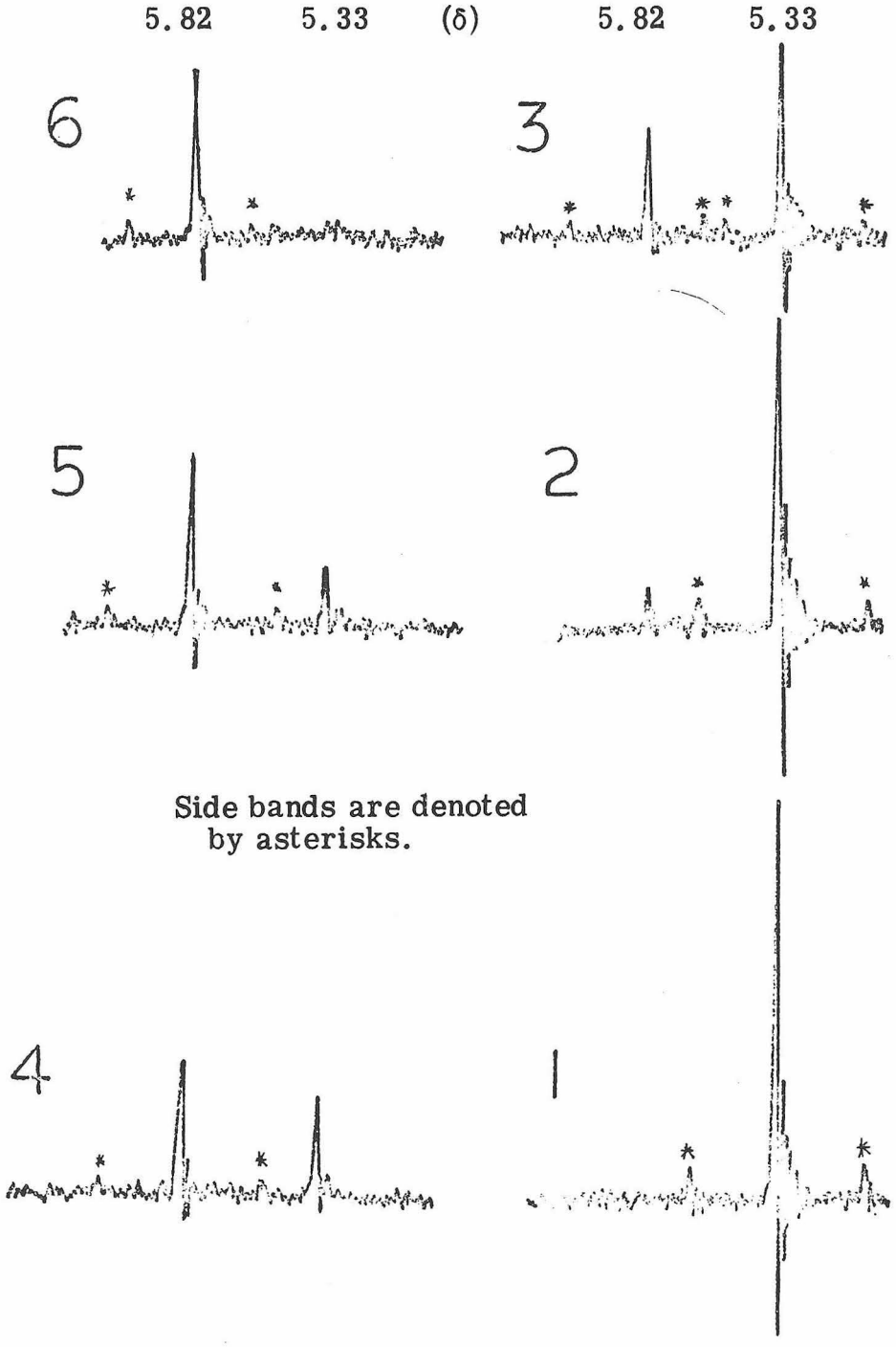

Side bands are denoted by asterisks.

Titration of $[(\pi\text{-}C_5H_5)Ru(CO)_2]_2$ with H_2SO_4 in CH_3CO_2H

Figure 50

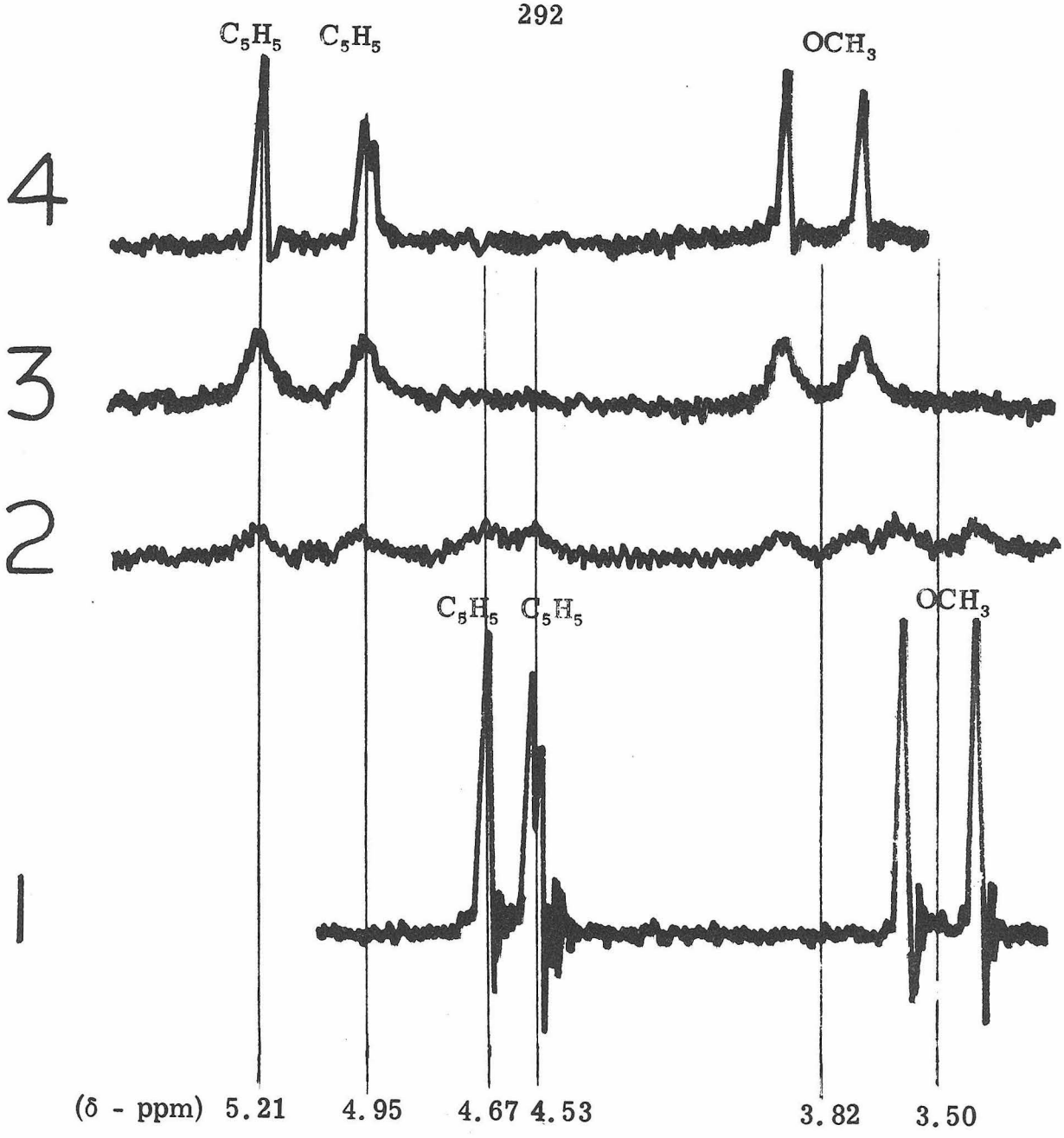

Titration of $(\pi\text{-}C_5H_5)(CO)Fe\text{-}\mu\text{-}(CO)_2\text{-}Fe[P(OCH_3)_3](\pi\text{-}C_5H_5)$ with H_2SO_4 in CH_3CO_2H

Figure 51

Our other NMR result of note came when we used ^1H NMR measurements to assay the deuterium content of $[(C_2H_5)_4N][DW_2CO_{10}]$. The spectrum of the ethyl protons of the cation (Figure 52) shows gorgeous ^{14}N-^1H coupling. The CH_3 peaks are all split into 1 : 1 : 1 triplets ($^3J_{^{14}N-^1H}$ = 1.9 Hz) and the broadening of the CH_2 lines allows us to estimate $^2J_{^{14}N-^1H} \approx$ 0.2 Hz.[94] The spectrum of the hydride region of $HW_2(CO)_{10}^-$ is very similar to that of Whitesides and Maglio,[93] showing τ_H = 22.51 ppm, $J_{^{183}W-^1H}$ = 42.7 Hz, $J_{^{13}C-^1H}$(cis) = 3.6 Hz, $J_{^{13}C-^1H}$(trans) $\approx$ 4.6 Hz. The weak trans ^{13}C satellites are not well resolved in our spectrum.

Potentiometric Base Strength Determination in Acetic Acid

As described fully in Chapter Seven, a base, B, will ionize in acetic acid solution as follows:

$$B + HOAc \underset{K_i}{\overset{\text{ionization}}{\rightleftharpoons}} [BH^+AcO^-] \underset{K_d}{\overset{\text{dissociation}}{\rightleftharpoons}} BH^+ + AcO^-$$

The only net equilibrium constant we can determine potentiometrically is

$$K_B = \frac{[BH^+][AcO^-]}{[B] + [BH^+AcO^-]} = \frac{K_iK_d}{1 + K_i}$$

Bruckenstein and Kolthoff[95] have determined K_B (and the analogous K_A for acids) for a number of compounds in acetic acid solution.

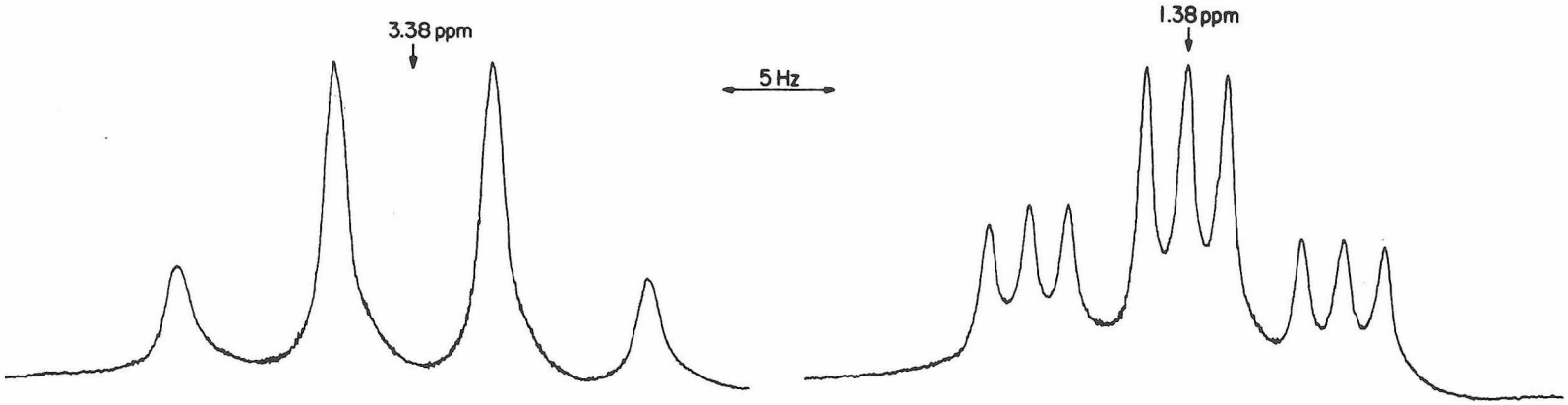

220 MHz NMR Spectrum of Ethyl Region of $[Et_4N][DW_2(CO)_{10}]$ in $(CD_3)_2CO$
(Suitable For Framing)

$^3J_{^1H-C-C-^1H} = 7.2$ Hz $\quad$ $^2J_{^{14}N-C-^1H} \approx 0.2$ Hz $\quad$ $^3J_{^{14}N-C-C-^1H} = 1.9$ Hz

Figure 52

Their meager results show a crude correlation of acid or base strength in acetic acid to strength in aqueous solution. We applied this technique, in a completely modified form described in the Experimental Section, to our iron compounds. The results (Table XXIII) agree with our NMR results. Namely, $[CpFe(CO)_2]_2$ and $[(\pi\text{-}CH_3C_5H_4)Fe(CO)_2]_2$ are of comparable base strength and are both much weaker bases than Fe_2P.

A Brief Excursion

In view of the controversy[96] surrounding the NMR behavior of H_2FeL_4 ($L = \phi P(OEt)_2$), we attempted to observe the spectra of the isoelectronic species $H_2CoL_4^+$ formed in situ by protonation of $HCoL_4$ with H_2SO_4. $HCoL_4$, obtained from Don Titus,[100] is a yellow crystalline solid which is very soluble in both polar and nonpolar organic solvents, giving yellow solutions. Addition of 98% H_2SO_4 at -78° in appropriate solvents results in a yellow solution of the protonated species $H_2CoL_4^+$. Slight warming of these unstable solutions results in the formation of a green color. On standing at room temperature for a month in a N_2 filled tube, an acetone solution of $HCoL_4$ and H_2SO_4 deposited a pink solid tentatively identified by its IR spectrum as either $CoSO_4$ or $Co(HSO_4)_2$ or a mixture of the two.

The NMR spectrum of $HCoL_4$ in C_6H_5Cl at 17°C is shown in Figure 53. This shows a quintet for the hydride at τ 24.4 ppm, $J_{^{31}P-^{1}H} = 22$ Hz. This spectrum is typical of a static square

Table XXIII

Base Strength in Acetic Acid Solution

Compound	pK_B (acetic acid)	pK_B (H_2O)
$[CpFe(CO)_2]_2$	7.5 ± 0.3	--
$[(\pi\text{-}CH_3C_5H_4)Fe(CO)_2]_2$	7.0 ± 0.3	--
$Cp(CO)Fe\text{-}\mu\text{-}(CO)_2\text{-}FeCp[P(OCH_3)_3]$	5.9 ± 0.3	--
Comparison Compounds[95]		
Tribenzylamine	5.36	--
N,N-Diethylamine	5.78	--
Pyridine	6.10	8.77
Potassium Acetate	6.10	9.25
Lithium Acetate	6.79	9.25
2,5-Dichloroaniline	9.48	--
Urea	10.24	13.82

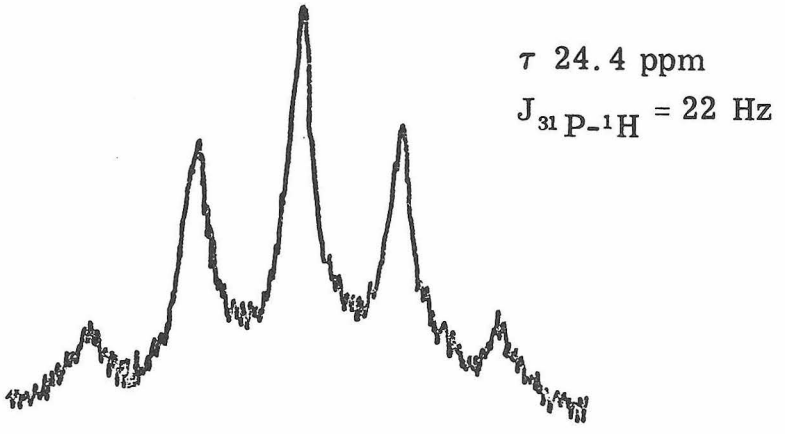

NMR Spectrum of $HCo[\phi P(OC_2H_5)_2]_4$ at 17°C

Figure 53

pyramidal structure or a fluxional structure of any geometry. We fully believe this to be a fluxional molecule.[101,102] The spectrum of $H_2CoL_4^+$ at several temperatures in $C_6H_5Cl/(CH_3)_2CO$ is shown in Figure 54. At -30° we barely resolve a quintet with $J_{^{31}P-^{1}H} \approx 45$ Hz centered at τ 22.3 ppm. All structure is lost as the peak broadens at lower temperature. We cannot say whether this broadening is due to fluxionalism or viscosity (or both). The mixture is solid at -78° so it is probably very viscous at -55°. Spectra run at high temperatures (-7°, $\omega_{\frac{1}{2}} = 180$ Hz; +17°, $\omega_{\frac{1}{2}} = 90$ Hz) were narrower but showed no structure. We cannot be certain that the samples were not decomposing at the higher temperatures. Meakin, et al.[103] have observed that the spectrum of $HCo(PF_3)_4$ shows a broad signal at

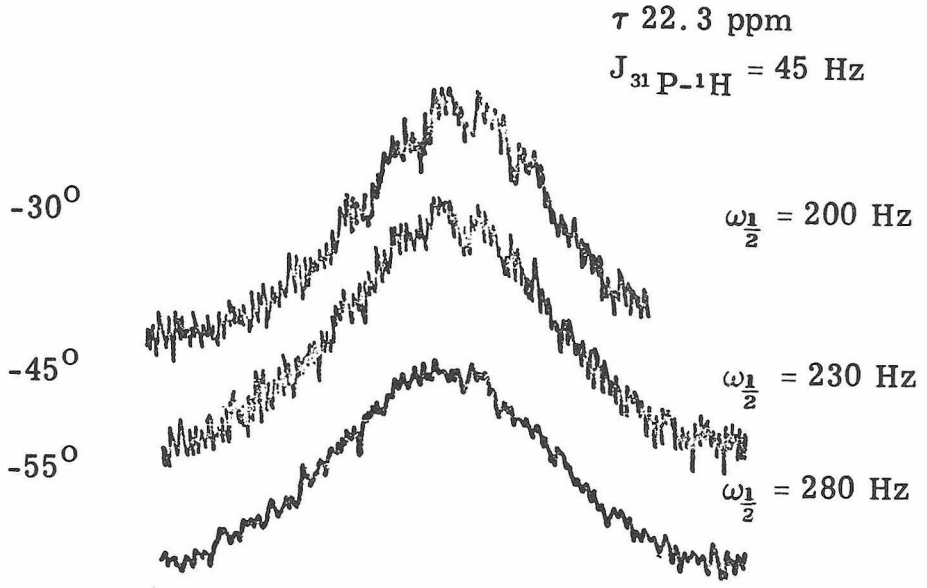

NMR Spectrum of $H_2Co[\phi P(OC_2H_5)_2]_4^+$

Figure 54

room temperature due to ^{59}Co quadrupole relaxation. At -60°, sharpening and structure are apparent, but at -110° some exchange process broadens the signal again. We may be observing similar behavior.

An attempt to observe the IR spectrum of $HCoL_4$ in CH_2Cl_2 at 80°K in a AgCl cell resulted in reduction of the AgCl surface to form a silver mirror. Spectra could be obtained in a sapphire cell, but no bands not present in solvent (CH_2Cl_2 or methylcyclohexane) were ever seen, even at 80°K, in the region 2500-1550 cm^{-1}. This behavior is similar to that of $HCo(N_2)$-$(P\phi_3)_3$ for which no Co-H absorption could be observed either.[104]

Experimental

General

All reactions and all handling of compounds was done under an atmosphere of nitrogen. The compounds $[CpFe(CO)_2]_2$, $[CpRu(CO)_2]_2$, $Cp_2(CO)_3Fe_2[P(OCH_3)_3]$, and $\{HCp_2(CO)_3Fe_2-[P(OCH_3)_3]^+\}\{B\phi_4^-\}$ could be handled in air with no apparent harm, but solutions were always protected by N_2. KBr pellets for spectra of air sensitive samples were prepared in a glove bag and loaded into the pellet die in a glove bag. NMR samples were protected from the air by a serum cap wired onto the NMR tube or samples were prepared under N_2 and sealed into tubes on the vacuum line. For Raman spectra, air sensitive solids were loaded into the Raman sample holder in a glove bag and a glass cover slip was placed over the sample using silicone stop-cock grease as glue. The grease was not in contact with the sample. All compounds were stored under N_2 at -20° in the dark when not being used. Solvents were deoxygenated by bubbling N_2 through or by several freeze-thaw cycles on the vacuum line. Acetone solutions of 98% H_2SO_4 should generally be handled at 0° to avoid acetone polymerization which produces an intense red product.

Chromium Family Compounds

$[Et_4N]_2[W(CO)_{10}]$ and $[Et_4N][HW_2(CO)_{10}]$ were prepared by the method of Hayter[32] by David Novikoff. Twice as much $NaBH_4$

as Hayter used was needed for the preparation of $HW_2(CO)_{10}^-$ to be complete in 1-2 days. Among all of the Cr and W compounds we handled, this is the most stable and could be handled in the air as a solid for short periods of time. $W_2(CO)_{10}^{2-}$ preparations required as long as 24 hours to go to completion using "Big Bertha" (a 130 W UV lamp with maximum output at 366 nm) as a light source. Crystallization from acetone-ethanol generally produced an oil prior to the formation of any crystals. The yellow salt slowly became contaminated by green impurity almost any time it was handled. In air, the salt $[Et_4N]_2[W(CO)_{10}]$ was usually pyrophoric.

The deuterated compound, $[Et_4N][DW_2(CO)_{10}]$ was also prepared by Novikoff, substituting $NaBD_4$ for $NaBH_4$ in Hayter's procedure.[32] All solvents were normal undeuterated materials and the product was crystallized three times from ethanol. NMR integration showed that this material was 80 (±10%) deuterated. Though the protio salt is yellow, the deuterio salt is light orange. Successive recrystallizations convinced me that these are the real colors of these materials and are not the results of impurities. Solution spectra of the protio and deuterio salts in ethanol are identical. The light orange color of the solid deuterio salt must be due to a very slight change in the bandshape of the spectrum. The effect of such a slight bandshape change would be greatly magnified at the concentration of a solid.

$[Et_4N][HCr_2(CO)_{10}]$ was also prepared by the method of Hayter.[32] One batch was moderately soluble in tetrahydrofuran (THF) but another batch was completely insoluble. We were unable to recrystallize this material and the spectra in this chapter were obtained with unrecrystallized material that had been washed with ethanol and dried in vacuo. Though the product is a beautifully crystalline yellow material as it forms in the reaction mixture, drying leaves a dirty yellow powdery product. Our faith in the visible absorption spectra presented in this chapter rests on the observation of identical spectra produced by several different samples with different histories in different solvents.

$Na_2[Cr_2(CO)_{10}]$ was prepared by Hayter's method[32] but required 84 hours' reaction time to produce an infrared spectrum similar to Kaska's[33] in THF. The reaction solution was centrifuged and the yellow liquid phase was filtered through celite to give clear yellow liquid from which beautiful yellow snowflake-like crystals of product grew at -78°. This material was washed with THF and dried in vacuo. After drying, a crudiferous brownish orange powder remained. An IR spectrum of this material in THF showed roughly equal bands due to both $Cr_2(CO)_{10}^{2-}$ and $HCr_2(CO)_{10}^{-}$. A visible absorption spectrum of this solution was very similar to that of plain $HCr_2(CO)_{10}^{-}$, so we conclude that the spectrum of each compound is similar.

$[Et_4N][MnCr(CO)_{10}]$[40] and $Mn_2(CO)_8(P\phi_3)_2$[72] were prepared by published procedures by David Novikoff. $MnCr(CO)_{10}^-$ could not be separated from a green impurity by crystallizations from 95% ethanol. It was placed in a filter under N_2 and extracted with absolute ethanol. This yellow solution could be treated with H_2O to grow well-formed yellow crystals of product. Attempts to protonate both compounds with 98% H_2SO_4 in acetone failed.

Attempted preparation of $W_2(CO)_8[P(OEt)_3]_2^{2-}$. Following the preparation of $Mn_2(CO)_8(P\phi_3)_2$,[72] David Novikoff was able to react 0.22 g $[Et_4N]_2[W_2(CO)_{10}]$ with 84 μl (2 equivalents) $P(OEt)_3$ in 10 ml ethanol <u>in vacuo</u> with UV irradiation for 6 hours. The reaction solution was maintained at room temperature by immersing it in a beaker of water which was constantly replaced as it warmed in the UV beam. The solid yellow starting material slowly dissolved and gas evolved to produce a greenish yellow solution. Removal of solvent <u>in vacuo</u> left a yellow oil which was treated with ethanol and water and set aside to crystallize. This solution turned green and never produced any crystals. A similar reaction using 0.14 g $[Et_4N]_2[W_2(CO)_{10}]$, 0.08 g $P\phi_3$ and 5 ml acetone for 3 hours of irradiation gave a yellow solution whose IR spectrum showed a single peak in the ν_{CO} region at 1944 cm^{-1} with several less intense shoulders. This is very similar to the spectra of axially disubstituted $Mn_2(CO)_8L_2$ compounds, so we believe

substitution did occur. All of my attempts to reproduce either of these two reactions failed as the yellow $W_2(CO)_{10}^{2-}$ starting material would not react and remained insoluble.

Iron Family Compounds

cis- and trans-$[CpFe(CO)_2]_2$[43] could be crystallized from ethyl acetate. A sample of commercial $[CpFe(CO)_2]_2$ (Alpha) was dissolved in boiling ethyl acetate and the liquid phase (after centrifugation) was set aside to crystallize at 0°. This produced black plates of trans isomer. The same solution from which the trans isomer grew was then cooled to -78° to deposit cis isomer. Comparison of the KBr pellet spectra to those of Bryan et al.[43] showed that the trans isomer was formed uncontaminated by cis isomer, but cis isomer sometimes contained some trans isomer. If this happens, you try try again.

$(Cp)_2(CO)_3Fe_2[P(OCH_3)_3]$[57] ("$Fe_2P$") was prepared in 27% yield after two crystallizations from benzene-hexane. 2.2 g $[CpFe(CO)_2]_2$ and 0.80 ml $P(OCH_3)_3$ were refluxed in 115 ml benzene for 24 hours. The mixture was centrifuged and the liquid phase was concentrated to dryness in vacuo. The black residue can be crystallized from 12 ml C_6H_6 and 18 ml hexane in stages down to -20°. Petroleum ether (BP 40-60°) was often used to wash the product or was used in place of hexane as the iron compound is less soluble in petroleum ether.

$\{H(Cp)_2(CO)_3Fe_2[P(OCH_3)_3]^+\}\{B\phi_4^-\}$. ("$Fe_2PHB\phi_4$").

0.25 g Fe_2P in 7.0 ml deoxygenated acetic acid was treated with

0.7 ml 98% H_2SO_4. The H_2SO_4 need not be degassed for this preparation. The red solution turns green on addition of H_2SO_4. This green solution was added to 0.28 g $NaB\phi_4$ dissolved in 14 ml H_2O to precipitate the product. The green powder is filtered, washed with water, and dried. The product is dissolved in 6 ml hot acetone, centrifuged, and the liquid phase is treated with 4.5 ml ethyl ether and set aside to crystallize in stages down to -20°. Yield = 74%. An analytical sample was crystallized a second time from 4 ml acetone/2 ml ether. MP 154-159 dec. Anal. Calcd. for $C_{40}H_{40}O_6Fe_2PB$: Fe, 14.50; C, 62.38; H, 5.23; B, 1.40. Found (Schwarzkopf): Fe, 16.11; C, 62.83; H, 5.14; B, 1.30.

$[CpRu(CO)_2]_2$.[60] "$RuCl_3 \cdot H_2O_x$" was obtained from Research Inorganic Chemicals. If your sample is not soluble in water, send it back. We prepared $[Ru(CO)_3Cl_2]_2$[107] by the method of Blackmore, et al.[60] (high-pressure carbonylation), but found the yield to be very poor. Instead, the procedure of Cleare and Griffith[108] gave good results. Unreacted material was saved and thrown in with the next reaction. Any material which did not react after two cycles was chemically inert. NaC_5H_5 was prepared by treating 15 ml cyclopentadiene (cracked at 190°, BP 40°) in 175 ml THF with 6 g Na to give a red solution after 4 hours stirring at room temperature. The liquid was placed in a fresh flask equipped with a reflux condensor and 6 g dry $[Ru(CO)_3Cl_2]_2$ in

200 ml THF was added. This was stirred and refluxed 19 hours and allowed to cool and settle. The solution was separated from the orange solid and concentrated to dryness on a rotary evaporator using N_2 in the evaporator. The orange residue was extracted twice with 100 ml portions benzene. The benzene extracts were centrifuged and the liquid phase concentrated in a rotary evaporator to leave several grams of pyrophoric orange residue. The only way we found to obtain pure product was by tedious sublimation of this residue in small aliquots at 160°/10μ. The residue must be loaded into the sublimation apparatus in a glove bag because it smolders on contact with air. Prior to loading it into the sublimer, it was pulverized in a mortar. This allowed as much sublimation as was going to occur to be over in ~3 hours. The first sublimate is a brownish orange material which can be handled in air. It was fractionally resublimed, first at 60°/10μ to remove yellow Cp_2Ru byproduct, and then at 160°/10μ to collect light orange product. Even purer material could be obtained after another fractional sublimation. To aid in assessing purity, the KBr pellet spectrum of Cp_2Ru is given in Figure 55. Bands appear at 3081 m, 1404 m, 1341 w, 1251 w, 1103 w, 1100 s, 1090 w, 1060 w, 1050 w, 1044 w, 1001 s, 993 s, 895 w, 862 m, 831 w, 817 s, 810 s, 704 w, 490 m, 473 w, 447 s, 380 w. Final light orange $[CpRu(CO)_2]_2$, MP 165-175 shrink, 175-176 melt, was very slightly contaminated by a hydrocarbon

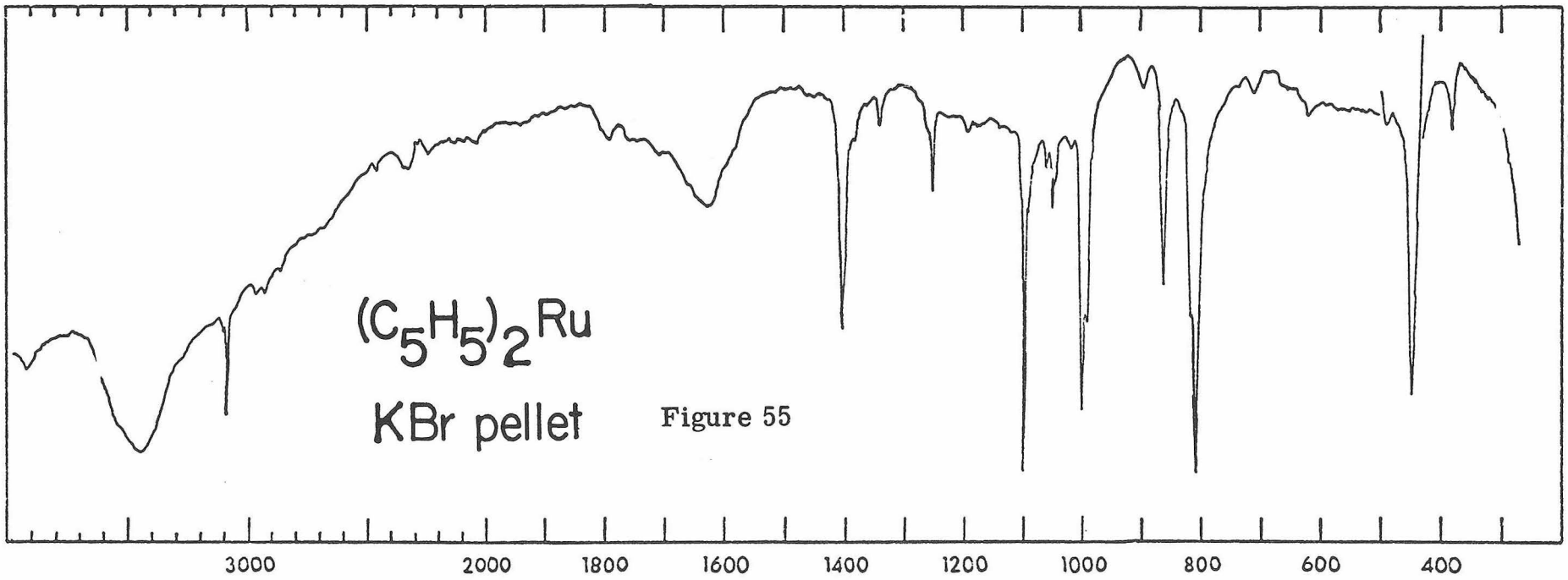
$(C_5H_5)_2Ru$
KBr pellet
3000
2000
1800
1600
1400
1200
1000
800
600
400

Figure 55

from which it could not be separated by sublimation. Raman spectrum: (70-1200 cm^{-1}) 75(6), 94(6), 110(37), 216(34), 252(5), 325 sh(21), 337(59), 439(15), 506(7), 1110(14). The sample slowly burned in the beam. Yield = 0.17g = 3%.

Attempts to protonate $[CpRu(CO)_2]_2$ in a manner analogous to that used for $[CpFe(CO)_2]_2$ gave a yellow product. This is incomprehensible because NMR protonation experiments show that protonated material is definitely green. The preparative scale protonation needs to be repeated.

Far IR spectra of several iron compounds are presented without comment in Figure 56. The preparation of paraffin pellets is described in Chapter Four.

The solution absorption spectra of $[CpFe(CO)_2]_2H^+$ shown in Figures 12 and 13 were obtained by adding 1.00 ml degassed 98% H_2SO_4 to 9.00 ml of a $[CpFe(CO)_2]_2$ solution of the proper concentration to record the spectrum. Solutions were cooled in an ice bath when acid was added.

Potentiometric Base Strength Determination in Acetic Acid Solution

The principle behind our potentiometric base strength determinations is appallingly crude. Solutions of "known" pH were prepared as will be described. An ordinary glass electrode and a calomel electrode (in which the aqueous KCl solution was replaced by a saturated solution of NaCl in HOAc) were then placed in the solutions and readings in an arbitrary millivolt

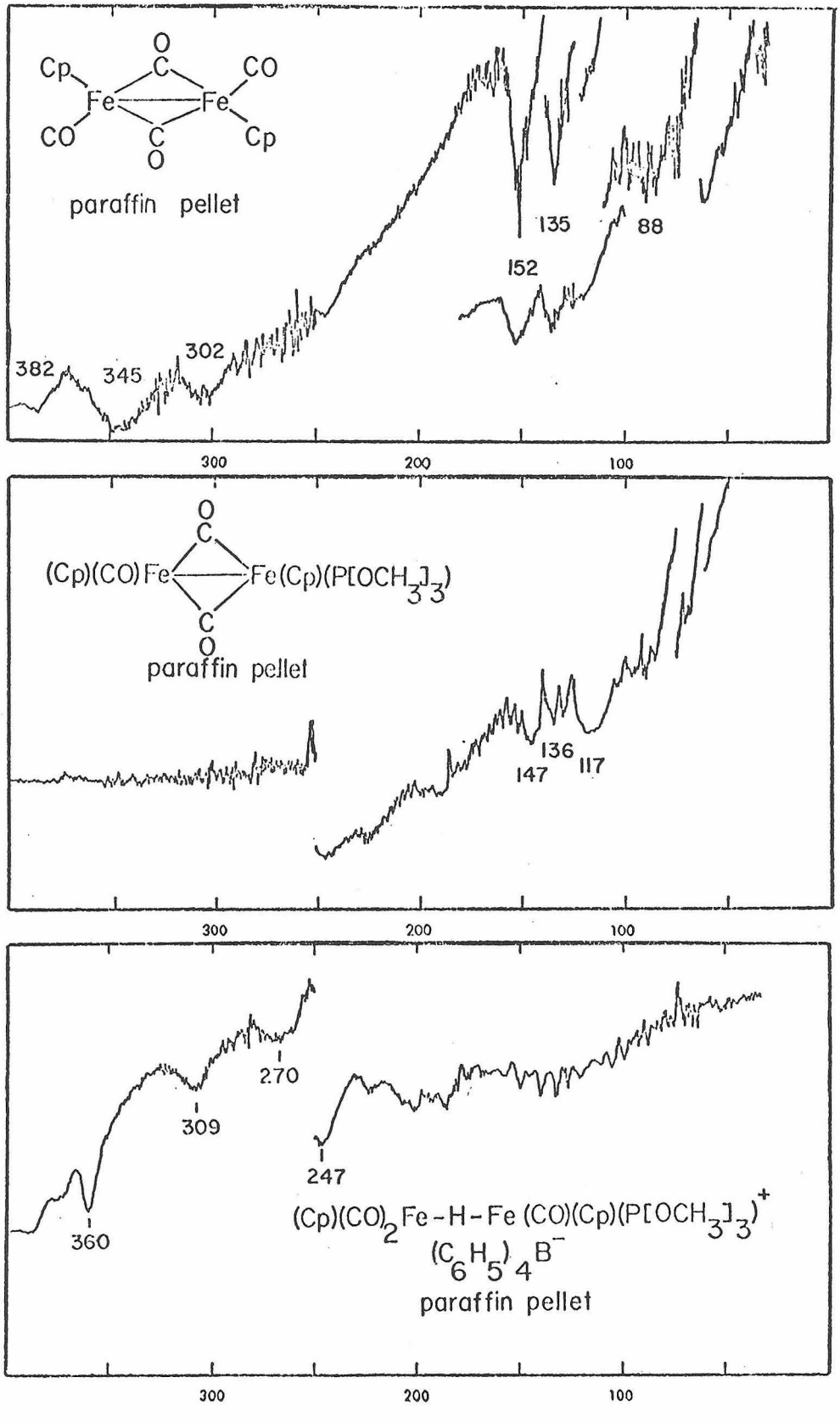
Cp
Fe
Fe
CO
CO
Cp
O
C
C
O
paraffin pellet
382
345
302
152
135
88
300
200
100
(Cp)(CO)Fe
Fe(Cp)(P[OCH3]3)
O
C
C
O
paraffin pellet
147
136
117
300
200
100
360
309
270
247
(Cp)(CO)2Fe-H-Fe(CO)(Cp)(P[OCH3]3)+
(C6H5)4B−
paraffin pellet
300
200
100

Figure 56

scale were recorded. Over a certain pH range, the response of these electrodes is linear in pH. A solution of a weighed amount of iron compound was then prepared and its potential was recorded with the electrodes. The reading in millivolts was compared to our calibration graph and used to determine the pH of the iron solution. This can then be used to calculate a pK_B value for the iron compound. We now describe the procedure in detail.

Reference bases were purified as follows:

Tribenzylamine: Eastman White Label material was crystallized once from hexane, M.P. 91-92°.

Potassium Acetate: Mallinckrodt Analytical Reagent was dried at 0.01 mm with P_2O_5 for 3 days.

Lithium Acetate: 30 g $LiOAc \cdot 2H_2O$ (Matheson, Coleman and Bell) was dissolved in 75 ml boiling acetic anhydride and 25 ml acetic acid was added. After cooling to room temperature, 50 ml C_6H_6 was added and the precipitate was collected and washed with C_6H_6. The sample was then dried at 0.01 mm for two days.

2,5-Dichloroaniline: A sample of Eastman Practical Grade was crystallized twice from hexane and sublimed twice at 1 mm/40°C. M.P. 48-50°.

Urea: Allied Chemical A.C.S. Reagent grade was dried overnight in a dessicator with $CaSO_4$.

The following solutions were then prepared:

Base	Concentration(M)	pH	mv	Point on Graph(Fig. 58)
$(\phi CH_2)_3N$	0.05	11.12	457	1
KOAc	0.05	10.75	434	2
	0.005	10.25	400	3
2,5-Dichloroaniline	0.05	9.04	341	7
	0.005	8.54	345	6
Urea	0.05	8.65	350	5
LiOAc	0.0073	9.98	383	4

The pH values were calculated from expression 4-48 of Laitinen's text which is given in Chapter Seven.

$$[H_2OAc^+] = \frac{K_S}{\sqrt{K_B(C_B)_t}} = \frac{10^{-14.45}}{\sqrt{K_B(C_B)_t}}$$

$(C_B)_t$ is the formal concentration of base-derived species in solution. Values of K_B were given in Table XXIII. The pH of an acetic acid solution is just - log $[H_2OAc^+]$.

Glass and modified calomel electrodes were then placed in these solutions and a mv reading was recorded. A sensitive digital pH meter proved useless for this purpose because of the extremely high noise level. An old Leeds and Northrup pH meter was borrowed from the freshman lab to cut down the sensitivity. Even this meter showed tremendous noise and readings were the eyeballed average of a swinging needle. We

estimate mv readings to be accurate to ± 5 mv (or a little better when the relative positions of Venus and Saturn were right).

The apparatus used for these measurements (Figure 57)

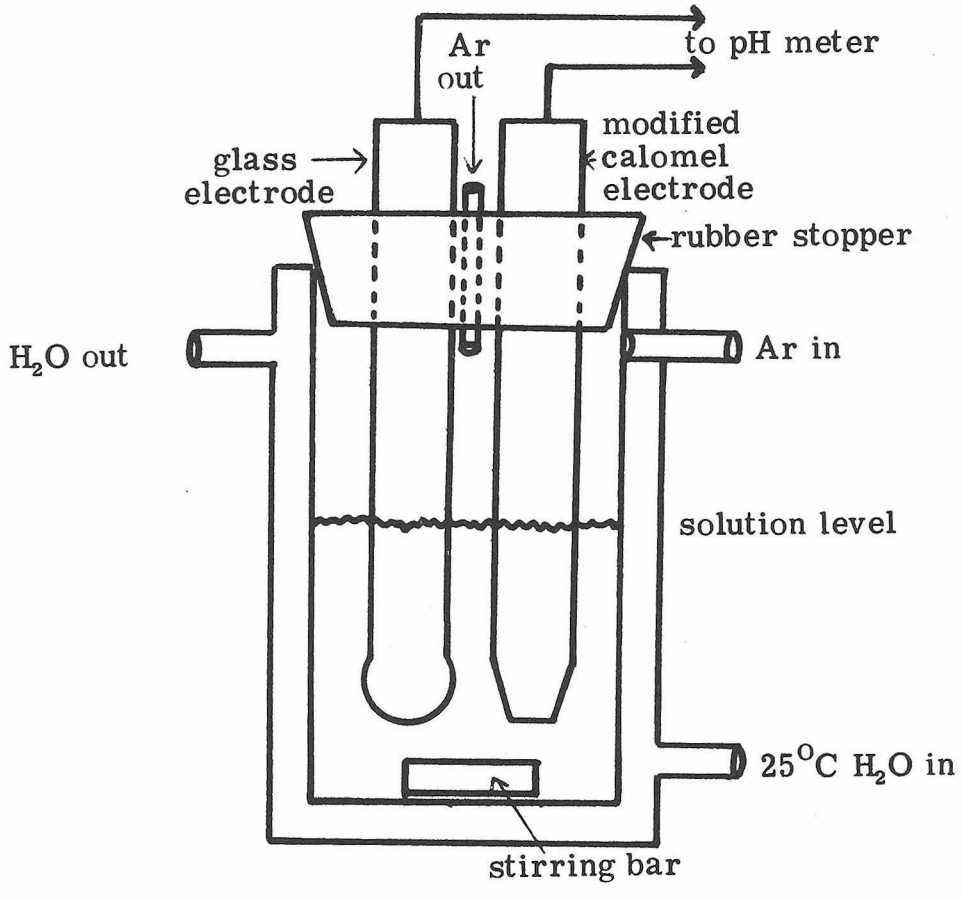

Apparatus for Potentiometric pK_B Determination.
Ar outlet is also solution inlet.

Figure 57

was thermostated at 25 °C and an Ar atmosphere was maintained for all measurements. Samples were introduced by pipette to minimize contact with the water vapor of the air. The solvent

was reagent grade acetic acid (99.7%) (3 liters mixed with 50 ml acetic anhydride) deoxygenated by a stream of argon.

The calibration curve constructed from these data (Figure 58) shows that the electrode response is linear in the pH region $\gtrsim 10$. Solutions of iron compounds then gave the results under "Experiment I" in Table XXIV. Data for Experiment II are plotted in Figure 59 and tabulated below.

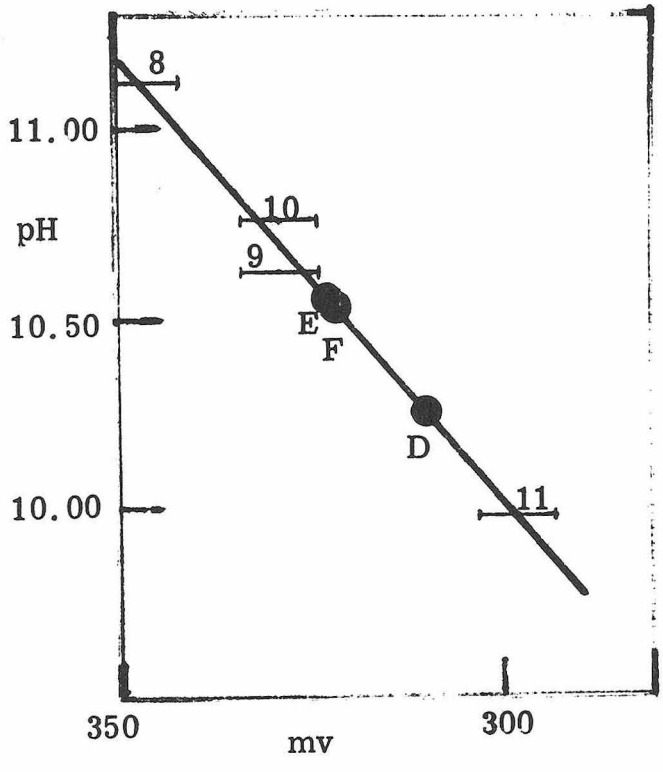

pH-mv Calibration Curve. Experiment II

Figure 59

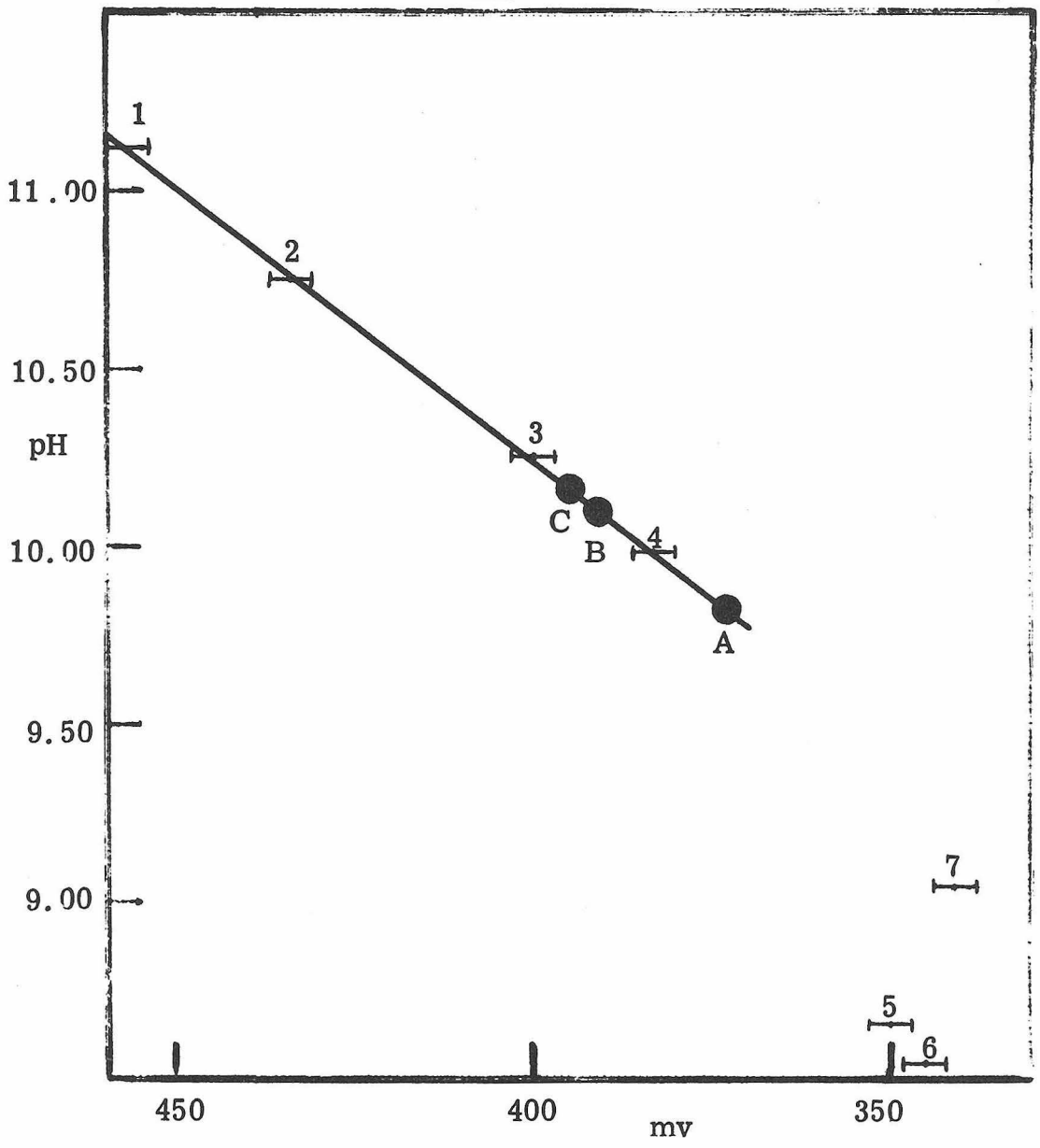

pH-mv Calibration Curve. Experiment I

Figure 58

Table XXIV

	Concentration (M)	mv Reading	Calculated pH	Calculated pK_B	Point on Graph
	Experiment I				
$[CpFe(CO)_2]_2$	0.0243	373	9.82	7.64	A
	0.0450	391	10.12	7.36	B
$[(\pi\text{-}CH_3C_5H_4)Fe(CO)_2]_2$	0.0304	395	10.16	7.06	C
	Experiment II				
$[(\pi\text{-}CH_3C_5H_4)Fe(CO)_2]$	0.0300	310	10.26	6.86	D
$(Cp)(CO)Fe\text{-}\mu\text{-}(CO)_2\text{-}Fe[P(OCH_3)_3]Cp$	0.00812	323	10.56	5.69	E
	0.0159	322	10.54	6.02	F

Data for Experiment II

Base	Concentration(M)	pH	mv	Point on Graph (Fig. 59)
$(\phi CH_2)_3N$	0.05	11.12	347	8
	0.005	10.62	328	9
KOAc	0.05	10.75	328	10
LiOAc	0.0073	9.98	298	11

The average pK_B value of the two determinations for each iron compound is reported in Table XXIII.

The 4.10 M H_2SO_4/HOAc solution used in the NMR titration of $[CpFe(CO)_2]_2$ (Table XXII) was standardized by titration of a known amount of potassium biphthalate in HOAc solution using the glass and modified calomel electrodes. A representative titration curve is given in Figure 60.

$HCo[\phi P(OEt)_2]_4$ Experiments

The NMR spectrum of $HCoL_4$ (Figure 53) was obtained with a sample of 81 mg $HCoL_4$ in 0.4 ml C_6H_5Cl at 17°C on a 220 M Hz spectrometer. The sample was prepared from deoxygenated solvent under N_2 at -78° and degassed *in vacuo* prior to sealing. The NMR spectrum of $H_2CoL_4^+$ (Figure 54) was obtained with 0.09 g $HCoL_4$ in 250 μl C_6H_5Cl, 190 μl acetone, 0.06 ml 98% H_2SO_4 and 15 μl TMS. $[H_2SO_4]/[HCoL_4] \approx 10$. This was prepared and sealed as the unprotonated sample was. The order in which the spectra of Figure 54 were run was -45° before -55° before -30°. The samples used for IR spectra in a 0.1 mm sapphire cell contained 20 mg $HCoL_4$/ml in CH_2Cl_2 and 60 mg/ml in methylcyclohexane.

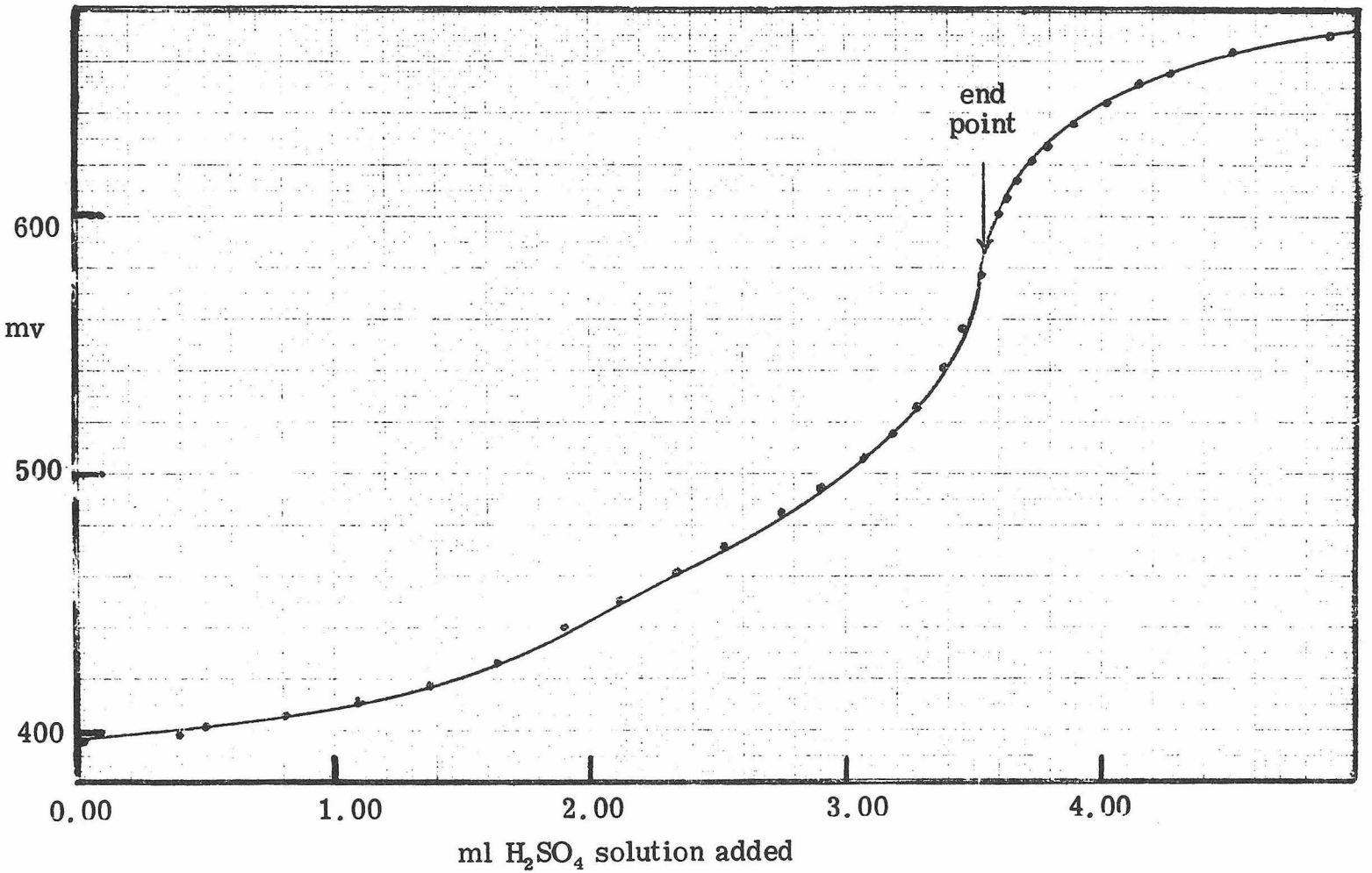

Potentiometric Titration of Potassium Biphthalate with H_2SO_4 in Acetic Acid

Figure 60

Additional Experiments

We attempted to study another Fe-Fe system not yet mentioned in this chapter. This is the system of pure carbonyl compounds. $Fe(CO)_5$ exhibits its first absorption maximum at 41 kK. In contrast, $Fe_2(CO)_9$ has a band at 26.2 kK which we believe is a consequence of the metal-metal bond (Figure 61). We prepared $HFe(CO)_4^-$ and $Fe_2(CO)_8^{2-}$ by the method of Farmery *et al.*[109] and attempted to prepare $HFe_2(CO)_8^-$ by their procedure. The suggested structures are shown below.

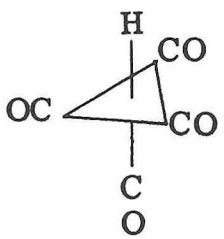

C_{3v}

$HFe(CO)_4^-$

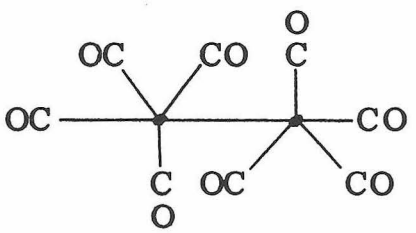

D_{3d}

$Fe_2(CO)_8^{2-}$

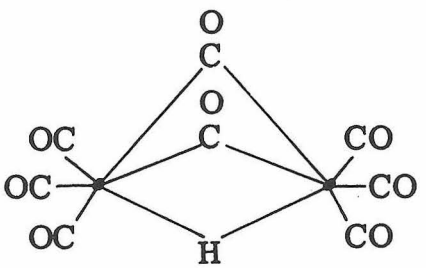

C_{2v}

$HFe_2(CO)_8^-$

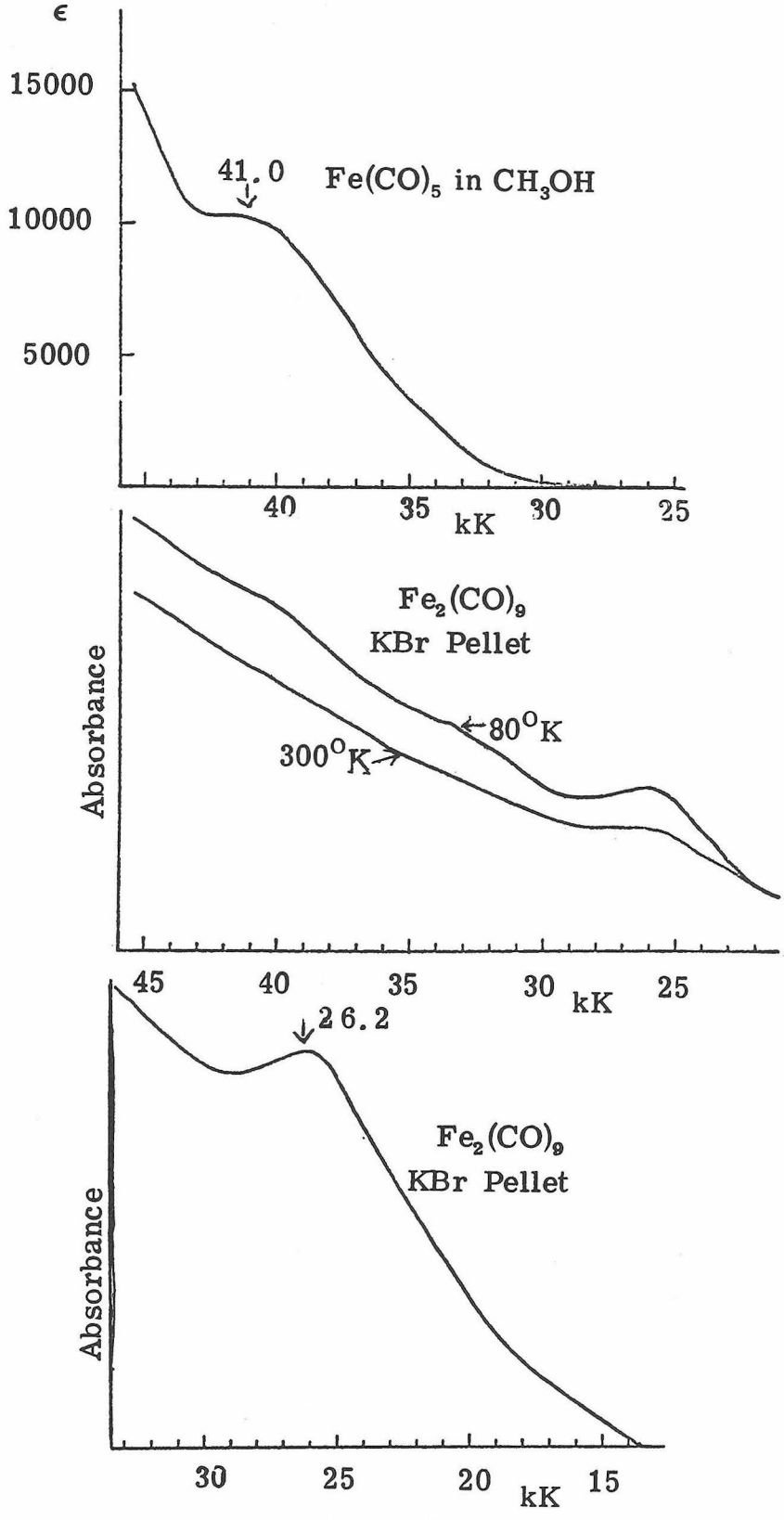
ε
15000
10000
5000
41.0
Fe(CO)5 in CH3OH
40
35
30
25
kK
Fe2(CO)9
KBr Pellet
Absorbance
←80°K
300°K→
45
40
35
30
25
kK
26.2
Fe2(CO)9
KBr Pellet
Absorbance
30
25
20
15
kK

Figure 61

The spectra of $HFe(CO)_4^-$ and $Fe_2(CO)_8^{2-}$ are shown in Figure 62. We were unable to prepare any material with an IR spectrum comparable to the one reported for $HFe_2(CO)_8^-$. In lieu of a solid sample, we added methanolic HCl to a pale red solution of $Fe_2(CO)_8^{2-}$ in methanol. The solution became a more intense red and the spectrum is shown in Figure 62. This red solution faded to a colorless solution within minutes.

Reference Spectra

To facilitate any future use of the IR spectra reported in this chapter, we give the KBr pellet spectra of Et_4NBr, $NaB\phi_4$ and ϕ_3P in Figures 63 through 65 and list them in Table XXV.

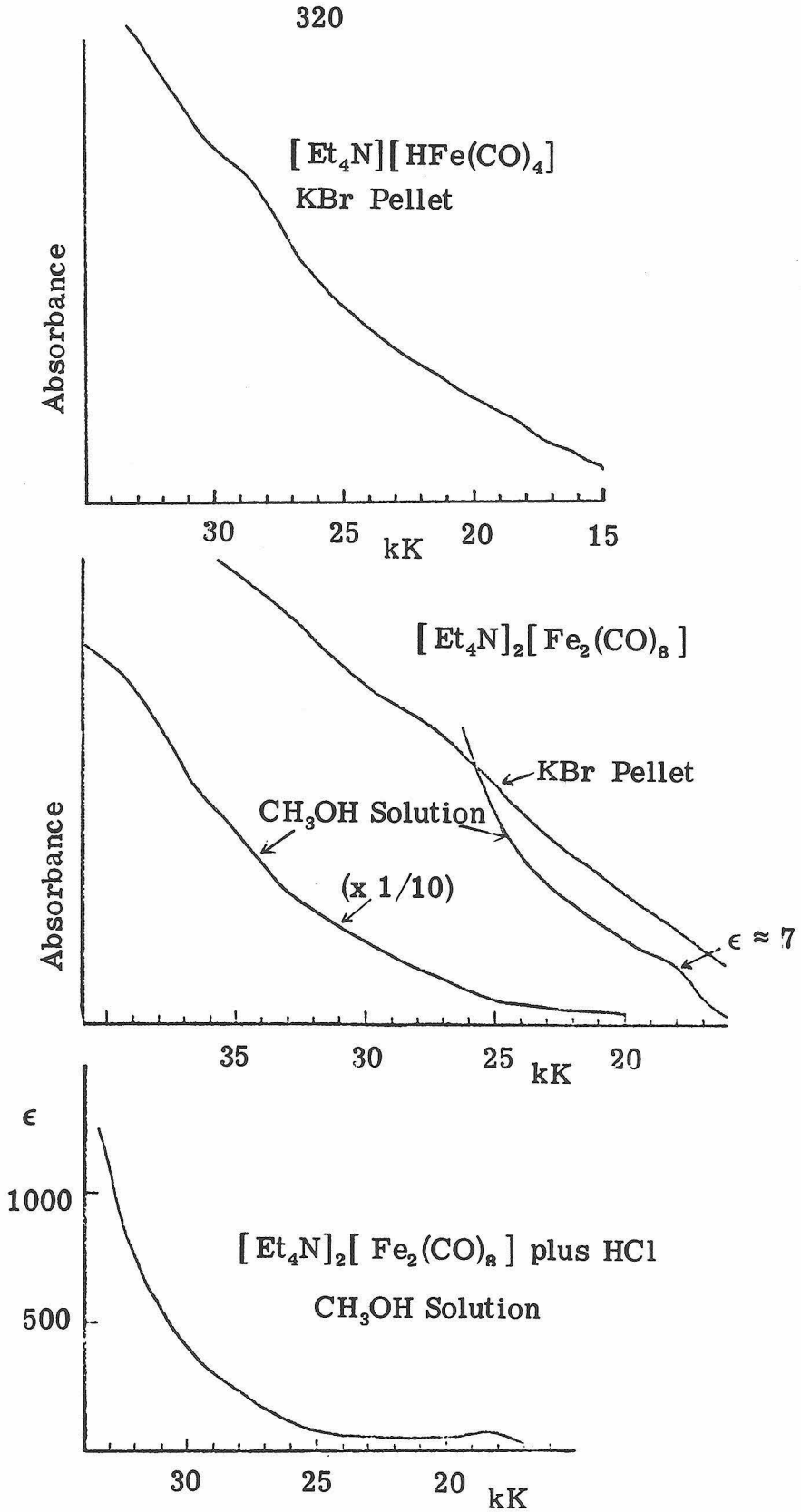
[Et4N][HFe(CO)4]
KBr Pellet
Absorbance
30
25
kK
20
15
[Et4N]2[Fe2(CO)8]
KBr Pellet
CH3OH Solution
(x 1/10)
ε ≈ 7
Absorbance
35
30
25
kK
20
ε
1000
500
[Et4N]2[Fe2(CO)8] plus HCl
CH3OH Solution
30
25
20
kK

Figure 62

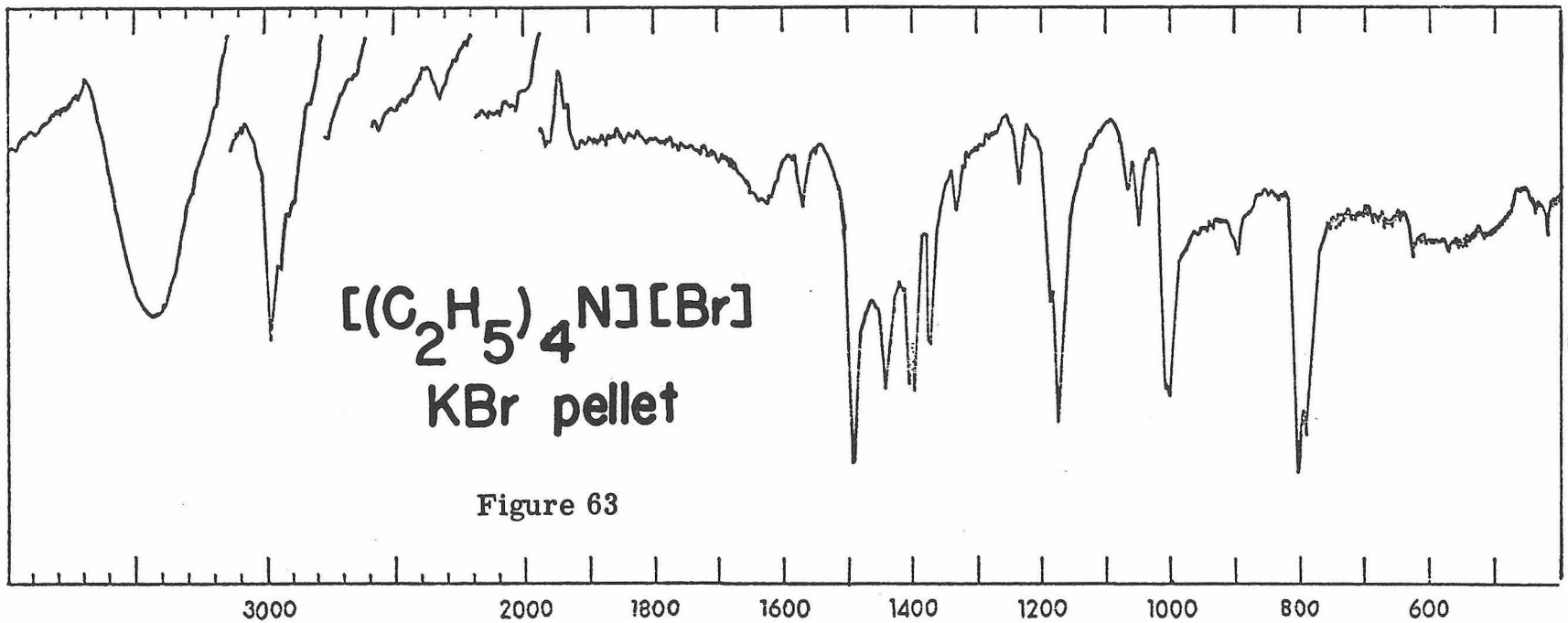
[(C2H5)4N][Br]
KBr pellet
3000
2000
1800
1600
1400
1200
1000
800
600

Figure 63

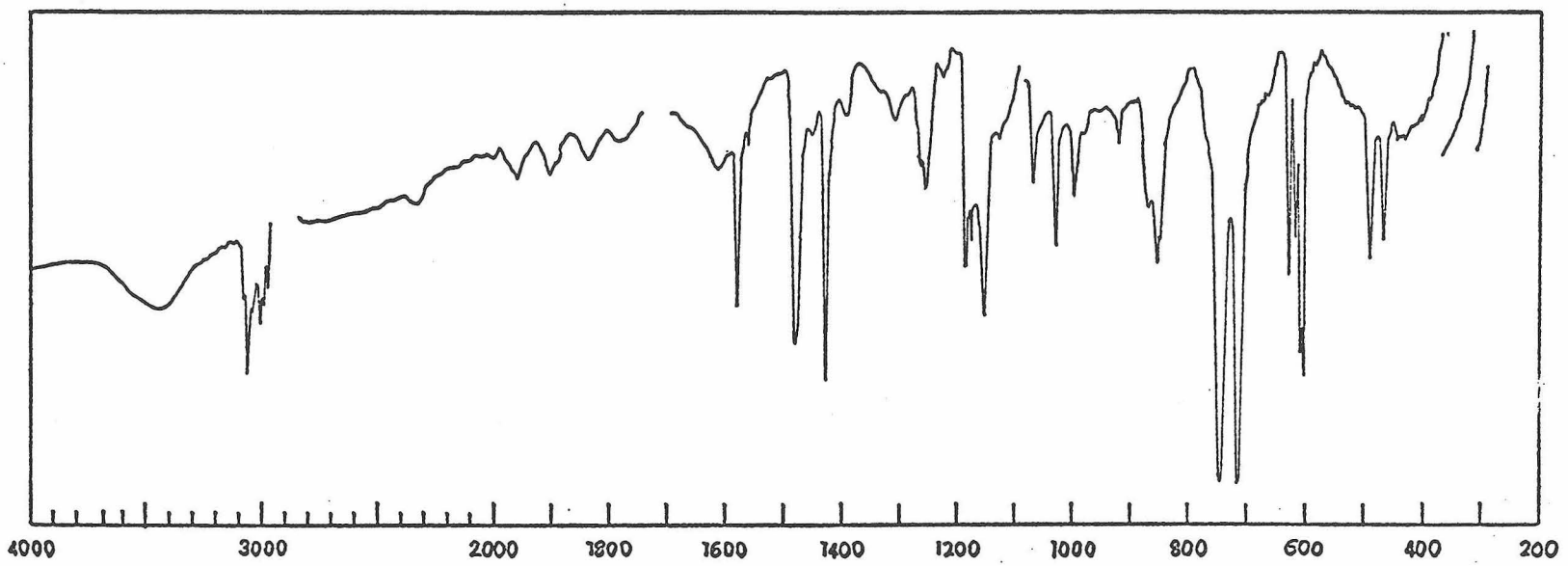

KBr Pellet Spectrum of $NaB(C_6H_5)_4$

Figure 64

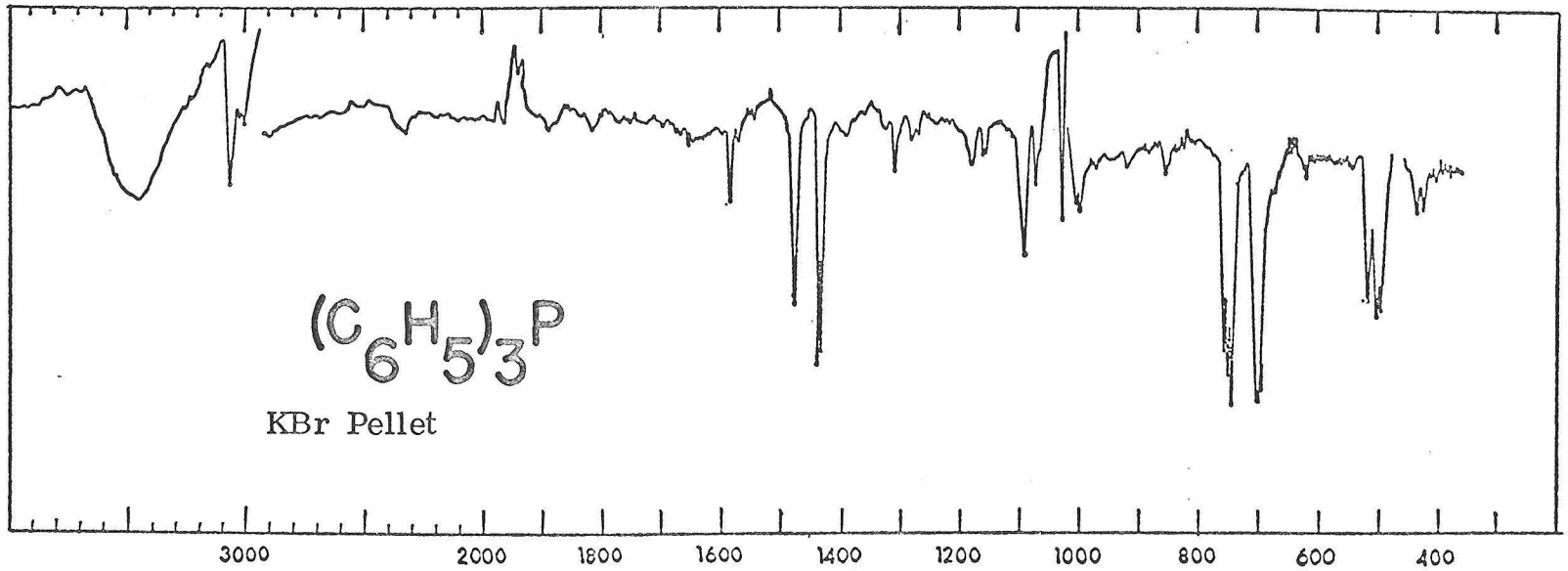
$(C_6H_5)_3P$
KBr Pellet
3000
2000
1800
1600
1400
1200
1000
800
600
400

Figure 65

Table XXV. Infrared Spectra

$[(C_2H_5)_4N][Br]$ 300° (4000-320 cm^{-1})	$(C_6H_5)_3P$ 300° (4000-340 cm^{-1})	$[Na][B(C_6H_5)_4]$ 300° (4000-300 cm^{-1})
3430 m,br	3460 m,br	3070 sh,w
2985 m	3055 m	3055 m
2940 m	3040 w	3035 w
2910 vw	3020 vw	3005 w
2890 vw	3000 vw	2985 w
2330 vw	2330 vw	2970 w
1635 w	1640 vw,br	1967 w
1569 w	1581 w	1900 w
1493 s	1569 vw	1835 w
1441 m	1476 m	1781 w
1406 m	1436 s	1610 w
1398 m	1430 s	1577 m
1374 m	1389 vw	1558 w
1333 w	1322 vw	1477 s
1236 w	1307 w	1449 w
1185 m	1289 vw	1426 s
1173 s	1277 vw	1389 w
1067 w	1178 vw	1260 m
1050 w	1156 vw	1251 m
1108 s	1090 m	1220 w
1002 s	1069 w	1181 m
898 vw	1025 m	1171 m
800 s	1000 sh,w	1151 m
787 s	996 w	1121 w
623 vw	852 vw	1064 w
419 vw	754 s	1026 m
	748 s	995 w
	742 s	918 w
	698 s	868 m
	692 s	851 m
	672 sh,vw	745 s
	619 vw	715 s
	513 m	626 m
	499 m	615 m
	491 m	606 s
	432 vw	601 s
	421 vw	488 m
		464 m
		438 w

References

1. a) A. J. Deeming, B. F. G. Johnson, and J. Lewis, J. Chem. Soc. A, 2517 (1970).

   b) For a later paper and references to other work in this whole series of papers, see A. J. Deeming, R. Ettorre, B. F. G. Johnson, and J. Lewis, Ibid., 2701 (1971).

2. The report of compounds with $\tau_H \approx 60$ ppm came a few months later.

   C. Masters, B. L. Shaw, R. E. Stainbank, Chem. Comm., 209 (1971).

3. A. Davison, W. McFarlane, L. Pratt, and G. Wilkinson, J. Chem. Soc., 3653 (1962).

4. D. A. Symon and T. C. Waddington, J. Chem. Soc. A, 953 (1971).

5. R. A. Levenson, Ph.D. Dissertation, Columbia University, 1970.

6. In this figure 3-PIP is a 6:1 (vol/vol) mixture of isopentane and 3-methylpentane.

7. L. F. Dahl and R. E. Rundle, Acta Cryst., 16, 419 (1963).

8. N. Flitcroft, D. K. Huggins, and H. D. Kaesz, Inorg. Chem., 3, 1123 (1964).

9. Polarizations of the ν_{CO} modes of $Mn_2(CO)_{10}$ are in excellent agreement with this structure in solution. Ref. 1, page 37.

10. a) R. E. Winters and R. W. Kiser, Inorg. Chem., 3, 699 (1964);

    b) Ibid., 4, 157 (1965).

11. N. A. Beach and H. B. Gray, J. Amer. Chem. Soc., 90, 5713 (1968).

12. H. J. Svec and G. A. Junk, Ibid., 89, 2836 (1967).

13. C. O. Quicksall and T. G. Spiro, Inorg. Chem., 8, 2363 (1969).

14. G. J. Wessel and D. J. W. Ijdo, Acta Cryst., 10, 466 (1957).

15. R. Saillant, R. B. Jackson, W. E. Streib, K. Folting, and R. A. D. Wentworth, Inorg. Chem., 10, 1453 (1971).

16. W. H. Watson and J. Wasser, Acta Cryst., 11, 689 (1958).

17. J. Lewis, R. S. Nyholm, and P. W. Smith, J. Chem. Soc. A, 57 (1969).

18. R. Saillant and R. A. D. Wentworth, Inorg. Chem., 7, 1606 (1968).

19. R. J. Ziegler and W. M. Risen, Jr., Inorg. Chem., 11, 2796 (1972).

20. P. W. Smith and A. G. Wedd, J. Chem. Soc. A, 2447 (1970).

21. R. Saillant, J. L. Hayden, R. A. D. Wentworth, Inorg. Chem., 6, 1497 (1967).

22. F. A. Cotton and J. G. Norman, Jr., J. Amer. Chem. Soc., 94, 5697 (1972).

23. L. Dubicki and R. L. Martin, Inorg. Chem., 9, 673 (1970).

24. M. J. Bennett, K. G. Caulton, and F. A. Cotton, Ibid., 8, 1 (1969).

25. J. V. Brencic and F. A. Cotton, Ibid., 8, 7 (1969).

26. F. A. Cotton and C. B. Harris, Ibid., 6, 924 (1967).

27. F. A. Cotton and C. B. Harris, Ibid., 4, 330 (1965).

28. A whole class of Chem 2 Trolls agrees with the $\delta \rightarrow \delta^*$ assignment.

29. F. A. Cotton, N. F. Curtis, B. F. G. Johnson, and W. R. Robinson, Ibid., 4, 326 (1965).

30. L. B. Handy, J. K. Ruff, and L. F. Dahl, J. Amer. Chem. Soc., 92, 7312 (1970).

30a. $Re_2(CO)_{10}$ is believed to adopt an eclipsed conformation above 92°C. P. Lemoine, M. Gross and J. Boissier, J. Chem. Soc. Dal., 1626 (1972).

31. L. B. Handy, P. M. Treichel, L. F. Dahl, and R. G. Hayter, J. Amer. Chem. Soc., 88, 366 (1966).

32. R. G. Hayter, Ibid., 88, 4376 (1966).

33. W. C. Kaska, Ibid., 90, 6340 (1968); 91, 2411 (1969).

34. E. Lindner, H. Behrens, and S. Birkle, J. Organomet. Chem., 15 165 (1968).

35. H. Behrens and W. Haag, Chem. Ber., 94, 312 (1961); Z. Naturforsch. B, 14, 600 (1959).

36. H. Behrens and W. Kleck, Z. Anorg. Allg. Chem., 292, 151 (1957).

37. H. Behrens and J. Vogl, Chem. Ber., 96, 2220 (1963).

38. U. Anders and W. A. G. Graham, Chem. Comm., 499 (1965).

39. J. K. Ruff, Inorg. Chem., 6, 2080 (1967).

40. U. Anders and W. A. G. Graham, J. Amer. Chem. Soc., 89, 539 (1967). These people also failed to observe any protonation product when $MnCr(CO)_{10}^-$ was treated with 90% H_3PO_4.

41. M. F. Bailey and L. F. Dahl, Inorg. Chem., 4, 1140 (1965).

42. R. F. Bryan and P. T. Greene, J. Chem. Soc. A, 3064 (1970).

43. R. F. Bryan, P. T. Greene, M. J. Newlands, and D. S. Field, Ibid., 3068 (1970).

44. J. G. Bullit, F. A. Cotton, and T. J. Marks, Inorg. Chem., 11, 671 (1972).

45. O. A. Gansow, A. R. Burke, and W. D. Vernon, J. Amer. Chem. Soc., 94, 2550 (1972).

46. A. R. Manning and P. A. McArdle, J. Chem. Soc. A, 1498 (1969).

47. A. R. Manning, Ibid., 1319 (1968).

48. T. S. Piper, F. A. Cotton, and G. Wilkinson, J. Inorg. and Nucl. Chem., 1, 165 (1955).

49. F. A. Cotton, A. D. Liehr, and G. Wilkinson, Ibid., 1, 175 (1955).

50. F. A. Cotton, H. Stammreich, and G. Wilkinson, Ibid., 9, 3 (1959).

51. N. Noack, Ibid., 25, 1383 (1963).

52. R. D. Fisher, A. Vogler, and K. Noack, J. Organomet. Chem., 7, 135 (1967).

53. N. Noack, Ibid., 7, 151 (1967).

54. F. A. Cotton and G. Yagupsky, Inorg. Chem., 6, 15 (1967).

55. E. Weiss, H. Hubel, and R. Merenyi, Chem. Ber., 95, 1155 (1962).

56. For IR studies of closely related compounds, see P. McArdle and R. Manning, J. Chem. Soc. A, 717 (1971); Ibid., 2119, 2123, 2133 (1970).

57. R. J. Haines and A. L. DuPreez, Inorg. Chem., 8, 1459 (1969).

58. For the synthesis of other phosphine substituted iron dimers, see

a) R. B. King, P. N. Kapoor, and R. N. Kapoor, Ibid., 10, 1841 (1971);

b) R. J. Haines and A. L. DuPreez, J. Organomet. Chem., 21, 181 (1970).

59. For interesting studies of the oxidation of these and closely related iron compounds see

a) J. A. Ferguson and T. J. Meyer, Inorg. Chem., 11, 631 (1972);

b) J. A. Ferguson and T. J. Meyer, Ibid., 10, 1025 (1971);

c) N. G. Connelly and L. F. Dahl, J. Amer. Chem. Soc., 92, 7472 (1970);

d) M. A. Neuman, Trinh-Toan, and L. F. Dahl, Ibid., 94, 3383 (1972);

e) Trinh-Toan, W. P. Fehlhammer, and L. F. Dahl, Ibid., 94, 3389 (1972).

60. T. Blackmore, M. I. Bruce, and F. G. A. Stone, J. Chem. Soc. A, 2158 (1968).

61. P. McArdle and A. R. Manning, Ibid., 2128 (1970).

62. For the synthesis of $[CpOs(CO)_2]_2$, see reference 52.

63. R. J. Haines and A. L. DuPreez, J. Chem. Soc. Dal., 944 (1972); J. Chem. Soc. A, 2341 (1970); J. Amer. Chem. Soc., 91, 769 (1969).

64. F. Bonati and G. Wilkinson, J. Chem. Soc., 179 (1964).

65. W. R. Cullen, D.J. Patmore, J. R. Sams, M. J. Newlands, and L. K. Thompson, Chem. Comm., 952 (1971).

66. S. R. A. Bird, J. D. Donaldson, A. F. LeC. Holding, B. J. Senior, and M. J. Tricker, J. Chem. Soc. A, 1616 (1971).

67. A. Davison, J. A. McCleverty, and G. Wilkinson, J. Chem. Soc., 1133 (1963).

68. Y. S. Sohn, D. N. Hendrickson, and H. B. Gray, J. Amer. Chem. Soc., 93, 3603 (1971). There is a mistake in Table II of this reference. Band II of $Fe(Cp)_2$ should have an ϵ value of 91.0 and not 9.10. This is clearly shown in Figure 2 of the same article.

69. H. D. Kaesz and R. B. Saillant, Chem. Revs., 72, 231(1972).

70. N. A. Paauwe, Ph.D. Thesis, Purdue University, 1968.

71. W. F. Edgell and N. A. Paauwe, Chem. Comm., 284 (1969).

72. A. G. Osborne and M. H. B. Stiddard, J. Chem. Soc., 634 (1964).

73. $Mn_2(CO)_8(P\phi_3)_2$ has only axial substitution. For the first confirmed report (X-ray study) of a compound with equatorial arsine substituents, see M. Laing, T. Ashworth, P. Sommerville, E. Singleton, and R. Reimann, Chem. Comm., 1251 (1972).

74. W. F. Edgell, J. W. Fisher, G. Asato, and W. M. Risen, Jr., Inorg. Chem., 8, 1103 (1969).

75. K. Nakamoto, "Infrared Spectra of Inorganic and Coordination Compounds," Wiley-Interscience, New York, 1970 ed., pages 10-16.

76. D. K. Ottesen (Ph.D. Thesis, California Institute of Technology, 1971) has shown that similar approximations used to derive the Mn-Mn force constant of $Mn_2(CO)_{10}$ are in serious error (a factor of two) because coupling to Mn-C modes is ignored.

77. Davison, et al.[3] assigned a weak band at 1767 cm^{-1} to ν_{as} (Fe-H-Fe) but Symon and Waddington[4] showed that this band is actually due to unprotonated starting material. Our own work agrees with Symon and Waddington. Studies of the

protonation and deuteration of $[CpFe(CO)_2]$ in $CHCl_3$ with HBr and DBr show no bands in the region 1000-2300 cm^{-1} that can be assigned to the Fe-H-Fe vibration. Davison[3] also observed weak bands at 1760 and 1270 cm^{-1} in the compounds $CpFe(CO)_2$-H-$Mn(CO)_5^+$ and $CpFe(CO)_2$-D-$Mn(CO)_5^+$ assigned as Fe-H-Mn and Fe-D-Mn modes, respectively. This observation has never been confirmed or denied since the initial report.

78. In the section on infrared spectra we discuss the possibility of other rotamers in different solvents. We have no infrared spectra of $[CpFe(CO)_2]_2H^+$ in the solvents used for UV-VIS absorption studies (acetone and acetic acid) so the trans (C_{2h}) structure has not been verified in our solutions.

79. M. I. Bruce, J. Howard, I. W. Nowell, G. Shaw, and P. Woodward, Chem. Comm., 1041 (1972).

80. M. I. Bruce, M. A. Cairns, and M. Green, J. Chem. Soc. Dal., 1293 (1972).

81. B. F. G. Johnson, R. D. Johnson, J. Lewis, B. H. Robinson, and G. Wilkinson, J. Chem. Soc. A, 2856 (1968).

82. R. C. Dobbie, M. J. Hopkinson, D. Whittaker, J. Chem. Soc. Dal., 1030 (1972).

83. C. J. Gilmore and P. Woodward, J. Chem. Soc. A, 3453(1971).

84. A. Cox and P. Woodward, Ibid., 3599 (1971).

85. B. E. Cavit, K. R. Grundy, and W. R. Roper, Chem. Comm., 60 (1972).

86. J. J. Hough and E. Singleton, Ibid., 371 (1972).

87. T. Blackmore, M. I. Bruce, and F. G. A. Stone, J. Chem. Soc. A, 2376 (1971).

88. A. J. Deeming, R. Ettorre, B. F. G. Johnson, and J. Lewis, Ibid., 1797 (1971).

89. In compounds of the type L_5M-X-ML_5 and L_5M-ML_5, the the linear bridged species are all eclipsed whereas the L_5M groups of L_5M-ML_5 are all staggered. This suggests that the barrier to rotation in the bridged species has a low contribution from interligand repulsion and is actually governed by interligand van der Waals attraction. See M. L. Katchner and G. L. Simon, Inorg. Chem., 11, 1651 (1972), and references cited therein.

90. Compounds assigned the structure below, with both bridging ^1H and bridging ^{31}P, show much smaller values of $J_{^{31}P-^1H}$. (P. M. Treichel, W. K. Dean and W. M. Douglas, Inorg. Chem., 11, 1609 (1972).) Notice that these compounds do not follow the correlation of large chemical shift for bridging hydrogen.

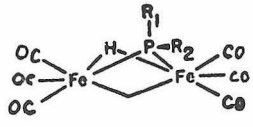

R_1	R_2	τ_H(ppm)	$J_{^{31}P-^1H}$(Hz)
C_6H_5	C_6H_5	12.58	11.0
C_6H_5	CH_3	12.56	11.0
CH_3	CH_3	12.20	13.0
C_2H_5	C_2H_5	12.20	12.0

These authors try to pass off IR bands near 3600 cm^{-1} as Fe-H vibrations. This is preposterous!

91. W. Jetz and W. A. G. Graham, Inorg. Chem., 10, 1159 (1971). An interesting note is that the compound XVII, is second only to $HClO_4$ as an acid in CH_3CN. It is a stronger acid than H_2SO_4!

92. ^{57}Fe-^{13}C and ^{57}Fe-^{31}P coupling has also been observed recently. See B. E. Mann, Chem. Comm., 1173 (1971).

93. G. M. Whitesides and G. Maglio, J. Amer. Chem. Soc., 91, 4980 (1969).

94. In the compound below, vicinal ^{14}N-^{1}H coupling is observed, but no geminal coupling is seen. This example is cited on page 442 of the third edition (yellow cover) of the Chem Two Bestiary. The source is a communication in J. Amer. Chem. Soc., prior to March 1971, but we have not been able to locate the article.

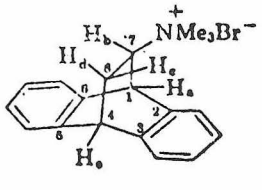

	$J_{^{14}N-^{1}H}$ (Hz)
H_a	≤ 0.3
H_b	--
H_c	2.7
H_d	0.8

95. S. Bruckenstein and I. M. Kolthoff, J. Amer. Chem. Soc., 78, 1, 10, 2974 (1956); 79, 1, 5915 (1957).

96. The controversy is between Muetterties, et al.[97-99] and a group of Caltech people who propose different species and different mechanisms to account for the fluxional behavior of H_2FeL_4 ($L = \phi P(OEt)_2$) and related compounds.

97. F. N. Teebe, P. Meakin, J. P. Jesson, and E. L. Muetterties, Ibid., 92, 1068 (1970).

98. P. Meakin, L. J. Guggenberger, J. P. Jesson, D. H. Gerlach, F. N. Tebbe, W. G. Peet, and E. L. Muetterties, Ibid., 92, 3482 (1970).

99. P. Meakin, E. L. Muetterties, F. N. Teebe, and J. P. Jesson, Ibid., 93, 4701 (1971).

100. L. J. Guggenberger, D. D. Titus, M. T. Flood, R. E. Marsh, A. A. Orio, and H. B. Gray, Ibid., 94, 1135 (1972).

101. The solid state structure of $HCoL_4$ is a distorted trigonal bipyramid or a face-capped tetrahedron. At -55° in methylcyclohexane only a single broad NMR absorption is observed. (D. D. Titus, A. A. Orio, R. E. Marsh, and H. B. Gray, Chem. Comm., 322 (1971).)

102. The fluxionalism of many similar five-coordinate compounds is discussed by P. Meakin, E. L. Muetterties, and J. P. Jesson, J. Amer. Chem. Soc., 94, 5271 (1972).

103. P. Meakin, J. P. Jesson, F. N. Tebbe, and E. L. Muetterties, Ibid., 93, 1797 (1971).

104. A. Yamamoto, S. Kitazume, L. S. Pu, and S. Ikeda, Ibid., 93, 371 (1971).

105. Evidence is presented in the section on infrared spectra that the protonated dimer, V, may exist in a cisoid C_{2v} conformation in $CHCl_3$.

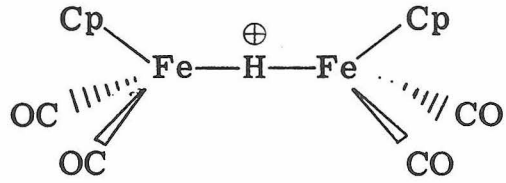

C_{2v}

In this conformation, the $\sigma \rightarrow \sigma^*$ transition is allowed. This may account for the 21 kK shoulder in the acetone spectrum listed in Table VIII.

106. A sample of $(Fe_2PH^+)(B\phi H_4^-)$ stored in a refrigerator (at 4°C) for 5 months gave an infrared spectrum with bands at 2057, 2032, 2011, 1981, and 1951 cm^{-1}, as well as weak bands at 1765 and 1730 cm^{-1}. An isomerization in the solid state apparently occurs to give the same isomers present in the PF_6^- salt.

107. The structure is presumed to be the one shown below by analogy to the structure of the bromine analog. (S. Merlino and G. Montagloni, Acta Cryst., 24B, 424 (1968).

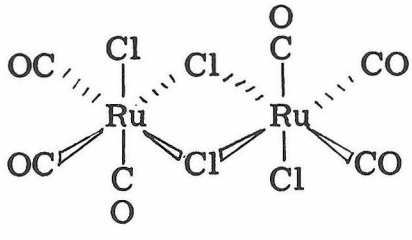

108. M. J. Cleare and W. P. Griffith, J. Chem. Soc. A, 372 (1969).

109. K. Farmery, M. Kilner, R. Greatrex, and N. N. Greenwood, Ibid., 2339 (1969).

Chapter Seven

Graphical Display of Pernicious Acid-Base Equilibria in Acetic Acid

There comes a point in most Ph.D. theses when the innate appeal of the subject matter can stifle even the most avid reader. If you have not found such a point yet, this is it. During the fleeting moment when acid-base equilibria in acetic acid solution were important to this work, a method was developed to depict such equilibria graphically. This method is analogous to the graphical techniques used for aqueous solutions. An excellent review of these techniques has been written by Sillén.[1] As the equilibria in acetic acid are much more complicated than those in water, a brief description of the aqueous solution treatment will be presented first.

Consider the case of dissolving enough base, B, in water to form a 10^{-3} F solution. Figure 1 is a plot of the logarithim of the concentration of each species in solution versis the pH. The relevant equilibria are

$$B + H_2O \overset{K_B}{\rightleftharpoons} BH^+ + OH^-$$

$$BH^+ + H_2O \overset{K_A}{\rightleftharpoons} B + H_3O^+$$

$$2H_2O \overset{K_W}{\rightleftharpoons} H_3O^+ + OH^-$$

$$K_BK_A = K_W$$

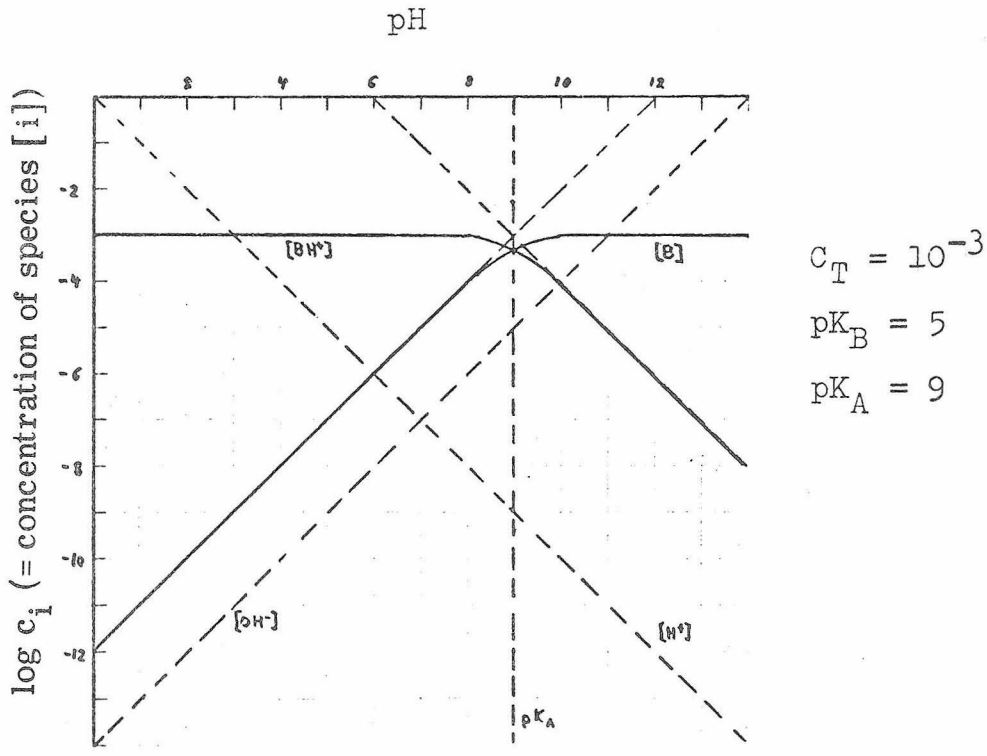

Figure 1. Log c_i vs. pH for aqueous solution

The salient features of Figure 1 include the following. At high pH ($pH \gg pK_A$) [B] approaches C_T, the total concentration of base derived species ($C_T = [B] + [BH^+]$). At low pH ($pH \ll pK_A$) $[BH^+]$ approaches C_T. At $pH = pK_A$, $[B] = [BH^+]$. At low pH [B] approaches an asymptote of slope +1 which passes through the point $C_T = pK_A$. At high pH $[BH^+]$ approaches an symptote of slope -1 which also passes through the point $C_T = pK_A$.

For the study of acid-base equilibria in any solvent, the overriding features of the solvent which determine the kind of

chemistry which can occur are the protic or aprotic nature of the solvent and the dielectric constant. That acetic acid is protic makes it similar to water. The solvent undergoes autoionization with an ionization constant remarkably similar to that of water:

$$2CH_3CO_2H = CH_3CO_2H_2^+ + CH_3CO_2^-$$

$$K_S = [CH_3CO_2H_2^+][CH_3CO_2^-] = 10^{-14.45} \ (25\,°C)$$

That acetic acid has a dielectric constant of 6.13 makes it abyssmally different from water. Dissociation of electrolytes into solvated ions is a severely limited possibility. It is this difference from water which changes the whole set of rules and regulations.

The important equilibria which occur in acetic acid when an acid or a base is dissolved were first delineated by Bruckenstein and Kolthoff.[2] A marvelous summary of the important equilibrium relationships has been written by Laitinen.[3] At this time the reader is remanded to the custody of a few pages lifted directly from Laitinen's book. It is necessary to understand this material if the present paper is to be meaningful. Good luck.

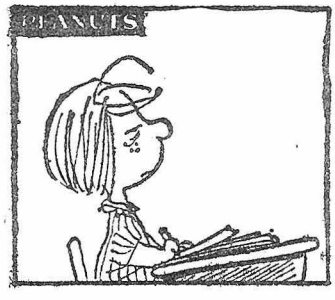

4-5. Acid-Base Equilibria in Glacial Acetic Acid

Glacial acetic acid is strongly acidic and very weakly basic compared with water. In addition, its dielectric constant is only 6.13; so there is a strong tendency toward incomplete dissociation of ion aggregates. It is important to distinguish between ionization and dissociation,[3] described by the following reactions for an acid HA and a base B:

$$\mathrm{HA} + \mathrm{HOAc} \underset{\text{Ionization}}{\rightleftharpoons} \mathrm{H_2OAc^+A^-} \underset{\text{Dissociation}}{\rightleftharpoons} \mathrm{H_2OAc^+} + \mathrm{A^-} \qquad (4\text{-}37)$$

$$\mathrm{B} + \mathrm{HOAc} \rightleftharpoons \mathrm{BH^+OAc^-} \rightleftharpoons \mathrm{BH^+} + \mathrm{OAc^-} \qquad (4\text{-}38)$$

As in any other solvent, the corresponding equilibrium constants can be written in terms of activities or approximately in terms of concentrations. However, owing to the low dielectric constant of glacial acetic acid, even "strong" electrolytes have dissociation constants only of the order of 10^{-5}, so that high ionic strengths are never encountered. Therefore, it is a good approximation to write concentrations rather than activities of all species.[4]

The ionization constant of an acid HA is written

$$K_i^{\mathrm{HA}} = \frac{[\mathrm{H_2OAc^+A^-}]}{[\mathrm{HA}]} \qquad (4\text{-}39)$$

From Reference 3. Used with permission of McGraw-Hill Book Company.

The dissociation constant is

$$K_d^{\mathrm{HA}} = \frac{[\mathrm{H_2OAc^+}][\mathrm{A^-}]}{[\mathrm{H_2OAc^+A^-}]} \qquad (4\text{-}40)$$

and the over-all dissociation constant is

$$K_{\mathrm{HA}} = \frac{[\mathrm{H_2OAc^+}][\mathrm{A^-}]}{[\mathrm{HA}] + [\mathrm{H_2OAc^+A^-}]} = \frac{[\mathrm{H_2OAc^+}][\mathrm{A^-}]}{C_{\mathrm{HA}}} = \frac{K_i^{\mathrm{HA}} K_d^{\mathrm{HA}}}{1 + K_i^{\mathrm{HA}}} \qquad (4\text{-}41)$$

where C_{HA} is the total concentration of undissociated acid, that is, $[\mathrm{HA}] + [\mathrm{H_2OAc^+A^-}]$.

Corresponding expressions for bases are:

$$K_i^{\mathrm{B}} = \frac{[\mathrm{BH^+OAc^-}]}{[\mathrm{B}]} \qquad (4\text{-}42)$$

$$K_d^{\mathrm{B}} = \frac{[\mathrm{BH^+}][\mathrm{OAc^-}]}{[\mathrm{BH^+OAc^-}]} \qquad (4\text{-}43)$$

$$K_{\mathrm{B}} = \frac{[\mathrm{BH^+}][\mathrm{OAc^-}]}{[\mathrm{B}] + [\mathrm{BH^+OAc^-}]} = \frac{[\mathrm{BH^+}][\mathrm{OAc^-}]}{C_{\mathrm{B}}} = \frac{K_i^{\mathrm{B}} K_d^{\mathrm{B}}}{1 + K_i^{\mathrm{B}}} \qquad (4\text{-}44)$$

where C_{B} is the total concentration of undissociated base, that is, $[\mathrm{B}] + [\mathrm{BH^+OAc^-}]$.

An acid may, rather arbitrarily, be called a strong acid in glacial acetic acid if $K_i^{\mathrm{HA}} \geq 1$. Thus perchloric acid is a strong acid; yet its over-all dissociation constant is only $10^{-4.87}$ because it exists largely as ion pairs.[1]

Bruckenstein and Kolthoff[1] used spectrophotometric and potentiometric measurements to establish an acidity scale and to determine dissociation constants of a number of acids and bases (Table 4-6). The autoprotolysis of acetic acid was found to be described by the equilibrium

$$2\mathrm{HOAc} \rightleftharpoons \mathrm{H_2OAc^+} + \mathrm{OAc^-} \qquad \mathrm{pK_s} = 14.45 \qquad (4\text{-}45)$$

Compared with their counterparts in water solution, acid-base titrations in glacial acetic acid are subject to several peculiar effects.[2] We shall consider here the several equilibria involved in the titration of weak base B with perchloric acid, assuming first that the change in acidity is indicated by the change in potential of an electrode, and then that an indicator is used.

Solution of a Base B. If the total undissociated base concentration is given by $C_{\mathrm{B}} = [\mathrm{B}] + [\mathrm{BH^+OAc^-}]$ and if the analytical concentration of base is designated $(C_{\mathrm{B}})_t$, then

$$(C_{\mathrm{B}})_t = C_{\mathrm{B}} + [\mathrm{BH^+}] = C_{\mathrm{B}} + [\mathrm{OAc^-}] \qquad (4\text{-}46)$$

TABLE 4-6. OVER-ALL DISSOCIATION CONSTANTS OF ACIDS, BASES, AND SALTS IN GLACIAL ACETIC ACID

	Compound	pK
Acids	Perchloric acid	4.87
	Sulfuric acid	7.24
	p-Toluene sulfonic acid	8.46
	Hydrochloric acid	8.55
Bases	Tribenzylamine	5.36
	N,N-Diethylaniline	5.78
	Pyridine	6.10
	Potassium acetate	6.10
	p,p'-N,N'-dimethylaminazobenzene	6.32
	Sodium acetate	6.58
	Lithium acetate	6.79
	2,5-Dichloroaniline	9.48
	Urea	10.24
Salts	Sodium perchlorate	5.48
	Diethylaniline perchlorate	5.78
	Tribenzylamine hydrochloride	6.71
	Diethylaniline hydrochloride	6.84
	Potassium chloride	6.88
	Urea hydrochloride	6.96
	Lithium chloride	7.08
	Dodecylamine hydrochloride	7.45

[With permission from Bruckenstein, S., and Kolthoff, I. M., *J. Am. Chem. Soc.*, **78**, 2974 (1956).]

and, from (4-44),

$$K_B = \frac{[OAc^-]^2}{C_B} = \frac{[OAc^-]^2}{(C_B)_t - [OAc^-]} = \frac{[OAc^-]^2}{(C_B)_t} \tag{4-47}$$

The approximation $C_B = (C_B)_t$ in Eq. (4-47) is generally valid because of the low degree of dissociation in glacial acetic acid. Setting $[H_2OAc^+] = K_s/[OAc^-]$, we have

$$[H_2OAc^+] = \frac{K_s}{\sqrt{K_B(C_B)_t}} \tag{4-48}$$

The hydrogen ion concentration varies inversely as the square root of the concentration of base. Thus, for a hundredfold increase in base concentration, the pH increase is 1 unit.[1-3]

Solution of Base B and Its Perchlorate. It is necessary to consider the dissociation equilibria of the salt $BH^+ClO_4^-$ and the acid as well as those of the weak base.

The dissociation of the salt is expressed by an equation analogous to (4-41) or (4-44):

$$K_{BHClO_4} = \frac{[BH^+][ClO_4^-]}{C_{BHClO_4}} \tag{4-49}$$

The electroneutrality expression is

$$[H_2OAc^+] + [BH^+] = [OAc^-] + [ClO_4^-] \tag{4-50}$$

And, to calculate $[H_2OAc^+]$, we can express the other concentrations in terms of the desired hydrogen ion concentration, as follows:

From Eqs. (4-44) and (4-45),

$$[BH^+] = \frac{K_B C_B}{[OAc^-]} = \frac{K_B C_B [H_2OAc^+]}{K_s} \tag{4-51}$$

From Eqs. (4-49) and (4-51),

$$[ClO_4^-] = \frac{K_{BHClO_4} C_{BHClO_4}}{[BH^+]} = \frac{K_{BHClO_4} C_{BHClO_4} K_s}{K_B C_B [H_2OAc^+]} \tag{4-52}$$

Combining Eqs. (4-45), (4-50), (4-51), and (4-52), we have

$$[H_2OAc^+] = \left\{ \frac{K_s(1 + K_{BHClO_4} C_{BHClO_4}/K_B C_B)}{1 + K_B C_B/K_s} \right\}^{1/2} \tag{4-53}$$

If the base is strong enough to give a detectable end point, $K_B C_B/K_s$ is much greater than 1; so Eq. (4-53) becomes

$$[H_2OAc^+] = \frac{K_s}{K_B C_B} (K_{BHClO_4} C_{BHClO_4} + K_B C_B)^{1/2} \tag{4-54}$$

Kolthoff and Bruckenstein[1] pointed out an interesting relationship for the case in which K_B and K_{BHClO_4} are approximately equal. Thus, for diethylaniline, both pK values are equal to 5.78 (Table 4-6). Now, if the titrant is relatively concentrated so that the sum of $C_B + C_{BHClO_4}$ remains sensibly constant and equal to C, Eq. (4-54) reduces to

$$[H_2OAc^+] = \frac{K_s}{C_B}\sqrt{\frac{C}{K_B}} = \frac{K'}{C_B} \tag{4-55}$$

where $K' = K_s\sqrt{C/K_B} \cong$ constant during titration. Thus the hydrogen ion concentration is inversely proportional to the concentration of untitrated base. If X is the fraction titrated, a plot of log $(1 - X)$ vs.

pH is a straight line, as is observed for a *strong acid–strong base* titration curve in water. Such a relationship was actually observed by Hall and Werner[1] for guanidine and for diethylaniline. It appeared paradoxical because the solution of the pure base behaved like a typical weak base upon dilution.

It will be noted that, for aqueous solution, the quantity $\log[(1 - X)/X]$ plotted against pH yields a straight line for the titration of a weak base with a strong acid. No relationship of this type exists in acetic acid. Therefore it is not possible to reason directly by analogy and use buffer formulas derived for aqueous solutions in acetic acid.

Ordinarily, Eq. (4-54) may be applied using stoichiometric concentrations instead of equilibrium concentrations for C_B and C_{BHClO_4}. This is analogous to applying the simple buffer formulas in water. For an equimolar mixture of base and its salt, such that $C_B = C_{BHClO_4} = C$, Eq. (4-54) becomes

$$[H_2OAc^+] = K_s\left(\frac{K_{BHClO_4} + K_B}{K_B^2 C}\right)^{1/2} \tag{4-56}$$

and, therefore, the hydrogen ion concentration increases tenfold for a hundredfold dilution. A similar result was observed also by Hall and Werner.[2]

If the base is very weak, K_{BHClO_4} is much greater than K_B, and Eq. (4-54) becomes

$$[H_2OAc^+] = \frac{K_s}{K_B C_B}\sqrt{K_{BHClO_4} C_{BHClO_4}} \tag{4-57}$$

If C_{BHClO_4} is set equal to X and C_B equal to $1 - X$, a plot of pH vs. $\log\{\sqrt{X}/(1 - X)\}$ should yield a straight line. Kolthoff and Bruckenstein[3] found this to be true for urea.

Solution of a Pure Salt. To calculate the acidity at the equivalence point, the equilibrium constant of the titration reaction is considered:

$$B + HClO_4 \rightleftharpoons BHClO_4 \qquad K_f^{BHClO_4} = \frac{C_{BHClO_4}}{C_B C_{HClO_4}} \tag{4-58}$$

where $K_f^{BHClO_4}$ is the formation constant of the salt $BHClO_4$. It follows from Eqs. (4-41), (4-44), and (4-45) that

$$K_f^{BHClO_4} = \frac{K_{HClO_4} K_B}{K_s K_{BHClO_4}} \tag{4-59}$$

Equation (4-54) can be simplified because, for most salts, $K_B C_B$ is negligible in comparison to $K_{BHClO_4} C_{BHClO_4}$, so that

$$[H_2OAc^+] = \sqrt{\frac{K_s^2 K_{BHClO_4} C_{BHClO_4}}{K_B^2 C_B^2}} \tag{4-60}$$

At the equivalence point $C_B = C_{HClO_4}$, and, from Eqs. (4-58) and (4-59),

$$C_B^2 = \frac{C_{BHClO_4}}{K_f^{BHClO_4}} = \frac{C_{BHClO_4} K_s K_{BHClO_4}}{K_{HClO_4} K_B}$$

which, when substituted into Eq. (4-60), gives

$$[H_2OAc^+] = \sqrt{K_s K_{HClO_4}/K_B} \tag{4-61}$$

Equation (4-61) yields the interesting conclusion that the hydrogen ion concentration of a pure salt solution is *independent of the concentration of salt.* On this basis Kolthoff and Bruckenstein suggested that titration to an equivalence potential should actually be more useful than determining the inflection point of a titration curve.

Solution of Salt plus Excess Acid. From Eqs. (4-58) and (4-59),

$$\frac{K_B C_B}{K_s} = \frac{K_{BHClO_4}}{K_{HClO_4}}\frac{C_{BHClO_4}}{C_{HClO_4}} \tag{4-62}$$

Substituting into Eq. (4-53),

$$[H_2OAc^+]^2 = \frac{K_s + K_{HClO_4} C_{HClO_4}}{1 + K_{BHClO_4} C_{BHClO_4}/K_{HClO_4} C_{HClO_4}} \tag{4-63}$$

which holds at all points of the titration. In the presence of an appreciable excess of acid, $K_{HClO_4} C_{HClO_4}$ is much greater than K_s, so that Eq. (4-63) becomes

$$[H_2OAc^+] = \frac{K_{HClO_4} C_{HClO_4}}{\sqrt{K_{HClO_4} C_{HClO_4} + K_{BHClO_4} C_{BHClO_4}}} \tag{4-64}$$

In the vicinity of the end point, C_{BHClO_4} is much greater than C_{HClO_4}. Either of the two terms under the square-root sign may be negligible in certain cases, depending upon the relative magnitudes of K_{HClO_4} and K_{BHClO_4}.

Let us establish the following nomenclature:

CH_3CO_2H	=	HS	acid	=	HA
$CH_3CO_2H_2^+$	=	H_2S^+	base	=	B
$CH_3CO_2^-$	=	S^-	salt	=	BHA

Laitinen's equations describe either the titration of B with HA or the titration of HA with B. We will examine a method for plotting the concentrations of all the pertinent species in either titration. It is convenient to choose perchloric acid ($pK_A = 4.87$) as the acid in all the examples which follow. I will outline a method for plotting the logarithm of the concentration of each species versus pH. Following the procedure will be an explanation of why it works.

<u>Titration of B with HA.</u> There are three cases:

(i) $K_B > K_{BHA}$

(ii) $K_{BHA} > K_B$

(iii) $K_B = K_{BHA}$

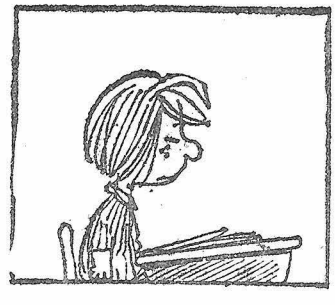

<u>Case (i).</u>

(a) The background for any of our plots will be a log-log plot showing $[H_2S^+]$ and $[S^-]$ vs. pH (Figure 2a.)

(b) The calculational input for this graphical technique involves four pH values, <u>viz</u> ∴

line (1): $[H_2S^+] = (K_{BHA}C_T)^{\frac{1}{2}}$

line (2): $[H_2S^+] = (K_S K_{HA}/K_B)^{\frac{1}{2}}$

line (3): $[H_2S^+] = K_S(K_{BHA}C_T)^{-\frac{1}{2}}$

line (4): $[H_2S^+] = K_S(K_B C_T)^{-\frac{1}{2}}$

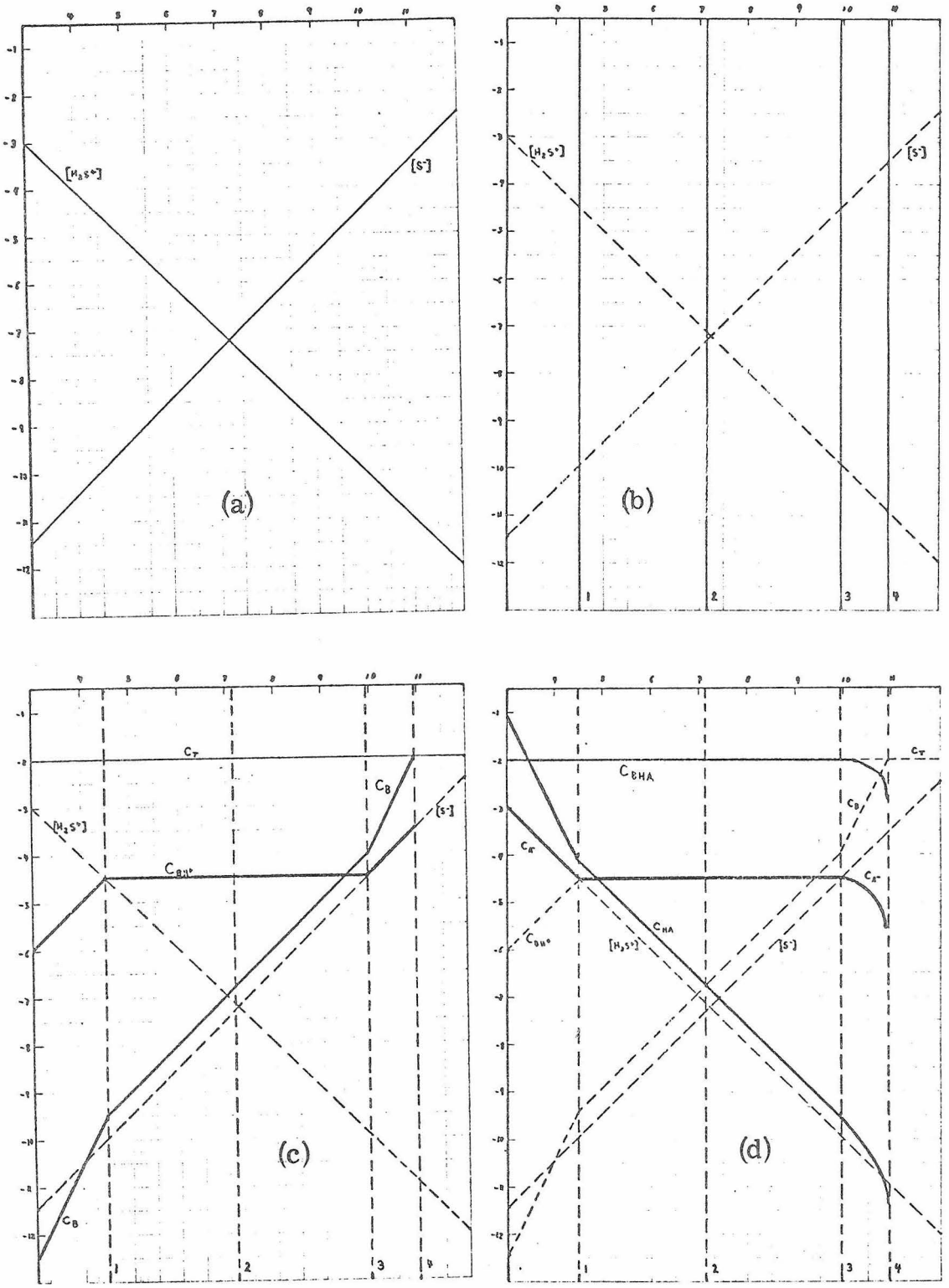

Figure 2. Log c_i vs. pH. Case (i).

These lines are shown in Figure 2b assuming the following values:

$C_T = 10^{-2}$

$K_B = 10^{-5}$

$K_{BHA} = 10^{-7}$

$K_{HA} = 10^{-4.87}$

(c) We will first plot the "idealized concentrations" of the base and its conjugate acid. By "idealized concentration" we generally mean the asymptotic concentrations but some of these lines are not true asymptotes. The significance of these lines will become clear with a few examples. The concentration of species i will hereafter be designated either [i] or C_i. The C_B plot starts at $C_B = C_T$ at line (4), the initial pH of the solution. This line goes down from line (4) with a slope of +2. At line (3) the slope changes to +1. At line (1) the slope reverts to +2. An actual plot of C_B would not have sharp corners at the slope changeover points. The C_B and C_{BH^+} lines are shown in Figure 2c. The C_{BH^+} line starts at the intersection of the $[S^-]$ line and line (4). Its slope is +1 until it reaches line (3) where the slope becomes zero. At line (1) (where the C_{BH^+} and $[H_2S^+]$ lines must meet) the slope goes to +1 again.

(d) Figure 2d shows C_{BHA}, C_{HA}, and C_{A^-}. The C_{BHA} line is level at C_T for most of the plot. It has an initial value of $10^{-\infty}$ at line (4) and crosses the C_B line at $C_B = C_{BHA} = C_T/2$. The C_{A^-} line also has an initial value of $10^{-\infty}$ at line (4). Between lines (3) and (1) it overlaps the C_{BH^+} line and the slope is -1 beyond line (1).

The C_{HA} line intercepts the C_B line at line (2), the end point pH. The C_{HA} line has a slope of -1 between lines (1) and (3). The initial value is again $10^{-\infty}$ at line (4) and to the left of line (1) the slope is -2.

Case (ii). We now choose the following constants:

$$C_T = 10^{-2}$$
$$K_B = 10^{-7}$$
$$K_{BHA} = 10^{-5}$$
$$K_{HA} = 10^{-4.87}$$

(a) Figure 3 is constructed as follows: lines (1), (2), and (4) have the same formulae as in case (i). Line (3) is given by:

$$[H_2S^+] = (K_S/K_B)(K_{BHA}/C_T)^{\frac{1}{2}}$$

(b) The C_B line has an asymptotic slope of zero between lines (3) and (4). At line (3), the slope changes to +1 and at line (1) the slope changes to +2. C_{BH^+} begins at the junction of $[S^-]$ and line (4) with an initial slope of -1. Then it changes to a slope of zero between lines (3) and (1). At line (1) the slope changes to +1. Again, the C_{BH^+} line intercepts the $[H_2S^+]$ line at line (1).

(c) C_{BHA} is constant at C_T at low pH and goes to $10^{-\infty}$ at line (4). Again, it intercepts C_B at $C_{BHA} = C_B = C_T/2$. C_{A^-} starts at $10^{-\infty}$, overlaps C_{BH^+} between lines (3) and (1), and overlaps $[H_2S^+]$ beyond line (1). The C_{HA} line intercepts the C_B line at the end point pH, line (2). It has a slope of -1 between lines (1) and (3) and goes to $10^{-\infty}$ at line (4). To the left of line (1) its slope is -2.

Case (iii). This is intermediate between the first two cases. Figure 4 shows a plot of the titration of N,N-diethylaniline with $HClO_4$. The significant point is that lines (3) and (4) overlap.

$$\text{initial pH} = K_S(K_BC_T)^{-\frac{1}{2}}$$

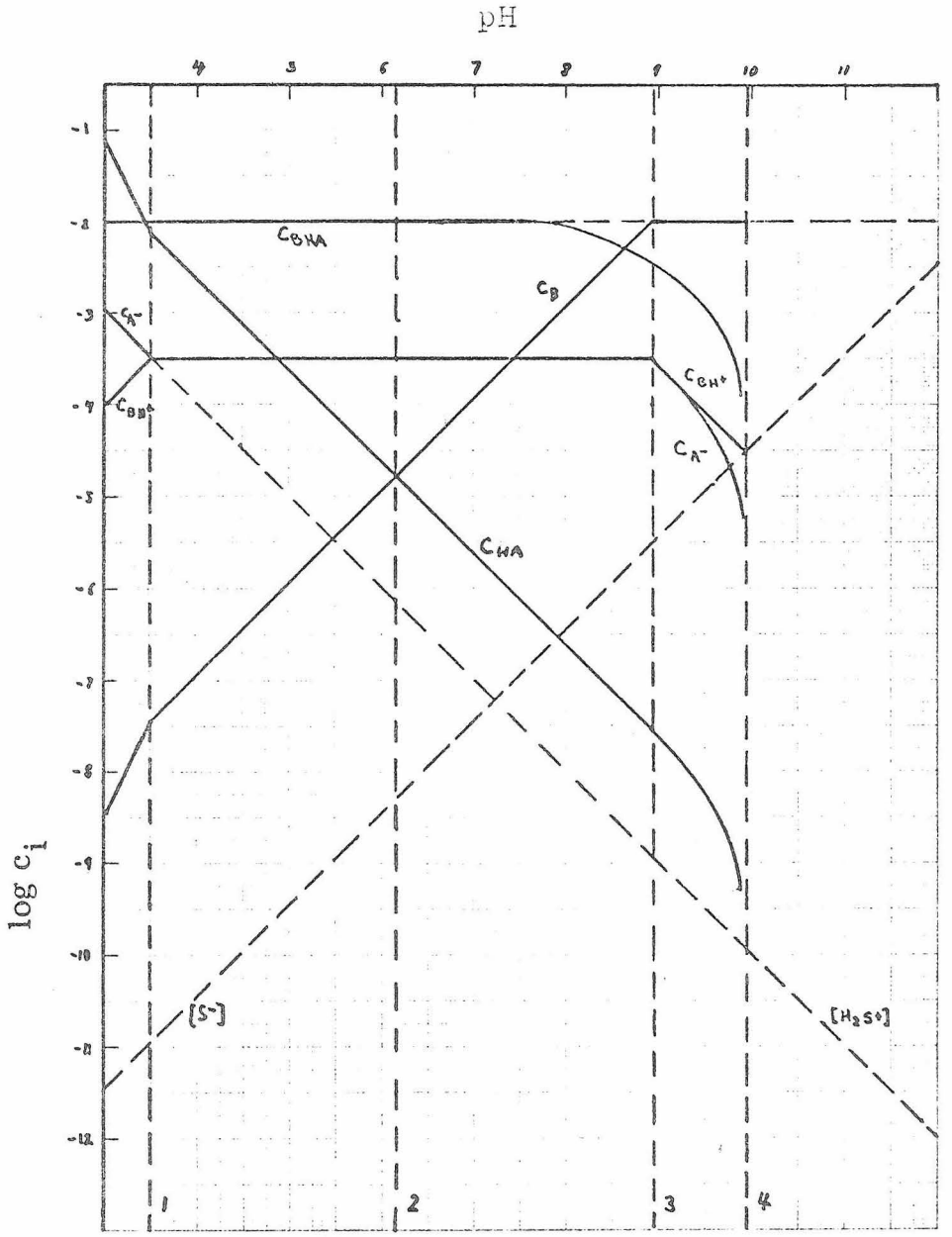

$C_T = 10^{-2}$

$K_B = 10^{-7}$

$K_{BHA} = 10^{-5}$

$K_{HA} = 10^{-4.87}$

Figure 3. Log c_i vs. pH. Case (ii)

line (1): $[H_2S^+] = (K_{BHA}C_T)^{\frac{1}{2}}$

line (2): $[H_2S^+] = (K_S K_{HA}/K_B)^{\frac{1}{2}}$

line (3): $[H_2S^+] = (K_S/K_B)(K_{BHA}/C_T)^{\frac{1}{2}}$

line (4): $[H_2S^+] = K_S(K_B C_T)^{-\frac{1}{2}}$

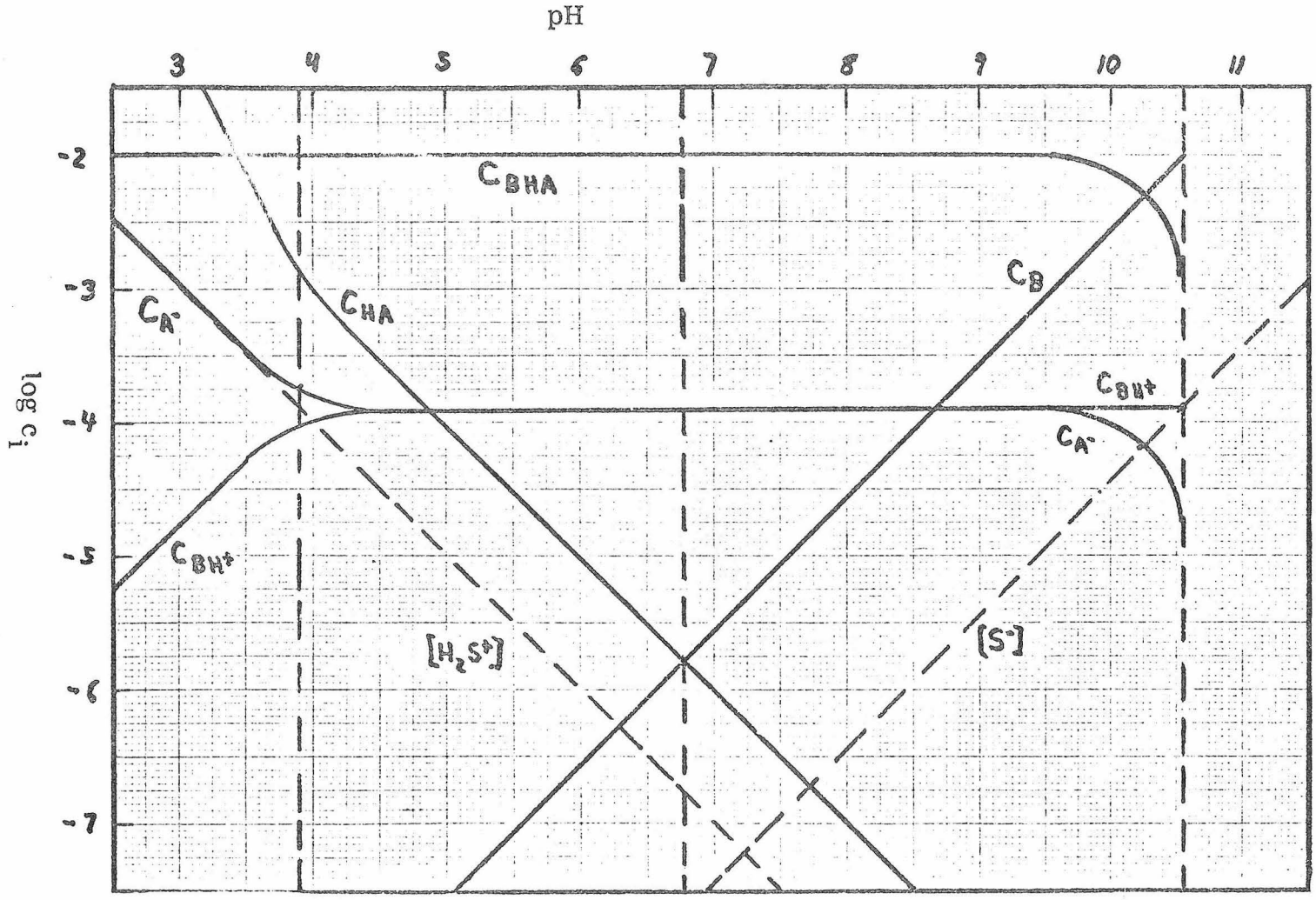

Figure 4. Log c_i vs. pH. Case (iii).

$C_T = 10^{-2}$ $K_B = 10^{-5.78}$ $K_{BHA} = 10^{-5.78}$ $K_{HA} = 10^{-4.87}$

Why do these plots look as they do? Let's examine case (i). Look at the C_B curve. The master equation is (4-53), viz.:

$$[H_2S^+] = \left\{ \frac{K_S \left(1 + \frac{K_{BHA}C_{BHA}}{K_B C_B}\right)}{1 + \frac{K_B C_B}{K_S}} \right\}^{\frac{1}{2}}$$

In the region to the right of line (1), $K_BC_B/K_S \gg 1$ and (4-53) reduces to (4-54).

$$[H_2S^+] = \frac{K_S}{K_BC_B} (K_{BHA}C_{BHA} + K_BC_B)^{\frac{1}{2}}$$

Between (3) and (4), $K_BC_B > K_{BHA}C_{BHA}$ and (4-54) reduces simply to

$$[H_2S^+] \approx \frac{K_S}{(K_BC_B)^{\frac{1}{2}}}$$

or

$$\log [H_2S^+] = \log K_S - \tfrac{1}{2} \log K_B - \tfrac{1}{2} \log C_B$$

$$pH = -\log K_S + \tfrac{1}{2} \log K_B + \tfrac{1}{2} \log C_B$$

$$\frac{d(\log C_B)}{d(pH)} = +2$$

The slope of the C_B line is +2 in this region. Further, the C_B line starts at the intersection of C_T and line (4), since (4) is just the initial pH of the solution. Between lines (1) and (3), $K_BC_B < K_{BHA}C_{BHA}$ and (4-54) reduces to

$$[H_2S^+] \approx \frac{K_S}{K_BC_B} (K_{BHA}C_{BHA})^{\frac{1}{2}} \approx \frac{K_S}{K_BC_B} (K_{BHA}C_T)^{\frac{1}{2}}$$

$$\frac{d(\log C_B)}{d(pH)} = +1$$

To the left of line (1) $K_BC_B/K_S \ll 1$ and (4-53) reduces to

$$[H_2S^+] \approx \{K_S(\frac{K_BC_B + K_{BHA}C_{BHA}}{K_BC_B})\}^{\frac{1}{2}}$$

$$\approx (\frac{K_S\, K_{BHA}C_{BHA}}{K_BC_B})^{\frac{1}{2}}$$

$$\frac{d\,(\log C_B)}{d\,(pH)} = +\,2$$

The C_B curve is finished.

Now look at the C_{BH^+} curve. (4-51) gives

$$[BH^+] = \frac{K_BC_B[H_2S^+]}{K_S}$$

$$\frac{[BH^+]}{C_B} = \frac{K_B}{K_S}[H_2S^+]$$

$$\frac{d(\log \frac{[BH^+]}{C_B})}{dpH} = -\,1$$

This says that the slope of the C_{BH^+} curve is <u>always</u> one unit less than the slope of the C_B curve. The electroneutrality condition is

$$[H_2S^+] + [BH^+] = [S^-] + [A^-]$$

At line (4), $[H_2S^+]$ is negligible and $[A^-] = 10^{-\infty}$. Hence $[BH^+] = [S^-]$. With this initial point and all of the slopes already determined, the C_{BH^+} line is done.

The C_{B^-} line is also easy now because

$$[A^-][BH^+] = C_{BHA}K_{BHA}.$$

In the region where $C_{BHA} \approx C_T$,

$$[A^-][BH^+] = C_T K_{BHA}$$

$$\frac{d[A^-]}{d(pH)} = -\frac{d[BH^+]}{d(pH)}$$

C_{A^-} must start at $10^{-\infty}$ at line (4) and at line (2), the end point, $[A^-] = [BH^+]$. This establishes the entire curve.

Finally, the C_{HA} curve comes from

$$K_{HA} = \frac{[H_2S^+][A^-]}{C_{HA}}$$

$$\frac{d(\log \frac{C_{HA}}{(A^-)})}{d\,(pH)} = -1$$

The slope of the C_{HA} line is always one unit less than the C_{A^-} curve. At the end point, line (2), $C_{HA} = C_B$ and the slope of C_{HA} is -1.

The pH values of lines (1) - (4) were determined as follows. Lines (2) and (4) are just the end point pH and initial pH, respectively. Line (3) is the pH at which a line of unit slope coming from the end point

C_B value intersects a line of slope +2 coming down from the starting point of the C_B curve at C_T. Line (1) is the pH at which a projection of the horizontal (BH^+) line would intersect the $[H_2S^+]$ line.

Now we will briefly examine the graph for case (ii). This is just like case (i) except between lines (3) and (4). Examine the C_B line. At the end point values of pH and C_B, the slope of the C_B line must be +1. Such a line intersects the C_T line at the pH of line (3). The C_B and C_{BHA} lines are very curved in the vicinity of line (3). The slope of the C_B line seemingly must approach zero in the (3) - (4) region in order to give the correct initial value before the titration is begun. Perhaps you can find a more satisfying argument for the slope in the (3) - (4) region but I have none yet. The remainder of the lines are determined exactly as in case (i) once the C_B curve is determined. The slopes in the various regions and one point on each curve is sufficient to determine each and every curve.

Case (iii) is the same as case (i) in which lines (3) and (4) coincide so that the initial slope of C_B is 1.

To determine the points on a titration curve graphically, just use stoichiometric values of C_B or C_{HA}. For example, Figures 5 and 6 show titration curves generated by cases (i) and (ii), respectively. The pH at 80% titration would be the pH at which the C_B line goes through $10^{-2.70}$ M in Figure 5. The pH of the 110% point on the curve comes from the value of pH at which $C_{HA} = 10^{-3}$M. The use of these graphs to determine the shape of a titration curve is exceedingly rapid.

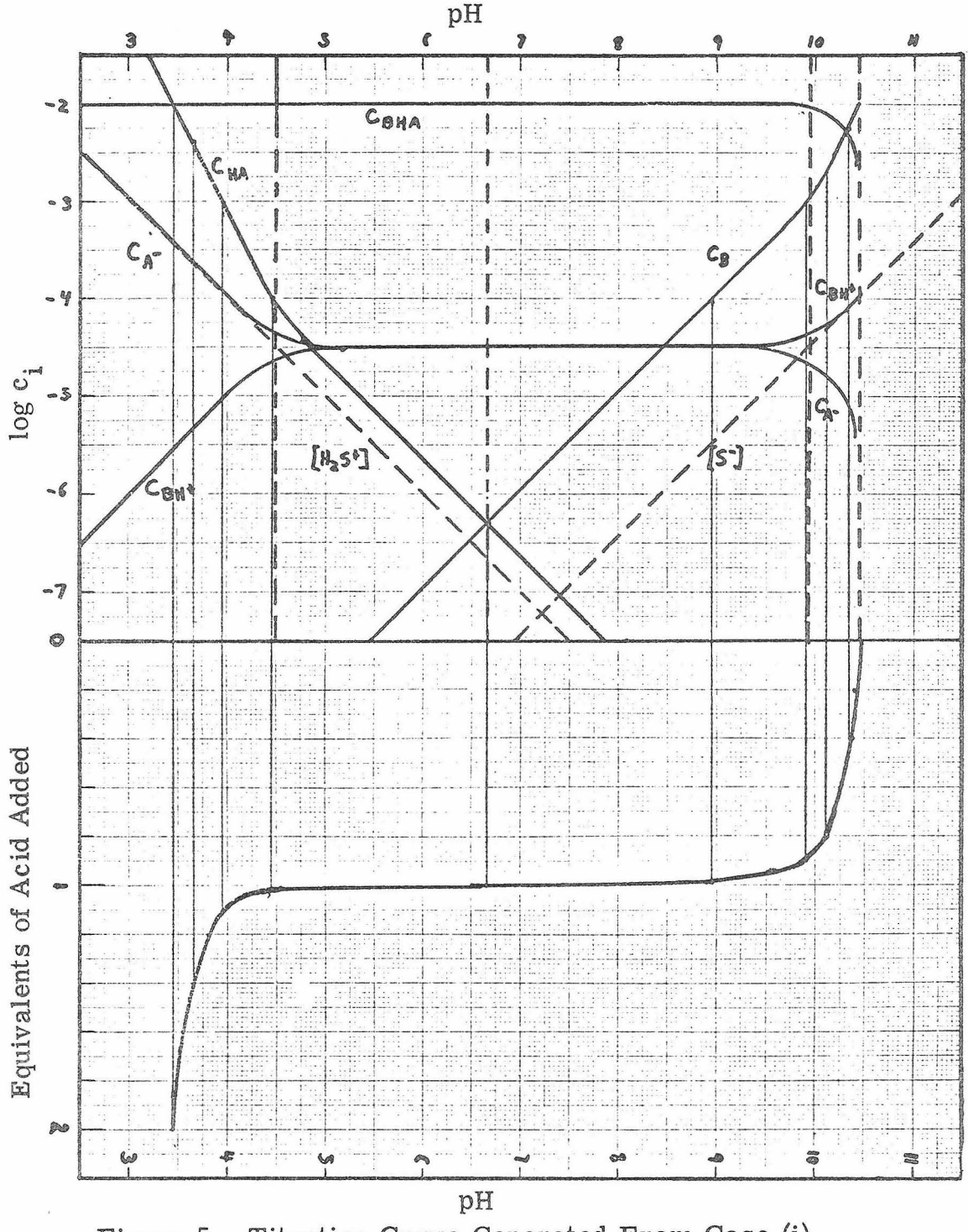

Figure 5. Titration Curve Generated From Case (i).

$C_T = 10^{-2}$ $K_B = 10^{-6}$ $K_{BHA} = 10^{-7}$ $K_{HA} = 10^{-4.87}$

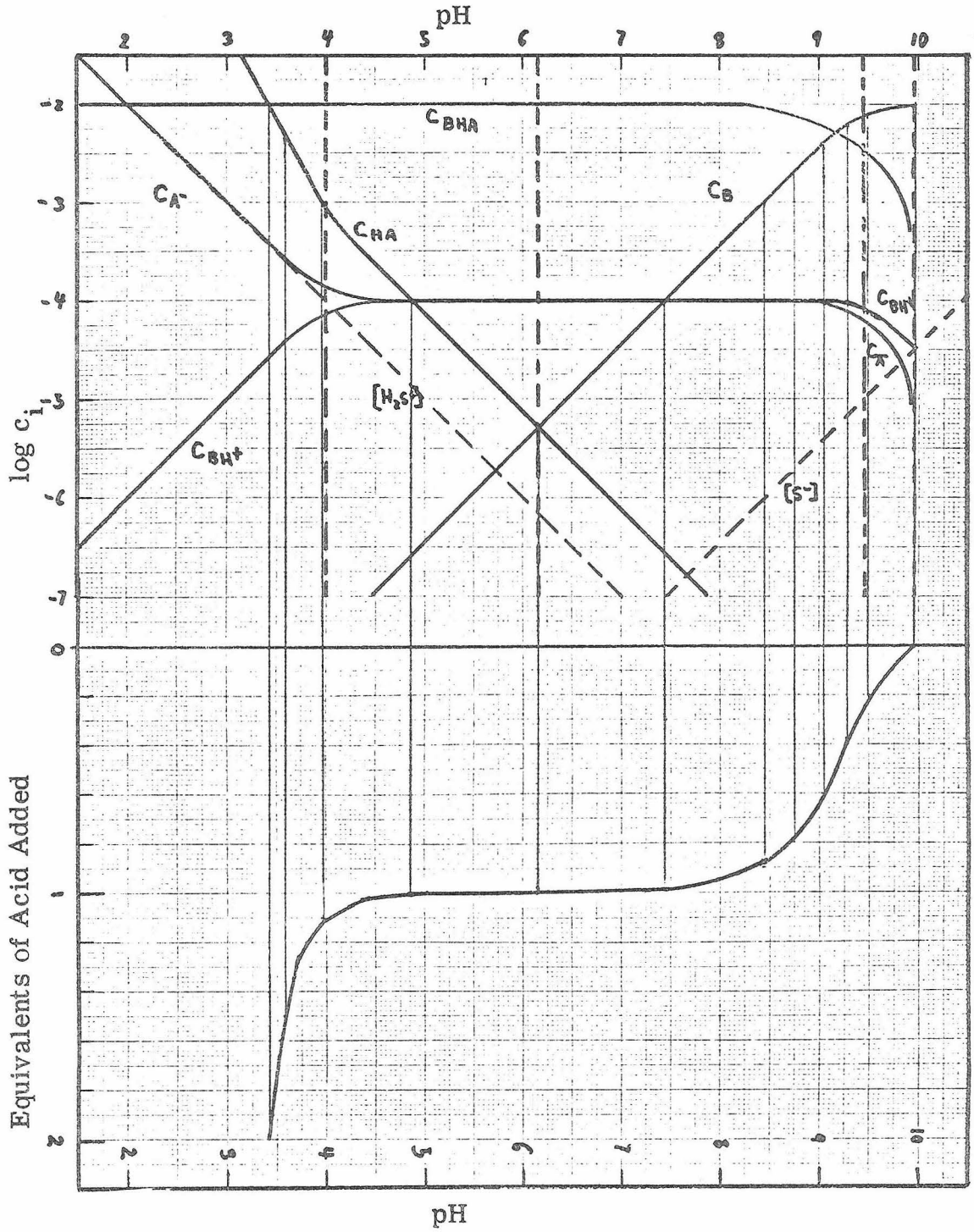

Figure 6. Titration Curve Generated From Case (ii).

$C_T = 10^{-2}$ $K_B = 10^{-7}$ $K_{BHA} = 10^{-6}$ $K_{HA} = 10^{-4.87}$

One can see what different shapes of curves are generated by various values of K_B, K_{BHA}, K_{HA}, and C_T. Case (ii) has a distinctly differently shaped titration curve from case (i). In practice, the rapidity of the drop of pH at the beginning of a titration should be able to tell you if you have a case (i) or a case (ii) system. One that drops rapidly is case (ii).

Titration of HA with B. The equations in Laitinen are adequate for this purpose also. Figure 7 is a plot of such a titration. The initial pH (line (1)) is determined from

$$[H_2S^+][A^-] = K_{HA}C_{HA} = K_{HA}C_T$$

Since initially $[H_2S^+] = [A^-]$,

$$[H_2S^+] = (K_{HA}C_T)^{\frac{1}{2}}$$

Line (3) is the endpoint pH. Lines (2) and (4) determine slope changes and come about as follows. The master equation is (4-63):

$$[H_2S^+]^2 = \frac{(K_S + K_{HA}C_{HA})(K_{HA}C_{HA})}{(K_{HA}C_{HA} + K_{BHA}C_{BHA})}$$

Between (1) and (2), $K_{HA}C_{HA} > K_S$ and $K_{HA}C_{HA} > K_{BHA}C_{BHA}$:

$$[H_2S^+]^2 = K_{HA}C_{HA} \qquad \text{(a)}$$

$$\frac{d\,(\log C_{HA})}{d(pH)} = -2$$

Between (2) and (4), $K_{HA}C_{HA} > K_S$, $K_{HA}C_{HA} < K_{BHA}C_{BHA}$ and $C_{BHA} \approx C_T$.

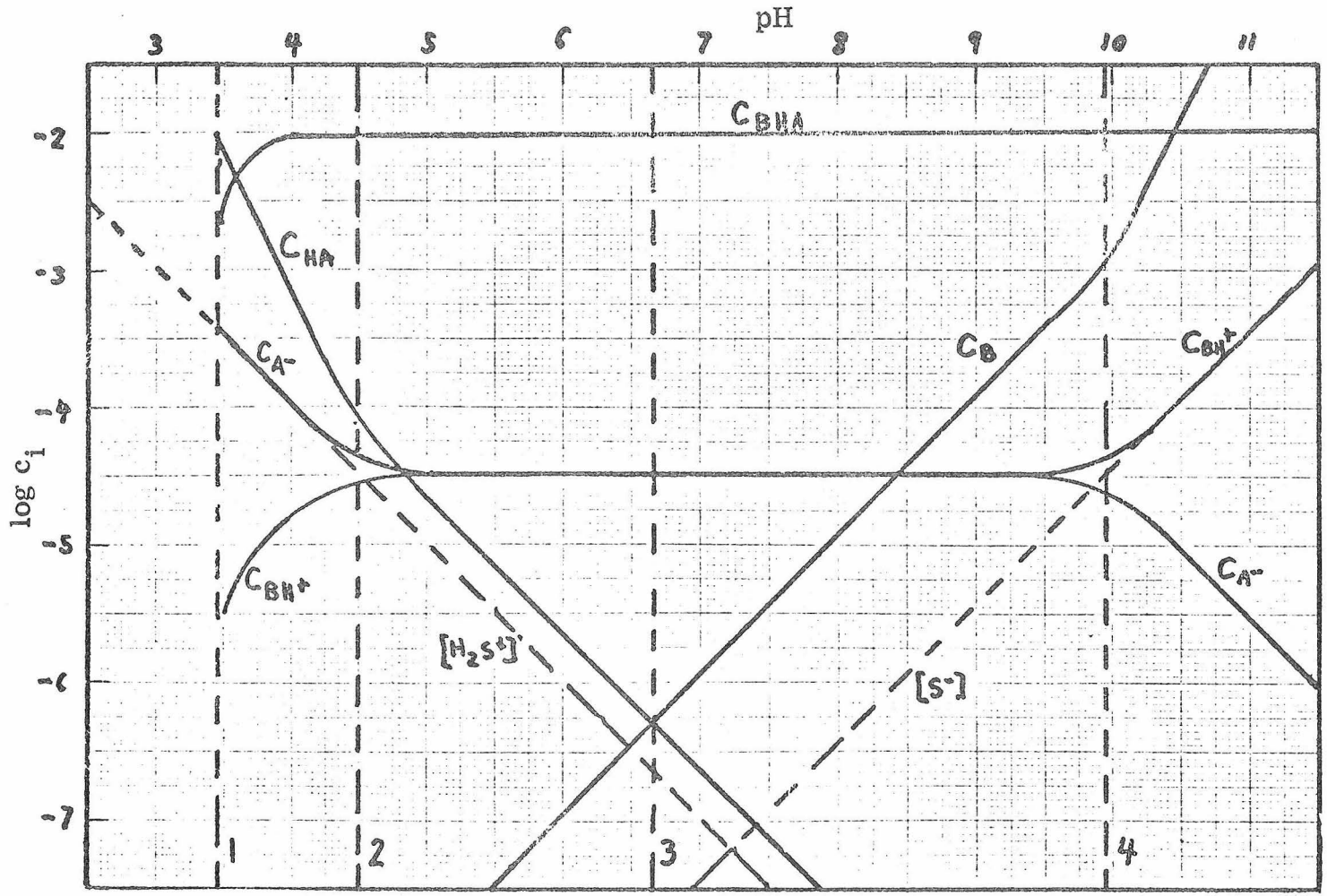

$C_T = 10^{-2}$

$K_B = 10^{-6}$

$K_{BHA} = 10^{-7}$

$K_{HA} = 10^{-4.87}$

Figure 7. Titration of HA with B

Line (1): $[H_2S^+] = (K_{HA}C_T)^{\frac{1}{2}}$

Line (2): $[H_2S^+] = (K_{BHA}C_T)^{\frac{1}{2}}$

Line (3): $[H_2S^+] = (K_S K_{HA}/K_B)^{\frac{1}{2}}$

Line (4): $[H_2S^+] = K_S(K_{BHA}C_T)^{-\frac{1}{2}}$

$$[H_2S^+]^2 = \frac{(K_{HA}C_{HA})^2}{K_{BHA}C_T} \qquad \text{(b)}$$

$$\frac{d\ (\log C_{HA})}{d\ (pH)} = -1$$

Beyond line (4) $K_{HA}C_{HA} < K_S$, $K_{HA}C_{HA} < K_{BHA}C_{BHA}$, and $C_{BHA} \approx C_T$.

$$[H_2S^+]^2 = \frac{K_S K_{HA} C_{HA}}{K_{BHA} C_T} \qquad \text{(c)}$$

$$\frac{d\ (\log C_{HA})}{d\ (pH)} = -2$$

The junctions (2) and (4) are just the junctions of the lines described by equations (a) and (b) and by (b) and (c), respectively. All the other lines on the graph come from the slope relationships developed for case (i) and the initial value of $[A^-] = [H_2S^+]$.

The Gran Titration. It is often useful to determine the end point of a real titration by a graphical technique. The method outlined below is analogous to the Gran titration described by Stumm and Morgan.[4] This method gives us information about the various equilibrium constants as well.

We divide the titration curve into basic and acidic regions.

Basic region: Case (i). (4-54) reduces to

$$[H_2S^+] \approx \frac{K_S}{(K_B C_B)^{\frac{1}{2}}}$$

$$C_B = \frac{K_S^2}{K_B} \frac{1}{[H_2S^+]^{\frac{1}{2}}}$$

But

$$C_B = \left(\frac{v_e - v}{v_o}\right) C_A$$

where

C_A = concentration of HA titrant solution

v_o = initial volume of basic solution

v_e = volume of acid needed to neutralize the base

v = volume of acid added

(These equations specifically neglect dilution. Sample calculations which follow are based on $v_o = 50$ ml, $C_T = 10^{-2}$ M, $C_A = 1$ M, so that only 0.5 ml acid is needed for the titration. None of the calculations in this paper consider dilution.)

Substituting for C_B above,

$$\left(\frac{v_e - v}{v_o}\right) C_A = \frac{K_S^2}{K_B[H_2S^+]^2} \qquad \text{(d)}$$

A plot of 10^{2pH} vs. v will have a slope of $-(C_A K_B / v_o K_S^2)$.

Case (ii): (4-54) reduces to

$$[H_2S^+] \approx \frac{K_S}{K_B C_B} (K_{BHA} C_{BHA})^{\frac{1}{2}}$$

$$\approx \frac{K_S}{K_B C_B} (K_{BHA} C_T)^{\frac{1}{2}}$$

This last equation is pretty abominable. Now substitute for C_B.

$$\left(\frac{v_e - v}{v_o}\right)\frac{C_A K_B}{K_S(K_{BHA}C_T)^{\frac{1}{2}}} \approx \frac{1}{[H_2S^+]} \qquad \text{(e)}$$

A plot of 10^{pH} vs. v will have a slope of $-(C_A K_B/v_o K_S(K_{BHA}C_T)^{\frac{1}{2}}$.

Case (iii): Since here $K_B = K_{BHA}$, (4-54) rigorously reduces to

$$[H_2S^+] = \frac{K_S}{C_B}\left(\frac{C_T}{K_B}\right)^{\frac{1}{2}}$$

$$\left(\frac{v_e - v}{v_o}\right)\frac{C_A}{K_S}\left(\frac{K_B}{C_T}\right)^{\frac{1}{2}} = \frac{1}{[H_2S^+]} \qquad \text{(f)}$$

A plot of 10^{pH} vs. v will have a slope of $-(C_A/v_o K_S)(K_B/C_T)^{\frac{1}{2}}$.

Acidic region. Perusal of several graphs indicates only two different cases.

(a) $K_{BHA} \ll K_{HA}$. (4-64) becomes

$$[H_2S^+]^2 \approx K_{HA}C_{HA}$$

Since

$$C_{HA} = \left(\frac{v - v_e}{v_o}\right) C_A,$$

$$[H_2S^+]^2 = K_{HA}C_A\left(\frac{v - v_e}{v_o}\right) \qquad \text{(g)}$$

A plot of 10^{-2pH} vs. v will have a slope of $K_{HA}C_A/v_o$.

(b) $K_{BHA} \approx K_{HA}$. (4-64) becomes

$$[H_2S^+] \approx \frac{K_{HA}C_{HA}}{(K_{BHA}C_T)^{\frac{1}{2}}}$$

$$[H_2S^+] \approx \frac{K_{HA}C_A}{(K_{BHA}C_T)^{\frac{1}{2}}} \left(\frac{v - v_e}{v_o}\right) \qquad \text{(h)}$$

A plot of 10^{-pH} vs. v will have a slope $K_{HA}C_A/v_o(K_{BHA}C_T)^{\frac{1}{2}}$. If HA is perchloric acid, the case in which $K_{BHA} > K_{HA}$ will not arise since perchloric acid is such a strong electrolyte. However, equation (h) applies even if $K_{BHA} > K_{HA}$.

Two Gran plots are shown in Figures 8 and 9. The titration curves were calculated numerically using the master equations. The slopes of Figure 8 are equal to the theoretical slopes predicted by equations (d) and (g). The limiting slopes of the plots in figure 9 are off by 0.06 and 0.07 log units from the theoretical slopes of equations (e) and (h).

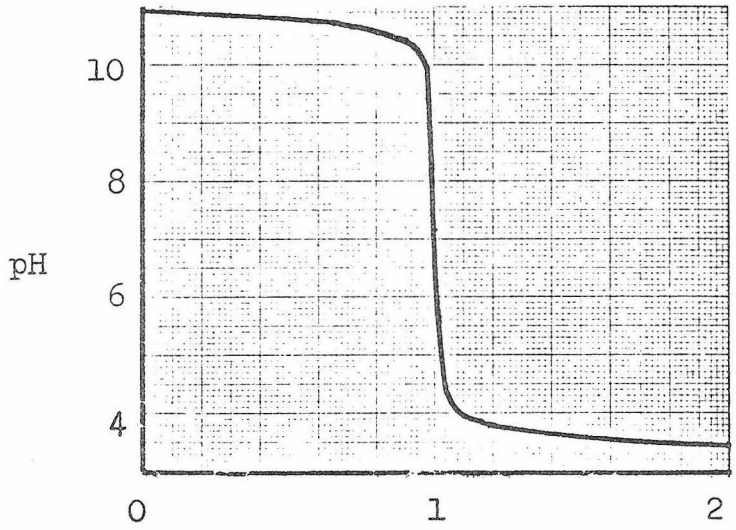

$C_T = 10^{-2}$

$K_B = 10^{-5}$

$K_{BHA} = 10^{-7}$

$K_{HA} = 10^{-4.87}$

$C_A = 1.00M$

$v_o = 50$ ml

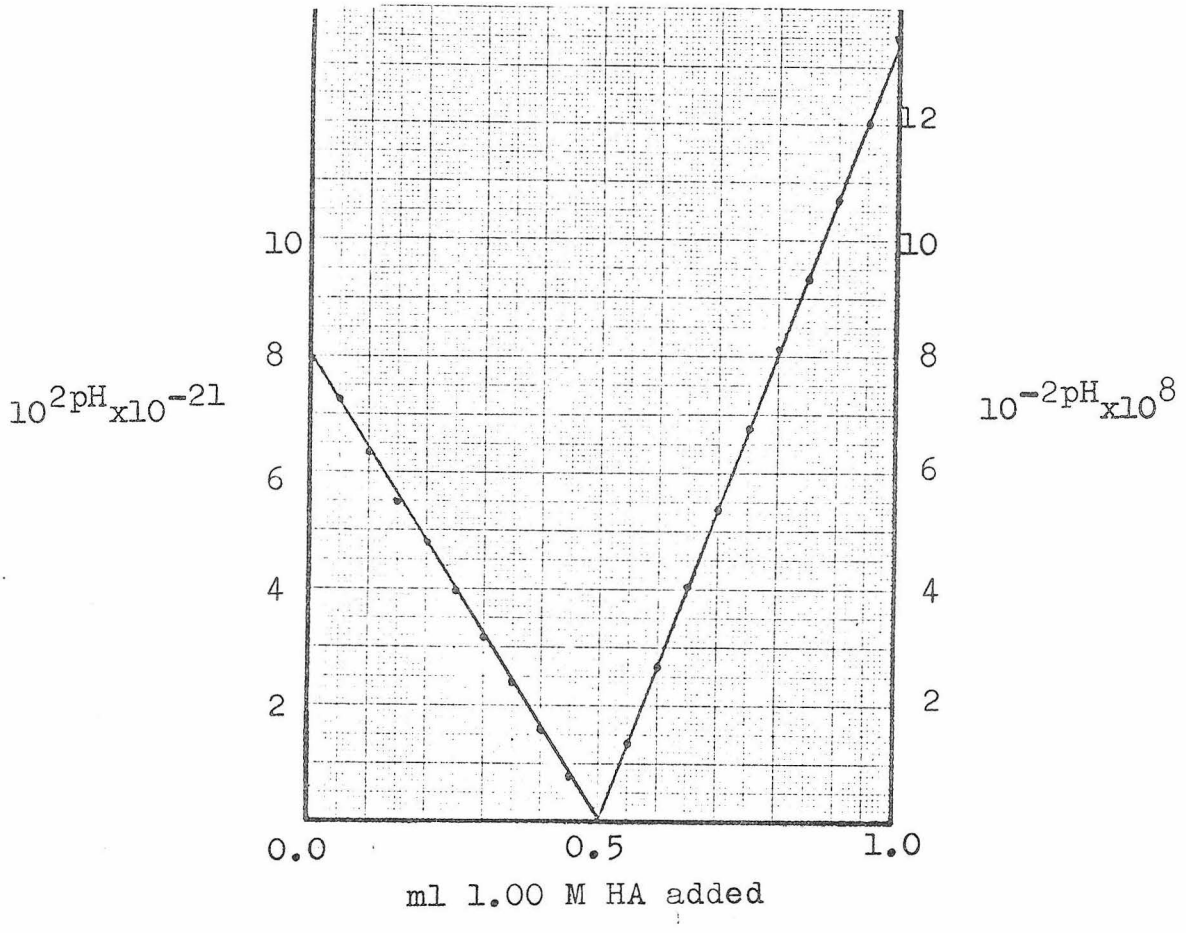

Figure 8. Gran Plot For Titration of B With HA.
Case (i). $K_B > K_{BHA}$.

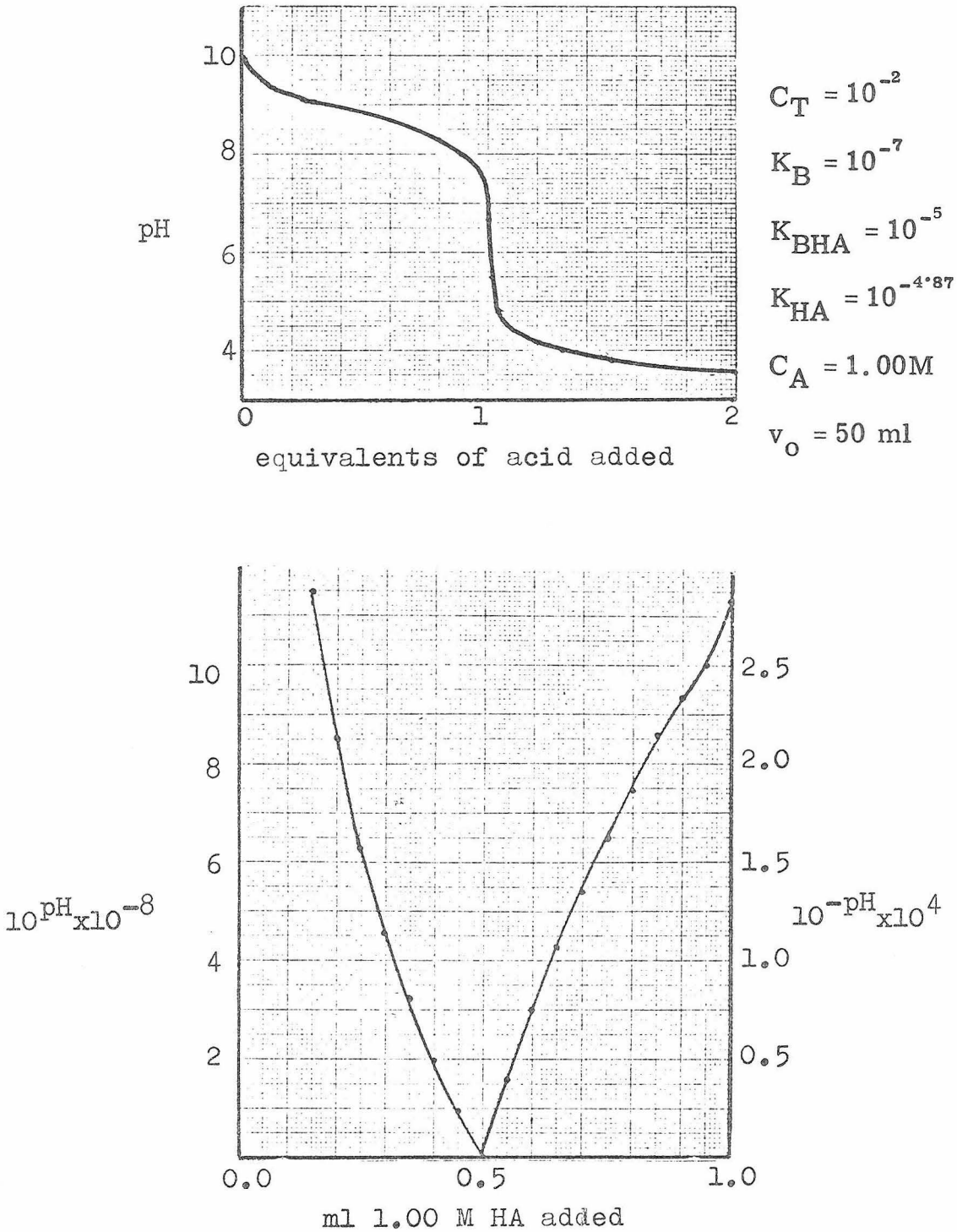

Figure 9. Gran Plot for Titration of B with HA.
Case (ii). $K_B < K_{BHA}$.

Data for Gran Plots

Figure 8. $C_T = 10^{-2}$ $K_B = 10^{-5}$ $K_{BHA} = 10^{-7}$ $K_{HA} = 10^{-4.87}$

Basic Region	$C_B \times 10^3$(M)	log C_B	pH	$10^{2pH} \times 10^{-21}$	v (ml)
	10	-2.000	10.95	7.94	0.00
	9	-2.046	10.93	7.24	0.05
	8	-2.097	10.90	6.31	0.10
	7	-2.155	10.87	5.49	0.15
	6	-2.222	10.84	4.79	0.20
	5	-2.301	10.80	3.98	0.25
	4	-2.398	10.75	3.16	0.30
	3	-2.523	10.69	2.40	0.35
	2	-2.699	10.60	1.59	0.40
	1	-3.000	10.45	0.79	0.45
Acidic Region	$C_{HA} \times 10^3$(M)		pH	$10^{-2pH} \times 10^7$	v (ml)
	10		3.43	1.35	1.00
	9		3.45	1.20	0.95
	8		3.48	1.07	0.90
	7		3.51	0.933	0.85
	6		3.54	0.813	0.80
	5		3.58	0.676	0.75
	4		3.63	0.537	0.70
	3		3.69	0.407	0.65
	2		3.78	0.269	0.60
	1		3.93	0.135	0.55

Figure 9. $B_T = 10^{-2}$ $K_B = 10^{-7}$ $K_{BHA} = 10^{-5}$ $K_{HA} = 10^{-4.87}$

Basic Region	$C_B \times 10^3$(M)	C_{BHA}	pH	$10^{pH} \times 10^{-9}$	v (ml)
	10	0	9.95	8.91	0.00
	9	1×10^3	9.38	2.40	0.05
	8	2	9.19	1.55	0.10
	7	3	9.06	1.15	0.15
	6	4	8.93	0.851	0.20
	5	5	8.80	0.631	0.25
	4	6	8.66	0.457	0.30
	3	7	8.51	0.324	0.35
	2	8	8.30	0.200	0.40
	1	9×10^3	7.98	0.0955	0.45
Acidic Region	$C_{HA} \times 10^3$(M)		pH	$10^{-pH} \times 10^4$	v (ml)
	10		3.55	2.82	1.00
	9		3.59	2.51	0.95
	8		3.63	2.34	0.90
	7		3.67	2.14	0.85
	6		3.73	1.86	0.80
	5		3.79	1.62	0.75
	4		3.87	1.35	0.70
	3		3.97	1.07	0.65
	2		4.12	0.759	0.60
	1		4.40	0.398	0.55

References

1. L. G. Sillén, in "Treatise in Analytical Chemistry," Part 1, Vol. 1., I. M. Kolthoff and P. J. Elving, Eds., Interscience, New York, 1959, pages 280-290.

2. S. Bruckenstein and I. M. Kolthoff, J. Amer. Chem. Soc., 78, 1, 10, 2974 (1956); 79, 1, 5915 (1957).

3. H. A. Laitinen, "Chemical Analysis," McGraw-Hill, New York, 1960, pages 72-77.

4. W. Stumm and J. J. Morgan, "Aquatic Chemistry," Wiley Interscience, 1970, pages 155-158. Also G. Gran, Analyst, 77, 661 (1952).

Chapter Eight

The Philosophy of Chem 2

Hellfire and damnation! Thunder, lightning and the Wrath of Zeus! At least a ponding. Such would be my fate as perpetrator of Chem 2 if the work load remained constant but the appeal of the subject matter were decreased.

Chem 2 is an advanced placement freshman chemistry course originally offered only to students with exceptional high school backgrounds in chemistry. When I began teaching the course I changed the prerequisite from exceptional background to exceptional motivation. Since the individual student has no control over the courses offered by his high school, background seems a poor basis for course selection. This argument probably does not apply to students of lesser intellectual capabilities than Caltech freshmen. Given a very heterogeneous group of backgrounds and varied interests linked only by a common burning interest in science in general, how does an instructor choose his subject matter? Two criteria for Chem 2 topics evolved: The topics must be excessively interesting and no previous knowledge can be required for presentation of that subject except what has preceded it in Chem 2. I reject the idea that freshman chemistry courses should seek to give students the basic knowledge necessary to deal with whatever little chemistry they eventually encounter. A freshman chemistry course should seek to give its students the <u>ability</u> to handle future chemical problems, but not the <u>knowledge</u>. I maintain that this thinking applies not only to Chem 2 but to any freshman chemistry course, subject to the limitations

of its students' capabilities and interests, or lack thereof. The vast majority (~90%) of Chem 2 students will not major in chemistry. They will use chemistry in their future lives to very varying degrees. Most will use it hardly at all. Since this is the case with most students in most freshman chemistry courses, why in hell's name do we spend so much time in most freshman courses with topics like the Nernst equation and the details of chemical equilibrium? Not only will these topics never be used in the future by almost all of the students, but they will be forgotten as quickly as humanly possible after the final exam. In selecting topics for Chem 2 I tried to choose those which were inherently very interesting and which would serve to give the students a basic "gut feeling" for the things molecules do-- and hence chemistry. When an engineer needs to know about chemical equilibrium for his work ten years after taking freshman chemistry, he will have the motivation to learn whatever he needs to know. As a freshman chemistry teacher, my job is to be sure he is able to do that, but not necessarily to have taught him that subject. And if the topic is dull and boring, why waste his time and "turn off" his feelings for any chemistry by including it in a freshman course? A freshman course should have the very best that chemistry can offer.

The curriculum of Chem 2 is in part an outgrowth of the sophomore "Structural Chemistry" course taught by Harry Gray and George Hammond at Caltech from 1968 to 1970. Mike Bertolucci, my co-conspirator in the founding of Chem 2, and I both share a contagious interest in spectroscopy which we feel is a sufficiently interesting and broad topic around which to build a freshman chemistry course. The contagion of a teacher's interests should be a prerequisite in the selection of freshman instructors. If the teacher is bored, all but the most interested students will be, too. If the teacher is interested but his feelings are not contagious, the result is still disaster. In order to teach half a year of spectroscopy, three months of more general, but decidedly interesting topics were deemed necessary. These topics are clearly a product of my own biases but serve to instill a "gut feeling" for chemistry, which I feel is an important product of Chem 2. My idea of a gut feeling for a molecule is to be able to envision the molecule in three dimensions and to understand how the arrangement of nuclei and electrons affects the

physical properties and reactivity of that molecule. With the hope of building such a gut feeling and of creating an interesting course, the curriculum of Chem 2 has evolved to the form outlined on the next page for the 1972-73 school year.

The text used for Chem 2a is "Inorganic Chemistry: Principles of Structure and Reactivity" by James E. Huheey. This text is designed for third or fourth year students and is therefore ideally suited for Chem 2. The level of Huheey's presentation is such that our students often need to think hard and ask questions to understand their reading. Huheey's book is very good in that it presents chemistry as an experimental science with many open questions. This view is magnified in class by my bias that chemistry is a string of experimental results connected by fuzzy theories which often fail under scrutiny. Few ideas presented in class are not scrutinized by my students. Undoubtedly my inability to defend many theories under intensive questioning in class has served to build my view that many of our theories are inadequate. Though we use an "inorganic chemistry" text, Chem 2 is in no way a course in inorganic chemistry. We pick and choose among all areas of chemistry to illustrate the topic under discussion. Huheey's text has been supplemented by handouts on Lewis structures and on valence shell electron pair repulsion rules as well as by reading in "Chemical Principles" by Dickerson, Gray and Haight. The spectroscopy part of the course is taught from "The Chem Two Bestiary" (wherein all is disclosed)-- a text written for this course by me and by Mike Bertolucci. Subject to the constraint that no topic may be presented which cannot be understood with the knowledge built previously in Chem 2, the depth of the Bestiary is startling. Perhaps this is epitomized by the vibronic analysis of the high resolution emission spectrum of benzene doped into a crystal of C_6D_6 at liquid helium temperature. That a topic such as this can be understood by a class of freshmen is nothing short of amazing to me.

You may be saying to yourself at this point that we have gone off the deep end in our own way just as some teachers go crazy with chemical equilibrium. My only answer is that we present these topics such that the students find them interesting and often exciting. Perhaps it is the same process by which Tom Sawyer convinced his friends that whitewashing a fence was really fun. But it works!

Outline of Chem 2
1972-1973

Chem 2a. General Chemistry

A. Atoms
   1. Wave properties
   2. Quantum mechanics
   3. Atomic structure
   4. Periodic properties of the elements

B. Ionic Compounds

C. Covalent Compounds
   1. Lewis structures
   2. Valence shell electron pair repulsion theory
   3. Molecular orbitals of diatomic molecules
   4. Hybridization and bonding in polyatomic molecules

D. Fundamentals of Thermodynamics
   1. Enthalpy and entropy
   2. Free energy and equilibrium

E. Fundamentals of Kinetics
   1. Rate laws
   2. Arrhenius law and activation parameters
   3. Kinetics and mechanisms of chemical reactions

F. Relation of Structure, Bonding and Reactivity
   1. Optical activity
   2. Funny things that molecules do
   3. Structure and strength of acids and bases

G. Topics in Transition Metal Chemistry
   1. Structure of organometallic compounds
   2. Crystal field theory and its applications

Chem 2b. Spectroscopy

A. Group Theory
   1. Symmetry operations
   2. Point groups
   3. Matrix representations of symmetry operations
   4. Character tables and their use

B. Vibrational spectroscopy
   1. Infrared and Raman spectra
   2. Vibration and rotation of diatomic molecules
   3. Normal modes of vibration of polyatomic molecules
   4. Selection rules and polarization
   5. Uses of vibrational spectra
      a. Functional group analysis
      b. Determination of stereochemistry
      c. Force constants

C. Neanderthal Orbital Theory
   1. Quantum techniques
   2. Diatomic molecules
   3. Selected polyatomic molecules
   4. Huckel method
   5. Woodward-Hoffman rules

Chem 2c. Spectroscopy and Selected Topics

A. Electronic spectroscopy
   1. Configurations and states
   2. Selection rules
   3. Electronic processes in polyatomic molecules
   4. Analysis of spectra
      a. Small molecules
      b. Absorption spectra of big molecules
      c. Emission spectra of big molecules
      d. Transition metal complexes

B. Nuclear magnetic resonance
   1. Theory
   2. Chemical shift
   3. Spin-spin splitting
   4. Spectra of nuclei other than ^{1}H
   5. The study of dynamic processes by NMR

C. Selected Topics
   (Probably including ion cyclotron resonance and topics of biological interest.)

Our philosophy of the lecture-learning process is reflected by the mechanics of the course. Chem 2 has two one-hour lectures each week and a problem session between every lecture. An assignment is given out at every lecture and is due by the next lecture. This follows from the fact (yes, fact) that the majority of students in any class work on an assignment only the night before it is due. Two assignments each week insure that the students will think about chemistry twice instead of once. This allows the student to digest less material each time and therefore understand and remember more of it than the usual weekly assignment would permit. Further, each assignment consists of reading the material for the next lecture as well as problems on the previous lecture and simple problems on the new reading assignment. To clarify this, the assignment given out at lecture 11 (due on the day of lecture 12) includes problems from lecture 11 and reading and problems for lecture 12. We feel that a student benefits very much more from a lecture if he has read about the topic and grappled with a relatively simple problem prior to that lecture. We absolutely reject the use of a lecture to regurgitate the text, or vice versa. Rather, they should amplify and reinforce each other. For this reason the examples and approach used in lecture are as different as possible from the examples and approach of the text. Problem sessions are used mainly for answering students' questions but sometimes to continue parts of a lecture. Only one midweek problem session was originally planned. This was not sufficient for many of the more interested people and they requested that a second problem session be held on Sunday night so as to have one problem session for each lecture. To my surprise, this Sunday night session proved fairly popular.

The grade for Chem 2a is based on a final exam (40%), two midterms (each 20%) and homework (20%). The weighting of homework is designed to encourage the student to do his homework but is not so heavy that I cannot use the homework as a learning experience for the students. (Every problem set turns out to be a learning experience for me.) Collaboration on homework is encouraged, short of just using someone else's answers. All tests are open-book with a specific time limit. As much as possible, tests are designed to test the student's knowledge and ability to apply that knowledge in new situations and

not his speed or ability to "twang" a slide rule. We do not always succeed in these goals but strive toward them. Though the official grade in a freshman course is only "Pass" or "Fail," each student receives the letter grade (A, B, C, D, F) that he would have earned.

Chem 2 b,c will also include two midterm exams but the final exam will be replaced by a library research project designed to familiarize the student with chemical journals. The goal of these papers, which allow a student to write about any topic he chooses, is to develop an appreciation of the state of chemical literature and, more importantly, to develop a critical frame of mind when reading about chemical research. When the student understands that most chemists are very fallible, he will understand the limitations of using chemical information and will strive to decrease those limitations in his own work -- hopefully. Clearly, this lesson transfers to any other experimental science. Chem 2b will also include a computer project on normal coordinate analysis. This is purely optional but more than half the class has expressed interest in it.

In summary, we have tried to make Chem 2 as interesting as possible. We make no effort to include all the topics that a "survey" course would include. Instead, we go into considerable depth in those topics we do cover. We have tried to instill a healthy skepticism in our students so that little is accepted on faith but everything must stand on its own merits.

As the single best indication of the methods and goals of Chem 2, we present, in reduced form, all of the problem assignments and exams of Chem 2a, 1972-73. When it is realized that this is the work of just eleven weeks, I think this is an impressive achievement on the part of both students and teacher.

A Problem Set Which May Bohr You To Death (#1)

Due Monday 2 October 1972

Reading: Huheey 20-35

1. (2 pts) CO absorbs IR radiation at about 2150 cm^{-1}. What is the energy of this radiation in kcal $mole^{-1}$, eV and joules? Useful physical constants are given on page 670 of Huheey.

2. (1 pt) What is the wavelength in nanometers (nm) of light sufficient to break a chemical bond with a bond dissociation energy of 100 kcal $mole^{-1}$? This is about the strength of a C-H bond.

3. (2 pts) Fill in the following table:

vacuum UV	UV	VIS	near IR	mid IR	far IR
λ (nm)	200	360	800		
$\bar{\nu}$ (cm^{-1})				5000	200
ν (sec^{-1})					

4. (1 pt) Compare the gravitational attraction in dynes (cgs units) between a proton and an electron separated by one Angstrom unit to their electrostatic attraction. This should convince you that gravity is of little importance to wayward trolls. This is what happened to the last person who badmouthed a troll:

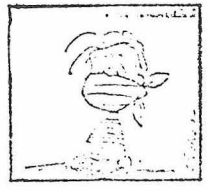

5. (2 pts) Calculate the radii (cm) and energies (cm^{-1} units) of the third and fourth Bohr orbits of a Li^{2+} ion. What is the energy in cm^{-1} and kcal $mole^{-1}$ of the transition $n=3 \rightarrow n=4$? In what region of the spectrum does this occur? Will the ion absorb or emit radiation during this transition?

6. (2 pts) Atomic orbitals are often named for Cartesian functions (e.g. $2p_x$, $3d_{xy}$, $4f_{y(z^2-x^2)}$.) You may be curious about the origin of these names. The Cartesian description of, say, a $3d_{xy}$ orbital comes from transforming the spherical polar form of the wavefunction.

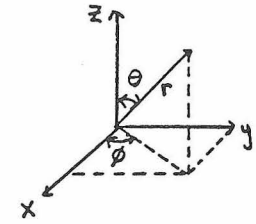

$$z = r\cos\theta$$
$$x = r\sin\theta\cos\phi$$
$$y = r\sin\theta\sin\phi$$

$$\psi_{3d_{xy}} = (81\sqrt{2\pi})^{-1}(Z/a_o)^{3/2}e^{-\sigma/3}\sigma^2\sin^2\theta\,\sin 2\phi$$

$\sigma = Zr/a_o$
Z = nuclear charge
a_o = radius of first Bohr orbit

$$\psi_{3d_{xy}} \propto r^2\sin^2\theta\,\sin 2\phi$$
$$\propto r^2\sin^2\theta\,\sin\phi\cos\phi \quad (\text{since } \sin 2\phi = 2\sin\phi\cos\phi)$$
$$= \underbrace{r\sin\theta\cos\phi}_{x}\,\underbrace{r\sin\theta\sin\phi}_{y}$$
$$\psi_{3d_{xy}} \propto xy$$

What are the quantum numbers n, l and m of a $3d_{xy}$ orbital? Using the polar graph paper provided by the generous Chem 2 staff, make a plot of the angular part of the $3d_{xy}$ wavefunction in the xy plane. (ie., $\theta = 90^o$) What you should plot is the function

$$\psi = \sin^2\theta\,\sin 2\phi$$

where ψ will be the distance from the origin of the graph and ϕ determines which radial of the graph paper you are working on. Plot this function for every 15° increment of ϕ from 0 - 360°. Get some sleep this weekend. Write the angular part of the $f_{y(z^2-x^2)}$ orbital. This is just the part containing r and sines and cosines. Don't mess with the normalization coefficient or the exponential factor and you don't even have to simplify your answer.

With Glee -- From Irwin Claus (#2)

Due Thursday 5 October

Reading: Huheey 38-53

1. (3 pts) Using the scheme of drawing a circle for each orbital, (the scheme used in class today) write the electron configuration for each element in Huheey, problem 2.4 and for each ion in problem 2.6. How many unpaired electrons will there be in the ground state of each of the above species? What is the ground state spin multiplicity of each of these species?

2. (7 pts) To get a real gut feeling for hydrogen wave functions, we are going to plot the radial parts of ψ_{4s} and ψ_{4f} as well as the probability functions $r^2\psi_{4s}^2$ and $r^2\psi_{4f}^2$. The radial wave functions for a bunch of orbitals are given below. Irwin Claus (a troll who will not show his face in Chem 2 until December) has gleefully provided a computer program to calculate the 4s, 4p, 4d and 4f radial wavefunctions in cgs units. This program and its output (values of ψ and $r^2\psi^2$ for r = 0.1 to r = 25.0 Å in increments of 0.1 Å) are given after this text. In the output ψ_{4s} and $r^2\psi_{4s}^2$, say, are given under the headings PSI4S and PROB4S, respectively. On the left are values of r in Angstroms. (Can any computer freak figure out why values of r stop after 9.90 Å ? Irwin Claus made a little mistake in his program.)

TABLE 6–3. The Hydrogen-like Radial Wave Functions $R_{nl}(r)$

$$\left(\rho = \frac{2Z}{na_0}r\right)$$

$n = 1$, K shell: $l = 0$, $1s$, $R_{10}(r) = \left(\frac{Z}{a_0}\right)^{3/2} 2e^{-\rho/2}$

$n = 2$, L shell: $l = 0$, $2s$, $R_{20}(r) = \frac{(Z/a_0)^{3/2}}{2\sqrt{2}}(2-\rho)e^{-\rho/2}$

$l = 1$, $2p$, $R_{21}(r) = \frac{(Z/a_0)^{3/2}}{2\sqrt{6}}\rho e^{-\rho/2}$

$n = 3$, M shell: $l = 0$, $3s$, $R_{30}(r) = \frac{(Z/a_0)^{3/2}}{9\sqrt{3}}(6-6\rho+\rho^2)e^{-\rho/2}$

$l = 1$, $3p$, $R_{31}(r) = \frac{(Z/a_0)^{3/2}}{9\sqrt{6}}(4-\rho)\rho e^{-\rho/2}$

$l = 2$, $3d$, $R_{32}(r) = \frac{(Z/a_0)^{3/2}}{9\sqrt{30}}\rho^2 e^{-\rho/2}$

$n = 4$, N shell: $l = 0$, $4s$, $R_{40}(r) = \frac{(Z/a_0)^{3/2}}{96}(24-36\rho+12\rho^2-\rho^3)e^{-\rho/2}$

$l = 1$, $4p$, $R_{41}(r) = \frac{(Z/a_0)^{3/2}}{32\sqrt{15}}(20-10\rho+\rho^2)\rho e^{-\rho/2}$

$l = 2$, $4d$, $R_{42}(r) = \frac{(Z/a_0)^{3/2}}{96\sqrt{5}}(6-\rho)\rho^2 e^{-\rho/2}$

$l = 3$, $4f$, $R_{43}(r) = \frac{(Z/a_0)^{3/2}}{96\sqrt{35}}\rho^3 e^{-\rho/2}$

$n = 5$, O shell: $l = 0$, $5s$, $R_{50}(r) = \frac{(Z/a_0)^{3/2}}{300\sqrt{5}}(120-240\rho+120\rho^2-20\rho^3+\rho^4)e^{-\rho/2}$

$l = 1$, $5p$, $R_{51}(r) = \frac{(Z/a_0)^{3/2}}{150\sqrt{30}}(120-90\rho+18\rho^2-\rho^3)\rho e^{-\rho/2}$

$l = 2$, $5d$, $R_{52}(r) = \frac{(Z/a_0)^{3/2}}{150\sqrt{70}}(42-14\rho+\rho^2)\rho^2 e^{-\rho/2}$

$l = 3$, $5f$, $R_{53}(r) = \frac{(Z/a_0)^{3/2}}{300\sqrt{70}}(8-\rho)\rho^3 e^{-\rho/2}$

$l = 4$, $5g$, $R_{54}(r) = \frac{(Z/a_0)^{3/2}}{900\sqrt{70}}\rho^4 e^{-\rho/2}$

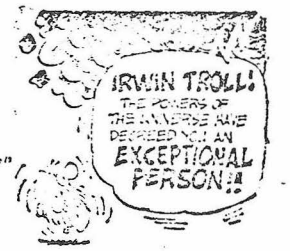

a. Make a plot of ψ_{4s} and $r^2\psi_{4s}^2$ from 0-25 Å on the same sheet of graph paper. Then do the same for ψ_{4f} and $r^2\psi_{4f}^2$ on a second sheet of paper. You should use as few points as possible to produce a decent plot. Don't use too many points! Pay particular attention to maxima, minima and nodes. You will need to calculate the value of ψ_{4s} at r = 0.

b. Fill in the following table where "maximum probability" is the distance in Å at which you are most likely to find an electron for each orbital. List the maxima to the nearest 0.05 Å.

	4s	4p	4d	4f
maximum probability				

For comparison, what is the radius of the fourth Bohr orbit of hydrogen?

A Note: In computer output, powers of ten are shown as follows:

$$4.3 \times 10^7 = 0.43 \times 10^8 = 0.43\ \text{E}\ 08$$

```
FORTRAN IV G LEVEL  20                    MAIN              DATE =   9/26/72      16:27:33
      C     THIS PROGRAM IS DESIGNED TO CONFUSE TROLLS?
      A = 0.529
      WRITE (6,101)
  101 FORMAT (1X,'R(A)      PSI4S        PROB4S        PSI4P        PROB4P
     1  PSI4D        PROB4D        PSI4F        PROB4F  ///)
  100 FORMAT (1X,F4.2,5E12.5)
      DO 10 I = 1,250
      R = 0.1*FLOAT(I)
      RPO = R/(2.0*A)
      PSI4S = (1.0/(96.0*A**1.5))*(24.0-36.0*RHO+12.0*RHO**2-RHO**3)*EXP
     1(-1.0*RHO/2.0)*1.0E12
      PSI4P = (1.0/(32.0*3.673*A**1.5))*(20.0-10.0*RHO+RHO**2)*RHO*EXP(-
     1 1.0*RHO/2.0)*1.0E12
      PSI4D = (1.0/(96.7*2.23*A**1.5))*(6.0-RHO)*RHO**2*EXP(-1.0*RHO/2.
     1 0)*1.0E12
      PSI4F = (1.0/(96.(*5.91*A**1.5))*(RHO**3)*EXP(-1.0*RHO/2.0)*1.0E1
     12
      PROB4S = (R**2)*(PSI4S**2)*1.0E-16
      PROB4P = (R**2)*(PSI4P**2)*1.0E-16
      PROB4D = (R**2)*(PSI4D**2)*1.0E-16
      PROB4F = (R**2)*(PSI4F**2)*1.0E-16
      WRITE (6,100)R,PSI4S,PROB4S,PSI4P,PROB4P,PSI4D,PROB4D,PSI4F,PROB4F
   10 CONTINUE
      STOP
      END
```

R(A)	PSI4S	PRCB4S	PSI4P	PROB4P	PSI4D	PROB4D	PSI4F	PRCB4F	
0.10	0.534635E 12	0.265355E 06	0.330543E 11	0.127915E 05	0.600935E 09	0.371125E 00	0.336558E 07	0.135585E-04	
0.20	0.433935E 12	0.759196E 06	0.654446E 11	0.171332E 05	0.228775E 10	0.209331E 02	0.281296E 08	0.316426E-02	
0.30	0.344116E 12	0.107855E 07	0.685956E 11	0.712735E 05	0.424945E 10	0.205412E 03	0.405452E 08	0.733816E-01	
0.40	0.270506E 12	0.115669E 07	0.107338E 12	0.184505E 06	0.905409E 10	0.103796E 04	0.204716E 09	0.670515E 00	
0.50	0.204335E 12	0.135443E 07	0.121276E 12	0.367654E 06	0.171802E 11	0.348206E 04	0.351375E 09	0.363161E 01	
0.60	0.146056E 12	0.174104E 06	0.131225E 12	0.615855E 06	0.159335E 11	0.913865E 04	0.626554E 09	0.142256E 02	
0.70	0.100205E 12	0.445355E 05	0.137756E 12	0.924853E 06	0.230325E 11	0.202431E 05	0.952410E 09	0.444168E 02	
0.80	0.555516E 11	0.226456E 06	0.141336E 12	0.127686E 07	0.249746E 11	0.395995E 05	0.135506E 10	0.117615E 03	
0.90	0.255522E 11	0.528875E 05	0.142464E 12	0.156435E 07	0.237455E 11	0.704225E 05	0.186411E 10	0.274555E 03	
1.00	[illegible]	[illegible]	[illegible]	[illegible]	[illegible]	[illegible]	[illegible]	[illegible]	1
1.10	[illegible]	[illegible]	[illegible]	[illegible]	[illegible]	[illegible]	[illegible]	[illegible]	
1.20	[illegible]	[illegible]	[illegible]	[illegible]	[illegible]	[illegible]	[illegible]	[illegible]	
1.30	[illegible]	[illegible]	[illegible]	[illegible]	[illegible]	[illegible]	[illegible]	[illegible]	
1.40	[illegible]	[illegible]	[illegible]	[illegible]	[illegible]	[illegible]	[illegible]	[illegible]	
1.50	[illegible]	[illegible]	[illegible]	[illegible]	[illegible]	[illegible]	[illegible]	[illegible]	
1.60	[illegible]	[illegible]	[illegible]	[illegible]	[illegible]	[illegible]	[illegible]	[illegible]	
1.70	[illegible]	[illegible]	[illegible]	[illegible]	[illegible]	[illegible]	[illegible]	[illegible]	
1.80	[illegible]	[illegible]	[illegible]	[illegible]	[illegible]	[illegible]	[illegible]	[illegible]	
1.90	[illegible]	[illegible]	[illegible]	[illegible]	[illegible]	[illegible]	[illegible]	[illegible]	
2.00	[illegible]	[illegible]	[illegible]	[illegible]	[illegible]	[illegible]	[illegible]	[illegible]	2
2.10	[illegible]	[illegible]	[illegible]	[illegible]	[illegible]	[illegible]	[illegible]	[illegible]	
2.20	[illegible]	[illegible]	[illegible]	[illegible]	[illegible]	[illegible]	[illegible]	[illegible]	
2.30	[illegible]	[illegible]	[illegible]	[illegible]	[illegible]	[illegible]	[illegible]	[illegible]	
2.40	[illegible]	[illegible]	[illegible]	[illegible]	[illegible]	[illegible]	[illegible]	[illegible]	
2.50	[illegible]	[illegible]	[illegible]	[illegible]	[illegible]	[illegible]	[illegible]	[illegible]	
2.60	[illegible]	[illegible]	[illegible]	[illegible]	[illegible]	[illegible]	[illegible]	[illegible]	
2.70	[illegible]	[illegible]	[illegible]	[illegible]	[illegible]	[illegible]	[illegible]	[illegible]	
2.80	[illegible]	[illegible]	[illegible]	[illegible]	[illegible]	[illegible]	[illegible]	[illegible]	
2.90	[illegible]	[illegible]	[illegible]	[illegible]	[illegible]	[illegible]	[illegible]	[illegible]	
3.00	[illegible]	[illegible]	[illegible]	[illegible]	[illegible]	[illegible]	[illegible]	[illegible]	3
3.10	[illegible]	[illegible]	[illegible]	[illegible]	[illegible]	[illegible]	[illegible]	[illegible]	
3.20	[illegible]	[illegible]	[illegible]	[illegible]	[illegible]	[illegible]	[illegible]	[illegible]	
3.30	[illegible]	[illegible]	[illegible]	[illegible]	[illegible]	[illegible]	[illegible]	[illegible]	
3.40	[illegible]	[illegible]	[illegible]	[illegible]	[illegible]	[illegible]	[illegible]	[illegible]	
3.50	[illegible]	[illegible]	[illegible]	[illegible]	[illegible]	[illegible]	[illegible]	[illegible]	
3.60	[illegible]	[illegible]	[illegible]	[illegible]	[illegible]	[illegible]	[illegible]	[illegible]	
3.70	[illegible]	[illegible]	[illegible]	[illegible]	[illegible]	[illegible]	[illegible]	[illegible]	
3.80	[illegible]	[illegible]	[illegible]	[illegible]	[illegible]	[illegible]	[illegible]	[illegible]	
3.90	[illegible]	[illegible]	[illegible]	[illegible]	[illegible]	[illegible]	[illegible]	[illegible]	
4.00	[illegible]	[illegible]	[illegible]	[illegible]	[illegible]	[illegible]	[illegible]	[illegible]	4
4.10	[illegible]	[illegible]	[illegible]	[illegible]	[illegible]	[illegible]	[illegible]	[illegible]	
4.20	[illegible]	[illegible]	[illegible]	[illegible]	[illegible]	[illegible]	[illegible]	[illegible]	
4.30	[illegible]	[illegible]	[illegible]	[illegible]	[illegible]	[illegible]	[illegible]	[illegible]	
4.40	[illegible]	[illegible]	[illegible]	[illegible]	[illegible]	[illegible]	[illegible]	[illegible]	
4.50	[illegible]	[illegible]	[illegible]	[illegible]	[illegible]	[illegible]	[illegible]	[illegible]	
4.60	[illegible]	[illegible]	[illegible]	[illegible]	[illegible]	[illegible]	[illegible]	[illegible]	
4.70	[illegible]	[illegible]	[illegible]	[illegible]	[illegible]	[illegible]	[illegible]	[illegible]	
4.80	[illegible]	[illegible]	[illegible]	[illegible]	[illegible]	[illegible]	[illegible]	[illegible]	
4.90	[illegible]	[illegible]	[illegible]	[illegible]	[illegible]	[illegible]	[illegible]	[illegible]	
5.00	[illegible]	[illegible]	[illegible]	[illegible]	[illegible]	[illegible]	[illegible]	[illegible]	5
5.10	[illegible]	[illegible]	[illegible]	[illegible]	[illegible]	[illegible]	[illegible]	[illegible]	
5.20	[illegible]	[illegible]	[illegible]	[illegible]	[illegible]	[illegible]	[illegible]	[illegible]	
5.30	[illegible]	[illegible]	[illegible]	[illegible]	[illegible]	[illegible]	[illegible]	[illegible]	
5.40	[illegible]	[illegible]	[illegible]	[illegible]	[illegible]	[illegible]	[illegible]	[illegible]	
5.50	[illegible]	[illegible]	[illegible]	[illegible]	[illegible]	[illegible]	[illegible]	[illegible]	
5.60	[illegible]	[illegible]	[illegible]	[illegible]	[illegible]	[illegible]	[illegible]	[illegible]	
5.70	[illegible]	[illegible]	[illegible]	[illegible]	[illegible]	[illegible]	[illegible]	[illegible]	
5.80	[illegible]	[illegible]	[illegible]	[illegible]	[illegible]	[illegible]	[illegible]	[illegible]	
5.90	[illegible]	[illegible]	[illegible]	[illegible]	[illegible]	[illegible]	[illegible]	[illegible]	
6.00	[illegible]	[illegible]	[illegible]	[illegible]	[illegible]	[illegible]	[illegible]	[illegible]	6
6.10	[illegible]	[illegible]	[illegible]	[illegible]	[illegible]	[illegible]	[illegible]	[illegible]	
6.20	[illegible]	[illegible]	[illegible]	[illegible]	[illegible]	[illegible]	[illegible]	[illegible]	
6.30	[illegible]	[illegible]	[illegible]	[illegible]	[illegible]	[illegible]	[illegible]	[illegible]	
6.40	[illegible]	[illegible]	[illegible]	[illegible]	[illegible]	[illegible]	[illegible]	[illegible]	
6.50	[illegible]	[illegible]	[illegible]	[illegible]	[illegible]	[illegible]	[illegible]	[illegible]	
6.60	[illegible]	[illegible]	[illegible]	[illegible]	[illegible]	[illegible]	[illegible]	[illegible]	
6.70	[illegible]	[illegible]	[illegible]	[illegible]	[illegible]	[illegible]	[illegible]	[illegible]	
6.80	[illegible]	[illegible]	[illegible]	[illegible]	[illegible]	[illegible]	[illegible]	[illegible]	
6.90	[illegible]	[illegible]	[illegible]	[illegible]	[illegible]	[illegible]	[illegible]	[illegible]	
7.00	[illegible]	[illegible]	[illegible]	[illegible]	[illegible]	[illegible]	[illegible]	[illegible]	7
7.10	[illegible]	[illegible]	[illegible]	[illegible]	[illegible]	[illegible]	[illegible]	[illegible]	
7.20	[illegible]	[illegible]	[illegible]	[illegible]	[illegible]	[illegible]	[illegible]	[illegible]	
7.30	[illegible]	[illegible]	[illegible]	[illegible]	[illegible]	[illegible]	[illegible]	[illegible]	
7.40	[illegible]	[illegible]	[illegible]	[illegible]	[illegible]	[illegible]	[illegible]	[illegible]	
7.50	[illegible]	[illegible]	[illegible]	[illegible]	[illegible]	[illegible]	[illegible]	[illegible]	
7.60	[illegible]	[illegible]	[illegible]	[illegible]	[illegible]	[illegible]	[illegible]	[illegible]	
7.70	[illegible]	[illegible]	[illegible]	[illegible]	[illegible]	[illegible]	[illegible]	[illegible]	
7.80	[illegible]	[illegible]	[illegible]	[illegible]	[illegible]	[illegible]	[illegible]	[illegible]	
7.90	[illegible]	[illegible]	[illegible]	[illegible]	[illegible]	[illegible]	[illegible]	[illegible]	
8.00	[illegible]	[illegible]	[illegible]	[illegible]	[illegible]	[illegible]	[illegible]	[illegible]	8
8.10	[illegible]	[illegible]	[illegible]	[illegible]	[illegible]	[illegible]	[illegible]	[illegible]	
8.20	[illegible]	[illegible]	[illegible]	[illegible]	[illegible]	[illegible]	[illegible]	[illegible]	
8.30	[illegible]	[illegible]	[illegible]	[illegible]	[illegible]	[illegible]	[illegible]	[illegible]	
8.40	[illegible]	[illegible]	[illegible]	[illegible]	[illegible]	[illegible]	[illegible]	[illegible]	
8.50	[illegible]	[illegible]	[illegible]	[illegible]	[illegible]	[illegible]	[illegible]	[illegible]	
8.60	[illegible]	[illegible]	[illegible]	[illegible]	[illegible]	[illegible]	[illegible]	[illegible]	
8.70	[illegible]	[illegible]	[illegible]	[illegible]	[illegible]	[illegible]	[illegible]	[illegible]	
8.80	[illegible]	[illegible]	[illegible]	[illegible]	[illegible]	[illegible]	[illegible]	[illegible]	
8.90	[illegible]	[illegible]	[illegible]	[illegible]	[illegible]	[illegible]	[illegible]	[illegible]	
9.00	[illegible]	[illegible]	[illegible]	[illegible]	[illegible]	[illegible]	[illegible]	[illegible]	
9.10	[illegible]	[illegible]	[illegible]	[illegible]	[illegible]	[illegible]	[illegible]	[illegible]	
9.20	[illegible]	[illegible]	[illegible]	[illegible]	[illegible]	[illegible]	[illegible]	[illegible]	
9.30	[illegible]	[illegible]	[illegible]	[illegible]	[illegible]	[illegible]	[illegible]	[illegible]	
9.40	[illegible]	[illegible]	[illegible]	[illegible]	[illegible]	[illegible]	[illegible]	[illegible]	
9.50	[illegible]	[illegible]	[illegible]	[illegible]	[illegible]	[illegible]	[illegible]	[illegible]	
9.60	[illegible]	[illegible]	[illegible]	[illegible]	[illegible]	[illegible]	[illegible]	[illegible]	
9.70	[illegible]	[illegible]	[illegible]	[illegible]	[illegible]	[illegible]	[illegible]	[illegible]	
9.80	[illegible]	[illegible]	[illegible]	[illegible]	[illegible]	[illegible]	[illegible]	[illegible]	
9.90	[illegible]	[illegible]	[illegible]	[illegible]	[illegible]	[illegible]	[illegible]	[illegible]	
10.00	[illegible]	[illegible]	[illegible]	[illegible]	[illegible]	[illegible]	[illegible]	[illegible]	10
10.10	[illegible]	[illegible]	[illegible]	[illegible]	[illegible]	[illegible]	[illegible]	[illegible]	
10.20	[illegible]	[illegible]	[illegible]	[illegible]	[illegible]	[illegible]	[illegible]	[illegible]	
10.30	[illegible]	[illegible]	[illegible]	[illegible]	[illegible]	[illegible]	[illegible]	[illegible]	
10.40	[illegible]	[illegible]	[illegible]	[illegible]	[illegible]	[illegible]	[illegible]	[illegible]	
10.50	[illegible]	[illegible]	[illegible]	[illegible]	[illegible]	[illegible]	[illegible]	[illegible]	
10.60	[illegible]	[illegible]	[illegible]	[illegible]	[illegible]	[illegible]	[illegible]	[illegible]	
10.70	[illegible]	[illegible]	[illegible]	[illegible]	[illegible]	[illegible]	[illegible]	[illegible]	
10.80	[illegible]	[illegible]	[illegible]	[illegible]	[illegible]	[illegible]	[illegible]	[illegible]	
10.90	[illegible]	[illegible]	[illegible]	[illegible]	[illegible]	[illegible]	[illegible]	[illegible]	
11.00	[illegible]	[illegible]	[illegible]	[illegible]	[illegible]	[illegible]	[illegible]	[illegible]	11
11.10	[illegible]	[illegible]	[illegible]	[illegible]	[illegible]	[illegible]	[illegible]	[illegible]	
11.20	[illegible]	[illegible]	[illegible]	[illegible]	[illegible]	[illegible]	[illegible]	[illegible]	
11.30	[illegible]	[illegible]	[illegible]	[illegible]	[illegible]	[illegible]	[illegible]	[illegible]	
11.40	[illegible]	[illegible]	[illegible]	[illegible]	[illegible]	[illegible]	[illegible]	[illegible]	
11.50	[illegible]	[illegible]	[illegible]	[illegible]	[illegible]	[illegible]	[illegible]	[illegible]	
11.60	[illegible]	[illegible]	[illegible]	[illegible]	[illegible]	[illegible]	[illegible]	[illegible]	
11.70	[illegible]	[illegible]	[illegible]	[illegible]	[illegible]	[illegible]	[illegible]	[illegible]	
11.80	[illegible]	[illegible]	[illegible]	[illegible]	[illegible]	[illegible]	[illegible]	[illegible]	
11.90	[illegible]	[illegible]	[illegible]	[illegible]	[illegible]	[illegible]	[illegible]	[illegible]	
12.00	[illegible]	[illegible]	[illegible]	[illegible]	[illegible]	[illegible]	[illegible]	[illegible]	12
12.10	[illegible]	[illegible]	[illegible]	[illegible]	[illegible]	[illegible]	[illegible]	[illegible]	
12.20	[illegible]	[illegible]	[illegible]	[illegible]	[illegible]	[illegible]	[illegible]	[illegible]	
12.30	[illegible]	[illegible]	[illegible]	[illegible]	[illegible]	[illegible]	[illegible]	[illegible]	
12.40	[illegible]	[illegible]	[illegible]	[illegible]	[illegible]	[illegible]	[illegible]	[illegible]	
12.50	[illegible]	[illegible]	[illegible]	[illegible]	[illegible]	[illegible]	[illegible]	[illegible]	
12.60	[illegible]	[illegible]	[illegible]	[illegible]	[illegible]	[illegible]	[illegible]	[illegible]	
12.70	[illegible]	[illegible]	[illegible]	[illegible]	[illegible]	[illegible]	[illegible]	[illegible]	
12.80	[illegible]	[illegible]	[illegible]	[illegible]	[illegible]	[illegible]	[illegible]	[illegible]	
12.90	[illegible]	[illegible]	[illegible]	[illegible]	[illegible]	[illegible]	[illegible]	[illegible]	
13.00	[illegible]	[illegible]	[illegible]	[illegible]	[illegible]	[illegible]	[illegible]	[illegible]	13
13.10	[illegible]	[illegible]	[illegible]	[illegible]	[illegible]	[illegible]	[illegible]	[illegible]	
13.20	[illegible]	[illegible]	[illegible]	[illegible]	[illegible]	[illegible]	[illegible]	[illegible]	
13.30	[illegible]	[illegible]	[illegible]	[illegible]	[illegible]	[illegible]	[illegible]	[illegible]	
13.40	[illegible]	[illegible]	[illegible]	[illegible]	[illegible]	[illegible]	[illegible]	[illegible]	
13.50	[illegible]	[illegible]	[illegible]	[illegible]	[illegible]	[illegible]	[illegible]	[illegible]	
13.60	[illegible]	[illegible]	[illegible]	[illegible]	[illegible]	[illegible]	[illegible]	[illegible]	
13.70	[illegible]	[illegible]	[illegible]	[illegible]	[illegible]	[illegible]	[illegible]	[illegible]	
13.80	[illegible]	[illegible]	[illegible]	[illegible]	[illegible]	[illegible]	[illegible]	[illegible]	
13.90	[illegible]	[illegible]	[illegible]	[illegible]	[illegible]	[illegible]	[illegible]	[illegible]	
14.00	[illegible]	[illegible]	[illegible]	[illegible]	[illegible]	[illegible]	[illegible]	[illegible]	14
14.10	[illegible]	[illegible]	[illegible]	[illegible]	[illegible]	[illegible]	[illegible]	[illegible]	
14.20	[illegible]	[illegible]	[illegible]	[illegible]	[illegible]	[illegible]	[illegible]	[illegible]	
14.30	[illegible]	[illegible]	[illegible]	[illegible]	[illegible]	[illegible]	[illegible]	[illegible]	
14.40	[illegible]	[illegible]	[illegible]	[illegible]	[illegible]	[illegible]	[illegible]	[illegible]	
14.50	[illegible]	[illegible]	[illegible]	[illegible]	[illegible]	[illegible]	[illegible]	[illegible]	
14.60	[illegible]	[illegible]	[illegible]	[illegible]	[illegible]	[illegible]	[illegible]	[illegible]	
14.70	[illegible]	[illegible]	[illegible]	[illegible]	[illegible]	[illegible]	[illegible]	[illegible]	
14.80	[illegible]	[illegible]	[illegible]	[illegible]	[illegible]	[illegible]	[illegible]	[illegible]	
14.90	[illegible]	[illegible]	[illegible]	[illegible]	[illegible]	[illegible]	[illegible]	[illegible]	
15.00	[illegible]	[illegible]	[illegible]	[illegible]	[illegible]	[illegible]	[illegible]	[illegible]	15
15.10	[illegible]	[illegible]	[illegible]	[illegible]	[illegible]	[illegible]	[illegible]	[illegible]	
15.20	[illegible]	[illegible]	[illegible]	[illegible]	[illegible]	[illegible]	[illegible]	[illegible]	
15.30	[illegible]	[illegible]	[illegible]	[illegible]	[illegible]	[illegible]	[illegible]	[illegible]	
15.40	[illegible]	[illegible]	[illegible]	[illegible]	[illegible]	[illegible]	[illegible]	[illegible]	
15.50	[illegible]	[illegible]	[illegible]	[illegible]	[illegible]	[illegible]	[illegible]	[illegible]	
15.60	[illegible]	[illegible]	[illegible]	[illegible]	[illegible]	[illegible]	[illegible]	[illegible]	
15.70	[illegible]	[illegible]	[illegible]	[illegible]	[illegible]	[illegible]	[illegible]	[illegible]	
15.80	[illegible]	[illegible]	[illegible]	[illegible]	[illegible]	[illegible]	[illegible]	[illegible]	
15.90	[illegible]	[illegible]	[illegible]	[illegible]	[illegible]	[illegible]	[illegible]	[illegible]	
16.00	[illegible]	[illegible]	[illegible]	[illegible]	[illegible]	[illegible]	[illegible]	[illegible]	16
16.10	[illegible]	[illegible]	[illegible]	[illegible]	[illegible]	[illegible]	[illegible]	[illegible]	
16.20	[illegible]	[illegible]	[illegible]	[illegible]	[illegible]	[illegible]	[illegible]	[illegible]	
16.30	[illegible]	[illegible]	[illegible]	[illegible]	[illegible]	[illegible]	[illegible]	[illegible]	
16.40	[illegible]	[illegible]	[illegible]	[illegible]	[illegible]	[illegible]	[illegible]	[illegible]	
16.50	[illegible]	[illegible]	[illegible]	[illegible]	[illegible]	[illegible]	[illegible]	[illegible]	
16.60	[illegible]	[illegible]	[illegible]	[illegible]	[illegible]	[illegible]	[illegible]	[illegible]	
16.70	[illegible]	[illegible]	[illegible]	[illegible]	[illegible]	[illegible]	[illegible]	[illegible]	
16.80	[illegible]	[illegible]	[illegible]	[illegible]	[illegible]	[illegible]	[illegible]	[illegible]	
16.90	[illegible]	[illegible]	[illegible]	[illegible]	[illegible]	[illegible]	[illegible]	[illegible]	
17.00	[illegible]	[illegible]	[illegible]	[illegible]	[illegible]	[illegible]	[illegible]	[illegible]	17
17.10	[illegible]	[illegible]	[illegible]	[illegible]	[illegible]	[illegible]	[illegible]	[illegible]	
17.20	[illegible]	[illegible]	[illegible]	[illegible]	[illegible]	[illegible]	[illegible]	[illegible]	
17.30	[illegible]	[illegible]	[illegible]	[illegible]	[illegible]	[illegible]	[illegible]	[illegible]	
17.40	[illegible]	[illegible]	[illegible]	[illegible]	[illegible]	[illegible]	[illegible]	[illegible]	
17.50	[illegible]	[illegible]	[illegible]	[illegible]	[illegible]	[illegible]	[illegible]	[illegible]	
17.60	[illegible]	[illegible]	[illegible]	[illegible]	[illegible]	[illegible]	[illegible]	[illegible]	
17.70	[illegible]	[illegible]	[illegible]	[illegible]	[illegible]	[illegible]	[illegible]	[illegible]	
17.80	[illegible]	[illegible]	[illegible]	[illegible]	[illegible]	[illegible]	[illegible]	[illegible]	
17.90	[illegible]	[illegible]	[illegible]	[illegible]	[illegible]	[illegible]	[illegible]	[illegible]	
18.00	[illegible]	[illegible]	[illegible]	[illegible]	[illegible]	[illegible]	[illegible]	[illegible]	18
18.10	[illegible]	[illegible]	[illegible]	[illegible]	[illegible]	[illegible]	[illegible]	[illegible]	
18.20	[illegible]	[illegible]	[illegible]	[illegible]	[illegible]	[illegible]	[illegible]	[illegible]	
18.30	[illegible]	[illegible]	[illegible]	[illegible]	[illegible]	[illegible]	[illegible]	[illegible]	
18.40	[illegible]	[illegible]	[illegible]	[illegible]	[illegible]	[illegible]	[illegible]	[illegible]	
18.50	[illegible]	[illegible]	[illegible]	[illegible]	[illegible]	[illegible]	[illegible]	[illegible]	
18.60	[illegible]	[illegible]	[illegible]	[illegible]	[illegible]	[illegible]	[illegible]	[illegible]	
18.70	[illegible]	[illegible]	[illegible]	[illegible]	[illegible]	[illegible]	[illegible]	[illegible]	
18.80	[illegible]	[illegible]	[illegible]	[illegible]	[illegible]	[illegible]	[illegible]	[illegible]	
18.90	[illegible]	[illegible]	[illegible]	[illegible]	[illegible]	[illegible]	[illegible]	[illegible]	

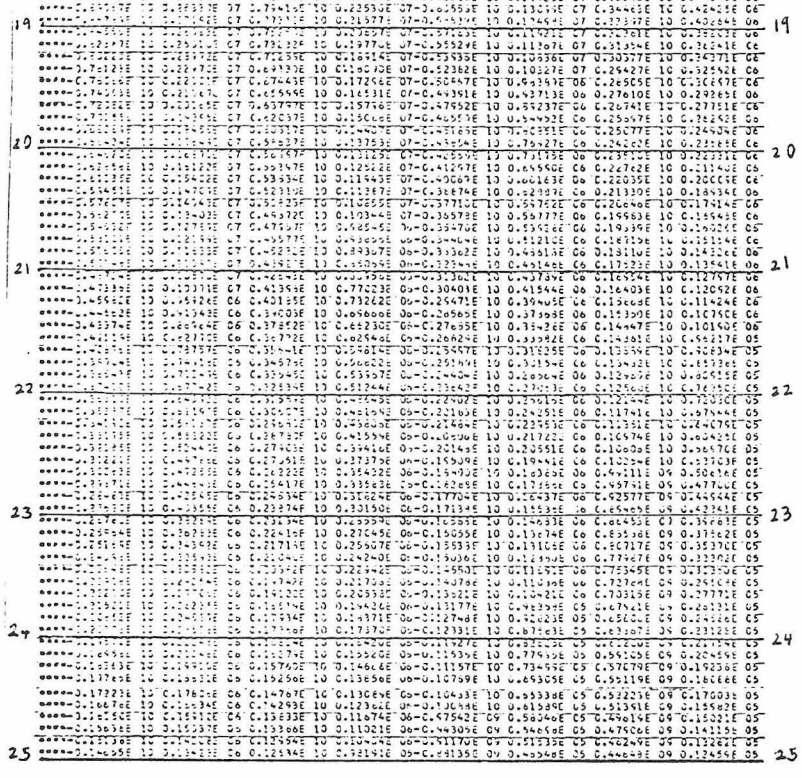

Chem 2 is Probably a Social Disease (#3)

Due Monday 9 October

Reading: Huheey 56-76

1. (3 pts) Work problem number 1 of the last problem set.

2. (4 pts) Make a plot similar to figure 2.20 including the elements F, Cl, Br and I for oxidation states from -1 to +3. Values of IP and EA needed for this graph can be found in tables 2.5A and 2.6. F and Cl are plotted in figure 2.20 so you can check your work against this figure to see if you are doing things right. These curves may be described by the equation

$$E = \alpha q + \beta q^2 + \gamma q^3 + \delta q^4 \qquad (1)$$

where the values for the constants are given for F and Cl below.

	α	β	γ	δ
F	12.66	8.70	-0.40	-0.083
Cl	9.83	5.65	-0.36	-0.0433

The slope of such curves at the origin (E = q = 0) is proportional to the electronegativity of the atom. (If you don't understand the meaning of the slope of a curve, ask someone to explain it to you.) The slope is given by

$$\text{slope} = dE/dq = \alpha + 2\beta q + 3\gamma q^2 + 4\delta q^3 \qquad (2)$$

At q = 0, the slope is just α.

a. By inspection of your graph, rank these four halogens in order of increasing electronegativity.

b. By evaluating equation (1) at q = -2, determine the energy for the following reaction for Cl and F :

$$X^- + e^- = X^{2-}$$

For which element is this process more favorable?

3. (2 pts) Plot the first eight ionization potentials of Al given in table 2.5A.

a. Explain the discontinuity in your graph.

b. Where would the next major discontinuity occur?

c. To which process below does the IP listed in table 2.5A under VIII refer?

i. $Al^{+7} = Al^{+8} + e^-$

ii. $Al = Al^{+8} + 8e^-$

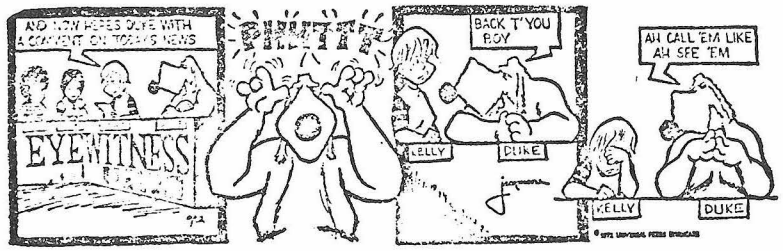

4. (4 pts) The K-Cl distance in a crystal of KCl is 3.14 Å.

a. Calculate the effective nuclear charge, Z*, for K^+ and for Cl^- using the method of Clementi and Raimondi. Pay attention to the fine print on page 71 when you do this.

b. With these values, estimate the ionic radii of K^+ and Cl^-.

To Be Born-Haber Is To Be Born Unlucky (#4)

Due Thursday 12 October

Reading: Lewis Structure handout and Huheey 138-142

1. (4 pts) Predict the enthalpy of formation, ΔH_f, of CaS by means of a Born-Haber cycle. Use crystal radii for Ca^{2+} and S^{2-} from Table 3.5. When calculating U_o, ignore any heat capacity corrections. You may wish to reproduce the value U_o (NaCl) = -180 kcal mole^{-1} using equation 3.11 to be sure that you understand how to use this equation. The units are especially important. To find ΔH_f(Ca(g)) and ΔH_f(S(g)), use Appendix 3 of the Chem 1 text which appears on the next page. (Save this table as we will use it occasionally throughout the year.) For the reaction X→Y, $\Delta H^o = \Delta H^o(Y) - \Delta H^o(X)$. Thus to find ΔH^o for the reaction $H_2O(l) \rightarrow H_2O(g)$, $\Delta H^o = (-57.798) - (-68.317) = +10.519$ kcal mole^{-1}. The sign is very important as it tells that you must put heat into this reaction to make it go. Be sure that the sign for ΔH for each step of your Born-Haber cycle makes sense. State any assumptions that you make when working this problem. Compare the calculated heat of formation of CaS with the experimental value found in the Handbook of Chemistry and Physics. What are the principal sources of error in your calculation besides your arithmetic mistakes?

A candid view of the Chem 2 staff preparing this problem set.

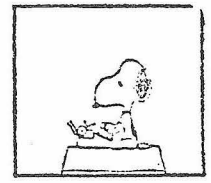

2. (2 pts) problem 3.6 of Huheey

3. (4 pts) Draw the single best Lewis structure for each compound below. The central atom is underlined in each case. Be sure to include any formal charges.

a. $\underline{Be}H_2$
b. CsI
c. $\underline{Tl}Br_3$
d. $\underline{Xe}OF_4$
e. $H\underline{C}N$
f. $\underline{Pb}O_2$

3 STANDARD ENTHALPIES AND FREE ENERGIES OF FORMATION, AND STANDARD THIRD LAW ENTROPIES, AT 298°K

This table gives the standard heat (ΔH°_f) and free energies (ΔG°_f) of formation of compounds from elements in their standard states and the thermodynamic or third law entropies (S°) of compounds, all at 298°K. The state of the compound is specified by (g) = gas, (l) = liquid, (s) = solid, (aq) = aqueous solution. Occasionally the crystal form of the solid is also specified. Compounds are arranged by the group number of a principal element, with metals taking precedence over nonmetals and O and H being considered least important.

This table is an abbreviated version of a more complete one in R. E. Dickerson, *Molecular Thermodynamics* (W. A. Benjamin, New York, 1969). Other convenient tabulations are found in the *Chemical Rubber Company Handbook of Chemistry and Physics* and in *Lange's Handbook of Chemistry*.

	Substance	ΔH°_f	ΔG°_f	S°
	H(g)	52.089	48.573	27.393
	H^+(aq)	0.0	0.0	0.0
	H_2O(l)	−68.317	−56.690	16.716
	H_2O(g)	0.0	0.0	31.211
IA	Li(g)	37.07	29.19	33.143
	Li(s)	0.0	0.0	6.70
	Li^+(aq)	−66.554	−70.22	3.4
	LiF(s)	−146.3	−139.6	8.57
	LiCl(s)	−97.70	−91.7	(13.2)
	LiBr(s)	−83.72	−81.2	(16.5)
	Na(g)	25.98	18.67	36.715
	Na(s)	0.0	0.0	12.2
	Na^+(aq)	−57.279	−62.589	14.4
	Na_2O(s)	33.97	24.85	55.92
	NaO_2(s)	−61.9	−46.5	–
	NaF(s)	−99.4	−90.0	17.4
	Na_2SO_4(s)	−1210.6	−1012.8	(19.9)
	NaCl(g)	−136.0	−129.3	14.0
	NaCl(s)	−98.232	−91.785	17.3
	NaBr(s)	−86.030	−85.1	–
	NaI(s)	−68.84	−56.7	–
	$NaClO_3$(s)	−270.3	−250.4	32.5
	K(g)	21.51	14.62	38.296
	K(s)	0.0	0.0	15.2
	K^+(aq)	−60.04	−67.46	24.5
	KCl(s)	−104.175	−97.592	19.76
	KCl(g)	−51.6	−59.2	57.24
	Rb(g)	20.51	13.35	40.828
	Rb(s)	0.0	0.0	16.6
	Rb^+(aq)	−58.9	−67.43	29.7
	RbF(s)	−131.9	−124.5	27.2
	RbCl(s)	−102.91	−98.8	–
	RbBr(s)	−93.03	−90.38	25.48
	RbI(s)	−78.5	−77.8	26.21
	Cs(g)	18.85	12.24	41.944
	Cs(s)	0.0	0.0	19.8
	Cs^+(aq)	−59.2	−67.41	31.8
	CsF(s)	−126.9	−119.5	–
	CsCl(s)	−103.5	−96.6	–
	CsBr(s)	−94.3	−91.6	29
	CsI(s)	−86.5	−79.7	31
IIA	Be(g)	76.63	67.60	32.543
	Be(s)	0.0	0.0	2.28
	Be^{++}(aq)	−93	−85.2	–
	Mg(g)	35.9	27.6	35.504
	Mg(s)	0.0	0.0	7.77
	Mg^{++}(aq)	−110.41	−108.99	−28.2
	$MgCl_2$(s)	−153.40	−141.57	21.4
	$MgCl_2 \cdot 6H_2O$(s)	−597.42	−505.93	47.5
	Ca(g)	46.04	37.98	36.99
	Ca(s)	0.0	0.0	9.95
	Ca^{++}(aq)	−129.77	−132.18	−13.2
	CaO(s, calcite)	−284.45	−269.78	22.2
	CaO(s, aragonite)	−288.49	−269.55	21.2
	SrO(g)	39.2	29.3	39.325
	SrO(s)	0.0	0.0	13.0
	Sr^{++}(aq)	−130.38	−133.2	−9.4
	BaO(g)	41.96	34.60	40.699
	BaO(s)	0.0	0.0	16
	Ba^{++}(aq)	−128.67	−134.0	3
	BaCl(g)	−205.56	−193.8	30
	$BaCl_2 \cdot H_2O$(s)	−278.4	−253.1	40
	$BaCl_2 \cdot 2H_2O$(s)	−349.55	−309.8	48.5
IVB	Ti(g)	112	101	43.069
	Ti(s)	0.0	0.0	7.24
	TiO_2(s, rutile III)	−218.0	−203.8	12.01
	TiO^{++}(aq)		−138	–
	Ti_2O_3(s)	−567	−546	18.83
	Ti_3O_5(s)	−584	−550	30.92
VIB	W(g)	201.6	191.6	41.552
	W(s)	0.0	0.0	8.0
VIII	Fe(g)	96.68	85.76	43.11
	Fe(s)	0.0	0.0	6.49
	Fe^{++}(aq)	−21.0	−20.30	−27.1
	Fe^{+++}(aq)	−11.4	−2.53	−70.1
	Fe_2O_3(s, hematite)	−196.5	−177.1	21.5
	Fe_3O_4(s, magnetite)	−267.9	−242.4	35.0
IB	Cu(g)	81.52	72.04	39.744
	Cu(s)	0.0	0.0	7.96
	Cu^+(aq)	(12.0)	12.0	(−9.6)
	Cu^{++}(aq)	15.39	15.53	−23.6
	CuO(s)	−184.00	−158.2	27.1
	Ag(g)	69.12	59.84	41.3221
	Ag(s)	0.0	0.0	10.206
	Ag(aq)	−30.362	−26.224	22.97
	$AgNO_3$(s)	−10.605	4.744	30.92
	$AgNO_3$(aq)	−29.43	−7.69	33.68
IIB	Hg(g)	14.54	7.59	41.80
	Hg(l)	0.0	0.0	18.5
	Hg_2Cl_2(s)	−53.0	−44.4	(34.5)
	$HgCl_2$(s)	−63.32	−50.35	46.8
IIIA	B(g)	97.2	86.7	36.649
	B(s)	0.0	0.0	1.56
	B_2O_3(s)	−302.0	−283.0	12.91
	B_2H_6(g)	7.5	19.8	55.66
	B_5H_9(g)	15.0	39.6	65.88
	BF_3(g)	−265.4	−261.3	60.70
	BF_3(aq)	−365	−345	40
	BCl(g)	−94.5	−90.9	69.29
	BCl_3(l)	−100.0	−96.6	50.0
	BBr_3(g)	−44.6	−51.0	77.49
	BBr_3(l)	−52.8	−52.4	34.7
	Al(g)	75.0	65.3	39.593
	Al(s)	0.0	0.0	6.769
	Al^{+++}(aq)	−125.4	−115.9	−74.9
	Al_2O_3(s)	−399.09	−376.77	12.186
	AlF(g)	−196.2	−152.2	49
	TlF(g)	[illegible]	−5	65.6
	TlF(s)	−297.7	−294.2	29.4
IVB	C(g)	171.698	166.845	37.761
	C(s, diamond)	0.4532	0.6850	0.5429
	C(s, graphite)	0.0	0.0	1.3609
	CO_2(g)	−393.517	−394.389	47.801
	CO_2(aq)	−419.26	−386.022	51.061
	CO_3^{--}(aq)	−677.14	−527.81	29.0
	CO(g)	−27.200	−32.810	47.30
	CH_4(g)	−17.889	50.8	44.499
	C_2H_6(g)	−20.236	−7.860	54.85
	C_3H_8(g)	−24.82	−5.61	64.51
	C_4H_{10}(g)	−29.81	−4.75	74.10
	C_5H_{12}(g)	−35.85	−8.39	83.42
	C_6H_{14}(g)	−39.959	0.064	92.90
	C_2H_4(g)	12.556	16.282	52.45
	C_2H_2(g)	226.731	209.970	48.000
	C_6H_6(l)	49.087	124.50	64.34
	C_6H_6(g)	82.927	129.66	64.34
	C_2H_5OH(l)	−277.63	−174.76	38.4
	C_2H_5OH(g)	−235.31	−168.49	67.9
	CH_3OH(l)	−238.66	−166.27	30.3
	CH_3OH(g)	−200.66	−162.00	57.5
	HCN(g)	135.1	124.7	48.2
	HCN(l)	108.9	112.8	26.7
	CH_3NH_2(g)	−5.5	32.8	57.7
	CH_3CN(l)	−37.9	−12.7	29.4
	CH_3CN(g)	−21.4	−5.4	59.3
	CH_3CO_2H(l)	−116.4	−93.8	38.2
	CH_3CO_2H(g)	−103.743	−95.31	–
	$CH_3CO_2^-$(aq)	−116.843	−89.92	–
	H_2CO(g)	−108.7	−102.5	52.3
	H_2CO_3(aq)	−167.0	−149.0	45.7
	HCO_3^-(aq)	−165.18	−140.31	22.5
	CO_3^{--}(aq)	−161.63	−126.22	−12.7
	CH_3OCH_3(g)	−184.1	−95.8	63.2
	CH_3CH_2OH(g)	−56.240	−38.79	76.8
	CH_3CHO(g)	−39.75	−32.89	63.1
	CH_3CHO(l)	−57.036	−39.75	30.3
	$CH_3CO_2CH_3$(l)	−98.72	−74.06	51.4
	$CH_3CO_2CH_3$(g)	−96.30	−77.76	79.1

in which there is no charge separation. (One is given. Just draw two more.) If all three structures contribute equally to the structure of the molecule, what is the bond order of each carbon-carbon bond in the molecule? Is this consistent with the known bond distances (in Angstroms) below?

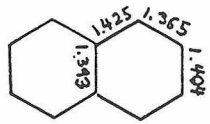

5. (2 pts) Using the VSEPR rules, draw a three dimensional structure for each species below.

a. SF_6 (sulfur hexafluoride)
b. $\underline{Xe}OF_4$ (tetrafluorooxoxenon(VI))
c. PCl_5 (phosphorus pentachloride)
d. PO_4^{3-} (phosphate)
e. $SnCl_3^-$ (trichlorostannite)
f. $\underline{Al}(OH)_3(H_2O)_3$ (t rihydroxytriaquo-aluminum(III))

There are two possible isomers of f. Draw only one.

(Thompson is in trouble?)

Will you please be sure to write both your first and last names legibly on your answer sheets. Some people are losing complete credit for their homework because we can't figure out who they are.

Mostly Molecular Stereochemistry

and

Why I Slugged a Molecular Orbital

or

Homonuclear Diatomics are Sometimes Gay (Part I) (#6)

Due Thursday 19 October

Reading: Huheey 93-113

A two hour, open book, take-home exam will be given out on Thursday, 19 October. It will be due on Monday, 23 October. Pleasant dreams.

1. (5 pts) Draw a clear, three-dimensional structure for each beastie below. Show the sites occupied by lone pairs. Draw one good Lewis structure for each one while you're at it. Central atoms are sometimes underlined.

a. SOF_4 tetrafluorooxosulfur(VI)
b. TeO_4^{2-} tellurate
c. $Se\underline{C}N^-$ selenocyanate
d. PbI_2 lead diiodide
e. SO_2Cl_2 sulfuryl chloride
e. $Sb(C_6H_6)_5$ pentaphenylantimony(V)
f. AsF_6^- hexafluoroarsenate(V)
g. $\underline{Sn}Cl_2(OH)_2$ dichlorodihydroxytin(IV)
h. $BeCl_2(NH_3)_2$ dichlorodiammineberyllium(II)
i. $(CN)_2CC(CN)_2$ tetracyanoethylene

In the case of pentaphenylantimony, don't draw out all of the phenyl ring atoms. Just call each phenyl group "L". Don't draw a Lewis structure for the phenyl rings either. Just draw a Lewis structure for the central SbL_5 group. Tetracyanoethylene has the following basic structure:

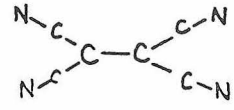

2. (2pts) Propose a structure for each species in the series XeF_2. XeF_3^-, XeF_4, XeF_5^- and XeF_6. Draw clear pictures showing all ligands and lone pairs.

3. (3 pts) Diatomic quickies. For the homonuclear diatomics Li_2-N_2 use the energy level scheme I below. For O_2 and F_2, scheme II is applicable. For heteronuclear diatomics, eg. CN, try both schemes and see if your result would be affected by the choice of schemes.

a. Match the reactions with their enthalpies.

i. $O_2^- = O^- + O$
ii. $O_2 = 2O$
iii. $O_2^+ = O^+ + O$

a. +149 kcal mole^{-1}
b. + 90 " "
c. +118 " "

b. Which is the most stable cation? N_2^+, NO^+, O_2^+, Li_2^+, Be_2^+

c. Which has the longest bond? CN^+, CN^-, CN, NO^+

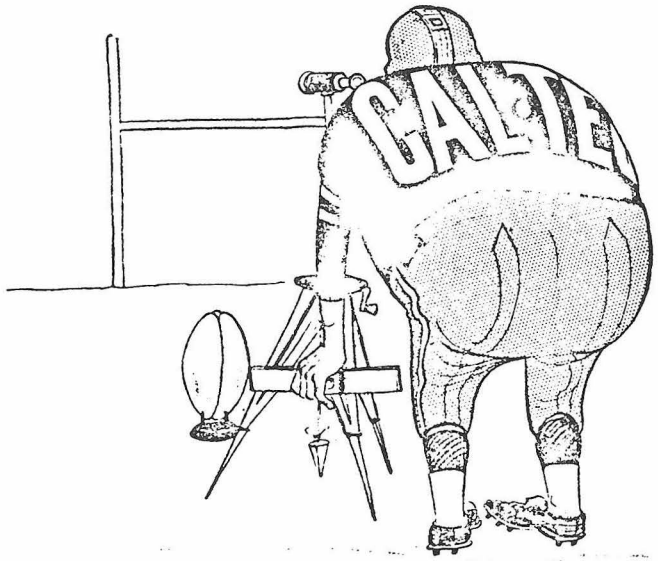

Scheme I

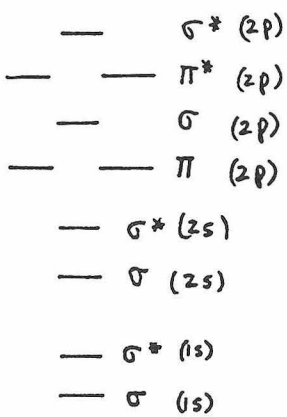

Scheme II

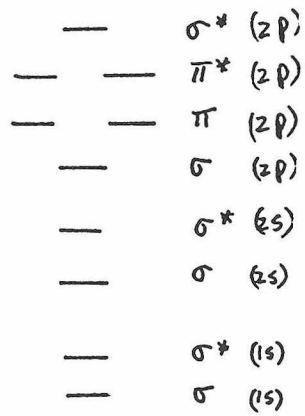

Chem 2 Strikes Back!

or

Disparage Your Local Chemist!

This titillating experience may last up to two hours but no more. You may use your textbook, your class notes, your homework and handouts. If you are desperate, you may even use your brain. No collaboration, naturally. Please put your answers in the blue exam books available at the book store. To further confuse you, the reading assignment to be done prior to Monday's class is Huheey 114-120, 130-138, 142-143. This test is due Monday 23 October. It is worth 100 points and your total grade for the quarter will come to 500 points.

1 (10 pts) Write the single best Lewis structure for each compound. Show all formal charges.

a. PF_5 (phosphorus pentafluoride)
b. H-N-N-H (diimide)

What is the oxidation state of each atom in these compounds?

2. (10 pts) Draw the electron configuration of each species below using circles for each orbital as we did in class and on a problem set. Venerate Hund and Pauli.

Nb Au^{+3} U^{+3} O^{-2}

3. (15 points) Draw a clear picture that Picasso would be proud of showing the stereochemistry of each species below. Sometimes the central atom is underlined. Indicate the stereochemical number in each case.

a. O-O-O (ozone)
b. $Te(CH_3)_4$ (tetramethyltellurium)
c. BO_3^{3-} (borate)
d. I-C-N (iodine cyanide)
e. $\underline{Xe}OF_2$ (difluorooxoxenon(IV))

In case (b) treat each methyl group as a monatomic ligand, L, in your picture.

4. (8 pts) Write the <u>sign</u> (<u>just</u> the sign) of ΔH for each reaction below taken from left to right.

a. $O(g) + e^-(g) = O^-(g)$
b. $O(g) + 2e^-(g) = O^{2-}(g)$
c. $CH_3(g) = CH_3^+(g) + e^-(g)$
d. $Mg^{2+}(g) + 2F^-(g) = MgF_2(s)$

5 (12 pts) Consider a He^+ ion bombing along in the sun's corona on a nice afternoon.

a. Write the ground state electron configuration of this atom. (<u>ie.</u>, tell how many electrons are in which orbitals.)

b. With appropriate alchemy, calculate the ionization energy (in ergs and kcal/mole) of this cation. This is the energy of the reaction

$$He^+(g) = He^{++}(g) + e^-(g)$$

c. If this energy is in the form of light, will a photon be absorbed or emitted during this process?

d. What is the wavelength (nm) and wavenumber (cm^{-1}) of this photon?

In part (b) you are asked to <u>calculate</u> this number, not to look it up.

6 (2 pts) Match each picture with an appropriate description. Do not justify your answer as I can't justify this question.

a. man's best friend
b. man's worst friend
c. an impostor
d. Chem 2 staff

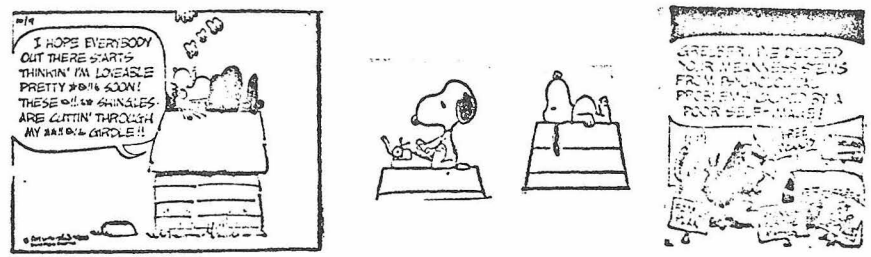

I II III IV

7. (10 pts) a. Write the n best resonance structures for each species. n is given in parentheses for each case.

i. CO (carbon monoxide) (2)
ii. H-O-I(=O)(=O) (iodic acid) (3)

b. The I-O distances in HIO_3 are 1.81 and 1.89 Angstroms. Label each I-O bond with its proper length.

8. (8 pts) In the figures below are shown contour diagrams of ψ_{3p_x} and $\psi^2_{3p_x}$.

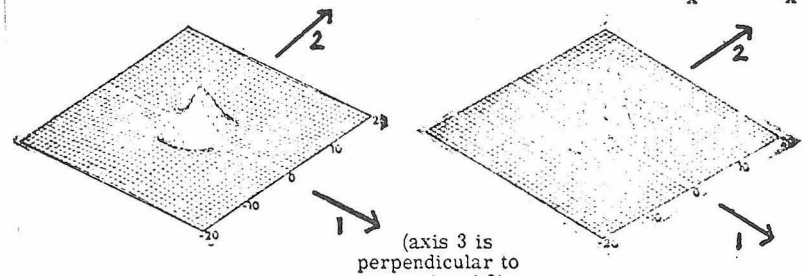

(axis 3 is perpendicular to axes 1 and 2)

a. Which one is ψ and which is ψ^2?

b. Match the axes 1, 2 and 3 with the Cartesian axes x, y and z.

c. Write an analytical expression for the radial (R) and angular ($\Theta\Phi$) parts of ψ_{3p_x}. These need not be normalized.

d. Which function, R, Θ or Φ, accounts for the spherical node in ψ_{3p_x}? Which accounts for the planar node?

9. (10 pts) The aluminum halides do not exist as monomers (AlX_3) in the gas phase at room temperature. Rather, the dimers (Al_2X_6) with the structures below are formed.

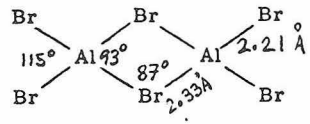

a. Write the Lewis structures for the reactants and products as shown below.

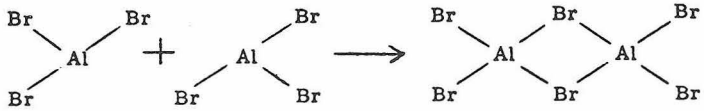

b. Indicate on your drawing how this reaction can be considered to be that of Lewis acids and Lewis bases.

c. What is the stereochemical number of Al in Al_2Br_6? Is this compound planar?

10. (15 pts) What is the value (sign and magnitude) of ΔH^o_{298} for the following reactions?

a. $Ca(g) + 2F(g) = CaF_2(s)$ ($CaF_2(s)$ is the mineral fluorite)

b. $Ca^{2+}(g) + 2F^-(g) = CaF_2(s)$

c. $Ca^{2+}(aq) + 2F^-(aq) = CaF_2(s)$

$\Delta H^o_{298}(CaF_2(s)\text{-fluorite}) = -290.3$ kcal/mole. Determine ΔH for the second reaction by the most accurate means available. Will fluorite be soluble in water?

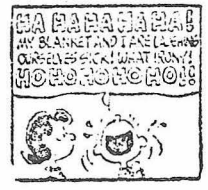

In Lieu of a Better Problem Set (#8)

(There is no problem set #7)

Due Thursday 26 October

Reading: Huheey 149-151, 155-169 (up to the bottom paragraph)

1. (1 pt) Propose a hybrid orbital bonding scheme for allene, C_3H_4 which explains its geometry. Before doing this, draw the single best Lewis structure of allene.

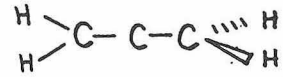

allene

2. (1 pt) Predict the geometry of the hypothetical C_4H_4 shown below using a hybrid orbital bonding scheme. All four C atoms are linear.

$$H_2C{=}C{=}C{=}CH_2$$

3. (2 pts) Acetic acid is a typical carboxylic acid which ionizes in water to give the acetate anion (a carboxylate anion).

$$CH_3\overset{O}{\overset{\|}{C}}OH \longrightarrow CH_3CO_2^- + H^+$$

Draw one good Lewis structure for acetic acid and two good structures for the anion. Propose a hybrid orbital bonding scheme for the anion Over which orbitals is the negative charge spread?

4. (3 pts) In this problem we will calculate the C-C bond hybridization of some interesting organic compounds based on experimentally determined C-H hybridizations. The C-H hybridizations were determined by nuclear magnetic resonance in a way which we will study this spring. In cyclopropane, C_3H_6, the C-H hybridization is known to be sp^2.

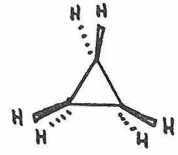

This just means the bond has $\frac{1}{3}$ s character and $\frac{2}{3}$ p character. We are only talking about the C atom as the H atom uses nearly pure 1s orbital. Now we have to divide up the remaining s and p character into two equal parts for the two remaining C-C bonds. The total s character of all four orbitals must add to unity as there is only one s orbital on C. The total p character must sum to 3 since there are three p orbitals.

C-H	$\frac{1}{3}$s	$\frac{2}{3}$p
C-H	$\frac{1}{3}$s	$\frac{2}{3}$p
C-C	xs	yp
C-C	xs	yp

$$2(\tfrac{1}{3})s + 2xs = 1s \Longrightarrow x = 1/6$$
$$2(\tfrac{2}{3})s + 2yp = 3p \Longrightarrow y = 5/6 \Longrightarrow sp^5$$

The C-C bonds have 1/6 s character and 5/6 p character so the hybridization is sp^5. Now do the same for cyclobutane, C_4H_8, and cubane, C_8H_8.

cyclobutane

cubane

The C-H hybridizations are sp^3 in cyclobutane and sp^2 in cubane. In these pictures there is one carbon at each vertex and hydrogens to go around such that each carbon atom is bonded to a total of four neighbors.

5. (2 pts) Sulfur is perfectly octahedral in SF_6. All S-F distances are the same and all angles are 90°. Using the coordinate system below, which six orbitals among the energetically feasible set 3s, 3p, 3d can combine to form six equivalent octahedral hybrid orbitals (ie., six hybrids, each of which points toward one of the ligands).

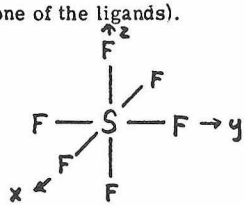

6. (1 pt) Huheey, problem 4.8.

In Memory of Jackie Robinson (#9)

Due Monday 30 October

It is a high form of honor to have a problem set dedicated in your name. It is something else again to have to do that problem set.

Reading: Chem 1 Text (Dickerson, Gray, Haight) 572-596. This assignment and the next one will be from chapter 14 of DGH. These will be the only assignments from DGH this year so don't go off and buy the book. Borrow one from a Chem 1 Toad who will be more than happy to be rid of it.

1. (4 pts) Which compounds are optically active?

a. CH_2ClBr

b. 2-chlorobutane

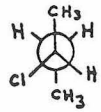

c.

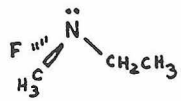

Note: Nitrogen compounds with a lone pair invert rapidly (10^3-10^5 sec^{-1}) as follows:

d. CH_3NHFCl^+

e. erythrose

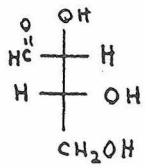

f.

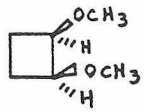

g. 1,3-dichloroallene HClC=C=CClH

2. (3 pts) The pK of a base is defined as follows:

$$B + H_2O = BH^+ + OH^-$$
$$K_b = [BH^+]\,[OH^-]/[B]$$
$$pK_b = -\log_{10}K_b$$

Here are some compounds and pK values.

$(CH_3)_3N$:

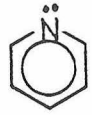

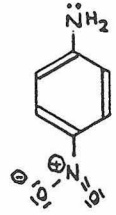

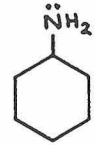

trimethylamine $pK_b = 4.26$

pyridine $pK_b = 8.8$

p-nitroaniline $K_b = 3.8 \times 10^{-10}$

cyclohexylamine $K_b = 4.4 \times 10^{-4}$

a. At what concentration of OH^- will trimethylamine be half protonated in aqueous solution? What about pyridine?

b. What is the pH (-log $[H^+]$) of each of these solutions?

c. Which is a stronger base?

d. Explain the relative basicities of trimethylamine and pyridine in terms of hybridization and electronegativity. Use no more than three sentences.

e. p-Nitroaniline is a much weaker base than cyclohexylamine. Draw just one important resonance structure of p-nitroaniline to illustrate why this is so. You may use no more than one sentence to show how your resonance structure explains the relative base strengths

3. (3 pts) If you really groove stereochemistry this is the problem for you. Cis- and trans-stilbene both react with chlorine to give the stilbene dichlorides. If chlorine adds in a cis fashion across the C=C bond it should form the meso dichloride from cis-stilbene and the d,l-dichloride from trans-stilbene:

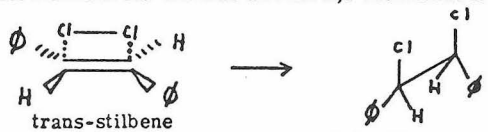

trans-stilbene

d,l-stilbene dichloride

(ϕ = phenyl)

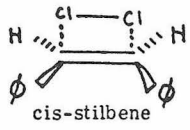

cis-stilbene

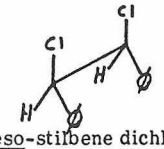

meso-stilbene dichloride

In order to test this prediction you need to determine whether d,l or meso product is formed from each isomer of stilbene. There is a way to distinguish the d,l from the meso product. It involves measuring the dipole moment of each. Consider the possible rotamers (rotational isomers) of each substance. Draw them all out and label the most stable rotamer of each compound. In doing this, only draw staggered conformations. To determine the most stable rotamer, consider the relative sizes of the substituents to be phenyl>Cl>H. Now look at the most stable rotamer of each compound and decide which one has the greater dipole moment. The dipole is due mainly to the C-Cl dipole. Remember to add the dipoles vectorially:

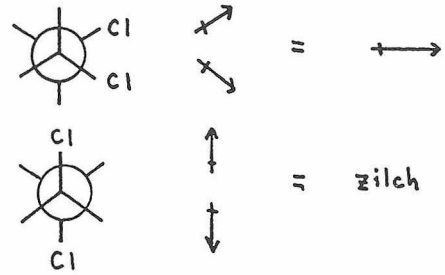

If the product from addition of chlorine to trans-stilbene has a dipole moment of 2.75D and that of cis-stilbene had a moment of 1.27D, was the addition of chlorine across the double bond cis as drawn above?

OPTIONAL Cyclohexane has two types of conformations known as the boat and the chair. Of these, the chair is more stable and we will only worry

boat

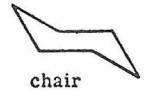

chair

about chairs in this problem. The chair form has axial and equatorial positions:

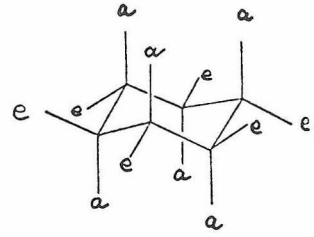

Generally, a substituent finds the equatorial position more hospitable.

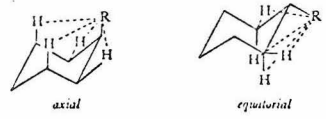

axial equatorial

Equatorial and axial monosubstituted cyclohexanes. Significant nonbonded interactions are indicated by dotted lines; these are more severe in the axial than the equatorial conformation.

But note that simple ring inversion can interchange all axial and equatorial positions.

(axial) (equatorial)

Cyclohexane itself inverts about 10^6 times each second at room temperature. The ring inversion of methylcyclohexane above has an equilibrium constant of 15 favoring the equatorial form. Though there is fifteen times as much equatorial form present as axial form in solution, each converts to the other many times each second.

Draw the cis and trans isomers of 1,3-dimethylcyclohexane in the chair form and draw the mirror image of each one. Are either the cis or trans forms optically active in the absence of ring inversion? What happens if there is rapid ring inversion?

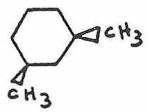

cis-1,3-dimethylcyclohexane

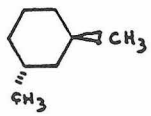

trans-1,3-dimethylcyclohexane

This Paper Was Better Off as a Tree (#10)

Due Thursday 2 November

Reading: DGH 597-620

1. (2 pts) Top exercise, page 584 DGH

2. (1 pt) Problem 2, page 627 DGH

3. (1 pt) Problem 8, page 628 DGH

4. (2 pts) Three moles of an ideal gas at 27° C expand isothermally and reversibly from 20 l to 60 l. Compute w, q and ΔE.

5. (2 pts) The stabilization (delocalization) energy of benzene is calculated to be 40 kcal/mole on page 585. Using bond energies, estimate the heat of formation of cyclooctatetraene. The experimental heat of formation is 1095 kcal/mole. What is the stabilization energy of cyclooctatetraene? In three sentences or less (perhaps with a good picture), explain the difference in stabilization energy between benzene and cyclooctatetraene in terms of geometry and bonding. Cyclooctatetraene exists in the "tub" form below.

cyclooctatetraene
C_8H_8

6. (2 pts) The residual entropy of deuteromethane (CH_3D) at absolute zero is 2.77 cal/deg/mole. Explain this in terms of Boltzmann's equation 14-10. Deuteromethane will be a crystalline solid at absolute zero.

OPTIONAL (Guaranteed to blow your little mind) The Cope rearrangement of a diene (two "enes" is two double bonds) proceeds as follows:

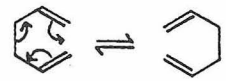

The geometry of this reaction is consistent with a chair-like transition state.

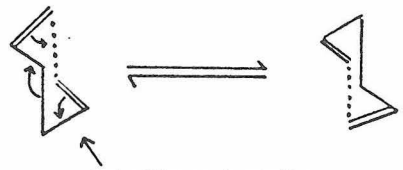

chair-like conformation

A boat-like transition state is also possible but it will be of higher energy. One chair-like rearrangement of a deuterium substituted compound is shown below. In this figure, the lines projecting from the basic carbon skeleton are understood to end in hydrogen atoms and they are not methyl groups.

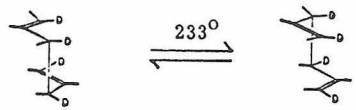

Draw the product of a boat-like rearrangement reaction starting with the compound on the left above. Molecular models are almost essential to working this problem.

Most of These Problems Have Solutions - For a Change (#11)

Due Monday 6 November

Reading: Huheey 1 82-205

Much to our mutual regret, there will be a second Chem 2a midterm exam given out on Thursday 9 November. It will be due on the following Monday. This test is guaranteed to be shorter than the last one.

Problems:

1. (1 pt) DGH page 629 #13
2. (2 pts) DGH page 629 #14
3. (2 pts) DGH page 629 #15
4. (2 pts) DGH page 629 #17
5. (2 pts) DGH page 630 #28
6. (1 pt) Huheey page 206 #5.5

A Challenge (Optional): The series of $C_{10}H_{10}$ hydrocarbons below interconvert with the application of heat(Δ) or light ($h\nu$). We can imagine how 1 goes to 34 by rearranging electrons as shown in the diagram on the right below. I challenge you first to understand what these drawings are telling you about how 1 goes to 37 goes to 38 goes to 34. I challenge you to show how bonds in 1 can be rearranged to go to 33. I challenge you to show how any of these other hydrocarbons can be interconverted. (Source: J. Am. Chem. Soc., 92, 3118 (1970).)

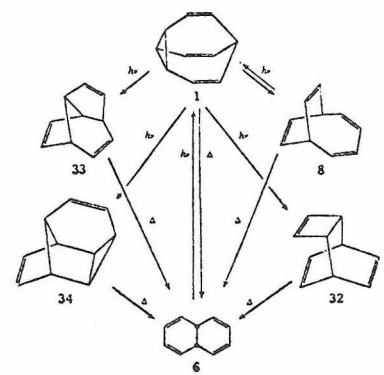

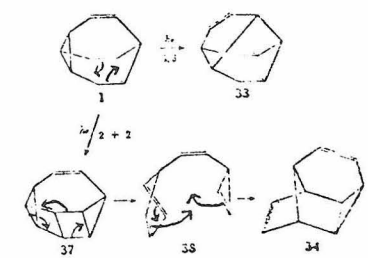

"If You're Old Enough to Vote and Old Enough to Fight For Your Country, You're Not Innocent Enough to be in Chem 2" or "You'll Need All The Innocence You Can Muster to Work This Set." (#12)

Due Thursday 9 November

Reading: Huheey 207-218, 225-230 and (optional) 230-235

Topics to study for the next midterm: MO theory of diatomic molecules, hybridization and bonding, optical activity, thermodynamics, chemical forces. Lewis structures and VSEPR will be used freely whenever needed.

1. (2 pts) Calculate the London energy (instantaneous dipole-induced dipole) in cgs units of two Ar atoms separated by 5 Angstrom units.

Molecule	Polarizability (α) (units are $10^{-24}cm^3$)	Dipole Moment(μ) (Debye)
He	0.203	0
Ne	0.392	0
Ar	1.63	0
Kr	2.46	0
Xe	4.01	0
H_2	0.81	0
N_2	1.72	0
O_2	1.55	0
CH_4	2.6	0
C_2H_6	4.5	0
$(CH_3)_2O$	6.0	1.30
NH_3	2.34	1.46
H_2O	1.59	1.85
CH_3OH	3.0	1.70
para-dichlorobenzene	-	0
meta-dichlorobenzene	-	1.72
ortho-dichlorobenzene	-	2.50

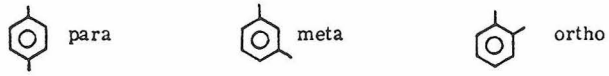

2. (2 pts) The BN and NC bond lengths in diphenylmethyleneaminodimesitylborane have been determined by x-ray crystallography.

R_2B ------ 1.40Å ------ N ------ 1.31Å ------ CR'_2 R' = phenyl, R = mesityl =

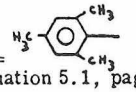

a. Calculate the length of single BN and NC bonds using equation 5.1, page 188.
b. Draw the best single Lewis structure of this compound.
c. Show the three-dimensional structure of the $R_2BNCR'_2$ unit.

3. (2 pts) The allignment of $Sb_2Br_9^{3-}$ and Br_2 in the crystal of tetramethylammonium nonabromodiantimonate(III)-dibromine, $[(CH_3)_4N]_3[Sb_2Br_9]\cdot Br_2$ is shown on the next page.

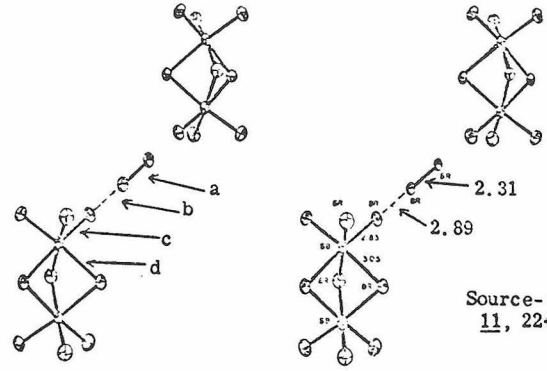

Source- Inorg. Chem., 11, 2247 (1972)

Molecular bromine bridging of $Sb_2Br_9^{3-}$ anions.

a. What is the charge on a tetramethylammonium cation?
b. Discuss the significance (or lack thereof) of the four bond lengths a-d shown above. Please keep your bullshitting to a minimum.

4. (1 pt) The heavier group III elements form the bridged dimeric species with which you are painfully familiar. The bonding in these compounds is

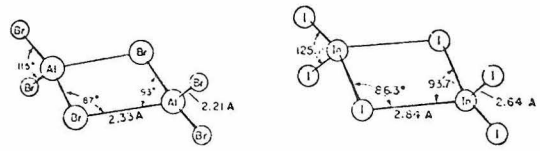

The structures Al_2Br_6 and In_2I_6

not electron deficient as in diborane. On your last midterm you showed that each bond contains two electrons. Will the bonding in $(CH_3)_6Al_2$ resemble that of Al_2Cl_6 or B_2H_6? Explain why.

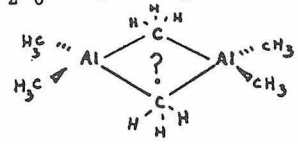

5. (1 pt) Boron compounds have some amazing structures. Try these:

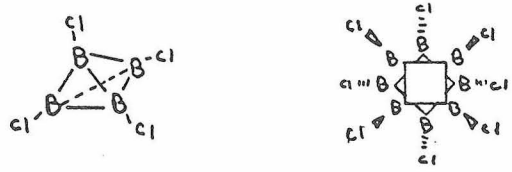

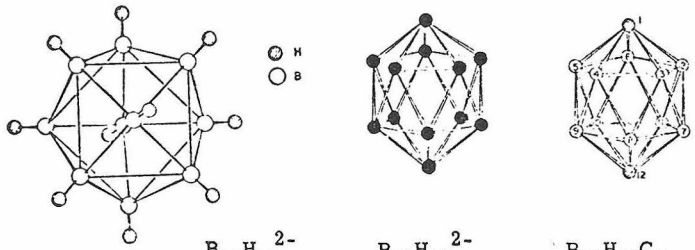

$B_{10}H_{10}^{2-}$ $B_{12}H_{12}^{2-}$ $B_{10}H_{12}C_2$

One isomer of carborane, $B_{10}C_2H_{12}$, is shown above. In this picture the filled circles are carbon atoms and the unfilled circles are boron atoms. Each atom of the cage structure also has a terminal hydrogen atom attached to it. Draw the only two other isomers of carborane not shown above.

6. (2 pts) The structures of P_4O_6 and P_4O_{10} are shown below. These are called

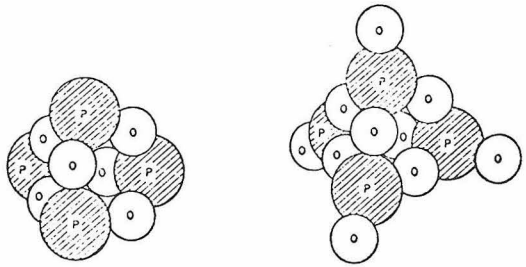

acid anhydrides because they are formally acids which lack the elements of water. Hydrolysis (reaction with water) leads to an acid:

$$P_4O_{10} + 6H_2O = 4\ H_3PO_4$$

The oxidation state of the phosphorus is unchanged in this reaction. What are the hydrolysis products of the following anhydrides?

a. N_2O_3
b. Sb_2O_5 (empirical formula only-structure unknown)
c. I_2O_5 (structure is O_2IOIO_2)
d. B_2O_3 (an infinite 3-dimensional network with B-O bonds)
e. $CH_3\underset{\underset{O}{\|}}{C}O\underset{\underset{O}{\|}}{C}CH_3$ (hint: this is called acetic anhydride)
f. SrO

The product of the SrO hydrolysis is actually a base. Metals generally form basic anhydrides. Al_2O_3, which dissolves in both acid and base, is amphoteric.

$$Al_2O_3 + 3H_2O = 2Al(OH)_3 \text{ (actually } Al(OH)_3(H_2O)_3)$$

$$\xrightarrow{OH^-} Al(OH)_4^- \qquad \xrightarrow{H^+} Al(OH)_2^+$$

HARRIS BATTERS FROSH

Pain Still Fresh

CALTECH IRKED

Two hours. Open Huheey and DGH. Open notes. Open Homework. Use blue books. Due Monday 13 November. Have log table handy. ln a = 2.303 log a. Models allowed but probably not necessary.

Reading: Huheey 276-294.

The Scoreboard

Me	Them
1	

1. (20 pts) Which compounds can be optically active?

a. 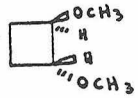

b. 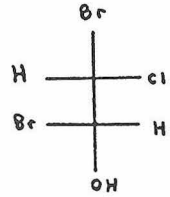

c. 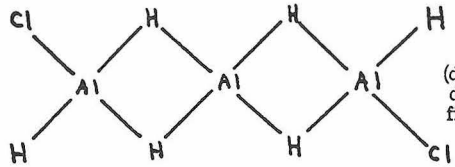

(determine the three-dimensional structure first)

d. 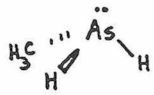

(Unlike compounds of nitrogen, compounds of the lower group V elements do not undergo rapid inversion.)

e. 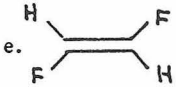

2. (20 pts) When two ideal gases are allowed to mix, the entropy increases because there is more disorder. The entropy increase is given by the equation

$$\Delta S = -R(x_1 \ln x_1 + x_2 \ln x_2)$$

where x_i is the mole fraction of component i in the final mixture. Imagine doing the following experiment in which each gas behaves as an ideal gas.

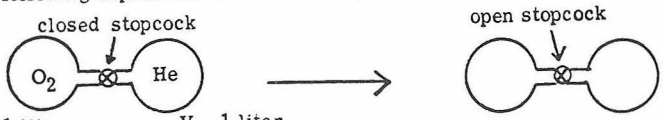

V = 1 liter	V = 1 liter	completely mixed gases
P = 0.002 atm	P = 0.001 atm	
T = 300°K	T = 300°K	

a. If the whole assembly is taken as a thermodynamic system, has any PV work been done by the system?

b. If the system is thermally isolated from its surroundings, what is the value of q?

c. What is the value of ΔE in kcal/mole?

d. What is the pressure of the final system?

e. Calculate ΔS in e.u.

f. Is ΔG positive, negative or zero in this process?

In answering these questions ignore any work involved in opening the stopcock.

3. (25 pts) The bond between a metal atom and a carbon monoxide molecule consists of two parts. There is a dative sigma bond in which CO donates two electrons to the metal.

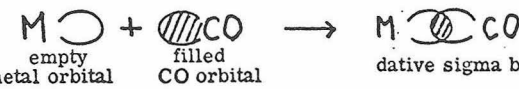

There is also pi back bonding from a filled metal d orbital to an empty CO π^* orbital:

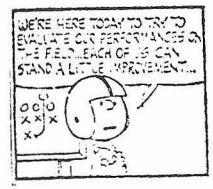

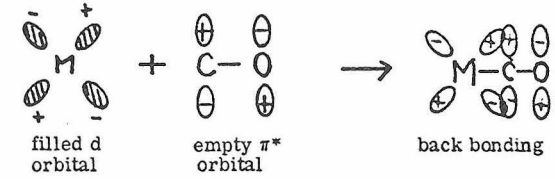

a. Given that CO has a bond order of three, write the Lewis structure consistent with the bond order. (Just the structure of plain CO)

b. Put the right number of electrons into the MO scheme below. What is the predicted bond order? Is CO diamagnetic or paramagnetic?

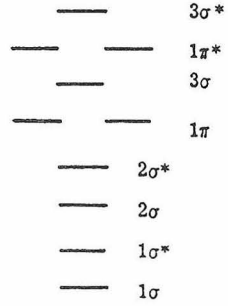

c. If $Mo(CO)_6$ is octahedral, what is the hybridization of Mo?

d. What is the hybridization of carbon in $Mo(CO)_6$? Draw a hybrid orbital bonding scheme for one Mo-C-O unit showing only the filled orbitals. Ignore the back bonding for the sake of this question. Use an unhybridized oxygen atom.

e. If back bonding occurs, does the CO bond order increase, decrease or remain the same as in free CO?

f. What is the Mo-C bond order in the absence or back bonding? How does this bond order change as back bonding increases?

g. Shown on the next page are plots of bond lengths vs. bond orders. For which point, A or B, is there more back bonding? For which point, C or D, is there more back bonding? These graphs come from data for a series of different metal carbonyl complexes. (A CO group is called a carbonyl group.)

Bond Length vs. Bond Order of Mo Carbonyls

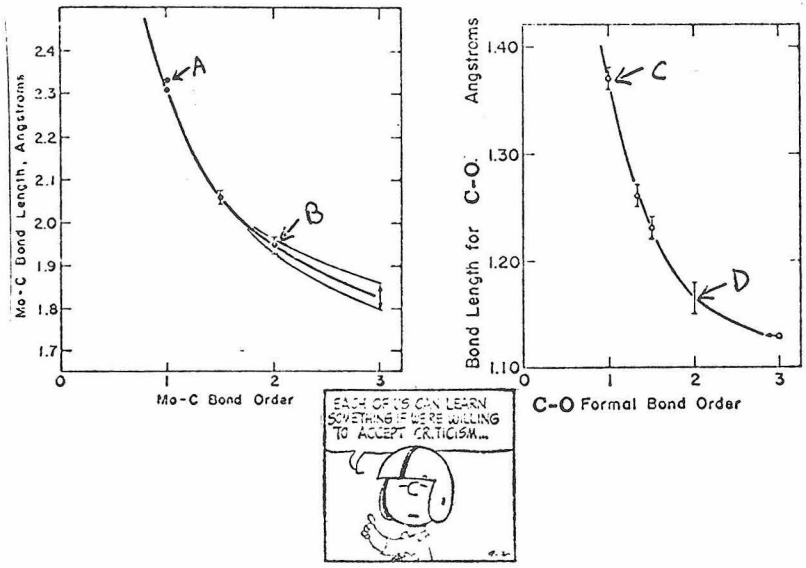

4. (15 pts) 1,2-difluorotetrachloroethane undergoes relatively free rotation at room temperature. Construct a schematic diagram of potential energy vs. rotation angle showing how the energy of the molecule varies as rotation occurs. (With a given constant total energy, what actually varies is the proportion of kinetic and potential energy. We will plot the potential energy.) Consider the rotation angle to be zero when the two fluorine atoms are eclipsed and that rotation of the front carbon occurs in a clockwise fashion as the rear carbon atom is held fixed. It will be easiest to look at the relative energy for every 60° of rotation.

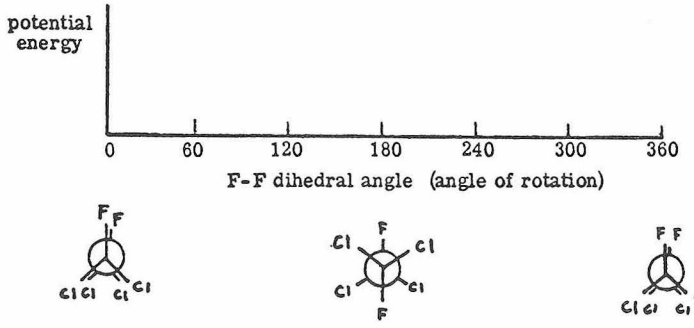

5. (20 pts) Hydrogen and carbon dioxide are in equilibrium with water and carbon monoxide at high temperature. This is called the water gas reaction.

$$H_2(g) + CO_2(g) = H_2O(g) + CO(g)$$

a. At 986°C and 1 atm total pressure, an equilibrium mixture corresponds to 47.51 mole % CO_2, 6.86 mole% H_2, 22.82 mole % H_2O and 22.82 mole % CO. Calculate the equilibrium constant under these conditions.

b. Calculate ΔG^{o}_{1259}.

When days were bold
And nights were old,
'Ere Chem 2 was invented,
This Problem Set Would Have Been Banned! (#14)

Due Thursday 16 November

Reading: Huheey 294-316

1. (2 pts) Huheey, problem 6.4, page 235.

2. (1 pt) How many chemically different kinds of protons (hydrogen atoms) are there in thioacac? Which are the most acidic?

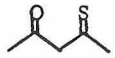

thioacetonylacetate (thioacac)

3. (1 pt) Which is a stronger acid?

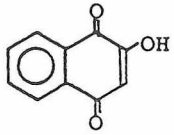

2-hydroxy-1,4-naphthoquinone

2-naphthol

4. (1 pt) Which is a stronger base?

$(H_2N)_2C(NH)$ guanidine

$(C_6H_5)NH_2$ aniline

5. (1 pt) Huheey, problem 8.1, page 370.

6. (1 pt) Huheey, problem 8.2, page 370.

7. (3 pts) Make a table like the one below and fill in the blank columns using valence bond theory. Et = ethyl, Ø = phenyl.

Let's try that again. Fill in the blanks in the table on the next page.

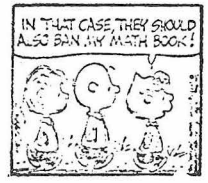

Complex	Number of Unpaired Electrons	Oxidation State of Metal	Number of Valence Electrons of Metal Ion	Ye Olde Diagramme	Hybridization	Geometry
CoF_6^{3-}	4	+3	6		sp^3d^2	octahedral
$Co(NH_3)_6^{3+}$	0	+3	6		d^2sp^3	octahedral
MnO_4^-	0	+7	0		d^3s	tetrahedral
$PdCl_4^{2-}$	0	+2	8		dsp^2	square planar
$Mn(H_2O)_6^{2+}$	5					
$Cr(NCS)_6^{3-}$	3					
CoI_4^{2-}	3					
$Ni(PEt_3)_2Cl_2$	0					
$Ni(PØ_3)_2Cl_2$	2					

d s p d

Trolls - 1: Bomber - 1
(Wait 'till the final!)

#15

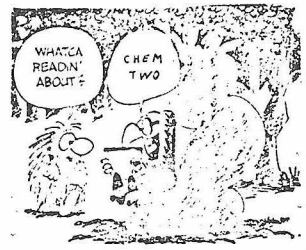

Reading: Huheey 316-337

1. (2 pts) Like d orbitals, p orbitals can also be considered subject to the electrostatic effects of the ligands. Indicate the degeneracies of the three p orbitals in an octahedral and a square planar environment. Draw an energy level diagram for each case and use the same coordinate system for each.

2. (2 pts) $Fe(H_2O)_6^{2+}$ is high-spin ($\Delta_o = 10,400\ cm^{-1}$). $Fe(CN)_6^{4-}$ is low-spin ($\Delta_o = 33,000\ cm^{-1}$). What can you say about the value of the spin pairing energy, P, for Fe(II)?

3. (2 pts) Huheey, problem 8.3 page 370.

4. (1 pt) Huheey, problem 8.4 page 370.

5. (1 pt) Huheey, problem 8.5 page 370. A eutectic mixture is just defined as that mixture of two substances which has the lowest melting point of any mixture of those two substances.

6. (1 pt) Huheey, problem 8.6 page 370.

7. (1 pt) Huheey, problem 8.7 page 370. Just work the following three cases:

$Co(CN)_6^{3-}$
$Rh(H_2O)_6^{3+}$
$Ir(en)_3^{3+}$

en is the abbreviation for ethylenediamine: $H_2NCH_2CH_2NH_2$. This is a bidentate ligand, ie., one which has two "teeth" or can bind itself to the transition metal from both nitrogen atoms. Before working this problem, draw a picture of one of the possible isomers of an $M(en)_6$ complex.

OPTIONAL The structure of the $Mo_2Ni_3(CO)_{16}^{2-}$ anion is illustrated on the right. (JACS., 93, 2159 (1971)) This cluster compound does not conform to the 18 electron rule for all the metal atoms. Can you determine how many electrons are formally associated with each metal atom in the cluster?

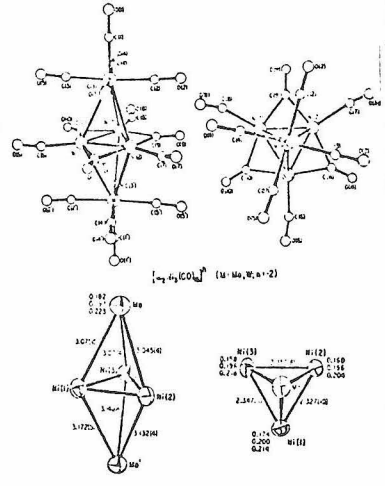

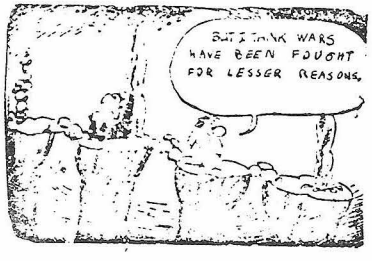

Another Turkey From the Staff of Chem Two (#16)

Due Monday 27 November

Reading: Huheey 371-385

Special Thanksgiving Instructions: Eat the Bird!

1. (2 pts) Show the d orbital splitting patterns for cubic and for square antiprismatic ML_8 complexes. Which geometry will $Mo(CN)_8^{6-}$ adopt and why?

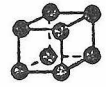

cubic

square antiprismatic

2. (2 pts) Starting with the ML_4 tetrahedral crystal field splitting diagram below, show how the energies of the five d orbitals change as the tetrahedron is distorted by elongation along the z axis.

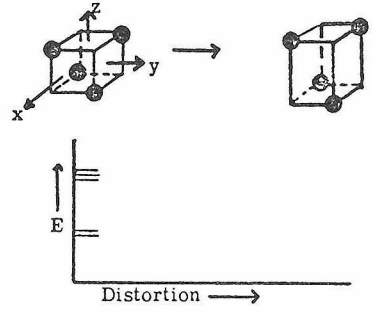

3. (2 pts) Using the diagram of f orbitals given out with Problem Set #2, show how these seven orbitals will be split by an octahedral crystal field. Note that these orbitals can be expressed (and drawn) in a different way on page 587 of Huheey and that the orbitals on page 587 could be harder to use for this purpose. This points up the fact that although the Schrödinger equation gives us seven solutions, we are free to combine them in many linear combinations to construct orbitals suitable to our needs.

What would be the f orbital splitting pattern for a cubic ML_8 complex?

4. (3 pts) In your own words, using no more than half a page, explain the significance of figure 8.20, page 312.

5. (1 pt) Which have a dipole moment?

a. HgI_3^-
b. chlorobis(thiourea)copper(I) - $Cu(tu)_2Cl$ tu = $H_2N\overset{S}{\overset{\|}{C}}NH_2$
c. molecule in figure 9.4a
d. molecule in figure 9.4b
e. pentachlorocuprate(II) (figure 9.5)
f. cyanotris(3-dimethylarsinopropyl)phosphinenickel(II) (figure 9.6)

VSEPR is applicable to elements with completely filled d orbitals. Is it applicable to any of these compounds?

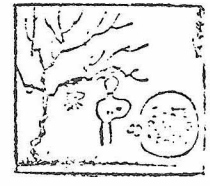

Isn't It Too Bad You Have But One Life To Give To Chem 2? (#18)

Reading: Huheey 401-417.

Optional Reading: DGH Chapter 19. This material deals with chemical kinetics which we will be doing in class for two lectures. The reading is not required as everything you will be responsible for will be presented in class. However, if you want additional background in kinetics or if the usual sterling lectures don't satisfy you, this is a good chapter to read.

1. (3 pts) For the first order reaction below, show that the time needed for 99.9% of the reaction to be complete is ten times the time needed for half the reaction to be complete.

$$A \xrightarrow{k} \text{products}$$

2. (3 pts) The observed rate law for the decomposition of N_2O_5 is

$$\frac{-d[N_2O_5]}{dt} = k_o[N_2O_5]$$

A mechanism postulated for this decomposition is

a. $N_2O_5 \xrightarrow{k_1} NO_2 + NO_3$

b. $NO_2 + NO_3 \xrightarrow{k_2} N_2O_5$

c. $NO_2 + NO_3 \xrightarrow{k_3} NO + O_2 + NO_2$

d. $NO + NO_3 \xrightarrow{k_4} 2NO_2$

Using the steady state approximation for [NO] and $[NO_3]$, verify that the decomposition follows first order kinetics and that the rate constant, k_o is given by

$$k_o = \frac{2k_3k_1}{2k_3 + k_2}$$

An orderly way to do this is as follows:

i. determine $-d[N_2O_5]/dt$ = ?

ii. determine $d[NO]/dt$ and solve for [NO]

iii. determine $d[NO_3]/dt$ and use the results of (ii) to simplify the expression.

iv. plug (iii) into (i) and hope for the best

3. (2 pts) Draw the two enantiomers (optical isomers) of $Co(phen)_3^{3+}$.

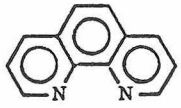

phen = 1,10-phenanthroline

Given a racemic (inactive) mixture of the enantiomers of $Co(phen)_3^{3+}$, say as the chloride salt, $Co(phen)_3Cl_3$, how might you isolate a sample enriched in one of the enantiomers? You may use one of the following naturally occurring optically active compounds in any way you see fit (except to poison your friendly Chem 2 staff.)

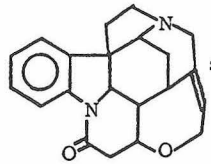

strychnine

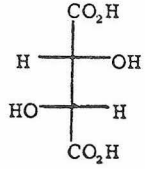

tartaric acid

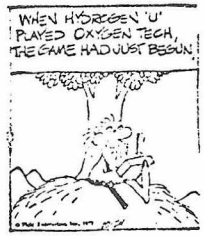

4. (2 pts) The equation for the net reaction between oxalate ion and $HgCl_2$ is

$$2HgCl_2 + C_2O_4^{2-} \xrightarrow{k_o} 2Cl^- + 2CO_2 + Hg_2Cl_2\downarrow$$

The rate of the reaction can be determined by weighing the Hg_2Cl_2 precipitated per unit time and the empirical rate law can be determined by measuring these rates at various initial concentrations of $HgCl_2$ and $C_2O_4^{2-}$. At 100°C we find:

$HgCl_2$ (moles/liter)	$K_2C_2O_4$ (moles/liter)	$d[Hg_2Cl_2]/dt$ (M/min)
0.0836	0.202	0.26
0.0836	0.404	1.04
0.0418	0.404	0.53

State the empirical rate law: $d[Hg_2Cl_2]/dt$ = ?

5. (0 pts) 'The atom has shells of electrons spinning in different directions around the nucleus. spdf signify the orbitals in which the electrons are kept. Only two electrons can inhibit an orbital. The atom is now thought of as dumbells. An electron moves around an atom sometimes close to the nucleus sometimes far away: the average is the medium, about a third of the way out from the nucleus. The concept now held about the atom can be explained the quantum method. At one time it was believed that electrons moved about the nucleus in a set pattern. The quantum idea has changed this to make it harder to explain. One is constantly subjected to the flat atomic model with the electron perfectly circumsizing the nucleus. One then has to be reindoctrinated to an atomic model that no one is sure of."

- J. Chem. Ed., 49, 774. (November 1972)

"What me worry?"

- who said that?

For Want Of A Title The Kingdom Was Lost (#19)

Due Monday 4 December

Reading: Huheey 401-417. (The reading assignment on Problem Set 18 should have been 385-401.)

1. (1 pt) The rate of ring inversion of 1,1-difluorocyclohexane has been measured by NMR. What must be the ratio k_1/k_{-1}? What is the value of the equilibrium constant for this reaction? What is the value of ΔG^o? Will the value of $\Delta G^{\mp}$ be positive, negative or zero?

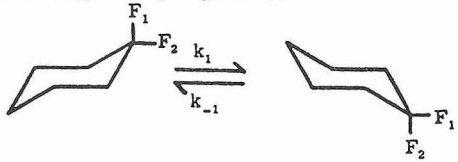

2. (4 pts) (Ref. J. Am. Chem. Soc., 92, 7056 (1970).) Draw the two optical isomers of $Cr(acac)_3$. This should be old hat by now. The rate at which the enantiomers interconvert has been measured recently. An Arrhenius plot for this interconversion is shown below. Determine E_a, logA and $\Delta S^{\mp}$ (at 100°C). For the entropy of activation use the relation

$$k = (ekT/h)\, e^{\Delta S^{\ddagger}/R}\, e^{-E_a/RT}$$

where k is the rate constant (units of sec^{-1} for a first order reaction) and k is Boltzmann's constant.

Table II. Rate Constants for Inversion of $Cr(acac)_3$ and $Co(acac)_3$ in Chlorobenzene Solution

Temp. °C	$Cr(acac)_3$ Concn × 10^4, mol/L	$k \times 10^4$,[a] sec^{-1}
96.1	1.20	0.134 ± 0.002[b]
	2.68	0.127 ± 0.005
116.0	1.14	1.48 ± 0.04
	3.03	1.42 ± 0.04
126.1	1.07, 3.30[c]	4.44 ± 0.31
	1.62, 9.90[c]	4.29 ± 0.32
135.0	1.07, 1.25, 2.89[c]	12.2 ± 0.5
	1.66, 1.69, 4.47[c]	13.0 ± 1.1

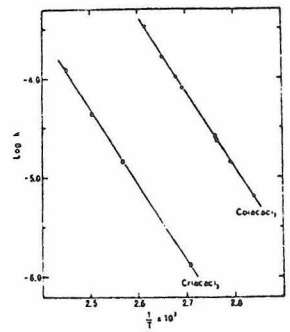

Figure 4. Arrhenius plots for inversion of $Cr(acac)_3$ and $Co(acac)_3$.

3. (2 pts) There exists an important principle of reaction mechanisms known as the Principle of Microscopic Reversibility. Quoting K. J. Laidler, this states that "in a system at equilibrium, any molecular process and the reverse of that process occur on the average at the same rate." This seems trivial but among its implications is that reaction along any path at equilibrium must go at the same rate in either direction. Thus the dominant path for the forward reaction must be the dominant path for the reverse reaction. The ratio of the rate constants in the forward and reverse directions must be equal to an equilibrium constant.

Consider the reaction

$$A \underset{k_{-1}}{\overset{k_1}{\rightleftharpoons}} B \underset{k_{-2}}{\overset{k_2}{\rightleftharpoons}} C$$

At equilibrium we have

$$\frac{[B]}{[A]} = k_1/k_{-1} \qquad \frac{[C]}{[B]} = k_2/k_{-2} \qquad \frac{[C]}{[A]} = k_1k_2/k_{-1}k_{-2} = K_1K_2 = K_{eq}$$

The rate of appearance of B at equilibrium must be zero, so:

$$d[B]/dt = k_1[A] - (k_{-1}+k_2)[B] + k_{-2}[C] = 0$$

$$[B]_{eq} = (k_1[A] + k_{-2}[C])/(k_{-1} + k_2)$$

Using this expression for $[B]_{eq}$, write an expression for the rate of appearance of A at equilibrium. Set this equal to zero and show that the rate equations predict that

$$\frac{[C]}{[A]} = k_1k_2/k_{-1}k_{-2} = K_{eq}$$

4. (3 pts) (Ref. J. Am. Chem. Soc., 92, 6425 (1970).) The iron substitution reaction below has been suggested to be a two step reaction with the following elementary steps:

$$\underset{A}{Fe(NO)_2I(P\phi_3)} + \underset{P}{P\phi_3} \underset{k_{-1}}{\overset{k_1}{\rightleftharpoons}} \underset{X}{Fe(NO)_2I(P\phi_3)_2} \xrightarrow{k_2} \underset{B}{Fe(NO)_2(P\phi_3)_2^{+}} + I^-$$

Assuming a steady state for the intermediate we get

$$0 = d[X]/dt = k_1[A][P] - (k_{-1} + k_2)[X]$$

$$[X] = k_1[A][P]/(k_{-1} + k_2)$$

$$\text{Rate} = d[B]/dt = k_2[X] = (k_1k_2/(k_{-1} + k_2))[A][P] \equiv k_{obs}[A][P]$$

It is found that at low temperatures $k_2 \gg k_{-1}$ so $k_{obs} \approx k_1$ and at high temperatures $k_{-1} \gg k_2$ so $k_{obs} \approx k_1k_2/k_{-1}$.

A table of second order rate constants (k_{obs}) is given on the next page.

T (°C)	k_{obs} (liter mole^{-1} sec^{-1})
60	3.31×10^{-4}
45	1.40×10^{-3}
20	1.50×10^{-3}
0	4.90×10^{-4}
-19	0.95×10^{-4}

Make a plot of log k vs. 1/T. In the low temperature region $k \approx k_1$. Use the slope in this region to determine E_{a1} for the Arrhenius equation

$$k_1 = A_1 e^{-E_{a1}/RT}$$

In the high temperature region $k \approx k_2 k_1/k_{-1} = k_2 K_1$ where K_1 is an equilibrium constant. Using an equation from thermodynamics we can write the following:

$$d(\log K_1)/d(1/T) = -\Delta H_1/2.303R$$

$$k \approx k_2 K_1$$

$$\log k \approx \log k_2 + \log K_1$$

$$d(\log k)/d(1/T) \approx -E_{a2}/2.303R - \Delta H_1/2.303R = -(E_{a2} + \Delta H_1)/2.303R$$

From the slope in the high temperature region determine the value of $(E_{a2} + \Delta H_1)$. What should be the sign of E_{a2}? What is the sign of ΔH_1? What, therefore, is an upper limit on ΔH_1? By Le Chatelier's principle does K_1 increase or decrease with increasing temperature?

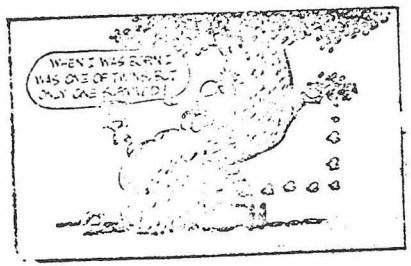

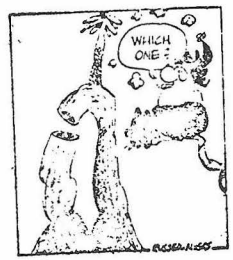

The Parting Blow of Chem 2a (#20)

Due Thursday 7 December

Reading: 418-425, 429-440.

The final exam, worth 200 of your 500 points, will be given out Thursday 7 December and will be due in the Bomber's mailbox in Noyes no later than 5:00 pm on Monday 11 December. Graded exams can be picked up outside my door (220 Noyes) on Tuesday. The letter grade appearing on the exam will be your total grade for the course. Though the Registrar will only see a P or F, you will see the actual grade you would have earned -- thanks to your loving Chem Two Staff.

1. (3 pts) A dissociative mechanism for hydrolysis of $Co(NH_3)_5X^{2+}$ in aqueous solution might be as follows:

$$Co(NH_3)_5X^{2+} \underset{k_{-1}}{\overset{k_1}{\rightleftharpoons}} Co(NH_3)_5^{3+} + X^-$$

$$Co(NH_3)_5^{3+} + H_2O \xrightarrow{k_2} Co(NH_3)_5(H_2O)^{3+}$$

The net rate of reaction will be the rate of the second step:

$$d[Co(NH_3)_5(H_2O)^{3+}]/dt = k_2[Co(NH_3)_5^{3+}][H_2O]$$

Assuming a steady state for $Co(NH_3)_5^{3+}$, show that the observed rate law will be of the form

$$\frac{d[Co(NH_3)_5(H_2O)^{3+}]}{dt} = \frac{k_a[Co(NH_3)_5X^{2+}]}{k_b[X^-] + 1}$$

and find k_a and k_b in terms of the various rate constants given above.

2(1.5 pts) The equilibria below illustrate the chelate effect.

$Ni^{2+} + 2NH_3 = Ni(NH_3)_2^{2+}$		logK = 5.00
$Ni^{2+} + 4NH_3 = Ni(NH_3)_4^{2+}$		logK = 7.87
$Ni^{2+} + 6NH_3 = Ni(NH_3)_6^{2+}$		logK = 8.61
$Ni^{2+} + en = Ni(en)^{2+}$		logK = 7.51
$Ni^{2+} + 2en = Ni(en)_2^{2+}$		logK = 13.86
$Ni^{2+} + 3en = Ni(en)_3^{2+}$		logK = 18.28

en = ethylenediamine

Writing K in terms of ΔH and ΔS, which you do masterfully from your vast knowledge of thermo, explain how these two factors contribute to the increased stability of the chelate complexes. Use no more than four sentences.

3. (2 pts) A possible mechanism for the E2 reaction might be

$$CH_3CH_2Cl + HO^- \overset{fast}{\rightleftharpoons} {}^-{:}CH_2CH_2Cl + H_2O$$

$${}^-{:}CH_2CH_2Cl \overset{slow}{\rightarrow} CH_2{=}CH_2 + Cl^-$$

This mechanism has been excluded for several halides by carrying out the reaction in deuterated solvents such as D_2O or C_2H_5OD. Explain how such experiments could be relevant to the reaction mechanism.

4. (1 pt) Write out the different staggered conformations of meso and d,l-2,3-dibromobutane. Show the structures of the alkenes that could be formed from each rotamer by a trans E2 elimination reaction of one mole of HBr with OH^-. Which alkene would more readily eliminate further to form dimethylacetylene?

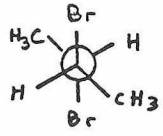

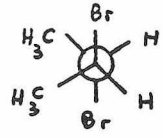

5. (1 pt) Huheey Problem 9.7, page 440

6. (1.5 pts) Huheey Problem 9.6, page 440

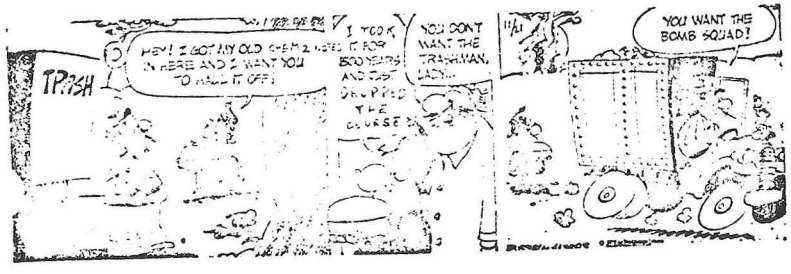

This test has 24 questions (very short answers) and is worth 200 points. Your strategy should be to skip any question for which you do not see the answer very quickly. You may use up to three hours in your never-ending quest to outguess me. Open Huheey, DGH, notes, homework. Closed everything else. ln a is still 2.303 log a. A periodic table appears in Huheey, page 39. Your slide rule should be handy. The computer is in Jorgensen and you can't use it.

Due in Bomber's mailbox in Noyes no later than 5:00 p.m. Monday, 11 December 1972. The letter grade on your test (available 12 December at 220 Noyes) will be your total grade for the course.

Reading for Thursday, 4 January 1973: Bestiary, pages 1-10. Stipulation: You may not do this assignment before 2 January 1973 unless you think you are Super Troll.

1. (8 pts) Given that CoF_6^{3-} is high spin, what would be the electronic configuration of $CoBr_6^{4-}$? For your answer draw an energy level diagram and place the right number of electrons with the right spins in the diagram.

2. (8 pts) The ion with the composition SbF_5 has the geometry below. (Inorg. Chem., 11, 2323 (1972).) Working backwards from the geometry, use VSEPR to figure out the charge on this ion.

"Colloids may be separated from crystalloids by filtering through a mucous membrane."

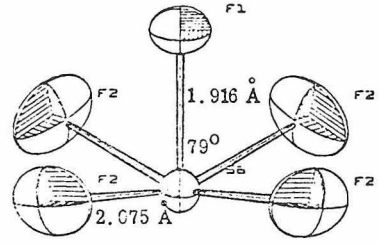

3. (8 pts) In the spectrochemical series of Huheey page 307, thiocyanate (SCN) appears twice. In one sentence or less, why?

4. (8 pts) For which compound below will the hydrogen bound to nitrogen be more acidic? You must show why to get credit for your answer. When drawing Lewis structures, be sure to include all electrons and all formal charges.

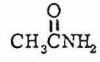

acetamide

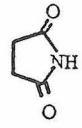

succinimide

5. (8 pts) In which complex, A or B, would you expect ^{35}Cl of complex to exchange faster with ^{37}Cl in solution? This illustrates the trans effect. Which ligand, Cl or $P(CH_3)_3$, has a larger trans influence?

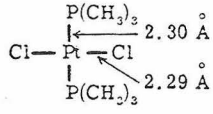

A

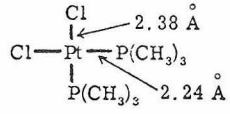

B

399

6. (8 pts) The chirping of tree crickets follows a good Arrhenius law. The slope of this graph is -2.67×10^3 deg. What is the activation energy for this process? (Ref. J. Chem. Ed., 49, 343 (1972).)

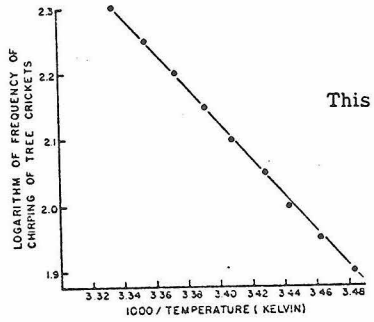

Arrhenius plot for the chirping of tree crickets.

This is real data.

Food for thought:

Of special interest are some applications of the Arrhenius law to rates of psychological processes. For example, Hoagland (*12, 2*) made studies of patients whose body temperatures varied over a few degrees. He had them count at what they believed to be one a second, and found the rates to be higher the higher the temperature. His Arrhenius plot is reproduced in Figure 4; the activation energy is 24.0 kcal/mole.

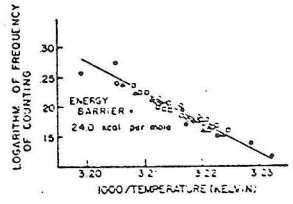

Arrhenius plot for rates of counting.

7. (8 pts) You are a government bureaucrat trying how best to waste the taxpayer's money. Pat Hagan proposes to synthesize C, Bernie Richman proposes to synthesize D and Dave Miller proposes to synthesize E. For whom will you provide research money? (Use no more than one sentence for your reason.)

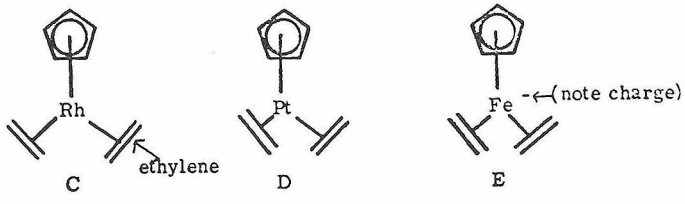

"Ammonia is a medicine administered to hysterical females."

8. (8 pts) Using VSEPR, what is the geometry about carbon in thiourea?

$S{=}C(NH_2)_2$ thiourea

9. (8 pts) $NiCl_2(P\phi_3)_2$ is paramagnetic but $PdCl_2(P\phi_3)_2$ is diamagnetic. How many isomers will there exist for each compound?

10. (6 pts) The crystal structure of $AgClO_4 \cdot 3(C_4H_4O_2)$ is shown schematically below. In this figure $C_4H_4O_2$ is dioxane and is drawn in the funny way shown here:

dioxane

Ref.: J. Chem. Soc., Dal., 1732 (1972).

In this crystal structure the dioxane is

a. ambidentate
b. bidentate
c. monodentate
d. polydentate
e. ambivalent
f. chelating
g. bridging
h. terminal

Choose whichever terms apply.

"Aqueous tension is that which enables flies to walk on water."

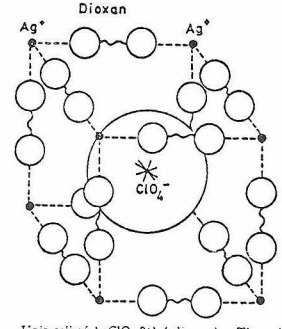

Unit-cell of $AgClO_4.3(1,4\text{-dioxan})$. The anion rotates freely and the dioxan molecules rotate about the O–O axes (Prosen and Trueblood, *Acta Cryst.*, 1956, 9, 741)

11. (10 pts) A plot of the radii of octahedrally coordinated M^{2+} ions is shown below. Using no more than five sentences, explain the appearance of this graph. The compounds referred to are all high spin.

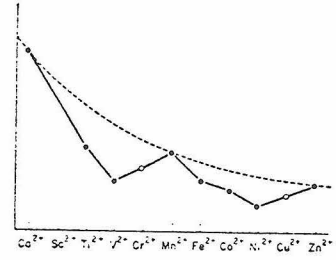

The relative ionic radii of divalent ions of the first transition series.

400

12. (10 pts) We used peroxodisulfate, $S_2O_8^{2-}$, to oxidize luminol in class. Hit me with two of the many very good resonance structures of this anion. What is the oxidation state of sulfur in peroxodisulfate?

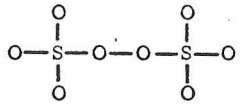

"If you should eat 50 pounds of bacon which produces 100,000 Calories, you would be some warm baby when you got through."

13. (12 pts) Draw an energy level diagram, populated with the right number of electrons with the right number of spins, of each of the following:

a. $CrCl_6^{3-}$ ($\Delta_O = 13,200\ cm^{-1}$, $P \approx 20,000\ cm^{-1}$)

b. $Mn(CN)_6^{4-}$ (Estimate Δ_O with equation 8.15, page 310. P can be estimated from Table 8.11, page 305.)

14 (8 pts) The quinuclidine-trimethylborane adduct is much more stable than the trimethylamine-trimethylborane adduct. In one sentence or less, suggest a reason for this.

(1) 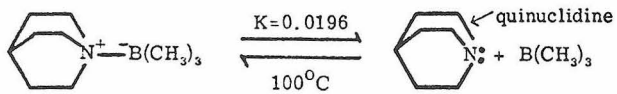

(2) $(CH_3)_3N^+{-}^-B(CH_3)_3 \underset{100^oC}{\overset{K=0.472}{\rightleftharpoons}} (CH_3)_3N: + B(CH_3)_3$

15 (8 pts) Calculate ΔG^o_{373} for reaction (2) directly above this line.

16 (8 pts) Will element number 118 be a solid or a gas? Estimate its first ionization energy ($\pm$ 1 eV).

17 (8 pts) The exchange of coordinated water of a metal complex with solvent water might be expected to go by a dissociative path.

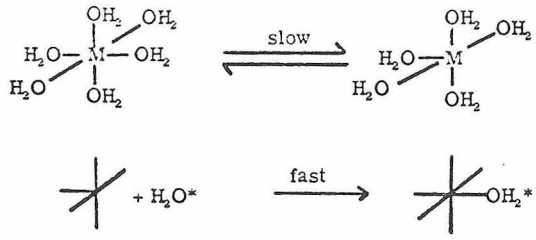

H_2O^* is water that was originally solvent.

The reaction coordinate diagram might therefore look something like this:

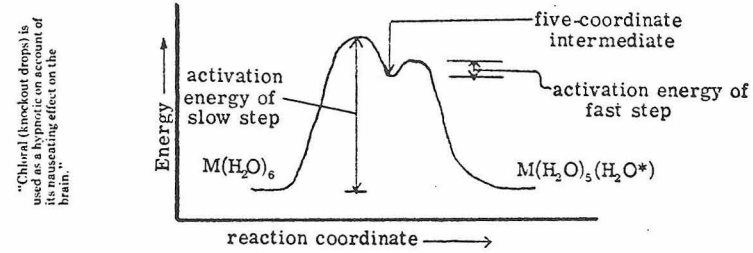

"Chloral (knockout drops) is used as a hypnotic on account of its nauseating effect on the brain."

Crystal field activation energies (in Dq) for dissociation mechanism Octahedral → square pyramid

System	Strong Fields: Octahedral	Strong Fields: Square Pyramid	Strong Fields: C.F.A.E.	Weak Fields: Octahedral	Weak Fields: Square Pyramid	Weak Fields: C.F.A.E.
d^0	0	0	0	0	0	0
d^1	4	4.57	−0.57	4	4.57	−0.57
d^2	8	9.14	−1.14	8	9.14	−1.14
d^3	12	10.00	2.00	12	10.00	2.00
d^4	16	14.57	1.43	6	9.14	−3.14
d^5	20	19.14	0.86	0	0	0
d^6	24	20.00	4.00	4	4.57	−0.57
d^7	18	19.14	−1.14	8	9.14	−1.14
d^8	12	10.00	2.00	12	10.00	2.00
d^9	6	9.14	−3.14	6	9.14	−3.14
d^{10}	0	0	0	0	0	0

We can get a very crude estimate of the activation energy of the slow (rate determining) step if we look at the change in crystal field stabilization energy on going from an octahedral ML_6 complex to a square pyramidal ML_5 complex. This difference in energy is called the crystal field activation energy. For which complex, $Cu(H_2O)_6^{2+}$ or $Ni(H_2O)_6^{2+}$, do you expect a faster rate of water exchange? The observed difference in rate is five orders of magnitude.

18. (8 pts) Which will be more acidic and why? (One sentence or less.)

ICH_2CO_2H $\qquad$ $ClCH_2CO_2H$

19. (10 pts) The substitution reaction below has a rate which is first order in $[XCo(CO)_4]$ and independent of [P]. In this reaction X = CH_3CO and P is a

$$XCo(CO)_4 + P \rightarrow XCo(CO)_3P + CO$$

phosphine. This rate law suggests a rate determining dissociation step:

$$\underset{A}{XCo(CO)_4} \underset{k_{-1}}{\overset{k_1}{\rightleftharpoons}} \underset{B}{XCo(CO)_3} + CO$$

$$XCo(CO)_3 + P \xrightarrow{k_2} \underset{C}{XCo(CO)_3P}$$

Assuming a steady state in B, derive a rate expression, d[C]/dt, and state what conditions must hold if this rate is independent of phosphine concentration.

20. (8 pts) In which solvent below will you find the highest column of liquid when you determine the molecular weight of 0.136 g/l of an unknown solute by osmotic pressure?

	Molecular Weight (g)	Boiling Point (°C)	Density (g/cc)
Benzene	78.11	80.1	0.879
Acetone	58.08	56.2	0.791
Water	18.01	100.0	1.00
Chloroform	119.38	61.2	1.49

21. (8 pts) The crystal field energy level scheme for a trigonal bipyramidal complex is given below. Will either Z-in or Z-out distortions ever be used to remove the degeneracy of the electronic ground state and satisfy the Jahn-Teller Theorem?

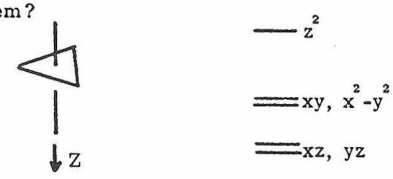

22. (6 pts) Using our favorite circles for orbitals, write out the electronic structure of Se^+.

23. (8 pts) When a molecule can't pull off a job by itself, it may call on a friend for assistance. The acetate anion is not a sufficiently strong nucleophile to displace bromide from the compound below. But if the acetate calls on Ag^+ for

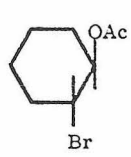

(Ac = $CH_3\overset{O}{\overset{\|}{C}}$-

(This picture only says we have a trans cyclohexane structure. It is not the actual three-dimensional geometry.)

help (it would merely yell "Hi Ho Ag^+! Away....") the Ag^+ can pull on the front of the Br while the incoming OAc attacks the rear in the usual S_N2 manner.

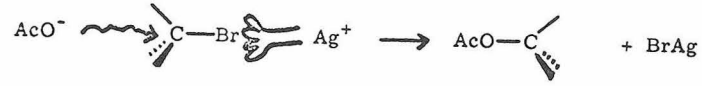

The net result is still inversion of configuration at carbon as shown above. Draw the stereochemistry of the product of attack of AcO^- on the compound above (on page 6). A drawing like the one on page 6 will be sufficient. Is the product diacetate cis or trans?

24. (10 pts) $N(SiR_3)_3$ compounds are planar and have a very low basicity toward protons or anything else. Some acceptable resonance structures to account for this are given below.

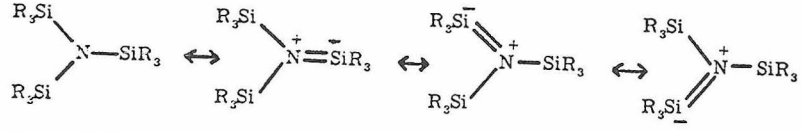

Draw a hybrid orbital scheme showing the N and just one Si bound to it. Show which orbitals participate in the sigma and pi parts of the bond. You may have to think twice about what the Si is doing in this compound.

25. (0 pts) The loving Chem Two Staff would appreciate any comments you care to offer at the end of your exam book after you are through with the test. Criticism which would improve the course is especially desirable. Personal slurs should be minimized.

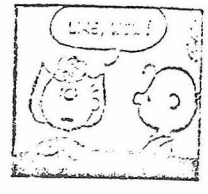

402